LEABHARLANN CHOLÁISTE NA TRÍONÓIDE, BAILE ÁTHA CLIATH | TRINITY COLLEGE LIBRARY DUBLIN
Ollscoil Átha Cliath | The University of Dublin

Terms and Conditions of Use of Digitised Theses from Trinity College Library Dublin

Copyright statement

All material supplied by Trinity College Library is protected by copyright (under the Copyright and Related Rights Act, 2000 as amended) and other relevant Intellectual Property Rights. By accessing and using a Digitised Thesis from Trinity College Library you acknowledge that all Intellectual Property Rights in any Works supplied are the sole and exclusive property of the copyright and/or other IPR holder. Specific copyright holders may not be explicitly identified. Use of materials from other sources within a thesis should not be construed as a claim over them.

A non-exclusive, non-transferable licence is hereby granted to those using or reproducing, in whole or in part, the material for valid purposes, providing the copyright owners are acknowledged using the normal conventions. Where specific permission to use material is required, this is identified and such permission must be sought from the copyright holder or agency cited.

Liability statement

By using a Digitised Thesis, I accept that Trinity College Dublin bears no legal responsibility for the accuracy, legality or comprehensiveness of materials contained within the thesis, and that Trinity College Dublin accepts no liability for indirect, consequential, or incidental, damages or losses arising from use of the thesis for whatever reason. Information located in a thesis may be subject to specific use constraints, details of which may not be explicitly described. It is the responsibility of potential and actual users to be aware of such constraints and to abide by them. By making use of material from a digitised thesis, you accept these copyright and disclaimer provisions. Where it is brought to the attention of Trinity College Library that there may be a breach of copyright or other restraint, it is the policy to withdraw or take down access to a thesis while the issue is being resolved.

Access Agreement

By using a Digitised Thesis from Trinity College Library you are bound by the following Terms & Conditions. Please read them carefully.

I have read and I understand the following statement: All material supplied via a Digitised Thesis from Trinity College Library is protected by copyright and other intellectual property rights, and duplication or sale of all or part of any of a thesis is not permitted, except that material may be duplicated by you for your research use or for educational purposes in electronic or print form providing the copyright owners are acknowledged using the normal conventions. You must obtain permission for any other use. Electronic or print copies may not be offered, whether for sale or otherwise to anyone. This copy has been supplied on the understanding that it is copyright material and that no quotation from the thesis may be published without proper acknowledgement.

PLATINUM AND TAXANE CHEMORESISTANCE MECHANISMS IN OVARIAN CANCER CELLS



TRINITY
COLLEGE
DUBLIN

A Thesis submitted to the University of Dublin for the degree of

Doctor of Philosophy (Ph.D.)

by

Steven Busschots (B.Sc)

Supervisors: Prof. John O'Leary, Dr. Sharon O'Toole & Dr. Britta Stordal

Department: Histopathology & Morbid Anatomy/Obstetrics & Gynaecology

University of Dublin

Trinity College

March 2015

Declaration

I hereby certify that the work in this thesis has not been submitted for any other degree or diploma at this, or any other university, and that all of the work described herein is entirely my own except where otherwise acknowledged. This thesis may be made available from the library for lending, consulting or copying.

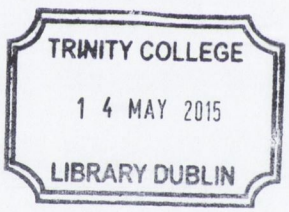

Thesis 10537

Steven Busschots

Summary

Ovarian cancer is the leading cause of death from a gynaecological malignancy, typically presenting at late stage due to difficult diagnosis and lack of suitable screening tools. The standard treatment of combination taxol/carboplatin chemotherapy often fails and patients relapse with chemoresistant disease. Patients have a median survival of two years following recurrence and will all eventually die from their disease. Patients with BRCA1 deficiencies have an increased lifetime risk of approx. 39-46% for developing ovarian cancer. There exists an inverse resistance relationship between platinum and taxane therapies in relation to BRCA1. Cells with non-functional BRCA1 are sensitive to platinums but resistant to taxanes. The opposite is true for cells with functional BRCA1. The focus of this study is to uncover a greater understanding of the mechanisms of ovarian cancer chemoresistance in order to contribute significantly to the improved treatment of ovarian cancer patients.

As part of this study we devised a clinically relevant comparative selection strategy to allow us to investigate the effects of resistance development on the inverse resistance relationship between platinum and taxane chemotherapy in relation to BRCA1 status. By selecting OVCAR8 (BRCA1-methylated) and UPN251 (BRCA1-wildtype) with different combinations of carboplatin and taxol treatments, we produced dual and singularly resistant models for carboplatin and taxol. Results indicated that resistance to both carboplatin and taxol developed quicker and more stably in UPN251 (BRCA1-wildtype) compared to OVCAR8 (BRCA1-methylated) and that taxol resistance developed quicker in BRCA1-wildtype and BRCA1-methylated cells models irrespective of BRCA1 status.

The resulting carboplatin and/or taxol-resistant UPN251 sublines were characterised using multiple methods including Affymetrix gene/miRNA screening in order to elucidate the mechanism of resistance that developed after clinically relevant selection. The main mechanisms of taxol resistance were, increased efflux of taxol via over-expression of P-glycoprotein, increased expression of PLAC8 and MAP3K15 and inability to decrease Bcl-2 resulting in resistance to apoptosis, circumvention of G2/M arrest and a reduction in growth rate. The main mechanisms of carboplatin resistance were increased expression of PLAC8 and MAP3K15, reduced expression of BMPR1B and BMP2 and inability to decrease Bcl-2/Bcl-XL resulting in resistance to apoptosis and resistance to changes in the cell cycle when exposed to carboplatin. Results regarding our dual carboplatin/taxol resistant models UPN251-6CALT and UPN251-6TALT indicated that the cytotoxic agent that a cell-line was exposed to first influenced

the mechanisms of resistance that developed. Also, as cross resistance to PARP inhibitors CEP8983 and veliparib did not develop in any of our resistant UPN251 models, they have been recommended as possible candidate drugs for the treatment of carboplatin/taxol resistant ovarian cancer.

Affymetrix gene/miRNA screening investigated expressional changes between carboplatin resistant subline UPN251-7C, taxol resistant subline UPN251-7T and parental cells. This provided an array of novel genes/miRNAs associated with the chemoresistance phenotype in ovarian carcinoma. The expression of the most promising of these markers (CCL20, GLI3, LIN28B, SRPX2, let-7i and miR-205) were examined in a pilot study which contained 32 clinical ovarian cancer samples. The patients were subdivided by their response to chemotherapy. GLI3 and the 6 markers in combination were found to be predictive of disease-free survival and overall survival in ovarian cancer patients and may represent important therapeutic targets for future investigation.

The above findings have contributed substantially to the current knowledge on ovarian cancer chemoresistance and have the potential to contribute to the improvement of ovarian cancer treatment in the future.

Acknowledgements

This study was funded by a PhD Scholarship from the Royal City of Dublin Hospital Trust (Steven Busschots), the Emer Casey Foundation (Steven Busschots) as part of the DISCOVARY Consortium, an Irish Cancer Society Postdoctoral Fellowship (Britta Stordal) and a Marie Curie Re-integration Grant from the European Union P7 programme (Britta Stordal). A special thank you goes to our funding bodies for supporting this work.

I would like to give a huge thank you to my supervisor Professor John J. O'Leary and my co-supervisors Dr. Sharon O'Toole and Dr. Britta Stordal. Each of you has given me the expertise, guidance and encouragement needed to be able to complete this research project to the highest possible standards. Your help has been invaluable in developing the project and myself to be a more independent and confident researcher. I really appreciate everything you have done for me over the last three years.

Another huge thank you is extended to both my family and family to be, for the love and support given to me throughout the duration of this endeavour. A special thank you goes to my beautiful fiancée Jenny Martin. You have been there for me to celebrate the good time but have also been there for me in my moments of weakness. Your endless love, support, motivation and belief have been my driving force in completing this project.

Thank you to Professor Orla Sheils. You have always proved to be a great person to turn to in times of need. Your knowledge, advice and understanding have helped me greatly over the past years.

Sincere thanks to all the people who have graced the Sir Patrick Dunns Research Laboratory over the past years especially, Louise Flynn, Lauren Brady, Dr. Paul Smith, Dr. Gordon Blackshields, Dr Stephen Finn, Dr. Orla Casey, Dr. Gary Sommerville, Denise Lawlor, Ben Doherty and Patricia Martin. Your help and friendship have guided me at every turn and the odd nights out with you have kept me sane.

A big thank you goes to Dr. Cathy Spillane for all her help and expertise regarding Affymetrix array platforms and qPCR analysis. I would also like to thank Dr. Gordon Blackshields for all the help and many hours spent working on bioinformatics related analyses.

Thanks to Dr Lorraine O' Driscoll and Dr Martin Barr for your critical analysis of my transfer report. Your suggestions and advice were a welcome contribution in strengthening this research project.

I would like to thank Dr. Bryan T. Hennessy and Dr. Angela Farrelly our collaborators in RCSI for expertise regarding ovarian cancer and BRCA1 and work which provided background to this project.

Thanks to everyone who has worked in the Obstetrics and Gynaecology Department especially Dr Lucy Norris, Dr Feras Saadeh, Dr Nadia Ibrahim, Dr Ream Langhe, Dr Fiona Martin and Anthony Cooney.

Also, thanks to everyone in the Coombe Molecular Pathology Laboratory especially Dr. Cara Martin, Dr. Cathy Spillane, Dr. Michael Gallagher, Dr. Brendan Ffrench, Dr. Victoria McEneaney, Dr. Katherine McAllister, Dr Helen Keegan, Mark Bates and Claudia Gasch.

Thanks to Dr Stephen Smith of the Microbiology Department in the CPL, for allowing us to use facilities and equipment. Thanks also to, Helen, Clodagh and Sam of the Microbiology Department for all the help over the years.

I would also like to thank Dr Eamon Breen for training and assistance in the use of the IMM Flow Cytometry Facility and to Dr Anthony Davies for training and assistance in the use of the IMM High Content Screening Facility.

Thanks to everyone in the Compounding Unit in St. James Hospital Pharmacy for the provisioning of cytotoxic drugs.

A big thank you goes to all the patients who consented in providing ovarian cancer tumour specimens for use in this research project. Thanks also to the gynaecology team, theatre staff and the gynaecological pathology team at St. James Hospital for help in the collection and identification of specimens.

List of figures

Figure 1.1 The female reproductive tract. 3

Figure 1.2 Structure of cisplatin (cis-diammine) platinum complex. 17

Figure 1.3 Structure of DNA adducts formed on DNA. 18

Figure 1.4 Efflux of platinum molecules from the cell by GSH. 23

Figure 1.5 Overview of the MMR system. 25

Figure 1.6 Overview of NER pathway. 27

Figure 1.7 Overview of homologous recombination. 30

Figure 1.8 Intrinsic pathway of cell death. 31

Figure 1.9 Extrinsic pathway of cell death. 34

Figure 1.10 Inverse resistance relationship between platinums and taxanes. 51

Figure 1.11 Overview of miRNA biogenesis. 56

Figure 2.1 Growth curves. The effects of insulin on doubling time. 67

Figure 2.2 Mycoplasma PCR. 70

Figure 2.3 High content screening growth curve images. 73

Figure 2.4 Glutathione assay standard curve. 74

Figure 2.5 Bradford 1X protein assay standard curve. 76

Figure 2.6 Cell cycle Phospho Histone H3 Assay. 80

Figure 2.7 Affymetrix suggested three day workflow (gene expression analysis). 90

Figure 2.8 Affymetrix GeneChip® Array. 98

Figure 2.9 ELOSA signal development. 104

Figure 3.1 T25 cardboard cover design for AF calculation method. 117

Figure 3.2 Example of images generated from the AF calculation method. 118

Figure 3.3 AF output photo analysis of newly seeded versus confluent flasks. 120

Figure 3.4 Correlation of AF method with cell counts using a haemocytometer. 121

Figure 3.5 Tracking cell recovery using AF. 122

Figure 4.1 Carboplatin and taxol IC_{50} for a panel of ovarian cancer cell lines.....138

Figure 4.2 OVCAR8 and UPN251 treatment strategy for the development of platinum/taxane resistant cell lines. 142

Figure 4.3 BRCA1 protein expression in UPN251 and OVCAR8 by Western blot. 144

Figure 4.4 Recovery plots for the dose finding evaluation.....146

Figure 4.5 Selection strategy recovery data.....148

Figure 4.6 Fold resistance to carboplatin/taxol compared to parental cell lines.....150

Figure 4.7 Fold resistance of sublines after defrosting.....151

Figure 4.8 Selection strategy fold resistance outcomes. 153

Figure 5.1 Post selection drug screen results. 171

Figure 5.2 Post selection drug screen results. 172

Figure 5.3 Total cellular glutathione assay. 174

Figure 5.4 High content growth curve analysis. 175

Figure 5.5 High content growth curve analysis. 177

Figure 5.6 A comparison of cells in mitosis after a 24hour taxol drug treatment. 179

Figure 5.7 Representative images of the cell cycle PHH3 assay for UPN251 and UPN251-7T taken by the Incell Analyzer. 180

Figure 5.8 FITC annexin V / PI apoptosis assay by FACS. 182

Figure 5.9 FITC annexin V / PI apoptosis assay by FACS (graphs). 183

Figure 5.10 FITC annexin V / PI apoptosis assay by FACS. 184

Figure 5.11 FITC annexin V / PI apoptosis assay by FACS (graphs). 185

Figure 5.12 PI cell cycle assay by FACS. 187

Figure 5.13 PI cell cycle assay by FACS. 188

Figure 5.14 Graphic representation of PI cell cycle assay by FACS. 189

Figure 5.15 P-glycoprotein (170kDa) Western blot. 192

Figure 5.16 ATP7A (180 kDa) Western blot.....193

Figure 5.17 CTR1 (30kDa) Western blot. 194

Figure 5.18 MRP2 (180kDa) & BRCA1 (220kDa) Western blot. 195

Figure 5.19 Bcl-2 (28kDa) Western blot.....196

Figure 5.20 Bcl-XL (30kDa) Western blot. 197

Figure 5.21 Dicer (220kDa) Western blot. 198

Figure 5.22 Drosha (160kDa) Western blot. 199

Figure 6.1 Visual quality control for HuGene 2.0 and miRNA-3.0 array chips. 234

Figure 6.2 Probe summarisation quality control metrics 235

Figure 6.3 Box plots of the relative log expression values (mRNA arrays). 236

Figure 6.4 Probe level quality control metrics (mRNA). 237

Figure 6.5 Individual probe level metrics. 238

Figure 6.6 Rank order of bac spike controls. 239

Figure 6.7 Box plots of the relative log expression values (miRNA arrays). 240

Figure 6.8 Probe level quality control metrics (miRNA). 241

Figure 6.9 Rank order of bac spike controls. 242

Figure 6.10 Spike-in control probe sets. 243

Figure 6.11 Pearson correlation of samples analysed using Affymetrix gene and miRNA arrays. 244

Figure 6.12 Clustering denogram of hierarchical clustering analysis of all samples run on the mRNA Affymetrix arrays. 246

Figure 6.13 Clustering denogram of hierarchical clustering analysis of all samples run on the miRNA Affymetrix arrays. 247

Figure 6.14 Overview of the deregulated gene expression from comparison A=UPN251 V UPN251-7C. 249

Figure 6.15 Overview of the deregulated miRNA expression from comparison A=UPN251 V UPN251-7C. 250

Figure 6.16 Overview of the deregulated gene expression from comparison B=UPN251_C V UPN251-7C_C. 251

Figure 6.17 Overview of the deregulated miRNA expression from comparison B=UPN251_C V UPN251-7C_C. 252

Figure 6.18 miRNA/mRNA interactions for comparisons A and B. 267

Figure 6.19 Overview of the deregulated gene expression from comparison C=UPN251 V UPN251-7T. 271

Figure 6.20 Overview of the deregulated miRNA expression from comparison C=UPN251 V UPN251-7T. 272

Figure 6.21 Overview of the deregulated gene expression from comparison D=UPN251_TL V UPN251-7T_TL. 273

Figure 6.22 Overview of the deregulated miRNA expression from comparison D=UPN251_TL V UPN251-7T_TL. 274

Figure 6.23 Overview of the deregulated gene expression from comparison E=UPN251_TL V UPN251-7T_TH. 275

Figure 6.24 Overview of the deregulated miRNA expression from comparison E=UPN251_TL V UPN251-7T_TH. 276

Figure 6.25 miRNA/mRNA interactions for taxol comparisons C, D and E. 288

Figure 7.1 Fold change of qPCR target expression in non-responder (NR) and partial-responder (PR) patient groups relative to the responder (R) patient group. 316

Figure 7.2 Δ CT values of qPCR targets in patient samples grouped by chemotherapy response. 318

Figure 7.3 Kaplan Meier survival curves depicting disease free survival (DFS) in patient samples grouped and compared by expressional data. 320

Figure 7.4 Kaplan Meier survival curves depicting disease free survival (DFS) in patient samples grouped and compared by expressional data. 321

Figure 7.5 Kaplan Meier survival curves depicting overall survival (OS) in patient samples grouped and compared by expressional data. 322

Figure 7.6 Kaplan Meier survival curves depicting overall survival (OS) in patient samples grouped and compared by expressional data. 323

Figure 7.7 Kaplan Meier analysis of DFS and OS between different expression patterns of a miRNA and predicted target gene 325

Figure 7.8 Analysis of DFS and OS between samples in the expected group and the un-expected group. 329

Figure 8.1 Characterisation of resistance mechanisms in taxol-resistant cell line UPN251-7T. 348

Figure 8.2 Characterisation of resistance mechanisms in carboplatin-resistant cell line UPN251-7C. 350

List of tables

Table 1.1 Epithelial ovarian cancer classification. 5

Table 1.2 FIGO staging of ovarian cancer. 12

Table 2.1 Cytotoxic drugs and Inhibitors 65

Table 2.2 Table of antibodies used for Western blotting. 77

Table 2.3 Final concentrations of Poly-A RNA controls when added to total RNA samples 91

Table 2.4 First-strand cDNA master mix components 92

Table 2.5 Second-strand cDNA master mix components 92

Table 2.6 IVT master mix components. 92

Table 2.7 Second-cycle ss-cDNA master mix components 95

Table 2.8 Fragmentation reaction sample preparation 96

Table 2.9 Fragmentation master mix components. 96

Table 2.10 Labelling reaction master mix components. 96

Table 2.11 Hybridisation cocktail master mix components (mRNA). 98

Table 2.12 Tailing master mix components. 101

Table 2.13 Hybridisation master mix components. 103

Table 2.14 Hybridisation cocktail master mix components (miRNA). 104

Table 2.15 List of probes for TaqMan qPCR 106

Table 2.16 Gene reverse transcription master mix components. 106

Table 2.17 MiRNA reverse transcription master mix components 107

Table 2.18 TaqMan master mix components. 108

Table 2.19 Results of small RNA sample input optimisation 110

Table 4.1 Acid phosphatase cytotoxicity assays. 145

Table 5.1 Resistance profile of UPN251 drug-resistant sublines. 169

Table 6.1 Overview of miRNAs associated with ovarian cancer chemoresistance 222

Table 6.2 Overview of deregulated genes and miRNA for carboplatin comparisons. 254

Table 6.3 Top five transcripts involved in ovarian cancer and/or resistance (carboplatin comparisons).....255

Table 6.4 DAVID carboplatin resistance pathway analysis. 259

Table 6.5 Deregulated genes in the hematopoietic cell lineages pathway. 260

Table 6.6 Deregulated genes in the axon guidance pathway.....262

Table 6.7 Deregulated genes in the cytokine-cytokine receptor interaction pathway. 263

Table 6.8 Deregulated genes in the hedgehog signalling pathway. 265

Table 6.9 Deregulated genes in the pathways in cancer pathway. 266

Table 6.10 MiRNA-Target Interactions for carboplatin comparisons. 268

Table 6.11 Overview of deregulated genes and miRNA for taxol comparisons.....278

Table 6.12 Top five transcripts involved in ovarian cancer and resistance (taxol comparisons).....280

Table 6.13 DAVID pathway analysis of deregulated genes found in comparisons D (Taxol).....285

Table 6.14 MiRNA-Target Interactions for taxol comparisons. 289

Table 6.15 Overview of deregulated genes and miRNA for first response comparisons. 292

Table 6.16 Comparison of de-regulated probes (gene and miRNA) between datasets. 296

Table 7.1 Patient details for pilot study. 304

Table 7.2 OVMARK results for candidate platinum/taxane resistance biomarkers.....309

Table 7.3 Mean fold change of target (gene/miRNA) in patient chemotherapy-response groups relative to responders group. 315

Table 7.4 Number of significant fold changes in NR or PR when compared to R.....317

Table 7.5 Fold change direction and survival.....326

Abbreviations

ABC – Adenosine triphosphate-binding cassette

ABCB1 (MDR1) – ATP-binding cassette, sub-family B (MDR/TAP), member 1

ACTION – Adjuvant chemotherapy in ovarian neoplasm

ADP – Adenosine diphosphate

AF – Area fraction

AGCC – Affymetrix GeneChip® command console

AGO – German consortium of gynaecological oncology

AKAP14 – A kinase (PRKA) anchor protein 14

AKT – Serine/threonine protein kinase Akt

ALK7 – Activin receptor-like kinase 7

ANPEP – Alanyl (membrane) aminopeptidase

AP – Alkaline phosphatase

APAF1 – Apoptotic peptidase activating factor *1*

AREG – Amphiregulin

ARID1A – AT rich interactive domain 1A

ARVC – Arrhythogenic right ventricle cardiomyopathy

ATG9A – Autophagy related 9A

ATM – Ataxia telangiectasia-mutated

ATP – Adenosine triphosphate

ATP7A/B – ATPase (copper transporting) alpha/beta polypeptide

AUC – Area under the concentration time curve

BAC – Bacterioopsin-associated chaperone

BAD – BCL-2-associated agonist of cell death

BARD1 – BRCA1 associated RING domain 1

BAX – BCL-2-associated X protein

BCL-(2/XL) – B-cell Lymphoma (2/extra large)

BCRP – Breast cancer resistance protein

BMP2 – Bone morphogenetic protein 2

BMPR1B – Bone morphogenetic protein receptor, type IB

BR1P1 – BRCA1-interacting protein 1

BRAF – V-raf murine sarcoma viral oncogene homolog B

BRCA1/2 – Breast cancer type 1/2 susceptibility protein

BSA – Bovine serum albumin

BSO – Buthionine sulphoximine

BTC – Betacellulin

CA125 – Cancer antigen 125

CA72-4 – Cancer antigen 72-4

CA9 – Carbonic anhydrase IX

CCD – Charge-coupled device

CCL(2\20) – Chemokine (C-C motif) ligand (2\20)

CCSG – Cancer centre support grant

CD24P4 – CD24 molecule pseudogene 4

CD55 – Decay accelerating factor for complement

CDH6 – Cadherin 6, type 2, K-cadherin (fetal kidney)

cDNA – Complimentary DNA

CHO – Chinese hamster ovary

CHST9 – Carbohydrate (N-acetylgalactosamine 4-0)

CLL – B-cell chronic leukaemia

CNN1 – Calponi 1, basic, smooth muscle

CRISPLD1 – Cysteine-rich secretory protein LCCL domain containing 1

cRNA – Complementary RNA

CSF1 (M-CSF) – Macrophage Colony-Stimulating Factor

CT – Computerized tomography

CTGF – Connective tissue growth factor

CTNNB1 – Catenin (Cadherin-associated protein) Beta 1

CTR1 – solute carrier family 31 (copper transporter) members 1

CTSS - Cathepsin S

$CuSO_4$ – Copper sulphate

DACH – 1,2-diaminocyclohexane

dATP – Deoxyadenosine triphosphate

DAVID – Database for annotation, visualization and integrated discovery

DD – Death Domain

DEPC – Diethylene Pyrocarbonate

DFS – Disease free survival

DFTR – Diffuse fluorescence temporal response

DHH – Desert hedgehog

DISC – Death-inducing signalling complex

DMSO – Dimethyl Sulfoxide

DNA – Deoxyribonucleic acid

DPP4 (CD26) – Dipeptidyl-peptidase 4

DS – Double strand

ds-cDNA – Double stranded complimentary DNA

dsRBD – Double-stranded RNA binding domain

dsRNA – Double stranded RNA

DTNB - Ellman reagent

dTTP – Deoxythymidine triphosphate

dUTP – Deoxyuracil triphosphate

DYSF – Dysferlin

ECM – Extra cellular matrix

EDN2 – Endothelin 2

EDNRA – Endothelin receptor type A

EEF1A2 – Eukaryotic translation elongation factor 1 alpha 2

EFNB2 – Ephrin B2

EGFR – epidermal growth factor

ELOSA – Enzyme linked oligosorbent assay

EME1 – Essential meiotic structure-specific endonuclease 1

EMT – Epithelial to mesenchymal transition

EPH – Ephrin

EPHA7 – EPH receptor A7

ER – Estrogen receptor

ERBB2 – V-Erb-B2 avian erythroblastic leukaemia viral oncogene homolog

ERCC1 – Excision repair cross-complementation group 1

EXO1 – Exonuclease 1

F2RL2 – Coagulation factor II (thrombin) receptor-like 2

FACS – Fluorescence-activated cell sorting

FADD – Fas-associated death domain

FCS – Foetal calf serum

FDA – US Food and Drug Administration

FDR – False discovery rate

FGF(18) – fibroblast growth factor (18)

FHIT – Fragile histidine triad

FIGO – The International Federation of Gynaecological Oncologists

FITC – Fluorescein isothiocyanate

FLIP – Anti-apoptotic FLICE inhibitory protein

FOLFOX – Folinic acid, fluorouracil and oxaliplatin chemotherapy regime

FOLR3 – Folate receptor 3 (gamma)

FWER – Family-wise error rate

GAPDH – Glyceraldehyde 3-phosphate dehydrogenase

GDF15 – Growth differentiation factor 15

GDP – Guanosine-5'-diphosphate

GEN1 – Holliday junction 5' flap endonuclease

GFR – glomerular filtration rate

GLI3 – GLI family zinc finger 3

GLTSCR2 – Glioma tumour suppressor candidate region gene 2

GOG – Gynaecological Oncology Group

GP6 – Glycoprotein VI (platelet)

GPC4 – Glypican 4

GSH – Glutathione

GST-pi – Glutathione S-transferase Pi

GTP – Guanosine-5'-triphosphate

GUCY1B3 – Guanylate cyclase 1, soluble, beta 3

HE4 – Human epididymis protein 4

HHIP – Hedgehog interacting protein

HIST1(H3F\H4B\H2BB) – Histone cluster 1, (H3F\H4B\H2BB)

HMG – High mobility group

HR – Hazard Ratio

HR – Homologous recombination

HRP – Horseradish peroxidise

Hsp90 – Heat shock protein 90

IHH – Indian hedgehog

IL(1\1β\1R1\6\8\8R1\23A) – Interleukin (1\1β\1 receptor 1\6\8\8R1\23A)

IOSE – Immortalised epithelial ovarian cancer

ITG(A2\A6\B6) – Integrin (Alpha-2\Alpha-6\Beta-6)

IV – Intravenous

IVT – *In vitro* transcription

JUP – Junction plakoglobin

KEGG – Kyoto encyclopaedia of genes and genomes

KITLG – KIT ligand

KNDC1 – Kinase non-catalytic C-lobe domain (KIND) containing 1

KRAS – Kirsten rat sarcoma viral oncogene homolog

LAM(A3\B3\C2) – Laminin, (A3\B3\C2)

LDH – Lactate dehydrogenase

LIN28B - lin-28 homolog B (C. elegans)

LMP – Low malignant potential

LOH – Loss of heterozygosity

LRP – Lipoprotein receptor-related protein

MACC1 – Metastasis associated in colon cancer 1

MAD2 – Mitotic arrest deficient-like 2

MAGE(2\6) – Melanoma antigen family A, (2\6)

MAL(2) – Mal, T-Cell Differentiation Protein (2)

MAMDC2 – MAM domain containing 2

MAP – Microtubule associated proteins

MAP3K15 – Mitogen-activated protein kinase 15

MAPK10 – Mitogen-activated protein kinase 10

MCL1 – Myeloid cell leukaemia 1

MCM3 – Mini-chromosome maintenance complex component 3

MDM2 – MDM2 oncogene, E3 ubiquitin protein ligase

MDR1 (ABCB2) – P-glycoprotein coding gene

miRNA – Micro RNA

MLH1 – MutL homolog 1

MMP(7\9) – Matrix metallopeptidase (7\9)

MMR – Mismatch repair

MRE11A – Meiotic recombination 11 homolog A

mRNA – Messenger RNA

MRP1/2 – Multidrug resistance-associated protein ½

MSH2/6 – MutS homolog 2/6

MTI – MiRNA-target interaction

MTT – 3-(4,5-Dimethylthiazol-2-Yl)-2,5-Diphenyltetrazolium Bromide

MUS81 – MUS81 structure-specific endonuclease subunit

MyD88 – Myeloid differentiation primary response 88

NADPH – Nicotinamide adenine dinucleotide phosphate

NAV3 – Neuron navigator 3

NBS1 – Nibrin

NCI – National cancer institute

NER – Nucleotide excision repair

NFkB – Nuclear factor kappa-B

NHEJ – Non-homologous end joining

NID1 – Nidogen 1

NMD – Nonsense-mediated mRNA decay

NPR3 – Natriuretic peptide receptor 3

NR – Non-responders group

NRG2 – Neuregulin 2

NSCLC – Non-small cell lung cancer

NT5E (CD73)– 5'-nucleotidase, ecto

NTC – Non-template control

NTN(1\4\G1) – Netrin (1\4\G1)

OATP – Organic anion transporting polypeptides

OCPP – Ovarian cancer prognostic profile

OS – Overall survival

OVMARK – A tool for correlating transcriptomic data to ovarian cancer patient survival

P21 – Cyclin-dependent kinase inhibitor 1

p53 – Tumour protein p53

P-gp – P-glycoprotein

PALB2 – Partner and localizer of BRCA2

PAR – Prostate apoptosis response protein

PARP – Poly ADP ribose polymerase

PBS – Phosphate buffered saline

PDGFRA – Platelet-derived growth factor receptor, alpha polypeptide

PDX – Patient derived xenografts

PFS – Progression free survival

PGK1 – Phosphoglycerate kinase 1

PGRMC1 – Progesterone receptor membrane component 1

PI – Propidium iodide

PIK3CA – Phosphatidylinositol-4,5-bisphosphate 3-kinase catalytic subunit alpha

PKP2 – Plakophilin 2

PLAC8 – Placenta-specific 8

PMS2 – Postmeiotic segregation increased 2

PODXL – Podocalyxin-like

POF1B – Premature ovarian failure, 1B

PPP(1R10\2R1A) – Protein phosphatase (1 regulatory subunit 10\2 regulatory subunit A alpha)

PR – Partial responders group

PSP94 – Prostatic secretory protein-94

PTEN – Phosphatase and tensin homolog

PTX3 – Pentraxin 3, long

qPCR – Quantitative PCR

QC – Quality control

R – Responders group

RB – Retinoblastoma

REAL – Revised European-American lymphoma

RECIST – Response evaluation criteria in solid tumours

RELN – Reelin

RHOBTB1 – Rho-related BTB domain containing 1

RIN – RNA integrity number

RISC – RNA-induced silencing complex

RLE – Relative log expression

RMA – Robust multichip average

RMI – Risk of malignancy index

RNA – Ribonucleic acid

ROBO1 – Roundabout, axon guidance receptor, homolog 1 (Drosophila)

ROCA – Risk of ovarian cancer algorithm

ROMA – Risk of ovarian malignancy algorithm

RPA – Replication protein A

rRNA – Ribosomal RNA

RT – Reverse transcription

RT-PCR – Reverse transcription PCR

SAC – Spindle assembly checkpoint

SD – Standard deviation

SEMA3A – Sema domain, immunoglobulin domain (Ig), short basic domain, secreted, (semaphorin) 3A

SERPINB7 – Serpin peptidase inhibitor, clade B (ovalbumin), member 7

siRNA – Small interfering RNA

SLC4(A1\A4) – Solute carrier family 4 (sodium bicarbonate cotransporter), (member 1\member 4)

SLC17A1 – Solute carrier family 17 (organic anion transporter), member 1

SLC34A2 – Solute carrier family 34 (type II sodium/phosphate contransporter), member 2

SLIPI – Sulpholipid immobilizing protein 1

SLIT(2\3) – Slit homolog (2\3)

SMAD7 – SMAD family member 7

SMO – Smoothened, frizzled class receptor

SMRP – Soluble mesothelin related peptide

snoRNA – Small nucleolar RNA

SNPs – Single nucleotide polymorphisms

SRPX2 – Sushi-repeat containing protein, X-linked 2

SSA – Sulfosalicyclic acid

SSA – Single strand annealing

ss-cDNA – Single stranded complimentary DNA

ss-cRNA – Single stranded complimentary RNA

ssDNA – Single stranded DNA

ssRNA – Single stranded RNA

STR – Short tandem repeats

SYNE1 – Spectrin repeat containing, nuclear envelope 1

TCGA – The Cancer Genome Atlas

TENM2 – Teneurin transmembrane protein 2

TFIIH – Transcription factor 2 human

TGF – Transforming growth factor

TIC – Tubal intra-epithelial carcinoma

TLR4 – Tool Like receptor 4

TMEM47 – Transmembrane protein 47

TNF(-R1) – Tumour necrosis factor (receptor 1)

TNFRSF9 (CD137\4-1BB) – Tumour necrosis factor receptor superfamily, member 9

TNFRSF11A (RANK) – Tumour necrosis factor receptor superfamily, member 11a, NFKB activator

TNFRSF19 (TROY) – Tumour necrosis factor receptor superfamily, member 19

TP53 – Tumour protein p53

TRAIL – Tumour necrosis-related apoptosis-inducing ligand

TRAMP – Tumour necrosis factor receptor-related apoptosis mediating protein

TRBP – TAR RNA binding protein

tRNA – Transfer RNA

TUBB3 – Beta 3 tubulin

TVS – Transvaginal sonography

VCAM1 – Vascular cell adhesion molecule 1

VEGF – Vascular endothelial growth factor

WIF1 – WNT inhibitory factor 1

WNT(2B\5A\7A\9\10B) – Wingless-type MMTV integration site family, member (2B\5A\7A\9\10B)

XIAP – X-linked inhibitor of apoptosis

XPA/C/F/G – Xeroderma pigmentosum, complementation group A/C/F/G

Xrcc2 – DNA repair protein XRCC2

Table of contents

Declaration i

Summary ii

Acknowledgements iv

List of figures vi

List of tables x

Abbreviations xii

Table of contents xxiii

Chapter 1 Introduction 2

1.1 Ovarian cancer 2

1.1.1 Definition 2

1.1.2 Prevalence, mortality and risk 4

1.1.3 Ovarian cancer onset 6

1.1.4 Detection and screening 8

1.2 Current treatment options 11

1.2.1 Early stage disease 11

1.2.2 Advanced stage disease 11

1.2.3 Relapse or recurrence of disease 14

1.3 Platinum chemotherapy 15

1.3.1 Cisplatin 15

1.3.2 Carboplatin 19

1.3.3 Oxaliplatin 19

1.4 Mechanisms of platinum resistance 20

1.4.1 Decreased accumulation of drug 21

1.4.1.1 Role of copper transporters 21

1.4.1.2 Role of adenosine triphosphate-binding cassette transporters 22

1.4.2 Drug deactivation 22

1.4.3 Decreased mismatch repair 24

1.4.4 Increased repair of DNA adducts 26

1.4.5 Inhibition of apoptosis 29

1.4.6 Mutations in p53 33
1.5 Taxane chemotherapy 35
1.5.1 Taxol and docetaxel 35
1.6 Mechanisms of taxane resistance 37
1.6.1 MDR1/P-glycoprotein (P-gp, p170) over-expression 37
1.6.2 β-tubulin protein isotypes 38
1.6.3 β-tubulin mutations 40
1.6.4 Genetic changes 40
1.7 BRCA1 43
1.7.1 BRCA1 mutation 45
1.7.2 Methylation of BRCA1 47
1.7.3 BRCA1 in chemo-sensitivity and chemo-resistance 48
1.8 Ovarian cancer biomarkers 50
1.8.1 MiRNAs as novel cancer biomarkers 52
1.8.2 MiRNA biosynthesis and function 54
1.8.3 MiRNA expression analysis in ovarian cancer 56
1.9 Aims and objectives 60
1.9.1 Hypotheses 60
1.9.2 Objectives 60
Chapter 2 General methods 64
2.1 General methods 64
2.1.1 Cytotoxic drugs 64
2.1.2 General solutions 64
2.1.3 Cell lines and tissue culture conditions 64
2.1.3.1 Media 64
2.1.3.2 Tissue culture conditions 66
2.1.3.3 Cell Lines 66
2.1.3.4 Cell line freezing and defrost protocols 67
2.1.3.4.1 Cell line freezing 67

2.1.3.4.2 Cell line defrost 68
2.1.4 Mycoplasma PCR assay 68
2.1.5 Cell counting for growth experiments 69
2.1.6 Acid phosphatase cell viability assay 69
2.1.7 Growth assay protocols 71
2.1.7.1 Manual growth assay 71
2.1.7.2 High content screening growth assay 71
2.1.8 Total cellular glutathione assay 72
2.1.9 Protein analysis 74
2.1.9.1 Preparation and quantification of total protein 74
2.1.9.2 Sodium dodecylsulphate-polyacrylamide gel electrophoresis (SDS-PAGE) 75
2.1.9.3 Western blotting 75
2.1.9.4 Western blot development 76
2.1.10 Cell cycle mitosis assay 78
2.1.11 Fluorescence-activated cell sorting (FACS) analysis 81
2.1.11.1 FITC annexin V / PI apoptosis assay 81
2.1.11.2 Cell cycle assay 81
2.1.12 RNA extraction 82
2.1.12.1 Solution preparation 82
2.1.12.2 Extracting RNA from frozen tissue 82
2.1.12.2.1 Tissue preparation 82
2.1.12.2.1.1 The mortar and pestle method 82
2.1.12.2.1.2 The TissueLyser method 83
2.1.12.2.2 Large and small RNA isolation (initial steps) 83
2.1.12.2.3 Small RNA enriched purification steps 84
2.1.12.2.4 Large RNA purification steps 84
2.1.12.3 Extraction of total RNA from cell lines 85
2.1.12.4 Quantification of RNA content 87
2.1.13 Evaluation of RNA integrity from cell line total RNA extracts 87
2.1.13.1 Preparing chip priming station 87
2.1.13.2 Preparing the Bioanalyzer 87
2.1.13.3 Preparing the RNA ladder 88

2.1.13.4 Agilent RNA 6000 nano assay protocol 88
2.1.14 Affymetrix gene expression analysis protocol 88
2.1.14.1 Preparation of total RNA and Poly-A controls 89
2.1.14.2 First -strand cDNA synthesis 89
2.1.14.3 Second-strand cDNA synthesis 91
2.1.14.4 cRNA synthesis by *in vitro* transcription 91
2.1.14.5 cRNA purification 93
2.1.14.6 Second-Cycle ss-cDNA synthesis 94
2.1.14.7 RNase H hydrolysis 94
2.1.14.8 Second-cycle ss-cDNA purification 94
2.1.14.9 Fragmentation of ss-cDNA 95
2.1.14.10 Labelling of fragmented ss-cDNA 95
2.1.14.11 Hybridisation 97
2.1.14.12 Fluidics station and scanner setup 97
2.1.14.13 Array washing and staining 97
2.1.14.14 Array scanning 99
2.1.15 MiRNA expression analysis 99
2.1.15.1 Poly (A) tailing 100
2.1.15.2 FlashTag™ biotin HSR ligation 100
2.1.15.3 Enzyme linked oligosorbent assay (ELOSA) QC assay 100
2.1.15.3.1 Coating wells with ELOSA Spotting Oligos 102
2.1.15.3.2 Washing and blocking 102
2.1.15.3.3 Sample hybridisation 102
2.1.15.3.4 SA-HRP binding 102
2.1.15.3.5 Signal development 102
2.1.15.4 Hybridisation 103
2.1.15.5 Array staining, washing and scanning 105
2.1.16 TaqMan® quantitative polymerase chain reaction (qPCR) 105
2.1.16.1 Reverse Transcription (genes) 105
2.1.16.2 Reverse Transcription (miRNA) 105
2.1.16.3 TaqMan® qPCR step 107
2.1.16.4 Optimisation of the quantity of small RNA input for reverse transcription 109
Chapter 3 The area fraction output method 114
3.1 Introduction 114

3.2 Methods 115
3.2.1 The area fraction output method 115
3.2.1.1 Image capture 115
3.2.1.2 Image analysis 116
3.2.1.2.1 Analysis steps (ImageJ) 116
3.2.1.2.2 Accuracy steps – count image vs. original image (ImageJ) 118
3.2.2 Area fraction output method validation 119
3.2.3 Example of area fraction output method: Tracking recovery of drug administration 119
3.3 Results 120
3.3.1 Area fraction output method validation 120
3.3.2 Example of area fraction output method: Tracking recovery of drug administration 121
3.4 Discussion 122
3.4.1 Comparison of area fraction output method to other microscopy-based measures of confluence 123
3.4.2 Comparison of area fraction output method to label-based methods of proliferation and cell viability 125
3.5 Conclusion 126
Chapter 4 Chemoresistant ovarian cancer cell line development 130
4.1 Introduction 130
4.1.1 Resistance cell models 130
4.1.1.1 Key decisions involved in planning a selection strategy 131
4.1.1.1.1 Parental cell line 131
4.1.1.1.2 Type of cell resistance model: High level laboratory or clinically relevant 132
4.1.1.1.3 Drug dose and strategy of administration for clinically relevant models 133
4.1.1.1.4 Risk reduction strategies 134
4.1.2 Aims and objectives 135
4.1.2.1 Hypotheses 135
4.1.2.2 Objectives 136

4.2 Cell selection strategy methods and design 136
4.2.1 Selection strategy design 136
4.2.2 Dose optimisation method 139
4.2.2.1 Dose optimisation of carboplatin 139
4.2.2.2 Dose optimisation of taxol 139
4.2.2.3 Dose finding method 140
4.2.3 Cell selection strategy method 141
4.3 Selection strategy related results 141
4.3.1 BRCA1 protein expression of parental cell lines 141
4.3.2 Cytotoxicity data of parental cell lines 143
4.3.3 Dose finding optimisation 143
4.3.4 Selection strategy recovery 147
4.3.5 Selection strategy fold resistance 149
4.3.6 Maintenance of resistance after cell defrost 149
4.4 Discussion 152
4.5 Conclusions 155
Chapter 5 Resistant cell line characterisation 160
5.1 Introduction 160
5.1.1 Cell selection strategies influence resistance development 160
5.1.2 Models of taxol resistance and related mechanisms 163
5.1.3 Models of carboplatin resistance and related mechanisms 164
5.1.4 Resistance biomarkers in the clinic for ovarian cancer 166
5.1.5 Aims and objectives 166
5.1.5.1 Hypotheses 166
5.1.5.2 Objectives 166
5.2 Methods 167
5.3 Results 168
5.3.1 Drug screen 168
5.3.2 Total cellular glutathione assay 173

5.3.3 High content growth assay 174
5.3.4 Cell cycle mitosis assay 178
5.3.5 Fluorescence activated cell sorting (FACS) analysis 178
5.3.5.1 Apoptosis assay 181
5.3.5.2 Cell cycle assay 186
5.3.6 Western blotting 190
5.4 Discussion 200
5.4.1 Mechanisms of taxol resistance 200
5.4.2 Mechanisms of carboplatin resistance 202
5.4.3 Combined resistance to platinums and taxanes 204
5.4.4 Resistance and miRNA biogenesis proteins 205
5.4.5 Treatment options for platinum/taxane resistant ovarian cancers 206
5.5 Conclusions 206
Chapter 6 Chemoresistant ovarian cancer biomarker discovery 210
6.1 Introduction 210
6.1.1 Microarray technology 210
6.1.2 Gene expression analysis in ovarian cancer 211
6.1.2.1 Molecular profiling and subtype identification 211
6.1.2.2 Biomarker for diagnosis and early detection 212
6.1.2.3 Biomarkers for prognosis, therapy and resistance 214
6.1.3 MiRNA expression analysis in ovarian cancer resistance 217
6.1.3.1 The miR-200 family and resistance 219
6.1.3.2 The Let-7 family and resistance 219
6.1.3.3 Contributions by the Discovary consortium to miRNA resistance 220
6.1.4 Aims and objectives 223
6.1.4.1 Hypotheses 223
6.1.4.2 Objectives 223
6.2 Methods 223
6.2.1 Sample selection for Affymetrix analysis 223
6.2.2 Sample preparation for Affymetrix platform 224

6.2.3 Quality control analysis for the Affymetrix platform 225
6.2.3.1 Probe level metrics 225
6.2.3.2 Probe set summarisations metrics 225
6.2.3.3 Individual probe level metrics 226
6.2.3.4 MiRNA array specific probe metrics 227
6.2.4 Affymetrix gene and miRNA array data analysis 227
6.2.4.1 RMA method 227
6.2.4.2 Differential gene and miRNA expression analysis 228
6.2.4.3 Analysis of target gene and miRNA lists 229
6.2.4.3.1 MiRNA-Target interactions (MTIs) analysis 232
6.3 Results - Affymetrix quality control and general clustering analysis 233
6.3.1 Array quality control 233
6.3.1.1 Visual quality control 233
6.3.1.2 Probe metric quality control 233
6.3.1.2.1 MRNA array probe metrics 233
6.3.1.2.2 MiRNA array probe metrics 238
6.3.2 Summary characteristics analysis of datasets 242
6.4 Results and discussion – Affymetrix gene/miRNA expression 248
6.4.1 Carboplatin resistance biomarker discovery 248
6.4.1.1 Top five deregulated genes and miRNAs 253
6.4.1.2 Pathway analysis by DAVID 258
6.4.1.2.1 Hematopoietic cell lineages 258
6.4.1.2.2 Axon guidance 261
6.4.1.2.3 Cytokine-cytokine receptor interaction 261
6.4.1.2.4 Hedgehog signalling pathway 261
6.4.1.2.5 Pathways in cancer 264
6.4.1.3 MiRNA-Target interactions (MTIs) for carboplatin resistance analyses 264
6.4.2 Taxol resistance biomarker discovery 270
6.4.2.1 Top five deregulated genes and miRNAs 277
6.4.2.2 Pathway analysis by DAVID 284
6.4.2.2.1 Extra cellular matrix (ECM)-receptor interaction 284
6.4.2.2.2 Arrhythogenic right ventricle cardiomyopathy (ARVC) 286
6.4.2.2.3 Pathways in cancer 286

6.4.2.3 MiRNA-Target interactions (MTIs) for taxol resistance analyses 287
6.4.3 First response biomarker discovery 291
6.4.4 Comparisons of de-regulation between datasets 294
6.5 Conclusions 297
Chapter 7 Resistance biomarkers clinical validation 302
7.1 Introduction 302
7.1.1 Aims and objectives 302
7.1.1.1 Hypotheses 303
7.1.1.2 Objectives 303
7.2 Methods 303
7.2.1 Patient sample details 303
7.2.2 Biomarker selection for clinical validation 305
7.2.3 Kaplan-Meier survival analysis 307
7.3 Results 308
7.3.1 Selection of targets for clinical validation 308
7.3.1.1 LIN28B 310
7.3.1.2 SRPX2 311
7.3.1.3 CCL20 311
7.3.1.4 GLI3 312
7.3.1.5 Let-7i 312
7.3.1.6 MiR-205 313
7.3.2 Target expression analysis 314
7.3.3 Survival analysis 314
7.4 Discussion 329
7.4.1 LIN28B as a marker of diagnosis and resistance 330
7.4.2 GLI3 as a marker of diagnosis and resistance 331
7.4.3 Potential biomarkers (alone and in combination) 333
7.5 Conclusions 334
Chapter 8 General discussion 338
8.1 Introduction 338

8.2 A novel investigation of chemoresistance in ovarian cancer 338

8.3 Contributions to the current knowledge on ovarian cancer resistance 343

8.3.1 Development of the novel area fraction output method 343

8.3.2 BRCA1 and the inverse resistance relationship 344

8.3.3 Mechanisms of resistance in ovarian cancer 345

8.3.3.1 Taxol Resistance 345

8.3.3.2 Carboplatin resistance 347

8.3.3.3 Combined platinum and taxol resistance models and their effects on resistance development 350

8.3.4 Ovarian cancer resistance biomarkers 351

8.3.5 Summary of contributions to current knowledge 354

8.4 Future directions 355

8.5 Publications and conference proceedings 359

8.5.1 Publications 359

8.5.2 Conference proceedings 359

8.6 Conclusions 361

References 364

CHAPTER 1

Introduction



TRINITY
COLLEGE
DUBLIN

Chapter 1 Introduction

1.1 Ovarian cancer

1.1.1 Definition

Ovarian cancer can be defined as cancerous growths that originate from the tissues of the ovary or fallopian tubes. Ovarian tissue includes one of a pair of female reproductive glands in which the ova, or eggs, are formed. The ovaries of the female reproductive system can be described as being two almond shaped organs residing in the pelvic region, one on either side of the uterus to which it is connected by the fallopian tubes. From puberty to menopause the ovaries alternate in releasing eggs (ova) which are transported to the uterus by the fallopian tubes. The ovaries also produce and secrete the hormones oestrogen and progesterone, which regulate the menstrual cycle, pregnancy and the development of secondary sexual characteristics in females (breasts, body hair and body shape) (*Lentz et al. 2014*). Figure 1.1 shows the architecture of the female reproductive track.

Ovarian cancer cells are extremely heterogeneous at both a cellular and molecular level. There are three main types of ovarian cancer classified by origin of the tumour. Epithelial, derived from surface cells of the ovary or fallopian tubes; germ cell, derived from the ovum producing cells within the ovary, and sex cord stromal cells, derived from connective tissue cells and the hormone producing cells of the ovary (*Cho et al. 2009*).

Sex-chord stromal tumours make up approximately 7-8% of ovarian tumours. They arise from two groups of cells with different embryological precursors, the stromal cells (fibroblasts, theca and leydig cells) and primitive sex chord cells (granulosa and sertoli cells). Tumours are usually made up of more than one cell type (*Outwater et al. 1998*).

Germ Cell tumours comprise of approximately 5% of ovarian tumours. They are rare malignancies that usually occur in young women. Histotypes include dysgerminoma, yolk sac tumour, embryonal carcinoma, polyembryoma, nongestational choriocarcinoma, teratomas and mixed cell tumours *(Matei et al. 2006)*.

The most common type of ovarian cancer is epithelial ovarian cancer. This is found to be the cause of 85-90% of ovarian cancer malignancies and will be the focus of this thesis (*Lentz et al. 2014*). 90% of epithelial ovarian cancers are clonal in nature and develop from single cell progenies that have accumulated genetic alterations over a

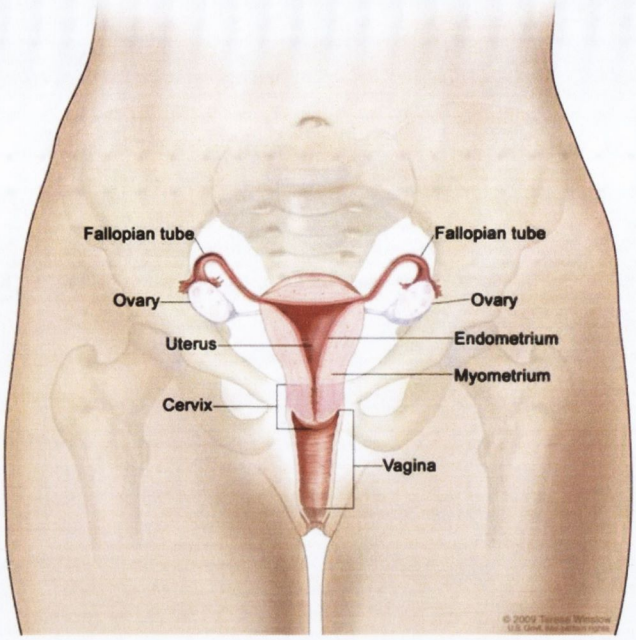

Figure 1.1 The female reproductive tract.

Adapted with permission from (*National Cancer Institute 2014*). © 2009 Terese Winslow, U.S. Govt. has certain rights.

period of time. Usually 5 or more genetic alterations have occurred from a repertoire of more than 30 tumour suppressor and oncogenes that have been associated with ovarian cancer. This repertoire drives changes in signalling pathways that induce proliferation, block apoptosis, stop anoikis, increase motility, adhesion and invasion and attracts stromal components (*Bast et al. 2009*). Epithelial ovarian cancer is split up into a number of histotypes; papillary serous (most common histotype, approximately 70% of tumours), endometrioid, mucinous, clear cell, transitional, squamous, mixed and undifferentiated subtypes. Classically, epithelial ovarian cancer is believed to arise from malignant transformations of the ovarian surface epithelium which is in contact with the peritoneal epithelium. Also, it can be derived from cells that line subsurface cortical inclusion cysts, developing from the ovarian surface epithelium (*Cannistra 2004*; *Feeley et al. 2001*). Recent evidence from morphological and molecular studies now indicates that a subset (possibly half) of high grade serous epithelial ovarian cancer can develop from cortical inclusion cysts that arise from tubal epithelium and not from the ovarian surface epithelium *(Kurman 2013).* Recently, epithelial ovarian cancer has been classified into two groups based on its histological grade, molecular

phenotype, and genotype. See Table 1.1. This is opposed to the traditional classification; well-, moderate- or poorly-differentiated tumours. Type I cancers are low grade of serous, mucinous, endometrioid and clear cell histotypes, that grow slowly, resist conventional chemotherapy, may respond to hormone therapy, and are often diagnosed at an early stage (I or II) (*Romero et al. 2012*). They are associated with mutations in ARID1A, BRAF, CTNNB1, ERBB2, KRAS, PIK3CA, PPP2R1A and PTEN genes (*Kurman 2013*; *Kurman et al. 2011*; *Vang et al. 2009*). Type II cancers are more prevalent and are high grade serous, endometrioid or undifferentiated histotypes that grow aggressively, respond to conventional chemotherapy, respond less often to hormonal treatment and are diagnosed at late stage (III or IV) (*Romero et al. 2012*). They are most commonly associated with mutations in TP53 and BRCA1/2 genes (*Kurman 2013*; *Kurman et al. 2011*; *Vang et al. 2009*).

1.1.2 Prevalence, mortality and risk

Ovarian cancer is the leading cause of death from a gynaecological malignancy. European cancer incidence statistics show that ovarian cancer was the 5th most common cancer for all European women in 2012. There was a reported estimate of more than 65,000 new cases and approximately 42,000 deaths (*Ferlay et al. 2013*). This gives a mortality rate of approximately 65% in Europe. Ireland had in excess of 350 reported cases in 2012 with approximately 260 deaths (*Ferlay et al. 2013*). This gives Ireland a mortality rate which is greater than the European average at approximately 75%. When compared to breast cancer, which is the most common cancer amongst European women, more than 460,000 cases were reported in Europe in 2012, with more than 130,000 deaths, giving a mortality rate of only 28% (*Ferlay et al. 2013*). This highlights the need for improved treatment of this disease.

One of the greatest risk factors associated with epithelial ovarian cancer is a family history of the disease. This is most often linked to germline BRCA1/2 mutations found in 8.6-13.7% of ovarian cancer patients (*Pal et al. 2005*; *Risch et al. 2001*; *Rubin et al. 1998*). A recent study, examining somatic and germline mutations in ovarian cancer, has revealed that incidences for BRCA1\2 mutations might be even higher at 18.3% (*Hennessy et al. 2010*). A woman with a BRCA1 mutation has a 39-46% chance of developing ovarian cancer in her lifetime, while a woman with BRCA2 has a 12-20% chance (*Hennessy et al. 2009*).

Other factors that are associated with increased or reduced risk are influenced by the reproductive history of a woman. This may be related to oestrogen and progesterone exposure. Nulliparity, early menarche, late menopause and infertility all seem to

Table 1.1 Epithelial ovarian cancer classification.

Classification	Type 1	Type 2
Histotypes	low grade of serous, mucinous, endometrioid and clear cell	High grade serous, endometrioid or undifferentiated
Growth rate	Slow	Aggressive
Chemotherapy response	Resistant	Responders
Hormone treatment response	May respond	Often poor response
Diagnosis	Early stage (I or II)	Late stage (III or IV)
Common mutated genes	ARID1A, BRAF, CTNNB1, ERBB2, KRAS, PIK3CA, PPP2R1A and PTEN	TP53 and BRCA1/2

increase the risk of developing ovarian cancer (*Hennessy et al. 2009*; *Jensen et al. 2009*; *Tworoger et al. 2007*). Reduced risk is associated with use of the oral contraceptive, pregnancy, increasing parity, lactation, hysterectomy and tubal ligation (*Collaborative Group on Epidemiological Studies of Ovarian Cancer 2008*; *Hankinson et al. 1993*; *Hennessy et al. 2009*; *Salehi et al. 2008*). In particular, a reduction in the incidences of ovarian cancer in Western Europe and the USA has been linked with the increased use of oral contraception. In regions such as Southern and Eastern Europe where the oral contraceptive pill has not had the same impact, there have been increased incidences of ovarian cancer *(Brewster 2005)*. Also, as with the majority of cancers, increasing age is also a risk factor. Pregnancy seems to have a protective effect against ovarian cancer, where the greater number of pregnancies a mother has had decreases the risk (*Pasalich et al. 2013*; *Riman et al. 2004*).

Hormone replacement therapy, which is often used to relieve menopausal symptoms, has been shown to increase risk by approximately 50%, compared to women who have not undergone this treatment (*Riman et al. 2004*). Infertility in women has been reported to increase the lifetime risk of ovarian cancer by 36-46%. This is not associated with the taking of fertility drugs (*Jensen et al. 2009*; *Tworoger et al. 2007*).

Other diseases, such as pelvic inflammatory disease, endometriosis, polycystic ovarian syndrome and mumps have been linked to increased risk, but this association is poorly understood and more studies are needed (*Riman et al. 2004*). It must also be mentioned that lifestyle choices such as smoking and obesity have also been linked with increased risk, but the evidence is not conclusive and again, more studies are needed in this area (*Jordan et al. 2006*; *Schouten et al. 2008*).

1.1.3 Ovarian cancer onset

There are four popular theories which have been proposed to explain the onset of ovarian cancer. The first is the 'incessant ovulation hypothesis' which suggests that genomic abnormalities may be accumulated by repeated wounding of the ovarian surface epithelium and cell proliferation after ovulation. Rupture of the ovulating follicle damages epithelial cells on the surface of the ovary, which then must be repaired. This continuous damage and repair results in an increased chance of errors occurring from replication *(Fathalla 1971)*. This is supported by evidence that the average number of ovulations in a women's lifetime has increased dramatically since the 19th century. This corresponds to increased incidences of ovarian cancer over this time period. Also, there is a correlation between decreases in ovulation through pregnancy or oral contraceptive use and decreased risk of developing ovarian cancer (*Jensen et al. 2009*; *Modan et al. 2001*; *Riman et al. 2002*; *Salehi et al. 2008*; *Titus-Ernstoff et al. 2001*; *Tworoger et al. 2007*). Arguments against this hypothesis include that the use of progestin-only contraceptive pill, which does not stop ovulation, better protects against the risk of developing epithelial ovarian cancer than ovulatory impeding contraceptives. Furthermore, some women with anovulatory infertility are at increased risk of developing epithelial ovarian cancer (*Fleming et al. 2006*).

The second hypothesis is the 'gonadotropin theory', suggesting that increases in pituitary gonadotropins during ovulation and persistently high concentrations of gonadotropins after menopause stimulate epithelial cells, causing the accumulation of genetic changes in response. This results in cancer progression (*Cramer et al. 1983*). This may be due to direct stimulation by gonadotropins on the surface epithelium or due to indirect stimulation due to the stimulation of oestrogen production (*Mohle et al. 1985*). Supportive evidence for this hypothesis includes; increasing gonadotropin levels with age (with high levels during menopause) and lower levels of circulating gonadotropin levels during pregnancy and during oral contraceptive use (*Beltsos et al. 1996*; *Risch 1998*). However, it must be noted that there are significant increases in oestrogen and human chronic gonadotropin levels during pregnancy, which is counter

to this theory (*Risch 1998*). Evidence against this theory also includes the observation that lactating women have increased levels of circulating follicle stimulating hormone and that some ovarian cancer patients have an increased risk of ovarian cancer, but have low levels of gonadotropin (*Fleming et al. 2006*).

The third theory suggests that inflammation and changes in redox potential during ovulation and surface epithelium repair contribute to the onset of ovarian cancer. It is suggested that this theory may explain the links of pelvic inflammatory disease, endometrosis, mumps and talc or asbestos exposure to the increased risk factors of ovarian cancer (*Cramer et al. 1983*; *Fleming et al. 2006*).

The fourth theory is the 'hormone' theory', which attempts to explain the conflict of evidence arising from the 'incessant ovulation' and 'gonadotropin' hypothesis. It suggests that excess androgen stimulation of epithelial ovarian cancer cells leads to an increased risk of ovarian cancer, while increased progesterone is protective (*Risch 1998)*. Androgens are produced in the ovary by developing follicles at a higher rate than estrogen and are the main sex steroids present within the fluid of growing follicles (*McNatty et al. 1979*). It may be the case that epithelia-lined inclusion cysts, which are close to developing follicles, experience high levels of androgens. Some evidence supporting this theory includes increased levels of androgen in polycystic ovarian syndrome, hirsutism and a history of acne which have all been linked to increased risk of ovarian cancer (*Schildkraut et al. 1996*; *Wynder et al. 1969*). In addition, the protective nature of the oral contraceptive pill has been linked with reduced levels of androgens and increased levels of progestins. Further to this, progestin-only pills, which do not suppress ovulation, are more protective than the combined pill (*Ho 2003*; *Rosenberg et al. 1994*). Pregnancy has also been suggested to be protective due to increased levels of progesterone which dwarf androgen levels, rather than the reduction in ovulation being the protective factor (*Risch 1998*).

The most recent theory for ovarian cancer's origin suggests that epithelial ovarian cancer can also arise from cells of the fallopian tubes. Most serous ovarian cancers present with preinvasive legions in the distal fallopian tube (*Erickson et al. 2013*). From a study examining tubal segments removed after bilateral salpingo-oophorectomy, from women with increased risk of ovarian cancer, it was found that out of 12 samples, five had areas of hyperplasic lesions and six had cellular dysplastic lesions in their tubal epithelium. These legions were histologically similar to that of high-grade serous ovarian cancer (*Piek et al. 2001*). Further studies from larger cohorts of patients harbouring BRCA1 mutations revealed that women who have undergone risk-reduction surgery had early tubal malignancies with an intraepithelial component (*Callahan et al.*

2007; *Cass et al. 2005*; *Leeper et al. 2002*). Thus, evidence suggests that patients have a higher risk of developing serous ovarian cancer from cells derived of the fallopian tube and not the ovary itself. A theory was subsequently put forward that the majority of hereditary serous ovarian cancer originates from the epithelium of the fallopian tube and that these cells translocate onto the surface of the ovary making it appear as if the malignancy originated from the ovary (*Piek et al. 2003*). Further studies, not limited to BRCA1 mutation carriers, have shown that 59% of patients with serous ovarian cancer had tubal intra-epithelial carcinoma (TIC), which is composed of regions of dysplasia within tubule epithelium (*Przybycin et al. 2010*). As TIC is not present in all cases of epithelial ovarian cancer, there appears to be a dual pathway where the majority of serous tumours originate from the distal fallopian tube, while the rest have ovarian origin (*Erickson et al. 2013*).

1.1.4 Detection and screening

Ovarian cancer has a high mortality rate due to poor detection at an early stage. When detected early, the 5-year survival rate is approximately 90%. However, cancer diagnosed at late stage has a 5-year survival rate of approximately 33% *(Clarke-Pearson 2009)*. Ovarian cancer typically presents at late stage. This is mainly because symptoms experienced from the onset of ovarian cancer are not specific to the disease and are often overlooked. Symptoms include abdominal pain, distension, early satiety or bloating, a feeling of fullness, dyspepsia, change in frequency of urination, pain during sex, back pain and irregular periods (*Bankhead et al. 2008*; *Goff et al. 2007*). The chances of detecting ovarian cancer at an early stage may be increased in women who have more than one symptom. For example, abnormal post-menopausal bleeding (although not a common symptom) and the presence of an abdominal mass are much more likely in women with ovarian cancer than those without. Therefore, these symptoms are good markers to warrant examination for the presence of ovarian cancer (*Hamilton et al. 2009*).

To date, no suitable screening program has been established to detect ovarian cancer at an early stage. The main strategies investigated are transvaginal sonography (TVS), serum markers, and a combination of both. TVS has been proposed as a strategy to detect changes in the size and architecture of the ovary, which precede symptoms or detection by a pelvic examination.

Cancer antigen 125 (CA125), a high-molecular-weight glycoprotein, is the most commonly used marker for ovarian cancer. Reports showed that 82% of patients with ovarian cancer had increased CA125 levels and that rises and falls in antigen levels

correlated to progression or regression of disease in 93% of cases. Screening for CA125 is not specific enough to permit early diagnosis. It can give false positive results, as CA125 is naturally up-regulated during both ovulation and many benign conditions, including endometriosis, fibroids, uterine myomas, cystadenomas, acute chronic salpingitis and pelvic inflammatory disease (*Jacobs et al. 1989*). Furthermore, in stage I ovarian cancer only 50% of patients express CA125 (*Jacobs et al. 1989*). Assessment of CA125 levels is currently used with other predictors of ovarian cancer, for example ultrasound and menopausal status, in order to calculate a Risk of Malignancy Index (RMI) (*Jacobs et al. 1990*). This method is not ideal due to CA125's aforementioned weaknesses. However, CA125 could be used in combination with other markers or strategies to increase its predictive value (*Bast, Jr. et al. 1983*). The Risk of Ovarian Cancer Algorithm (ROCA) was developed in order to improve CA125's predictive power. It measures the relative closeness of a woman's long-term CA125 pattern to the change-point profile in women with ovarian cancer compared with the flat profiles obtained from women without ovarian cancer. With this method only a small fraction of women are sent for TVS (*Skates et al. 2001*; *Skates et al. 2003*).

In a large randomised clinical trial, annual screening with TVS alone was compared to the efficiency of ROCA in combination with TVS screening in the early detection of ovarian cancer (UK Collaborative Trial of Ovarian Cancer Screening) (*Menon et al. 2009*). The trial randomly assigned 638 postmenopausal women (50-74 years old) to both groups. Although both strategies resulted in an encouragingly high sensitivity in detecting ovarian cancer at an early stage, ROCA in combination with TVS was more sensitive and resulted in fewer repeat tests and surgery. Although two-staged strategies, like ROCA in combination with TVS, promises to be more cost effective, only 82% of ovarian cancers express CA125. This highlights the need for more specific detection strategies to be developed.

Human Epididymis protein 4 (HE4) is a serum biomarker which shows much promise in ovarian cancer screening. This protein is found to be transcriptionally up-regulated in ovarian cancer patients by nuclear factor-κB. It is part of the disulfide-core protein group encoded by the WFDC2 (HE4) gene. It is an 11kDa protein which acts as a precursor protein to the epididymal secretory protein 4E. It was found to be up-regulated to a much lesser extent in benign disease compared to CA125 as was seen in a study by *Moore et al. (2008)* where HE4 was tested along with a panel of other biomarkers. As a single marker, HE4 shows high sensitivity in stage I ovarian cancer, higher than other markers tested, such as CA125, SMRP, CA72-4, inhibin, activin, osteopontin, epidermal growth factor (EGFR), and ERBB2 (Her2). However, when HE4

was combined with CA125 the highest sensitivity (76.4%) and specificity (95%) was seen. The addition of other biomarkers to this combination had minimal effect. The study showed that the combination of HE4 and CA125 was a more accurate predictor of malignancy than either marker on its own and could be useful in a biomarker panel. A subsequent study was carried out to compare RMI to the Risk of Ovarian Malignancy Algorithm (ROMA) using a combination of CA125 and HE4 values and menopausal status to predict ovarian cancer. It was found that ROMA, using CA126 and HE4 values, achieved higher overall sensitivity than RMI 85.3% compared to 64.7%, which strengthens the case for using CA125 in combination with HE4 as a screening tool (*Moore et al. 2010*). More recently it has been reported that including CT scans in a workflow in combination with ROMA could improve HE4's predictive potential for women with a pelvic mass (*Stiekema et al. 2014*).

It is thought that a combination of serum markers will be needed to detect all cases of ovarian cancer. The combination of haemoglobin, haptoglobin and apolipoprotein E with CA125 has been shown to improve sensitivity and specificity in all stages of ovarian cancer (*Kim et al. 2012b*). A new serum-based screening test which shows promise and has been approved by the US Food and Drug Administration (FDA) in 2009 is called the OVA1 test (*Fung 2010*). This is used in order to identify patients who are at risk for ovarian cancer who have presented with an adnexal mass. It was not designed as a standalone test but rather to assist physicians in tandem with physical and radiological findings. It uses a panel of 5 markers (CA125, β2-microglobulin, apolipoprotein A1, transferrin, transthyretin) which are measured and fed into an algorithm which gives an overall OVA1 score. This test gives >90% sensitivity with a 90% negative predictive value for women with ovarian tumours. Some sources suggest that consumer pressure may lead to the OVA1 test becoming a screening tool (*Muller 2010)*. As OVA1 was not designed for this purpose, it may lead to a higher rate of false positive results and costly interventions. It is a high cost test and has not yet been tested for patient screening to detect early-stage ovarian cancer (*Rein et al. 2011*).

To summarise, much research is being put into the development of new serum biomarkers for the detection of ovarian cancer which will improve detection and screening. CA125, the most widely used marker, is not specific enough for early detection. However, ongoing research is working on improving sensitivity, specificity and positive predictive value for detection and screening by looking at other markers, such as HE4, or using a combination of markers.

1.2 Current treatment options

The primary goal of treatment in epithelial ovarian cancer is to cure a patient of the disease or prolong a patient's survival. Treatment strategies will depend on the stage of disease at presentation. Disease stage has been defined by FIGO. See Table 1.2

1.2.1 Early stage disease

Only 20-25% of patients present with early stage disease (FIGO I or II) (*Ozols 2005*). At this stage, while the tumour is still restricted to the pelvis, there is a good chance of patient survival (*Ozols 2005*). Patients who present in stage IA or IB with well differentiated tumours are treated with surgery alone. The surgery usually consists of the removal of the uterus, fallopian tubes and ovaries (hysterectomy with bilateral salpingo-oophorectomy). Cure rate at this stage is >90%. Early stage patients with poorly differentiated tumours (typically stage IC and II) have a high relapse rate of about 40-50% after treatment. It is not certain what the optimum treatment for this group of patients is. Options include treating patients with surgery alone, treating patients with surgery and adjuvant chemotherapy, or treating patients with chemotherapy only after a re-occurrence. This has been investigated in two large, randomised, parallel clinical trials, the International Collaborative Ovarian Neoplasm (ICON) and Adjuvant Chemotherapy in Ovarian Neoplasm (ACTION) (*Trimbos et al. 2003a*) and by the 'Adjuvant chemotherapy in ovarian neoplasm trail' (*Trimbos et al. 2003b*). With the knowledge obtained from these trials, the current standard for the treatment of early stage ovarian cancer from the German Consortium of Gynaecological Oncology (AGO), which was recommended in 2009, is 3-6 cycles of platinum based adjuvant chemotherapy for stages I-IIA excluding stage IA who benefits greater from surgery alone. Appropriate surgical staging must be performed to gain benefit from these guidelines. This improves recurrence free and overall survival. In the case of chemotherapy, it is not clear whether carboplatin mono-therapy or carboplatin/taxane combination therapy is the optimal treatment (*Burges et al. 2011*).

1.2.2 Advanced stage disease

Patients with advanced disease are classified as FIGO stage III or IV. The current standard for treatment for these stages is surgical debulking, followed by intravenous combination of platinum and taxane-based chemotherapy. The most effective platinum agents used for ovarian malignancies are carboplatin and cisplatin and the most effective taxane agents are taxol and docetaxel (*Cannistra 2004*). The most efficient combination with the least adverse effects is three hour intravenous (IV) administration

Table 1.2 FIGO staging of ovarian cancer.

STAGE I	**Tumour is limited to the ovary / ovaries**
IA	Only one ovary is affected by the tumour, the ovary capsule is intact No tumour detected on the external surface of the ovary No Malignant cells can be detected in ascites or peritoneal washings
1B	Both ovaries are affected by the tumour, the ovary capsule is intact No tumour detected on the external surface of the ovaries No Malignant cells are detected in ascites or peritoneal washings
IC	The tumour is in stage IA or IB but with any of the following: The ovary capsule is ruptured The tumour is detected on the ovary surface Positive malignant cells are detected in the ascites or peritoneal washings
STAGE II	**Tumour involves one or both ovaries and has extended to other pelvic organs or surfaces**
IIA	The tumour has extended and/or implanted into the uterus and/or the fallopian tubes. No Malignant cells are detected in ascites or peritoneal washings
IIB	The tumour has extended to another organ in the pelvis No Malignant cells are detected in ascites or peritoneal washings
IIC	Tumours are as defined in IIA/B, but malignant cells are detected in the ascites or peritoneal washings
STAGE III	**The tumour involves one or both ovaries with microscopically confirmed peritoneal metastasis outside the pelvis and/or regional lymph node metastasis.** **Includes liver capsule metastasis.**
III A	Microscopic peritoneal metastasis beyond the pelvis to abdominal peritoneal surfaces or the omentum
III B	Same as IIIA above but Microscopic peritoneal metastasis beyond the pelvis 2 cm or less in size
III C	Same as IIIA above but Microscopic peritoneal metastasis beyond the pelvis more than 2 cm in size and/or lymph node metastases to inguinal, pelvic or para-aortic areas observed
STAGE IV	**Distant metastasis beyond the peritoneal cavity. And, liver parenchymal metastasis.**

Adapted from (*Heintz et al. 2006*)

of taxol (175mg/ml^2) and carboplatin (area under the concentration time curve (AUC) 5), every 3 weeks for 6 cycles. Meta-analyses show that the combination of these two agents is superior to platinum mono-therapy (*Covens et al. 2002*). Optimal surgical debulking prior to chemotherapy is a key factor in prolonging recurrence-free and overall survival. An optimal residual tumour of less than 1cm can be achieved in 50-85% of advanced stage ovarian patients (*Bristow et al. 2002*).

The combination of cisplatin and taxol became the initial standard chemotherapy regime following the results of a number of clinical trials. This regime was replaced by the current standard of carboplatin and taxol as this combination had lessened non-hematologic toxicity associated with it (*du Bois et al. 2003*; *McGuire et al. 1996*; *Ozols et al. 2003*; *Piccart et al. 2000*). The combination of docetaxel and carboplatin may be even more favourable as less neuropathy is seen with this regime, when compared to taxol and carboplatin (*Cannistra 2004*). Recently clinical trials such as the GOG-0218 (*Burger et al. 2011*) and the ICON7 (*Perren et al. 2011*) have shown that chemotherapy administered with bevacizumab (Avastin) improves progression free survival for patients with advanced ovarian cancer compared to the current standard chemotherapy regimes. However, there have been no reports that the drug improves overall survival. Based on this data, Bevacizumab in combination with chemotherapy has been approved for treatment of advanced ovarian cancer in Europe and Japan. Bevacizumab works by inhibiting angiogenesis. It binds to vascular endothelial growth factor (VEGF) in the tumour's micro-environment and stops it binding to target receptors on the tumour surface, thus inhibiting angiogenic signalling (*Wang et al. 2004*). Ordinarily, angiogenesis is tightly regulated in adult humans and only occurs during ovulation and wound repair. Tumours, which are greater than 1mm in size, require angiogenesis to grow further and activity stimulate this process. This presents an attractive target for intervention in ovarian cancer. Blocking this process may prevent growth of tumours and improve survival.

With current treatments, complete clinical remission occurs in 50% of treated patients with advanced ovarian cancer. These patients are closely monitored for any indication of relapse. Even with invasive surgery and treatment with highly active chemotherapeutics, 20-30% of patients show no remission whatsoever and have sustained residual or progressive disease (*Cannistra 2004*). Approximately 75% of treated patients will have recurrence of disease after treatment with cytoreductive surgery and combination chemotherapy with a median survival of 2 years following the recurrence. All relapsed patients eventually die from their disease (*Ozols 2005*).

1.2.3 Relapse or recurrence of disease

Cancer is recurrent when the disease re-appears after initial treatment regimes. The recurrence can be local (in or near the same position as original tumour) or distant (tumour is in other organs). The focus of recurrent ovarian cancer treatment is to manage the symptoms, increase quality of life, and to extend survival for as long as possible. An optimum treatment strategy for this group of patients has not yet been found. The first indication of re-occurrence is usually a sequential increase in serum CA125 levels (*Rustin et al. 1996*; *Rustin et al. 2004*). There are a number of considerations to take into account when choosing a treatment strategy for second-line chemotherapy. An important factor is the time taken for the disease to re-occur after responsiveness to the initial therapy.

Patients who show progression during platinum treatment are classified as platinum refractory. Patients who relapse before 6 months are classed as platinum resistant. Patients that relapse after 6 months are considered to be platinum sensitive and patients who relapse after 18 months can be considered very platinum sensitive (*Armstrong 2002*; *Markman et al. 2000*). Other factors to take into account are the previous agents used in first-line treatment, the patient's performance status including the presence of further conditions, toxicities experienced, and cost-effectiveness of treatments. With all these factors taken into account, the two main groupings for treatment are considered to be patients who relapse within 6 months (non-responders) and patients who relapse after 12 months (responders) (*Salzberg et al. 2005*). Response indicators are also examined, which include histology, tumour size and the platinum-free interval.

In order to increase the platinum-free treatment interval, patients who relapse within 6 months are resistant to platinum and these patients are usually treated with non-platinum containing regimes including gemcitabine, topotecan, pegylated liposomal doxorubicin, vinorelbine, oral etoposide or weekly taxane treatments (taxol or docetaxel) (*Armstrong 2002; Ozols 2005*). Longer gaps in platinum treatment give better response rates in subsequent platinum treatment regimes. This is because tumours gain acquired resistance to treatment agents. Acquired resistance is generally unstable, therefore the resistance can be lost over time (*Armstrong 2002*). For patients treated with first-line chemotherapy including platinum and/or taxol agents, a second-line treatment with pegylated liposomal doxorubicin results in longer overall survival and improved quality of life with fewer adverse side effects than patients who are treated with topotecan or other non-platinum agents (*Thigpen et al. 2005*). In platinum-containing, taxane-free first-line chemotherapy regimes, taxol and pegylated liposomal

doxorubicin can both be used effectively. However, both drugs have adverse side effects associated with their administration. By modulating the dosing schedule and closely monitoring tolerability these side effects can be managed (*Armstrong 2002*).

Patients who relapse after 12 months are generally sensitive to platinum treatment, as enough time has passed to lose much of the acquired resistance to platinum. The main choice for therapy in this patient group is platinum and taxane combination or platinum and gemcitabine combination.

1.3 Platinum chemotherapy

The first platinum drug approved for clinical use was cisplatin in 1978. It was approved by the FDA for the use in testicular and ovarian cancers and has now become one of the most widely used anticancer drugs (*Higby et al. 1974*). There was little progress in improving mortality rates in ovarian cancer between the 1950's and 1960's. The introduction of cisplatin improved ovarian cancer treatment dramatically (*Piccart et al. 2001*). Cisplatin is used in many types of cancer treatments, including testicular, ovarian, bladder, osteogenic sarcoma, head and neck, endometrial and cervical and small cell lung cancers (*Reedijk J 1987*). Some treatment challenges are that cancers can have an intrinsic resistance to cisplatin (such as ovarian, colorectal and non-small cell lung cancer) or develop acquired resistance (as seen in ovarian or small cell lung cancer) (*Fuertes et al. 2003a*). Cisplatin treatment is also associated with severe side effects, which include nephrotoxicity, neurotoxicity, ototoxicity, nausea and vomiting (*Giaccone 2000*). In order to improve on cisplatin's therapeutic ability, a number of analogs have been synthesized. These have been investigated via clinical trial to identify possible improvements in toxicity, cross resistance and pharmacological aspects of prospective drugs when compared to cisplatin. To date only carboplatin and oxaliplatin have been accepted as possible alternatives (*Weiss et al. 1993*).

1.3.1 Cisplatin

The anti-tumour potential of cisplatin was first discovered during experiments carried out by *Rosenberg et al.* in the 1960's who were studying the growth of E-coli bacteria under the influence of electric fields. The inhibition of cell division in E-coli was observed in the presence of an electric field, which caused filamentous growth of the bacteria. It was found that the inhibition of cell division by cell cycle arrest was caused by the presence of group VIIIB transition metal compounds. The most stable and most active of these compounds was a cis-Pt(II) species characterized and developed as

cis-diamminedichloroplatinum(II) now known as cisplatin (*Rosenberg et al. 1967*). The structure of the cisplatin angent is presented in Figure 1.2.

It is widely accepted that the main mechanism of action for cisplatin is its binding to nuclear DNA causing accumulation of adducts on DNA strands, which interferes with transcription and DNA replication processes. This in turn can initiate cytotoxic processes within the cell leading to cell death (*Fuertes et al. 2003b*). Cancer patients receive cisplatin compounds intravenously. Cisplatin is carried around the body by the blood before diffusing into tissue and reaching the tumour cells. Platinum compounds have a high affinity for sulphur and thiol groups of amino acids such as cysteine. Approximately 90% of platinum becomes inactivated by binding to blood plasma proteins (mainly albumin) before reaching its target cells (*Judson et al. 2000*). It must be noted that cisplatin will also be taken up by normally functioning cells. It is thought that cancer cells are more susceptible to the DNA damage induced by cisplatin due to a possible reduced ability to repair the DNA damage or via inhibition during replication, which is a key part of cell division and must occur frequently in rapidly dividing cells like cancer cells (*Reedijk J 1987*).

The cisplatin molecule can be actively taken into the cell by copper transporter CTR1. A hydrolysis reaction occurs upon entering the cell by the substitution of a chloride group with a water molecule (aquation). One or both chloride groups may be removed in this reaction resulting in a mono or diaquo positively charged cisplatin species (*Jamieson et al. 1999*). The structure of cisplatin is seen in Figure 1.2. Aquation is inhibited in the blood serum due to high concentrations of chloride. The resulting species of cisplatin are very reactive towards nucleophile centres of biomolecules. Because of this reactivity, cisplatin will bind to a number of intracellular molecules including cytoskeletal microfilaments, RNA and thiol-containing proteins and peptides (*Jordan et al. 2000*). The most important non-DNA molecule that cisplatin binds with is the tripeptide glutathione (GSH). GSH is present in high concentrations within the cell and binds rapidly to cisplatin upon entering the cell. The binding of cisplatin to these non-DNA molecules within the cell may have a role to play in its cytotoxicity by blocking these molecules from carrying out important cellular functions. For example, binding of cisplatin to methionine 1 and/or histidine 68 of ubiquitin might inhibit the degradation of intracellular proteins by blocking the ubiquitin-proteasome pathway. This can cause deregulation of many important cellular functions (*Peleg-Shulman et al. 2001*). Cisplatin is also known to inhibit heat shock protein 90 (Hsp90) by binding to and blocking its C-terminus ATP binding site. Hsp90 is an ATP-binding chaperone involved in cell cycle regulation and signal transduction (*Soti et al. 2002*).

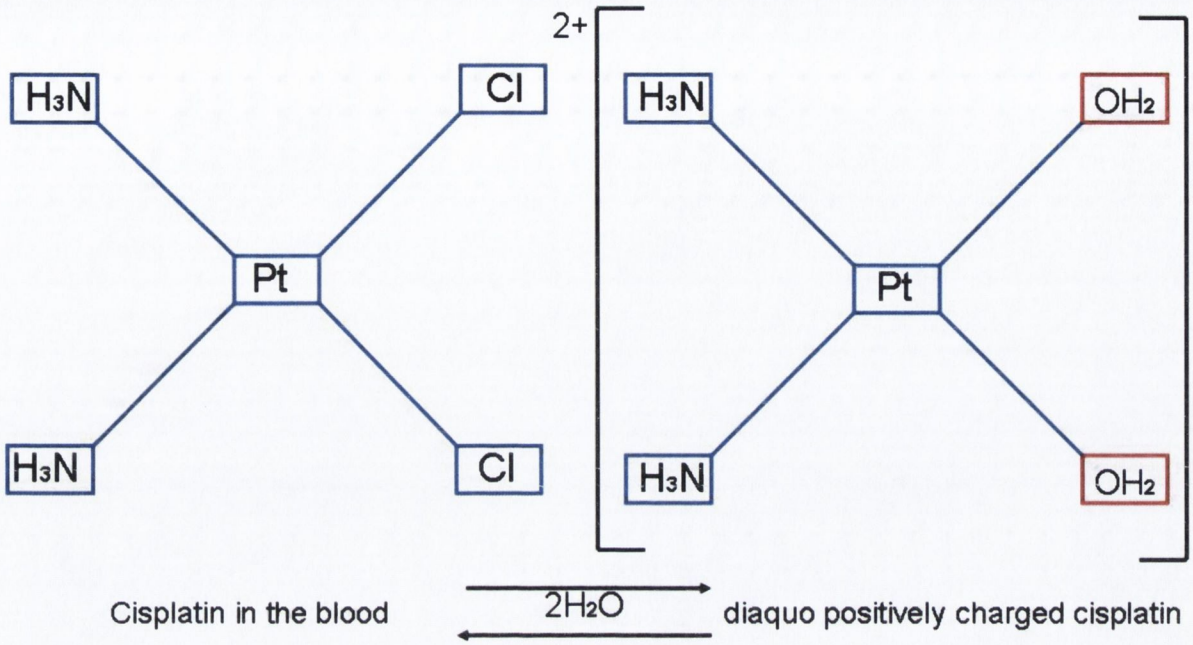

Figure 1.2 Structure of cisplatin (cis-diammine) platinum complex.

On the left is the structure of cisplatin as it appears in the blood and on the right is the structure of cisplatin after aquation in the cytoplasm. Red boxes indicate changes to the structure after aquation. Adapted from (*Piccart et al. 2001*).

Cisplatin that reaches the nucleus of the cell can bind to nuclear DNA and form adducts (*Jamieson et al. 1999*), although 99% of the cisplatin will have bound to other extracellular and intracellular molecules prior to reaching the nucleus. It has the highest affinity for the nucleophilic N7 atoms of guanine and adenine in the major groove, as this is the most reactive site for metal binding (*Yang et al. 1999*). There are a number of different types of adduct that can be formed by Cisplatin-DNA binding. Cisplatin can form 1,2-intrastrand cross-links, interstrand cross-links, monofunctional adducts and protein-DNA cross-links (*Fuertes et al. 2003b*). See Figure 1.3. Formation of adducts on the DNA strand causes contortion and bending towards the major groove (*Fuertes et al. 2003a*). Monoadducts are first formed by the loss of one water molecule. 90% further react to form intrastrand adducts the majority of those being 1,2-intrastrand adducts (*Rabik et al. 2007*). It is the 1,2-intrastrand adducts that are believed to be most important in the cytotoxic action of cisplatin. This notion is not proven but is

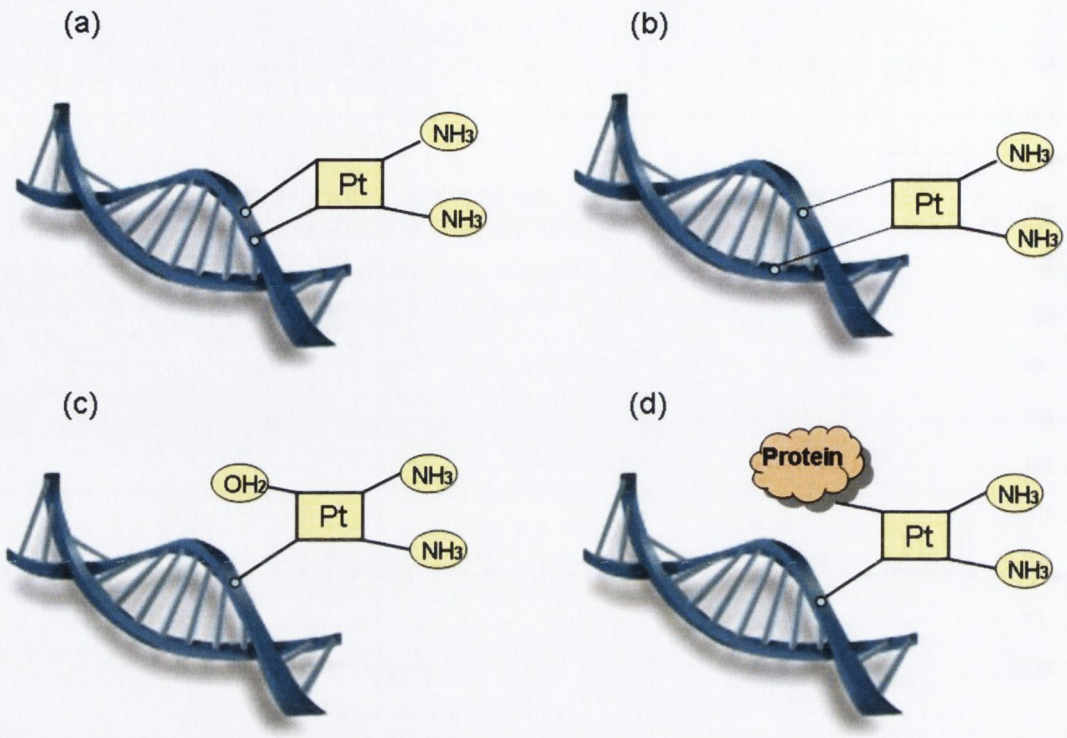

Figure 1.3 Structure of DNA adducts formed on DNA.

Structure of main DNA adducts formed by cisplatin: (a) 1,2 intrastrand cross-link (b) interstrand cross-link (c) monofunctional adduct (d) protein-DNA cross-link. Adapted from (*Cepeda et al. 2007*)

supported by the discovery of High Mobility group (HMG) proteins that specifically recognize this type of adduct and may be involved in regulating the processing of these adducts (*Pil et al. 1992*). HMG proteins are composed of basic domains of 80 amino acids containing three α-helical domains. The binding of HMG proteins blocks replication machinery and has been shown to block Nucleotide Excision DNA repair (NER) components from repairing the DNA lesions (*Rabik et al. 2007*). Also the NER recognises and repairs 1,3 intrastrand adducts formed on DNA to a much greater extent than it locates and repairs 1,2 intrastrand adducts (*Zamble et al. 1996*). This strengthens the theory that 1,2-intrastrand adducts are the most important in the mechanism of action of cisplatin. The other adducts formed by cisplatin may also play an important role in cytotoxicity. Interstrand adducts will cause deformation of DNA

structure through the bending of the helical axis towards the minor groove and DNA unwinding (*Malinge et al. 1999*). The distortions in the DNA caused by platinum adducts and intra/inter-strand crosslinks can be recognised by DNA binding proteins which can either initiate DNA repair or signal a cell to undergo apoptosis (triggered by the impeded separation of DNA strands impairing replication and DNA synthesis) (*Siddik 2003*).

1.3.2 Carboplatin

Carboplatin was first approved for use in treatment in the mid 1980's. It has a similar method of action to cisplatin. The same positively charged acquated species of platinum are formed when carboplatin or cisplatin undergo hydrolysis reactions upon entering a cell. Also carboplatin causes the formation of the same DNA adducts as cisplatin which have been previously described in section 1.3.1.1 (*Go et al. 1999*). However, carboplatin causes less severe side effects than cisplatin. It is more tolerable due to less nephrotoxicity and neurotoxicity and causes less nausea and vomiting. Carboplatin is also more stable and binds less to proteins. Although it has these advantages over cisplatin, it has much less efficiency in treating germ cell tumours, head and neck cancers and bladder and oesophageal cancers. However, It does seem to have the same efficiency when treating advanced non-small cell lung cancers and most stages of small cell lung cancer along with the same ability in suboptimally debulked ovarian cancer tumours (*Pasetto et al. 2006*).

1.3.3 Oxaliplatin

As a derivative of cisplatin, oxaliplatin structure is similar to that of cisplatin, except for that the ammine ligands have been replaced by a DACH group, which appears to inhibit alkylating-agent resistance. Because of this difference in structure, oxaliplatin has been seen to have activity in some cisplatin resistant cancers, including ovarian cancer (*Piccart et al. 2001*). However, it must be noted that this activity is limited to highly cisplatin-resistant models. In low-level cisplatin-resistant models cross resistance to oxaliplatin is seen (*Stordal et al. 2006*). This is based on responses from patients and evidence from *in vitro* models (*Stordal et al. 2007c*). Oxaliplatin can be useful in treating cisplatin resistance clinically when combined with other therapeutic agents. This may suggest that it is the combination of drugs that has activity against cisplatin resistance rather than oxaliplatin as a single agent. Other clinical benefits of oxaliplatin over cisplatin is that its toxicity profiles are more favourable (*Stordal et al. 2007c*).

Oxaliplatin's method of action is similar to that of other platinum compounds. Again, its main method of action is the formation of DNA adducts causing disruption in transcription and DNA replication processes, causing the initiation of cytotoxic pathways. It forms the same type of DNA adducts previously described but with different chemical conformation. These adducts seems to be better at inhibiting DNA replication due to its bulky DACH compound and is better at withstanding DNA repair as it is less recognized by mismatch repair proteins (MMR) (*Raymond et al. 1998*). Interestingly, oxaliplatin seems to have a secondary mechanism of action by which the compound induces the immune system to target and kill tumour cells. *Tesniere et al. (2010)* have carried out experiments on murine and human colon cancer cells. They have shown that exposing colon cancer cells to oxaliplatin causes the cells to release immunogenic signals from their surface before they undergo platinum-mediated cell death. This caused an immune response against the cancer cell in the form of interferon γ production by T-cells and interaction with toll like receptor 4 of dendritic cells. In advanced colon cancer patients treated with oxaliplatin, patients with a defective Toll like receptor 4 gene (TLR4), causing a loss of function, had significantly lower progression free and overall survival when compared with those having functional TLR4 (*Tesniere et al. 2010*).

1.4 Mechanisms of platinum resistance

Although initial response to platinum chemotherapy is high in ovarian cancer, most patients will relapse with platinum resistant disease. Several platinum drug resistance mechanisms have been identified *in vitro*. Numerous reviews on platinum and chemotherapeutic resistance show a number of mechanisms for resistance to platinating agents (*Piccart et al. 2001*; *Rabik et al. 2007*; *Stordal et al. 2007a*; *Vasey 2003*). A tumour cell which has a resistant phenotype can utilize multiple mechanisms of resistance. The most common of these mechanisms are:

- Decreased accumulation of the drug in the cell
- Deactivation of the drug within the cell
- Loss or decrease in Mismatch repair (MMR)
- Increased repair of DNA adducts
- Inhibition of apoptosis
- Mutations in p53

1.4.1 Decreased accumulation of drug

Reduced accumulation of the drug within cells can be attributed to decreased influx, increased efflux or both. It has long been postulated that platinum compounds enter the cell by passive diffusion as cells cannot become saturated or inhibited by structural analogs (*Judson et al. 2000*). However, other mechanisms such as active transport could play a role in intracellular drug accumulation. For example, cisplatin import is blocked by the ouabain molecule which inhibits the action of the membrane sodium/potassium ATPase pump. This suggests that cisplatin transport may be dependent on the membrane potential of the cell (*Andrews et al. 1988*).

1.4.1.1 Role of copper transporters

CTR1, the major copper influx transporter, has been found to regulate cisplatin, carboplatin and oxaliplatin intake, while ATP7A and ATP7B, two copper efflux transporters, are involved in efflux of these platinum compounds from the cell. Copper transporters within the cell, which are involved in copper homeostasis, have been found to be have the ability to sequester platinums into different subcellular compartments, preventing their reaction with DNA (*Safaei et al. 2005*). Exposing ovarian cancer cell lines to cisplatin has been shown to cause down regulation of CTR1 protein expression by internalization of the transporter from the surface membrane. This results in diminished accumulation of the drug within the cell in a time-dependent manner (*Holzer et al. 2004*). Over expression of ATP7B has been shown to increase resistance to cisplatin in ovarian cancer cell lines. Studies carried out by (*Nakayama et al. 2001*) on a panel of 9 ovarian cancer cell lines showed high expression of this cellular pump in SKOV3, OMC6 and PA1. This over expression correlated with increased cisplatin resistance. SKOV3 had the highest expression of ATP7B. Prognosis in ovarian cancer patients is poor when ATP7B is highly expressed in tumours in contrast to better prognosis when expression is low (*Rabik et al. 2007*). In a follow up study, 82 ovarian carcinomas were profiled for a number of genes known to play a part in cisplatin resistance using RT-PCR (reverse transcription PCR). From this gene list only ATP7B could be linked to resistant phenotypes in the majority of ovarian carcinomas. It had significantly increased expression in moderately or poorly differentiated tumours treated with cisplatin and could be used as a marker of cisplatin resistance (*Nakayama et al. 2002*). ATP7A has been found to sequester cisplatin, carboplatin and oxaliplatin into vesicles. Over expression of this molecule has been found in ovarian cisplatin resistant cell lines A2780/CP and 2008/C13 *5.25 when compared to their non-resistant parent cell lines. Ovarian cancer patients who show

increased levels of ATP7A after platinum treatment have poorer survival rates than patients who do not show elevated levels (*Katano et al. 2002*).

1.4.1.2 Role of adenosine triphosphate-binding cassette transporters

Members of the MRP-related transport proteins may be linked to active efflux of platinums from cells. MRP proteins are members of the adenosine triphosphate-binding cassette (ABC) family which transport anticancer drugs from the cell (*Choudhuri et al. 2006*). The MRP family consists of 12 members but in particular MRP1 and MRP2 have been linked with multidrug resistance. MRP2 over expression has been linked with platinum resistance in ovarian cancer and a number of other cancers types. It is deemed to be a good determinant of tumour sensitivity (*Kool et al. 1997*; *Korita et al. 2010*).

1.4.2 Drug deactivation

It has been previously noted that when platinum compounds enter the cell they become a positively charged aqueous species that has high reactivity for thiol-containing proteins and peptides including GSH and metallothioneins. Increased levels of these compounds can be correlated to cisplatin resistance. Studies carried out on eight ovarian cancer cell lines have shown an inverse relationship between intracellular GSH levels and platinum sensitivity (*Mistry et al. 1991*). Platinum's are inactivated by the substitution of thiol for platinum. There are many mechanisms in which the GSH system may act in conferring cisplatin resistance or sensitivity. Three of these mechanisms are described by (*Chen et al. 2010*). The first is via the formation of cisplatin-GSH complexes by GSH-S-transferase π. These complexes are inactivated and effluxed from the cell via the MRP2 membrane protein, a member of the ABCC2 transporter family. Cisplatin cannot be effluxed from the cell on its own in this way but requires GSH (*Paulusma et al. 1999*). Both GSTπ and У-glutamylcycteine synthetase contribute to cisplatin resistance in ovarian, lung and cervical cancer cell lines (*Kavanagh et al. 2005*; *Li et al. 2009*; *Sakamoto et al. 2001*). This mechanism is shown in Figure 1.4.

The second proposed mechanism involves the role of glutathione as a cytoprotector in cisplatin resistance. It has been discovered that resistant cells often over express glutathione and y-glutamylcysteine synthesis, the rate limiting enzyme for glutathione synthesis. The more GSH that is within the cell, the more that is present to bind and inactivate platinum compounds. Increased Metallothionein II levels in the cell have also been correlated to cisplatin resistance in a number of cell lines. This protein is involved

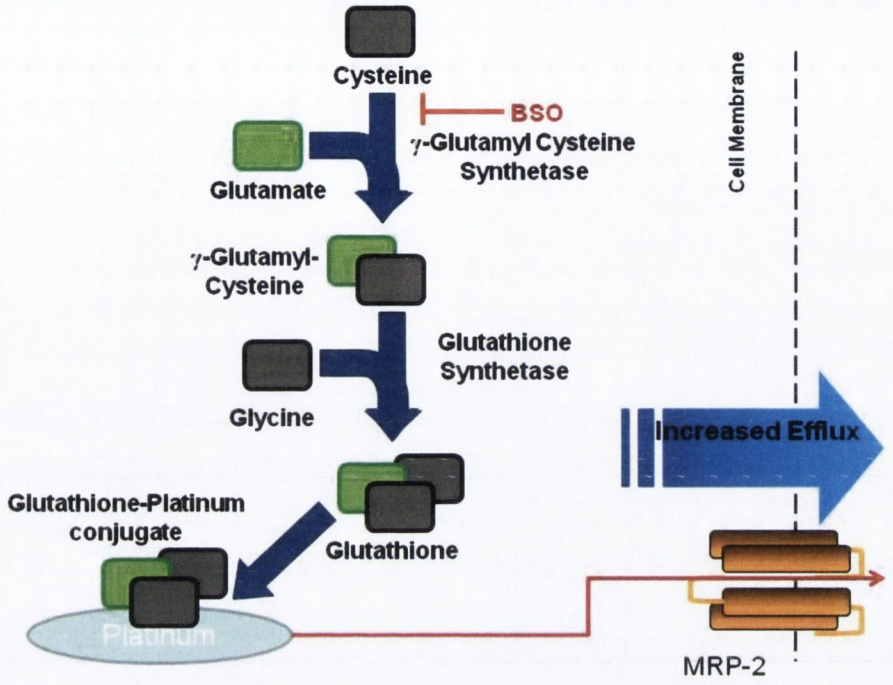

Figure 1.4 Efflux of platinum molecules from the cell by GSH.

The building blocks of GSH are cysteine, glutamate and glycine which are assembled into GSH by Y-Glatamyl Cysteine Synthetase and Glutathione Synthetase. GSH can then bind platinums and form a Glutathione-Platinum conjugate which can be effluxed by the cell via membrane protein pump MRP-2. Glutathione synthesis can be inhibited by Buthionine sulphoximine (BSO).

in the detoxification of heavy metal ions. Platinums bind to this molecule and become inactive and no longer able to carry out its cytotoxic mechanisms of action within the cell. Cancers that have been shown to have acquired resistance by this mechanism include bladder and oesophageal cancers and transitional primary cell carcinomas. However, this mechanism is tissue specific and speculated to play only a minor role in platinum resistance (*Rabik et al. 2007*).

The final mechanism described indicates how GSH up-regulation can confer sensitivity to platinums. Up-regulated expression of GSH causes diminished copper levels within the cell, which is needed for biological processes. This, in turn, causes the expression of CTR1 which can influx platinum compounds into the cell facilitating platinum

mediated cell death through accumulation of platinum within the cell (*Safaei et al. 2005*; *Song et al. 2008*).

1.4.3 Decreased mismatch repair

DNA mismatch repair (MMR) is a strand specific mechanism in which the cell fixes incorrectly paired nucleotides and mismatch loops after the cell has replicated its DNA. It fixes the errors made by DNA polymerase after replication. The proteins which recognize and bind these mismatched nucleotides are MLH1 and MSH2, MSH2 binding DNA and MLH1 binding the DNA/MSH2 complex. The PMS2 protein acts in stabilising this complex (*Fishel et al. 1995*). Firstly, the MSH2:MSH6 complex bind the effected DNA area containing a mismatched DNA nucleotide. This complex will undergo a conformational change by phosphorylation of ATP. This complex will then recruit the MLH1:PMS2 complex in another ATP driven reaction. This assembled complex is able to translocate in either direction along the DNA strand. When it reaches a strand discontinuity it will stop and bind PCNA. Recruitment of the EXO1 exonuclease causes the degradation of the interrupted DNA strand in a 5' direction towards the mismatched nucleotide. The gap produced will be stabilized by RPA. The MSH2:MSH6:MLH1:PMS2 complex is able to disassociate during this process but binding of other complexes will continue until the mismatched nucleotide is reached and removed. Replicative DNA polymerase fills in the single strand gap stabilised by RPA and DNA ligase anneals the cut in the DNA strand to finish the process (*Dzantiev et al. 2004*; *Genschel et al. 2003*) See Figure 1.5 for overview of the MMR system.

The MMR system is able to recognise DNA adducts that are formed by cisplatin or carboplatin DNA binding. It is thought that recognition of these adducts causes cellular signalling that leads to apoptosis (*Meyers et al. 2004*). When the system is inactivated, an accumulation of unpaired deletions in mononucleotide and dinucleotide repeats occur, which leads to variable length repeats. This is known as microsatellite instability and could be caused by genetic or epigenetic inactivation, which in turn has been given a possible marker for MMR deficient cells. The loss of DNA repair by the system is attributed to a tolerance of DNA damage in the cell. This loss and tolerance to damaged DNA leads to cisplatin and carboplatin resistance. This correlates to the loss of apoptotic signalling by the MMR pathway. Cancer cells with loss of MMR function have been shown to be 2-3 fold more resistant to cisplatin than cells with functioning MMR (*Stojic et al. 2008*). No changes in resistance occur with oxaliplatin where MMR is functional or non-functional. For this reason it is speculated that the MMR system does not recognise the novel adducts formed by this platinum species

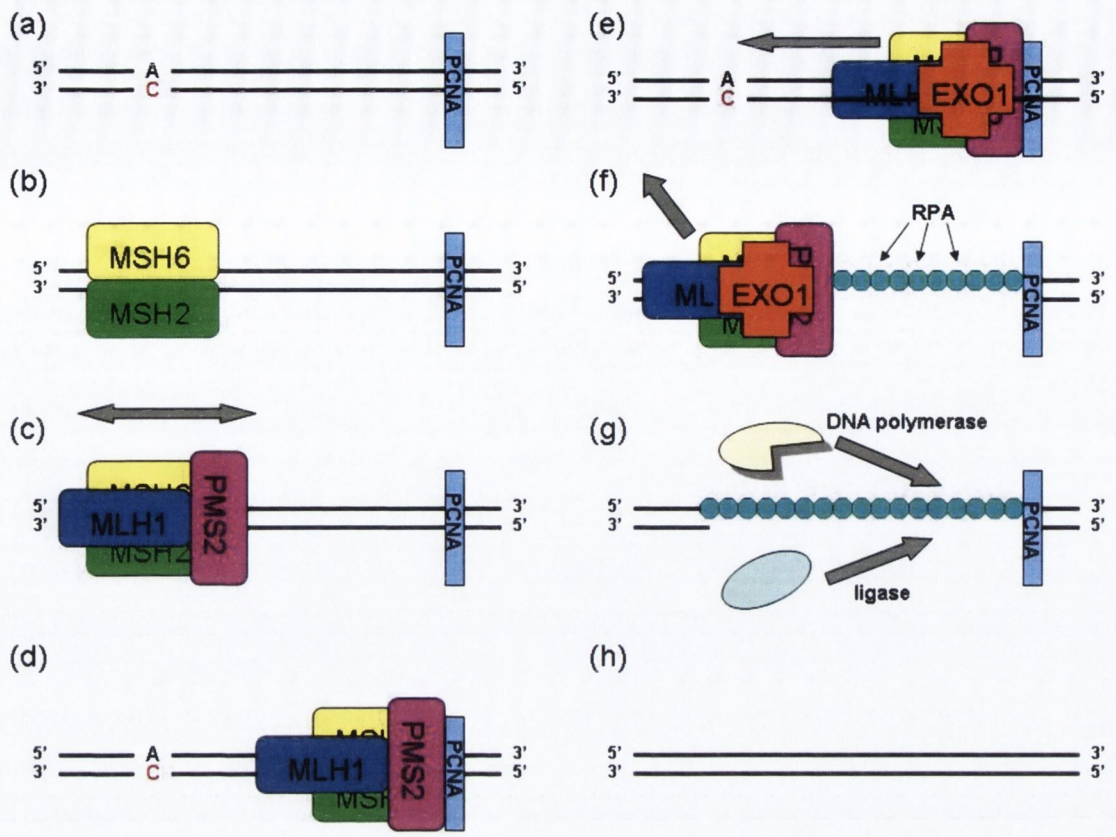

Figure 1.5 Overview of the MMR system.

(a) DNA strands with mismatched nucleotide shown in red. (b) MSH2:MSH6 complex bind the effected DNA area containing a mismatched DNA nucleotide. (c) The MSH2:MSH6 complex recruits the MLH1:PMS2 complex in an ATP driven reaction. The complex is able to translocate in either direction along the DNA strand shown by directional arrows. (d) Complex has reached a strand of discontinuity. (e) EXO1 exonuclease is recruited and degrades interrupted DNA strand in a 5' direction. (f) The gap produced is stabilised by RPA. The MSH2:MSH6:MLH1:PMS2 complex is able to disassociate during this process, but binding of other complexes will continue until the mismatched nucleotide is reached and the complex disassociates from the DNA strands. (g) DNA polymerase fills in the single strand gap and DNA ligase anneals the cut in the DNA (h) Repaired mismatched DNA strand. This figure was adapted from (*Stojic et al. 2008*)

(*Fink et al. 1996*). The loss of MMR function could be a mechanism of acquired resistance in ovarian cancer after platinum chemotherapy. It has been suggested that Methylation of MLH1 in plasma DNA, one of the proteins involved in recognising mismatch errors, will result in loss of MMR and in turn contribute to platinum resistance in ovarian cancer after chemotherapy with carboplatin and taxol (*Gifford et al. 2004*).

The majority of MMR-deficient cancers have mutations in MLH1 or MSH2 which recognised mismatched proteins and initiate repair. One study examined tumour sections for MLH1 and MSH2 expression from 54 ovarian cancer patients before and after platinum based chemotherapy. They used immunohistochemical staining to seek for associations between protein expression of these MMR proteins and clinical parameter of prognostic significance as well as treatment response and overall survival. It was found that the tumour mass changed after chemotherapy and gave a selective pressure for cells expressing lower levels of MLH1 and MSH2 proteins (*Samimi et al. 2000*). This reduction in expression may be due to hypermethylation of the promoter regions of these proteins and in theory demethylating agents like decitabine could be used to sensitise tumours and inhibit tumour growth (*Brown et al. 2004*). To date, however, only a small number of studies have given conclusive links to platinum resistance and MMR inactivation in cellular models (*Fink et al. 1998*; *Gifford et al. 2004*; *Helleman et al. 2006b*; *Watanabe et al. 2001*). The pathway is only thought to be linked to 10% of ovarian tumours from a systematic review of the literature from articles published on the PubMed electronic database on August 31 2009 (*Murphy et al. 2011*).

1.4.4 Increased repair of DNA adducts

Nucleotide excision repair (NER) is a major pathway associated with DNA repair. It is one of the main pathways involved in the development of platinum resistance due to increased repair of DNA adducts. NER is used in a cell in order to repair DNA lesions formed by exposure to chemicals or radiation or by protein addition to DNA (*Sancar et al. 2004*). NER detects DNA damage via the distortion detection factor XPC and the XPA and RPA proteins which form a complex that binds to damaged DNA. TFIIH binds to this complex and is involved in the initiation of repair (*Sancar 1996*). All intrastrand crosslinks that are a result of platinum adduct formation are recognized by NER although 1, 2 crosslinks are less efficiently repaired when compared to 1, 3 crosslinks. These adducts are primarily formed by cisplatin and support the theory that 1, 2 adducts are cytotoxic (*Moggs et al. 1997*). Adducts are removed by the action of 2 structure specific endonucleases. XPG will cut the DNA strand on the 3' side of the lesion while ERCC1/XPF will cut the DNA strand at the 5' side of the lesion. Excision fragments range from 24 to 32 nucleotides. A new DNA strand is synthesised by PCNA-dependant DNA polymerase completing the NER process (*Sancar 1996*). See Figure 1.6 for an overview of the NER pathway.

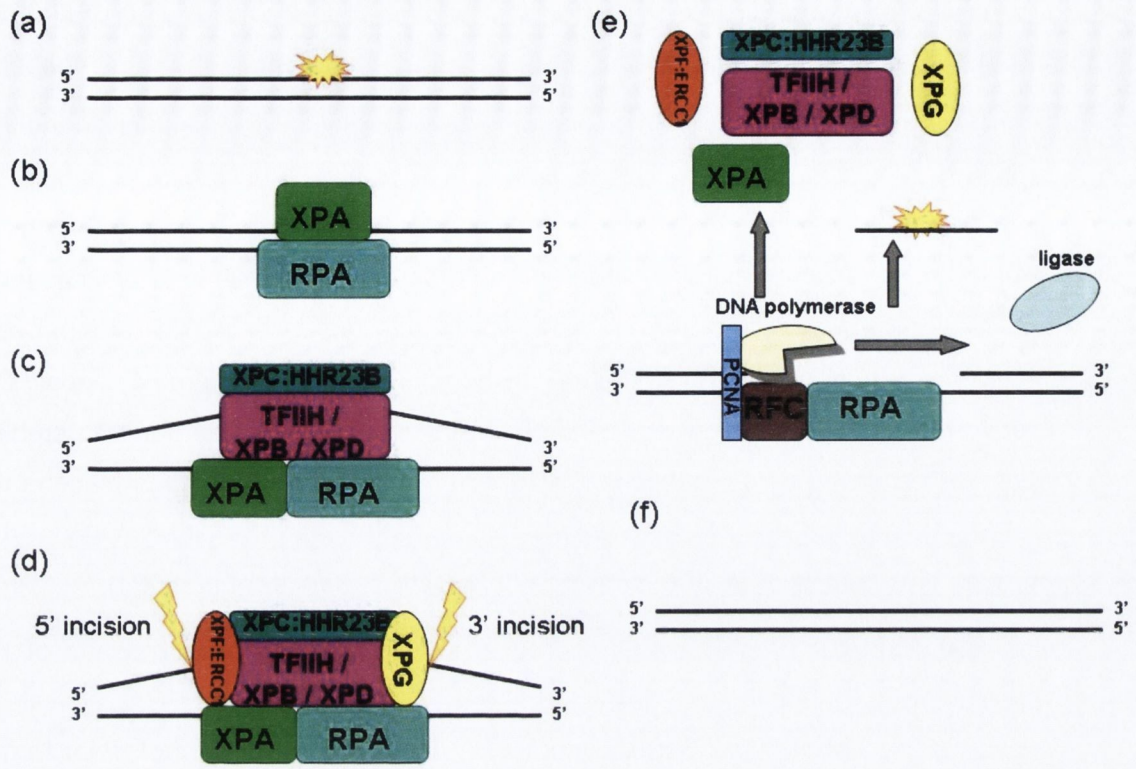

Figure 1.6 Overview of NER pathway.

(a) DNA strand with an adduct. Adduct is represented by yellow object. (b) Adduct or damaged DNA is recognized by the XPA:RPA complex which binds to the effected region. (c) TFIIH is recruited by XPA:RPA and unwinds the DNA leaving it exposed. XPC:HHR23B is recruited through interactions with TFIIH and XPA and binds to the exposed DNA. (d) Recruitment of XPG occurs by RPA and TFIIH. XPG makes an incision in the 3' side of the effected DNA. XPF:ERCC1 is then recruited by XPA, XPF and TFIIH and makes an incision to the 5' side of the effected DNA. (e) Damaged DNA is released. RFC causes the disassociation of the post-incision complex. RFC recruits PCNA which associates with DNA polymerase ε or δ. DNA polymerase fills in the gap and ligase joins the DNA strand back together. (f) Repaired DNA strand. This figure is adapted from (*Sancar 1996*).

In ovarian cancer increased expression of XPA and ERCC1/XPF genes has been found in tumours from cisplatin resistant patients. This suggests an increase in NER in cisplatin resistant patients (*Dabholkar et al. 1994*). Other studies in ovarian cancer cell lines have also shown that elevated levels of ERCC1 mRNA are linked to increased levels of DNA repair of cisplatin induced DNA damage, resulting in drug resistance (*Selvakumaran et al. 2003*). Supporting this evidence, there are low levels of XPA and

ERCC1 gene expression in Testicular cancer, which is generally very responsive to cisplatin treatment (*Welsh et al. 2004*).

Homologous recombination (HR) is another DNA repair process which is involved in repairing DNA damage induced by platinum adducts. HR is used to repair double stranded (DS) breaks in DNA strands. DS breaks are very damaging to the cell and a large volume of breaks will lead to cell death signalling. DS Breaks are caused by a collapse in the replication fork after the replication machinery meets platinum adducts bound to the DNA strands. HR uses the homologous chromosome to repair the DS break ensuring that the right sequence is maintained keeping the genome stable. It is generally regarded as a highly conserved, error free system that takes place in the G2 and S phase of the cell cycle. However, this leads to loss of heterozygosity at the site of repair (*Hartlerode et al. 2009*; *Helleday et al. 2007*; *Sancar et al. 2004*).

The RAD50:MRE11:NBS1 (MRN) complex acts early on in the process of HR by recognising and binding to damaged DNA from DS breaks. MRN activates and increases the ataxia telangiectasia-mutated (ATM)'s affinity for its molecular targets by undergoing conformational changes and directly interacting with ATM kinase and Nbs1 (*Lee et al. 2004*). ATM kinase will then phosphorylate and activate a number of targets which include NBS1, H2AX, FANCD2 and BRCA1 which are involved in DNA repair (*Jacquemont et al. 2007*; *Savic et al. 2009*). BRCA1 binds and phosphorylates CtIP which aids in the processing of DS break ends and results in 3' overhangs of single-stranded DNA (ssDNA) (*Chen et al. 2008a*). RPA has high affinity for ssDNA and so is quick to coat it. BRCA2 is involved in displacing RPA and loading RAD51 into its place (*Jensen et al. 2010*). The RAD51 protein is important in strand invasion and recognising homologous sequences in the neighbouring chromosome. RAD51 actively searches for homologous sequences in DNA (*Bianco et al. 1998*). The invading 3' strand sets up a D-loop intermediate and initiates DNA synthesis using the homologous DNA strand as a template. If the D-loop is successful in capturing the second end of the broken DNA strand a Holiday Junction forms. RAD54 is a strong candidate for the promotion of branch migration, as it can bind many substrates which resemble one end of the D-Loop. This promotes branch migration in either a 3'-5' direction or a 5'-3' direction (*Bugreev et al. 2006*). The resolution of the Holiday Junction can be mediated by a number of different complexes. BLM, a protein translated from the Bloom's syndrome gene in complex with topoisomerase IIIa, is able to dissolve double Holiday Junctions and form non-crossover products (*Wu et al. 2003*). Also Holiday Junctions can be cleaved by the MUS81-EME1 complex resulting in crossovers with an exchange in flanking markers (*Constantinou et al. 2002*). Lastly, the resolvase GEN1

can mediate Holiday Junction resolution through symmetrical cleavage (*Ip et al. 2008*). Figure 1.7 illustrates the process of HR.

Proteins involved in HR may be useful as markers of resistance. For example, RAD51 has already proven to be a useful marker for platinum resistance in non-small cell lung cancer (NSCLC). It was found that the RAD51 protein, in combination with the ERCC1 protein, can be an effective marker of resistance from surgically excised tissue samples taken from 41 NSCLC patients (*Takenaka et al. 2007*). Further evidence for RAD51's role in platinum resistance comes from a pilot study examining RAD51 protein expression in head and neck cancers. It was concluded that high expression of the RAD51 protein lead to poor long term survival and could be used as a resistance marker (*Connell et al. 2006*). From a study on ovarian cancer cell lines, it was found that BRCA1 is required for the recruitment of RAD51 to DNA damage sites induced by platinum exposure. This process may be a contributing factor in platinum resistance in ovarian cancer (*Zhou et al. 2005*). Germline mutation of BRCA1 and BRCA2 of the HR machinery are one of the main risk factors associated with ovarian cancer (*Pal et al. 2005*; *Risch et al. 2001*; *Rubin et al. 1998*). A recent study has revealed that 18.3% of ovarian cancer patients will have germline BRCA1/2 mutations (*Hennessy et al. 2010*). 90% of inherited epithelial ovarian tumours have BRCA1/2 mutation and are linked to having better prognosis than cells with functional HR due to increased sensitivity to platinum compounds (*Ben David et al. 2002*; *Cass et al. 2003*; *Tan et al. 2008*). However, BRCA1/2 mutated patients also develop resistance. This is thought to be a result of secondary mutations in the intrinsic region of BRCA1/2 genes that re-align the open reading frame. This results in a functional protein that re-establishes HR function (*Edwards et al. 2008*; *Sakai et al. 2008*; *Sakai et al. 2009*; *Swisher et al. 2008*). However, this is not the case in all BRCA1/2 resistant cells. Further studies are required in this area. BRCA1/2 and resistance will be further discussed in section 1.7.3.

Other mechanisms of repairing DS breaks include non homologous end joining (NHEJ) and single strand annealing (SSA). NHEJ directly ligates broken ends of DNA strands causing deletions or mutations in DNA sequence, while SSA anneals both sides of the complementary DNA on broken strands causing loss of repeats and DNA sequences between repeats (*Hartlerode et al. 2009*; *Helleday et al. 2007*; *Sancar et al. 2004*).

1.4.5 Inhibition of apoptosis

Platinum resistance can be mediated via the inhibition of apoptotic signalling. There are two main signalling pathways for apoptosis; the intrinsic (mitochondrial) and extrinsic pathways (receptor mediated).

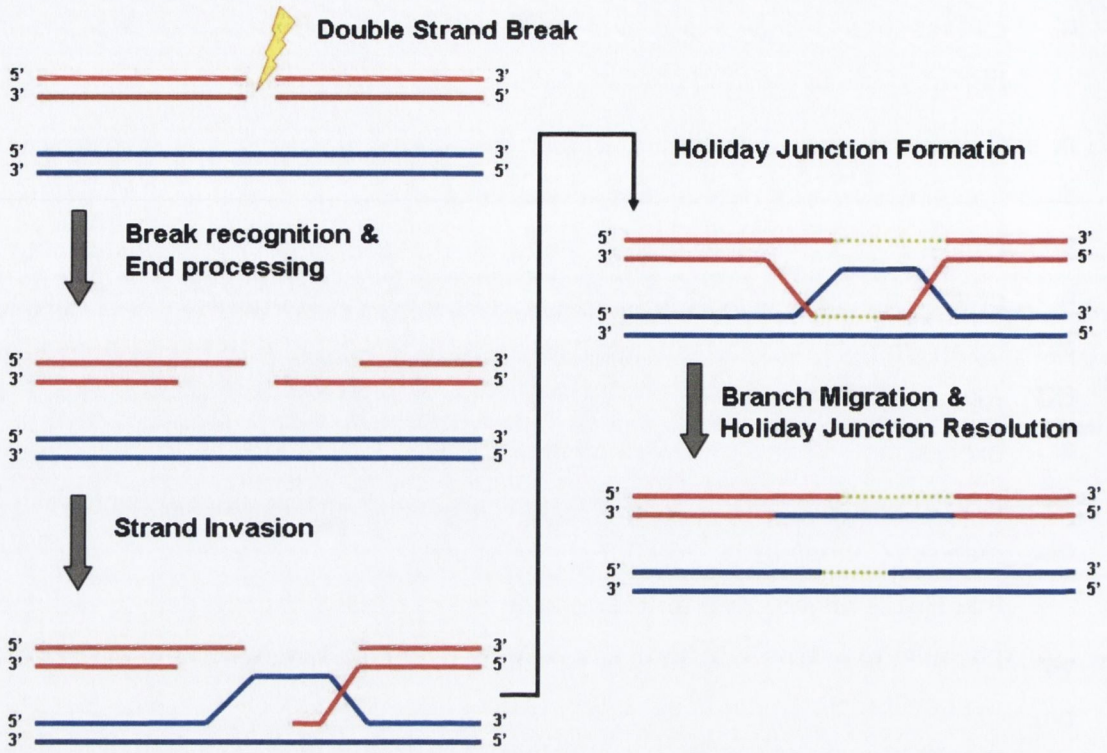

Figure 1.7 Overview of homologous recombination.

Adapted from (*Helleday et al. 2007*)

The intrinsic pathway can be induced by DNA damage caused by platinum therapy. Most chemotherapy drugs in clinical use target the intrinsic pathway of apoptosis (*Pennington et al. 2010*). We see in the intrinsic pathway, the mitochondria release of Cytochrome C in response to apoptotic stimuli. Cytochrome C will bind to Apaf-1 in the cytoplasm, which results in ologomerisation and further binding to procaspase-9. This complex, termed the apoptosome, gathers procaspase-9 molecules closely together and causes the activation of effector caspases-3, -6 and -7 via self activation recruitment of the enzymes. This process will eventually end in cell death (*Pennington et al. 2010*). See Figure 1.8.

The activation of the PI3k/Akt pathway can increase resistance in ovarian cancer. About 30% of ovarian cancers show activation of this pathway and it is believed to be one of the early events in cancer initiation and progression (*Landen et al. 2008*). The activation of the PI3k/Akt pathway results in the expression of NFkB, which inhibits Bcl-2 family member Bad, a pro-apoptotic factor that inhibits apoptosis. Cisplatin chemoresistance in ovarian cancer cell lines has been shown to be diminished when PI3k/Akt pathway is inhibited (*Yang et al. 2006*).

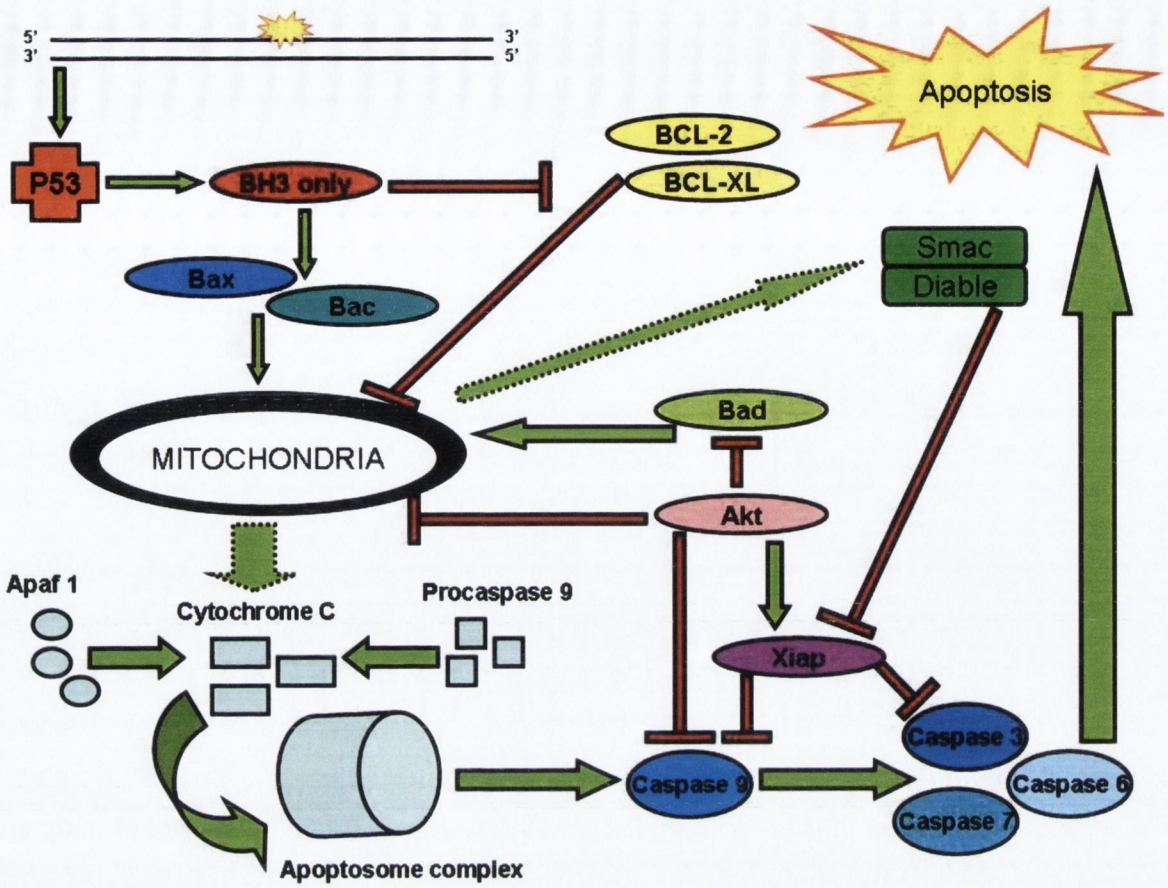

Figure 1.8 Intrinsic pathway of cell death.

DNA damage triggers the action of p53, which leads to BH3-only proteins activation. BH3-only proteins are able to activate pro-apoptotic proteins Bax or Bac or can sequester BCL-2 and BCL-XL, which are anti-apoptotic factors. Bax and Bad can act on the mitochondria causing increased permeability of its outer membrane, allowing for the release of cytochrome C and Smac/Diablo. Cytochrome C will form a complex with apaf-1 and procaspase-9 molecules to form the apoptosome complex. This complex will cause auto-activation of caspase-9 which activates downstream caspases-3, -6 and -7 which lead to cell death by apoptosis. This pathway is regulated by Xiap and Akt. Xiap inhibits the activation of caspases. Akt has a number of modulatory roles. Akt can inhibit caspase-9 and also cause the expression of Xiap to further inhibit caspase activity. It also reduces the mitochondrial release of cytochrome C and Smac/Diable and can block Bad activity, which causes increased permeability of the mitochondrial outer membrane. Smac/Diable can also regulate the system by binding to and inhibiting Xiap. Figure adapted from (*Pennington et al. 2010*)

Aberrant expression levels of Bcl-2 family members, which regulate cytochrome C release, have been shown to influence chemoresistance. Over expression of Bcl-2, Bcl-XL and Mcl-1, which are anti-apoptotic proteins in the Bcl-2 family, are associated with increased resistance to cisplatin chemotherapy. In particular, in ovarian cancer, amplified expression of Bcl-XL and Mcl-1 shows strong correlation to chemoresistance. Cisplatin chemotherapy is improved *in vitro* by inhibiting these two proteins (*Brotin et al. 2010*; *Villedieu et al. 2007*). Furthermore, down-regulation or mutations in certain Bcl-2 family members can confer resistance to chemotherapy. For example, down-regulated expression or mutated expression of the BAX gene shows poor response to chemotherapy and reduces survival in metastatic breast cancer patients (*Krajewski et al. 1995*).

It has been shown that differential function of apaf-1 can play a role in chemo resistance in ovarian cancer. It has been found from cystolic extracts of ovarian carcinoma cell lines and primary tumour samples that the ability to activate procaspase-9 in the presence of cytochrome C and dATP was deficient when compared to control extracts. In particular, SKOV3 which has reduced apoptosome activity was more resistant to chemotherapy-induced apoptosis when compared to cell lines with functional Apaf-1 activity. This shows that the ability to form a functioning apoptosome inhibits activation of caspase-9 which normally induces cell death and renders cells more chemoresistant (*Liu et al. 2002*). As well as the apoptosome influencing procaspase-9 activation, the Xiap protein can also block caspase-9's apoptotic ability. Xiap is a member of the Iap family of proteins, which are inhibitors of apoptosis through caspase interaction. Under expression of Xiap renders cells more chemo-sensitive and improves cisplatin treatment (*Cheng et al. 2002*). Xiap protein over expression has been linked to cisplatin mediated chemoresistance in ovarian cancer cell lines (*Li et al. 2001*).

The extrinsic apoptotic pathway is activated through specific ligands binding to specific receptors that initiate apoptotic signalling. The receptors in question belong to the tumour necrosis family or the nerve growth factor receptor superfamily. Members include tumour necrosis factor receptor 1 (TNF-R1), tumour necrosis factor receptor-related apoptosis mediating protein (TRAMP), tumour necrosis-related apoptosis-inducing ligand (TRAIL) and FAS. The main ligands associated with these receptors and activation of this pathway are FAS, TNF and TRAIL. Binding of these ligands causes the activation through trimerization of receptors. The cytoplasmic domain of the receptor, termed the death domain (DD), recruits adaptor proteins to the death-inducing signalling complex (DISC) to which they bind. This activated complex will

recruit pro-caspase-8 and pro-caspase-10 which, upon activation through autocatalysis, will ultimately activate effector caspases -3, -6 and -7. This will lead to apoptosis (*Pennington et al. 2010*). See Figure 1.9.

There are a number of ways that the extrinsic pathway could influence chemoresistance. One way is by over-expressing decoy receptors on the cellular surface. DcR3 has been found on the surface of a large amount of different cancer cell types. DcR1, DcR2 and DcR3 have no intracellular signalling domain and bind Apo2L/TRAIL ligands. Sequestration of ligands by decoy receptors and blocking the apoptotic signal is speculated to be one form of chemoresistance for cancer cells (*Ashkenazi 2002*).

The Fas-associated death domain (FADD) is one of the adaptor proteins that may be recruited to the DD in order to form the DISC. The anti-apoptotic FLICE inhibitory protein (FLIP) can block apoptotic signalling by competing with pro-caspase-8 and pro-caspase-10 by binding to FADD. It can also inhibit pro-caspase-8 by associating with it and inhibiting its binding to FADD (*Krueger et al. 2001*). It has been found that cisplatin chemotherapy in ovarian cancer cell lines causes the ubiquitination and subsequent degradation of FLIP, thus rendering it unable to inhibit apoptosis. However, Akt can block cisplatin ubiquitination of FLIP in a p53-dependent manner promoting chemoresistance (*Abedini et al. 2008*).

1.4.6 Mutations in p53

A mutation causing inactivation of gene product in the TP53 tumour suppressor gene occurs in 50-70% of ovarian cancer patients (*Ferreira et al. 1999*). p53 the protein product of this gene acts as a transcription factor. The main functions of p53 are to block cell cycle progression and initiate DNA repair, and initiate apoptosis in response to cellular stresses such as DNA damage that can be inflicted by platinating agents (*Hanahan et al. 2000*). In this way, p53 acts to maintain genetic stability. Therefore, when a cell is exposed to DNA damaging agents, there are two possible scenarios depending on the response by p53. In one scenario, p53 can mediate chemosensitivity by inducing apoptosis, while in the second scenario chemoresistance can be the result of cell cycle arrest and initiation of DNA repair (*Ferreira et al. 1999*). Loss of function mutation in p53 can therefore cause chemoresistance through loss of p53-mediated apoptosis or halting the progression of damaged cells through the cell cycle. It has been shown that mutation in p53 is associated with a lack of response to high-dose cisplatin chemotherapy in advanced ovarian carcinoma (*Righetti et al. 1996*). However, it must be noted that cellular p53 function is not straightforward and it is

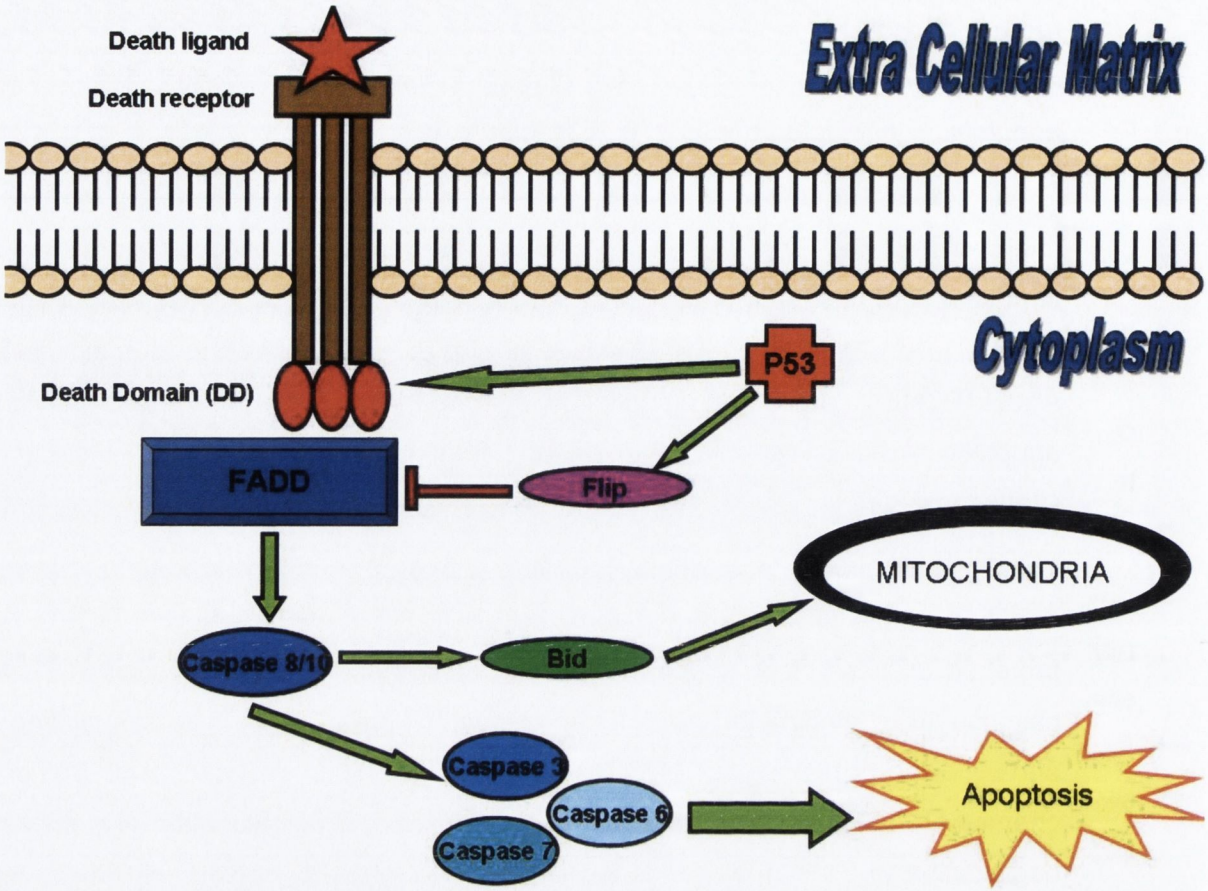

Figure 1.9 Extrinsic pathway of cell death.

Binding of ligand to receptor causes trimerization of the receptor and recruitment of adapter molecule FADD. Active FADD will bind procaspase-8 or -10 which will become auto activated and consequently activate downstream effector caspases-3, -6 and -7. Caspase-8 can also cause the cleavage of Bid a member of the Bcl-2 family to its active form. Bid allows for crosstalk between the extrinsic and intrinsic pathway. FLIP can regulate the extrinsic pathway by competitively binding FADD and blocking the binding and activation of pro-caspase-8. Figure adapted from (*Pennington et al. 2010*).

involved in many different cellular pathways. Therefore, its response to chemotherapeutics is not always the same, depending on the cell's state or preferential mechanism of p53 activity. In some models, *In vitro* studies have revealed that inactivation of p53 leads to cellular resistance (*Fan et al. 1994*), while in other models loss of p53 function can incur chemosensitivity to DNA damaging agents (*Fan et al. 1995*).

1.5 Taxane chemotherapy

1.5.1 Taxol and docetaxel

The first taxane agent to be found to have activity in human carcinomas was paclitaxel (Taxol), which was first isolated and characterized in 1971. It was originally extracted from the bark of the rare Pacific yew tree, *T. Brevifolia,* in the late 1960's as part of the National Cancer Institute (NCI) screening program to identify anticancer agents from thousands of plant species. Its chemical formula is $C_{47}H_{51}O_{14}$ and it has a molecular weight of 853.9. Taxol has a complex structure in the form of a ring system that is linked to a four-member oxetan ring at positions C_4 and C_5 and to an ester side chain at C_{13}. Its structure ensures that it is lipophilic, is insoluble in water and melts at 217°C. In 1979 it was found that cell division was prevented in cancer cells exposed to the agent by the promotion of microtubule assembly (*Sciff et al. 1979*).

Initially taxol's potential as an anticancer agent was not recognised as it did not seem to be more effective than other agents that were in use at the time. Also, the procurement of this scarce natural product was deemed to be too cost and labour intensive. It was not until the 1980's that its true potential was recognised, as it had great activity in nude mice with human tumour xenographs. It was then entered into phase I clinical trials by the NCI (*Oberlies et al. 2004*). Due to the scarcity of this agent, taxol has since been generated in a semi-synthetic process, which involves a precursor 10-deacetylbaccatin taken from the needles of other yew species including the readily available European yew *T. baccata* (*Rowinsky 1997*).

After the success of deriving taxol in the above semi-synthetic route, further research began to derive taxoid analogues that might be more efficient and less toxic than taxol. The most notable analogue to have been developed to date is docetaxel (Taxotere). Docetaxel was developed in a semi-synthetic manner in a similar way to taxol. It also involves the 10-deacetyl baccatin III precursor extracted from the needles of the European yew *T. baccata*. The main structural differences between docetaxel and taxol are that docetaxel show two modifications. A hydroxyl group replaces an acetyl group in the 10 position of the baccatin III and a OC(CH3)3 moiety replaces a benzamide phenyl group at the 3' position on the C13 side chain (*Bissery et al. 1995*).

The main mechanism of action utilised by taxanes is the binding of the agent to β-tubulin subunit of microtubules within the cell. Structurally, microtubules are hollow tubes of about 25nm diameter that extend from the microtubule-organizing centre of the centrosome in the cytoplasm of cells in interphase (*Nogales 2001*). Microtubules

are made up of a backbone of tubulin dimers and microtubule associated proteins (MAPs) (*Kirschner 1978*). Alpha- and beta-tubulin peptides form tubulin dimers, stiochiometrically switching between growing and shrinking phases. There are a number of different alpha- and beta-tubulin isoforms (six for each in total), which have slightly different amino-acid sequences with functional specificity. Microtubules have many important functions within the cell. They play a role in cell division, intracellular transport, axonemal motility, morphogenesis and migration. The dynamic behaviour of microtubules in these functions is hugely important. They are able to assemble and disassemble in a matter of seconds to a number of hours. These dynamics are due to the biochemical properties of the αβ-heterodimer which comprises the basic elements of microtubules. The dynamics of the microtubule assembly and disassembly is controlled by an array of biochemical entities and MAPs which can be modified by different reagents and drugs (*Nogales 2001*). Ordinarily, after assembly of the αβ-heterodimer GTP bound to β-tubulin can hydrolyze to GDP allowing disassembly of the microtubule structure. The binding of taxol and other taxanes to the N-terminal 31 amino acid of β-tubulin subunit results in an unusually stable and rigid structure that resists depolymerisation. This can occur even when GTP and microtubule-associated proteins are not present, which are normally needed for the process of tubule polymerization (*Manfredi et al. 1984*; *Rao et al. 1995*). Lag time in microtubule assembly is reduced in the presence of taxanes promoting the assembly of microtubules with a rigid structure. Thus the highly dynamic behaviour of microtubules is disrupted, which can result in abnormal mitosis, ultimately leading to initiation of cell death signals (*Xiao et al. 2006*). Docetaxel has been found to have a 1.9 fold higher affinity for binding to β-tubulin than taxol and causes tubulin polymerization at a 2.1 fold lower critical tubulin concentration. The initial rate at which polymerization occurs and the amount of polymer formed is greater for docetaxel. It does, however, bring greater toxicity due to its greater potency (*Diaz et al. 1993*).

Disruption of mitosis is the main cause of cytotoxicity after exposure to taxanes. Spindle formation, chromosome segregation or completion of mitosis can all be affected which can cause the activation of mitotic or DNA-damage checkpoints blocking cell cycle progression and activating specific apoptotic pathways. A number of different microtubule processes can be affected by taxane's method of action, depending on the cell cycle stage. Its main mechanism of action is disorganisation of microtubules, which causes cellular arrest at the G2/M phase of the cell cycle. This results in apoptotic signalling (*Downing 2000*; *Jordan et al. 1998*). Casase-3 and -8, hyperphosphorylation of Bcl-2 and in increase in Bax expression are linked to taxol

cytotoxicity. These are all proteins of the apoptotic pathway (*Ganansia-Leymarie et al. 2003*; *Wang et al. 1999*). Disruption of cell growth and metabolism by taxanes can also result in cell death signalling. It has been suggested that taxanes could cause impairment of centrosome function, leading to abnormal monopolar and multipolar spindles. This causes abnormal mitosis and cell death through apoptosis (*Abal et al. 2003*).

1.6 Mechanisms of taxane resistance

Taxane-containing regimens in ovarian cancer chemotherapy can cause relapse with taxane-resistant disease. Some of the most extensively reported on mechanisms of taxane resistance are the expression of different isotypes of the β-tubulin subunit (*Kavallaris 2010*), the over-expression of the MDR1 gene (*Gottesman et al. 2002*; *O'Connor 2007*), and the mutation in the gene that codes for β-tubulin. Further to this, transcriptomic changes in the transcriptome may also play a role in taxane resistance.

1.6.1 MDR1/P-glycoprotein (P-gp, p170) over-expression

The over-expression of P-gp is one of the main documented methods of taxane resistance. P-gp is a product of the MDR-1 gene. This gene is a part of a family of genes known as the adenosine triphosphate binding cassette genes, which can be found on chromosome 7. P-gp is a transmembrane ATP-dependant efflux pump. It has been shown to confer resistance to a wide variety of drugs including vinca alkaloids, anthracyclines, epipodophyllotoxins and taxanes by efficiently removing them from the cell (*Juliano et al. 1976*; *Ueda et al. 1987*).

The pump functions by the activation of ATPase activity by the substrate binding to the transmembrane region of the pump. This causes a conformational change that transports the substrate to the outer layer of the cell membrane and allows it to diffuse into the extracellular matrix. (*Ramachandra et al. 1998*) In order for the pump to be reset so that it can bind more substrate, hydrolysis at the second ATP site must occur. This completes one catalytic cycle for the transporter (*Sauna et al. 2000*).

There is significant evidence that points towards taxol being a substrate of P-gp and also that P-gp over-expression plays a role in taxol resistance. For example, it has been shown that taxol accumulates in the brain and gut of P-gp-deficient mice where P-gp expression had been knocked out. This shows how P-gp is responsible for preventing taxol from entering the brain through the blood brain barrier and for the biliary elimination of taxol from the gut (*Schinkel et al. 1997*). P-gp inhibitors, such as verapamil and elacridar, can sensitise cancer cell lines to taxol treatment (*Hyafil et al.*

1993; *Reinecke et al. 2000*). Futhermore, elevated levels of MDR1 mRNA and P-gp itself have been documented in a wide variety of taxol resistant cancer cell lines, implicating its role in taxane resistance profiles. The national cancer institute carried out a study using 60 cancer cell lines (NCI-60 panel) to correlate MDR1 expression with drug sensitivity profiles. It found that taxol sensitivity had a high negative correlation (-0.896) with MDR1 expression (*Alvarez et al. 1995*). Increasing levels of either MDR1 mRNA or P-gp has been shown to confer resistance to taxol in a number of cancer cell lines (*Bhalla et al. 1994*; *Duan et al. 1999c*; *Parekh et al. 1997a*; *Schondorf et al. 2002*). P-gp itself has also been put forward as being a useful indicator for taxol-based resistance in ovarian cancer (*Duan et al. 1999c*; *Kamazawa et al. 2002*; *Parekh et al. 1997a*; *Schondorf et al. 2002*). Over-expression of this protein is heavily linked with bad prognosis for patients with ovarian and breast cancers, sarcomas and other malignant disease (*Hoffmann et al. 2010*; *Nakayama et al. 2002*; *Rodrigues et al. 2008*).

Resistance to taxanes can also be mediated by other transporters that can be involved in changing the intracellular concentration of the drug by increasing drug efflux or reducing drug uptake. MRP1, BCRP, LRP have been linked to taxane resistance as efflux pumps of taxane molecules in a number of cancer cells, including ovarian cancer (*Borst et al. 2000*; *Cole et al. 1994*; *Duan et al. 1999c*; *Lee et al. 2000*; *Litman et al. 2000*; *O' Driscoll et al. 2007*; *Roy et al. 2007*). OATP1B1 and OATP1B3 have affinity for taxol and are expressed in ovarian cancer patient tissues and cell lines. Reduced uptake of taxol by OATP1B1 and OATP1B3 could be a mechanism of taxol resistance in ovarian cancer by reducing intracellular concentrations (*Svoboda et al. 2011*).

1.6.2 β-tubulin protein isotypes

There is a wide variety of different β-tubulin protein isotypes that have been documented to date. These isotypes include βI, βII, βIII, βIVa, βIVb, βV, βVI. They are all expressed by different genes and found on different chromosomes throughout the genome. Some of these have tissue or cellular specific expression. They can also be acted on by post-translational modifications, which will change the way that MAPS interact with them, thus changing microtubule function. These changes are conserved in evolution and help the microtubule carry out specific microtubule based functions and also play a role in regulating microtubules specific properties, including stability and structure (*Hammond et al. 2008*). Because of the wide array of different isotypes, with varying functions available to the cell, it is not difficult to see how differential expression of β-tubulin isotypes could have a role to play in cancerous phenotypes. In

fact, aberrant expression of β-tubulin isotypes have been shown to play a role in a number of different cancers resistant to taxanes, including ovarian, breast, non-small-cell-lung cancer, head and neck, pancreatic, gastric and pancreatic cancers.

In ovarian cancer tumours, increased expression in βIII tubulin protein has been observed in taxol resistance and has been shown to be associated with poor overall survival. Elevated levels of βIII tubulin protein in taxol resistant epithelial ovarian cancer were first documented in work carried out by *Kavallaris et al. (1997).* When compared to untreated primary ovarian tumours, it was found that tumours displaying taxol resistance had elevated levels in βI, βIII and βIVa tubulin protein isotypes. This was proposed to play a role in conferring resistance to taxol (*Kavallaris et al. 1997*).

A study by *Panday et al. (1999)* set out to find the main mechanisms involved in patients with taxol resistance by investigating three of the main mechanisms found in taxol resistance. They investigated over-expression of MDR1, mutations in α and β tubulin genes and over-expression of β-tubulin isotypes. They found that over-expression of β-tubulin isotype βIII in ovarian tumour tissue was the main mechanism involved in taxol resistance for ovarian cancer patients (*Panday et al. 1999*). Backing up this work, poor overall survival in ovarian cancer has been linked with βIII tubulin isotype protein over-expression. *Ferrandina et al. (2006)* found that the βIII tubulin protein was expressed in 82.2% of assessed patients with advanced ovarian cancer in their study after surgical debulking and prior to chemotherapy. After chemotherapy those expressing a higher amount of βIII were found to have poor outcomes. It is suggested that evaluation of βIII could be used as a marker to identify poor prognosis patients to be able to prescribe more aggressive and/or more targeted therapies (*Ferrandina et al. 2006*). Originally, it was believed that the βIII tubulin isotype de-stabilised the dynamics of microtubules, thus counteracting taxane's main mechanism of action (microtubule stabilisation) and conferring resistance (*Derry et al. 1997*). More recently, it has been put forward that the expression of this isotype may be an adaptive mechanism of survival for the cell when in unfavourable environments, particularly in oxygen-poor conditions and low nutrient environments. The protein isotype confers resistance by giving pro-survival signalling by being involved in a signalling cascade with other molecules (*De Donato et al. 2012*).

As well as βIII tubulin over-expression, loss of βII tubulin expression has been linked to shorter progression-free survival in ovarian cancer. A study carried out by *Ohishi et al. (2007)* shows that elevated levels of βIII tubulin protein and loss of βII tubulin protein correlate with earlier recurrence of resistant tumours after taxane treatment (*Ohishi et al. 2007*).

1.6.3 β-tubulin mutations

There is noteworthy *in vitro* evidence to demonstrate that mutations in β-tubulin can be a mechanism of taxane resistance. Work carried out on taxol-requiring mutants of the Chinese hamster ovary (CHO) was among the first pieces of work indicating that mutation in β-tubulin can affect functionality of microtubules when subjected to taxol. These cell lines assemble low amounts of microtubule polymers and need taxol in order to carry out cell division. Due to mutations at amino acids 250-300 in Tax-18 a taxol-requiring mutant CHO cell line, cells were unable to form a full spindle apparatus in the absence of taxol. Normal spindles and mid bodies were able to be produced in the presence of taxol (*Cabral et al. 1983*).

In subsequent years *Giannakakou et al. (1997)* developed two taxol-resistant human ovarian cancer sublines from the 1A9 cell line that showed impaired taxol-driven polymerisation. It was found that point mutations had occurred in the HM40 isotype of β-tubulin in the two sublines. One had a mutation at nucleotide position 810 and the other at position 1092. All cells lines were able to retain taxol as normal and no MDR-1 mRNA was detected. Exposure to taxol in parental cell lines caused increased polymerisation, while this was not the case in the resistant sublines. The reason for the resistance phenotype was hypothesised to be due to weakened interactions between β-tubulin and taxol caused by the mutations in β-tubulin (*Giannakakou et al. 1997*).

More recently, studies have produced increasing evidence supporting the link of mutations in β-tubulin and taxane resistance. In a study carried out by *Yin et al. (2010),* mutations of β-tubulin found in ovarian cancer patients were studied for their ability to induce resistance to chemotherapy drugs. It was found that three out of the four mutations were able to confer taxol resistance. These mutations were shown to counteract the effects of taxol on microtubule stability (*Yin et al. 2010*).

Taxol resistant CHO cell lines show a high frequency of mutations in β-tubulin. These mutations have been shown to confer taxol resistance in a number of cases (*Yin et al. 2007*). However, one recent study has revealed that mutation in β-tubulin can also cause sensitivity to taxol. An amino acid mutation at L215 in β-tubulin was found to enhance taxol sensitivity in CHO cells. It is hypothesised that L215I substitution enhances the effectiveness of taxol binding to β-tubulin (*Wang et al. 2005*).

1.6.4 Genetic changes

Genetic instability caused by the cancerous phenotype can result in mutations that can cause both sensitivity and resistance to chemotherapeutics. Work on p53 status in

taxol-resistant cell lines has revealed that loss of functional p53 may increase sensitivity to taxane therapy. Work carried out by *Vasey at al. (1996)* revealed that after transfecting a dominant p53-negative mutant into the A2780 ovarian cancer cell line with wild type p53, the cell line remained sensitive to taxol chemotherapy. Also, in this study, immature thymocytes taken from mice with non-functional p53 were demonstrated to be taxol sensitive (*Vasey et al. 1996*). This data suggests that screening for loss of p53 function could be a marker for taxol activity in otherwise resistant patients. Other studies have also shown that aberrant p53 function could confer increased taxol sensitivity. Using parental human colorectal cancer cell lines with wild type p53 and two transfected colorectal cancer cell lines with inactive p53, it was demonstrated that the cell lines with knocked out p53 function had significantly increased sensitivity to taxol (*Rakovitch et al. 1999*). The author suggested that this was not correlated with an increase in taxol-mediated mitotic arrest as in other studies but linked the method of cell killing to be via cytotoxicity in a p53 independent manner. Another study, using the IGROV-1 ovarian cancer cell line, developed a cisplatin resistant subline (IGROV-1/Pt1) with mutant p53. This also showed increased sensitivity to taxol. In this case it was concluded that the mechanism of cell death imposed on the cells was due to loss in p53 dependant post mitotic spindle checkpoint resulting in delayed apoptosis (*Cassinelli et al. 2001*).

The methods by which cells lacking p53 function confer sensitivity to taxol are suggested to be many. It is thought that lack of p53 can increase the expression of microtubule associated protein 4. This results in increased microtubule polymerisation and increased taxol-associated binding to β-tubulin (*Zhang et al. 1999*). It has been elucidated that taxol can initiate apoptosis through the checkpoint of mitotic spindle assembly, changes in cyclin dependent kinase activation, and the c-Jun N-terminal kinase/stress-activated protein kinase. One of the main methods of taxol sensitivity, related to the loss of p53 function, may be that loss of p53 mediated G1 arrest could stimulate cells in reaching the G2/M phase of the cell cycle, causing cells to then enter mitotic arrest. Further to this, p21 cannot be expressed when p53 is not present to act as a transcription factor. This means that cells cannot be teased out of mitotic arrest in a p21 mediated fashion (*Wang et al. 2000*). It has also been suggested that cytotoxicity could be imposed by loss in p53-dependant post mitotic spindle checkpoint resulting in delayed apoptosis (*Cassinelli et al. 2001*).

The effects of aberrant expression of both Bcl-2 and Bcl-XL, two anti-apoptotic proteins, and Bax and Bad, two pro-apoptotic proteins, all of the Bcl family of proteins, have been shown to play a role in taxol resistance and sensitivity. The over-expression

of Bcl-2 and Bcl-XL of the intrinsic pathway of apoptosis can be shown to mediate taxol resistance. For example, *Sharma et al. (2000)* carried out a study to investigate what factors are involved in taxol sensitivity in colon cancer. They found resistance to taxol to be multi-factorial. They showed that an increase in Bcl-2 expression was one of the causes for taxol resistance (*Sharma et al. 2000*). In another study, significant increases in Bcl-2 and Bcl-XL were found in taxol resistant leukaemia cell lines. In Bcl-2 and Bcl-XL transfectants of the ALM HL-60 cell line, a very high expression of the two proteins (5-fold for Bcl-2 and 10-fold for Bcl-XL) was needed to confer taxol resistance. This could mean that resistance mediated by these proteins only occurs after a certain threshold (*Huang et al. 1997*). Also, Bcl-2 has been shown to play a role in taxol resistance in breast cancer mediated by the Estrogen Receptor (ER) pathway. A study carried out by (*Tabuchi et al. 2009*) extensively shows that ER negative cells were sensitive to taxol and ER positive cells are resistant to taxol. It was shown that this resistance was coupled with an over-expression of Bcl-2, while ER negative cells sensitive to taxol showed no expression of Bcl-2. Expression of pro-apoptotic protein Bax was also examined in the ER positive and negative cells, but showed no significant differences in expression.

The combined over-expression of Bcl-2 and MDR1 has been shown to be a possible marker for predicting inefficiency in taxol chemoradiotherapy in NSCLC patients. Over-expression of both markers correlated to poor response and reduced progression free survival when treated with chemotherapy regimens, which include taxol (*Maraz et al. 2011*).

Many studies have demonstrated how over-expression of Bax and Bad is correlated to taxol sensitivity. It is of particular interest that Bax has been shown to reduce resistance in ovarian cancer in cells resistant to taxol. The authors speculate that the development of analogues to Bax could be used in order to target cells which are resistant to taxol (*Strobel et al. 1998*). Further evidence for Bad can be shown in a study investigating the effects of certain protein levels on cisplatin and taxol sensitivity in human head and neck squamous cell carcinoma. It was found that strong expression levels of Bax correlated with significantly higher sensitivity of cells to taxol (*Taguchi et al. 2004*). Recent studies by *Craik et al. (2010)* have re-enforced the evidence that Bad over-expression is linked to taxane sensitivity *in vitro* and can act as a prognostic indicator for survival in breast cancer patients. The study has also found that the mechanism by which Bad infers taxane sensitivity is not linked to mitochondrial apoptotic signalling in breast cancer. Instead, it is indirectly involved by stimulating cell

proliferation (*Craik et al. 2010*). This helps the mechanisms of taxane cytotoxicity, as taxanes target actively proliferating cells.

It has been shown that changes in spindle assembly checkpoint (SAC) protein Mad2 effects sensitivity to taxol. Research has been conducted on ovarian cancer cell lines A2780 (taxol sensitive) and SCOV3 (taxol resistant) where Mad2 was knocked out. The contrast in taxol sensitivity was measured by MTT assays and was found to be significantly different. It was shown that reduced Mad2 expression resulted in a weakened spindle check point and caused aberrant expression in Bcl-2 proteins and conferred taxol resistance in the ovarian cancer cells. The involvement of Bcl-2 proteins is believed to play a major part in this process of resistance (*Hao et al. 2010*). A subsequent study has shown that low expression of Mad2 is associated with poor progression free survival in ovarian cancer patients and may be a good marker for taxol resistant ovarian cancer (*Furlong et al. 2012*).

A number of studies have shown that MyD88 is an important prognostic factor for taxane resistance in ovarian cancer. This protein is an adaptor protein for TLR-4 signalling, which is known to be involved in taxol resistance. High MyD88 expression predicts poor response to taxol chemotherapy and results in shorter disease free and overall survival and has been significantly correlated to tumour metastasis in ovarian cancer patients (*Kim et al. 2012a*; *Silasi et al. 2006*; *Zhu et al. 2012*).

The above studies and evidence all show how genetic changes in an unstable genome have the potential to affect taxane therapy by causing changes that affect sensitivity to taxane drugs.

1.7 BRCA1

BRCA1 is a tumour suppressor gene that is located on chromosome 17q21 and encodes a nuclear protein of 220kDa in weight and 1863 amino acids long. It contains an amino terminal RING finger domain which is highly conserved and involved in DNA binding and an acidic carboxyl terminal domain which is seen in many transcription factors (*Monteiro et al. 1996*).

BRCA1 was the first gene to be identified in breast cancer to be linked to susceptibility to the disease (*Hall et al. 1990*). By the age of 70, a BRCA1 mutation carrier has a risk of 50-70% of developing breast cancer (*King et al. 2003*). Furthermore, patients with BRCA1 mutations are at higher risk of developing ovarian cancer. Patients can have hereditary germline mutations or can develop spontaneous somatic mutations. The chances of having a hereditary mutation vary between different populations. Individuals

with BRCA1 mutations have a lifetime risk of approximately 39-46% for developing ovarian cancer. It has been reported that about 10-15% of ovarian cancer patients will have BRCA1/2 mutations (*Hennessy et al. 2009*). A more recent study carried out by *Hennessy et al. 2010* revealed that the incidence of BRCA1/2 mutations might be even higher in ovarian cancer patients. 235 samples from ovarian cancer patients were examined and it was found that 18.3% of these had BRCA1/2 mutations. Germline DNA was available for 28 of these patients and it was found that 39% of these did not have a BRCA1/2 mutation. Therefore, these patients developed somatic BRCA1/2 mutations (*Hennessy et al. 2010*).

BRCA1 function has not been fully elucidated but it has been shown to have roles in a number of cellular functions including DNA damage repair (homologous recombination (HR) and mismatch repair (MMR)), initiation of apoptosis (if cell has too much damaged DNA), cell cycle regulation (including checkpoint function and chromatin remodelling), transcriptional control and ubiquitination (*Kennedy et al. 2002*; *Murphy et al. 2010*). The role of BRCA1/2 in HR and MMR function is described in sections 1.4.3 and 1.4.4 respectively. Its involvement in key DNA repair pathways renders cells with BRCA1 mutation more sensitive to DNA damaging agents, such as platinums used in ovarian cancer treatment. Functional BRCA1 has recently been shown to play a role in the removal of bulky adducts from stalled replication forks inflicted by UV damage (*Pathania et al. 2011*). It plays a crucial role in enabling damage excision, damage repair, suppression of translational synthesis and correct progression past the G2/M checkpoint after UV damage.

Poly ADP ribose polymerase (PARP) inhibitors are a novel class of drug that are currently being trialled in BRCA1/2 deficient cancer cells. PARP1 is involved in the repair of single strand nicks in DNA. Failure to repair these nicks before replication will result in the replication process itself causing double stand breaks when these single strand breaks are reached (*McGlynn et al. 2002*). Cells which are BRCA1/2 deficient will be less capable of repairing double strand breaks due to the loss of BRCA1 mediated HR. Thus, by inhibiting PARP1 from repairing single stand nicks, an accumulation of double strand breaks will occur, which will result in cell death signalling. This mechanism of action is known as 'synthetic lethality', as two separate repair pathways are inactivated resulting in cell death (*Yap et al. 2011*). The results of proof of concept clinical trials of the PARP inhibitor olaparib in breast and ovarian cancer patients with germline BRCA1/2 mutations have been encouraging as a chemotherapy intervention (*Audeh et al. 2010*; *Tutt et al. 2010*).

It is the loss of genomic integrity that is thought to be the main cause of tumourigenesis in BRCA1/2 deficient cells (*Silver et al. 2012*). Loss of HR may result in cells that rely on the more error prone mechanisms of DNA repair such as non-homologous end joining (NHEJ). This will result in many genomic wide mutations and instability. It has been shown that loss of BRCA1 leads to the production of telomeric chromosomal fragments that are no longer connected to centromeres, giving high levels of allelic imbalance extending from telomeric regions. This has been observed in both sporadic triple negative breast cancer and ovarian cancer and is thought to be an important event in the development of these tumours (*Birkbak et al. 2012*).

1.7.1 BRCA1 mutation

Familial BRCA1 mutations are most often minor changes. These mutations can occur along the full length of the gene. Most commonly, mutation results in a truncated protein that is the result of the mutation causing a premature stop codon. Also mRNA transcribed from a mutated BRCA1 gene could be degraded by nonsense-mediated mRNA decay (NMD) or be subject to exon skipping. This would mean the loss of gene product as result of missense or nonsense mutation (*Liu et al. 2001*). Mutations can also affect domains that are known to interact with other proteins such as BARD1, BRIPI and PALB2, which are also predictors of breast and ovarian cancer susceptibility. BRCA1 forms complexes with a number of proteins by which it carries out many of its functions.

The reversion of this mutation to wild type may be a mechanism for chemotherapeutic resistance in ovarian cancer patients that have presented with a mutated non-functional BRCA1 gene. This mechanism has been reported in platinum-resistant ovarian carcinomas. Initially, patients will be more sensitive to DNA damaging agents as they have defective DNA repair machinery due to non-functional BRCA1. Excessive DNA damage with the inability to repair it will result in apoptotic signalling and cell death. However, this susceptibility to DNA damage makes it possible to gain a second mutation in the BRCA1 gene, which could restore the open reading frame. This results in a functional BRCA1 protein after treatment with a DNA damaging agent. This would give these cells a selective advantage over cells without functioning BRCA1 as they would be able to repair damaged DNA more easily and survive. In theory, this would mean that these cells could outcompete other tumour cells with dysfunctional BRCA1, resulting in an overall tumour mass resistant to DNA damage associated agents, such as platinums and PARP inhibitors.

Another theory suggests that BRCA1/2 resistance may arise in BRCA1/2 deficient tumours from a small subpopulation of cells in a tumour mass that have functional BRCA1/2. Drug treatment of the tumour selects for the resistant cells and kills off those deficient in DNA repair, leaving an overall tumour mass with functional BRCA1, which is resistant to chemotherapy. This theory stems from evidence obtained in the treatment of lung cancer and chronic myelogenous leukaemia (*Dhillon et al. 2011*; *Ikeda et al. 2003*). These cancers have been seen to have subpopulations of cells harbouring resistant mutations to their respective chemotherapy drugs, which become the main bulk of the tumour after selection by drug exposure, thus conferring resistance.

Evidence for acquired resistance from secondary reversion mutations in ovarian cancer has been shown in a study carried out by *Swisher et al. (2008)* who observed this phenomenon in a laboratory setting using clinical samples. The team analysed nine samples of recurrent BRCA1-mutated ovarian cancer patients that had been previously treated with platinum. Five cases were initially platinum sensitive but became resistant and one case was initially resistant to platinum chemotherapy. Three out of the five tumours with acquired resistance and the initially resistant tumour, had a secondary mutation in the BRCA1 gene. Conversely, none of the remaining three sensitive samples had secondary changes in the BRCA1 gene. This study shows that secondary BRCA1 mutations occur frequently in platinum-resistant patient samples suggesting the above theories are plausible mechanisms of resistance.

Reversion mutations for BRCA2 conferring resistance have often been observed. BRCA2 is also largely important in DNA repair and is critical for HR like BRCA1. For example, deletions in the BRCA2 gene were shown to re-align the open reading frame in PARP-inhibitor and carboplatin acquired resistance (*Edwards et al. 2008*). Another study also published in Nature in the same year confirmed that secondary mutation in BRCA2 is a mechanism for acquired resistance to cisplatin (*Sakai et al. 2008*). The team's evidence for this mechanism includes a secondary change in the BRCA2-mutated breast cancer cell line HCC1428, which re-established BRCA2 function. Cisplatin resistance in BRCA2 mutated Capan-1 cells was shown to be a result of five possible mutations in BRCA2 that restored the open reading frame. Another piece of evidence highlighted that all clones of cells with secondary BRCA2 mutations were resistant to both cisplatin and the PARP inhibitor AG14361. Lastly, recurrent ovarian cancer patients with primary BRCA2 mutation which had acquired cisplatin resistance were shown to have reversion of BRCA2 to wild-type due to secondary mutation (*Sakai et al. 2008*). A follow up study by the same group also showed reversion mutations in

ovarian cancer patients with acquired resistance. *Saki et al. (2009)* used three ovarian cancer cell lines (PEO1. PEO4 and PEO6), which were serially derived from a BRCA2 mutated ovarian cancer patient with acquired resistance to cisplatin. PEO1 was BRCA2 deficient and sensitive to cisplatin. However, PEO4 and PEO6 were BRCA2 proficient due to a secondary mutation which re-established the BRCA2 open reading frame. It was of great interest that the development of drug resistance to cisplatin and AG14361 in PEO1 resulted in cells that were BRCA2 wild-type due to another mutation in BRCA2 and were also cross resistant to both chemotherapeutic agents (*Sakai et al. 2009*).

The frequency of BRCA1/2 reversion mutations conferring platinum resistance in BRCA1/2 mutation carriers with ovarian cancer was investigated by *Norquist et al. (2011).* They found that 12 out of 26 platinum-resistant recurrent ovarian cancer patients had secondary mutations restoring the BRCA1/2 reading frame. This accounted for the patients that were platinum resistant in the presence of a reversion to wild-type mutation (approximately 46%). Only one in 19 platinum-sensitive patients had a reversion mutation (approximately 5%). This suggests that this may be a frequent event in BRCA1/2 mutation carriers who develop platinum resistance and it could be a predictor of platinum resistance. The authors also speculated that this may also be the case with resistance to PARP inhibitors but this was only investigated in six platinum-resistant ovarian cancer patients that were treated with PARP inhibitors (*Norquist et al. 2011*). The three patients with a BRCA1/2 reversion had non/partial responses to PARP treatment, while the other three patients with no reversion had complete and partial responses.

1.7.2 Methylation of BRCA1

In ovarian cancer, it has been shown that the loss of BRCA1 gene product may be due to hyper-methylation of the promoter region of the gene and could be a component in cancer initiation or cancer progression. The first case in which hyper-methylation of a tumour suppressor gene was linked to carcinoma initiation was the methylation of the RB gene in sporadic retinoblastoma (*Sakai et al. 1991*). This phenomenon has since been seen in a number of different diseases. Recent examples include the tumour suppressor gene BLU, which is down-regulated by promoter hyper-methylation in myelodysplastic syndrome. Hyper methylation is thought to contribute highly to the development and etiology of the disease (*Yang et al. 2012*). The tumour suppressor gene PTX3 has shown similar evidence of down-regulation by hypermethylation in human oesophageal squamous cell carcinoma (*Wang et al. 2011*). For BRCA1 *Rice et al (2000)* has correlated reduced levels of BRCA1 mRNA with methylation of the

promoter region in clinical human breast cancer cells. The hyper-methylation of BRCA1 seems to be tumour specific and has been solely detected in sporadic ovarian and breast cancers which are the same tissues where familial mutation occurs (*Rice et al. 2000*). One exception is sporadic lung cancer where hypermethylation has been detected in BRCA1 (*Esteller et al. 2001*).

In a population-based study it was shown that 12 out of 98 ovarian cancer patient samples (12.2%) had methylation of the BRCA1 promoter region (*Baldwin et al. 2000*). Methylation was not seen in patients with a family pre-disposition for the disease. For this reason it seems that this only happens in sporadic cases. From the population of sporadic cases sampled 12 out of 81 were methylated (15%) (*Baldwin et al. 2000*). Recently, a study on a panel of 41 ovarian cancer cell lines showed that there was remarkably less BRCA1 methylation than observed in the clinic. Two out of 41 cell lines (4.9%) had promoter methylation (*Stordal et al. 2013*). The study by *Baldwin et al. (2000)* also found that methylation status was stable in recurrent ovarian cancer. Of the six matched samples where recurrent ovarian tissues were available, two of the primary tumours were methylated and four were un-methylated. The methylation status remained identical in all six samples after recurrent disease (*Baldwin et al. 2000*).

It may be possible that promoter de-methylation of BRCA1 could also be under a similar selective pressure as seen with BRCA1 secondary mutations that causes drug resistance. In theory, de-methylation of the promoter region allowing for the re-expression of a functional BRCA1 gene product, could be a possible mechanism of acquired chemotherapeutic drug resistance.

1.7.3 BRCA1 in chemo-sensitivity and chemo-resistance

BRCA1 can influence chemotherapeutic responses. It has been shown that down-regulation of BRCA1 causes sensitivity to DNA damaging agents such as platinums (*Foulkes 2006*; *Yuan et al. 1999*). This down-regulation may be due to mutation in the BRCA1 gene causing loss of function or methylation of the gene promoter region. In an ovarian cancer study the response profile of cancer therapy drugs were tested, in relation to BRCA1 status, in a subpopulation of randomly selected Ashkenazi Jewish women, who have high percentage of hereditary BRCA1 mutation. It was found that patients receiving platinum chemotherapy had an improved prognosis when the BRCA1 mutation was present (*Cass et al. 2003*). It is believed that DNA adducts formed by platinums can cause the collapse of replication forks during DNA synthesis. This results in double-strand breaks, which are extremely unfavourable for cell viability. As BRCA1 plays a major part in homologous recombination, cells deficient in functional

BRCA1 will be unable to repair the DNA damage, which explains their sensitivity to platinums. Other compelling evidence to indicate that BRCA1 down-regulation is correlated with platinum sensitivity became evident in the study by *Lafarge et al. (2001),* which showed that decreased expression of BRCA1 leads to cisplatin sensitivity in the breast cancer cell line HBL100. Interestingly, this same study showed that a decrease in BRCA1 conferred resistance to microtubule-interfering agents such as taxol (*Lafarge et al. 2001*). Chemoresistance was suggested to be linked to inhibition of the JNK pathway by transcriptional modification due to lack of BRCA1 gene product.

In contrast to this, up-regulation of BRCA1 causes resistance to DNA damaging agents like cisplatin and sensitivity to microtubule-interfering agents such as taxol. A study using cisplatin resistant variants of the breast cancer cell line MCF7 (MFC7-CDDP/R) and ovarian cancer cell line SKOV3 (SKOV3-CDDP/R) gives evidence that cisplatin-resistance is a result of BRCA1 up-regulation. The study found increased levels of BRCA1 in these resistant variants and found that SKOV3-CDDP was more proficient in DNA damage repair compared to parental cells. By knocking out BRCA1 expression in this cell line, increased sensitivity to cisplatin was seen due to reduced efficiency in repairing DNA damage and higher rates of apoptosis (*Husain et al. 1998*). Another study using HCC1937 human breast cancer cells, which were BRCA1-deficient due to a mutation in the coding region, demonstrated that by re-expressing the BRCA1 protein, cells reverted to being resistant to cisplatin and sensitive to taxol and docetaxel. These cells were originally more intrinsically sensitive to cisplatin and more resistant to the taxanes (*Tassone et al. 2003*). Evidence of sensitivity to microtubule interfering agents comes from the study of *Righetti et al. (1996).* It was reported that BRCA1 induces a more than 1000 fold increase in sensitivity to taxol. This study also shows that the G2/M arrest is mediated by BRCA1 in response to both DNA damage and microtubule interfering agents inferring differential function of BRCA1 by either inhibition or induction of apoptotic signalling (*Righetti et al. 1996*).

The above evidence shows that BRCA1 may have a major part to play in an 'inverse resistance relationship' between platinums and taxanes. The inverse relationship between cisplatin and taxol in cell models was examined through systematic review of the literature by *Stordal et al. (2007b).* It was found that in the majority of cellular models that had acquired drug resistance and reported sensitivities to platinums or taxanes, had an inverse resistance relationship between cisplatin and taxol. Other combinations of drug were also reported to have this relationship such as carboplatin and taxol, carboplatin and docetaxel and cisplatin and docetaxel. Observations were all

independent of cancer type, reported mechanism of resistance or agents that were used to develop resistance. Clinical trials of platinum and taxane salvage chemotherapy were also investigated. It was found that clinical responses to platinums and taxanes in ovarian cancer mirror that of cellular models displaying this inverse resistance relationship (*Stordal et al. 2007b*). A subsequent systematic review by the same team set out to investigate the major genetic players involved in this relationship. It was found that BRCA1 was the gene that was most associated with the inverse resistance relationship between cisplatin and taxol (*Stordal et al. 2009*). See Figure 1.10 for graphic representation of the inverse resistance relationship between platinums and taxanes.

1.8 Ovarian cancer biomarkers

As ovarian cancers are extremely heterogeneous at a molecular level, the identification of biomarkers that could aid in improving treatment and outcome is a huge challenge. Contributing to the challenge is the lack of high-quality normal and cancerous tissue and biofluid specimens available for research that have well documented clinical data associated with them (*Suh et al. 2009*). Improvements in tissue banking will help in rectifying these issues and make biomarker research more accessible (*Suh et al. 2010*). Over the last two decades, a number of potential biomarkers have been discovered for ovarian cancer, but only a small number have made it into the clinical setting. This may be due to the fact that the majority of these markers were only tested in cell line models and retrospective formalin-fixed paraffin-embedded biospecimens.

The majority of current biomarkers only predict what is already predictable by established clinical methods. Therefore, pathologists do not see the need to implement these in the clinic (*Suh et al. 2010*). The future scope for biomarker discovery should focus on finding stratified and predictive biomarkers. Aims for improving clinical methods in the future are to include molecular profiles into routine clinical workflows. In order to achieve this, researchers must identify a robust set of biomarkers that can be accepted by pathologists in medical centres with no ambiguity. Biomarkers can comprise of a combination of genes, proteins, miRNAs, SNPs and mutations that are derived from tissue and biofluids (*Suh et al. 2010*). Many potential biomarkers are currently undergoing development and are being entered into preclinical and clinical trials. These biomarkers have not yet lead to established panels that can be used for diagnosis, prognosis and efficiency platforms. In the future, a variety of combined biomarkers stemming from genomic (genes, mutations, SNPs, miRNA), proteomic (peptides, proteins and modifications) and metabolomic (small, molecular

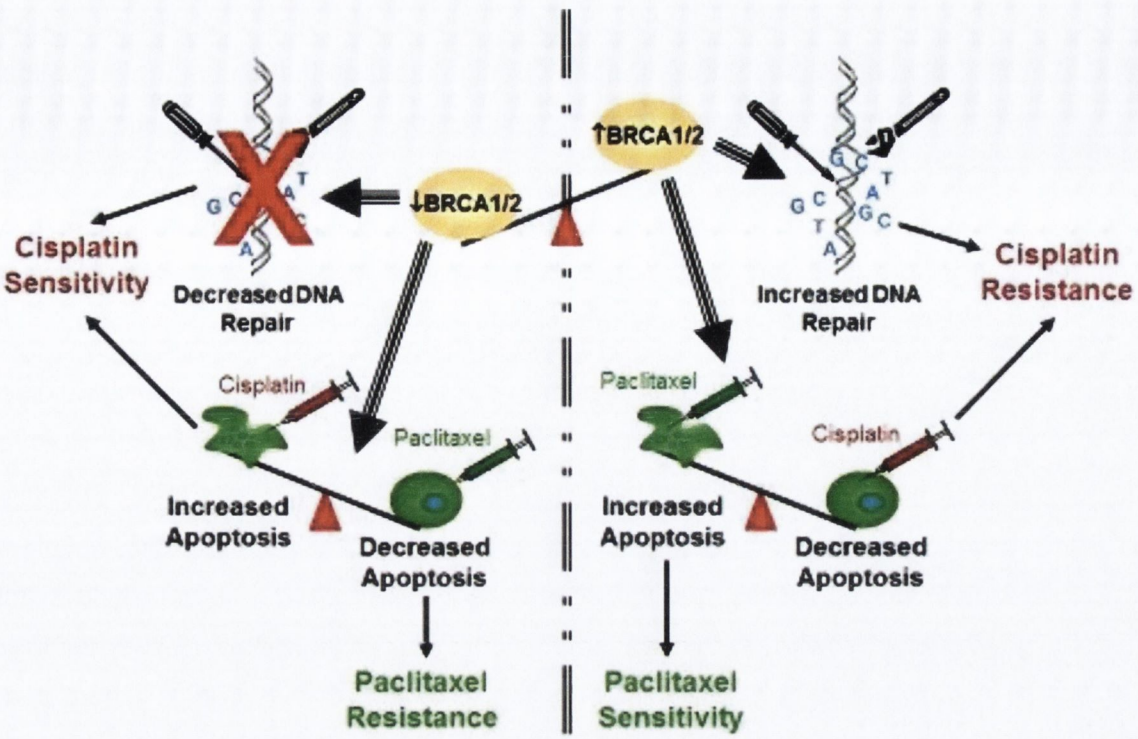

Figure 1.10 Inverse resistance relationship between platinums and taxanes.

The left of the diagram represents reduced expression of BRCA1. This will mean reduced ability of the cell to carry out DNA repair. This results in sensitivity to cisplatin through increased apoptotic signalling and resistance to taxol by reduced apoptotic signalling. On the right hand side of the diagram we see the inverse occurring. Elevated expression of BRCA1 means that cellular DNA repair will be functional. This results in resistance to cisplatin by decreased apoptotic signalling and sensitivity to taxol by increasing apoptotic signalling. Diagram was adapted from (*Stordal et al. 2009*) with permission from the author.

intermediates, hormones, systemic compounds) studies will provide the clinic with suitable assay platforms for tailoring patient treatment, depending on the specific signature an individual patient with ovarian cancer displays (*Suh et al. 2010*). This will positively impact ovarian cancer treatment and should improve 5-year survival and overall survival. An example of a study that shows promise in the discovery of a biomarker panel for early detection of ovarian cancer comes from *Mor et al. (2005)*. The team used protein microarray analysis to look at expression levels of 169 proteins in serum samples from 28 healthy women and 18 women with newly diagnosed ovarian cancer. There were significant differences in the expression of proteins between healthy and diseased patients. ELISA assays found four proteins (eptin, prolactin, osteopontin, and insulin-like growth factor-II) that could distinguish between

healthy individuals and ovarian cancer patients, including patients who were diagnosed with stage I or II disease (*Mor et al. 2005*). These proteins were further validated in a blind cross-validation study of 106 healthy individuals and 100 patients with ovarian cancer from stage I-IV disease. On their own, each protein was unable to distinguish between healthy individuals and diseased patients, but in combination they could discriminate between them with 95% sensitivity, 95% positive predictive value, 95% specificity and 94% negative predictive value.

The two main areas in ovarian cancer that limit clinicians' ability to cure the disease are late diagnosis due to inadequate screening (discussed in section 1.1.4), and the persistence of drug resistant cells (*Bast et al. 2009*). Approximately 70% of ovarian cancers will respond to initial chemotherapy, however, 75% of treated patients will have recurrence of disease after treatment with cytoreductive surgery and combination chemotherapy with a median survival of two years following the recurrence. All relapsed patients eventually die from their disease (*Ozols 2005*). In more than half of the patients who relapse, residual cancer cannot be detected using imaging studies or the current set of serum biomarkers available after the first five months of treatment. A small number of drug resistant cells can persist for many months remaining dormant in the peritoneal cavity. They will then progressively grow, which leads to the death even after aggressive treatment of the recurrent decease. These mechanisms of resistance in ovarian cancer are poorly understood. The main aim of this thesis is to elucidate these mechanisms by discovering a novel set of biomarkers for chemoresistant disease using micro RNAs (miRNA) and mRNA. Measurement of miRNA expression is much more sensitive than that of protein expression for example. They frequently target entire pathways and for this reason may be superior drug targets than genes or proteins (*Pritchard et al. 2012*). A robust overview of possible ovarian cancer resistance biomarkers could be obtained from the combination of mRNA and miRNA expression profiling (*Miles et al. 2012*). MiRNA represent a new frontier in cancer biomarkers that will aid in finding new molecular targets for chemoresistant disease and ultimately improve treatment and therapy response.

1.8.1 MiRNAs as novel cancer biomarkers

MiRNAs are small non-coding RNA molecules that are approximately 19-20 nucleotides in size. They are encoded by the genome of plants, invertebrates and vertebrates. It has recently been discovered that miRNAs are an important class of gene regulators in the human genome. Approximately 1-5% of the human genome comprises of miRNAs and about 30% of human genes are regulated by miRNA

function by interacting with mRNA targets as a post transcriptional regulator of gene expression (*Lewis et al. 2005*). They are involved in the regulation of diverse ranges of cellular processes including cell proliferation, cell differentiation, cell growth, cell cycle regulation and stress responses (*Bartel 2004*).

MiRNA are part of a number of small endogenous RNA molecules, which include ribosomal RNA (rRNA), transfer RNA (tRNA), small nucleolar RNA (snoRNA) and small interfering RNA (siRNA). MiRNA and siRNA are very similar. They are biochemically and functionally identical. They are the same length (19-20 nucleotides), they have the same 5'-phosphate and 3' hydroxyl ends and are both assembled into the RNA-induced silencing complex (RISC) to regulate gene target expression (*Ambros et al. 2003*; *Kim 2005*). The element that separates them is their origins. While miRNA is derived from the double stranded region of a 60-70 nucleotide hairpin loop precursor known as a pri-miRNA, the siRNA molecule is derived from long double-stranded RNA (dsRNA) (*Ambros et al. 2003*; *David 2004*; *Kim 2005*). Initially, all RNA molecules that are assembled into RISC to mediate post transcriptional gene silencing were known as siRNA, but now siRNA and miRNA are classified and distinguished between.

The miRNA class of gene regulators was first discovered by *Lee et al. (2003)* who were studying the larval development of C. elegans. They discovered that the lin-4 gene transcribed a small 22 nucleotide non-coding RNA that regulated the lin-14 gene product via RNA-RNA interaction in its 3' untranslated region. This interaction blocked translation of lin-14 mRNA regulating its expression at a post transcription stage and consequently regulating the timing of early stage larval events (*Lee et al. 1993*). For many years after this finding was made, it was believed that the biogenesis of this small non-coding RNA as a gene regulator was an isolated event, as there was no evidence for the existence of any other similar non coding RNAs in nematodes or any other organisms. It was deemed to be a simple discovery. This view changed after the discovery of another 22 nucleotide RNA product of the Let-7 gene that targets mRNAs with complimentary 3' untranslated regions. As Let-4 acts early in development, Let-7 has a similar function in late development. Soon after this finding, many homologues of Let-7 were found in a variety of species including vertebrates, ascidian, hemichordates, molluscs, annelids and arthropods (*Pasquinelli et al. 2000*).

Through bioinformatics and microarray studies, it has been found that a single miRNA can bind up to 200 separate mRNA targets where each target can regulate many diverse functions in the cell. This highlights the extent of miRNA's regulatory capacity (*Lewis et al. 2003*). Another study suggests that a single miRNA can have up to one thousand mRNA targets (*Miranda et al. 2006*). This again highlights the huge

regulatory capacity that a single miRNA may have in the cell, but also shows the complexity in developing targeted therapies.

It has been shown that aberrant miRNA expression plays a significant role in tumourigenesis where miRNAs can be defined to have both oncogenic and tumour suppressor functions (*Di Leva et al. 2010*). Their genes are often found in genomically unstable regions including loss of heterozygosity (LOH) regions, fragile sites or regions that are often subjected to deletions or amplifications (*Garzon et al. 2009*). They play central roles in cancer biology by influencing the regulation of cancer-stem-cells, angiogenesis, epithelial to mesenchymal transition (EMT), metastasis and drug resistance. Deregulation of miRNA will affect their target mRNA expression, which has a knock on effect on protein translation. This presents the opportunity to exploit this aberrant expression by examining miRNA expression profiles of germline versus tumour cells and improving the diagnosis and treatment of many human diseases, including ovarian cancer (*Shah et al. 2009*; *Zhang et al. 2006*). This idea can also be applied to chemotherapeutic resistance. Novel markers for resistance could be found by examining miRNA expression profiles of resistant cell lines and comparing these to parental tumour cells with the intention of specifying treatments to particular resistance profiles and increasing chances of improving progression free survival.

The first published study that linked aberrant miRNA expression to cancer was a study carried out by (*Calin et al. 2002*) in B-cell chronic lymphocytic leukaemia (CLL). Their study revealed that miR-15 and miR-16 were down-regulated through the deletion of a region in chromosome 13q14 where the genes for these miRNAs reside. This deletion occurs in more than 50% of CLL cases. These genes are either deleted or down-regulated in about 68% of all CLL cases. The first study that linked miRNA expression to ovarian cancer was *Zhang et al (2006).* It showed that 37.1% of genomic loci containing known miRNA's had altered DNA copy number (*Zhang et al. 2006*).

1.8.2 MiRNA biosynthesis and function

The biogenesis of miRNA begins with the transcription of pri-miRNA in the form of long primary transcripts more than 1kb in size in a stem loop structure from miRNA coding regions. MiRNAs in the genome are most often found in clusters and spread out in various different regions. Transcription and regulation of miRNA will differ depending on their location. Most commonly, miRNA coding regions are found in intergenic regions and introns of protein coding genes. It is presumed that intergenic miRNAs are transcribed by their own promoters and can result in one pri-miRNA being processed into a number of mature miRNAs. MiRNAs that are transcribed from intronic regions

are transcribed in tandem with the primary transcript by the same promoter (*Rodriguez et al. 2004*; *Saini et al. 2007*; *Ying et al. 2010*).

After transcription from an intergenic region, one end of the pri-miRNA is processed in the nucleus by the endonuclease Drosha RNase III and double-stranded RNA binding domain (dsRBD) protein DGCR8 (*Han et al. 2004*). Drosha cleaves both strands in a staggered manner at about 11bp from the base leaving a two nucleotide overhang at the 3' end, making a 60-70 nt sequence in a hairpin loop (*Han et al. 2006*). This cleaved product is termed pre-miRNA. This acts as a precursor to miRNA. The cut made by drosha makes one end of the mature miRNA (*Lee et al. 2003*). Pre-miRNA is then transported to the cytoplasm by the export receptor Exportin-5 and Ran-GTP (*Lund et al. 2004*). For intronic transcripts there are two theories for the generation of the pre-miRNA; it may occur simultaneously or independently of the mRNA transcript (*Kim et al. 2007*).

After active transport to the cytoplasm, another RNase III endonuclease called dicer processes the opposite end of the pre-miRNA, that drosha had previously cleaved while in the nucleus. Dicer's function in miRNA processing was first elucidated from work carried out on C. elegans (*Grishok et al. 2001*; *Ketting et al. 2001*). Dicer binds to the 3' overhang created by drosha by its PAZ domain along with another dsRBD protein TRBP, which allows it to position the pre-miRNA correctly for cleavage (*Chendrimada et al. 2005*). Dicer can then cleave off the terminal base pairs and the loop of the pre-miRNA. Cleavage of pre-miRNA results in an approx 22 nt duplex, which is made up of the mature miRNA transcript and a fragment made up of the opposing arm of the pre-miRNA. The duplex is characterized by having a 5' phosphate and a 2 nt 3' overhang, which is characteristic of RNase III processing (*Lee et al. 2002*). This duplex is short lived and is taken up by the RISC. This complex is made up of dicer, ago and TRPB (*Gregory et al. 2005*). Helicase separates the two RNA strands resulting in the mature miRNA strand being retained in the RISC. The other strand is degraded.

RISC is involved in identifying target mRNAs through perfect or near perfect complimentary base-pairing of the miRNA bound to RISC and the target mRNA. Perfect binding will result in the degradation of mRNA through endonuclease mediated cleavage of nucleotides pairing at residue 10 and 11. Non perfect base-pairing results in a translational block for the mRNA in a process which is not yet known. These two scenarios confer post-transcriptional gene silencing by miRNAs (*Elbashir et al. 2001a*; *Elbashir et al. 2001b*; *Hammond et al. 2000*). An overview of miRNA biogenesis can be seen in Figure 1.11.

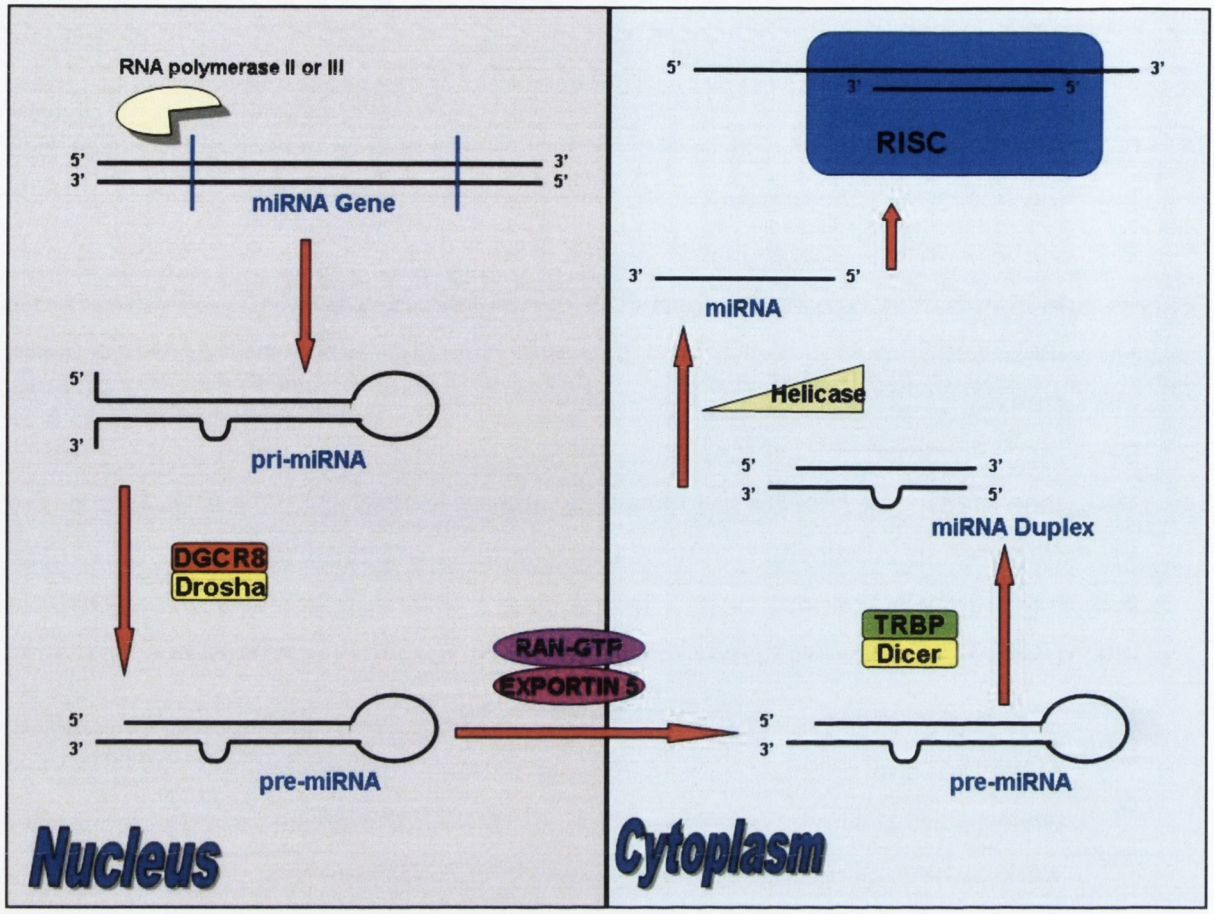

Figure 1.11 Overview of miRNA biogenesis.

In the nucleus RNA polymerase II or III transcribes pri-miRNA from a miRNA gene. This is then acted on by drosha and DGCR8. Drosha cleaves the pri-miRNA to form pre-miRNA. The pre-miRNA is transported from the nucleus to the cytoplasm my exportin5 and ran-GTP. In the cytoplasm dicer and TRBP act on the pre-miRNA. Dicer cleave the miRNA to form a miRNA duplex. Helicase then separated the strands of the duplex and one of the miRNA strands gets taken up by the RISC complex. The miRNA can now target specific mRNAs due to complementarities of the miRNA sequence and the 3' end of the mRNA sequence. Depending on how strong the strands sequences complement each other the mRNA will either become blocked from translation or degraded.

1.8.3 MiRNA expression analysis in ovarian cancer

Aberrant expression of miRNAs can result in disease phenotypes such as carcinoma (*Di Leva et al. 2010*). This aberrant miRNA expression presents us with an opportunity to characterise these changes and link miRNA expression to particular disease states. A study carried out by *Lu et al. (2005)* showed the potential of miRNA profiling. It

analysed the expression patterns of 217 mammalian miRNA's in 334 samples and found that there was generally a down-regulation of miRNA's in tumour tissues when compared to normal tissue. The study was able to successfully classify poorly differentiated tumour samples with miRNA profiling where mRNA profiling failed on the same samples (*Lu et al. 2005*).

The first study to link miRNA expression to ovarian cancer was undertaken by *Zhang et al. (2006)* which showed that 37.1% of miRNA genes in ovarian cancer exhibited DNA copy number alterations, which correlated to altered expression of miRNA (*Zhang et al. 2006*). In 2008, our group and others showed that low expression levels of dicer, drosha and eIF6, involved in the miRNA biogenesis machinery, were linked to poor clinical outcome in ovarian cancer (*Flavin et al. 2008*; *Merritt et al. 2008b*).

Numerous studies have taken place since miRNA expression patterns were first linked to ovarian cancer. One of these studies aimed to profile miRNA signatures in human ovarian cancer shortly after this discovery by using specialised miRNA microarrays (*Iorio et al. 2007*). The team of scientists found that they could clearly differentiate between normal and cancerous ovarian tissue by examining the miRNAs that were differentially expressed between them. The most significant changes found were over-expression of miR-200a, miR-141, miR-200c and miR200b and under-expression of miR-199a, miR-140, miR-145 and miR-125b-1 in tumour tissue compared to normal ovarian tissue. They were also able to identify specific miRNAs that may be involved in bio-pathogenic features such as histotype, lymphovascular and organ invasion and modifications to the ovarian surface. They concluded by remarking that their results demonstrate how miRNAs could be involved in tumour pathogenesis in epithelial ovarian cancer. They postulated that miRNA's may be involved in the development, but not progression, of ovarian cancer and that a possible mechanism for the aberrant expression of miRNA may be due to altered miRNA gene methylation. Demethylation treatments revealed that miR21, miR203 and miR-205 became up-regulated.

Subsequently, *Dahiya et al. (2008)* carried out a different study profiling miRNA expression in ovarian cancer using miRNA microarrays. Their study found a number of miRNA's such as miR-221 and miR-146b that were over-expressed and miR-21 and let-7f that were under-expressed in ovarian cancer cell lines and tissue compared to ovarian surface epithelial cell-lines immortalised with E6 and E7. This study yielded many different results when compared to previous studies. The authors suggest that the results of their study could be a more accurate predictor of miRNAs that are likely to be linked with ovarian cancer than previous studies. This was because the team used immortalised ovarian surface epithelial (IOSE) cells as a control while other

studies (such as *Iorio et al. (2007)*) used whole ovaries (*Dahiya et al. 2008*). The use of whole ovaries is not believed to be an appropriate control, as the bulk of the ovary contains many different cell types and only a small portion being epithelial cells. They then identified mRNA targets for the differentially expressed miRNA but found that there was little overlap between predicted targets and targets found in the experiment or between experimental targets and pathways found using different cell lines. This highlights the complexity of miRNA target selection.

Two other studies were published in 2008 using IOSE as normal controls. *Yang et al. (2008a)* found 23 miRNAs that were differentially expressed in ovarian cancer. They found that the most frequently deregulated of these were miR-214, miR199a, miR-200a and miR100. It was found in this study that miR-214 has a role to play in cisplatin resistance, which is discussed later in section 6.1.4 (*Yang et al. 2008a*). Also, *Zhang et al. (2008a)* found a number of miRNAs to be deregulated. Significantly different changes were seen between early and late stage disease. Down-regulation of miRNA was characteristic of tumour initiation and progression. The study suggested that genomic loss played a role in the down-regulations as deletions of genomic loci containing miRNA occurs in 15% of the down regulated miRNAs. Also, epigenetic alterations can be linked to a third of down-regulated miRNAs. They also showed evidence that Dicer and Drosha, key proteins in the miRNA biogenesis pathway, do not contribute to deregulation in ovarian cancer as has been found in other tumour types (*Zhang et al. 2008a*). Finally, the study revealed a cluster of miRNAs that may act together as tumour suppressor genes. This miRNA cluster may have a role to play in embryonic development. It was found that tumours with lower expression of the cluster had an increased proliferation index and shorter survival. The cluster is found on chromosome 14 (Dlk1-Grl2 domain) and contains eight miRNAs of interest which have also played a part in breast cancer, colon cancer and bladder cancer. Their down-regulation is associated with up-regulation of many potential mRNA targets of the cluster, which play a role in late-stage epithelial ovarian cancer.

Also, in 2008, 23 aberrantly expressed miRNAs were identified from a study by *Nam et al. (2008)* using microarray technology to investigate markers for ovarian cancer prognosis in 60% of examined patients. MiR-21 was the most up-regulated miRNA in 85% of samples and miR-125b was the most down-regulated miRNA in 95% of samples. Up-regulation of miR-200, miR-141, miR-18a, miR-93, and miR-429, and down-regulation of let-7b, and miR-199a was strongly associated with a poor prognosis (*Nam et al. 2008*). The following year (*Eitan et al. 2009*) found that miR-200a, miR-34a and miR-449b were the most down-regulated miRNAs in advanced ovarian tumours,

which was contrary to the findings of *Nam et al. (2008)* and *Yang et al. (2008a)*. They also found that miR200a was associated with improved overall survival in early stage disease. This finding agrees with *Hu et al. (2009)* who found miR200a to be correlated to favourable outcome. MiR-200c, another member of the miR-200 family, has been linked with favourable outcome. Down-regulation of this miRNA has been linked with improved progression-free and overall survival (*Hu et al. 2009*). The same study found 11 miRNAs that were differentially expressed in relapsed patients compared with non-relapsed patients.

A miRNA signature was also assessed as part of TCGA project (*The Cancer Genome Atlas Network 2011*). Expressional analysis of 11,846 genes was successful in identifying four robust expressional subtypes within high-grade serous ovarian cancer. These subgroups were termed Immunoreactive, Differentiated, Proliferative and Mesenchymal, based on gene clustering data. Clustering analysis of miRNA expression identified three subtypes within high-grade serous ovarian cancer (subtype 1-3). The miRNA subtype 1 overlapped with the mRNA proliferative subtype and miRNA subtype 2 overlapped with the mRNA mesenchymal subtype. This shows that miRNA expression has the ability to differentiate between subtypes as well as genetic expression. Survival analysis by Kaplan Meier was found to be significantly different between all the miRNA subtypes, with miRNA subtype 1 having significantly longer survival.

MiRNAs circulate freely in body fluids in a highly stable, cell free form. They are tissue specific and are accurate indicators of the origin of metastasis, making them ideal candidates for non-invasive biomarkers in cancer (*Chen et al. 2008b*; *Cheng et al. 2012*; *Mitchell et al. 2008*). A number of studies have shown that circulating miRNAs have been associated with ovarian cancer detection (miR-21, miR-92 and miR-93), staging (miR-92 and miR-221), grading (miR-221) and outcome (miR-221 and miR-92) (*Guo et al. 2013*; *Hong et al. 2013*; *Resnick et al. 2009*; *Xu et al. 2013*). Our research team has shown that a miRNA signature derived from the serum of ovarian cancer patients is capable of distinguishing between malignant and benign ovarian cancer lesions (*Langhe et al. 2014*). Four miRNAs (let-7i-5p, miR-152, miR-122-5p and miR-25-3p) were found to be down-regulated in the serum of ovarian cancer patients with malignant disease compared to those with benign lesions.

Numerous genome wide miRNA screens have been undertaken in the literature. These have linked aberrant miRNA expression to many aspects of ovarian cancer including histological subtypes, tumour stage and grade, prognosis, BRCA1 mutation/epigenetic changes, resistance, recurrence and survival (*Boren et al. 2009*; *Creighton et al. 2010*;

Dahiya et al. 2008; *Eitan et al. 2009*; *Gallagher et al. 2009*; *Hu et al. 2009*; *Iorio et al. 2007*; *Kim et al. 2010b*; *Laios et al. 2008b*; *Lee et al. 2009*; *Liu et al. 2013b*; *Marchini et al. 2011*; *Nam et al. 2008*; *Resnick et al. 2009*; *Sorrentino et al. 2008*; *Vaksman et al. 2011*; *Vecchione et al. 2013*; *Vilming Elgaaen et al. 2014*; *Wyman et al. 2009*; *Yang et al. 2008a*; *Yang et al. 2008b*; *Zhang et al. 2008a*) . An overall summary of the findings from these studies is published in two separate review articles relating to miRNA in ovarian cancer biology (*Di Leva et al. 2013*; *van Jaarsveld et al. 2010*). These reviews indicate that there is minimal overlap in all the various genome wide studies. Some reasons put forward for this may be that different specimens were used in the studies (Cell lines, tissue, and serum), histological subtypes, origin of tumour cells, RNA isolation protocols and detection platforms (Deep sequencing and miRNA arrays). Another issue, which was mentioned previously, would be the use of different controls, some of which may be more appropriate than others.

1.9 Aims and objectives

The mechanisms of chemoresistance and relapse are poorly understood in ovarian cancer. The primary goal of this project was to elucidate these mechanisms in order to find new drug targets and ultimately improve treatment.

1.9.1 Hypotheses

The hypothesis examined in this study stated that;

- Due to the inverse resistance relationship that exists between platinums and taxanes, cells with BRCA1 defects will develop resistance to platinums slower than taxanes, as they are more sensitive to DNA damage. The reverse being true for cells with functional BRCA1.

- When treating cells with alternating treatments of platinums and taxanes, resistance will develop more slowly or not at all when compared to treatment with single-agent taxane or platinum.

- A miRNA signature is associated with chemoresistance in ovarian cancer, which differs from chemosensitive non-resistant disease.

1.9.2 Objectives

The aim of this project was to develop novel chemoresistant ovarian cancer cell lines from established ovarian cancer cell lines using a comparative selection strategy. UPN251 (BRCA1 wild-type) and OVCAR8 (BRCA1 methylated) were used in order to

investigate the development of chemoresistance in relation to BRCA1 status. We examined how the development of resistance was effected by BRCA1 in relation to:-

- The inverse resistance relationship between platinums and taxanes.
- The effects of alternating doses of platinums and taxanes.

The secondary aim was to examine and evaluate the mechanisms of resistance which developed in resultant resistant cell lines. Affymetrix miRNA and mRNA arrays were used on the developed chemoresistant cell lines in order to find a novel miRNAs signature, which were associated with the development of chemoresistance in ovarian cancer. The mRNA array data was used to complement findings from the miRNA arrays and profile mechanisms of drug resistance. Validation of novel target biomarkers was carried out by quantitative polymerase chain reaction (qPCR) amplification of clinical specimens. This enabled us to develop a miRNA signature for chemoresistant ovarian cancer that was of clinical relevance and aided in the elucidation of chemoresistant mechanisms. This will ultimately improve treatment strategies through the development of novel targeted therapies. This study has further expanded the body of knowledge that governs chemoresistance in ovarian cancer.

CHAPTER 2

General Methods



TRINITY
COLLEGE
DUBLIN

Chapter 2 General methods

2.1 General methods

Analytical and molecular biology grade reagents were used in this study. All solutions were prepared in ultrapure deionised water. The source of all media, antibodies, enzymes and commercially available kits used are described in the relevant sections of this chapter and other methods sections.

2.1.1 Cytotoxic drugs

All of the cytotoxic drugs and inhibitors used in this project were obtained from commercial suppliers or from the St. James's Hospital pharmacy. Drugs and manufacturers are listed in Table 2.1.

2.1.2 General solutions

Phosphate Buffered Saline (PBS) DulbeccoA (Gibco®, Biosciences, Ireland)

NaCl (8.0 g/L); KCl (0.2 g/L); NaH_2PO_4 (1.15 g/L); KH_2PO_4 (0.2 g/L), made from 1 tablet per 100ml of distilled water, pH 7.2, stored at room temperature or 4°C.

Diethylene Pyrocarbonate (DEPC) Water

500ul of DEPC (Sigma-Aldrich, UK) was added per 500ml of autoclaved water. The bottle was placed on a magnetic stirrer for 1-2 hours at room temperature. Water was re-autoclaved to inactivate DEPC.

2.1.3 Cell lines and tissue culture conditions

2.1.3.1 Media

55ml of foetal calf serum (FCS) (Lonza, UK) was added to a 500ml bottle of RPMI 1640 with L-glutamine (Sigma-Aldrich, UK).

Media RPMI 1640 with L-glutamine and 10% FCS, free of antibiotics, was used to grow the human ovarian cancer cell lines UPN251 and OVCAR8 (MD Anderson Cancer Center, Houston, Texas, USA). Insulin was not added. UPN251 is traditionally grown in RPMI 1640 medium with 10% FCS and 0.25U/ml insulin, while OVCAR8 uses the same media and supplements, but in the absence of insulin. As UPN251 and OVCAR8 needed to be grown together for an extended period of time in subsequent experiments, it was deemed useful to investigate whether both cell lines could be

Table 2.1 Cytotoxic drugs and Inhibitors.

All cytotoxic drugs and Inhibitors including their source, molecular weight (MW), stock concentration (Conc) and formulation.

Cytotoxic Drug	Solvent / Formulation	Stock (Conc)	MW	Source
Buthionine Sulphoximine (BSO)	Weighed then dissolved in H_2O and filter sterilised	50mM	222.31	Sigma-Aldrich, UK
Carboplatin	Used directly from vial containing H_2O and mannitol	10mg/ml	371.25	Teva Pharma B.V., The Netherlands
CEP8983	Weighed then dissolved in DMSO	5mg/ml	306.32	Cephalon, USA
Cisplatin	Used directly from vial containing H_2O, NaCl, HCl and mannitol	1mg/ml	300.05	Hospira UK Ltd., Warwickshire, UK
Copper Sulphate ($CuSO_4$)	Weighed then dissolved in H_2O and filter sterilised	100mM	159.62	Sigma-Aldrich, UK
Docetaxel	Weighed then dissolved in DMSO	0.1mg/ml	807.88	Sigma-Aldrich, UK
Doxorubicin	Used directly from vial containing H_2O, NaCl and HCl 0.1M	2mg/ml	579.98	Actavis UK Ltd., Devon, UK
Elacridar	Weighed then dissolved in DMSO	2mg/ml	563.64	Santa Cruz Biotechnology, USA
Olaparib	Whole vial dissolved in DMSO	5mg/ml	434	Selleck Chemicals, USA
Oxaliplatin	Used directly from vial containing H_2O, C4H6O6 and NaOH	5mg/ml	397.29	Hospira UK Ltd., Warwickshire, UK
Taxol	Whole vial dissolved in DMSO	0.1mg/ml	853.9	Sigma-Aldrich, UK
Veliparib	Whole vial dissolved in DMSO	5mg/ml	244.29	Selleck Chemicals, USA
Vinblastine	Used directly from vial containing H_2O and NaCl	10mg/ml	810.9	Hospira UK Ltd., Warwickshire, UK

grown optimally in the same media and supplements, i.e. RPMI 1640 medium with 10% FCS (without insulin). For this reason growth curves were set up for both cell lines, where cells were grown in medium with insulin versus media without insulin. Doubling time of both treatments were statistically analysed for any significant differences in growth rate. Average doubling times for each treatment is shown in Figure 2.1. OVCAR8 showed a minor change in doubling time, while UPN251 showed no change at all. These observations were confirmed by t-test statistical analysis. P values were 0.8 and 1 for OVCAR8 and UPN251 respectively. Therefore, it was concluded that growing cell lines in media without insulin did not significantly affect their growth rate and RPMI + 10% FCS was used for the experiments.

2.1.3.2 Tissue culture conditions

Tissue culture was carried out in an ADS laminar flow hood (OPTIMALE 18) adhering to aseptic technique. All cells were maintained in a humidified atmosphere of 5% CO_2 at 37°C. Only cells at log phase of growth were used in experiments. Cell lines were routinely checked for mycoplasma and were mycoplasma-free. See section 2.1.4 for mycoplasma detection protocol.

2.1.3.3 Cell Lines

The human ovarian cancer cell lines UPN251 and OVCAR8 were sourced from the MD Anderson cancer center (Houston, Texas, USA). UPN251 originated from a patient who had failed first line chemotherapy and had relapsed after subsequent treatment of 8 rounds of taxol chemotherapy (personal communication, Dr. Thomas Hamilton). UPN251 is BRCA1 wild-type due to a secondary reversion mutation (*Stordal et al. 2013*). OVCAR8 was taken from a patient who had undergone treatment with high-dose carboplatin who exhibited progressive ovarian cancer (*Schilder et al. 1990*). OVCAR8 is BRCA1 wild-type but is methylated in the promoter region (*Stordal et al. 2013*). Methylation status was examined and confirmed by Myriad Genetics (Salt Lake City, Utah, USA). Both are adherent cells lines that grow in a monolayer and are of epithelial serous histotype. All cell lines were originally fingerprinted in the MD Anderson Cancer Center Support Grant (CCSG) supported cell line characterisation core to establish identity. Cell lines were subsequently re-fingerprinted by Source Biosciences (Nottingham, UK) to confirm identity by examining standard DNA microsatellite short tandem repeats (STR). The metrics used was a strict 80% cut-off with the allowance of using a difference of up to one STR, as used in the finger printing of the NCI-60 cell line panel (*Lorenzi et al. 2009*). Results from Source Biosciences

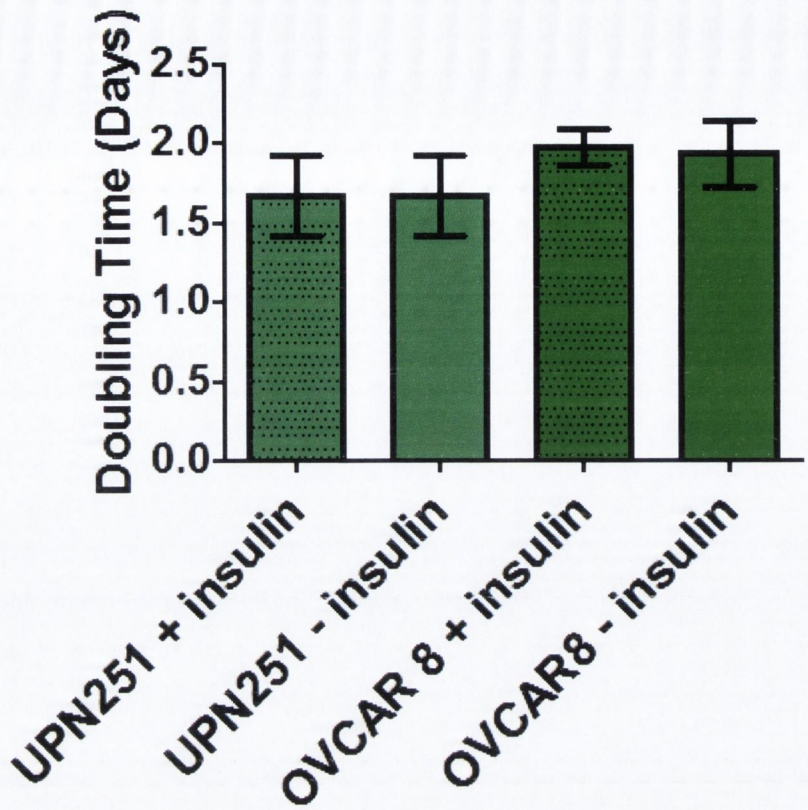

Figure 2.1 Growth curves. The effects of insulin on doubling time.

The doubling times of UPN251 ± insulin and OVCAR8 ± insulin are graphed for a minimum of n=3 replicates.

correlated with results originally obtained from MD Anderson CCSG supported cell line characterisation core.

2.1.3.4 Cell line freezing and defrost protocols

2.1.3.4.1 Cell line freezing

Cell freezing mixture

45% RPMI 1640 (Sigma-Aldrich, UK), 45% FCS (Lonza, UK), 10% DMSO (Gibco®, Biosciences, Ireland), stored at -80 degrees and in liquid nitrogen.

After the subculture of a T75 flask (Sarstedt, Germany) cells were centrifuged for 5mins at 180 x g and re-suspended in 6ml of cell freezing mixture. 1ml of cells suspended in cell freezing mixture was pipetted into a 2ml cryovial and stored at -80°C (short term storage) or in liquid nitrogen (long term storage).

2.1.3.4.2 Cell line defrost

Warm media (10ml) was added to a 15ml centrifuge tube. A pasture pipette was used to transfer cells to the tube of media. The transfer was achieved by adding warm media to the cryovial containing the cells in freezing mixture and mixing up and down until the contents of the cryovial had defrosted and its contents could be fully transferred to the tube containing media. The newly suspended cells in media were spun in a centrifuge at 180 x g for 5mins. The pellet was re-suspended in 5ml of media and transferred to a T25 flask. The media was changed after 24 hours. When confluence was reached the cells were transferred to a T75 flask.

2.1.4 Mycoplasma PCR assay

This protocol was adapted from (*Young et al. 2010*) and covers a range of mycoplasma species and other mollicutes including; *Achileplasma laidlawii, M. arginini, Mycoplasma fermentans, M. hyothinis, M. orale, M. pneumonia, Mycoplasma gallisepticum, Mycoplasma synoviae and Spiroplasma citri.* This represents an optimal selection for mycoplasma detection based on the guidelines provided by the European Pharmacopoeia. 1ml of media was collected from a confluent cell culture flask and stored at -20ºC until needed in a 15ml tube. The tube was defrosted at room temperature and spun at 720 x g to pellet cellular debris. The top of the suspension was pipetted when the sample was added to the PCR reaction tube. PCR reactions were set up with a mastermix as follows:

- 12.5µl of green 2x GoTaq (Medical Supply Company)
- 0.5µl of forward primers (10µM) (Sigma-Aldrich, UK)
  - 5'-GGGAGCAAACAGGATTAGATACCCT-3'
- 0.5µl of reverse primers (10µM) (Sigma-Aldrich, UK)
  - 5'-TGCACCATCTGTCACTCTGTTAACCTC-3'
- 10.5µl of DNase free water (Sigma-Aldrich, UK)
- Total volume 24µl

1µl of sample is added to each reaction. A positive control (1µl from an infected cell line) and a negative control (1µl of DNase free water) were always included. PCR was run in the GeneAmp® PCR system 9600 (Perkin Elmer, USA) thermal cycler with a heated lid with the following cycles:

- 95ºC for 5mins
- 40 cycles of 94 ºC for 0.5mins, 55 ºC for 0.5mins and 72 ºC for 1min
- 72 ºC for 10mins

- Holding at 4 °C until plate was removed.

The PCR product was run on 2% agarose gel (100mL 1X TBE (Fisher Scientific, Ireland) and 2g of agarose), which was dissolved in a microwave and had 10µl of Cyber safe (10,000 X concentrations in dimethyl sulfoxide (DMSO)) (Thermo Fisher Scientific Inc., USA) added. The gel was left at room temperature until set. The gel was then submerged in 1X TAE and 6µl of GelPilot 100bp ladder (Qiagen, UK) and 10µl of PCR product was added to separate lanes. The gel was run for 1 hour at 100V. The PCR product size was 270bp. The gel was imaged under UV light using the Biorad Gel Doc system using the Quantity One software analysis package.

Detection for mycoplasma contamination was carried out routinely on the cell lines for the duration of the project. The cell lines and developed sublines were found to be mycoplasma free on all occasions. Figure 2.2 shows a representative fluorescent photograph of a gel ran after mycoplasma PCR. The positive control can be seen clearly while no staining is seen in the other lanes containing samples and negative control.

2.1.5 Cell counting for growth experiments

Cell counting for growth curve experiments was performed in six well plates (Sigma-Aldrich, UK) and T25 flasks (Starstedt, Germany). Media was removed from each well of a six well plate or from each T25 to be counted. 500µl (6 well plate) or 2ml (T25 flask) of PBS was added to each well to wash cells. PBS was discarded and 500µl (6 well plate) or 2ml (T25 flask) of warmed trypsin (Gibco® by Life Technologies, USA) was added to each well and incubated in a humidified atmosphere of 5% CO_2 at 37°C for 5-10mins in order to allow cells to detach. Cells were examined under an inverted light microscope (Nikon TMS) to ensure all cells had detached. 500µl (6 well plate) or 2ml (T25 flask) of media was added to each well to inactivate the trypsin. 2µl (6 well plate) or 8µl (T25 flask) of trypan blue stain 0.4% (Invitrogen™, Thermo Fisher Scientific Inc, USA) was added to each well or flask and counted at least 4 times using a heamocytometer to obtain a mean value.

2.1.6 Acid phosphatase cell viability assay

Sodium acetate buffer

0.1M Sodium Acetate, 0.1% Triton X-100, pH 5.5 adjusted with concentrated NaOH.

The resistance of cell lines to cytotoxic drugs was evaluated using the acid phosphatase cell viability assay (*Yang et al. 1996*). This assay works by the hydrolysis

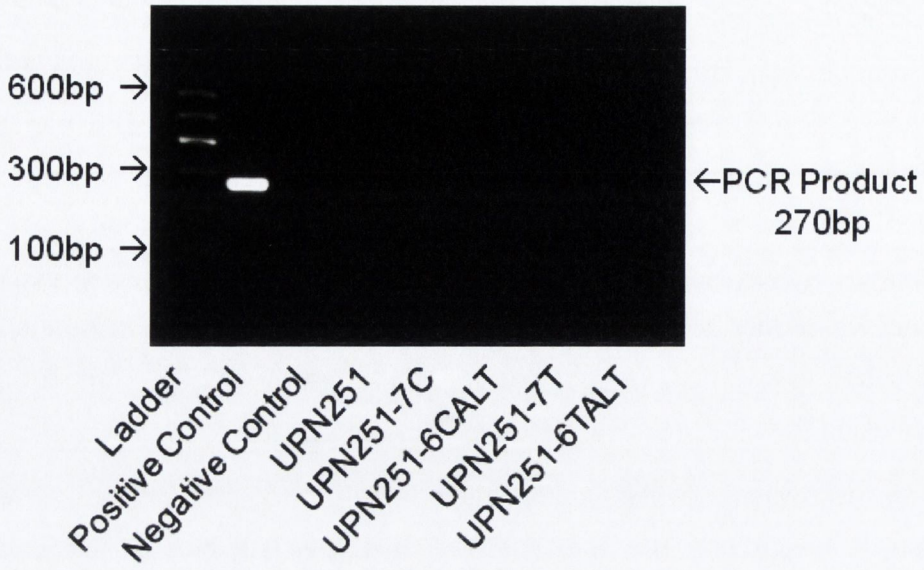

Figure 2.2 Mycoplasma PCR.

A representative fluorescence photograph of mycoplasma PCR result.

of p-nitrophenyl phosphate by intracellular acid phosphatases in viable cells which produce p-nitrophenyl. In brief, 100µl of cells growing at an exponential rate were plated into flat-bottomed 96-well microtitre plates (Nunc, Sigma-Aldrich, UK) at a cell density of $1x10^4$ cells/well. Cells were left to attach overnight and treated with cytotoxic drugs the following day. Cell treatments were setup in triplicate with 2-fold serial dilutions of drug making up to a total final volume of 200µl per well. Each assay contained a drug-free control. Plates were incubated at 37°C in a humidified atmosphere with 5% CO_2 for 3 or 5 days depending on desired exposure. The plates were washed twice with PBS and 100µl of acid phosphate substrate (0.00263g phosphate substrate (Sigma-Aldrich, UK) /ml sodium acetate buffer) was added to each well. The plates were further incubated for 2 hours (OVCAR8) or 1 hour (UPN251). 50µl of 1M NaOH (Sigma-Aldrich, UK) was added to each well in order to stop the reaction. The absorbance of the plates was read at 405nm using the FLUOstar OPTIMA (BMG LABTECH, Germany) multifunctional microplate reader. Cell viability was calculated as a percentage of the control absorbance values as outlined in Equation 2.1.

Equation 2.1 % cell viability

$$\frac{\textit{(Average absorbance of triplicate wells)} * 100}{\textit{(Average absorbance of triplicate control wells)}}$$

The 50% inhibitory concentration (IC_{50}) was defined as the concentration of drug that gave a 50% decrease in cell viability. The relative resistance of sublines produced was calculated using Equation 2.2

Equation 2.2 Relative resistance

$$\frac{(IC_{50} \text{ of resistant subline})}{(IC_{50} \text{ of parental cell line})}$$

2.1.7 Growth assay protocols

2.1.7.1 Manual growth assay

The cells that were growing at an exponential rate were plated in duplicate into a flat-bottomed 6-well (Nunc, Sigma-Aldrich, UK) microtitre plate at a cell density of $1x10^4$ cells/well in 2ml of media. Four identical plates were set up in this format. The plates were left in an incubator for 24 hours to allow cells to attach in a humidified atmosphere of 5% CO_2 at 37°C. After this time one of the four 6-well plates were taken down and cell counted using a heamocytometer. The remaining plates were stored as above and were taken down and cell counted one at a time over subsequent 24-hour periods. Averages and standard deviations were calculated for cell counts over each 24-hour time point and graphed as cell number versus time (hours) in GraphPad prism 5. The doubling time for each cell line was extrapolated from the graph as the amount of hours taken for cells to grow to $2x10^4$ cells/well.

2.1.7.2 High content screening growth assay

100µl of cells were plated into flat-bottomed 96-well microtitre plate (Nunc, Sigma-Aldrich, UK) at a cell density of $2x10^4$ cells/ml. 1 control and 7 drug treatment wells were plated in triplicate for each cell line. Cells were allowed to attach overnight in a humidified atmosphere of 5% CO_2 at 37°C. Cell confluence was read using the cell confluence protocol stored on the Cellavista system (Synen Tec, Germany). Default settings were used for image capture with the exception of exposure time, which was adjusted to 20% during preparation steps. The captured images were processed using Cellavista software giving a percentage cell confluence for each well. After the first reading treatment wells were drugged with 4 different doses of carboplatin (10, 2.5 and 0.625 (µg/ml)) and taxol (200, 50, 12.5 and 3.125 (ng/ml)), making up a total final volume of 200µl per well. Control wells received 100µl of drug free media. The plates were stored at 5% CO_2 at 37°C and were re-measured 3 further times over 24 hour periods. Percentage confluence versus time was graphed using GraphPad Prism 5 for

each treatment and the time to reach 4 times the initial % confluence (quadrupling time) was extrapolated from the graph. Figure 2.3 shows an example of the images captured over 4 days on parental UPN251 cells.

2.1.8 Total cellular glutathione assay

Glutathione phosphate buffer

250nM Na_2HPO_4

An analysis of total cellular levels of glutathione (GSH) was carried out from a method adapted from (*Suzukake et al. 1982*). $3.12x10^5$ cells were seeded into a T75 flask (Sarstedt, Germany) and exposed to the desired drug treatments for 3 days. The cells were then centrifuged at 180 x g for 5mins, washed with 10ml PBS, centrifuged again, resuspended and transferred to a sterile eppendorf tube (pellets could be stored at -20°C at this point). The cell pellets were then re-suspended in 150µl deionised H_2O and lysed with a sonicator at 10amps for 15 seconds. Disruption of samples was confirmed through microscopic examination. 12.5µL of 30% sulfosalicyclic acid (SSA) (Sigma-Aldrich, UK) was added to each sample and mixed by vortexing. The samples were incubated on ice for 15mins to allow protein precipitation to take place and then centrifuged at 12,000g for 5mins. The protein-free supernatant was stored at -20°C until analysis.

The assay reaction was carried out in triplicate in a flat-bottomed 96-well microtitre plate (NUNC, Sigma-Aldrich, UK). A standard curve was run with the samples using standards of glutathione (Sigma-Aldrich, UK) made up in 3% SSA ranging from 0-40µg/ml in order to ensure that the enzymatic reaction was linear over the concentration range (Figure 2.4). Each well for the assay reaction contained 20µl sample lysate or standard, 20µl 1M triethanolamine buffer pH 8.0 (Sigma-Aldrich, UK), 120µl 1mM NADPH (Sigma-Aldrich, UK) in GSH phosphate buffer and 20µl 6mM DTNB (Sigma-Aldrich, UK) in GSH phosphate buffer.

The plate was equilibrated at 30°C for 3mins and 0.3 units of glutathione reductase (Sigma-Aldrich, UK) were added to each reaction. The plate was read at 412nm for 9 measurements over an 8min period using the FLUOstar OPTIMA (BMG LABTECH, Germany) multifunctional microplate reader. The velocity of the reaction was calculated for each sample.

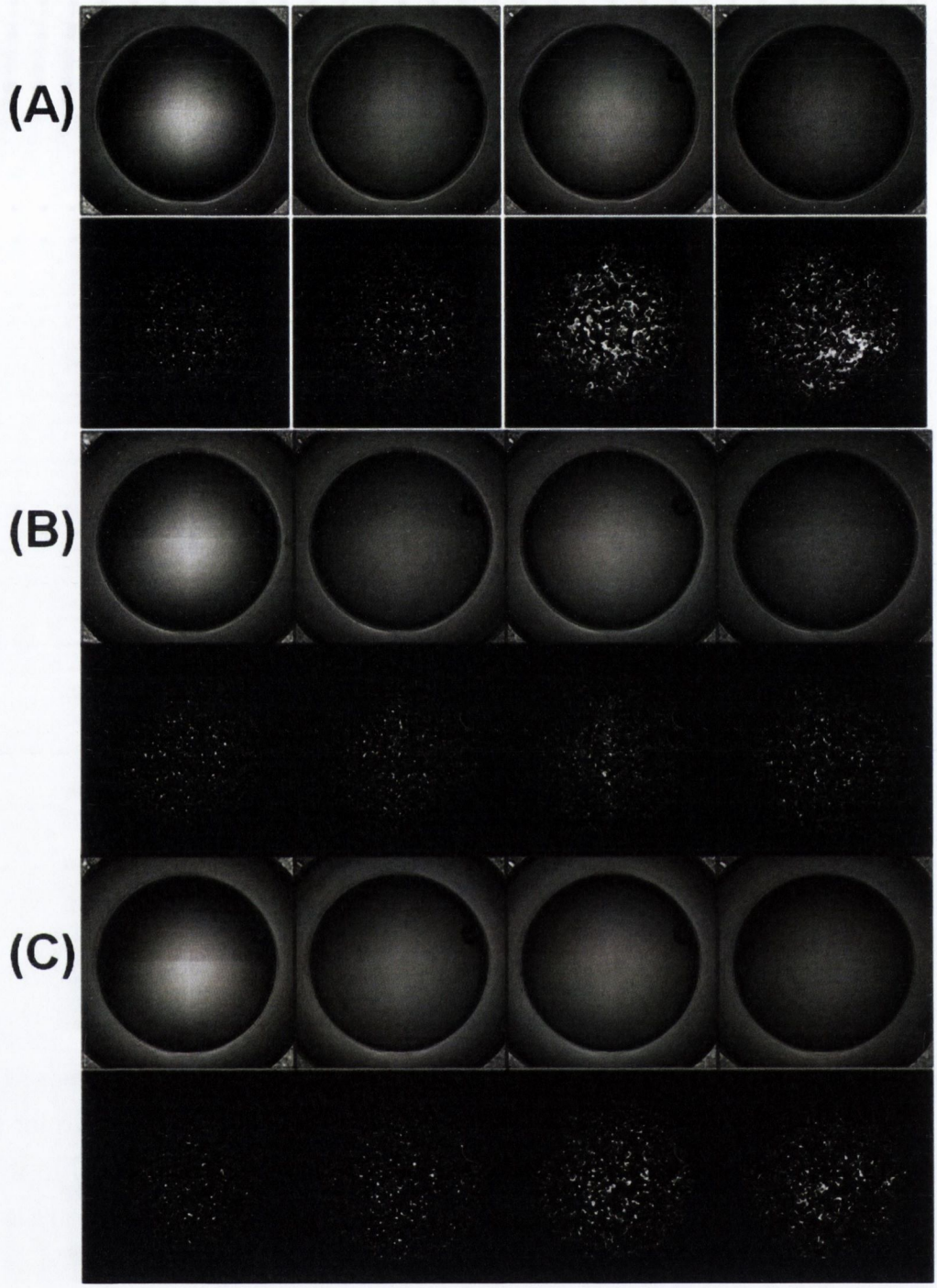

Figure 2.3 High content screening growth curve images.

All images were taken with the Cellavista system at 10x magnification. Cell confluence of a single representative well is shown through a progression of 24 hour time points for three different drug treatments on UPN251 cells. Day 1-4 is shown from left to right in each case. (A-C) show 3 different drug treatments on UPN251 cell lines. The top 4 images in each set are bright field images taken at each 24 hour time point. The bottom 4 images show the 'results image' used to calculate a measure of confluence by the Cellavista associated analysis software for each bright field image. (A) UPN251 control. (B) UPN251 carboplatin 10µg/ml (C) UPN251 taxol 50ng/ml.

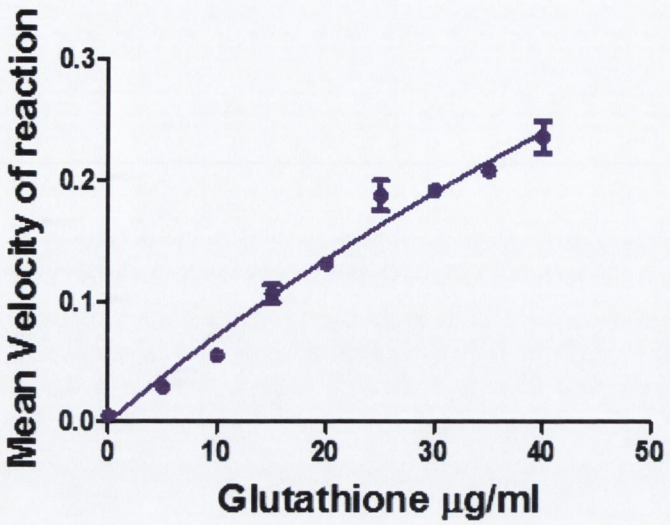

Figure 2.4 Glutathione assay standard curve.

Glutathione standards (plotted points) ranging from 0-40 µg/ml, prepared in 3% SSA were assayed. Means and standard deviations of triplicate wells are shown

2.1.9 Protein analysis

2.1.9.1 Preparation and quantification of total protein

Cell lysis buffer

0.1M Tris/HCl, pH7.4, prepared in deionised water, stored at 4°C.

$7.2x10^5$ Cells were seeded into a T175 (Sarstedt, Germany) flask and exposed to the desired drug treatments for 3 days. Cells were then centrifuged at 180 x g for 5mins, washed with 10ml PBS, centrifuged again, resuspended and transferred to a sterile eppendorf tube (pellets could be stored at -20°C at this point). 100µl of cell lysis buffer and 4µl of protease inhibitor (CPI 25X (Roche, Ireland)) was added to the eppendorfs immediately preceding sonication. The samples were sonicated on ice for 2mins using a Soniprep 150 sonicator (MSE Ltd, UK) for 15 seconds intervals, on and off, at 10amps. The cells were checked under a microscope to confirm cell disruption.

In order to ensure that protein was loaded equally on gels, protein concentrations were determined using a protein assay. A standard curve ranging from 0-1µg/ml of protein was prepared with bovine serum albumin (BSA, Sigma-Aldrich, UK) diluted with deionised water. Total protein extracts were diluted 1:40 with deionised water. 10µl of diluted samples and BSA standards were aliquoted into a flat-bottomed 96-well

microtitre plate in duplicate. A control of 10µl of cell lysis buffer was added to the plate in duplicate. 200µl of Bradford 1X (Bio-rad Laboratories Inc, USA) was added to each well. The samples were mixed for 15mins on a rocking platform. The plates were read at 595nm using a FLUOstar OPTIMA (BMG LABTECH, Germany) multifunctional microplate reader. Linear regression and extrapolation of protein concentrations from the standard curve was performed using GraphPad Prism 5 software. Figure 2.5 displays an example of a standard curve generated in this fashion. Equal concentrations of protein with 50µl 2X loading buffer (Sigma-Aldrich, UK) were made up in deionised water to a total volume of 100µl. This was sufficient for 10 western blots. The concentration of protein was made to contain 40µg of protein per gel.

2.1.9.2 Sodium dodecylsulphate-polyacrylamide gel electrophoresis (SDS-PAGE)

Electrophoresis running buffer

0.024M Tris, 0.192 glycine, 0.1%SDS, pH8.3, stored at 4°C.

The Mini-Protean® Tetra System (Bio-rad Laboratories Inc, USA) was used as per system protocol. Briefly prepoured gradient 4-20% Tris/glycine gels (Lonza, UK) were loaded into gel tanks. Running buffer was poured between gel inserts to ensure they had no leaks. Samples were heated for 3mins in a heating block at 95°C. Running buffer was poured into the tank ensuring the bottom of the gels containing slits was fully covered. 5µl of protein ProSieve QuadColor marker (Lonza, UK) was loaded onto one well of the gel. 10µl of each protein samples was loaded into the remaining, desired wells. The samples were electrophoresised for approximately 90mins at 100V.

2.1.9.3 Western blotting

Transfer buffer

25µM Tris/glycine, pH8.2 adjusted, 20% methanol, stored at 4°C.

The Mini-Protean® II system (Bio-rad Laboratories Inc, USA) was used to electrotransfer the gels to 0.45µm nitrocellulose membrane (Bio-rad Laboratories Inc, USA) for 90mins at 100V in the cold transfer buffer. The Western blots were then stained with ponceau-s-red solution (Sigma-Aldrich, UK) to ensure protein had transferred correctly and to enable quantification of loading in each lane. Ponceau stains were photographed using a Fujifilm LAS-4000 luminescent image analyser as a record.

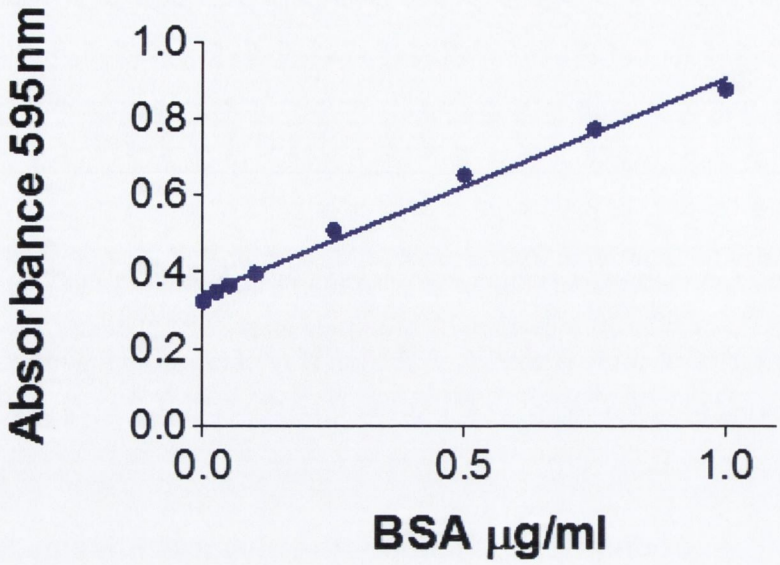

Figure 2.5 Bradford 1X protein assay standard curve.

BSA standards (plotted points) ranging from 0-1 µg/ml protein was prepared in deionised water and analysed. Means and standard deviations are shown for duplicate wells.

2.1.9.4 Western blot development

Blocking solution

5% skimmed milk (Biorad, USA) in PBS with 0.1% Tween.

Antibody solution

3% skimmed milk (Biorad, USA) in PBS with 0.1% Tween.

The blocking solution was added to the nitrocellulose membranes in weigh boats and left on a rocking platform for 2 hours, ensuring the solution covered the membranes while rocking. The blocking solution was removed and 10ml of an antibody solution with a specific concentration of primary antibody was added and incubated at 4°C overnight on a rocking platform, ensuring that the membrane was covered. A table of antibodies and specific dilutions used are shown in Table 2.2. The following day, the antibody solution was poured off and the membranes were washed in PBS 0.3% Tween 3 times for 10mins. The secondary antibody was added and incubated at room temperature on a rocking platform for 1 hour. The secondary antibody was poured off and washed as before. 1ml of Western Blotting Luminol Reagents (Santa Cruz, USA), solution A and solution B, were added to each blot and incubated at room temperature for 1 min. For low abundance proteins, 1ml of ECL Select Western blotting detection

Table 2.2 Table of antibodies used for Western blotting.

Protein	kDa	Host	Supplier	Catalogue #	Dilution
ATP7A	180	Rabbit	Gift from professor Anthony Monaco (*Cobbold et al. 2002*)	N/A	1:1,000
Bcl-2	26	Rabbit	Cell Signalling Technology, USA	4223	1:1,000
Bcl-XL	30	Rabbit	Cell Signalling Technology, USA	2762	1:1,000
BCRP	72	Mouse	Alexis Biochemicals, USA	AXL-801-029-C250	1:250
BRCA1	220	Rabbit	Cell Signalling Technology, USA	9010	1:500
β-Actin	42	Mouse	Sigma-Aldrich, UK	A5441	1:10,000
CTR1	30	Rabbit	Novus, USA	NB100-402	1:1,000
Dicer	220	Rabbit	Cell Signalling Technology, USA	5362	1:1,000
Drosha	160	Rabbit	Cell Signalling Technology, USA	3410	1:1,000
GAPDH	36	Rabbit	Sigma-Aldrich, UK	G9545	1:1,000
MRP2	180	Mouse	Alexis Biochemicals, USA	AXL-801-016-C250	1:250
P-glycoprotein	170	Mouse	Alexis Biochemicals, USA	AXL-801-002-C100	1:250
PAR	116	Rabbit	BD Pharmingen, USA	551813	1:1,000
Anti-mouse HRP	N/A	Sheep	Sigma-Aldrich, UK	A6782	1:1,000
Anti-rabbit HRP	N/A	Goat	Sigma-Aldrich, UK	A4914	1:1,000
Anti-mouse AP	N/A	Rabbit	Sigma-Aldrich, UK	A4312	1:1,000
Anti-rabbit AP	N/A	Goat	Sigma-Aldrich, UK	A3687	1:1,000

AP = Alkaline Phosphatase, ATP7A = ATPase, CU++ transporting, alpha polypeptide, BCL-2/XL = B-cell Lymphoma 2/extra large, BCRP = Breast cancer resistance protein, BRCA1 = Breast cancer susceptibility protein, CTR1 = Solute carrier family 31 (copper transporter), member 1, GAPDH = Glyceraldehyde 3-phosphate dehydrogenase, HRP-Horseradish peroxidise, MRP2-Multidrug resistance-associated protein 2, PAR- Prostate apoptosis response protein

reagents (GE Health Care, USA), luminal solution and peroxide solution, were added and incubated at room temperature for 1 min.

Developed Western blots were photographed using a Fujifilm LAS-4000 luminescent image analyser (GE Health Care, USA) taking light and chemoluminescent photographs. Files were saved in .tif format and analysed using Quantity One software (Biorad, USA). The samples were normalised to GAPDH, used as a loading control.

In order to develop GAPDH on the same blots as a loading control, after the imaging step above, the blots were re-blocked with blocking solution as before for 2 hours at room temperature. The blots were then exposed to GAPDH primary antibodies (Sigma-Aldrich, UK) overnight in an antibody solution as before. The following day the antibody solution was poured off and the membranes were washed in PBS 0.3% Tween 3 times for 10mins. The secondary antibody (Anti-rabbit AP) was added and incubated at room temperature on a rocking platform for 1 hour. The secondary antibody was poured off and washed as before. During the last wash, one alkaline phosphatase substrate tablet (Fast BCIP/NBT, Sigma-Aldrich, UK) was dissolved and mixed well by vortexing in 10ml of distilled water and then poured into a weigh boat. The washed membranes were placed in the alkaline phosphatase substrate solution until GAPDH bands became visible. The blots were immediately placed into a new weigh boat with distilled water to prevent over exposure. The blots were then photographed using a Fujifilm LAS-4000 luminescent image analyser (GE Health Care, USA).

2.1.10 Cell cycle mitosis assay

PBS + 1% BSA

1g BSA to 100ml PBS (Stored at 4°C)

Fixation solution (4% Formaldehyde + 0.1% Triton X-100)

11.1ml of 36% formaldehyde stock, 100ul Triton X-100, 88.8ml ultrapure water (Stored at 4°C)

Antibody Solution

10ul Antibody solution (vial 2, green cap) to 5ml PBS + 1% BSA (immediately before use)

Nuclei Dye Mixture

5ul Nuclei Dye (vial 1, blue cap) to 5ml PBS (immediately before use)

The quantification of mitotic cell fraction was carried out using the Phospho Histone H3 Imaging Kit (Roche, Ireland). 100µl of cells were plated into flat-bottomed 96-well

microtitre plates (NUNC) at a cell density of $2x10^4$cells/ml and were allowed to attach overnight. Parental cells received doses of 800, 200, 50, 12.5 and 3.125 (ng/ml) of taxol and sublines received doses of 800 and 50 (ng/ml) of taxol to a final volume of 200µl in triplicate (control wells received only media). After 24hours, the plate was prepared for florescence imaging as per the protocol. In brief:

1. 180ul of supernatant (90%) was removed from each well of the 96-well plate.
2. 180ul of fixation solution was added to each well to fix the cells. (Incubated at room temperature for 10mins).
3. Fixation solution was removed from each well.
4. 200ul PBS was added to each well (Incubated at room temp for 5mins).
5. PBS was removed from the wells entirely.
6. 50ul of antibody solution was added to each well (Incubated for 60mins at 23-27°C in the dark).
7. 50ul of nuclei dye mixture was added to each well and mixed up and down slowly using a pipette. (Incubated for 10mins at 23-27°C in the dark).
8. All solution was removed using a pipette.
9. 200ul of PBS was added and then removed.
10. Another 200ul of PBS was added.

The cells were analysed using the InCell Analyser 6000 (GE Healthcare, USA). A 10x objective lens and diffuse fluorescence temporal response (DFTR) filters were used during fluorescent image capture. 10 fields were captured in each well. A total cell count was obtained by measuring the nuclei dye channel (Ex Max: 361nm, Em Max: 486nm). The number of cells in mitosis was obtained by measuring the antibody channel (Ex Max: 495nm, Em Max: 519nm). Figure 2.6 shows a single image taken for UPN251 cells over both channels. For each sample the % true values (percentage of cells in mitosis) were calculated as shown in Equation 2.3. For drug treated cells, the fold difference in % true cells were calculated compared to drug free controls, as seen in equation 2.4.

Equation 2.3 % true

$$\frac{\text{(Mitotic cells)*100}}{\text{(Total cell number)}}$$

Equation 2.4 % true fold change

$$\frac{\text{\% true - drug treated cells}}{\text{\% true - untreated cells}}$$

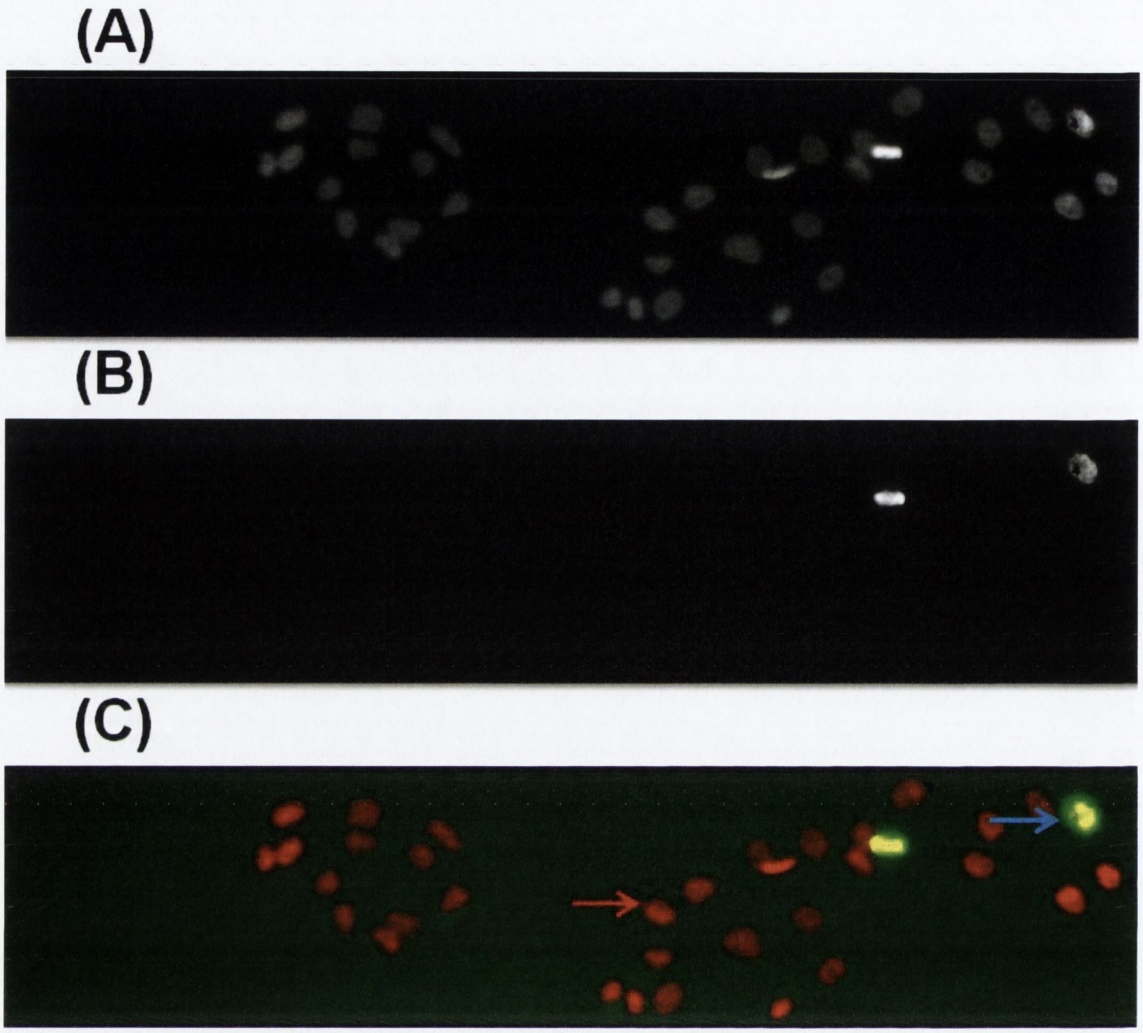

Figure 2.6 Cell cycle Phospho Histone H3 Assay.

Images were taken using the InCell fluorescence imager at 10x magnification. The above images represent 1 out of 10 fields taken from a single well of a 96 well plate containing UPN251 control treatment cells. (A) Total cell fluorescent dye image (Nuclear stain). This is used to determine the total number of cells present by labelling cell nuclei (Excitation max.=361nm, Emission max.=486nm) (B) Mouse anti-human phospho histone H3 antibody image. Antibodies were conjugated to the Alexa Flour® Dye for flourimetric quantification of mitotic cells (Excitation max.=495nm, Emission max.=519nm) (C) Fused image of A and B. Red arrow indicated cell stained with nuclear dye only. Blue arrow indicates cell in mitosis ladled with Alexa Flour® Dye.

2.1.11 Fluorescence-activated cell sorting (FACS) analysis

The cells were plated at $12.48x10^5$ cells/T75 flask and left to attach overnight and treated with cytotoxic drugs the following day. The cells received a carboplatin dose of 350µg/ml and a taxol dose of 100ng/ml for 24 hours. The CyAn™ ADP Analyser (Beckman Coulter, Ireland) was used to carry out flow cytometry. Summit v4.3 software was used to visualise and analyse the data.

2.1.11.1 FITC annexin V / PI apoptosis assay

The percentage cells undergoing apoptosis was measured using a Fluorescein isothiocyanate (FITC) annexin V and propidium iodide (PI) apoptosis assay. In brief, cells were trypsinised, washed with PBS and trypsin was inactivated with fresh media. 10^6 cells were then transferred to a 15ml tube, washed with PBS and resuspended in 1ml of 1X Annexin Binding Buffer (BD Pharmingen, USA). From the first sample (used as a calibrator control), 100µl of cells were transferred to four separate 5ml round bottom polypropylene tubes (Greiner Bio One, Germany). The first tube received no stain, the second received 1µl of PI stain only, the third received 5µl of FITC annexin V stain (BD Pharmingen, USA) only and the fourth tubes received both stains. 100µl of all other samples were transferred to separate polypropylene tubes and both dyes were added. All samples were incubated in the dark for 15mins. 800µl of Annexin Binding Buffer was added to each sample and analysed by FACS. PI was read using the PE-Texas Red laser and annexin was read using the FITC laser. 40,000 events were collected for each sample.

2.1.11.2 Cell cycle assay

PI staining solution

Per ml: 1ml PBS, 1µl Triton X100 (Sigma-Aldrich, UK), 10µl 1mg/ml PI stock

In brief, cells were trypsinised, washed with PBS and trypsin was inactivated with fresh media. 10^6 cells were then transferred to a 15ml tube, washed with PBS and resuspended in 1ml of PI staining solution. Solution was then transferred to a polypropylene tube and incubated for 10mins at room temperature. The samples were analysed by FACS. PI was read using the PE-Texas Red laser and 40,000 events were collected for each sample.

2.1.12 RNA extraction

Intact pure RNA free of DNA and protein was extracted using the miRNeasy® Mini Kit (Qiagen Ltd, UK).

2.1.12.1 Solution preparation

- QIAzol Lysis Reagent (Qiagen Ltd, UK) was wrapped in aluminum foil to protect from light.
- Chloroform was filtered through a 20µm membrane using a syringe into a sterile container.
- 100% ethanol was filtered through a 20µm membrane using a syringe into a sterile container.
- 96-100% ethanol was added to Buffer RWT and Buffer RPE concentrates to create working solutions.
- Solid DNase I (1500 kunitz units, Qiagen Ltd, UK) was dissolved in 550µl of RNase-free water and mixed gently by inverting the tube (This was not vortexed as DNase is sensitive to physical denaturation). Stock solution was removed from the glass vile and divided into single use working aliquots and stored at -20°C for up to 9 months. Thawed aliquots were suitable for use up to 6 weeks stored at 2-8°C. Once defrosted aliquots were not refrozen. DNase 1 was prepared in buffer RDD (10µl DNase added to 70µl Buffer RDD) and kept in fridge until needed.
- Diethylene Pyrocarbonate (DEPC) water was prepared. Briefly, 1000ml bottles were filled with ultrapure water and autoclaved. 1000µl of DEPC was added to each bottle and incubated at room temperature for 1-2 hours then re-autoclaved to deactivate the DEPC making the water RNase free.
- A liquid nitrogen (LN_2) container was rinsed with DEPC water, dried in an oven and left at 4°C in order to be cooled before use.

2.1.12.2 Extracting RNA from frozen tissue

2.1.12.2.1 Tissue preparation

2.1.12.2.1.1 The mortar and pestle method

This method was used for small amounts of tissue. A mortar and pestle was autoclaved, treated with RNase inhibitor RNase Away (Molecular Bio-products, USA), rinsed with DEPC to inactivate ribonucleases by covalent modification, placed in an oven to dry and cooled in a fridge. Prior to extraction they were placed in an ice box with tinfoil and pre-cooled with LN_2. The tissue was transferred from the -80°C freezer

directly to a sterile plate and cut with a sterile blade to a maximum amount of 30mg. The tissue was then immersed in the LN_2 in the mortar. The LN_2 was allowed to evaporate, but the tissue was not allowed to thaw. The tissue was then homogenised by thoroughly grinding it in the liquid nitrogen until it was ground into a fine powder. At this time, the mortar and pestle were moved into the fume hood for further homogenisation. Using a new pestle, 700µl of QIAzol lysis reagent was added. Grinding continued until the powder was liquefied (disruption). The cell lysate was pipetted into the purple shredder column in a 2ml collection tube and centrifuged in the ALC micro CENTRIFUGETTE 4204 (ALC international, Italy) at the maximum speed for 2mins to homogenise. The supernatant was pipetted into a new 2ml collection tube and the pellet was discarded.

2.1.12.2.1.2 The TissueLyser method

This method was used for large amounts of tissue. A stainless steel ball of 5mm (mean diameter) was added to 700µl of QIAzol Lysis Reagent in a 2ml collection tube. The tissue was transferred from the -80°C freezer directly to a sterile plate and cut with a sterile blade to a maximum amount of 50mg and transferred to the 2ml collection tube. The tube was closed and placed into the TissueLyser II as per manufacturer's instructions in the TissueLyser II (Qiagen Ltd, UK) handbook. The tissue was homogenised on the TissueLyser for 2mins at 20Hz. The TissueLyser rack was rotated 180° and run for another 2mins at 20Hz to allow for even homogenisation. The homogenate was transferred to a new microcentrifuge tube by pipette and the stainless steel bead was discarded.

2.1.12.2.2 Large and small RNA isolation (initial steps)

1. The tube containing the homogenate from the tissue preparation steps was placed on the benchtop at room temperature (15-25°C) for 5mins. This promotes dissociation of the nucleoprotein complexes. 140µl of chloroform was added to the homogenate, capped securely and shaken vigorously for 15secs.
2. The tube containing the homogenate was placed on the benchtop at room temperature for 2-3mins.
3. The homogenate was then centrifuged for 15mins at 12,000 x g at 4°C. After centrifugation the sample is separated into 3 phases: an upper, colourless, aqueous phase containing RNA; a white interphase; and a lower, red, organic phase. The volume of the aqueous phase will be approx 350µl.
4. The upper aqueous phase was pipetted to a new 2ml reaction tube. 1 volume of 70% ethanol was added (usually 350µl) and mixed thoroughly by vortexing. The next

step was proceeded to immediately without delay.

5. The sample (approximately 700µl) was pipetted into a mini-spin column and placed in a 2ml collection tube (including any precipitate that may have formed). The lid was closed and centrifuged at 8000 x g for 15secs at room temperature. The flow through was pipetted into a new 2ml collection tube. This contains the miRNA. The spin column was placed in a new 2ml collection tube and stored at 4°C or at room temperature to be used later in purifying for large RNA.

2.1.12.2.3 Small RNA enriched purification steps

1. 450µl of 100% ethanol (0.65 volumes) was added to the flow through from section 2.1.12.2.2 above and mixed thoroughly by vortexing. The next step was proceeded to immediately without delay.

2. 700µl of the sample was pipetted into a MinElute spin column (Qiagen, UK) placed in a 2ml collection tube. The lid was closed and centrifuged at 8000 x g at room temperature for 15secs. The flow through was discarded. This step was repeated until the entire sample had been loaded into the spin column with flow through discarded each time.

3. 500µl of Buffer RPE was pipetted into the MinElute spin column. The lid was closed and centrifuged at 8000 x g at room temperature for 15secs. The flow through was discarded.

4. 500µl of 80% ethanol was pipetted into the MinElute spin column. The lid was closed and centrifuged at 8000 x g at room temperature for 2mins to dry the spin column membrane. The flow through and collection tube was discarded. When removing the MinElute spin column, care should be taken not to contact the flow through as this would result in ethanol carryover.

5. The MinElute spin column was placed in a new 2ml collection tube. The lid was opened and centrifuged at 8000 x g at room temperature for 5mins.

6. The MinElute spin column was placed in a 1.5ml collection tube and 14µl of RNase free water was pipetted directly onto the spin column membrane. The lid was closed and centrifuged at 8000 x g for 1min to elute the miRNA enriched fraction. This tube can be stored at -80°C prior to quantification.

2.1.12.2.4 Large RNA purification steps

1. 350µl of Buffer RWT was pipetted into the Mini spin column set aside from section 2.1.14.2.2 above and centrifuged at 8000 x g for 15secs to wash. The flow through was discarded.

2. 10µl of DNase 1 stock solution was added to 70µl of Buffer RDD and mixed

gently by inverting the tube. This was not vortexed.

3. The DNase 1 incubation mix (80µl) was pipetted directly onto the Mini spin column membrane and placed on the benchtop for 15mins at 20-30°C.

4. 350µl of Buffer RWT was pipetted into the Mini spin column and centrifuged at 8000 x g for 15secs. The flow through was discarded.

5. 500µl of Buffer RPE was pipetted into the Mini spin column and centrifuged at 8000 x g for 15secs to wash the spin column membrane. The flow through was discarded.

6. Another 500µl Buffer RPE was pipetted into the Mini spin column and centrifuged at 8000 x g for 15secs to wash the spin column membrane. The flow through and column was discarded.

7. The Mini spin column was placed into a new 2ml collection tube and centrifuged at full speed for 1min with the lid open.

8. The Mini spin column was placed into a new 1.5ml collection tube and 30µl of RNase free water was pipetted directly onto the spin column membrane. This was then centrifuged at 8000 x g for 1min to elute the large RNA fraction.

9. If the expected yield was more than 30µg step 8 was repeated with the same volume of RNase free water into the same collection tube.

10. This tube was stored at -80°C prior to quantification.

2.1.12.3 Extraction of total RNA from cell lines

1. $3.12x10^5$ cells were seeded into a T75 and exposed to the desired drug treatments for 3 days. The cells were then centrifuged at 180 x g for 5mins, washed with 10ml PBS, centrifuged again, resuspended and transferred to a sterile eppendorf tube (pellets could be stored at -80°C at this point)

2. The cell pellets were taken from storage in the -80 freezer and allowed to thaw on ice. They were loosened thoroughly by flicking the tube and 700µl of QIAzol Lysis Reagent was added to the sample and mixed by vortex for 1 min.

3. The cell lysate was pipetted into the purple shredder column in a 2ml collection tube and centrifuged at max speed for 2mins to homogenise.

4. The supernatant was pipetted into a new 2ml collection tube and the pellet was discarded.

5. The tube containing the homogenate was placed on the benchtop at room temperature (15-25°C) for 5mins promoting dissociation of the nucleoprotein complexes.

6. 140µl of chloroform was added to the homogenate, capped securely and shaken vigorously for 15secs. Thorough mixing was important for subsequent phase

separation.

7. The tube containing the homogenate was placed on the benchtop at room temperature for 2-3mins.

8. The homogenate was then centrifuged for 15mins at 12,000 x g at 4°C. After centrifugation, the sample is separated into 3 phases: an upper, colourless, aqueous phase containing RNA; a white interphase; and a lower, red, organic phase. The volume of the aqueous phase will be approx 350µl.

9. The upper aqueous phase was transferred to a new collection tube and 1.5 volumes (approx 525µl) of 100% ethanol was added and mixed thoroughly by pipetting up and down a number of times. The sample was not centrifuged and the next step was carried out immediately.

10. 700µl of the sample, including any precipitate that may have formed was transferred to an RNeasy Mini spin column in a 2ml collection tube. The lid was closed and centrifuged at 12,000 x g for 15 seconds at room temperature. The flow through was discarded.

11. Step 10 was repeated using the same collection tube until the entire sample was used.

12. 350µl of Buffer RWT was pipetted into the Mini spin column and centrifuged at 12,000 x g for 15secs to wash. The flow through was discarded.

13. 10µl of DNase 1 stock solution was added to 70µl of Buffer RDD and mixed gently by inverting the tube. This should not be vortexed.

14. The DNase 1 incubation mix (80µl) was pipetted directly onto the Mini spin column membrane and placed on the benchtop for 15mins at 20-30°C.

15. 350µl of Buffer RWT was pipetted into the Mini spin column and centrifuged at 12,000 x g for 15secs. The flow through was discarded.

16. 500µl of Buffer RPE was pipetted into the Mini spin column. The lid was closed and centrifuged at 12,000 x g for 15 seconds to wash the column. The flow through was discarded.

17. Another 500µl of Buffer RPE was pipetted into the Mini spin column. The lid was closed and centrifuged at 12,000 x g for 15 seconds to dry the column. The flow through was discarded.

18. The Mini spin column was placed into a new 2ml collection tube and centrifuged at full speed for 1min with the lid open.

19. The Mini spin column was placed into a new 1.5ml collection tube and 40µl of RNase free water was pipetted directly onto the spin column membrane. This was then centrifuged at 12,000 x g for 1min to elute the total RNA.

20. If the expected yield was more than 30µg, step 19 was repeated with the same

volume of RNase free water into the same collection tube.

21. This tube can be stored at -80°C prior to quantification.

2.1.12.4 Quantification of RNA content

The amount and integrity of RNA in extracted samples was measured using a traditional spectrometer (Eppendorf BioPhotometer (Hamburg, Germany)) at 260nm. Total RNA content in ng/µl and sample integrity using 260/280 and 260/230 ratios were recorded.

2.1.13 Evaluation of RNA integrity from cell line total RNA extracts

The integrity of the total RNA samples extracted from UPN251 and sublines were measured using microfluidic analysis. Chips from the RNA 6000 Nano kit (Agilent Technologies, USA) were run on the Agilent 2100 Bioanalyzer as per the protocol. An RNA Integrity Number (RIN) was obtained from this procedure which acted as a measure of RNA integrity. RIN values above 7 were deemed suitable to use in downstream gene expression analysis. The RNA 6000 Nano kit protocol is described in brief.

2.1.13.1 Preparing chip priming station

With each new kit the old syringe on the chip priming station was replaced. After the old syringe was unscrewed the plastic cap on the new syringe was removed and it was inserted into the clip. It was then slid into the hole of the luer lock adapter and screwed tightly to the chip priming station. The base plate of the chip priming station was moved to position 'C'. After this, the syringe clip was adjusted so that it was at its highest position.

2.1.13.2 Preparing the Bioanalyzer

The lid of the bioanalyser was opened to ensure that the electrode cartridge was inserted. Any chip from a previous run was removed and the chip selector was moved to position (1). Before each run, the electrodes were decontaminated by filling the electrode cleaner chip with 350µl of RNase Away (Molecular Bio-products, USA) and placing it into the Agilent Bioanalyzer 2100 for 1 min. Another electrode cleaner was filled with 350µl RNase-free water and placed into the Bioanalyzer for 10secs. The lid was left open for 10secs after to allow water to evaporate. After each run the electrodes were cleaned with RNase free water (Sigma-Aldrich, UK) as above.

2.1.13.3 Preparing the RNA ladder

After kit arrival the ladder was pipetted into an RNase free vial. The ladder was heat denatured for 2mins at 70°C and then cooled on ice. Aliquots were made and stored at -80°C. Aliquots were thawed on ice before use.

2.1.13.4 Agilent RNA 6000 nano assay protocol

1. All reagents were equilibrated to room temperature before use. 550µl of the gel matrix (Red) was placed into the top receptacle of a spin filter. The spin filter was micro-centrifuged for 10mins at 1500 x g. 65µl of filter gel was aliquoted into 0.5ml RNase free tubes for storage at 4ºC for up to one month.
2. The dye concentrate (blue) was vortexed for 10secs. 1µl was added to a 65µl aliquot of filtered gel and vortexed thoroughly. The tube was spun for 10mins at room temperature at 18300 x g.
3. A new RNA Nano chip was placed on the chip priming station and 9µl of the gel-dye mix was pipetted into the bottom of the well marked 'G'. The plunger of the chip priming station was set to 1ml and then closed. The plunger was pushed down slowly until it was held by the clip for exactly 30secs before being released and allowed to move back to 1ml position. 0.9µl of the gel-dye mix was then pipetted into the two wells above the well marked 'G'.
4. 5µl of the marker (green) was loaded into the ladder well and each sample well. 1µl of the RNA ladder was pipetted into the ladder well and then 1µl of each sample was pipetted into each sample well (12 total).
5. The chip was vortexed in the IKA vortex mixer (IKA®, Germany) for 1min at 2400rpm and then placed into the bioanalyzer within 5mins to start the run.
6. The chip was analysed using the 2100 expert software running the Eukaryotic Total RNA Nano assay.

2.1.14 Affymetrix gene expression analysis protocol

The Affymetrix GeneChip® Human Gene 2.0 ST Arrays were used for the analysis of gene expression. These chips offer a comprehensive transcriptome coverage including >30,000 coding transcripts and >11,000 long intergenic non-coding transcripts. They measure alternative splicing event/transcript variants and have probes designed to have maximum coverage of exons. They show high reproducibility with a signal correlation coefficient of ≥ 0.99. They provide the ability to assess whole-transcriptome gene-expression at gene and exon levels.

The entire process was completed over a three day work flow, as seen in Figure 2.7. Initial total RNA samples were first quantified using a traditional spectrometer and then bioanalysed to ensure samples were of suitable RNA integrity before commencement of this protocol (see section 2.1.13). In brief, the Affymetrix GeneChip® WT PLUS Reagent Kit was used during the first two days of sample preparation from total RNA samples. The poly-A controls were prepared first. This was followed by first-strand cDNA synthesis, then second strand cDNA synthesis. Next *in vitro* transcription was used in order to produce cRNA. This was then purified and the cRNA yield was assessed. Second cycle ss-cDNA was then synthesised and hydrolysed using RNase H. The second cycle ss-cDNA was then purified and the yield was obtained. The GeneChip® WT Terminal Labelling and Hybridisation User Manuals were used in order to fragment, label and hybridise the ss-cDNA to the HuGene 2.0 chips. Finally, on day three the GeneChip® Expression Wash, Stain and Scan User Manual was used to wash, stain and scan the chips. All master mixes used in this process were prepared prior to each step of the protocol to improve reproducibility. Enzyme solutions were flick-mixed and spun down in a centrifuge before each PCR step.

2.1.14.1 Preparation of total RNA and Poly-A controls

The recommended concentration of total RNA per sample to be used in this protocol was 50-500ng. For this study 250ng of total RNA was used. Poly-A RNA spikes were used as exogenous positive controls. Each chip contains probe sets for several *B. subtilis* genes that are absent in eukaryotic samples (*lys, phe, thr* and *dap*). The controls were *in vitro* synthesised and premixed at staggered concentrations. The controls were amplified and labelled with the total RNA samples. The hybridisation intensities of the controls provide quality control for sample preparation and help monitor labelling and hybridisation.

The Poly-A stock was serially diluted with Poly-A control dilution buffer to the final concentration listed in Table 2.3. The dilution factors were calculated appropriately for starting RNA concentration in this study. 2µl of the final dilution was added to 3µl of total RNA sample in a nuclease free tube (250ng total RNA in RNase free water).

2.1.14.2 First -strand cDNA synthesis

Total RNA samples were reverse transcribed with primers containing a T7 promoter sequence. The reaction synthesises ss-cDNA with a T7 promoter sequence at its 5' end.

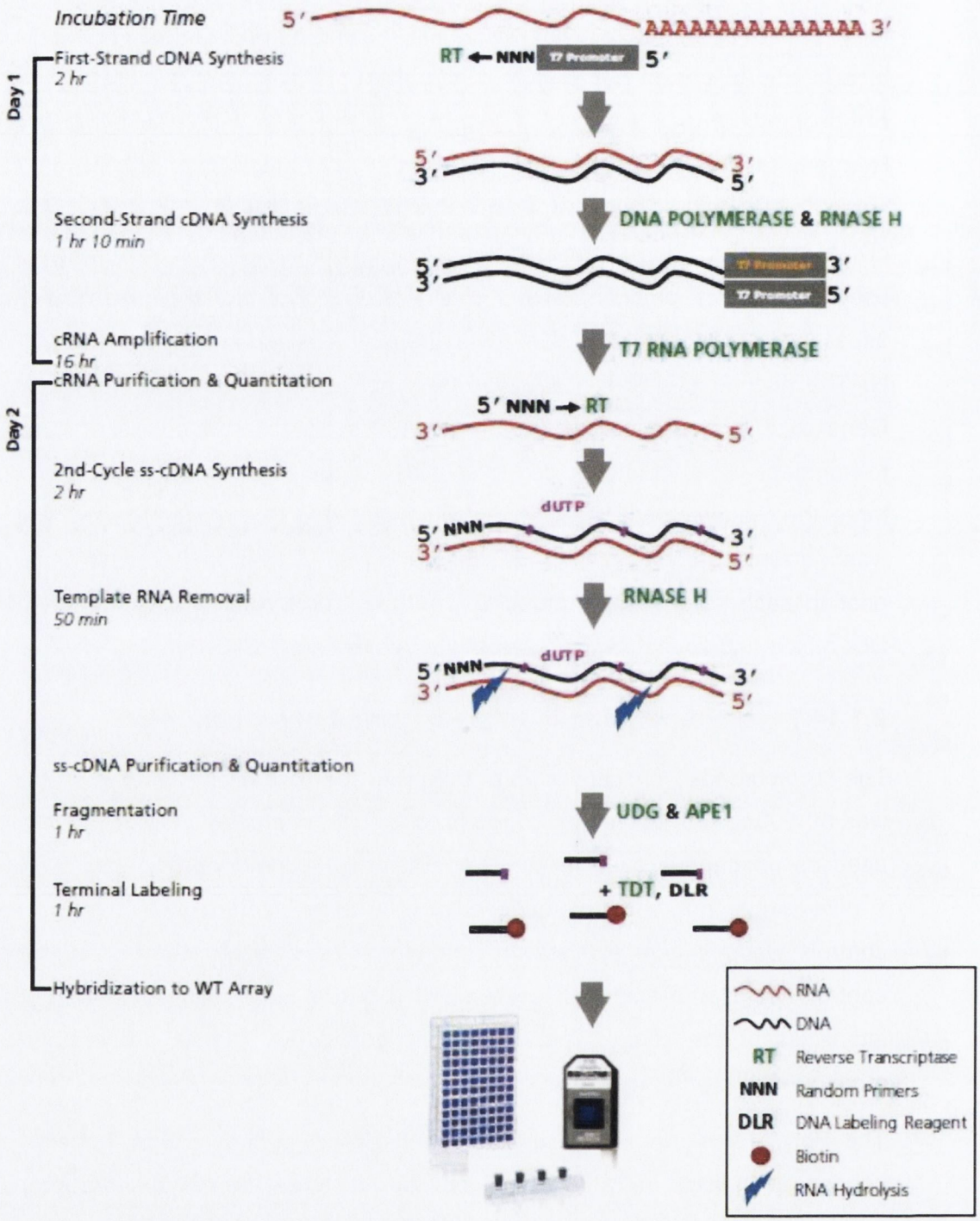

Figure 2.7 Affymetrix suggested three day workflow (gene expression analysis).

Table 2.3 Final concentrations of Poly-A RNA controls when added to total RNA samples

Poly-A RNA Spike	Final Concentration (Ratio of copy number)
Lys	1:100,000
Phe	1:50,000
Thr	1:25,000
Dap	1:6,667

Reagents were thawed and placed on ice. A master mix was prepared on ice as per Table 2.4. On ice 5µl of the master mix was added to 5µl of sample containing total RNA and Poly-A controls to a total reaction volume of 10µl. Tubes were vortexed, spun down and incubated for 1 hour at 25°C, 1 hour at 42°C and 2mins at 4°C in a thermal cycler with heated lid. Following incubation tubes were centrifuged briefly and placed on ice.

2.1.14.3 Second-strand cDNA synthesis

In this step, ss-cDNA was converted to ds-cDNA. This acted as a template for *in vitro* transcription. The reaction used DNA polymerase and RNase H to degrade the RNA and synthesise second-strand cDNA. Reagents were thawed and placed on ice. A master mix was prepared on ice as per Table 2.5. On ice 20µl of the master mix was added to 10µl of sample containing the first-strand cDNA to a total reaction volume of 30µl. Tubes were vortexed, spun down and incubated for 1 hour at 16°C, 10mins at 65°C and 2mins at 4°C in a thermal cycler with the lid off. Following incubation tubes were centrifuged briefly and placed on ice.

2.1.14.4 cRNA synthesis by *in vitro* transcription

Antisense RNA (cRNA) was synthesised and amplified by *in vitro* transcription (IVT) of the second-strand cDNA template using T7 RNA polymerase. This T7 IVT method was based on the Eberwine or RT-IVT method (*Van Gelder et al. 1990*). Reagents were thawed and placed on ice. A master mix was prepared on ice as per Table 2.6. On ice, 30µl of the master mix was added to 30µl of sample containing the second-strand cDNA to a total reaction volume of 60µl. Tubes were vortexed, spun down and incubated for 16 hours at 40°C and 2mins at 4°C in a thermal cycler with heated lid. Following incubation tubes were centrifuged briefly and placed on ice.

Table 2.4 First-strand cDNA master mix components.

Each component was added in sequence with 5% excess prepared in order to allow for pipetting loss.

Components	Volume for one reaction (µl)
First-Strand Buffer	4
First-Strand Enzyme	1
Total Volume	5

Table 2.5 Second-strand cDNA master mix components.

Each component was added in sequence with 5% excess prepared in order to allow for pipetting loss.

Components	Volume for one reaction (µl)
Second-Strand Buffer	18
Second-Strand Enzyme	2
Total Volume	20

Table 2.6 IVT master mix components.

Each component was added in sequence with 5% excess prepared in order to allow for pipetting loss.

Components	Volume for one reaction (µl)
IVT Buffer	24
IVT Enzyme	6
Total Volume	30

2.1.14.5 cRNA purification

The produced cRNA was purified in order to remove elements from the samples, which may have compromised RNA stability (salts, inorganic phosphates, unincorporated nucleotides and enzymes). Prior to purification, 50µl of nuclease free water per sample was heated to 65ºC for at least 10mins. Purification beads were mixed thoroughly by vortexing for 3mins to ensure all beads were fully dispersed and 100 µl of per sample (plus ~ 10% extra for pipetting loss) was transferred to a nuclease free tube. Fresh dilutions of 80% ethanol wash solution were prepared from 100% ethanol and nuclease free water. Approximately 600µl (plus ~ 10% extra for pipetting loss) was prepared. Purification of cRNA was carried out at room temperature.

For each sample, the previously mixed and separated purification beads were briefly vortexed again to re-suspend any magnetic particles that may have settled. 100µl of the purification beads were added to 60ul of cRNA sample and mixed up and down 10 times before transferring to the well of a U-bottom plate. The sample was then incubated at room temperature for 10mins to allow the cRNA to bind to the purification beads. The plate was then moved to a magnetic stand in order to capture the purification beads. After approximately 5mins the mixture appeared transparent and the purification beads formed pellets against the magnets of the magnetic stand. The supernatant was carefully aspirated without disturbing the pellets while still on the magnetic stand. The purification beads were washed three times by addition and removal of 200µl of 80% ethanol wash solution for 30 second incubations. After the final wash, the 80% ethanol wash solution was completely removed and left to air dry until no liquid was visible yet the beads appeared shiny. Care was taken not to over dry the beads, as this would have reduced the elution efficiency. If over dried, the bead surface will appear dull and may be cracked. After drying, the plate was removed from the magnetic stand and 50µl of the preheated (65ºC) nuclease free was added to the sample for 1min to elute the cRNA from the beads. The samples were mixed well by pipetting up and down 10 times, after which the plate was moved back to the magnetic stand for 5mins to capture the purification beads. The resulting supernatant which contained the eluted cRNA was transferred to a nuclease free tube and placed on ice. The cRNA yield of each sample was then assessed using the NanoDrop spectrophotometer.

2.1.14.6 Second-Cycle ss-cDNA synthesis

The cRNA was reverse transcribed to produce sense-strand cDNA using second cycle primers. The sense-strand cDNA contains deoxyuracil triphosphate (dUTP) at a fixed ratio relative to deoxythymidine triphosphate (dTTP).

Reagents were thawed and placed on ice. On ice, 625ng/µl (15µg) of cRNA was made up to a final volume of 24µl in nuclease-free water. 4µl of second cycle primers were added to the cRNA samples and mixed thoroughly by vortexing, then centrifuged briefly. The samples were incubated for 5mins at 70°C, 5mins at 25 °C and 2mins at 4°C in a thermal cycler with heated lid. Following incubation, tubes were centrifuged briefly and placed on ice.

A master mix was prepared on ice as per Table 2.7. On ice 12µl of the master mix was added to 28µl of sample to a total reaction volume of 40µl. The tubes were vortexed, spun down and incubated for 10mins at 25°C, 90mins at 42 °C, 10mins at 70°C and 2mins at 4°C in a thermal cycler with a heated lid. Following incubation, tubes were centrifuged briefly and placed on ice.

2.1.14.7 RNase H hydrolysis

The cRNA template was degraded by RNase H, leaving free ss-cDNA.

On ice, 4µl of RNase H was added to the ss-cDNA samples and mixed thoroughly by vortexing, then centrifuged briefly. The samples were incubated for 45mins at 37°C, 5mins at 95 °C and 2mins at 4°C in a thermal cycler with a heated lid. Following incubation, tubes were centrifuged briefly and placed on ice. On ice, 11µl of nuclease-free water was added to each sample. The tubes were mixed by vortexing and centrifuged briefly.

2.1.14.8 Second-cycle ss-cDNA purification

The produced ss-cDNA was purified in order to prepare samples, by removing salts, unincorporated nucleotides and enzymes.

The purification of second-cycle ss-cDNA was the same as purification of cRNA (section 2.1.14.5) samples with some slight modifications:

- After the transfer of 100µl of purification beads to the samples and transfer to U-bottomed plate, 150µl of 100% ethanol was added to the samples and pipetted up and down for thorough mixing. The sample was then incubated for 20mins to allow the ss-cDNA to bind to the purification beads.

Table 2.7 Second-cycle ss-cDNA master mix components.

Each component was added in sequence with 5% excess prepared in order to allow for pipetting loss.

Components	Volume for one reaction (µl)
Second-cycle ss-cDNA Buffer	8
Second-cycle ss-cDNA Enzyme	4
Total Volume	12

- After drying, the plate was removed from the magnetic stand and 30µl of the preheated (65°C) nuclease free water was added to the sample for 1min to elute the ss-cDNA from the beads.

The resulting supernatant that contained the eluted ss-cDNA was transferred to a nuclease free tube and placed on ice. The ss-cDNA yield of each sample was then assessed using the NanoDrop Spectrophotometer.

2.1.14.9 Fragmentation of ss-cDNA

In order to fragment the ss-cDNA, a fragmentation reaction was set up as per Table 2.8 in 0.2ml strip tubes. The fragmentation master mix was set up using Table 2.9. 16.8µl of the reaction master mix was added to the prepared samples of 5.5µg ss-cDNA. The tube was gently vortexed, centrifuged briefly, and incubated for 60mins at 37°C, 2mins at 93°C and 2mins at 4°C in a thermal cycler with a heated lid. Following incubation, tubes were centrifuged briefly and 45µl of the sample was transferred to a new 0.2ml strip tube.

2.1.14.10 Labelling of fragmented ss-cDNA

In order to label the fragmented ss-cDNA, 15µl of the labelling reaction master mix prepared as per Table 2.10 was added to 45µl of sample prepared in section 2.1.14.9. The samples were then flick-mixed, spun down and incubated for 60mins at 37°C, 10mins at 70°C and 2mins at 4°C in a thermal cycler with a heated lid. Following incubation, the tubes were centrifuged briefly.

Table 2.8 Fragmentation reaction sample preparation.

Components	Volume/Amount in one reaction
ss-cDNA	5.5g
RNase-free water	Up to 31.2µl
Total Volume	31.2µl

Table 2.9 Fragmentation master mix components.

Each component was added in sequence with 5% excess prepared in order to allow for pipetting loss.

Components	Volume for one reaction (µl)
RNase-free water	10
10X cDNA Fragmentation Buffer	4.8
UDG, 10U/µl	1
APE 1, 1,000U/µl	1
Total Volume	16.8

Table 2.10 Labelling reaction master mix components.

Each component was added in sequence with 5% excess prepared in order to allow for pipetting loss.

Components	Volume for one reaction (µl)
5X TdT Buffer	12
TdT	2
DNA Labelling reagent, 5mM	1
Total Volume	15

2.1.14.11 Hybridisation

In preparation for hybridisation, three heating blocks were set up at 65ºC, 99ºC and 45ºC. The stocks of eukaryotic hybridisation controls were heated to 65ºC for 5mins to completely re-suspend the cRNA before aliquoting. 109µl of the hybridisation cocktail master mix (as per Table 2.11) was added to 41µl of the labelled and fragmented ss-cDNA (~25ng/µl) to a total volume of 150µl in 1.5ml RNase-free tube. The tube was gently vortexed and spun down, then heated at 99ºC for 5mins and immediately cooled to 45ºC for 5mins. The cocktail was then centrifuged at max speed for 1min in the microcentrifuge 5417C (Eppendorf, Germany). The HuGene 2.0 ST array chips were equilibrated to room temperature before use and labelled with the name of the sample to be hybridised to the chip. 130µl of the specific sample was injected into the array through one of the septa (Figure 2.8). Two pipette tips were required to fill the probe array cartridge; one for filling and the second to allow venting of air from the hybridisation chamber. It is important that the bubble in the hybridisation chamber after filling moves freely upon rotation to ensure that the hybridisation cocktail makes contact with all parts of the array. Arrays were placed in a hybridisation oven at 45ºC and incubated for 17 hours ± 1 hour at 60rpm.

2.1.14.12 Fluidics station and scanner setup

Sample files were created using the Affymetrix GeneChip® Command Console (AGCC) software for all samples. The Affymetrix GeneChip® fluidics station 450 was set up using the AGCC software and primed to insure all lines contained the correct fluids before commencing the staining process.

2.1.14.13 Array washing and staining

The staining reagents were prepared for each array by adding 600µl of Stain Cocktail 1 to an amber 1.5ml microcentrifuge vial, 600µl of Stain Cocktail 2 to a clear 1.5ml microcentrifuge vial and 800µl of Array Holding Buffer to a clear 1.5ml microcentrifuge vial. Tubes were spun at max speed for 1min in the microcentrifuge 5417C (Eppendorf, Germany) to remove any air bubbles present. The arrays were removed from the hybridisation oven. The hybridisation cocktail was removed through one septum, while air was vented through the other, as was done previously in section 2.1.14.12. The hybridisation cocktail was stored at -20ºC in the event that problems arouse with the hybridisation procedure. The array was filled with 160µl of wash buffer A and kept at room temperature. The fluidics station was capable of staining four arrays per run and took approximately 90mins. Additional arrays were kept at 4ºC for up to 4hours and

Table 2.11 Hybridisation cocktail master mix components (mRNA).

Each component was added in sequence with 5% excess prepared in order to allow for pipetting loss.

Components	Volume for one reaction (µl)	Final Concentration
Control Oligonucleotide B2 (3nM)	2.5	50pM
20X Eukaryotic Hybridisation Cont (bioB, bioC, bioD and cre)	7.5	1.5,5,25 and 100pM respectively
2X Hybridisation Mix	75	1X
DMSO	10.5	7%
Nuclease-Free Water	13.5	
Total Volume	109	

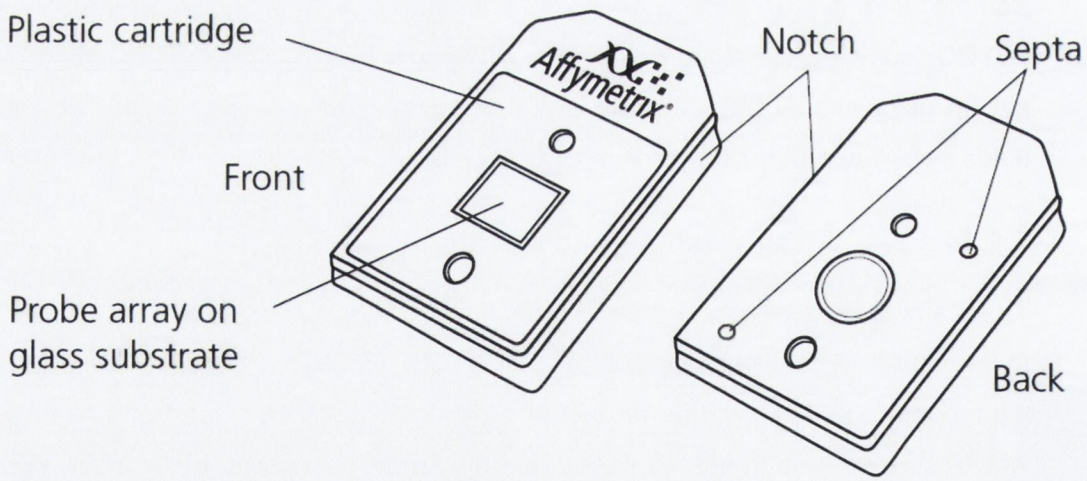

Figure 2.8 Affymetrix GeneChip® Array.

The sample is pipetted into the array through one of the septa on the back of the chip. Air is vented from the chip by placing a pipette tip in the other septa on the back of the chip while sample is being pipetted in. A bubble which is seen to float freely should be seen in order to allow the hybridisation cocktail to contact the entire probe surface.

were re-equilibrated to room temperature 45mins before staining. The AGCC fluidics control software was used to programme the wash solutions within the fluidics station. The arrays were inserted into the wash blocks in each wash station and the on-screen instructions were followed for loading the staining solutions.

2.1.14.14 Array scanning

Following staining in the fluidics station, the arrays were removed and checked for air bubbles. If no bubbles were present, they were moved to the Affymetrix GeneChip® Scanner 3000. If air bubbles were present, the arrays were replaced into the fluidics station and on-screen instructions were followed to remove bubbles. The scanner was switched on 10mins prior to a run to warm up. If any dust or dirt was present on the glass surface of the array, it was carefully removed using tissue or blowing. The septa were covered using 'tough spot' stickers to prevent the holding array buffer from leaking out. The arrays were placed into the scanner and the AGCC scanner control software was used to begin scanning. When scanning was complete, the arrays were removed from the scanner and stored at room temperature.

2.1.15 MiRNA expression analysis

The Affymetrix GeneChip® miRNA 3.0 Arrays were used for the analysis of miRNA expression. These chips provide complete coverage of the miRBase v17 and give snoRNA and scaRNA probes on the same chip. The design allows for independent interrogation of pre-miRNA and mature miRNA in the same experiment with high sensitivity (detects 94% of miRNA transcripts at 1.0 amol) and high reproducibility (0.95 inter- and intra-lot).

Sample preparation using the Affymetrix FlashTag™ Biotin Labelling Kit takes approximately 45mins to complete. The initial total RNA samples were first quantified using a traditional spectrometer (Eppendorf BioPhotometer (Hamburg, Germany)) and then bioanalyzed to ensure samples were of suitable RNA integrity before commencement (see section 2.1.13). This protocol can utilise samples with severely degraded RNA and low molecular weight RNA. In brief, 1000ng of total RNA samples were poly A tailed and biotinylated signal molecules were ligated to the target RNA. An Enzyme Linked Oligosorbent Assay (ELOSA) was carried out to confirm that the Affymetrix FlashTag Biotin Labelling Kit had performed appropriately in the biotin labelling process. The samples were then hybridised to the Affymetrix GeneChip® miRNA 3.0 Arrays overnight. The Affymetrix GeneChip® Expression Wash, Stain and Scan User Manual were used to wash stain and scan the chips.

All master mixes used in this process were prepared prior to each step of the protocol to improve reproducibility.

2.1.15.1 Poly (A) tailing

1mM Tris (pH8)

49.95ml nuclease free water, 50ul 1M Tris-HCl (USB), pH8

1000ng of total RNA was made up in 8µl of nuclease free water and placed on ice. 2µl of the RNA spike control oligos (vial 8) were added to each sample. The ATP Mix (vial 3) was diluted 1:500 in 1mM Tris (pH 8.0). A tailing master mix was prepared on ice (Table 2.12). 5µl of the master mix was added to the 10µl of RNA/Spike control oligos for a final volume of 15µl. The samples were mixed gently and heated at 37°C for 15mins.

2.1.15.2 FlashTag™ biotin HSR ligation

The samples were microcentrifuged briefly and placed on ice. 4µl of 5X FlashTag Biotin HSR Ligation mix (vial 5) was added to each sample. 2µl of T4 DNA Ligase (vial 6) was then added to each sample. The T4 DNA Ligase was not vortexed and was taken from storage immediately prior to use and kept on ice. The samples were mixed gently and microcentrifuged briefly after the components were added and then incubated at room temperature for 30mins. The reaction was stopped by adding 2.5µl HSR Stop Solution (vial 7) and then mixed and microfuged. 2µl of the biotin-labelled sample was removed for use in the Enzyme Linked Oligosorbent Assay (ELOSA) QC Assay. The remaining sample can be stored on ice for 6 hours or at -20°C for 2 weeks prior to hybridisation to the Affymetrix® GeneChip® miRNA arrays.

2.1.15.3 Enzyme linked oligosorbent assay (ELOSA) QC assay

This optional quality control step is used to ensure that the Affymetrix FlashTag™ Biotin HSR Labelling Kit has performed appropriately as a biotin labelling process. The ELOSA detects RNA Spike Control Oligos which are part of the Affymetrix FlashTag™ biotin HSR labelling reactions via a colorimetric ELOSA assay. It detects the hybridisation of the biotin-labelled RNA Spike Control Oligos to the complementary ELOSA Spotting Oligos immobilised onto the microtitre plate wells (Nunc Flat bottom Immobilizer™ Amino – 8 well strips, Fisher Scientific, Ireland) 2ul of each sample was saved after completion of the Affymetrix FlashTag™ biotin HSR ligation step (2.1.15.2) to be run on the ELOSA.

Table 2.12 Tailing master mix components.

Each component was added in sequence with 5% excess prepared in order to allow for pipetting loss. PAP enzyme was not vortexed and was and taken from storage immediately before use.

Components	Volume for one reaction (µl)
10X Reaction Buffer (vial 1)	1.5
25mM $MnCl_2$ (vial 2)	1.5
Diluted ATP Mix (vial 3 dilution)	1
PAP Enzyme (vial 4)	1
Total Volume	5

25% dextran sulphate

5ml 50% dextran sulphate (Merck Millipore, Ireland), 5ml nuclease free water, vortexed thoroughly

1X PBS

100ml 10X PBS (Applied Biosystems, USA), 900ml nuclease free water, pH7.4

1X PBS, 0.02% Tween-20

100ml 10X PBS (Applied Biosystems, USA), 0.2ml Tween-20 (Sigma-Aldrich, UK), 899.8ml nuclease free water, pH 7.4

5% BSA in 1X PBS

2g powdered BSA (Sigma-Aldrich, UK), 1X PBS (Applied Biosystems, USA) to final volume of 40ml vortexed. Stored as 8 5ml aliquots at -20°C for up to 6 months.

5X SSC, 0.05% SDS, 0.005% BSA

2.5ml 20X SSC (Applied Biosystems, USA), 0.05ml 10% SDS (Applied Biosystems, USA), 0.01ml 5% BSA in 1X PBS, nuclease free water to a final volume of 10ml. Stored as 10 1ml aliquots at -20°C for up to 6 months. Once thawed, aliquots were stored for 1 week at 4°C.

2.1.15.3.1 Coating wells with ELOSA Spotting Oligos

The ELOSA Spotting Oligos (vial 9) were diluted 1:50 in 1X PBS (Applied Biosystems, USA). 75µl of the diluted ELOSA Spotting Oligos were transferred to each well of the plate, ensuring the pipette tip did not touch the bottom of the wells. The plate was covered with an adhesive plate sealer (VWR) and incubated overnight at 4°C. Plates can be stored in this way for up to 2 weeks.

2.1.15.3.2 Washing and blocking

The ELOSA Spotting Oligos were removed by expelling the liquid into a sink. Wells were washed twice with 1X PBS, 0.02% Tween-20 and blotted dry. 150µl of 5% BSA in 1X PBS was added to each well. The plate was covered and incubated for 1 hour at room temperature.

2.1.15.3.3 Sample hybridisation

A hybridisation master mix was prepared as per Table 2.13. The master mix was gently vortexed until the dextran sulphate was in solution and briefly microcentrifuged. The positive control was prepared by adding 2µl of vial 10 to 50.5µl of master mix. The negative control was prepared by adding 2µl of water to 50.5µl of master mix. Each sample was prepared by adding 50.5µl of master mix to the 2µl of saved biotin labelled sample from section 2.1.15.2. The BSA blocking solution was removed from the plate by expelling the liquid into a sink. 52.2µl of the hybridisation solution was then added to each designated well. The plates were then covered and incubated for 1 hour at room temperature.

2.1.15.3.4 SA-HRP binding

The SA-HRP (Thermo Fisher Scientific Inc, USA) was diluted 1:4000 in 5% BSA in 1X PBS. The hybridisation solution was removed by expelling liquid into a sink. The wells were washed 3-4 times with 1X PBS, 0.02% Tween-20 and blotted dry. 75µl of the diluted SA-HRP was added to each well. Wells were covered and incubated for 30mins at room temperature.

2.1.15.3.5 Signal development

The SA-HRP was removed by expelling liquid into a sink. The wells were washed 3 times with 1X PBS, 0.02% Tween-20. 100µl of TMB Substrate (Thermo Fisher Scientific Inc, USA) was added to each well. The plate was covered and incubated at room temperature for 30mins in the dark. The substrate turned blue for positive results. At this stage, the TMB stop reagent was added for quantitation.

Table 2.13 Hybridisation master mix components.

Each component was added in sequence with 5% excess prepared in order to allow for pipetting loss.

Components	Volume for one reaction (µl)
5X SSC, 0.05% SDS, 0.005% BSA	48.0
25% Dextran sulphate	2.5
Total Volume	50.5

The blue substrate was converted to a yellow colour (see Figure 2.9). The plate was then read on a plate reader at 450nm. A reading greater than 0.1 OD over the negative control was considered positive.

2.1.15.4 Hybridisation

After achieving positive results from the above ELOSA assay, hybridisation of samples to the Affymetrix GeneChip® miRNA 3.0 arrays was carried out. In preparation for the hybridisation procedure, three heating blocks were set up at 65°C, 99°C and 45°C. The 20X Eukaryotic Hybridisation controls were heated for 5mins at 65°C. All reagents needed for the hybridisation cocktail (shown in Table 2.14) were brought to room temperature and a hybridisation cocktail was prepared. 110.5µl of the hybridisation cocktail master mix was added to 21.5µl of the biotin labelled samples (from section 2.1.15.2) to a total volume of 132µl in 1.5ml RNase-free tube. The tube was gently vortexed and spun down, then heated at 99°C for 5mins, and immediately cooled to 45°C for 5mins. The cocktail was then centrifuged at maximum speed for 1min. The Affymetrix GeneChip® miRNA 3.0 array chips were equilibrated to room temperature before use and labelled with the name of the sample to be hybridised to the chip. 130µl of the specific sample was injected into the array through one of the septa (Figure 2.8 (section 2.1.14.11)). Two pipette tips were required to fill the probe array cartridge, one for filling and the second to allow venting of air from the hybridisation chamber. It is important that the bubble in the hybridisation chamber after filling moves freely upon rotation to ensure that the hybridisation cocktail makes contact with all parts of the array. Arrays were placed in a hybridisation oven at 48°C and incubated for 17 hours ± 1 hour at 60rpm.

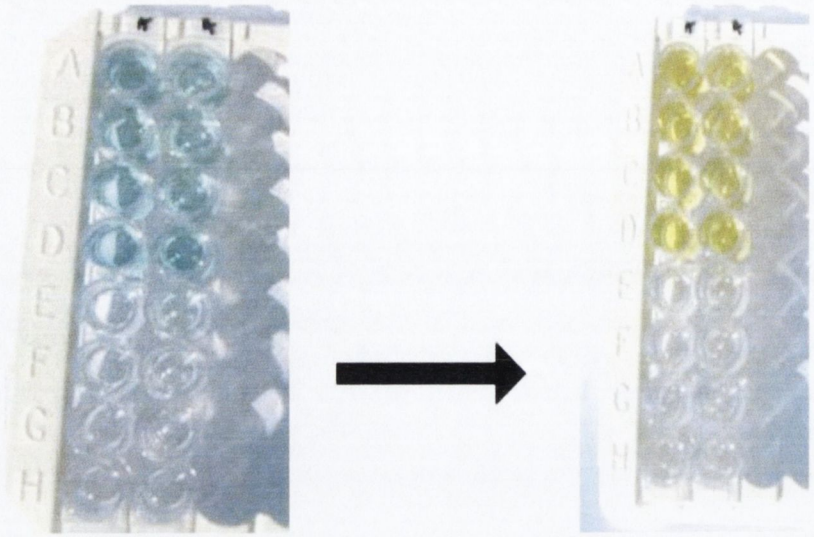

Figure 2.9 ELOSA signal development.

TMB substrate turns from blue to yellow after addition of TMB stop reagent if positive result is obtained.

Table 2.14 Hybridisation cocktail master mix components (miRNA).

Each component was added in sequence with 5% excess prepared in order to allow for pipetting loss.

Components	Volume for one reaction (µl)	Final Concentration
Control Oligonucleotide B2 (3nM)	2.2	50pM
20X Eukaryotic Hybridisation Controls (bioB, bioC, bioD and cre)	6.6	1.5,5,25 and 100pM respectively
2X Hybridisation Mix	66	1X
DMSO	10	9.7%
27.5% Formamide (vial 12)	19.2	4%
Nuclease-Free Water	3.7	
Total Volume	110.5	

2.1.15.5 Array staining, washing and scanning

Fluidics station and scanner setup, array washing and staining and array scanning for the Affymetrix GeneChip® miRNA 3.0 array chips were carried out as per the same methods used for the Affymetrix GeneChip® Human Gene 2.0 ST arrays chips following sections 2.1.14.12, 2.1.14.13 and 2.1.14.14 respectively.

2.1.16 TaqMan® quantitative polymerase chain reaction (qPCR)

TaqMan® quantitative PCR (qPCR) was carried out for genes and miRNAs of interest. Table 2.15 gives a list of all the probes used in this study.

2.1.16.1 Reverse Transcription (genes)

cDNA was reverse transcribed from extracted large RNA samples using the High Capacity cDNA Reverse Transcription Kit (Applied Biosystems, USA). In brief, a reverse transcription master mix was prepared on ice, as per Table 2.16, in a 2ml eppendorf tube. This master mix contains universal primers and performs a global reverse transcription for all of the large RNA in a given sample. The master mix was mixed gently. For each reaction, 10µl of the reverse transcription master mix and 10µl of RNA sample (300ng of RNA made in 10µl of nuclease-free water) was added to a 0.2ml PCR tube (Fisher Scientific, Ireland) and kept on ice. The PCR tubes were briefly centrifuged to spin down contents and eliminate air bubbles. The tubes were then incubated at 25°C for 10mins, 37°C for 2hours, 85°C for 5mins and held at 4°C in a thermal cycler. The samples (cDNA) were then stored at -20°C. This step results in one cDNA sample of 20µl for each large RNA sample reverse transcribed.

2.1.16.2 Reverse Transcription (miRNA)

cDNA was reverse transcribed from extracted small RNA samples using the TaqMan® MicroRNA Reverse Transcription Kit (Applied Biosystems, USA). In brief, a miRNA reverse transcription master mix was prepared on ice for each miRNA target of interest, as per Table 2.17. Only the target miRNA of interest was reverse transcribed in each reverse transcription reaction due to the specific 5X primer sets added to each mastermix. The master mixes were mixed gently. The concentration of the small RNA sample was estimated from the corresponding large RNA sample, as the small RNA sample could not be directly measured. For each reaction (one for each target of interest), 14µl of each specific miRNA reverse transcription master mix was added to separate 0.2ml PCR tubes (Fisher Scientific) and kept on ice. 1µl of small RNA sample (where the corresponding large RNA sample had up to 200ng/µl) was added to each

Table 2.15 List of probes for TaqMan qPCR.

All probes were obtained from Applied Biosystems, USA.

Probe	Target type	Assay code
CCL20	Gene	Hs01011368_m1
GAPDH	gene (endogenous control)	Hs99999905_m1
GLI3	Gene	Hs00609233_m1
LIN28B	Gene	Hs01013729_m1
SRPX2	Gene	Hs00997580_m1
Let-7i	miRNA	002221
miR-205	miRNA	000509
U6	snRNA (endogenous control)	001973

Table 2.16 Gene reverse transcription master mix components.

Each component was added in sequence with excess reactions prepared in order to allow for pipetting loss.

Components	Volume for one reaction (µl)
10X RT Buffer	2
25X dNTP mix (100nM)	0.8
10X RT Random Primers	2
Multiscribe™ Reverse Transcriptase	1
Nuclease-Free Water	4.2
Total Volume	10

Table 2.17 MiRNA reverse transcription master mix components.

Each component was added in sequence with excess reactions prepared in order to allow for pipetting loss.

Components	Volume for one reaction (µl)
10X RT Buffer	1.5
100nM dNTP mix (with dTTP)	0.15
Multiscribe™ Reverse Transcriptase, 50 U/µl	1
RNase Inhibitor, 20 U/µl	0.19
5X RT primers	3
Nuclease-Free Water	8.16
Total Volume	14

PCR tubes containing 14µl of each specific mastermix. If the large RNA sample was greater than 200ng/µl, the corresponding small RNA sample was diluted to a factor that would bring the corresponding large RNA sample to a concentration below 200ng/µl if the same dilution was applied. 1µl of the small RNA dilution was then added. The PCR tubes were briefly centrifuged to spin down contents and eliminate air bubbles. The PCR tubes were then incubated at 16°C for 30mins, 42°C for 30mins, 85°C for 5mins and held at 4°C in a thermal cycler. Samples (cDNA) were then stored at -20°C.

2.1.16.3 TaqMan® qPCR step

TaqMan® qPCR was carried out by following the TaqMan® Gene Expression Assay Protocol (Applied Biosystems, USA) for target genes and the TaqMan® Small RNA Assays Protocol for target miRNAs. qPCR of genes and miRNAs were discussed together below as this step was similar in both protocols.

In brief, a TaqMan mastermix was prepared on ice for each target gene/miRNA of interest preparing enough for each sample in triplicate (Table 2.18). Applied Biosystems Universal Master Mix II (without UNG, uracil-DNA glycosylase) was used in preparing each mastermix. This contains the DNA polymerase needed to carry out

Table 2.18 TaqMan master mix components.

Each component was added in sequence with excess reactions prepared in order to allow for pipetting loss.

Components	Volume for one reaction (µl) Gene Target	Volume for one reaction (µl) miRNA Target
2X Universal master mix II	10	10
20X TaqMan gene expression assay	1	1
Nuclease-free water	8	7.66
Total	19	18.66

amplification. The gene expression assays contain the primers and MGB probe for the target gene/miRNA of interest.

19µl of each gene TaqMan mastermix was aliquoted in triplicate into separate wells for each cDNA sample (section 2.1.16.1) on a 96-well fast plate (Applied Biosystems, USA). 1µl of cDNA sample was added to each well containing TaqMan master mix. An endogenous control for each sample (GAPDH) and a non-template control (NTC) for each target gene (1µl of nuclease-free water added to 19µl of TaqMan mastermix in place of cDNA) was run on each 96-well plate.

18.66µl of each miRNA TaqMan mastermix was aliquoted in triplicate into separate wells for each cDNA sample (section 2.1.16.2) on a 96-well fast plate (Applied Biosystems, USA). 1.34µl of cDNA miRNA target sample was added to each well containing TaqMan master mix. Each small RNA sample had a separate reverse transcription reaction from section 2.1.16.2 for each miRNA target of interest being investigated. An endogenous control (U6) for each sample and a NTC for each target miRNA (1.34µl of nuclease-free water added to 18.66µl of TaqMan mastermix in place of cDNA) was run on each 96-well plate.

All plates were sealed using optical adhesive film (Applied Biosystems, USA) and centrifuged briefly to remove air bubbles and to ensure the reaction mixture was at the bottom of the plate. The plates were run on the Applied Biosystems Fast 7500 Real-Time PCR System under the following conditions; hold at 50°C for 2mins, hold at 95°C for 10mins and 40 cycles of 95°C for 15secs followed by 60°C for 1min. When the run

was completed the data was analysed using the Data Assist software (v3.0, Applied Biosystems, USA) and Microsoft Excel.

2.1.16.4 Optimisation of the quantity of small RNA input for reverse transcription

As the small RNA sample could not be directly measured, the quantity of sample to be added to the miRNA reverse transcription mastermix was estimated from its corresponding large RNA sample. Small and large samples were separated into separate fractions during RNA isolation (section 2.1.12.2). This was investigated by running the full TaqMan® qPCR protocol for U6 endogenous control on four samples; two samples using 1µl of small RNA sample input and two samples using 4µl of small RNA sample input. Also, two of the samples had a relatively low concentration of large RNA in their corresponding large RNA samples and two had relatively high concentrations of large RNA in their corresponding large RNA samples. Table 2.19 shows the average CT values for U6 obtained from each sample and indicates sample input amount and concentration of corresponding large RNA samples. From these results, it was deemed that 1µl of small RNA sample input was optimal as both concentrations of large RNA sample (26 (high) and 32 (low)) gave similar average CT values (17.5 and 19.2 respectively). Sample 48 had 4µl input of small RNA sample and high concentration in corresponding large RNA sample, but had a low average CT value of 12.4. This was too low to give reliable results. For these reasons, 1µl of small RNA sample (where the corresponding large RNA sample had up to 200ng/µl) was added to each PCR tubes containing 14µl of the miRNA reverse transcription mastermix prepared in section 2.1.16.2. If the large RNA sample was greater than 200ng/µl, the corresponding small RNA sample was diluted to a factor that would bring the large RNA sample to a concentration below 200ng/ml if the same dilution was applied. 1µl of the small RNA dilution was then added. By using this estimation, a minimal amount of variation would occur in the concentration of small RNA entering the initial reverse transcription reaction. The endogenous control was used to normalise each sample. U6 was used as the endogenous control in this study as it has been widely published as a suitable control in tissue studies of miRNA expression (*Boyerinas et al. 2012*; *Nishimura et al. 2013*).

Table 2.19 Results of small RNA sample input optimisation

Sample	Small RNA Sample input (µl)	Large RNA sample concentration (ng/µl)	Average CT value of U6 (3 replicates)	SD of CT values (3 replicates)
26	1	186.6	17.5	0.2
31	4	17	19.3	0.2
32	1	19.6	19.2	0.3
48	4	303.6	12.4	0.1

CHAPTER 3

The Area Fraction Output Method



TRINITY
COLLEGE
DUBLIN

Chapter 3 The area fraction output method

3.1 Introduction

In chapter 4, the details of our cell selection strategy will be discussed. This cell selection strategy was optimised and developed in order to investigate a number of hypotheses which were put forward in chapter 1 (Section 1.9). During its optimisation, a new method, the area fraction output method (Accepted for publication in MethodsX, a peer reviewed journal), was developed that was deemed to be useful. This method provided a non-invasive, objective measurement of cell count that indicated when cells within a cell culture flask had reached a certain level of confluence. This was required to accurately measure the cells recovery from drugging after each round of selection. The values returned were used as a parameter to help elucidate the time taken for recovery from each round of drug treatment in our cell selection strategy (Chapter 4).

Measuring cell proliferation is a commonly used analytical technique in the biological field. It is particularly used in oncology, stem cell biology and immunology to measure cytotoxicity and effects of drug administration to cells. Many assays or protocols used for measuring the growth of cells *in vitro* are invasive and destructive in nature. They can only be used as end point assays. They do not allow for the continued undisturbed growth of cells *in vitro* within a cell culture flask and often use indirect methods for measuring proliferation. An example of this is the commonly used crystal violet proliferation assay (*Gillies et al. 1986*). Crystal violet is a triphenylmethane dye used to stain DNA in order to identify cell number. Different variations of the original protocol can be used to determine cell viability, cell proliferation and cytotoxicity or cell death. In general, crystal violet protocols are endpoint, use indirect metabolic measures and are invasive and destructive.

In order to analyse cell proliferation in a non-invasive or non-destructive manner, microscopy can be used. Image capture and analysis of adherent cells growing in cell culture flasks can be done using expensive equipment and software algorithms. These techniques may not be suitable for small projects, short-term projects or laboratories with small budgets or research grants. For example, quantitative phase microscopy can be used to analyse bright-field images for confluence in a non-invasive, non-destructive and label free manner. However, this requires the purchase of specialised equipment that may not be within a researcher's budget (*Curl et al. 2004*).

The following method of 'Area Fraction (AF) output' calculation is an affordable way of attaining measurements that correlate to cell count in order to consistently estimate a measure of confluence from adherent cell lines growing in cell culture flasks in a non-invasive, non-destructive fashion. This technique is label free, rapid, eliminates sample manipulation (for example trypsinisation), is non-invasive, non-destructive and means that cells can continue to grow undisturbed. The rate of cell proliferation can be measured over time and in response to the administration of drugs. This is particularly useful for cell selection strategies for the development of drug resistance where cells need to be maintained in culture and continually monitored. Also, it only requires standard equipment, an inverted phase contrast light microscope with digital camera and camera lens adaptor and use of downloadable ImageJ freeware for analysis using existing confluence analysis protocols.

3.2 Methods

3.2.1 The area fraction output method

This is a novel, non-invasive and non-destructive method developed to calculate a measure of confluence for growing adherent cells without disturbing growth. The result is known as an area fraction (AF) output which represents the amount of surface area that cells cover within a photographed area of a flask, representing an approximate value of cell count for the flask as a whole. This method can be used in order to monitor cells growing in T25 flasks or other cell culture plastics to detect objectively when they have reached a certain cell count as an estimation of cell confluence. It is important to note that the primary use of the AF method is to track recovery of small numbers of cells with normal morphology in drug-free media. The author does not advocate using the AF method for cells when they are exposed to drug treatment, as in this period, cellular debris can be present which can give a false result. The method can be broken down into two distinct parts; image capture and image analysis.

3.2.1.1 Image capture

T25 flasks of interest containing growing adherent cells in a monolayer were photographed under an inverted Nikon (TMS) phase contrast light microscope (Nikon, Surrey, UK) using a Nikon Coolpix 4500 camera (Nikon, Surrey, UK) with a Nikon Coolpix Camera Lens Adapter (eBay Inc US, seller-imaging_apparatus, USA). A 4x objective lens was used. The camera lens adaptor was screwed onto the camera's lens. The other end of the adaptor was placed into the ocular tube of the microscope. The camera was zoomed in to a focus point of F4.0. The microscope was focused so

that a clear image of the cell nuclei was obtained on the camera's LCD display. A cardboard cover slip was designed to fit the bottom of the T25 flask having 1cm² holes close to the top and the bottom of the flask. See Figure 3.1. This was placed onto the bottom of the T25 flask of interest to allow images to be taken consistently in the same position of the flask. One image from the top and bottom of each flask was taken using the cover slip and stored for analysis with ImageJ software (downloadable from: http://imagej.nih.gov/ij/download.html).

3.2.1.2 Image analysis

The software used to analyse the images was ImageJ 1.45s (*Schneider et al. 2012*). A step by step guide is presented below for analysing photos obtained from section 3.2.1.1 above. The analysis steps describe the method of image analysis. The accuracy steps ensure that the count generated from the analysis steps is a good fit for the amount of cells in the original photograph. This is done by overlaying the generated image onto the original image to see if the black count outlines from the generated image match the cells seen in the original image. The images generated from the accuracy steps should result in an image where black outlines are inverted to red, which outline the edges of cells from the original image. See Figure 3.2.

3.2.1.2.1 Analysis steps (ImageJ)

1. Open image – (file: open) – Figure 3.2 (a) is an example of an unanalysed image

2. Convert image to 16-bit - (Image: Type: 16-bit)

3. Subtract image background – (Process: Subtract Background...) – Set "Rolling ball radius" ="20.0 pixels" – Tick "Light background" and "preview" – Click "OK"

4. Adjust threshold – (Image: Adjust: Threshold...) – Set Bottom bar between "65528" and "65532" whichever value gives the best cover for the image – Click "Apply"

5. Separate overlaps – (Process: Binary: Watershed)

6. Set measurements to analyse – (Analyse: Set Measurements) – Tick "Area", "Standard deviation", "Min & max gray value", "Integrated density", "Area fraction", "Mean gray value", "Perimeter" and "Median"

7. Carry out cell count – (Analyze: Analyze Particles) – Set "Size"="100-Infinity", "Circularity"="0.00-1.00" and "Show"="Outlines" – Tick "Display results", "Summarise" and "Include holes" – Click "OK" – Figure 3.2 (b) shows an example of the resultant generated image "Drawing of X.JPG" showing the cells that have been counted.

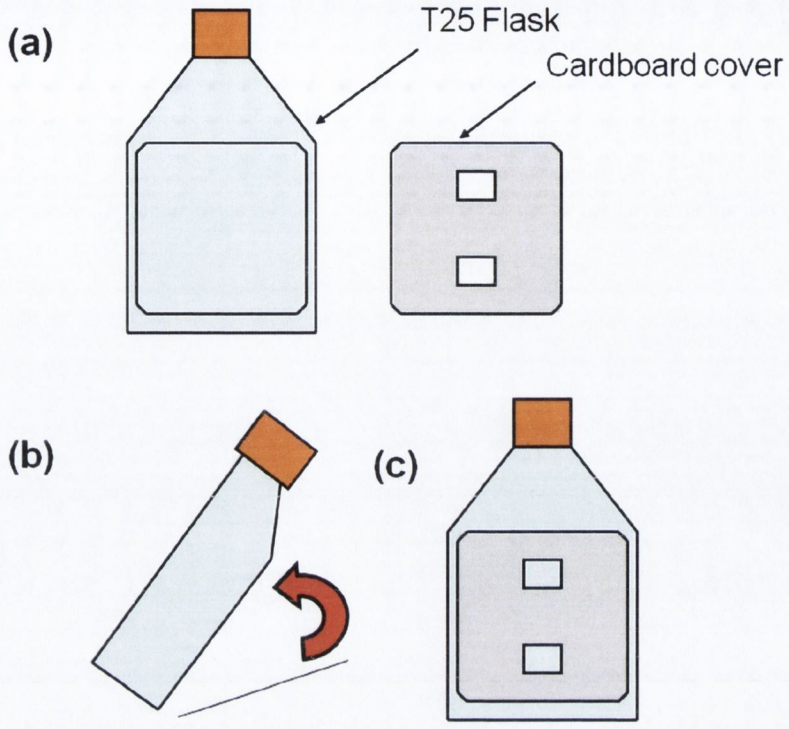

Figure 3.1 T25 cardboard cover design for AF calculation method.

(a) Shows the cardboard cover design next to T25 flask. (b) & (c) show how cover is placed onto a T25 flask before photography.

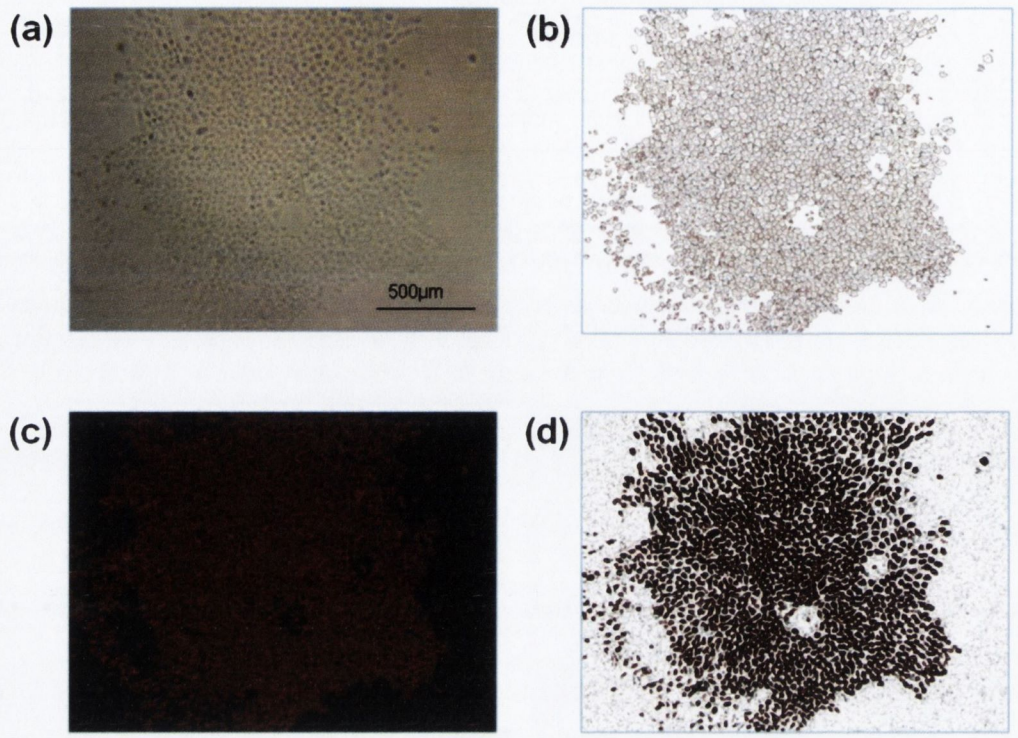

Figure 3.2 Example of images generated from the AF calculation method.

(a) Original image generated from section 2.3.1.1 of UPN251 cells. (b) Image 'Drawing of X.JPG' generated after analysis step 7, represents the cells counted from the analysis of original image. (c) Image 'Drawing of X.JPG' after accuracy step 5. This is the image that is used in the overlay onto the original image, to check for accuracy of the generated count versus the cells present in original image. (d) The result of the merged images ('a' and 'c') after completion of accuracy steps. In this case the count looks accurate as each cell is labelled with red numbering.

8. Save results – Save "Results" and "Summary" as Excel worksheets.

3.2.1.2.2 Accuracy steps – count image vs. original image (ImageJ)

1. Select generated image from analysis - Click on image generated from step 7 e.g. "Drawing of X.JPG"

2. Invert image - (Image: Lookup Tables: Invert LUT)

3. Change color to red - (Image: Lookup Tables: Red)

4. Invert image again - (Image: Lookup Tables: Invert LUT)

5. Change Both Images to RBG Color (Image: Type: RBG Color) – Figure 3.2 (c) shows "Drawing of X.JPG" after accuracy steps 1-5.

6. Merge images and see overlay (Process: Image calculator...) - Set "Image1"="Original image", "Operation"="Add" and "Image2"="Generated image" – Tick "Create new window" – Click "OK"

7. Save image if accurate. Figure 3.2 (d) shows an example of an accurate overlay. Otherwise step 4 (adjusting threshold) and step 7 ("size" parameter) of the analysis steps can be adjusted for more cell line specific measurements until a good fit is obtained.

Analysis and accuracy steps can be automated by using the record macros option in ImageJ. All steps were taken for both photographs of a flask (one from the top and one from the bottom), giving two area fraction output values. Each area fraction output is stored in the summary file. The average of the two area fractions was calculated in order to give an area fraction that represents an approximate measure for surface area cover or confluence over the flask as a whole. From our observations of UPN251 and OVCAR8 cells, an AF value of 30 or above was deemed to represent a T25 flask that had reached a level of confluence that required subculture to continue logarithmic growth (AF of 30=Approximately 70% confluence). Figure 3.3 shows pictures of OVCAR8 cells before and after analysis for newly seeded and confluent flasks.

3.2.2 Area fraction output method validation

OVCAR8 and UPN251 cells were plated into eight T-25 flasks at a cell density of $2.6x10^4$ cells per flask. The flasks were left in an incubator for 24 hours to allow cells to attach. After this time two of the flasks were removed and photographed, followed by AF calculation. The two flasks were then trypsinised and cells counted using a haemocytometer. The remaining flasks were incubated and the same procedure was used over subsequent 24 hour periods. AF output data was compared to cell count data using a Spearman correlation to see if the data sets correlated.

3.2.3 Example of area fraction output method: Tracking recovery of drug administration

Cells were plated into T25 flasks at a cell density of $2.6x10^4$ cells per flask and drugged with carboplatin on day 2. The doses of carboplatin used were 2µg/ml for UPN251 and 4µg/ml for OVCAR8. These doses caused a similar level of death in the cell lines due to different intrinsic resistances to the drug. On day 5, drugged media was removed and replaced with fresh drug free media. Over the subsequent days, all T25 flasks were examined using the AF output method to indicate when the cells had reached a predefined value of AF as an estimation of cell confluence. Upon reaching this

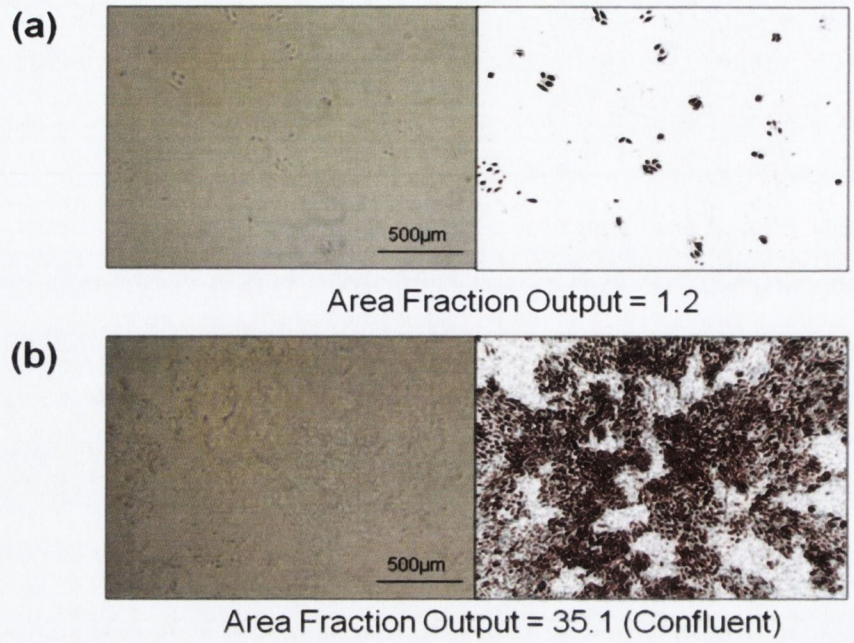

Figure 3.3 AF output photo analysis of newly seeded versus confluent flasks.

The left image is the original phase contrast photograph; the right is after analysis with ImageJ software. (a) OVCAR8 cells after seeding. AF value of 1.2 was achieved in this case. (b) OVCAR8 upon reaching confluence. AF value of 35.1 was achieved in this case.

predefined value of AF, the cells were re-seeded into T75 flasks. Once all cells had recovered, the next round of drugging commenced following the same format as above (provided the cells were 4 weeks after drugging, otherwise drugging was delayed until this time).

3.3 Results

3.3.1 Area fraction output method validation

In order to see if the AF method was an accurate representation of cell number within a T25 flask, it was compared to cell counting using a haemocytometer. AF calculation was found to be highly correlated with cell count results using a haemocytometer. The average correlation co-efficient value obtained from a Spearman correlation test for n=3 replicates was 0.99 ± 0.008 for OVCAR8 and 0.99 ± 0.01 for UPN251 with a p-value of 0.01 for both cell lines. See Figure 3.4. This shows that AF calculation is a reliable measure for surface area cover of cells within a T25 flask tested and that this corresponds to cell count. The ranges of cell counts by haemocytometer that have been validated by this method are within the linear range from 15,888-377,500 for

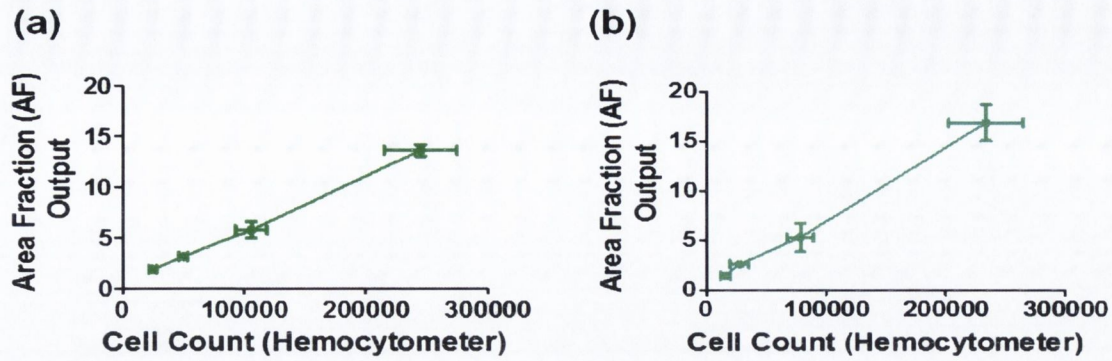

Figure 3.4 Correlation of AF method with cell counts using a haemocytometer.

The average total cell count per T25 flask for each day of a four day growth curve is shown on the x-axis of each graph and the AF output average for the same T25 flask for each day is shown on the y-axis. For each graph error bars represent the Standard Deviation. (a) Shows a representative experiment for OVCAR8 (n=3, r^2=0.99±0.02, p=0.01). (b) Shows a representative experiment for UPN251 (n=3, r^2=0.99±0.02, p=0.01).

UPN251 and 25,000-318,750 for OVCAR8. This corresponds to AF values ranging from 1.4-37.8 and 1.9-33.7 respectively.

3.3.2 Example of area fraction output method: Tracking recovery of drug administration

One example where the application of the AF method was useful was in the development of drug resistant cell models *in vitro*. AF can be used to track cell recovery in an objective manner to see consistently when cells have recovered after drug exposure. Figure 3.5 shows the recovery of UPN251 and OVCAR8 ovarian cancer cells after carboplatin exposure (2 and 4 µg/ml respectively) over a number of rounds of drugging during a selection strategy to produce carboplatin resistant models. The doses of carboplatin that were used, were selected from testing a range of carboplatin doses on each cell line and selecting the dose which exhibited a large amount of cell death followed by a return to logarithmic growth (covered in more detail in chapter 4). Each cell line received 3-day exposures to carboplatin every 4-5 weeks, with each dose of drug received denoting a new round of drugging (Round 1-6). With the AF output method, recovery from drugging was measured in a consistent manner giving meaningful data on recovery. Generally, as the amount of rounds of drug

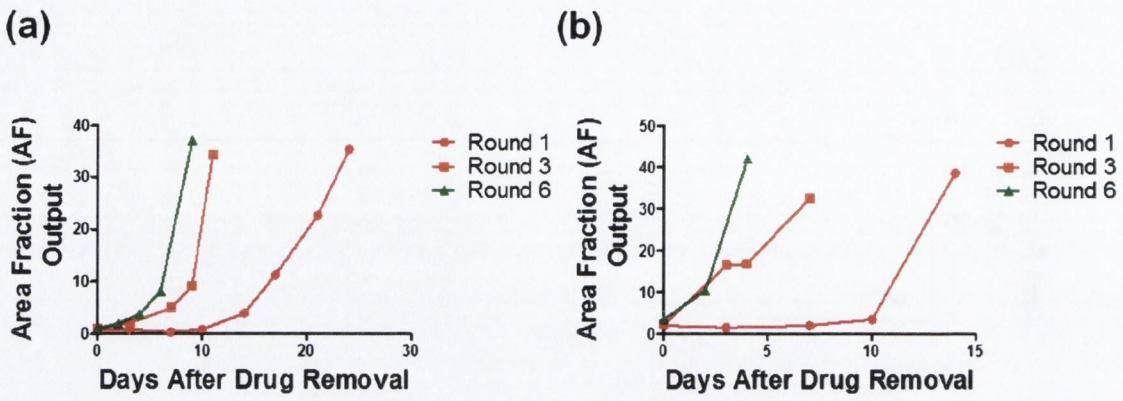

Figure 3.5 Tracking cell recovery using AF.

Graphs show the recovery of cells over a period of days after carboplatin exposure. The cells received 3-day exposures to carboplatin every 4-5 weeks. Each dose of drug received, denotes a new round of drugging (Round 1-6). The x-axis shows the days after the drug has been removed from the cells and the y-axis gives the AF output at each time point measured. (a) OVCAR8 cells after exposure to 4μg/ml carboplatin. (b) UPN251 cells after exposure to 2μg/ml carboplatin.

administration increased the time taken for cells to recover decreased. This was an indication that cells were becoming more resistant to carboplatin as the number of rounds of drug treatment increased over time. The AF output method was used in a similar fashion for our selection strategy in chapter 4 to develop carboplatin and taxol resistant cell lines under a number of different conditions in OVCAR8 and UPN251 cell lines.

3.4 Discussion

Microscopy can be used to evaluate cell viability or proliferation in adherent cells. These techniques normally require the addition of damaging fluorescent dyes to cells in order to take a clear image for analysis. This means that cells need to be manipulated and disturbed. In this case, continued growth of cells is not an option. Purchasing equipment for both image capture (microscope and camera systems) and analysis software can also be expensive and not in the scope of some laboratories or projects. The area fraction method provides an inexpensive means of tracking cellular growth over time. It gives an objective measure of when cells reach a certain level of cell number, used as an accurate estimation of confluence without disturbing the cells in culture. In our example in section 3.2.3, the AF method was used in this way during the

development of carboplatin-resistant cell lines. Cell recovery and the time taken to reach confluence must be assessed in a non-destructive manner over many different time points (ruling out destructive end point assays). This can be achieved non-objectively by examination under a microscope. However, this will result in the cells being deemed to have reached confluence at different levels and will, therefore, be inconsistent. The validated method of AF examination provides not only an objective measure of when cells reach a given cell count, which corresponds to cell confluence in the flask, but also gives recordable data on the length of time taken to reach confluence.

However, this method does have certain limitations. It is only suitable for adherent cell lines that grow in a monolayer. One caveat to the findings is that, the method has only been tested and validated in two epithelial ovarian cancer cell lines that have rounded morphology by the author. However, another team of researchers have further validated the AF method by comparing it to heamocytometer counts using two other epithelial ovarian cancer cell lines (CAOV3 (r^2=0.98, p=0.02) and UWB1.289 WT (r^2=0.97, p=0.02)) *(personal communication, Roshni Kalachand, Royal College of Surgeons in Ireland).*

Other morphologies, such as spindled or elongated cells, have not yet been tested by this method. By adjusting the AF cut-off value, an estimated measure of confluence could be obtained for these morphologies, but this must be experimentally validated. Another example could be cells with a smaller nuclei and larger cell body. The AF output cut-off value could be lowered in ImageJ, in this case to reflect this.

Another caveat that has the potential to skew results is cells that grow unevenly in a clumpy morphology. In this case, it is recommended that the largest colony of cells is identified within the 1cm holes of the cover slip and tracked for the duration of the experiment. By the time the cells have reached the desired level of cell count, as an estimation of confluence, the colonies will have grown together sufficiently to give an accurate estimation for confluence over the whole flask.

3.4.1 Comparison of area fraction output method to other microscopy-based measures of confluence

The 'cell screen' system uses microscopic imagery to quantify suspension cell confluence in a fully automated manner (*Brinkmann et al. 2002*). The author's method only measures adherent cells lines. Therefore, this protocol may act as a suitable alternative for experiments using suspension cells. This method is label free and non-invasive, but does require manipulation of cells into 96 well plates. For this reason, this

method is not suitable for protocols that need to measure cells directly in tissue culture flasks. This system has high precision and counting accuracy with high correlation to other established methods of counting, such as manual cell counting with trypan blue (*Tennant 1964*) and automatic cell counting using the Cedex System (*Gudermann et al. 1997*). The 'cell screen' system requires specialised equipment in the form of an inverse microscope equipped with 10x objective and a back-illuminated charge-coupled device (CCD) camera which is operated by special application software (*Brinkmann et al. 2002*). This system is an attractive option under certain circumstances, but may not be suitable for laboratories operating with modest budgets.

Quantitative phase microscopy can be used to analyse bright-field images. This offers a non-invasive, non-destructive, label free confluence measure for adherent monolayer cells (*Curl et al. 2004*). Values obtained from this technique have been directly compared to manual counts using a haemocytometer and correlate closely, as with the AF method. Again, this technique requires the purchase of specialised equipment which may not be in a researcher's budget. *Curl et al. (2004)* use a CCD camera mounted on an inverted microscope using a 10 x objective and QPm software in order to analyse images by creating phase maps. This is a good alternative to the AF method, if cost is not an obstacle.

It is possible to analyse phase-contrast images in order to obtain a reliable measure of confluence from growing myoblast cells, without the use of florescent dyes or manipulation (*Juneau et al. 2013*). This process uses a segmentation algorithm that is fast, simple to use, and of high accuracy and could be adapted to other cell lines. With adequate tuning, this algorithm could be used to monitor cell cultures in real time. However, one drawback would be that the microscope used in this analysis has an automated/motorised stage and an incubator attached throughout the experiment. The experiment also needs to be controlled by the metamorph® image analysis software package. The cost incurred by availing of this equipment is much higher than our proposed method.

Digital holography is a non-invasive, label-free method for determining cell counts in adherent cells growing in a monolayer. The technique can track cell growth and give confluence measures that are as accurate as manual cell counts using a haemocytometer. However, specialised equipment is needed in the form of a microscope that combines phase contract microscopy with holography (e.g. Holomonitor™ M2). Image analysis requires automated software algorithms based on the Fresnel approximation. Again, cost will be an issue to some researchers if this method is to be implemented (*Molder et al. 2008*).

Two recent studies have provided microscopy based methods of measuring adherent cell confluence which are quick, cheap, non-destructive and non-invasive (*Drey et al. 2013*; *Topman et al. 2011*). These studies measure cell confluence in 12 well plates and petri dishes. Neither of these studies measured cells directly in tissue-culture flasks as in the AF method. This novel aspect of the AF method makes it suitable for measuring cells directly in tissue culture flasks without disturbing growth.

Another recent publication provides an alternative method for analysing phase contrast microscopy images that is cheap, fast and accurate (*Jaccard et al. 2014*). The software toolbox (PHANTAST) that bundles together different algorithms, while providing a user friendly interface, has been made freely available. This may be a viable alternative to using ImageJ freeware as was used in the AF method.

3.4.2 Comparison of area fraction output method to label-based methods of proliferation and cell viability.

Classical membrane integrity assays are not suitable for the continued undisturbed growth of adherent cells in culture. Cell counting with a haemocytometer, trypan blue assay (*Tennant 1964*) or automatic trypan blue method (*Louis et al. 2011*), lactate dehydrogenase (LDH) leakage (*Allen et al. 1994*) and florescent dyes (e.g. ethidium bromide, acridine orange and propidium iodide (*Jones et al. 1985*; *Ribble et al. 2005*) all call for invasive cell manipulations.

Some alternative colourimetric assays to crystal violet mentioned in the introduction are MTT, Resazurin and BrdU.

The MTT assay was first described by *Mosmann (1983)*. It measures metabolic function. Water soluble MTT (3-(4,5-dimethylthiazol-2-yl)-2,5-diphenyltetrazolium bromide) is converted into an insoluble formazan.2-4 in living cells. Solubilised formazan is measured with a micro plate reader. Therefore, this method provides an indirect quantification of cell number and viability using metabolic products in a destructive manner (*Mosmann 1983*). This is only suitable as an endpoint assay.

The resazurin assay also known as the Alamar Blue assay is also based on metabolic activity (*Anoopkumar-Dukie et al. 2005*). Viable cells reduce resazurin (a redox dye) to resorufin and dilhydro-resorufin which occurs intracellularly. This reduction is coupled to cell growth causing resazurin to be converted from a non-fluorescent blue form to a reduced fluorescent red form, which can be measured using a microplate reader. The rate of dye reduction is directly proportional to viable cell number (*O'Brien et al. 2000*). This assay is non-toxic and stable in culture medium, meaning that cells can remain

viable for multiple measurements. However, it can still only be used as an end point assay after manipulation into 96 well plates.

The BrdU assay is an invasive label-based proliferation assay (*Muir et al. 1990*). BrdU (5-bromo-2'-deoxiuridine), a synthetic nucleoside analog of thymidine, is added to cell culture and is incorporated into the DNA of proliferating cells in the place of thymidine. Florescent probes in the form of monoclonal antibodies targeting BrdU can be used to quantify the amount of proliferating cells present. This method is again invasive and only useful as an endpoint assay. *Vega-Avila and Pugsley (2011)* provide a more in depth review of these colorimetric assays (*Vega-Avila and Pugsley 2011*).

3.5 Conclusion

The described AF output method of objectively measuring cell count as an estimate of cell confluence is ideal for adherent cells in cell culture flasks that require undisturbed continued growth. It is fast, accurate, cheap, non-destructive and non-invasive. It also provides an objective, consistent measure of when cells reach confluence. This method is correlated to data obtained by manual cell counts using a haemocytometer. Other common methods of measuring cell number or confluence such as colorimetric assays, membrane integrity assays and the use of microscopic systems can be expensive, destructive, invasive, and laborious and often use indirect measurements. This makes our method ideal for labs on a small budget. It can be adapted easily for equipment that is readily available and inexpensive.

The AF output method was developed for the present study to measure the time taken for cells to reach confluence after drug administration in the author's selection strategy (chapter 4). This was required in order to meet the aforementioned criteria, which could not all be met by other methods described in the discussion above. Namely, AF is an affordable method that is able to consistently measure an AF output value, correlated to cell count, which represents an objective estimate of when cells reach confluence in adherent cell lines that was non-invasive, non-destructive, accurate and objective in nature.

CHAPTER 4

Chemoresistant Ovarian Cancer Cell Line Development



TRINITY
COLLEGE
DUBLIN

Chapter 4 Chemoresistant ovarian cancer cell line development

4.1 Introduction

4.1.1 Resistance cell models

The development of chemotherapy drug-resistant cancer cell lines is a long established approach for investigating the mechanisms of cytotoxicity and resistance to chemotherapy agents. One of the first publications to describe the development of an anti-cancer drug resistant *in vitro* model, which exhibited acquired resistance to chemotherapy drugs, was published in 1970 (*Biedler et al. 1970*). Resistant cell lines were developed from parental Chinese hamster cells using treatment with actinomycin D. The selection strategy used was the stepwise increase in the concentration of the drug over time when exposed to parental cells. This gave a fold resistance to the drug in the developed model of up to 2500 times greater than parental cells. These resistant cell lines were also cross resistant to a number of other chemotherapy drugs such as vinblastine and daunorubicin. This was the first time that a multidrug resistant (MDR) phenotype was reported in the literature. Some earlier drug-resistant cell lines were developed in the 1950 and 1960s using *in vivo* mouse models. The earliest recorded example of a development strategy where a resistant cell model was produced was a study involving leukaemia cells implanted into mice (*Burchenal et al. 1950*). Leukaemia cells resistant to methotrexate were developed from a mouse strain implanted with AK 4 leukaemia cells. It was reported that the morphology of the resistant cells that were developed were the same as the sensitive original strains of cells. Immediately after this study, numerous resistant variants were developed primarily in leukaemia, but also in solid tumours. Another example is a study in 1951 where leukaemia cells resistant to the guanine analog, 8-Azaguanine, were developed (*Law 1951*). In this case the cell model was developed by transplantation of cells into mice receiving the maximum tolerated dose of the drug. Other important research from the 1960s using drug resistant models includes a study examining mouse derived tumour cells developed to be methotrexate resistance by prolonged exposure to the drug (*Roberts et al. 1965*). In 1968, a study described the use of P815/VLB cells which was a subline of P815 mouse leukaemia cells selected for vinblastine resistance. This study also used P388/38280 and P388/57155 cells which were sublines of P388 mouse leukaemia cells selected for resistance to terephthalanilide derivatives (*Kessel et al. 1968*).

Cell line models have pros and cons associated with them. Some of the advantages of using cell models are that they are widely used, readily available and easy to handle, maintain, and manipulate at a relatively low cost. Also, they initially have a high degree of similarity with the initial tumour. Some disadvantages are that they can be genomically unstable, which may lead to a change in cellular characteristics, and they are maintained in a different environment than the tumour from which they were originally derived. Therefore, cell models do not receive the same signals that the original tumour receives from its surrounding microenvironment and may act differently to certain stimuli (*Ferreira et al. 2013*). Another concern is that a number of studies have shown that cell lines retained in cell culture undergo a drift at the transcriptomic level, making cell lines more similar to each other regardless of the tissue of origin, than to the clinical samples they are supposed to model (*Gillet et al. 2013*). However, other studies have come to the opposite conclusion. They suggest the need for larger cell line panels to better capture the heterogeneity of tumours (*Gillet et al. 2013*). With these concerns in mind, cell models are still regarded as a good starting point for translational studies and drug testing. Results from cell line models are usually extrapolated to *in-vivo* models for further testing to confirm findings (*Ferreira et al. 2013*). These considerations were taken into account when the present study was designed. Cell line resistance models fulfilled the needs of this project and were used as a major component in order to fulfil our research objectives.

Publications in this research field usually place little emphasis on how the drug-resistant cell lines were established in the laboratory. The development of drug-resistant cell lines can take anywhere from 6 to 18 months in the laboratory and many decisions are taken during this time. This chapter will outline the decisions made in the development of a number of resistant sublines derived from two different parental ovarian cancer cell lines. It will also outline the time taken for resistance to develop and the extent of the resistance developed. Some of the key decisions involved in developing chemotherapy resistant cancer cell lines are outlined in a review by our research group and the key decisions that needed to be considered in the development of our selection strategy are discussed further below following the guidelines of this review (*McDermott et al. 2014*).

4.1.1.1 Key decisions involved in planning a selection strategy

4.1.1.1.1 Parental cell line

The choice of parental cell line is very important as this will influence all experiments stemming from the selection work. The researcher embarking on this task should be

familiar with growing the parental cells, if possible. This will make it easier to see changes in the developing resistant cells after they have been stressed with drug treatment. Thus, the decisions made on when to subculture cells can be intelligently made, ensuring that the cells will be healthy enough so survive manipulation. The chosen parental cells should be easy to maintain in culture, as the developing resistant sublines will become more challenging to grow (*McDermott et al. 2014*).

Another important consideration is the patient from which the parental cell line has been derived from. It is best to select cell lines from chemotherapy and radiation naïve patients, if possible, as these treatments will already have evoked changes in resistance associated pathways that may have changed drug resistance markers, which may not be relevant to the agent being studied (*Benard et al. 1985*; *Emoto et al. 1999*; *Langdon et al. 1988*). Another option would be to select a cell line which as a relatively low baseline IC_{50} to the drug of interest. This can act as a suitable model to examine small fold changes in resistance within a clinically relevant range.

4.1.1.1.2 Type of cell resistance model: High level laboratory or clinically relevant

Drug-resistant cell models can be divided into two categories; clinically-relevant resistance models and high-level laboratory resistance models. Both types of models have pros and cons associated with them regarding their utility for research. Before commencing, a researcher must decide which type of model they wish to produce. Both models will typically have different drug doses and exposures associated with them.

Clinically relevant resistance models aim to mimic conditions that cancer patients experience during chemotherapy. Drug exposures are at low concentrations and a pulsed treatment strategy is often used where the cells recover in drug-free media. This aims to mimic patients receiving cycles of chemotherapy drug in the clinical setting. The dose administered is influenced by data obtained from the clinical administration of the drug. Models will have minimal escalation of drug dose to keep it in the clinical range. Some drawbacks to using clinically relevant models are that resistance developed can be unstable, resistance is often at low levels and can involve small molecular changes, which can be more difficult to detect and analyse (*Breen et al. 2008*; *Davey et al. 1995*; *Stordal et al. 2006*). An example of a clinically-relevant resistance model derived from ovarian cancer cells is seen in the development of IGROVCDDP (*Ma et al. 1998*). In this case a pulsed exposure with cisplatin was used on the parental ovarian cell line IGROV-1. A stepwise increase of drug concentration

was used to generate IGROVCDDP over 9 months and 28 passages. IGROVCDDP had an 8.4 fold increase in resistance to cisplatin and the resistance model is deemed to be in the clinically relevant range.

High-level laboratory resistance models aim to understand the potential mechanisms of toxicity and resistance to chemotherapy agents by using high concentration of the drug. Treatment doses are often escalated over time and either the cells are grown under continuous exposure to the drug or highly drug-resistant clones are isolated from a mixed population. Usually, the drug concentrations used will start in the clinical range, but escalations bring it far beyond this to invoke large fold changes in resistance. High-level models usually produce a more stable resistance, which is easy to maintain in culture and can be used for long periods after selection work has finished. The levels of resistance produced are often very high. Therefore, the molecular changes are also at a higher level, making them easier to detect and link to resistance. The drawback associated with this model is that the high levels of resistance produced do not reflect the clinical setting (*McDermott et al. 2014*). An example of a high level model used in cervical cancer is seen in the development of KB-8-5-11 from parental KB-3-1 cells (*Akiyama et al. 1985*). In this case, a continuous dose of colchicine was administered in a stepwise and mutagenic fashion in order to produce a subline that had 40 fold higher resistance compared to parental cells.

4.1.1.1.3 Drug dose and strategy of administration for clinically relevant models

When designing a clinically relevant resistance model, it is important to know how the chemotherapy agent being used is administered in the clinic for the type of cancer being modelled.

When administering chemotherapy by the I.V. route, the amount of drug being given to a patient is expressed in mg/m^2. By consulting pharmacokinetic studies, the relevant dose of the drug in mg/m^2 can be converted into µg/ml or µM by looking at the measurements of drug concentration in the blood stream. This will give a broad range of doses achieved in the blood stream over time. The highest concentration of drug will present directly after the bolus injection of drug. This will then decrease over a number of hours or days, depending on the rate of drug elimination and excretion. This, in turn, gives a broad dose range that has clinical relevance. A higher dose given for a number of hours could mimic concentrations associated with the bolus of the drug, while a lower dose over a longer period could mimic lowering concentrations of the drug due to

the excretion of the drug from the body (*McDermott et al. 2014*). An example of this is cisplatin given by I.V. Following I.V. bolus injection of the drug at 100 mg/m², peak plasma levels of approximately 6 µg/ml are reached but this quickly decreases to less than 2µg/ml after 2 hours (*Himmelstein et al. 1981*). Clearance of cisplatin from the body is triphasic and distribution half-life is 13mins, elimination half-life is 43mins and terminal half life is 5.4 days (*Vermorken et al. 1984*). After 24 hours, 25% of the initial cisplatin dose has been eliminated from the body with renal clearance accounting for 90%.

4.1.1.1.4 Risk reduction strategies

A risk reduction strategy must be implemented in order to mitigate failure to develop drug resistance in the development of a cell line models. This is more common than might be expected. Frequently drug treatment can result in daughter cells that have no significant fold resistance changes relative to the parental cells (*Breen et al. 2008*; *Stordal et al. 2006*). For this reason, a comparative selection strategy should be performed where a number of cell lines are used, or a number of different treatments with chemotherapeutic agents are run in parallel. By using this comparative strategy, it is hoped that at least one arm of the selection strategy will produce daughter cells with a stable and significant resistance. The comparative strategy, therefore, reduces the chances of not developing a stably resistant model (*Breen et al. 2008*; *McDermott et al. 2014*; *Stordal et al. 2006*). Also, it is important to note that contamination is a risk when working in a cell culture environment. At each round of selection, frozen stocks should be made of all cells being selected in order to negate this risk.

A good example of using a comparative selection strategy as risk reduction comes from a study by *Tegze et al. (2012).* The team used two breast cancer cell lines (MDA-MB-231 and MCF-7) and aimed to develop 40 drug-resistant cell lines using two different selecting agents (doxorubicin and taxol). After 18 months of continuous treatment with increasing concentrations of drug in the clinically relevant range, 29 drug-resistant models were successfully produced. There were 6 doxorubicin and 9 taxol-resistant MDA-MB-231 cell lines and 10 doxorubicin and 4 taxol-resistant MCF-7 cell lines produced in total (*Tegze et al. 2012*).

The team was then able to compare and contrast the cell lines which produced resistance and examine the mechanisms of resistance that arose in each case. Interestingly, they concluded that the heterogeneity of the cell lines caused multiple resistant sublines with different resistance characteristics and that only a small amount of these mechanisms were needed to achieve resistance in a single subline. This

highlights the need to have a number of different comparisons in any selection strategy as combinations of different mechanisms may cause resistance in the clinical setting. Those mechanisms that arise frequently in different cell lines may have a good chance of being a major mechanism in the clinic and may give good biomarkers or could act in providing drug targets.

Multiple mechanisms of resistance exist for each chemotherapy drug. Cisplatin has been widely studied for many years in drug-resistant cell models. A number of different mechanisms of resistance have been identified including decreased accumulation of drug, increased drug efflux, inactivation of drug and increased DNA repair (*Stordal et al. 2007a*). Not all of these mechanisms need to occur in a model to make it drug resistant. A single, or small number of, different resistance mechanisms can act together to render cells drug resistant. Treating the same cell line with a certain chemotherapeutic agent under the same conditions may produce different or similar mechanisms of resistance in independent treatments. This shows the randomness of natural selection and shows how important it is to have a good risk reduction strategy in place with many different treatments running in parallel to mitigate failure to produce resistance.

4.1.2 Aims and objectives

This chapter examines the development of a number of chemotherapy resistant ovarian cancer cell lines by the application of a comparative selection strategy. The cell lines produced acted as a model for ovarian cancer resistance. They were used to examine the development of resistance in relation to BRCA1 status and to examine the mechanisms of resistance that arose in the cell lines which became resistant to their selecting agents.

4.1.2.1 Hypotheses

The hypotheses examined in this chapter stated that:

- Due to the inverse resistance relationship that exists between platinums and taxanes (chapter 1 section 1.7.3), cells with BRCA1 defects will develop resistance to platinums slower than taxanes, as they are more sensitive to DNA damage. The reverse should be true for cells with functional BRCA1.

- When treating cells with alternating treatments of platinums and taxanes, resistance will develop more slowly or not at all when compared to treatment with single-agent taxane or platinum.

4.1.2.2 Objectives

The objective of this chapter was to develop novel chemoresistant ovarian cancer cell lines from established ovarian cancer cell lines using a comparative selection strategy. The selection strategy was designed to be as clinically relevant as possible in order to mimic the mechanisms of resistance that may arise in the clinical setting. UPN251 (BRCA1 wild-type) and OVCAR8 (BRCA1 methylated) were used in order to investigate the development of chemoresistance in relation to BRCA1 status. How the development of resistance was effected by BRCA1 was then examined in relation to:-

- The inverse resistance relationship between platinums and taxanes;
- The effects of alternating doses of platinums and taxanes.

Resistant sublines, developed using the selection strategy, were ultimately used to screen for chemoresistance biomarkers.

4.2 Cell selection strategy methods and design

4.2.1 Selection strategy design

A number of key decisions were made when designing the selection strategy. As our goals were to find novel chemoresistant biomarkers in ovarian cancer cell lines and to examine chemoresistance development in relation to BRCA1 status, the cell lines were chosen from a panel of 41 ovarian cancer cell lines for which BRCA1 mutation analysis was carried out (*Stordal et al. 2013*).

In order to address the hypotheses relating to BRCA1 status two cell lines chosen, OVCAR8 (BRCA1 methylated) and UPN251 (BRCA1 wild-type) which had different BRCA1 expression status. OVCAR8 was taken from a patient who had undergone treatment with high-dose carboplatin who exhibited progressive ovarian cancer (*Schilder et al. 1990*). OVCAR8 is BRCA1 wild-type, but is methylated in the promoter region blocking mRNA transcription (*Stordal et al. 2013*). UPN251 originated from a patient who had failed first line chemotherapy and had relapsed after subsequent treatment of 8 rounds of taxol chemotherapy (personal communication, Dr. Thomas Hamilton). UPN251 is BRCA1 wild-type due to a secondary reversion mutation allowing the expression of a functional BRCA1 protein (*Stordal et al. 2013*). These cell lines were not chemo-naïve but were, however, exposed to the same drugs used in this study. Therefore, the signalling pathways that may already have been evoked by chemotherapy are relevant for this study. The IC_{50} of both cell lines to carboplatin were relatively low compared to other ovarian cancer cell lines in the panel from which

carboplatin resistance data was available (see Figure 4.1 (A)). This was desirable and could act as a suitable model to examine small fold changes in carboplatin resistance within a clinically relevant range. The cells were relatively highly resistant to taxol when compared to other ovarian cancer cell lines in the panel, from which taxol resistance data was available (see Figure 4.1 (B)). This high level of taxol resistance and low level of carboplatin resistance may be due to the inverse resistance relationship between platinums and taxanes in cell lines (section 4.1.2). Therefore, these cell lines may act as suitable models to examine taxol/carboplatin resistance in relation to the inverse resistance relationship.

Carboplatin and taxol were chosen to be used as selecting agents in the selection strategy. This was because these two agents are used in the clinic in the treatment of advanced ovarian cancer. The current standard treatment of advance ovarian cancer is surgical debulking followed by intravenous administration of combination carboplatin and taxol chemotherapy over 3-6 cycles, 3-4 weeks apart (*Hennessy et al. 2009*; *Ozols 2005*). These drugs were also chosen to look at the inverse resistance relationship between platinums and taxanes in relation to ovarian cancer chemotherapy. This is because carboplatin is from the platinum family of drugs (*Pasetto et al. 2006*) and taxol is from the taxane family of drugs (*Sciff et al. 1979*).

The next major consideration was whether to design a clinically relevant or a high-level laboratory resistance model. A clinically relevant resistance model was chosen in order to accurately model what happens in the clinical setting. It was desired that small molecular changes were modelled that may also occur in the clinical setting. This would enable the team to find highly relevant clinical biomarkers as opposed to high-level resistance models that produce large scale biochemical changes. These changes may not have the potential to arise in the clinic, within the dose ranges safely and routinely administered to patients (*Clynes et al. 1992*; *Liang et al. 2003*; *Shen et al. 1995*). The chances of developing a stably resistant model are reduced in a clinically relevant model, so a number of different treatments were performed as part of a risk reduction strategy. Risk reduction was achieved by carrying out the selection strategy on two different cell lines in parallel. Also, a number of treatments were carried out in parallel with two different selecting agents, the details of which will be outlined in section 4.2.3 to follow. The cells were exposed to drugs for three days and then allowed to recover in drug free media. A pulsed treatment strategy was used and the cells were treated with drug every 4-5 weeks. This attempted to mimic the clinic closely where drugs are administered over 3-6 cycles every 3-4 weeks by intravenous

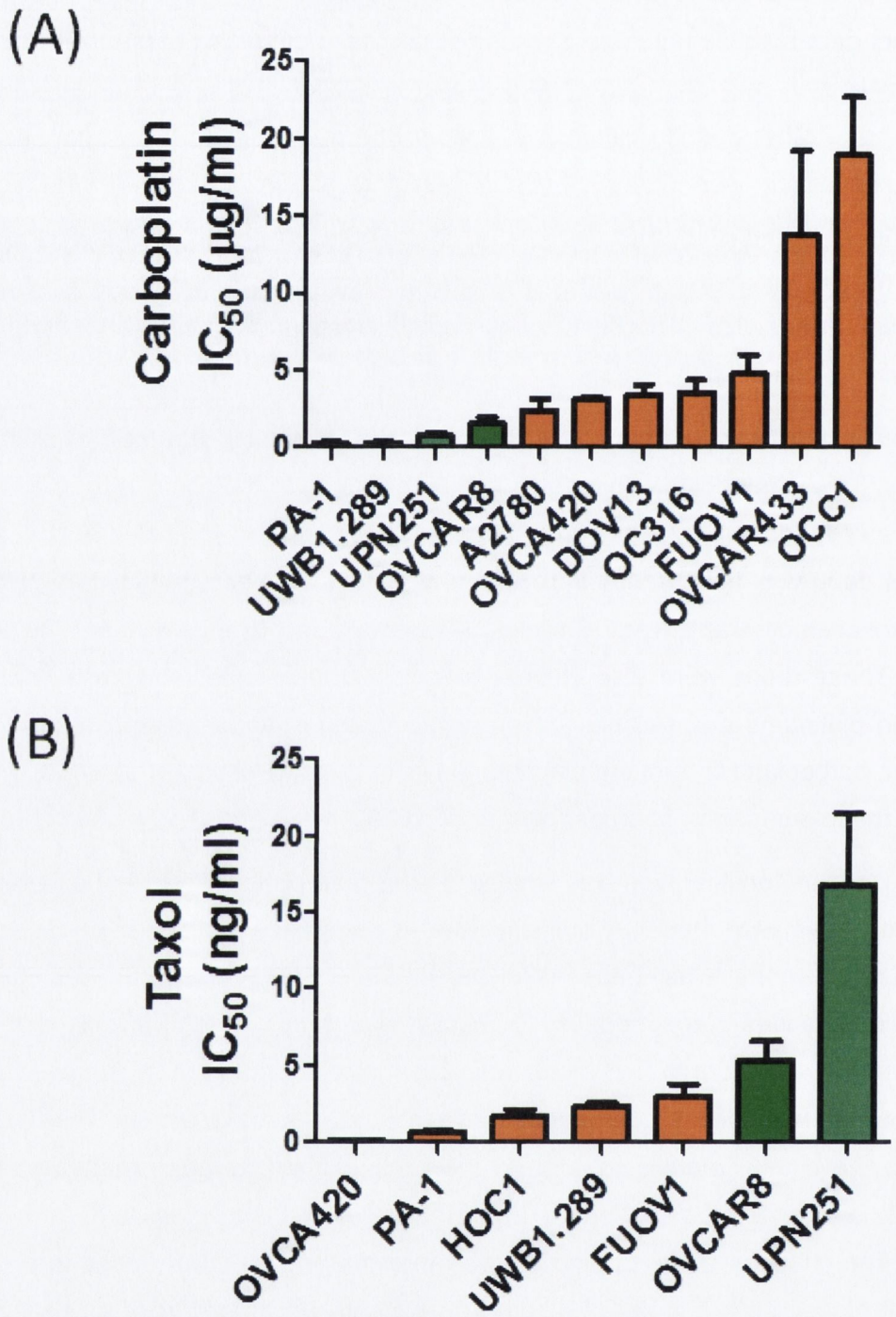

Figure 4.1 Carboplatin and taxol IC_{50} for a panel of ovarian cancer cell lines.

(A) X-axis gives 11 different ovarian cancer cell lines (OVCAR8 in green, UPN251 in blue and others in orange) and Y-axis indicated their fold resistance to carboplatin in µg/ml. (B) X-axis gives 7 different ovarian cancer cell lines (OVCAR8 in green, UPN251 in blue and others in orange) and Y-axis indicated their fold resistance to taxol in ng/ml. OVCAR8 and UPN251 show relatively low carboplatin IC_{50} and high taxol IC_{50} compared to other ovarian cancer cell lines. The experiments were performed by Dr. B Stordal and Dr. A. Farrelly.

bolus injection (*Hennessy et al. 2009*; *Ozols 2005*). The model had minimal escalation of drug dose to keep it in the clinical range.

4.2.2 Dose optimisation method

In order to select suitable starting doses of carboplatin and taxol for the selection strategy, that lies in a clinically relevant range, clinical trial data was examined to find doses that were often used in a clinical setting. Pharmacokinetic studies were then used to translate these doses into usable doses in the laboratory.

4.2.2.1 Dose optimisation of carboplatin

Clinical trial publications for carboplatin administration showed that a dose of carboplatin at the area under the concentration time curve (AUC) 5 was most often used for patients with advanced ovarian cancer as a single-agent (*Markman et al. 2010*; *Pfisterer et al. 2006b*). AUC is the ratio of the amount of drug that reaches the systemic circulation and the clearance of the drug, which correlates to its clinical efficiency and toxicity. A formula has been devised based on glomerular filtration rate (GFR), which is the main route of carboplatin elimination from the body, in order to calculate a suitable dose for patients, where the required AUC value can be achieved. This equation is known as the "Calvert Formula". The equation is written as Total Dose (mg) = (target AUC) x (GFR + 25) (*Calvert et al. 1989*). As the maximum GFR estimation for any patient at AUC5 is capped at 125mL/min, irrespective of what formula is used to calculate the GFR, the maximum permitted dose given to a patient will be 750mg for AUC5. A pharmacokinetic study by (*Gaver et al. 1988*) gives peak plasma values for doses ranging from 435-740mg or 170-500 mg/m². At 400mg/m², peak plasma was found to be 50µg/ml. Another pharmacokinetic study gives peak plasma for 375mg/m² as 39µg/ml dropping to 9µg/ml after 2 hours (*Oguri et al. 1988*). Considering that 90% of carboplatin is cleared from the body after 24 hours (*Go et al. 1999*), this would leave approximately 3.9µg/ml for a dose of 375mg/m² and 9µg/ml for a dose of 400mg/m². As these values are mid-range for AUC 5, it is reasonable to say that a range of 1-20µg/ml is clinically relevant.

4.2.2.2 Dose optimisation of taxol

Clinical trial publications for single-agent taxol administered to advanced ovarian cancer patients indicate that a dose of 175 mg/m² was commonest (*du Bois et al. 1997*; *ICON3 2002*; *Ozols et al. 2003*; *Rowinsky 1997*; *Vasey et al. 2004*). A pharmacokinetic study for patients administered with this dose shows a peak plasma concentration of 10,000ng/ml, followed by a steep drop off to 50ng/ml after 24 hours (*Mross et al. 2000*).

Another study gave an approximate peak plasma concentration of 4,000ng/ml for a typical female patient suffering from a solid tumour (NSCLC, ovarian and others) approximately 1 hour post administration (*Joerger et al. 2006*). This will decrease to a much lower level after 24 hours. From this evidence, 1-100ng/ml is a reasonable range to facilitate a clinically relevant dose.

4.2.2.3 Dose finding method

The doses of drug that were used in the selection strategy were evaluated separately. Doses of carboplatin for OVCAR8 and UPN251 and taxol for OVCAR8 and UPN251 were selected from a range of 2.3-18.5µg/ml, 0.7-2µg/ml, 2.3-14ng/ml and 10-100ng/ml respectively. Ranges were selected from the results of cytotoxic assays on parental cell lines initially encompassing inhibitory concentration (IC) values ranging from IC_{20}-IC_{80}. Clinical relevance was validated by investigating clinical trial publications and using pharmacokinetic studies to translate doses from the clinic into usable doses in the laboratory. These ranges could be extended depending on the outcome of dose testing.

On day 1, 1ml of media and cells were plated in duplicate into 5 separate 6 well plates (Sigma-Aldrich, UK) at a cell density of $1x10^4$ cells per ml. A control plate was set up separately, also with duplicate wells. On day 2, 1ml of media with a test dose of chemotherapy was added to all the plates excluding the control that received drug free media to the same volume. On day 5, the media was changed on all the plates and replaced with drug-free media. The control plate and one drugged plate were taken down and cell counted. The cell counts for the control were compared to the drug treatment. A percentage cell survival was calculated in order to see the effects of drug treatment on cell growth/survival. See equation 4.1.

Equation 4.1 Percentage cell survival

$$\frac{\text{(Average cell number of drugged cells)}}{\text{Average cell number of control cells}} \times 100$$

Over subsequent days, one plate for each drug dose was observed under a light microscope to see when normal growth had returned. When cells were deemed to have returned to confluence, this plate was cell counted to confirm recovery. Percentage cell survival was either above or climbing towards 100%. The time taken for cells to resume growth and return to confluence was recorded.

4.2.3 Cell selection strategy method

The cell lines were treated with carboplatin or taxol as per Figure 4.2. The sublines were named in the format of "(Parental cell line)-(Round)(Treatment)". For example, UPN251-4T refers to "(UPN251)-(Round 4)(Single-agent taxol treatment)". The parental cell line parameter can be UPN251 or OVCAR8. The round parameter can take the values 1-7 describing which round of selection the subline originates from. Finally, the treatment parameter can be (C) - single-agent carboplatin, (CALT) - alternating treatment starting with carboplatin in round 1, (T) - single-agent taxol and (TALT) - alternating treatment starting with taxol in round 1. This describes the treatment that this subline received. Treatments were 4-5 weeks apart, allowing for all cells to recover before subsequent drugging.

For each round of selection:-

Cells were plated into a T25 flask (Sarstedt, Germany) at a cell density of $2.6x10^4$ cells per flask and drugged on day 2 as per the selection strategy outline. On day 5, drugged media was removed and replaced with fresh drug free media. Over subsequent days, all T25 flasks were examined for confluence using a novel method to calculate an area fraction (AF) output (see chapter 3). Upon reaching confluence, cells were re-seeded into a T75 flask (Sarstedt, Germany). Leftover cells were used to freeze stocks. Cytotoxicity assays were performed at 1 week intervals for 3 weeks and were compared to the parental lines in order to calculate fold resistance. Once all cells had recovered, the next round of drugging commenced following the same format as above (provided the cells were 4 weeks after drugging, otherwise drugging was delayed until this time).

Equation 4.2 Relative fold resistance

$$\frac{IC_{50} \text{ of resistant subline}}{IC_{50} \text{ of parental cell line}}$$

4.3 Selection strategy related results

4.3.1 BRCA1 protein expression of parental cell lines

The BRCA1 protein expression of OVCAR8 (BRCA1 methylated) and UPN251 (BRCA1 un-methylated) was confirmed by Western blotting. The results were normalised to β-actin for n=3 samples. When BRCA1 results were normalised to

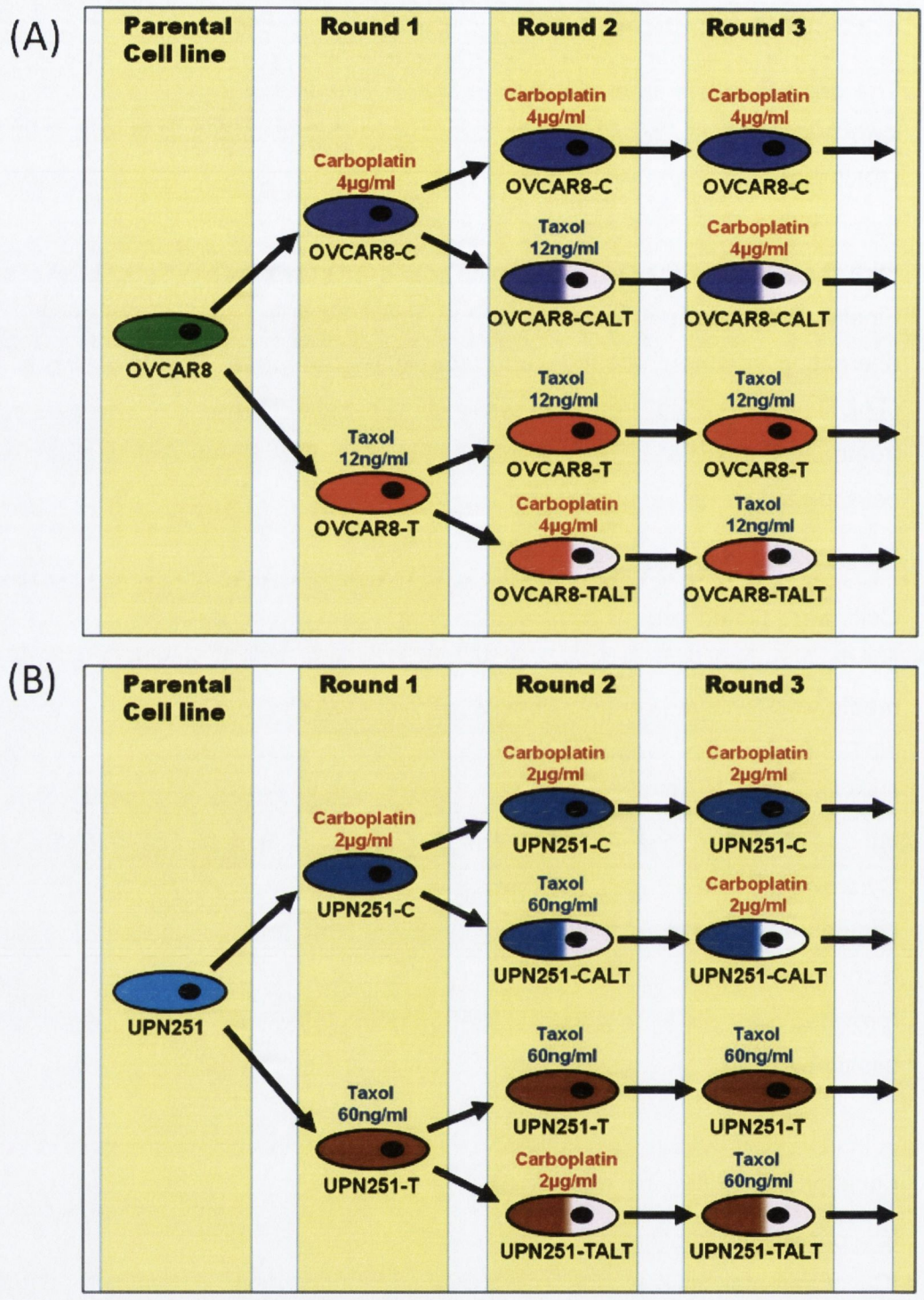

Figure 4.2 OVCAR8 and UPN251 treatment strategy for the development of platinum/taxane resistant cell lines.

In each case arrows represent progression to the next round with a drug treatment of either single-agent taxol or carboplatin as indicated. Resultant cells are shown from round 1-3 with the drug treatment they received in red (carboplatin) or blue (taxol) above cells and cell name given in black below cells. Rounds 4-7 progressed in the same pattern as shown. (A) OVCAR8 parental cells represented in green with resultant sublines in red and purple. (B) UPN251 parental cells represented in light blue with resultant sublines in dark blue and brown.

UPN251, it could be seen that BRCA1 expression was much lower in OVCAR8 when compared to UPN251. OVCAR8 shows 26 ± 7% of the expression of UPN251 ($p=3.3x10^{-4}$). See Figure 4.3. This finding supports the evidence from Myriad Genetics that OVCAR8 has reduced BRCA1 expression due to methylation of the promoter region of the BRCA1 gene (*Stordal et al. 2013*).

4.3.2 Cytotoxicity data of parental cell lines

Cytotoxicity assays for taxol and carboplatin were carried out on both UPN251 and OVCAR8 cell lines. Cell lines were subjected to 3-day and 5-day exposures to drug. The results for all cytotoxicity assays can be seen in Table 4.1. In 3 of the 4 treatments, we can see that higher doses of drug are needed for 3-day assays compared to 5-day assays in order to achieve an IC_{50}. This was an expected result. Student t-test analysis gave significant p-values for OVCAR8 taxol, OVCAR8 carboplatin and UPN251 carboplatin respectively when comparing 3-day and 5-day exposure to drug. The one exception was UPN251 treated with taxol. In this case, approximately the same dose of taxol was needed to achieve an IC_{50} over both 3 and 5 day exposures. The IC_{50} values were deemed to be not statistically significant with a p-value of 0.53 after Student t-test analysis. This may indicate that taxol's mechanism of action was being induced rapidly in UPN251 with two extra days of exposure having little effect on toxicity.

4.3.3 Dose finding optimisation

The dose optimisation method was used to find suitable doses to use in the selection strategy. Doses that displayed an initially large percentage cell death or growth inhibition compared to a control grown in drug-free media were selected, provided they were able to return to logarithmic growth after drug removal. A large percentage cell death from the cell population allows for the selection of resistant cells, as these cells are better able to survive exposure to cytotoxic drugs than those that have undergone apoptosis or necrosis. Allowing the remaining cells to return to logarithmic growth ensures that cells have recovered fully from the drugging before the next round commences.

Carboplatin doses of 4µg/ml and 2µg/ml and taxol doses of 12ng/ml and 60ng/ml were chosen for OVCAR8 and UPN251 respectively. See Figure 4.4 for recovery plots. The selected taxol doses saw less than 10% cell survival for both cell lines on the first day after drug exposure (compared to untreated control cells). They remained at this low level of survival over a number of days before cells returned quickly to logarithmic growth. UPN251 cells recovered quicker that OVCAR8 cells. This is likely because

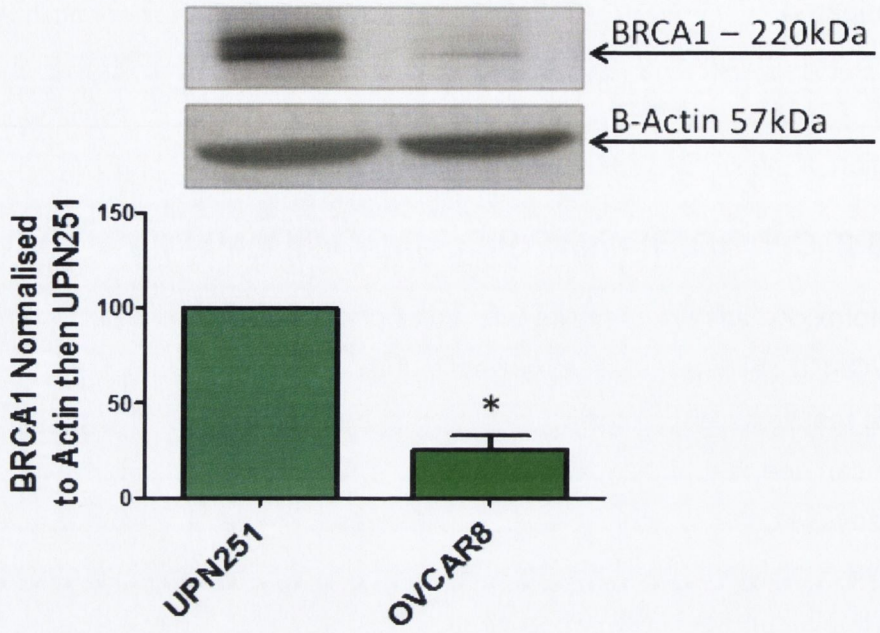

Figure 4.3 BRCA1 protein expression in UPN251 and OVCAR8 by Western blot.

Densitometry on n=3 biological replicates was carried out using Quantity One software (Biorad). Abundance of protein in arbitrary units was normalized to β-actin loading control for each sample and then each biological series was normalized to UPN251 control expression.

* Significant down regulation of BRCA1 in OVCAR8 compared to UPN251 with $p<0.05$.

Table 4.1 Acid phosphatase cytotoxicity assays.

IC50 data for UPN251 and OVCAR8 for 3-day and 5-day exposures. P-values are representative of Student t-test analysis between 3-day and 5-day exposures to drug.

	Drug	Exposure (Days)	N	IC50 (Mean)	IC50 (SD)	IC50 (%SD)	P-values
OVCAR8	**Carboplatin (µg/m)**	3	4	27.2	3.3	12.3	$5x10^{-6}$
		5	4	1.3	0.1	8.5	
	Taxol (ng/ml)	3	5	2.9	0.5	16.7	$8x10^{-5}$
		5	5	1.2	0.2	16.3	
UPN251	**Carboplatin (µg/ml)**	3	3	2.4	0.5	22.4	$7x10^{-3}$
		5	3	0.8	0.1	7.3	
	Taxol (ng/ml)	3	6	24.0	1.5	6.1	$5x10^{-2}$
		5	6	24.0	6.0	25.1	

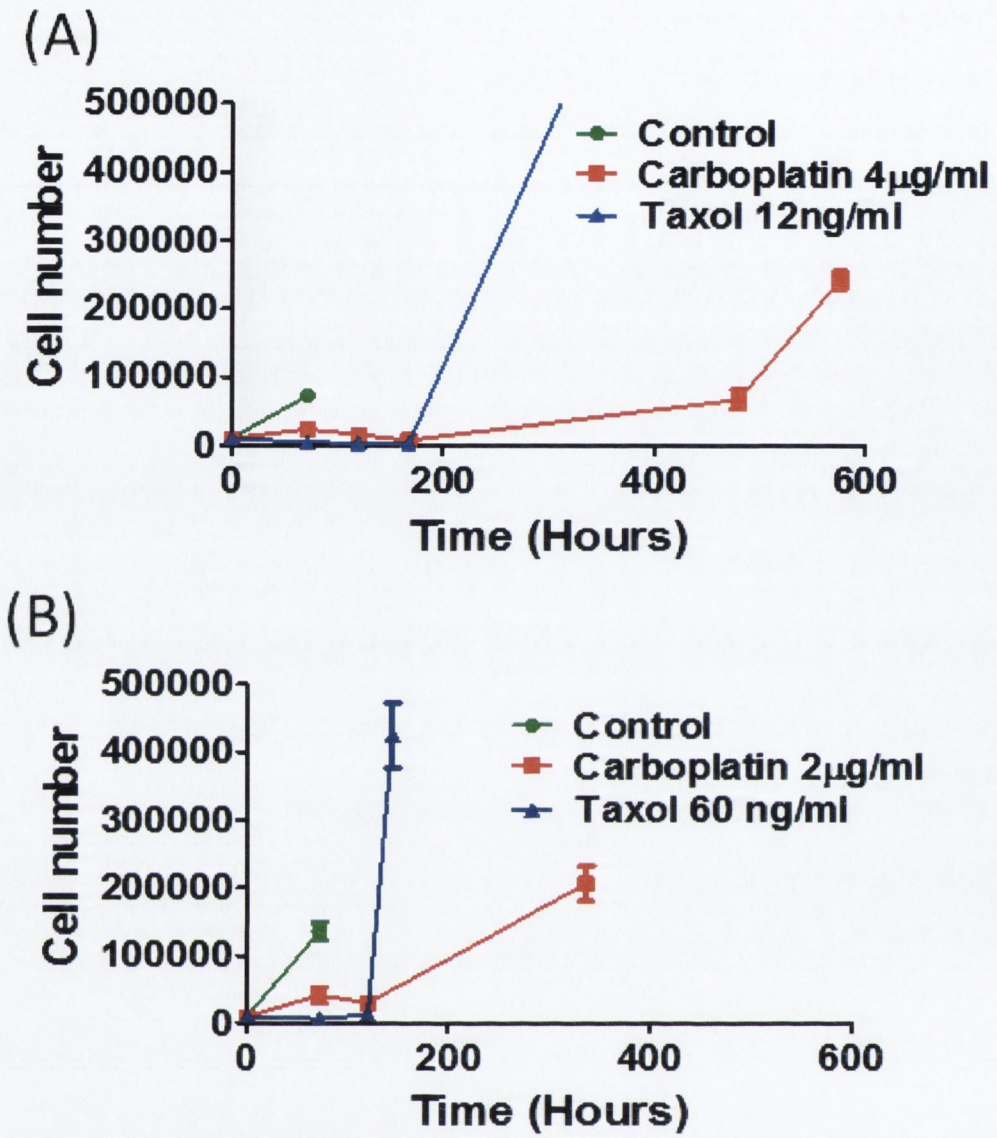

Figure 4.4 Recovery plots for the dose finding evaluation.

Graphs were generated using the dose finding method section 4.2.2.3 for selection strategy optimisation). Each graph is a representative of 1 of at least 3 biological repeats and shows cell number graphed over time (Hours). The control treatments are the cell lines grown in the absence of drug. Control treatments were cell counted on day 1 of the protocol. Once drugged treatments exceeded this number they were deemed to have recovered (A) Selected dose for carboplatin and taxol on OVCAR8. (B) Selected dose for carboplatin and taxol on UPN251.

patient from which UPN251 was derived had been exposed to taxol therapy, while the patient from which OVCAR8 was derived was taxol naïve. The UPN251 cells are more resistant to taxol and better able to deal with the drug's cytotoxic effects (Table 4.1). This would explain the higher dose needed on UPN251 to see a similar growth inhibition, followed by recovery (60ng/ml (UPN251) and 12ng/ml (OVCAR8)).

The recovery of cells with the selected carboplatin doses also showed similar trends in both cell lines, but recovered differently than the selected taxol doses. They showed an initial cell survival of between 20-50% after drug exposure. Cell survival decreased over the next 4-5 days dropping to between 10-20%. After this time, the cells slowly recovered and returned to logarithmic growth. Doses of carboplatin higher than the selected carboplatin doses caused the cells to have an initially low percentage cell death, followed by a decline in survival over the next 4-5 days, as seen in the selected doses. However, after this time, the cells died and could not return to logarithmic growth. OVCAR8 took longer to recover than UPN251 from the selected carboplatin doses, as was also seen in the selected taxol doses. However, this could not be explained by the patient's pre-exposure to the drugs as the patient from whom OVCAR8 was derived received high dose carboplatin treatment, while the UPN251 patient was carboplatin naïve. OVCAR8 requires a higher dose than UPN251 to see a similar growth inhibition and then recovery (2µg/ml (UPN251) and 4µg/ml (OVCAR8)), which would infer that OVCAR8 is slightly more resistant to carboplatin than UPN251. This is probably due to its pre-exposure to carboplatin. It may be that OVCAR8 has a different mechanism of dealing with carboplatin and taxol exposure, resulting in slower recovery in OVCAR8. This may be linked to their BRCA1 status.

The selected carboplatin concentrations were taken from a range of 0.7-18.5 µg/ml and the selected taxol concentrations from a range of 2.3-100ng/ml, which lie within the range of clinically relevant doses obtained from pharmacokinetic studies discussed in section 4.2.2.

4.3.4 Selection strategy recovery

As a general trend, the cells recovered quicker after drugging as the rounds of selection progressed. Figure 4.5 (A) shows recovery plots for each cell line grouped per ascending rounds of selection. In round 7, single-agent treatments received twice the usual dose of carboplatin or taxol and consequently recovery time increased accordingly. UPN251 cells recovered quicker than OVCAR8 cells and in both cell lines it took longer to recover from carboplatin treatments than taxol. Figure 4.5 (B) shows the sublines that were treated with carboplatin in each round of selection grouped

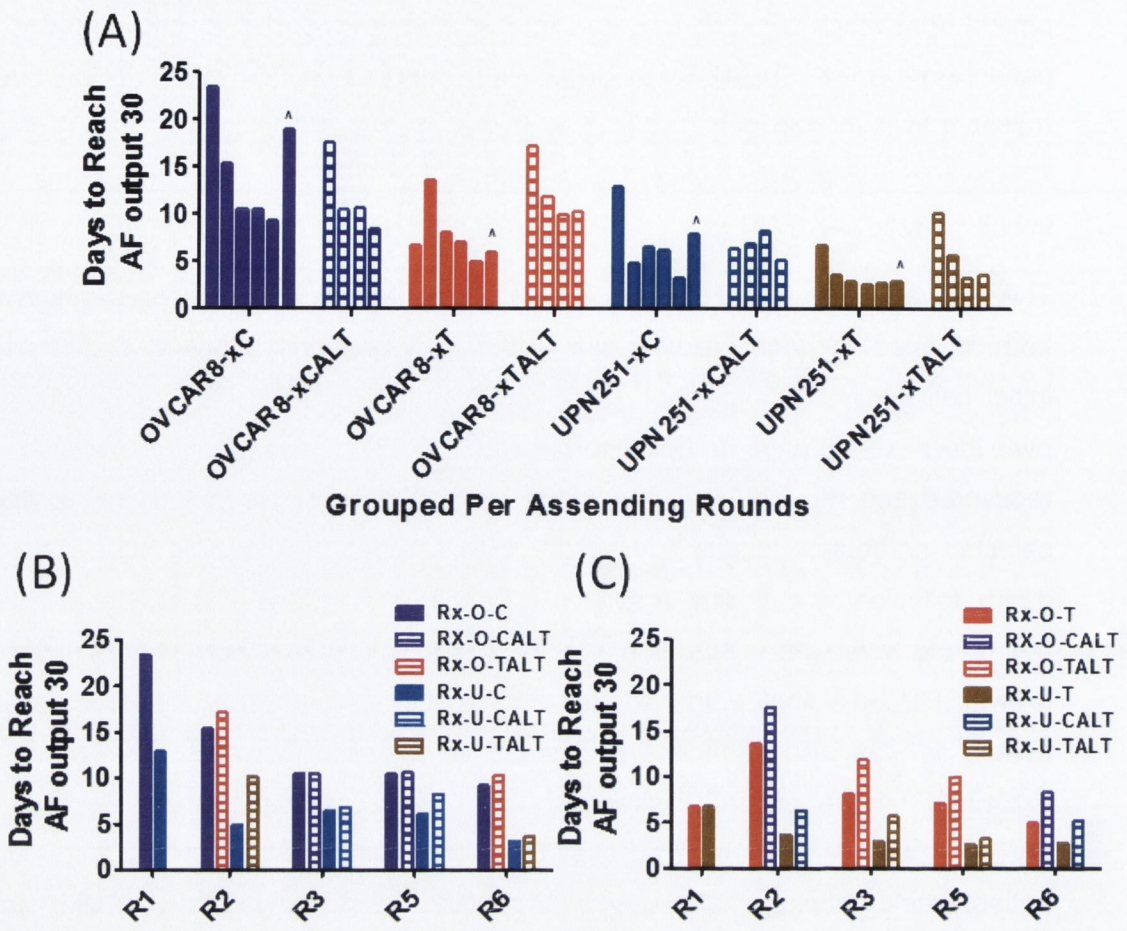

Figure 4.5 Selection strategy recovery data.

Recovery was indicated by days to reach AF output 30 (See chapter 3 for AF output method) shown on y-axis. (A) Recovery plots for each cell line (x in cell line name denotes that it represents all rounds of selection) grouped per ascending round of selection (1-7) Round 4 was excluded from the summery. (B) Recovery of carboplatin-treated cells in each round. (C) Recovery of taxol treated cells in each round.

^Received double dose of drug

together for comparison purposes. Single-agent carboplatin treatments were compared with alternating treatments that received carboplatin in each round. There was little difference in recovery between alternating and single-agent treatments receiving carboplatin. Round 2 was the only exception to this. Figure 4.5 (C) shows the same as above, but for taxol treatments. In this case, alternating treatments always took longer to recover than single-agent treatments when receiving taxol.

4.3.5 Selection strategy fold resistance

The fold resistance of each subline at weekly intervals for 3 weeks in each round of selection for carboplatin is shown in Figure 4.6 (A) and for taxol in Figure 4.6 (B). Significant fold resistance between parent and subline was assessed using Student t-test analysis. By round 6, UPN251-6T treated solely with taxol displayed the highest level of resistance (7-fold, $p=0.1x10^{-5}$). The sublines developed from UPN251 showed higher levels of resistance compared to those developed from OVCAR8. UPN251-6CALT, UPN251-6T and UPN251-6TALT all had significant resistance to taxol (4-8 fold, $p=0.4x10^{-6}$-$0.6x10^{6}$) while OVCAR8-6CALT, OVCAR8-6T and OVCAR8-6TALT all had significant resistance to taxol but to a lower extent (1.5-2.5 fold, $p=0.02$-$0.2x10^{-6}$). All UPN251 sublines, after their final round of selection (including UPN251-7T treated only with taxol), had significant resistance to carboplatin (1.6-3.5 fold, $p=0.3x10^{-3}$-$0.5x10^{-6}$). Only OVCAR8-7C and OVCAR8-6TALT had significant resistance to carboplatin in the OVCAR8 sublines (1.3-2.6 fold, $p=0.04$-$0.3x10^{-3}$). Again, this was lower than in UPN251 sublines. In as early as the first round of selection, UPN251-1C and UPN251-1T was significantly resistant to carboplatin (1.5-fold, $p=0.3x10^{-2}$) and taxol (1.7-fold, $p=0.8x10^{-2}$) respectively. These sublines retained significant resistance with fold resistance increasing from round to round. All UPN251 sublines receiving the opposite selecting agent in round 2 retained some degree of significant resistance to carboplatin, except UPN251-2TALT. However, this regained a significant level of resistance by round 3.

4.3.6 Maintenance of resistance after cell defrost

In order to see if the resistant sublines generated from the selection strategy would keep their developed resistance, they were screened with taxol and carboplatin cytotoxicity assays every week for 9 weeks, after they were defrosted. In general, alternating treatments lost some initial resistance and fluctuated more than single-agent treatments, but remained at an elevated level of resistance. Single-agent treatments showed stable resistance in the first 6 weeks. After this time, fold resistance started to decrease (See Figure 4.7).

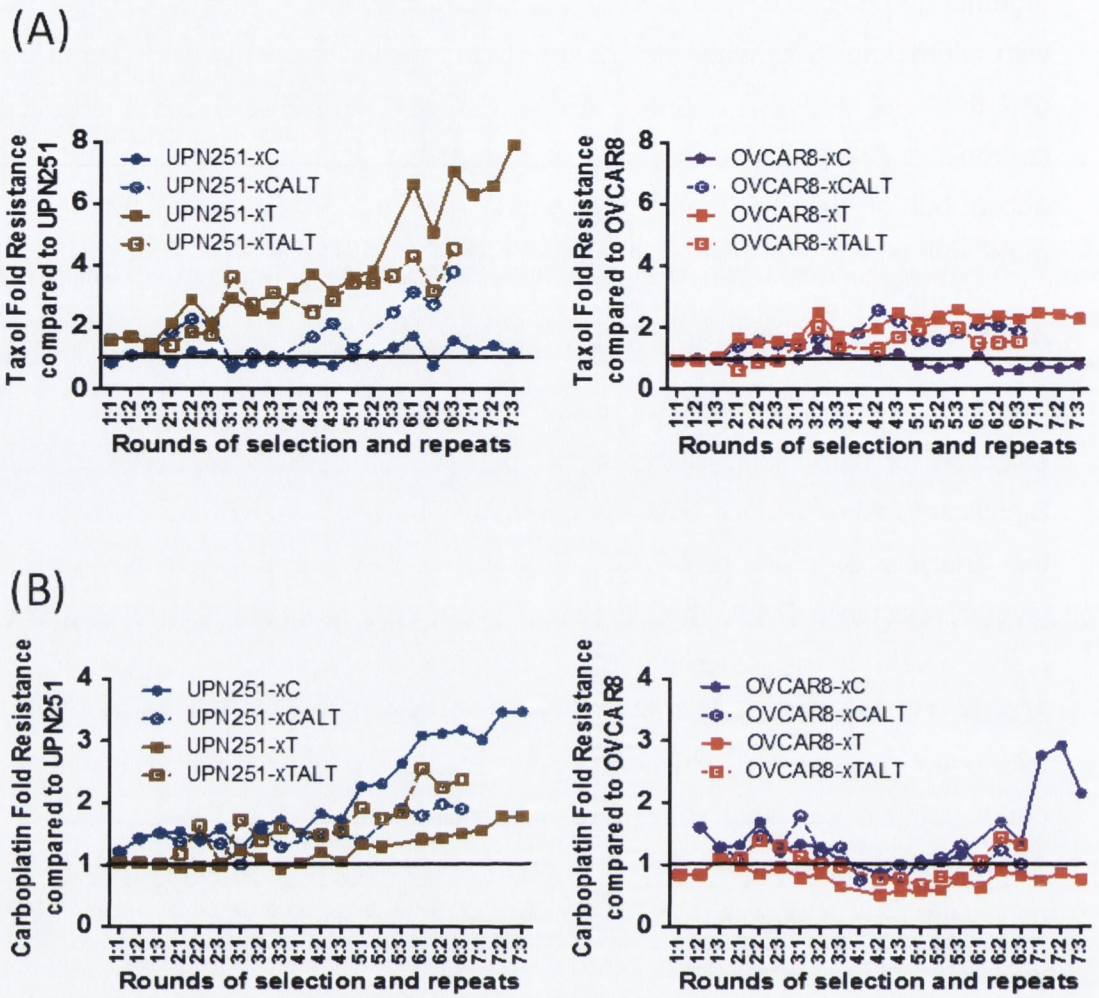

Figure 4.6 Fold resistance to carboplatin/taxol compared to parental cell lines.

Fold resistance to (A) carboplatin and (B) taxol are given for each subline from rounds 1-7. The x-axis gives a time progression for 3 weekly cytotoxicity assay in seven rounds of selection ((round number):(assay number)). The y-axis indicates fold resistance compared to parental cells assessed by equation 2.2, section 2.1.6 (Acid Phosphatase cell viability assay). The horizontal black bar indicates a fold resistance ratio of 1 (No difference to parent cells).

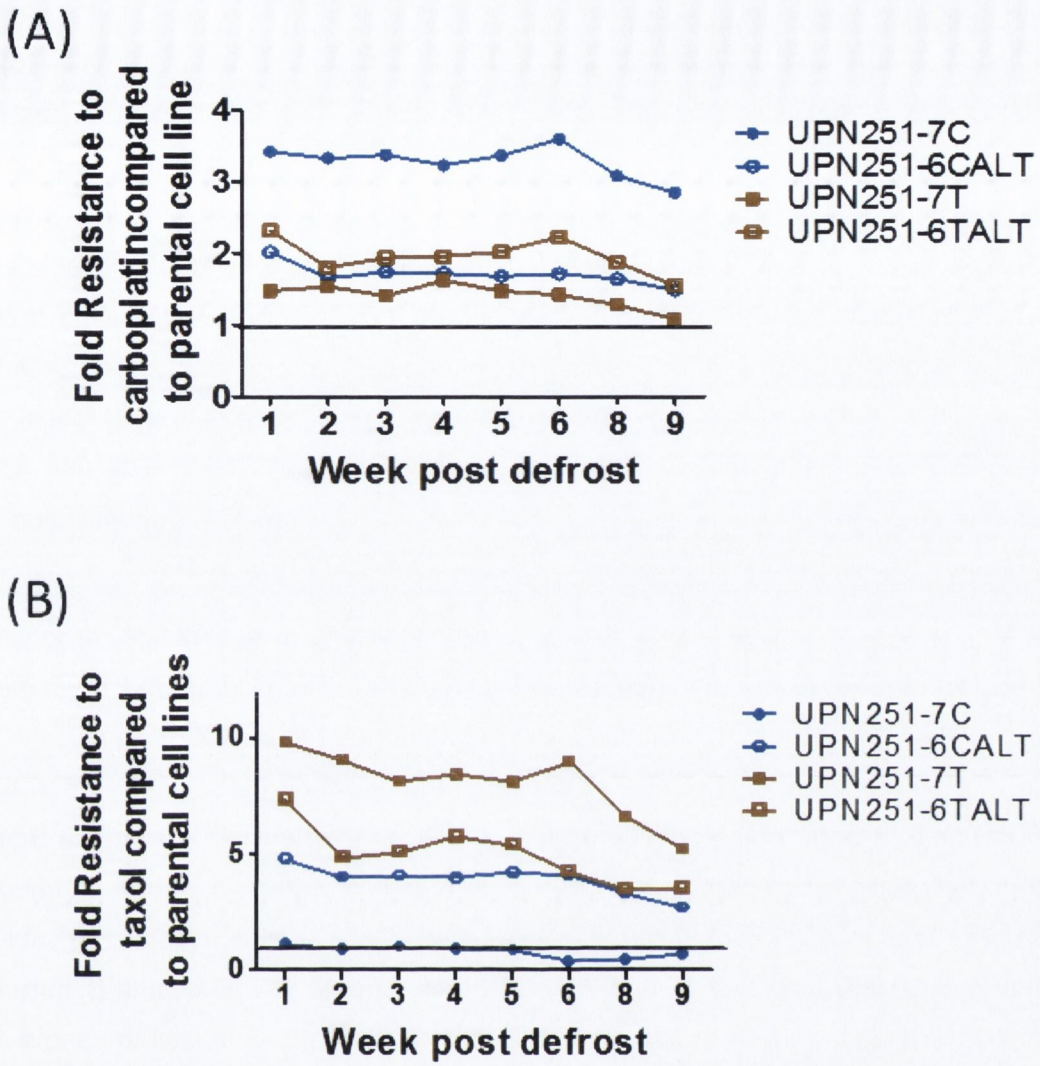

Figure 4.7 Fold resistance of sublines after defrosting.

Each graph represents fold resistance data for UPN251 sublines over a number of weeks after defrosting. The x-axis shows the number of weeks after defrost while the y-axis shows the fold resistance of the subline compared to UPN251. The Horizontal bar indicates a fold resistance ratio of 1 (No difference to parent cells). (A) Data from carboplatin cytotoxicity assays. (B) Data from taxol cytotoxicity assays.

4.4 Discussion

It was hypothesised that ovarian cancer cells with BRCA1 defects (OVCAR8) would develop resistance to platinums slower than taxanes, with the opposite being true for cells with functional BRCA1 (UPN251). Figure 4.8 (A) shows the extent of resistance development after 6 rounds of selection for single-agent treatments. This hypothesis holds true for OVCAR8 sublines, but not for UPN251 sublines, as taxol resistance developed quicker in both models irrespective of BRCA1 status. Possible reason for this occurrence was that taxol treated cells recover quicker than carboplatin-treated cells and, therefore, resistance can develop faster in taxol-treated cells. Slower recovery was seen for carboplatin treatments for both OVCAR8 and UPN251 compared to taxol treatments. This was noted in both the dose optimisation results (Figure 4.3) and the selection strategy recovery results (Figure 4.4).

Also it was hypothesised that cells receiving alternating treatments of carboplatin and taxol should develop resistance slower or not at all when compared to single-agent treatments. On first inspection, this seems to hold true. Figure 4.8 (B) shows the results of fold resistance after 6 rounds of selection for taxol and carboplatin. It can be seen from these graphs that single-agent treatments had higher fold resistance than all of the alternating treatments. However, the opposite conclusion could be reached, if the extent of resistance development was examined at point in time when each subline had received 3 doses of taxol (Figure 4.8 (C) (i)), or 3 doses of carboplatin (Figure 4.8 (C) (ii)). In UPN251, despite the fact that alternating treatments received the same amount of taxol or carboplatin over a longer period of time when compared to single-agent treatments (5 or 6 rounds in alternating versus 3 rounds for the single-agent), resistance development was higher in alternating treatments when compared to single-agent treatments. In OVCAR8, alternating and single-agent treatments are at a similar resistance level. This ambiguity in the results may stem from an inability to directly compare the results of the 2 drugs due to their different mechanisms of action and speed of recovery from drug treatment.

An interesting finding from the selection strategy was that cells treated with taxol, that received carboplatin in the previous round, displayed large increases in taxol resistance. This was larger than the increase in taxol resistance that was seen in cells that had only received taxol. Also, cells with carboplatin pre-treatment took longer to recover, compared to cells that had only received taxol, as was seen from our area fraction data (Figure 4.5 (C)). Therefore, carboplatin seems to enhance a cell's capacity to become taxol resistant.

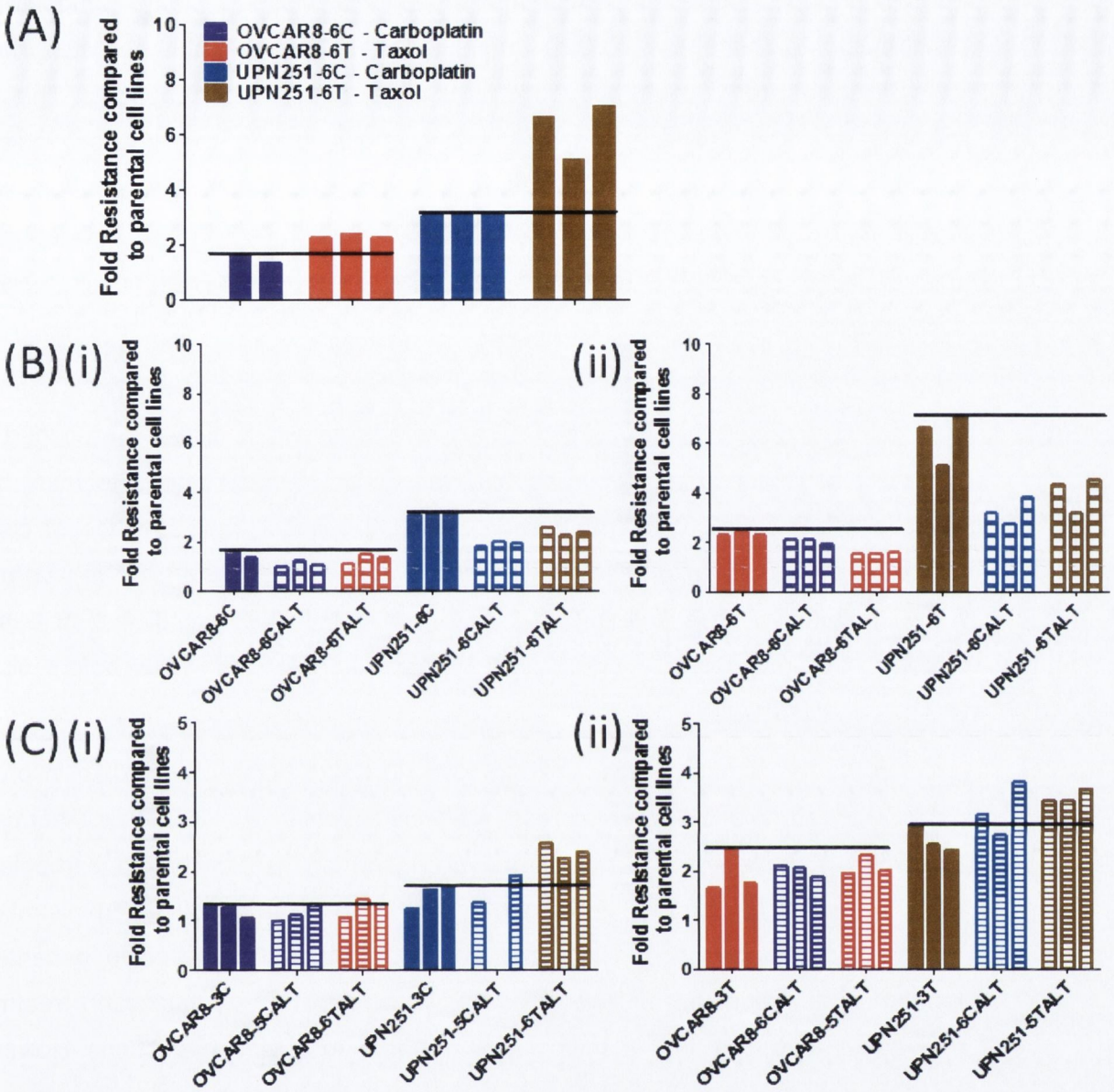

Figure 4.8 Selection strategy fold resistance outcomes.

Presented graphs show visual comparisons of fold resistance development between sublines to allow conclusions to be drawn in relation to the resistance development hypothesises (section 4.1.3.1). In each graph the y-axis shows fold resistance compared to parental cell lines. The x-axis shows resistant sublines. In Graph (A) it also indicates the drug used in cytotoxicity assay represented in the graph. Grouped bars represent cytotoxicity assays for 3 weeks following recovery. In (A) horizontal lines are used to show relative differences in carboplatin and taxol resistance development, while in (B) & (C) they show relative differences in carboplatin or taxol single-agent resistance development compared to alternating treatments. (A) Development of resistance to single-agent taxol and carboplatin for both OVCAR8 and UPN251. (B) Fold resistance to (i) carboplatin and (ii) taxol when compared to parental cell lines in round 6 of selection. (C) Fold resistance to (i) carboplatin and (ii) taxol when compared to parental cell lines when each cell line had received 3 doses of either carboplatin or taxol.

Further to this, alternating treatments generally displayed notable jumps in taxol resistance in a round in which they received taxol. This is usually greater than the increase in resistance seen per round from single-agent taxol treatments. This is the opposite of what we would have predicted, considering the inverse resistance relationship between platinum and taxanes (*Stordal et al. 2009*). We hypothesised that pre-treatment with one agent would sensitise to the other. There was no evidence of an opposite effect. Taxol pre-treatment did not affect the amount of carboplatin resistance developed.

Evidence of taxol treatment becoming less effective due to carboplatin pre-treatment is seen in the literature. An *in vitro* study showed that when cisplatin preceded taxol treatment, a lessened antitumor activity was seen when compared to taxol before cisplatin (*Kano et al. 1996*). In ovarian cancer cell lines, the sequence of cisplatin before taxol reduces taxol induced apoptosis (*Judson et al. 1999*). An *in vivo* mouse study showed that this sequence (cisplatin then taxol) had significant increases in morbidity and mortality associated with it when compared with taxol before cisplatin (*Milross et al. 1995*).

In the clinic for ovarian cancer, taxol is given 3 hours before carboplatin in order to circumvent carboplatin's myelosupressive affects (*Ozols et al. 2003*). Taxol reduces the proportion of bone marrow precursors circulating at the time when carboplatin is administered, which reduces toxicity when compared to the opposite administration. In non-small cell lung cancer clinical studies, with chemotherapy naïve patients, the sequence of carboplatin, followed by taxol administration in combination treatments, showed no sequence-dependant toxicities or pharmacokinetic interactions. However, it is unclear whether the different sequences affected the response data (*Giaccone et al. 1995*; *Huizing et al. 1997*).

OVCAR8 (BRCA1-methylated) developed much less resistance to carboplatin or taxol over the same time period as UPN251 (BRCA1-wildtype), after an identical cytotoxic drug treatment strategy. All OVCAR8 sublines were less than 2-fold resistant to carboplatin and less than 2.5-fold resistant to taxol after 6 rounds of selection. This may be due to the BRCA1 methylation status of the cells. Cells deficient in BRCA1 have reduced efficiency in repairing DNA damage caused by cytotoxic agents. It has been shown that hypermethylation of the BRCA1 promoter region causes increased sensitivity to platinum drugs (*Teodoridis et al. 2005*). Also, in two ovarian cancer cell lines, decreasing BRCA1 mRNA using inhibition assays correlated to increased sensitivity to platinums (*Quinn et al. 2007*). They also show that patients with low/intermediate levels of BRCA1 mRNA have a significantly improved overall survival

following platinum-based chemotherapy, compared to patients with high levels of BRCA1 mRNA. It has also been shown that the ovarian cancer cell line SNU251, having a mutation in BRCA1 inhibiting its sub-nuclear assembly, increased its sensitivity to taxol compared to the same cell line where BRCA1 wildtype was ectopically reintroduced (*Zhou et al. 2003*). Also, UPN251 and OVCAR8 may have had different baseline sensitivities to the drugs used as they originated from patients who had had different levels of exposures to carboplatin and taxol.

One caveat to our ability to directly compare resistance developed between carboplatin and taxol was that these drugs may not be directly comparable to each other, due to their different rates of recovery after drugging. This was seen in the dose finding experiment for the selection strategy (Figure 4.4) and in the selection strategy (Figure 4.5). The cells treated with taxol showed high initial cell death followed by fast recovery, while carboplatin showed much slower recovery with slight elevations in cell number after drugging, followed by cell death and slow recovery. This could be due to the differences in platinum and taxane mechanisms of action. Platinums act mainly by forming nuclear platinum adducts on DNA strands (*Fuertes et al. 2003b*; *Go et al. 1999*), while taxanes act by stabilising microtubules within the cell (*Manfredi et al. 1984*; *Rao et al. 1995*).

4.5 Conclusions

It was hypothesised that ovarian cancer cells with BRCA1 defects (OVCAR8) would develop resistance to platinums slower than taxanes with the opposite being true for cells with functional BRCA1 (UPN251). This did not hold true in the models. The development of taxane resistance was not slower than the development of platinum resistance in cells with functional BRCA1. Taxol resistance developed quicker in BRCA1-wildtype and BRCA1-methylated cells models irrespective of BRCA1 status. Both resistance to carboplatin and taxol developed quicker and more stably in UPN251 (BRCA1-wildtype) compared to OVCAR8 (BRCA1-methylated). Therefore, the BRCA1 status of an ovarian cancer patient may affect treatment outcome. Screening for BRCA1 defects in patients may be beneficial in improving patient survival. If patients have BRCA1 defects they will benefit more from standard chemotherapy than patients who have functional BRCA1. Alternate treatment may benefit patients with functional BRCA1 due to the development of carboplatin and taxol resistance. As the majority of patients will have functional BRCA1, it highlights the importance of developing new targeted treatments for ovarian cancer patients so that treatment can move away from

damaging chemotherapy regimens, to which the patient will ultimately develop resistance.

It was also hypothesised that cells receiving alternating treatments of carboplatin and taxol should develop resistance slower or not at all when compared to single-agent treatments. Results from this were ambiguous, depending on the logic used to draw conclusions. If this statement was found to hold unequivocally true, it would have pointed towards changing the way chemotherapy is currently administered to patients to reduce resistance development. However, this hypothesis was shown to be true or false under different conditions. Carboplatin and taxol treatment delayed, but did not prevent resistance development when compared to single agent administration. For this reason, the evidence produced was not strong enough to suggest changing the combined administration of carboplatin and taxol to alternating administration.

Finally, it was noted that UPN251 sublines developed greater fold resistance than OVCAR8 for both taxol and carboplatin. These relatively high fold changes within a clinically relevant dose range make the UPN251 sublines interesting candidates for further study. The mechanisms of resistance that had developed in these cell lines were investigated in chapter 5. OVCAR8 sublines were not further investigated due to the low-level unstable resistance achieved in comparison to UPN251 sublines.

CHAPTER 5

Resistant Cell Line Characterisation



TRINITY
COLLEGE
DUBLIN

Chapter 5 Resistant cell line characterisation

5.1 Introduction

This chapter deals with the characterisation of the resistance mechanisms that have developed in our UPN251 derived taxol and carboplatin resistant ovarian cancer sublines. The major mechanisms of carboplatin and taxol resistance from the literature have been discussed in Chapter 1 (section 1.4 and section 1.6 respectively). A number of these resistance mechanisms were investigated in this chapter. These mechanisms of resistance were deemed likely to play a role in our sublines' developed resistance phenotypes.

5.1.1 Cell selection strategies influence resistance development

The mechanism of resistance in a drug-resistance model can differ, depending on the method of selection used. The commonest methods of selection used to model resistance are increasing continuous administration (*Liu et al. 2010*; *Smith et al. 2002*; *Vandier et al. 2000*) and low-dose intermittent incremental inducement (*Godwin et al. 1992*; *Kars et al. 2006*; *Teicher et al. 1986*).

In the resistance models that use increasing continuous administration, the drug of choice is exposed to the cells in a continuous fashion and is periodically increased over many months in order to develop resistant sublines. Human colon cancer cells resistant to oxaliplatin have been developed using this strategy (*Liu et al. 2010*). SW620 and LoVo human colon cancer cell lines were initially exposed to 10mg/ml of oxaliplatin. This concentration was increased over 10 months to develop SW620/L-OHP and LoVo/L-OHP. SW620/L-OHP was 21-fold resistant to oxaliplatin and was maintained in a concentration of 2μg/ml and LoVo/L-OHP was 13.8-fold resistant to oxaliplatin and was maintained in a concentration of 2μg/ml. An example of ovarian cancer cells developed using this method is the development of cisplatin-resistant cell line A2780-E(80) from the parental A2780(1A9) ovarian cancer cell line (*Vandier et al. 2000*). A2780 (1A9) was initially exposed to a concentration of 1.7μg/ml cisplatin and periodically increased to a final concentration of 266.6μg/ml cisplatin. They were maintained at this concentration. The final dose given was 160 times greater than that of the initial dose. The relative fold resistance to cisplatin of these cells as determined by a cytotoxicity assay was not presented in this study.

In the resistance models that use low-dose intermittent incremental inducement, cells are exposed sporadically to increasing doses of drug over time. A number of resistant

human breast cancer cell lines were developed from MCF-7 cells using this method, which were resistant to taxol (MCF-7/Pac), docetaxel (MCF-7/Doc), doxorubicin (MCF-7/Dox) and vincristine (MCF-7/Vinc). The doses were increased from 0.1ng/ml to 140.5ng/ml for taxol, 0.1ng/ml to 99ng/ml for docetaxel, 17.2ng/ml to 1034.5ng/ml for doxorubicin and 2.4ng/ml to 48.5ng/ml for vincristine. Resistant cell lines were between 11.3-17.3-fold resistant to their selecting agents (*Kars et al. 2006*). An example of ovarian cancer cells developed using this method is the development of cisplatin-resistant cell lines from parental A2780 cell line. The A2780 cells were exposed to increasing concentrations of cisplatin ranging from 26.7µg/ml-233.3µg/ml to produce the cisplatin resistant cell line A2780/CP8-CP70. The A2780/CP70 cell line had a fold resistance to cisplatin of 29 fold.

The above strategies often produce high fold resistances and may be classed as high-level laboratory selection strategies. This, as discussed in chapter 4, may not emulate mechanisms of resistance that are produced from the low levels of drug concentrations administered in the clinic. However, they produce stable resistance often with large molecular changes which are easier to detect and maintain.

A number of studies have used a pulsed strategy of resistance development in an attempt to mirror the clinical setting more closely for certain drugs (*Glynn et al. 2004*; *Liang et al. 2004*; *Ying et al. 2012*). The pulsed strategy is used more seldom because it often gives low, unstable fold resistance when compared to other strategies. This normally involves a short drug exposure of approximately 4 hours over long intervals (for example weekly intervals), which may take place over a number of weeks. In a study by *Glynn et al. (2004)* the MDA-MB-435S-F human breast cancer cell line was exposed to IC_{90} values of doxorubicin (120ng/ml) or taxol (15ng/ml) for 4 hours once a week for 10 weeks. Taxol variants were further exposed to a higher dose of taxol (125ng/ml) for 4 hours once per week for 4 weeks and doxorubicin variants were further exposed to a higher dose of doxorubicin for (200ng/ml) 4 hours once per week for 10 weeks. The taxol selected variants MDA-MB-435S-F/Taxol-10p and MDA-MB-435S-F/Taxol-10p4p were 9.2 and 31.8-fold-resistant to taxol respectively. The doxorubicin selected variants MDA-MB-435S-F/Adr-10p and MDA-MB-435S-F/Adr-10p4p were 1.2 and 1.4-fold resistant to doxorubicin respectively (*Glynn et al. 2004*). Similarly, *Ying et al. (2012)* exposed MCF-7 and MDA-MB-231 cells to taxol for 4 hours once per week for 10 weeks at a dose of 234ng/ml and 117ng/ml respectively. The resistant variant 231-TIM10 had 11.9-fold resistance to taxol and MCF-7-TIM10 was 5.5-fold resistant to taxol (*Ying et al. 2012*).

A comparative study by *Yan et al. (2007)* compared the differences in using a pulse versus intermittent incremental strategy in the same ovarian cancer cell lines. SKOV3 ovarian cancer cell lines were subjected to cisplatin and taxol by each method over a 16 month period. For the pulsed strategy, SKOV3/CDDP-P and SKOV3/Taxol-P were produced by exposing the cells to cisplatin (30μg/ml) and taxol (2.13μg/ml) for 2 and 1 hour periods respectively, 20 times over the 16 month period. For the intermittent incremental strategy, SKOV3/CDDP80 was intermittently selected by a small dosage of cisplatin at 3, 6, 12 and 25μg/ml and 10 times each dosage. The cells were in a cisplatin-containing medium for 48 hour exposures. Similarly, SKOV3/Taxol-25 was intermittently selected by a small dosage of taxol at 8.5, 12.8 and 21.3ng/ml and 10 times each dosage was used. The cells were in a taxol-containing medium for 24 hour exposures. The cells selected by the intermittent incremental strategy had much higher levels of resistance than that of patients in the clinic, whereas the pulsed strategy produced smaller changes, but to a more similar level to that which is generally observed in the clinic. For this reason it was assumed that the pulsed strategy more closely mirrored the clinical setting. Morphology, growth rate, and proliferation indexes differed between cells selected with the different strategies. Also, genes known to be involved in resistance (MDR1, MRP1, LRP and GST-pi) differed in expression between the different cell models. Inconsistent results were obtained between the same cells, despite being resistant to the same agent, only differing from method of selection used. The team showed that different approaches of selection can lead to distinct expression of genes associated with drug resistance. Mechanisms of drug resistance were different for dissimilar methods of drug treatment, indicating the importance of model selection in gaining clinically relevant resistance mechanisms from a selection strategy. The consensus was that although the intermittent incremental strategy produced higher levels of fold resistance, the mechanisms evolved using the pulse strategy were closer to the mechanisms seen in the clinic and serves as a more 'appropriate' model in studying drug resistance in ovarian cancer (*Yan et al. 2007*). Therefore, mechanisms produced from this study have the potential to closely mirror the clinical mechanisms of resistance that arise in ovarian cancer patients.

In the clinic, ovarian cancer patients receive drug infusion every 3-4 weeks (*Ozols 2005)*. The model described in chapter 4 had one prolonged pulse over three days and then recovery in drug free media for 4-5 weeks. This is a more accurate representation of the clinical setting in ovarian cancer than other selection methods, including the typical pulsed strategies with shorter treatment intervals.

5.1.2 Models of taxol resistance and related mechanisms

Taxol resistance cell models are very common and many have been developed for ovarian cancer cell lines (*Duan et al. 1999b*; *Duan et al. 1999c*; *Hari et al. 2006*; *Parekh et al. 1997b*; *Zhang et al. 2012a*). Most of these models use different variations on the aforementioned intermittent incremental inducement and increasing continuous administration strategies. Our work is novel, as a pulsed strategy which closely mirrors the clinic has not been used before in ovarian cancer to our knowledge. Also, a model of taxane-resistance has not been previously developed in UPN251, to our knowledge.

The over-expression of P-glycoprotein (P-gp), a product of the MDR-1 (ABCB1) gene, is a common mechanism of taxane resistance. P-gp is a transmembrane ATP dependent efflux pump of the adenosine triphosphate binding cassette (ABC) gene family, which has many members. It has been shown to confer resistance to a wide variety of drugs, including taxanes, by efficiently removing them from the cell (*Juliano et al. 1976*; *Ueda et al. 1987*). The up-regulation of this protein is linked with poor prognosis for patients with ovarian and breast cancers, sarcomas and other malignant disease (*Hoffmann et al. 2010*; *Nakayama et al. 2002*; *Rodrigues et al. 2008*). However, other studies have indicated that strong P-gp over-expression is uncommon in the clinic, even if it is strongly correlated with poor outcome and relapse (*Materna et al. 2004*; *McGown et al. 1994*; *Penson et al. 2004*).

This will be examined in our UPN251 sublines to try and elucidate the major mechanisms of resistance that is driving change in our cell line panel. Increased levels of MDR1 mRNA and P-gp at a protein level have been demonstrated in a wide variety of taxol-resistant cancer cell lines, implicating its role in taxane resistance profiles (*Bhalla et al. 1994*; *Duan et al. 1999c*; *Parekh et al. 1997b*; *Schondorf et al. 2002*). It has also been put forward as being a useful indicator for taxol-based resistance in ovarian cancer (*Duan et al. 1999c*; *Kamazawa et al. 2002*; *Naniwa et al. 2007*; *Parekh et al. 1997b*; *Rutledge et al. 1990*; *Schondorf et al. 2002*). A recent ovarian study indicated that high P-gp expression, in treated recurrent patient samples, occurred more frequently than in primary ovarian tumour samples (43% versus 24% from 105 patient samples tested in this study) (*Zajchowski et al. 2012*). In combination with ERCC1, which is connected to carboplatin drug response, P-gp may have a useful application as a biomarker of relapse where changing expressions could affect secondary treatment choice and improve response (*Zajchowski et al. 2012*).

P-gp inhibitors, such as elacridar, can sensitise cancer cell lines to taxol treatment (*Hyafil et al. 1993*; *Reinecke et al. 2000*). This inhibitor was used in this study to

investigate P-gp mediated resistance in the resistant sublines. P-gp inhibitors have not been effective in the clinical setting to date. Mainly, this has been due to their non-specific action on P-gp and their non-selective distribution to non-target organs, which leads to adverse side effects by the P-gp inhibitors at the doses needed for P-gp to work when administered systemically (*Binkhathlan et al. 2013*). Further to this, elimination of anticancer drugs is reduced and toxicity of the drugs is increased when co-administered with P-pg inhibitors (*Binkhathlan et al. 2013*).

5.1.3 Models of carboplatin resistance and related mechanisms

Carboplatin-resistant ovarian cancer cell lines are rare in the literature. More than likely, this is because a combination of cisplatin and taxol was used as a standard chemotherapy treatment for advanced ovarian cancer up until 2003. Carboplatin and taxol was then introduced as the new standard of treatment as it was deemed more favourable due to reduced toxicities being associated with carboplatin administration *(du Bois et al. 2003; Ozols et al. 2003)*. A publication by *Li et al. (2004)* reports on the development of 5 resistance cell models for ovarian cancer cell lines (2 carboplatin, 2 cisplatin and 1 taxol) *(Li et al. 2004)*. They found a number of genes that were differentially expressed compared to parental cells across all resistant models. To our knowledge, a model of carboplatin-resistance has not been previously developed in UPN251 making this study novel.

One study developed carboplatin-resistant sublines from human larynx carcinoma cell line Hep 2 by continuous 5 day exposure of increasing doses of carboplatin. All of the 3 sublines developed had elevated levels of glutathione (GSH), but only one of these had significant elevations (*Osmak et al. 1995*). Elevated levels of GSH compounds can be correlated to platinum resistance. For example, a study carried out on eight ovarian cancer cell lines has showed a positive relationship between intracellular GSH levels and platinum resistance (*Mistry et al. 1991*). There are many mechanisms in which the GSH system may act in conferring cisplatin resistance (*Chen et al. 2010*). One mechanism involves the formation of cisplatin-GSH complexes by GSH-S-transferase π. These complexes are inactivated and effluxed from the cell via the MRP2 membrane protein, which is a member of the ABCC2 transporter family. Cisplatin cannot be effluxed from the cell on its own in this way but requires binding to GSH (*Paulusma et al. 1999*). This mechanism is shown in Figure 1.4 (chapter 1). Another mechanism is the GSH mediated up-regulation of copper transporter CTR1, which can efflux platinum compounds (*Safaei et al. 2005*; *Song et al. 2008*). GSH can also act as a cytoprotector in cisplatin resistance. It has been discovered that resistant cells often

increase synthesis of GSH and γ-glutamylcysteine synthetase, the rate limiting enzyme for glutathione synthesis. The more GSH that is within the cell, the more that is present to bind and inactivate platinum compounds (*Rabik et al. 2007*). GSH levels will be examined in the UPN251 resistant sublines in this study.

Aberrant expression of membrane transporters was also investigated in the sublines in this study. Increased expression of copper efflux transporters ATP7A and ATP7B and decreased expression of copper influx transporter CTR1 has been shown to confer platinum resistance in ovarian cancer. ATP7A has been found to sequester cisplatin, carboplatin and oxaliplatin into vesicles. Over-expression of the ATP7A protein has been found in platinum-resistant ovarian cancer cell lines and in ovarian cancer patients linked to poor survival rates after carboplatin treatment (*Katano et al. 2002*; *Samimi et al. 2004*). Also, *Doherty et al. (2014)* found decreased protein expression of ATP7A in platinum-sensitive ovarian cancer cell lines (*Doherty et al. 2014*). Elevated levels of ATP7B has also been linked to platinum resistance in ovarian cancer cell lines (*Nakayama et al. 2001*) and poor survival rates following platinum treatment (*Rabik et al. 2007*). CTR1 protein down-regulation has been shown to occur in ovarian cancer cell lines after exposure to cisplatin, resulting in diminished cisplatin accumulation in the cell (*Holzer et al. 2004*). This process is concentration and time dependent and occurs rapidly. Exposure to as little as 0.15ng/ml cisplatin for 5mins reduced CTR1 levels with ≥ 0.6ng/ml, causing almost complete disappearance of the protein in A2780 ovarian cancer cells. Another mechanism of cisplatin resistance involving CTR1 is the internalisation of the CTR1 protein from the surface membrane to the cytoplasm of the cell in response to cisplatin treatment. This was also shown in cisplatin-resistant IGROVCDDP ovarian cancer cells (*Stordal et al. 2012*).

MRP proteins, which are members of the ABC transporter family have been linked with multidrug resistance (*Choudhuri et al. 2006*). MRP2 gene and protein over-expression has been related with platinum resistance in ovarian cancer and a number of other cancer types. MRP2 over-expression is deemed to be a good determinant of tumour sensitivity (*Kool et al. 1997*; *Korita et al. 2010*).

Suppression of apoptosis is another major mechanism of resistance development that was investigated in the cell line models in this study. In particular, aberrant expression levels of Bcl-2 family members, which regulate cytochrome C release, have been shown to influence chemoresistance. In ovarian cancer, over-expression of Bcl-XL and Mcl-1 are strongly correlated to chemoresistance. Inhibition of these proteins can show marked improvement in cisplatin chemotherapy *in vitro* (*Brotin et al. 2010*; *Villedieu et*

al. 2007). Also, over-expression of the Bcl-2 gene has been shown to confer resistance in ovarian cancer cell lines (*Yu et al. 2004*).

5.1.4 Resistance biomarkers in the clinic for ovarian cancer

Drug resistance in ovarian cancer has been comprehensively studied. However, it has proved to be complex, with ovarian cancer being inherently heterogeneous. There has been an array of resistance biomarkers discovered to date for both platinum and taxane resistance in ovarian cancer at the transcriptomic and proteomic level. A number of these markers mentioned in section 1.1.3 and 1.1.4 were used to characterise the developed carboplatin and taxane resistant UPN251 sublines from chapter 4. However, these markers have had limited success in the clinic. Due to the inherent heterogeneity of ovarian cancer, they have not proved to be sufficiently robust or specific enough to date to be adopted by clinicians in the treatment and screening of ovarian cancer patients. There remains a need to discover novel markers for chemotherapy resistance in ovarian cancer that can be specific and robust enough to aid clinicians or aid in the development of targeted therapies to overcome chemoresistance.

5.1.5 Aims and objectives

This chapter aimed to characterise the major mechanisms of ovarian cancer resistance that had developed in our UPN251-derived taxol and carboplatin resistant ovarian cancer sublines (developed in chapter 4).

5.1.5.1 Hypotheses

The hypothesis examined in this chapter stated that:

- A number of carboplatin and taxol resistance mechanisms have developed within our ovarian cancer UPN251 resistant subline, which mirrors ovarian cancer patients in the clinic due to the clinically relevant selection strategy used during their development.

5.1.5.2 Objectives

The main objective of this chapter was to elucidate the major resistance mechanisms that have developed within our UPN251-derived carboplatin and taxol resistant sublines. The mechanisms that were examined include P-gp over-expression, de-regulation of copper and MRP transporters, elevated GSH levels and inhibition of apoptosis. This was achieved by carrying out a drug screen to examine cross

resistance to other drugs, looking at total GSH levels under different conditions, examining protein expression levels, cell cycle regulation, growth rate and suppression of apoptosis.

5.2 Methods

A number of techniques were used in order to characterise our chemoresistant UPN251 ovarian cancer sublines (UPN251-7C, UPN251-6CALT, UPN251-7T and UPN251-6TALT).

- The sublines' cross resistance profiles to a number of cytotoxic drugs was assessed by using acid phosphatase cell viability assays (chapter 2, section 2.1.6).
- A total cellular glutathione (GSH) assay was performed in order to see the effects of cellular GSH levels following carboplatin treatment (chapter 2, section 2.1.8).
- The growth rate of the sublines, with and without carboplatin and taxol, was assessed using a high content screening growth assay to allow for the testing of a range of different drug concentrations with high throughput (chapter 2, section 2.1.7.2).
- A cell cycle mitosis assay was carried out in order to investigate the amount of cells that were in the mitotic phase of the cell cycle and, as such, in a cell cycle arrest in the G2/M phase (chapter 2, section 2.1.10). Taxol is known to induce cell cycle arrest at the G2/M phase of the cell cycle, resulting in apoptosis as part of its mechanism of action (*Long et al. 1994*).
- Apoptosis and cell cycle assays were run in parallel using the same samples, using fluorescence-activated cell sorting (FACS) (chapter 2 section 2.1.11).
    - A FITC annexin V / (Propidium iodide) PI apoptosis assay was carried out on the UPN251 parental and resistant sublines to see the effect of high-dose drug exposure on initiation of apoptosis (chapter 2, section 2.1.11.1).
    - A cell cycle assay was carried out to see the effect of high dose drug exposure on the cell cycle (chapter 2, section 2.1.11.2).
- Protein expression levels for a number of known biomarkers of carboplatin and taxol resistance was examined by carrying out Western blotting (chapter 2, section 2.1.9).

5.3 Results

5.3.1 Drug screen

A drug screen was performed on the UPN251-derived resistant cell line panel in this study in order to evaluate cross resistance to other drugs and to help elucidate resistance mechanisms that have developed in the cells. 11 drugs and 2 inhibitors were used. Inhibitors included, buthionine sulphoximine (BSO), an inhibitor of GSH synthesis (*Drew et al. 1984*), and elacridar, an inhibitor of P-glycoprotein (P-gp) a member of the ATP binding cassette (ABC) transporter family (*Hyafil et al. 1993*). Other platinums/heavy metals (cisplatin, oxaliplatin and $CuSO_4$) and taxanes (docetaxel) were examined to see if the cells had cross resistance to the same class of drugs used in their selection (carboplatin and taxol). PARP inhibitors (Olaparib, Veliparib and CEP-8983), a new class of drug in the treatment of ovarian cancer, were also screened for cross resistance (*Davar et al. 2012*). A vinca alkaloid (vinblastine), a class of dug which inhibits microtubule formation in the cell (*Moudi et al. 2013*), and an anthracycline (doxorubicin), a class of drug which inhibits DNA/RNA synthesis, transcription and replication, while causing cell damage and deregulating DNA damage response, the epigenome and transcriptome were also selected (*Weiss 1992*). Table 5.1 gives a summary of all cytotoxicity data collected. This is also presented diagrammatically in Figure 5.1 and Figure 5.2.

All of the sublines developed from UPN251 were significantly resistant to carboplatin ($p=0.2x10^{-2}$-$0.5x10^{-8}$, fold change=1.5-3.2), with single-agent carboplatin developed UPN251-7C being the highest. The addition of 12.5µg/ml BSO had the effect of lowering IC_{50} values across all UPN251 sublines. UPN251 and all sublines (except UPN251-7T) showed significant decreases (p=0.0003-0.008, Figure 5.1 (A)). Fold resistance, however, stayed at a similar level. Significant cross resistance to cisplatin and copper sulphate ($CuSO_4$) was also seen in sublines developed with carboplatin during selection (Figure 5.1 (B) & (C)). One exception to this is UPN251-6TALT, which was not resistant to $CuSO_4$. Oxaliplatin showed significant cross resistance for single agent treatments while alternating treatments show no significant cross resistance. However, UPN251-6TALT showed significant cross sensitivity to oxaliplatin (p=0.01, Figure 5.1 (D)).

The UPN251 sublines, developed with taxol during selection, had significant taxol resistance ($p=0.5x10^{-3}$-$0.2x10^{-7}$, fold change=4.3-8.9). UPN251-7T had the highest fold resistance of 8.9-fold (Figure 5.1 (E)). UPN251-7C developed with carboplatin was not resistant to taxol. A dose of 0.25µg/ml of elacridar has been shown to successfully

Table 5.1 Resistance profile of UPN251 drug-resistant sublines.

UPN251-7C and UPN251-7T were developed using single agent carboplatin and taxol respectively, while UPN251-6CALT and UPN251-6TALT were developed using alternating treatments of carboplatin and taxol. UPN251-6CALT received carboplatin in round 1 of drugging and UPN251-6TALT received taxol.

	Parent		Carboplatin Single Agent			Alternating Carboplatin First			Taxol Single Agent			Alternating Taxol First		
Drug (Units)	**UPN251 IC_{50}**		**UPN251-7C IC_{50}**			**UPN251-6CALT IC_{50}**			**UPN251-7T IC_{50}**			**UPN251-6TALT IC_{50}**		
	Mean ± SD	**n**	**Mean ± SD**	**n**	**F**	**Mean ± SD**	**n**	**F**	**Mean ± SD**	**n**	**F**	**Mean ± SD**	**n**	**F**
Platinums and heavy metals														
Carboplatin (µg/ml)	1.0 ± 0.0	3	3.5 ± 0.1 8***	3	3.3	1.8 ± 0.0 ***	3	1.7	1.6 ±0.1 **	3	1.5	2.0 ± 0.1 ***	3	**2.0**
+ BSO (12.5µg/ml)	0.8 ± 0.0 ###	3	2.9 ± 0.2 ##	3	3.4	1.6 ± 0.1 ##	3	1.8	1.3 ±0.2	3	1.5	1.7 ± 0.1 ##	3	**2.1**
Cisplatin (µg/ml)	0.15 ± 0.01	3	0.48 ± 0.08 **	3	3.3	0.21 ± 0.02 **	3	1.6	0.15 ± 0.01	3	1.0	0.27 ± 0.04 **	3	**1.9**
Oxaliplatin (µg/ml)	0.08 ± 0.01	3	0.2 ± 0.03 **	3	2.1	0.08 ± 0.02	3	1.0	0.12 ± 0.0 *	3	1.3	0.04 ± 0.0 *	3	**0.6**
$CuSO_4$ (ng/ml)	15.3 ± 1.7	5	28.5 ± 11.4 *	5	1.9	34.7 ± 10.6 **	5	2.3	17.0 ± 2.9	5	1.1	15.0 ± 1.3	5	**1.0**
Taxanes														
Taxol (ng/ml)	14.9 ± 1.9	3	14.9 ± 1.7	3	1.0	63.6 ± 4.4 ***	3	4.3	133.3 ± 4.7 ***	3	8.9	84.4 ± 11.6 ***	3	**5.7**
+ Elacridar (0.14µg/ml)	1.8 ± 0.3 ###	3	1.8 ± 0.3 ###	3	1.0	1.9 ± 0.2 ###	3	1.1	1.9 ± 0.2 ###	3	1.0	2.9 ± 0.5 ###	3	**1.6**
Docetaxel (ng/ml)	4.1 ± 0.3	3	1.5 ± 0.6 **	3	0.4	8.5 ± 1.5 **	3	2.1	20.3 ± 4.0 **	3	4.9	9.0 ± 2.6 *	3	**2.2**
Parp Inhibitors														
Olaparib (µg/ml)	1.7 ± 0.4	4	3.3 ± 0.9 *	4	2.0	3.9 ± 0.7 **	4	2.3	5.4 ± 1.0 ***	4	3.2	3.7 ± 0.4 ***	4	**2.2**
+ Elacridar (0.14µg/ml)	1.3 ± 0.1	4	2.5 ± 0.6	4	1.8	1.7 ± 0.4 ##	4	1.2	1.3 ± 0.2 ###	4	1.0	1.4 ± 0.1 ###	4	**1.0**
Veliparib (µg/ml)	13.1 ± 2.9	3	14.5 ± 0.7	3	1.1	14.6 ± 1.3	3	1.1	10.4 ± 1.6	3	0.8	14.7 ± 1.6	3	**1.1**
+ Elacridar (0.14µg/ml)	13.7 ± 2.8	3	15.2 ± 1.8	3	1.1	14.0 ± 1.9	3	1.0	10.7 ± 1.8	3	0.8	14.3 ± 1.6	3	**1.0**
CEP-8983 (µg/ml)	1.4 ± 0.1	3	1.7 ± 0.3	3	1.2	1.3 ± 0.2	3	0.9	1.1 ± 0.3	3	0.8	1.3 ± 0.2	3	**0.9**
Vinca Alkaloids														
Vinblastine (ng/ml)	9.9 ± 1.1	4	11.9 ± 2.8	4	1.2	29.2 ± 4.5 ***	4	3.0	62.1 ± 3.8 ***	4	6.3	31.2 ± 11.1 **	4	**3.2**
+ Elacridar (0.14µg/ml)	3.2 ± 0.6 ###	4	5.4 ± 0.7 ##	4	1.7	3.3 ± 0.7 ###	4	1.1	4.6 ± 1.2 ###	4	1.5	3.6 ± 0.7 ##	4	**1.1**

Anthracyclines														
Doxorubicin (ng/ml)	39.1 ± 10.2	5	46.8 ± 3.0	5	1.2	62.8 ± 3.0 **	5	1.6	117.9 ± 20.2 ***	5	3.0	59.6 ± 6.4 **	5	**1.5**
Inhibitors														
BSO (μM)	5.1 ± 1.9	4	14.4 ± 2.1 ***	4	2.8	7.6 ± 0.2	4	1.5	7.9 ± 2.8	4	1.5	29.2 ± 11.1**	4	**5.7**
Elacridar (μg/ml)	**2.5 ± 0.4**	**5**	**1.5 ± 0.3 ** **	**5**	**0.6**	**0.8 ± 0.2 *** **	**5**	**0.3**	**1.3 ± 0.5 ** **	**5**	**0.5**	**0.8 ± 0.2 *** **	**5**	**0.3**

* Indicates a significant difference between UPN251 parent and UPN251 drug-resistant sublines ($p<0.05$ students t-test)

** Indicates a significant difference between UPN251 parent and UPN251 drug-resistant sublines ($p<0.01$ students t-test)

*** Indicates a significant difference between UPN251 parent and UPN251 drug-resistant sublines ($p<0.001$ students t-test)

# Indicates a significant difference on the addition of a modulator ($p<0.05$ students t-test)

Indicates a significant difference on the addition of a modulator ($p<0.01$ students t-test)

Indicates a significant difference on the addition of a modulator ($p<0.001$ students t-test)

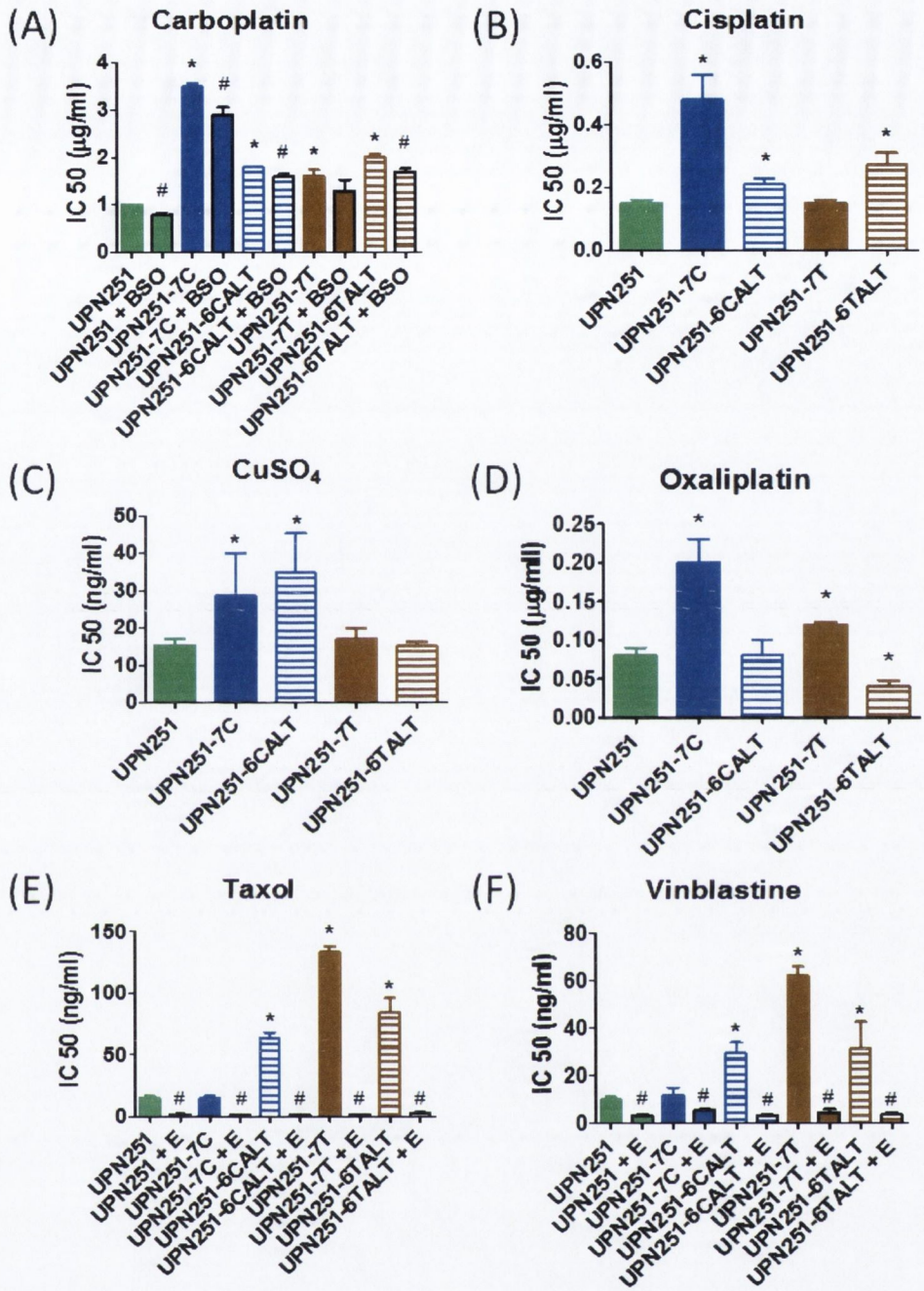

Figure 5.1 Post selection drug screen results.

Each graph represents mean IC50's of cells after cytotoxicity assays for an array of cytotoxic drugs with a minimum of 3 biological replicates. Error bars represent SD. In each graph the x-axis represents the cell lines ± an inhibitor and the y axis gives mean IC50 values and units. (A) Carboplatin ± Buthionine sulphoximine (B) Cisplatin (C) CuSO4 (D) Oxaliplatin (E) Taxol± Elacridar (F) Vinblastine ± Elacridar. This method is described in Chapter 2 section 2.1.6.

* Indicates a significant difference between resistant subline and UPN251 ($P<0.05$, student T-test)

# Indicates a significant difference between resistant subline and resistant subline with addition of inhibitor ($P<0.05$, student T-test)

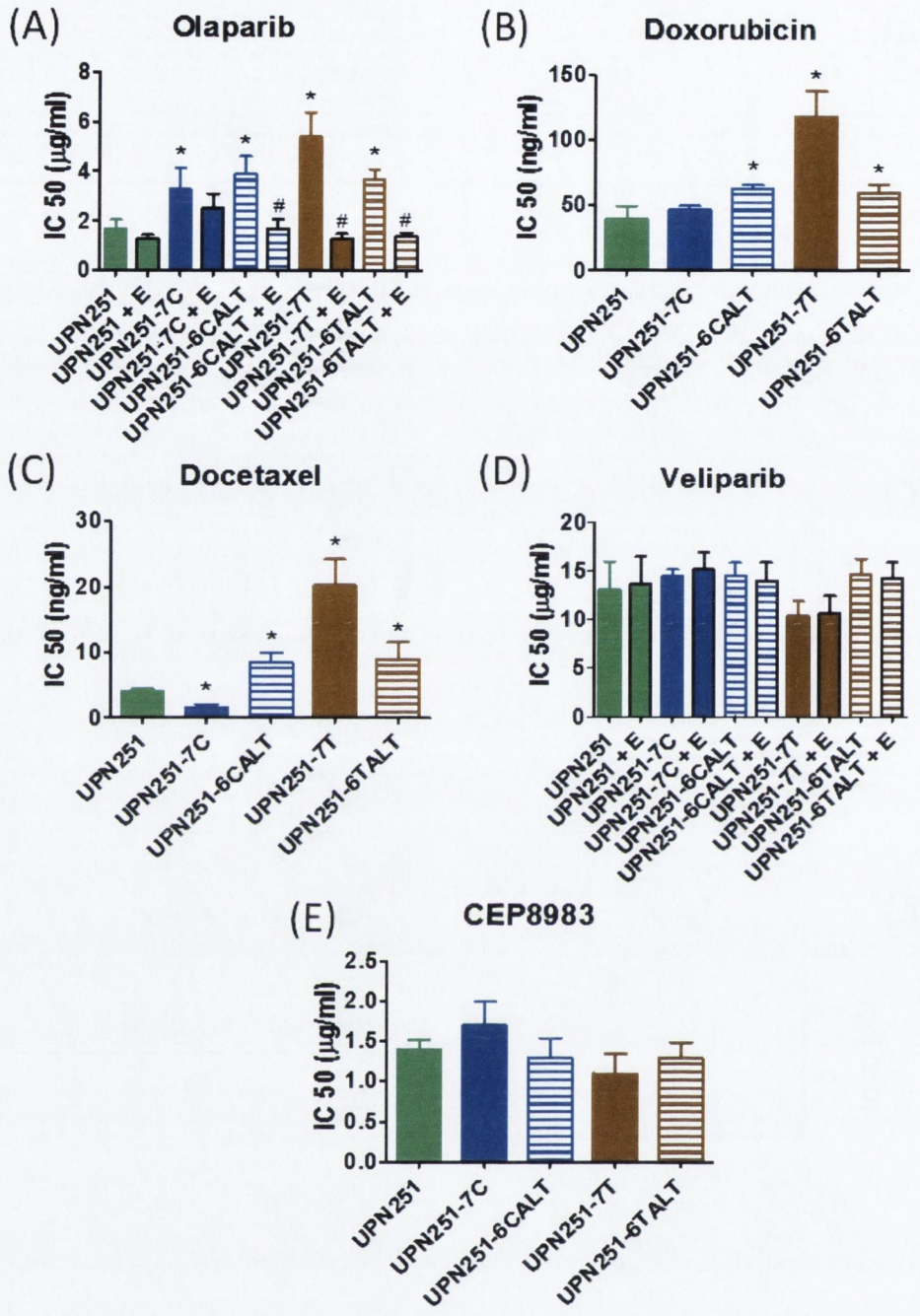

Figure 5.2 Post selection drug screen results.

Each graph represents mean IC50's of cells after cytotoxicity assays for an array of cytotoxic drugs with a minimum of 3 biological replicates. Error bars represent SD. In each graph the x-axis represents the cell lines ± an inhibitor and the y axis gives mean IC50 values and units. (A) Olaparib± Elacridar (B) Doxorubicin (C) Docetaxel (D) Veliparib ± Elacridar (E) CEP8983. This method is described in Chapter 2 section 2.1.6.

* Indicates a significant difference between resistant subline and UPN251 ($P<0.05$, student T-test)

# Indicates a significant difference between resistant subline and resistant subline with addition of inhibitor ($P<0.05$, student T-test)

reverse P-gp function (*Hyafil et al. 1993*; *Lawlor et al. 2014*; *Stordal et al. 2012*). Comparing taxol, with and without 0.25μg/ml of the P-gp inhibitor elacridar, across all cell lines reveals significant drops in IC_{50} values ($p=0.1x10^{-3}$-$0.4x10^{-7}$). UPN251-7C saw no changes in taxol fold resistance with the addition of elacridar, while sublines treated with taxol during development saw large decreases in taxol fold-resistance. UPN251-7T treated with taxol was 8.9 fold resistant to taxol while UPN251-7T treated with taxol and elacridar was identical to UPN251 parental cells. An almost identical trend was seen with vinblastine, which is also known to be transported by P-gp (Choudhuri et al. 2006) ($p=0.001$-$0.4x10^{-6}$, Figure 5.1 (F)). There was also a drop in IC_{50} when olaparib (another P-gp substrate (Lawlor et al. 2014)) was used instead of taxol or vinblastine. In this case, only significant drops in IC_{50} were seen in sublines developed with taxol during selection ($p=0.002$-$0.4x10^{-6}$, Figure 5.2 (A)). These results collectively point towards P-gp as a resistance mechanism in taxol treated sublines. UPN251-7C was also resistant to single agent olaparib ($p=0.01$, fold change=2), while no resistance was seen in UPN251-7C with the other P-gp substrates (taxol and vinblastine). The addition of 0.25μg/ml elacridar, in this case, saw no significant changes in IC_{50} or fold resistance. Doxorubicin, which is a member of the anthracycline family of drugs, also displayed significant cross resistance in sublines developed with taxol ($p=0.005$-$0.5x10^{-6}$, Figure 5.2 (B)). Also, significant cross resistance to docetaxel was seen in sublines developed with taxol ($p=0.03$-0.002) and a significant degree of sensitivity was noted in UPN251-7C ($p= 0.002$, Figure 5.2 (C)).

PARP inhibitors veliparib and CEP8983 both showed no significant change in IC_{50} when compared to the parental cell lines and could both be candidates for use in therapies for platinum/taxane-resistant ovarian cancer (Figure 5.2 (D) & (E)).

5.3.2 Total cellular glutathione assay

Using a total cellular glutathione (GSH) assay (Figure 5.3) no significant difference in GSH levels was observed when the UPN251 resistant sublines were treated with 2μg/ml carboplatin. However, UPN251 parental cells saw a significant 3-fold increase in total cellular GSH levels with the addition of 2μg/ml carboplatin ($p=0.02$) for a 3-day exposure. Treatment with 12.5μmol BSO for a 3 day exposure gave significantly reduced levels of GSH for UPN251 and its sublines, when compared to treatment-free control cells ($p=0.5x10^{-2}$- 0.02, fold reduction=9.3-27.8). This was the same dose of BSO that was used in our drug screen indicating that GSH synthesis was successfully inhibited in our cytotoxicity assays by BSO and had no effect on carboplatin resistance (Figure 5.1 (A), Table 5.1).

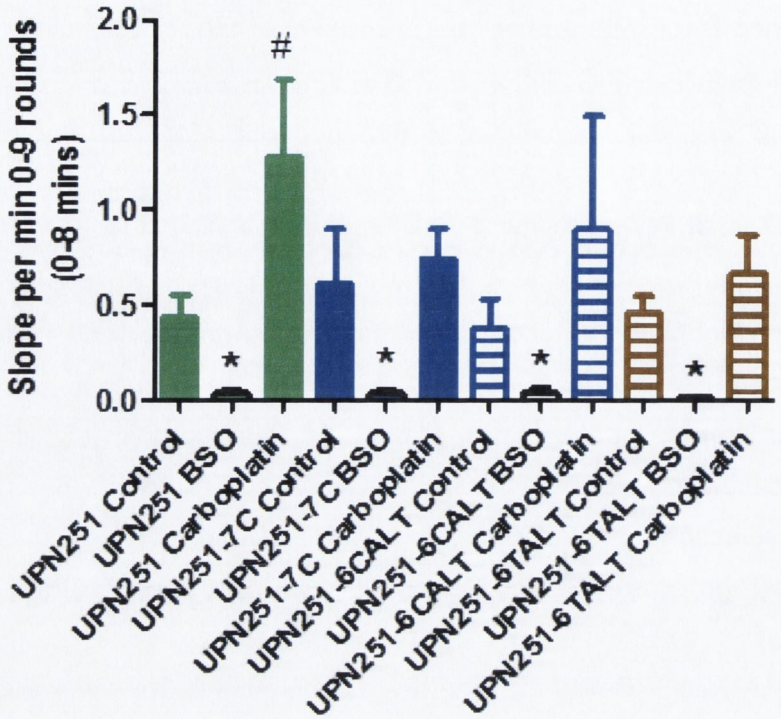

Figure 5.3 Total cellular glutathione assay.

Parental cells UPN251 and resistant sublines are shown on x-axis as control, BSO (12.5µmol) or carboplatin (2µg/ml) treated. The y-axis gives slope per minute of 0-9 rounds of the assay run over 8mins. 3-day exposures to drug were used in this experiment. This method is described in Chapter 2 section 2.1.8.

* Indicates a significant difference between control and BSO treatment ($P<0.05$, student T-test)

# Indicates a significant difference between control and Carboplatin treatment ($P<0.05$, student T-test)

5.3.3 High content growth assay

Growth assays were carried out on the UPN251 resistant sublines to see if there were any changes in growth rate compared to UPN251 parental cells. Growth assays were also carried out to see if growth was affected by different drug treatments of carboplatin and taxol.

When the cell lines were grown in the absence of drug, UPN251-6CALT, UPN251-7T and UPN251-6TALT took significantly longer to reach quadrupling time (between approximately 16-18 hours) than UPN251 ($P=0.01\text{-}0.9\times10^{-3}$, Figure 5.4 (A) and (B)). UPN251-7C had a similar growth rate to UPN251 cells.

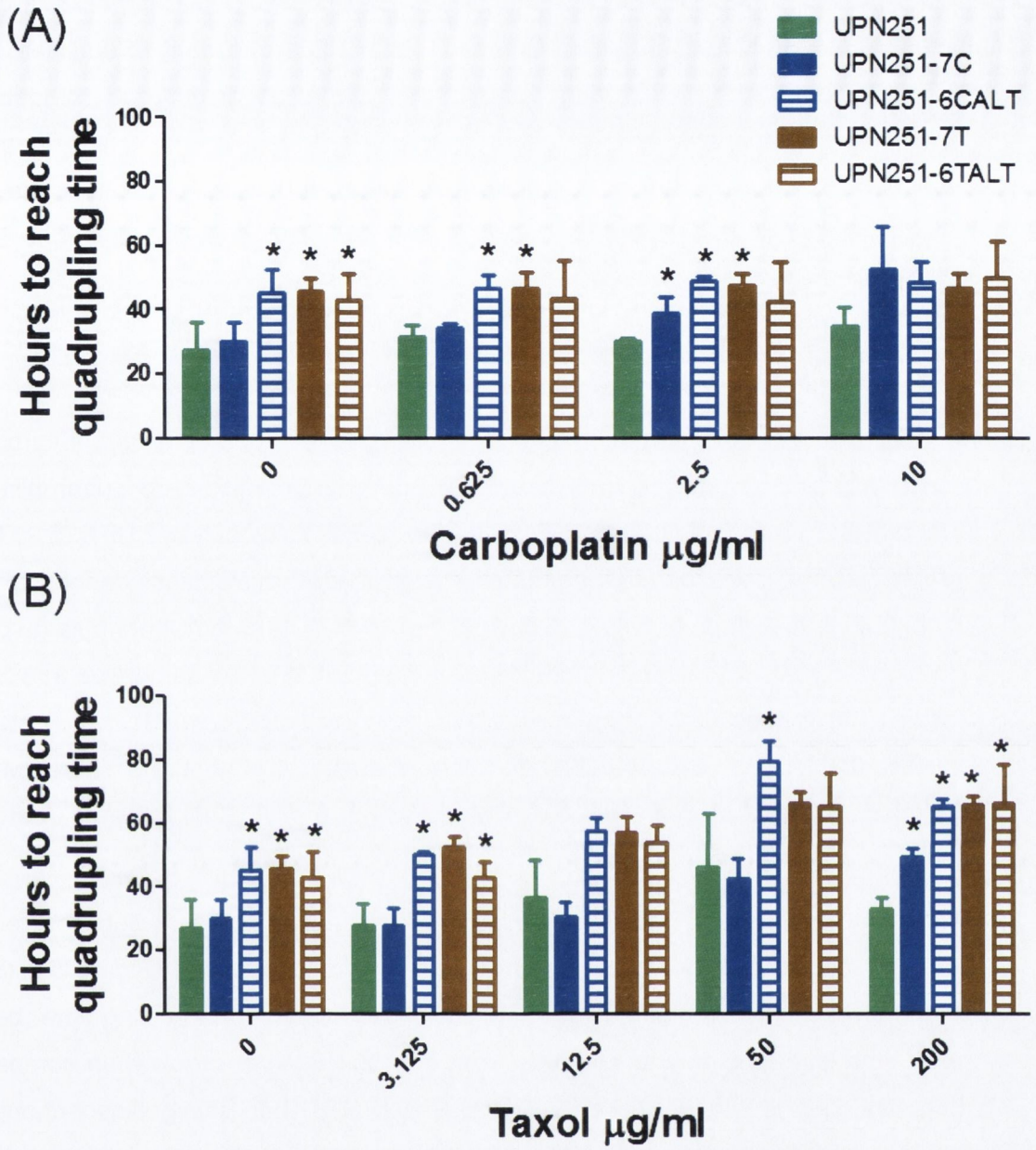

Figure 5.4 High content growth curve analysis.

This figure indicates the time taken for UPN251 and derived sublines to reach quadrupling when exposed to a range of drug doses (carboplatin (0-10µg/ml), taxol (0-200ng/ml)). (A) Different doses of carboplatin (0-10µg/ml) are shown together for each cell line tested for comparison purposes. (B) Different doses of taxol (0-200ng/ml) are shown together for each cell line tested for comparison purposes. This method is described in Chapter 2 section 2.1.7.2.

*Indicates a significant difference in quadrupling time UPN251 and resistant subline receiving the same drug dose ($P<0.05$, student T-test).

The experiment was optimised to test dose ranges of between 0-10µg/ml of carboplatin and 0-200ng/ml of taxol, to see their effect on UPN251 and derived sublines' growth rates. Doses outside of this range caused the cells to either undergo cell death and never reach quadrupling time or grow so slowly that they did not reach quadrupling time in the 80 hour window of measurement. Quadrupling time was taken as the growth cut off instead of the traditional doubling time as differences in growth were more obvious at this time using this method.

In general, no difference in growth rate was recorded for the cell lines receiving doses of carboplatin compared to the same cells grown in the absence of carboplatin Figure 5.5 (A). One exception was UPN251-7C. This subline, receiving 10µg/ml carboplatin, took significantly longer (approximately 22 hours longer) to reach quadrupling time compared to untreated UPN251-7C ($p=0.008$). UPN251-6CALTand UPN251-7T cells, treated with a dose of 0.625µg/ml carboplatin, took significantly longer to reach quadrupling time (approximately 15 hours) than UPN251 treated with the same dose of carboplatin ($p=0.008$ and 0.01 respectively, Figure 5.4 (A). The same was true for both cell lines at a dose of 2.5µg/ml carboplatin, along with UPN251-7C, which also took significantly longer ($p=0.04\text{-}0.3\times10^{-6}$, approximately 12-14 hours). There were no significant differences in growth rate between any of the UPN251 sublines treated with 10µg/ml carboplatin and UPN251 treated with 10µg/ml carboplatin.

Significant changes in growth rate occurred between all resistant sublines receiving taxol compared to the same cells grown in the absence of taxol (Figure 5.5 (B)). All UPN251 resistant sublines took significantly longer to reach quadrupling time (between approximately 12-35 hours) within the range of 50-200ng/ml taxol when compared to drug free controls ($p=0.03\text{-}0.2\times10^{-3}$). However, UPN251 had no significant changes for any dose of taxol tested. UPN251-6CALT and UPN251-7T also had a significant reduction of growth rate at lower dose ranges of taxol. UPN251-6CALT took significantly longer to reach quadrupling time at a range of 12.5-200ng/ml taxol ($p=0.03\text{-}0.2\times10^{-3}$, approximately 12-35 hours) and UPN251-7T at a range of 3.125-200ng/ml taxol ($p=0.04\text{-}0.2\times10^{-3}$, approximately 12-21 hours) when compared to untreated control cells of the same cell line. UPN251-6CALT, UPN251-7T and UPN251-6TALT took significantly longer to reach quadrupling time (between approximately 15 and 25 hours) than UPN251 at a dose of 3.125ng/ml taxol, the lowest dose tested ($p=0.04\text{-}0.004$, Figure 5.4 (B)). For a dose range of 12.5-50ng/ml taxol, there were no significant changes in the UPN251 sublines compared to UPN251 receiving the same drug dose. One exception was UPN251-6CALT which took significantly longer to reach quadrupling time (approximately 34 hours) at a dose of

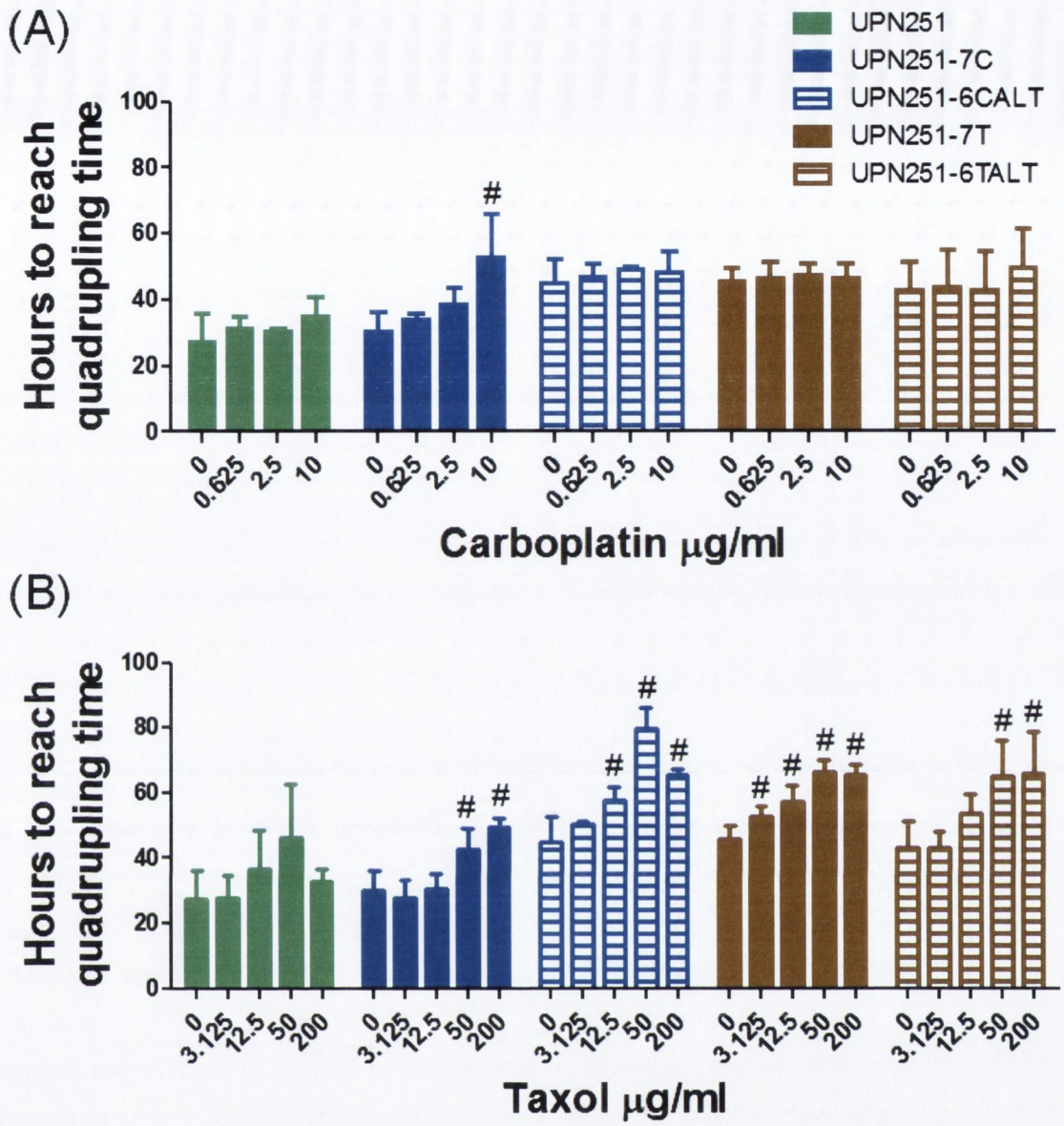

Figure 5.5 High content growth curve analysis.

This figure indicates the time taken for UPN251 and derived sublines to reach quadrupling when exposed to a range of drug doses (carboplatin (0-10µg/ml), taxol (0-200ng/ml)). (A) Drug concentrations of carboplatin increasing from 0-10µg/ml is shown separately for each cell line for comparison purposes. (B) Drug concentrations of taxol increasing from 0-200ng/ml is shown separately for each cell line for comparison purposes. This method is described in Chapter 2 section 2.1.7.2.

#Indicates a significant difference in quadrupling time between control cells (no drug) and the same cell line treated with a specific dose of carboplatin or taxol ($P<0.05$, student T-test).

50ng/ml taxol than UPN251 (p=0.03). Finally, all UPN251 resistant sublines took significantly longer to reach quadrupling time (between approximately 16-33 hours) than parental UPN251 when treated with the highest tested dose of 200ng/ml taxol ($p=0.01\text{-}0.1x10^{-3}$).

5.3.4 Cell cycle mitosis assay

A cell cycle mitosis assay was carried out in order to investigate the amount of cells that were in the mitotic phase of the cell cycle and, as such, in a cell cycle arrest in the G2/M phase. How this cell cycle response differed between resistant sublines receiving doses of taxol was investigated. Figure 5.6 (A) shows different biological replicates of UPN251 cells treated with a range of taxol doses from 0-800ng/ml with a 24hour exposure. The number of cells in mitosis remained below 10% for doses ranging from 0-50ng/ml. The highest dose (800ng/ml) showed an increase in the number of mitotic cells. This dose had between 20-30% of cells in mitosis. In general, an increase in taxol dose correlated with an increase in the % true cells (% of cells in mitosis). Figure 5.6 (B) shows the average % true fold change for UPN251 and resistant sublines receiving 50 and 800ng/ml of taxol for 24 hours. Both UPN251-7T and UPN251-6TALT showed significant decreases in % true fold change (8-fold and 2-fold respectively) for a dose of 800ng/ml taxol when compared to the % true fold change of UPN251, while receiving the same dose ($p=0.7x10^{-6}$ and $p=0.5x10^{-3}$ respectively).This indicates that fewer cells were stuck in a cell cycle arrest in G2/M for this high dose in UPN251-7T and UPN251-6TALT compared to parental UPN251 cells. There were no significant changes seen for the 50ng/ml dose. A representative image (1 of 10 photos taken from a single well) for the cells captured by the InCell analyser across both the nuclear dye channel and antibody channel is given in Figure 5.7 for UPN251 and UPN251-7T. For a dose of 800ng/ml, only a small number of cells were shown to survive in UPN251, all of which were in mitosis (Figure 5.7 (C)). More cells survived in UPN251-7T only a fraction of which were in mitosis (Figure 5.7 (F)).

5.3.5 Fluorescence activated cell sorting (FACS) analysis

Doses for the FACS experiments were chosen from a range of doses tested, between (25 and 100ng/ml) for taxol and (100 and 400µg/ml) for carboplatin over 24 hour exposures. Chosen doses (100ng/ml taxol and 350 µg/ml carboplatin) were selected, as they showed a clear impact on drug exposure on parental UPN251 cells, but also had enough cells present after drugging for experimentation.

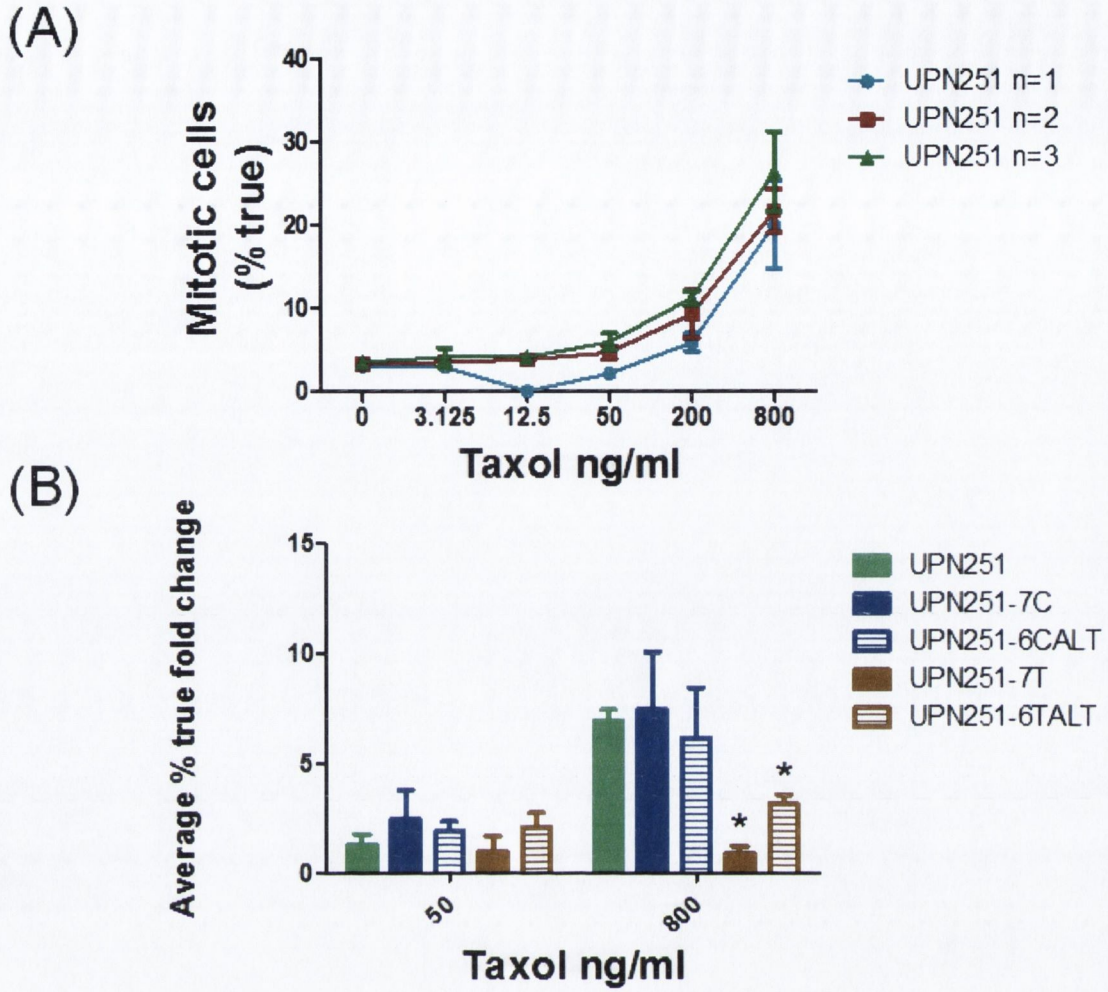

Figure 5.6 A comparison of cells in mitosis after a 24hour taxol drug treatment.

(A) The graph represents the number of mitotic cells (% true) for UPN251 parental cell lines over a range of taxol treatments (0-800ng/ml) for a 24 hour exposure. Three biological replicates are shown. Error bars give SD of three technical replicates. (B) The graph represents the average % true fold change (equation 2.4, chapter 2) of the UPN251 resistant sublines treated with 50 and 800ng/ml taxol. Error bars indicate SD of biological replicates.

* Indicates a significant reduction in the average % true fold change between UPN251 and resistant subline treated the same dose of taxol ($P<0.05$, student T-test).

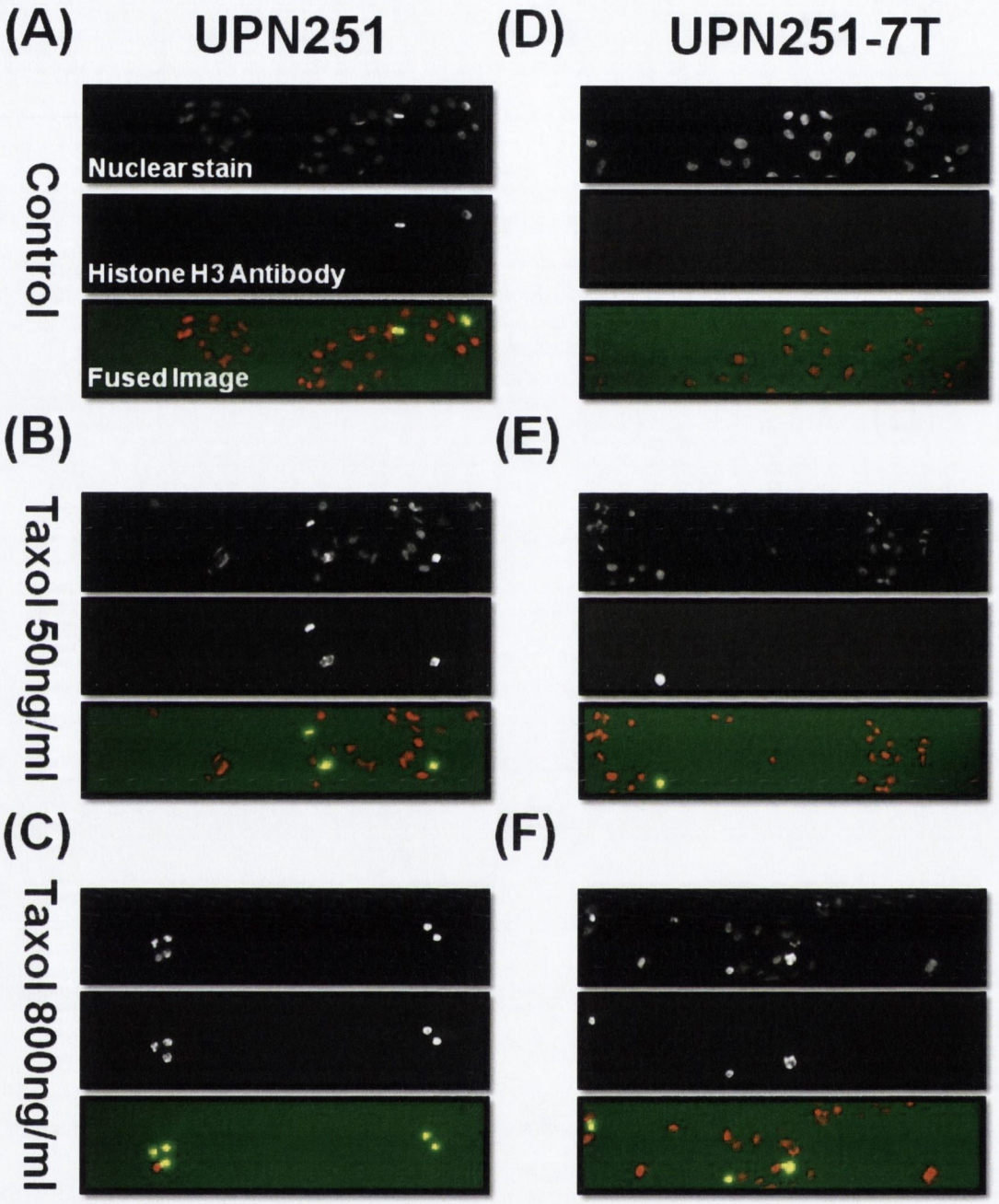

Figure 5.7 Representative images of the cell cycle PHH3 assay for UPN251 and UPN251-7T taken by the Incell Analyzer.

Images were taken using the Incell fluorescence imager at 10x magnification. The above images represent 1 out of 10 fields taken from a single well of a 96-well plate. For (A-F) the top image represents the total number of cells present captured by fluorescent nuclear staining, the middle image represents cells in mitosis imaged from staining of the mouse anti-human phospho histone H3 antibody and the last image is a fused image of both afore mentioned images. (A) UPN251 Control (B) UPN251 Taxol treated (50 ng/ml) (C) UPN251 Taxol treated (800 ng/ml) (D) UPN251-7T Control (E) UPN251-7T Taxol treated (50 ng/ml) (F) UPN251-7T Taxol treated (800 ng/ml). Method described in chapter 2 section 2.1.10.

5.3.5.1 Apoptosis assay

A FITC annexin V / PI apoptosis assay was carried out on the UPN251 parental and resistant sublines to see the effect of high-dose drug exposure on initiation of apoptosis.

Figure 5.8 shows the results obtained from exposing UPN251 (parent), UPN251-7C (carboplatin resistant subline) and UPN251-7T (taxol resistant subline) to 100ng/ml of taxol for 24 hours and comparing them to their untreated control cells using Summit v4.3 software. The results of n=3 replicates are given graphically in Figure 5.9. There was little change in the amount of necrotic cells present in the cell populations when comparing taxol treated cells and untreated cells (Figure 5.9 (A)). Only UPN251-7C showed a significant increase in necrotic cells when treated with taxol ($p=0.01$, fold increase=1.9). This is represented by region R2 in the diagrams shown in figure 5.8. All cell lines showed a significant increase in the number of cells that were in late stage apoptosis/necrosis when comparing taxol treated and untreated cells (Figure 5.9 (B), region R3 Figure 5.8). However, UPN251 cells showed a larger significant increase ($p=0.006$, fold increase=1.8) compared to UPN251-7C ($p=0.02$, fold increase=1.7)) and UPN251-7T ($p=0.04$, fold increase=1.5)). Only UPN251 and UPN251-7C showed a significant decrease in the number of cells that were living when comparing taxol treated and untreated cells ($p=0.7\times10^{-3}$ & 0.003 respectively, fold decrease=0.9) (Figure 5.9 (C), region R4 Figure 5.8). UPN251-7T saw no significant decreases in the amount of living cells present. Similarly, only UPN251 and UPN251-7C showed a large significant increase in the number of cells undergoing early stage apoptosis when comparing taxol treated and untreated cells ($p=0.003$ & 0.004, fold increase=3.8 & 3.5 respectively) (Figure 5.9 (D), region R5 Figure 5.8). UPN251-7T saw no significant increases in the amount of cells undergoing early stage apoptosis.

Figure 5.10 shows the results obtained from exposing UPN251, UPN251-7C and UPN251-7T to 350µg/ml of carboplatin for 24 hours and comparing them to their untreated control cells using Summit v4.3 software. The results of n=3 replicates are given graphically in Figure 5.11. There were no significant changes in the amount of necrotic cells present in the cell populations when comparing carboplatin treated and untreated cells (Figure 5.11 (A), region R2 Figure 5.10). Only UPN251 showed large significant increases in the number of cells undergoing late stage apoptosis/necrosis after carboplatin treatment ($p=0.4\times10^{-6}$, fold increase=2.5), while carboplatin and taxol resistant sublines UPN251-7C and UPN251-7T showed no significant difference (Figure 5.11 (B), region R3 Figure 5.10).

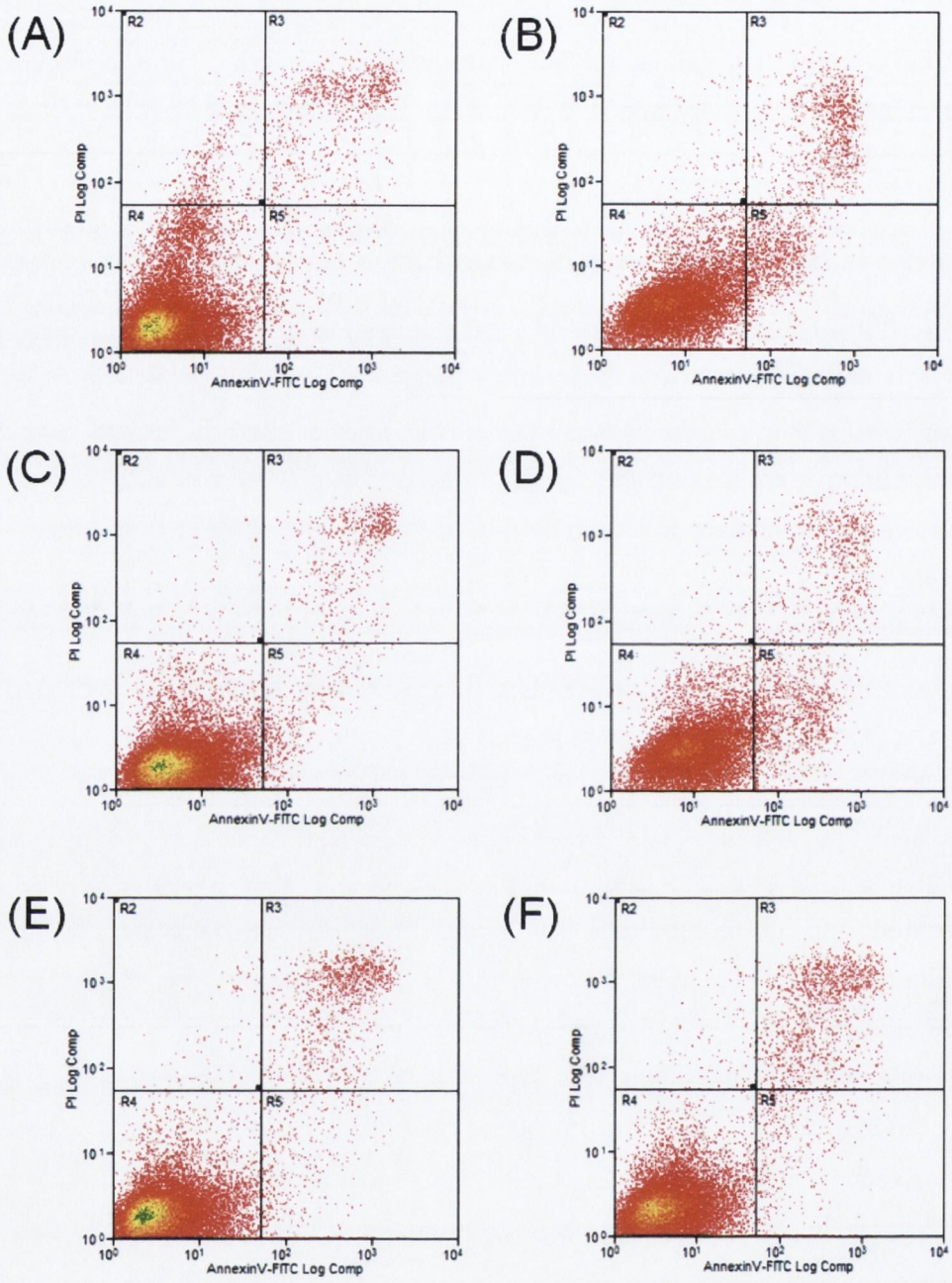

Figure 5.8 FITC annexin V / PI apoptosis assay by FACS.

Untreated (Control) and taxol (100ng/ml) treated for 24 hours in UPN251, UPN251-7C and UPN251-7T is shown for 1 representative replicate of n=3 biological replicates. Each graph gives Log of Annexin V-FITC (compensated) V Log of PI (compensated) for the gated cells. R2=Necrotic cells, R3=Necrotic/Late apoptotic cells, R4=Live cells and R5=Early apoptotic cells. (A) UPN251 control (B) UPN251 taxol treated (C) UPN251-7C control (D) UPN251-7C taxol treated (E) UPN251-7T control (F) UPN251-7T taxol treated. The method is described in chapter 2 section 2.1.11.1.

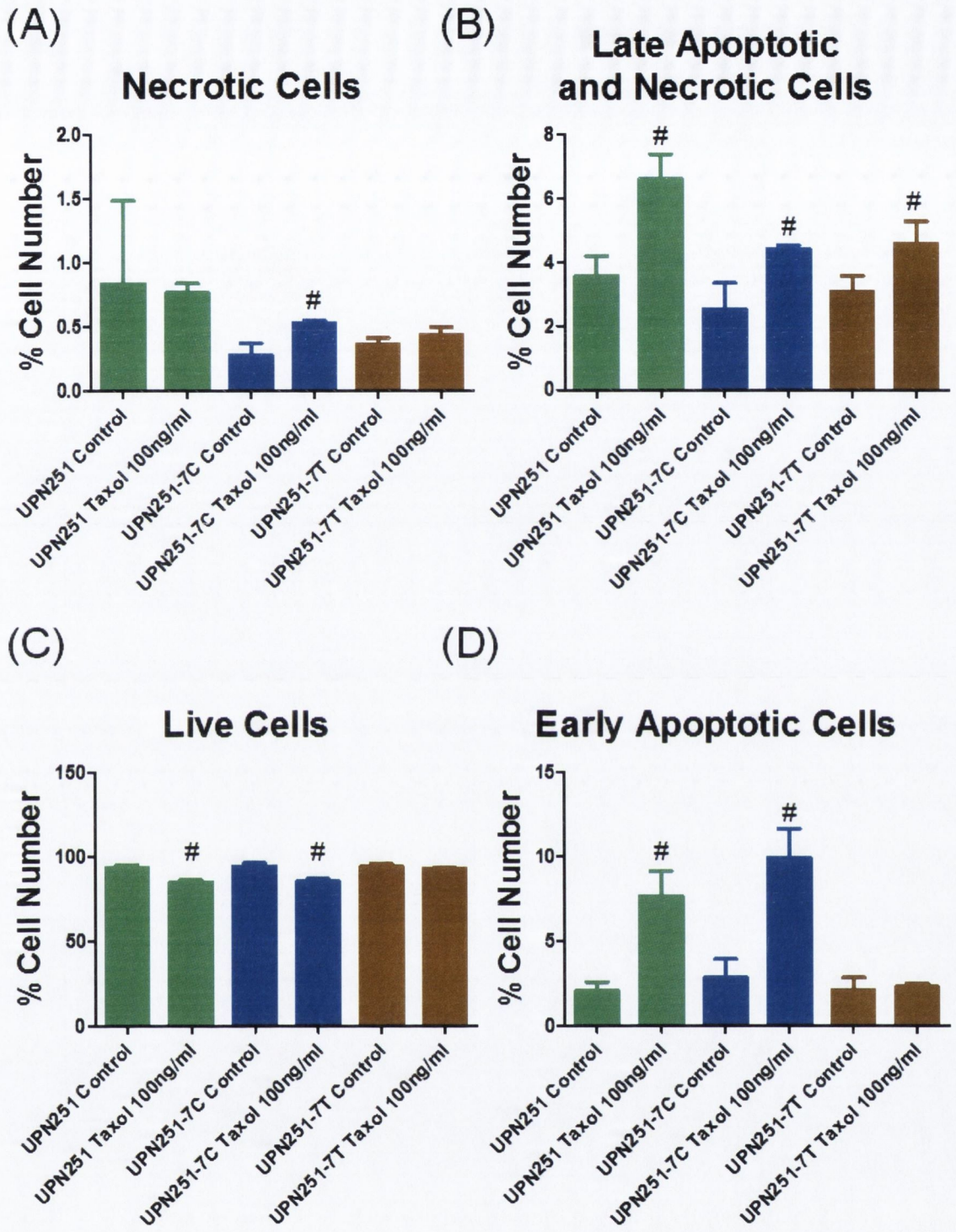

Figure 5.9 FITC annexin V / PI apoptosis assay by FACS (graphs).

Untreated (Control) and taxol (100ng/ml) treated for 24 hours in UPN251, UPN251-7C and UPN251-7T. Each graph gives the percentage number of cells which are; (A) Necrotic (B) Late stage apoptotic and necrotic (C) Living (D) Early stage apoptotic. Error bars represent SD for n=3 replicates.

# Indicates a significant difference in the percentage number of treated cells compared to untreated control cells ($P<0.05$, student T-test).

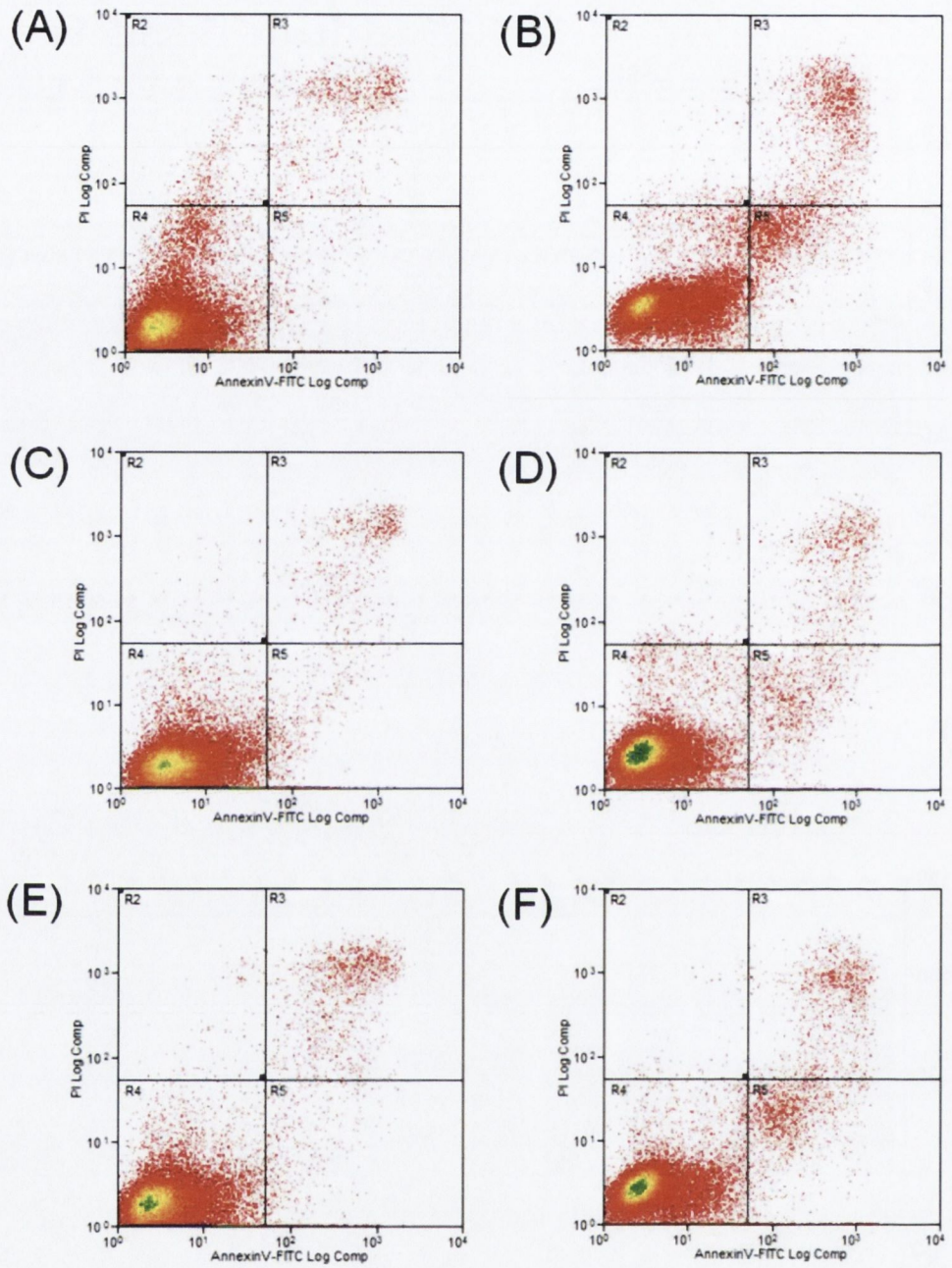

Figure 5.10 FITC annexin V / PI apoptosis assay by FACS.

Untreated (Control) and carboplatin (350µg/ml) treated for 24hours in UPN251, UPN251-7C and UPN251-7T is shown for 1 representative replicate of n=3 biological replicates. Each graph gives Log of Annexin V-FITC (compensated) V Log of PI (compensated) for the gated cells. R2=Necrotic cells, R3=Necrotic/Late apoptotic cells, R4=Live cells and R5=Early apoptotic cells. (A) UPN251 control (B) UPN251 carboplatin treated (C) UPN251-7C control (D) UPN251-7C carboplatin treated (E) UPN251-7T control (F) UPN251-7T carboplatin treated. The method is described in chapter 2 section 2.1.11.1.

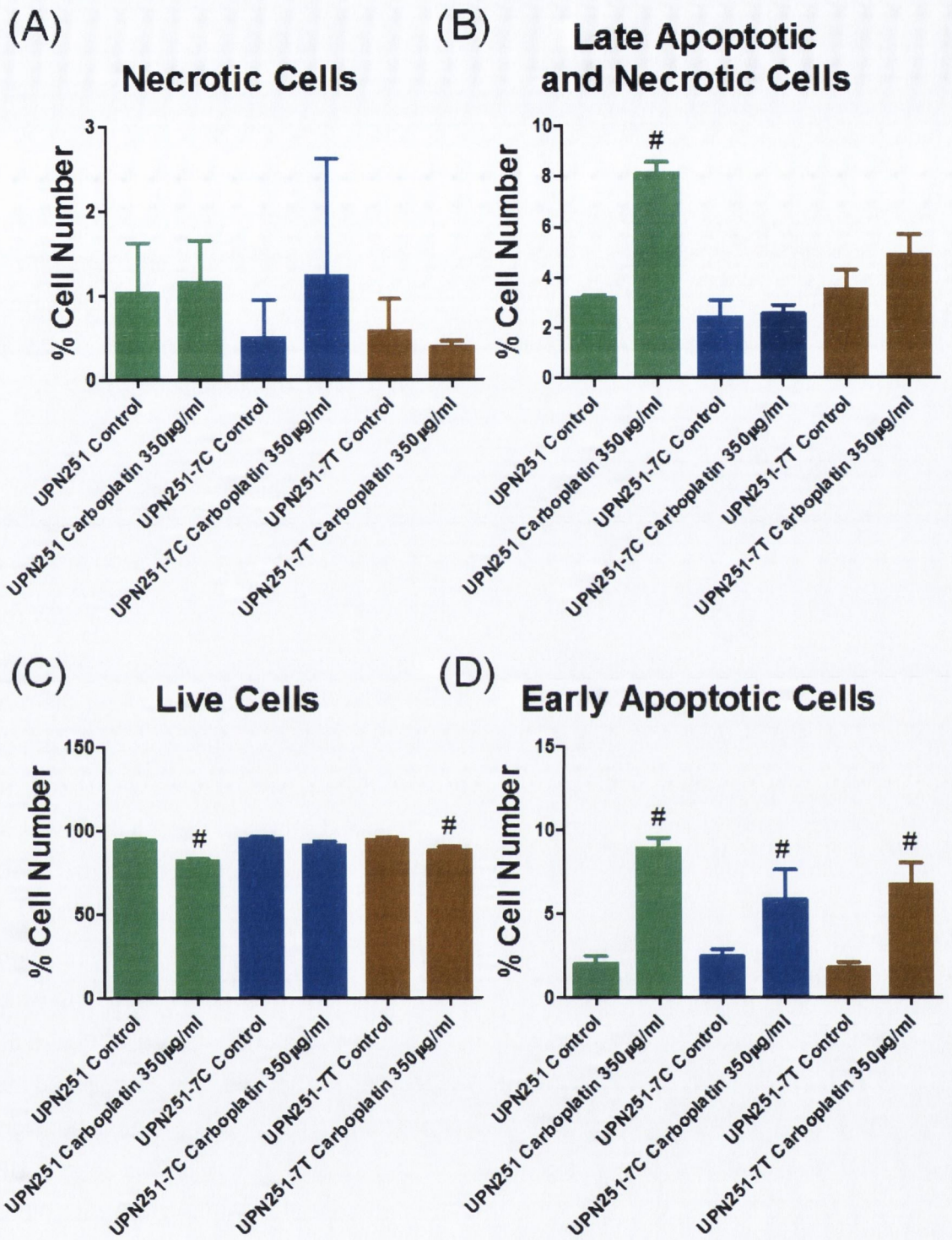

Figure 5.11 FITC annexin V / PI apoptosis assay by FACS (graphs).

Untreated (Control) and carboplatin (350µg/ml) treated for 24 hours in UPN251, UPN251-7C and UPN251-7T. Each graph gives the percentage number of cells which are; (A) Necrotic (B) Late stage apoptotic and necrotic (C) Living (D) Early stage apoptotic. Error bars represent SD for n=3 replicates.

# Indicates a significant difference in the percentage number of treated cells compared to untreated control cells ($P<0.05$, student T-test).

UPN251-7T showed some elevation that was trending towards significance (p=0.09, fold increase=1.4), while in UPN251-7C there was no change whatsoever. Only UPN251 and UPN251-7T showed a significant decrease in the number of cells that were living, when comparing carboplatin treated and untreated cells ($p=0.3x10^{-3}$ & 0.01 respectively, fold decrease=0.9) (Figure 5.11 (C), region R4 Figure 5.10). UPN251-7C saw no significant decreases in the amount of living cells present. All cell lines had a large significant increase in the number of cells undergoing early stage apoptosis when comparing carboplatin treated and untreated cells (Figure 5.11 (D), region R5 Figure 5.10). UPN251 and UPN251-7T had larger increases ($p=0.1x10^{-3}$ & 0.005, fold increase=4.5 & 3.9 respectively) than UPN251-7C (p=0.02, fold increase=2.4).

5.3.5.2 Cell cycle assay

The cell cycle assay was carried out alongside the apoptosis assay using the same samples. This was done to see the effect of high-dose drug exposure on the cell cycle.

Figure 5.12 and Figure 5.13 show the results obtained from exposing UPN251 (parent), UPN251-7C (carboplatin resistant subline) and UPN251-7T (taxol resistant subline) to 100ng/ml of taxol or 350µg/ml carboplatin for 24 hours and comparing them to their untreated control cells using Summit v4.3 software. These results are shown graphically for all replicates in Figure 5.14. When treating cells with taxol, a large significant reduction in the amount of cells in the G1 phase of the cell cycle was seen in UPN251 and UPN251-7C when compared to untreated control cells ($p=0.7x10^{-3}$ and $0.5x10^{-6}$, fold decrease=0.5 & 0.4 respectively) (Figure 5.14 (A), region R2 Figure 5.12). No significant change was seen in UPN251-7T. There were no significant changes in the S or G2/M phase for taxol treatments, except UPN251-7C which had significantly more cells in the G2/M phase compared to untreated cells (Figure 5.14 (B) & (C), region R3 and R4 Figure 5.12 respectively). This had only a small fold increase (1.7) with a p-value of 0.01. When treating cells with carboplatin, a small but significant reduction in the amount of cells in the G1 phase of the cell cycle was seen in UPN251 and UPN251-7T when compared to untreated control cells (p=0.006 and 0.008, fold decrease=0.8 & 0.9 respectively) (Figure 5.14 (D), region R2 Figure 5.13). No significant change was seen in UPN251-7C. A small but significant increase in the amount of cells in the S phase of the cell cycle was seen in UPN251 and UPN251-7T when compared to untreated control cells (p=0.04 and 0.02, fold increase=1.2 & 1.4 respectively) (Figure 5.14 (E), region R3 Figure 5.13). Again, there was no significant change in UPN251-7C. Finally, a significant decrease in the amount of cells in the G2/M phase of the cell cycle was seen in UPN251 and UPN251-7T when compared to

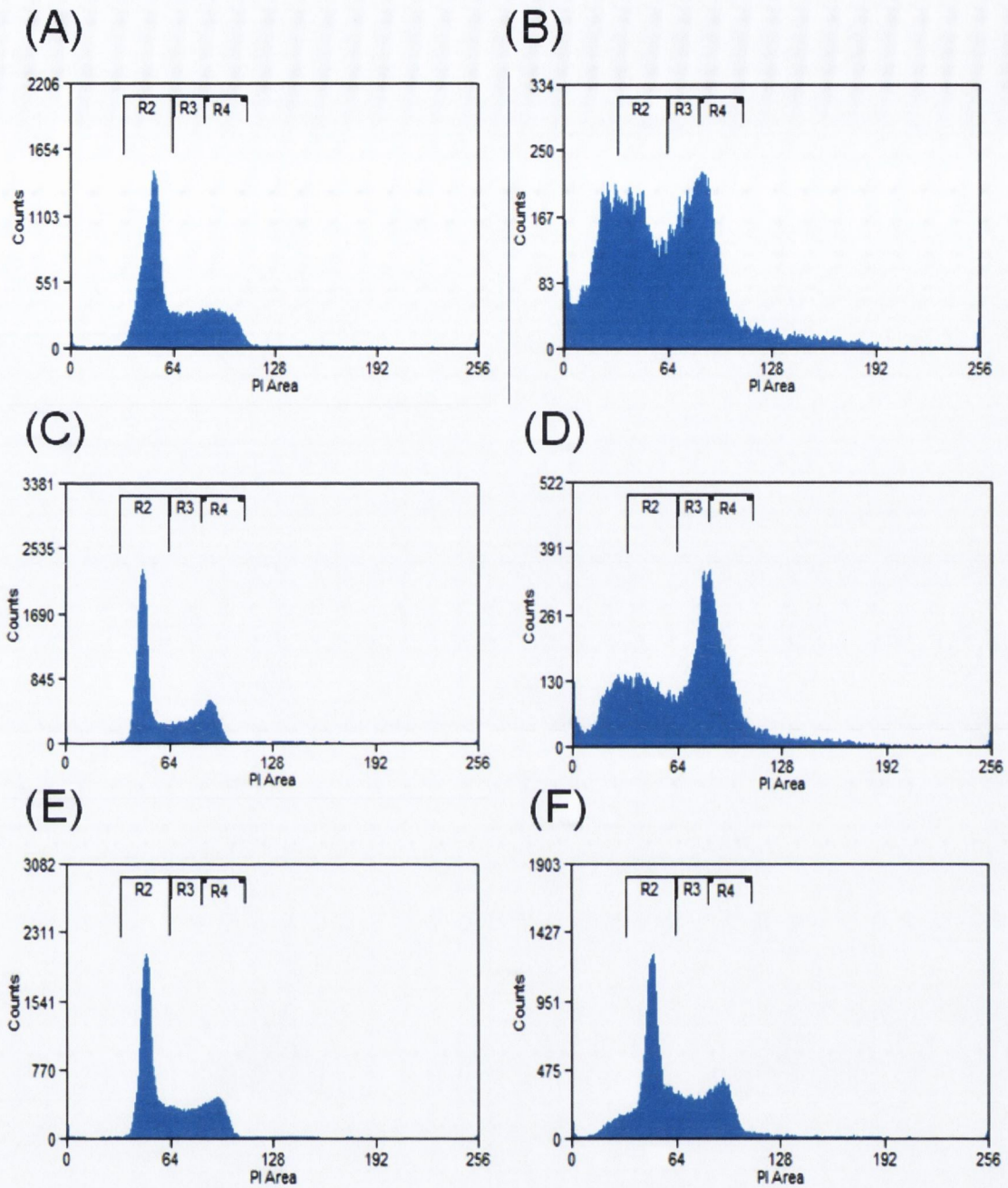

Figure 5.12 PI cell cycle assay by FACS.

Untreated (Control) and taxol (100ng/ml) treated for 24 hours in UPN251, UPN251-7C and UPN251-7T is shown for 1 representative replicate of n=3 biological replicates. For each diagram PI area is plotted against cell counts for the gated cells. R2=G1 phase, R3=S phase, R4=G2/M phase. (A) UPN251 control (B) UPN251 taxol treated (C) UPN251-7C control (D) UPN251-7C taxol treated (E) UPN251-7T control (F) UPN251-7T taxol treated. The method is described in chapter 2 section 2.1.11.2.

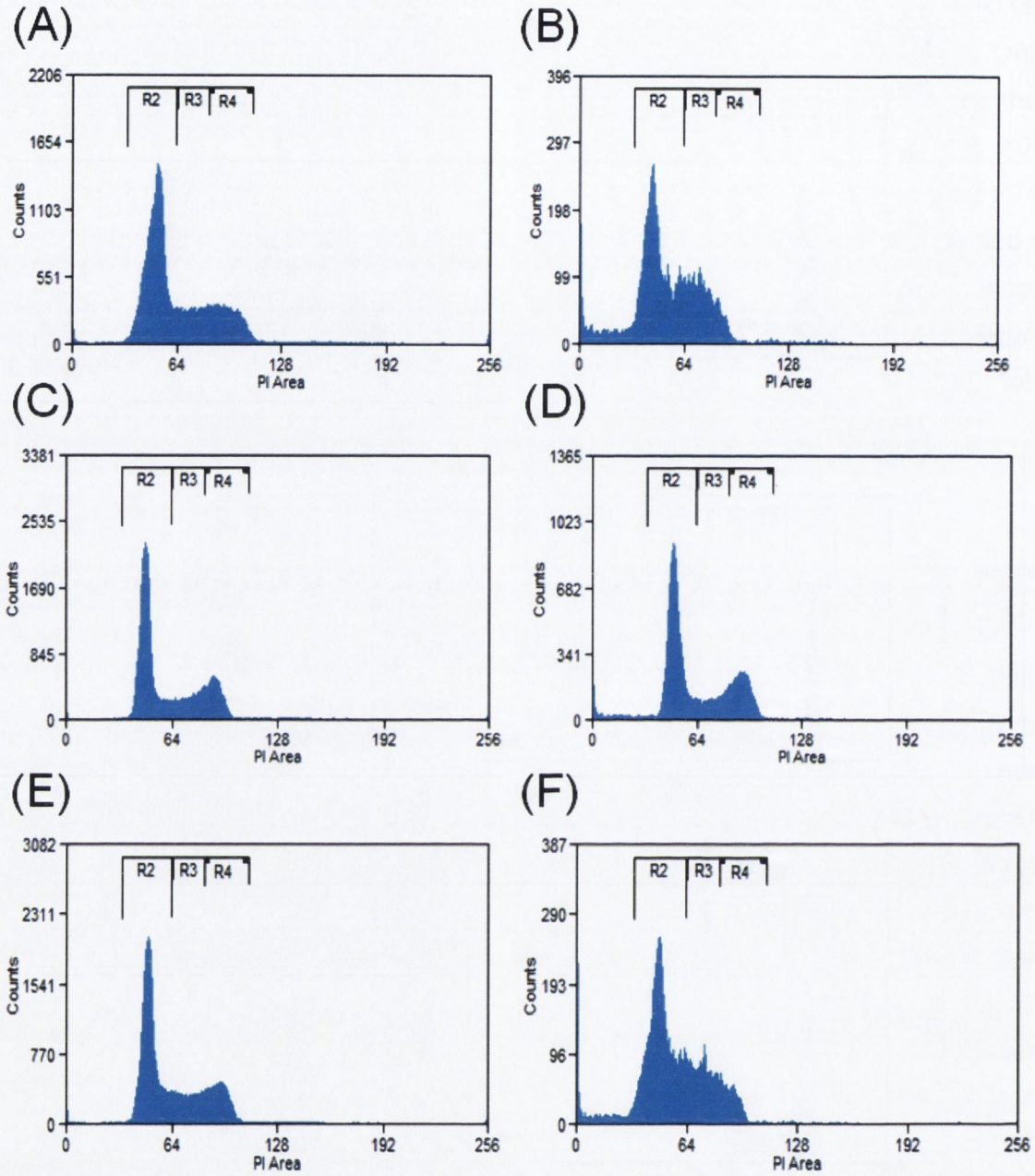

Figure 5.13 PI cell cycle assay by FACS.

Untreated (Control) and carboplatin (350µg/ml) treated for 24 hours in UPN251, UPN251-7C and UPN251-7T is shown for 1 representative replicate for n=3 biological replicates. For each diagram PI area is plotted against cell counts for the gated cells. R2=G1 phase, R3=S phase, R4=G2/M phase. (A) UPN251 control (B) UPN251 carboplatin treated (C) UPN251-7C control (D) UPN251-7C carboplatin treated (E) UPN251-7T control (F) UPN251-7T carboplatin treated. The method is described in chapter 2 section 2.1.11.2.

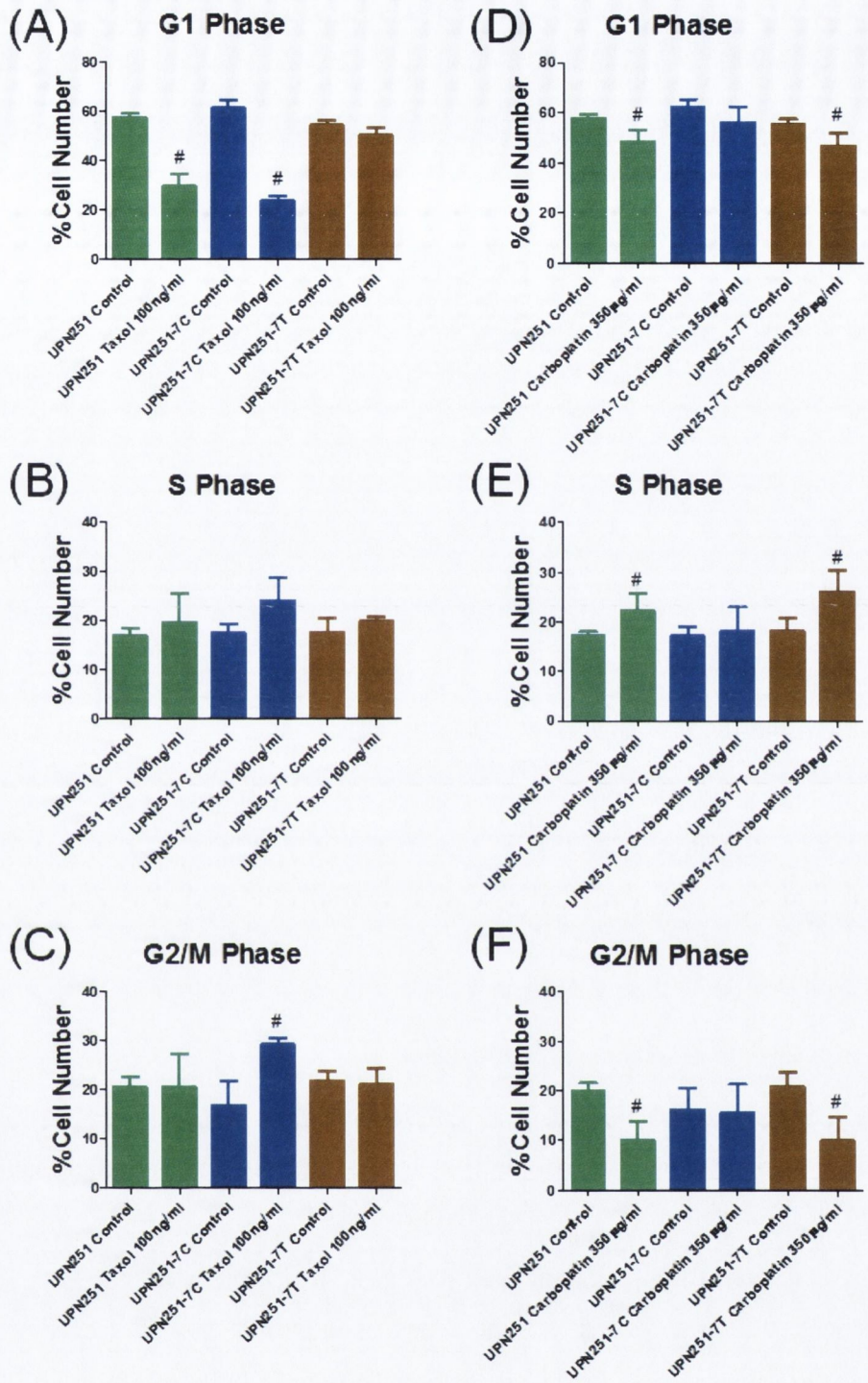

Figure 5.14 Graphic representation of PI cell cycle assay by FACS.

Untreated (Control) V taxol (100ng/ml) treated or carboplatin (350µg/ml) treated for 24 hours in UPN251, UPN251-7C and UPN251-7T. Each graph gives the percentage number of cells which are; (A) G1 phase (taxol treatments) (B) G1 phase (carboplatin treatments) (C) S phase (taxol treatments) (D) S phase (carboplatin treatments) (E) G2/M phase (taxol treatments) (F) G2/M phase (carboplatin treatments) . Error bars represent SD for n=3 replicates.

# Indicates a significant difference in the percentage number of treated cells compared to untreated control cells ($P<0.05$, student T-test).

untreated control cells (p=0.004 and 0.008 respectively, fold decrease=0.5) (Figure 5.14 (F), region R4 Figure 5.13). Again, UPN251-7C had no significant change.

It must be noted from the cell cycle analysis that no significant changes occurred at any stage in the cell cycle for UPN251-7T treated with taxol and UPN251-7C treated with carboplatin when compared to untreated controls. All other cell lines and treatments saw some disruption of the cell cycle with changes in all or some of the phases (G1, S or G2/M). The drug-resistant cell lines are resisting changes in their cell cycle in response to their own selecting agent. In contrast, the same cell lines are making changes to their cell cycle in response to the alternate drug, not used in their selection.

5.3.6 Western blotting

Parental UPN251 and all resistant sublines (UPN251-7C/6CALT/7T/6TALT) were examined by Western blotting for a number of different proteins known to be involved in ovarian cancer drug resistance;

- P-glycoprotein (P-gp) – See section 1.6.1
- ATP7A – See section 1.4.1.1
- CTR1 – See section 1.4.1.1
- MRP2 – See section 1.4.1.2
- Bcl-2 – See section 1.4.5 and 1.6.4
- Bcl-XL – See section 1.4.5 and 1.6.4

Also, dicer and drosha involved in miRNA biosynthesis (section 1.8.2) were examined in order to see if the development of carboplatin or taxol chemoresistance had any effect on their protein expression.

Cell pellets were made for at least n=3 biological replicates, for both untreated cells and the same cells treated with the drugs used during their selection in chapter 4, e.g. for UNP251-6CALT, 3 pellets were made; an un-treated control, a carboplatin treated and a taxol treated pellet. UPN251 was treated with both carboplatin and taxol for comparison purposes. Cells selected with carboplatin received 2µg/ml carboplatin, the same dose given in the selection strategy for three day exposure to drug. Cells selected with taxol received 15ng/ml taxol for three day exposure to drug. This was lower than the dose given in the selection strategy, as 60ng/ml did not allow enough cells to survive in UPN251 to examine protein expression. This allowed us to examine the effects of protein expression on first response to drug exposure in UPN251 and the response to drugs in resistant sublines. The gels were run in two series; a carboplatin

and taxol selected series. The carboplatin selected series contained UPN251 and all cells selected with carboplatin during the selection strategy in chapter 4, including both untreated cells and cell treated with carboplatin. The taxol series was the same for taxol treated cell lines and treatments.

P-gp protein expression for UPN251-6CALT and UPN251-7T (control and taxol treated) and UPN251-6TALT (taxol treated) was significantly up-regulated when compared to UPN251 control (fold change= 2.3±0.9 - 7.3±2.8, p=0.04-0.003, Figure 5.15). P-gp is significantly decreased in UPN251-7C (carboplatin treated) when compared to UPN251 control cells.

There were no significant changes in protein expression for the two copper transporters tested, ATP7A (Figure 5.16) and CTR1 (Figure 5.17) compared to UPN251 control. Also, MRP2 had no detectable protein expression in UPN251 parental cells or resistant sublines (Figure 5.18 (A)). An MRP2 transfected cell line (2008/MRP2) was used as a positive control in order to demonstrate efficient binding of the anti-MRP2 antibody to its intended target.

A number of significant changes occurred in the protein expression of Bcl-2 and Bcl-XL, which are members of the apoptosis pathway (Figure 5.19 and 5.20 respectively).

Small, but significant reductions of Bcl-2 protein expression is evident in UPN251 treated with carboplatin and taxol (fold change=0.7±0.2 & 0.6±0.2 respectively, p=0.02) compared to untreated UPN251 cells. Both UPN251-6CALT and UPN251-6TALT treated with carboplatin also have significantly reduced expression of Bcl-2 (fold change=0.6±0.2 and 0.4±0.07, p=0.03 and $0.2x10^{-3}$ respectively) when compared to UPN251 control. Untreated UPN251-7T and UPN251-6TALT have small, but significant over-expression of Bcl-2 (fold change=1.1±0.05 and 1.4±0.1, p=0.04 and 0.007 respectively) when compared to UPN251 control cells. In the case of Bcl-XL, all treated and untreated UPN251 and resistant sublines had reduced expression (fold change=0.6±0.2 – 0.8±0.09, p=0.05-$0.8x10^{-6}$) when compared to UPN251 control cells, except UPN251 (taxol treated), UPN251-7C (carboplatin treated) and UPN251-6TALT (carboplatin treated) which showed no change.

Dicer and Drosha showed no significant changes in protein expression (Figure 5.21 and 5.22 respectively). The only exceptions were a significant increase in UPN251 treated with taxol and a significant reduction in UPN251-6TALT treated with taxol.

There was also no change in BRCA1 protein expression between UPN251 parental cells and UPN251-7C and UPN251-7T resistant sublines (Figure 5.18 (C), (D) and (E)).

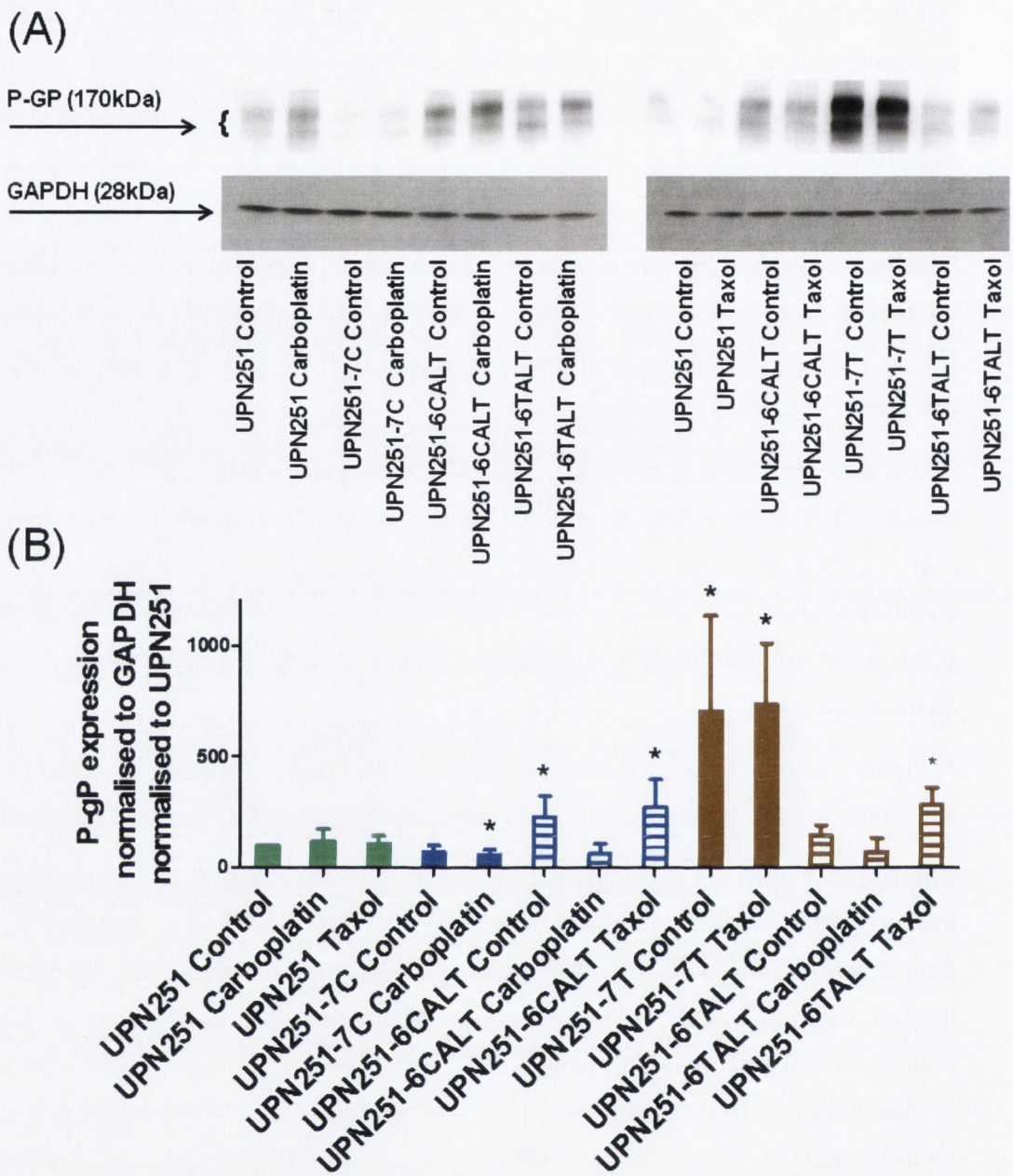

Figure 5.15 P-glycoprotein (170kDa) Western blot.

(A) Representative image of chemoluminescent photographs taken of target protein and GAPDH loading control. UPN251 cells and resistant sublines are given; both untreated (control) and treated with carboplatin (2μg/ml) or taxol (15ng/ml) for 3-day exposure to drug. (B) The target protein expression was normalised to GAPDH and then normalised to UPN251 control cells is shown on y-axis. This graph represents the mean and SD of at least 3 biological replicates.

*Indicates a significant change in protein expression compared to UPN251 control ($P<0.05$, student T-test).

# Indicates a significant change in protein expression compared to parental control ($P<0.05$, student T-test).

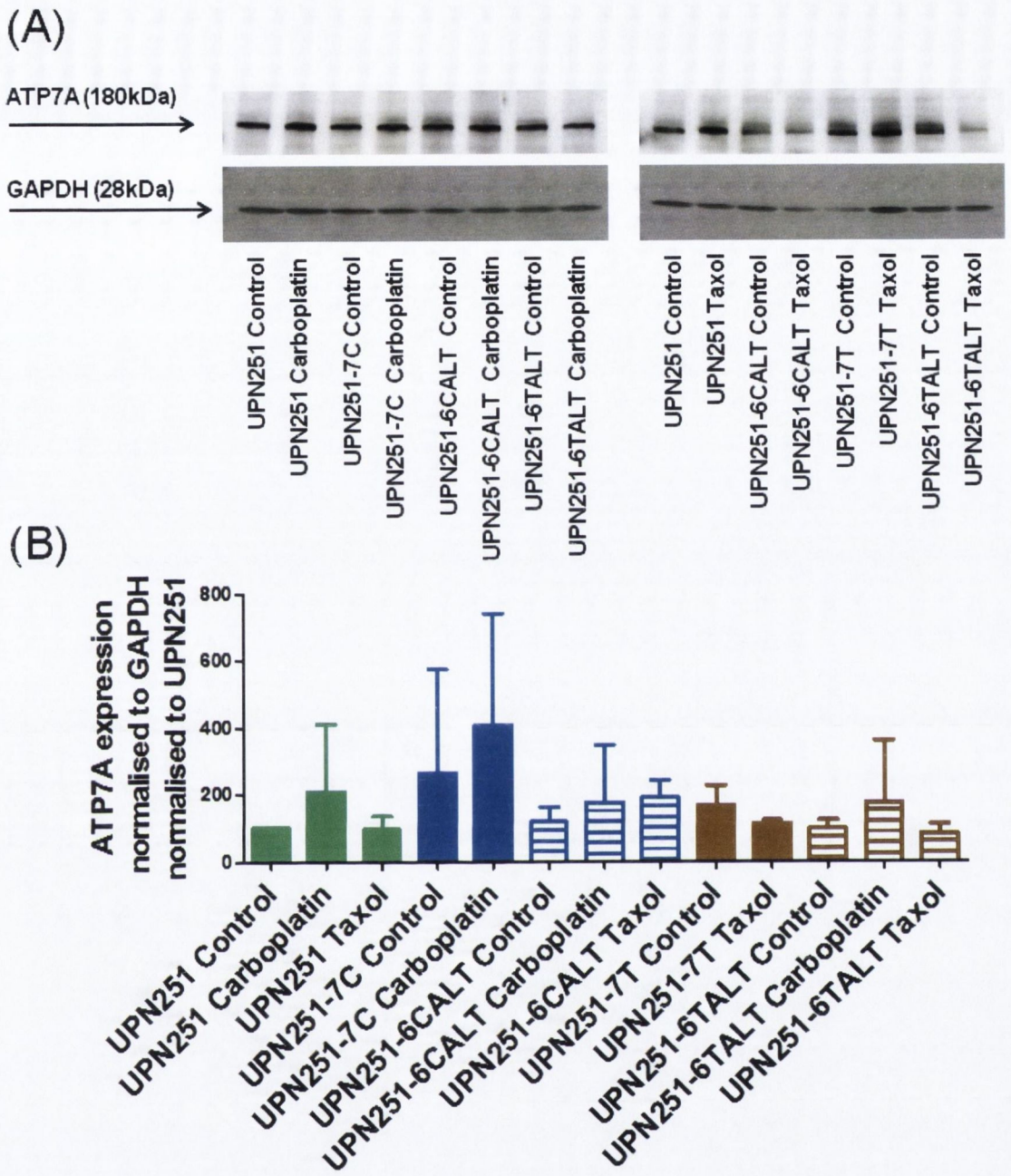

Figure 5.16 ATP7A (180 kDa) Western blot.

Representative image of chemoluminescent photographs taken of target protein and GAPDH loading control. UPN251 cells and resistant sublines are given; both untreated (control) and treated with carboplatin (2μg/ml) or taxol (15ng/ml) for 3-day exposure to drug. (B) The target protein expression was normalised to GAPDH and then normalised to UPN251 control cells is shown on y-axis. This graph represents the mean and SD of at least 3 biological replicates.

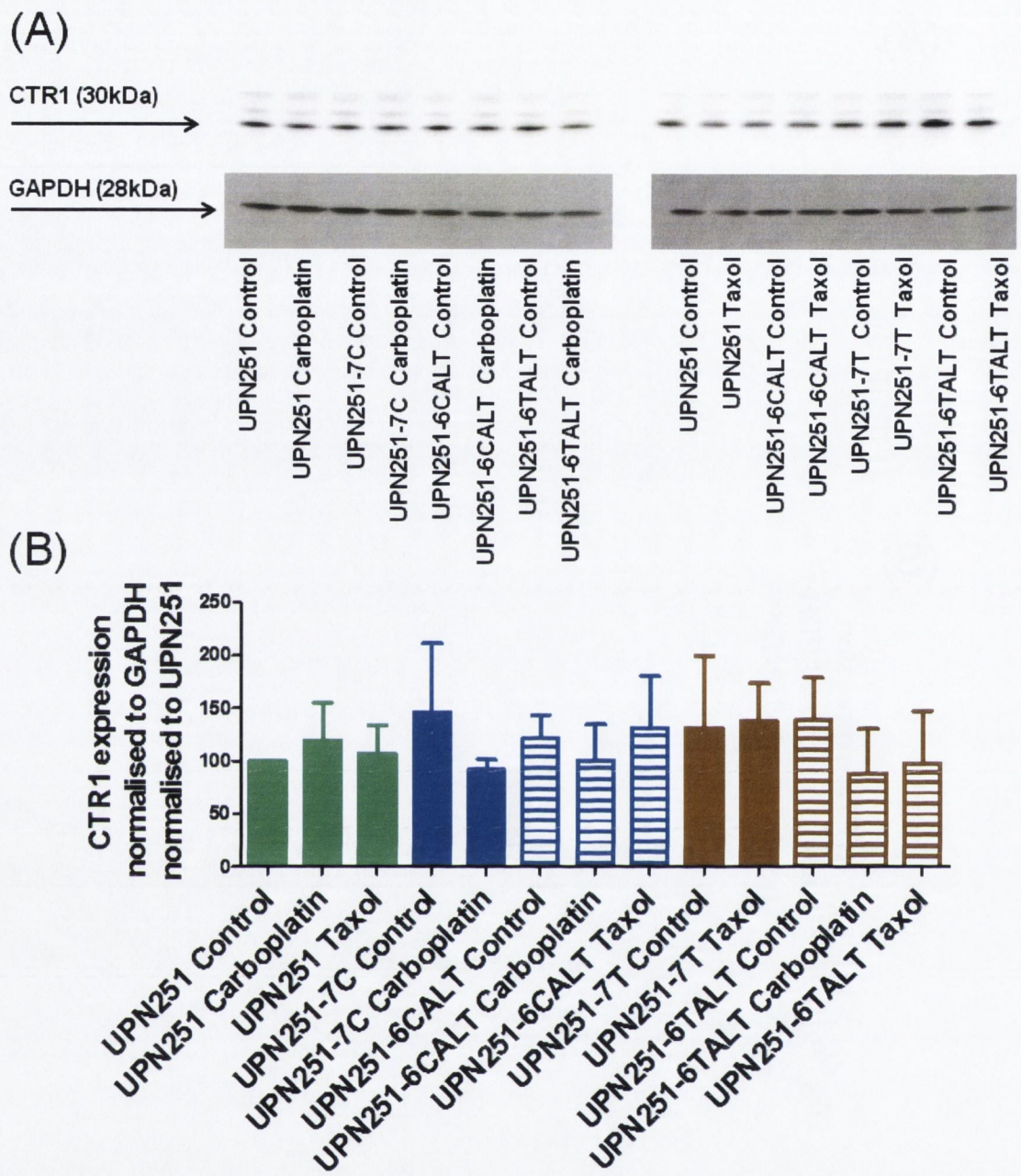

Figure 5.17 CTR1 (30kDa) Western blot.

Representative image of chemoluminescent photographs taken of target protein and GAPDH loading control. UPN251 cells and resistant sublines are given; both untreated (control) and treated with carboplatin (2μg/ml) or taxol (15ng/ml) for 3-day exposure to drug. (B) The target protein expression was normalised to GAPDH and then normalised to UPN251 control cells is shown on y-axis. This graph represents the mean and SD of at least 3 biological replicates.

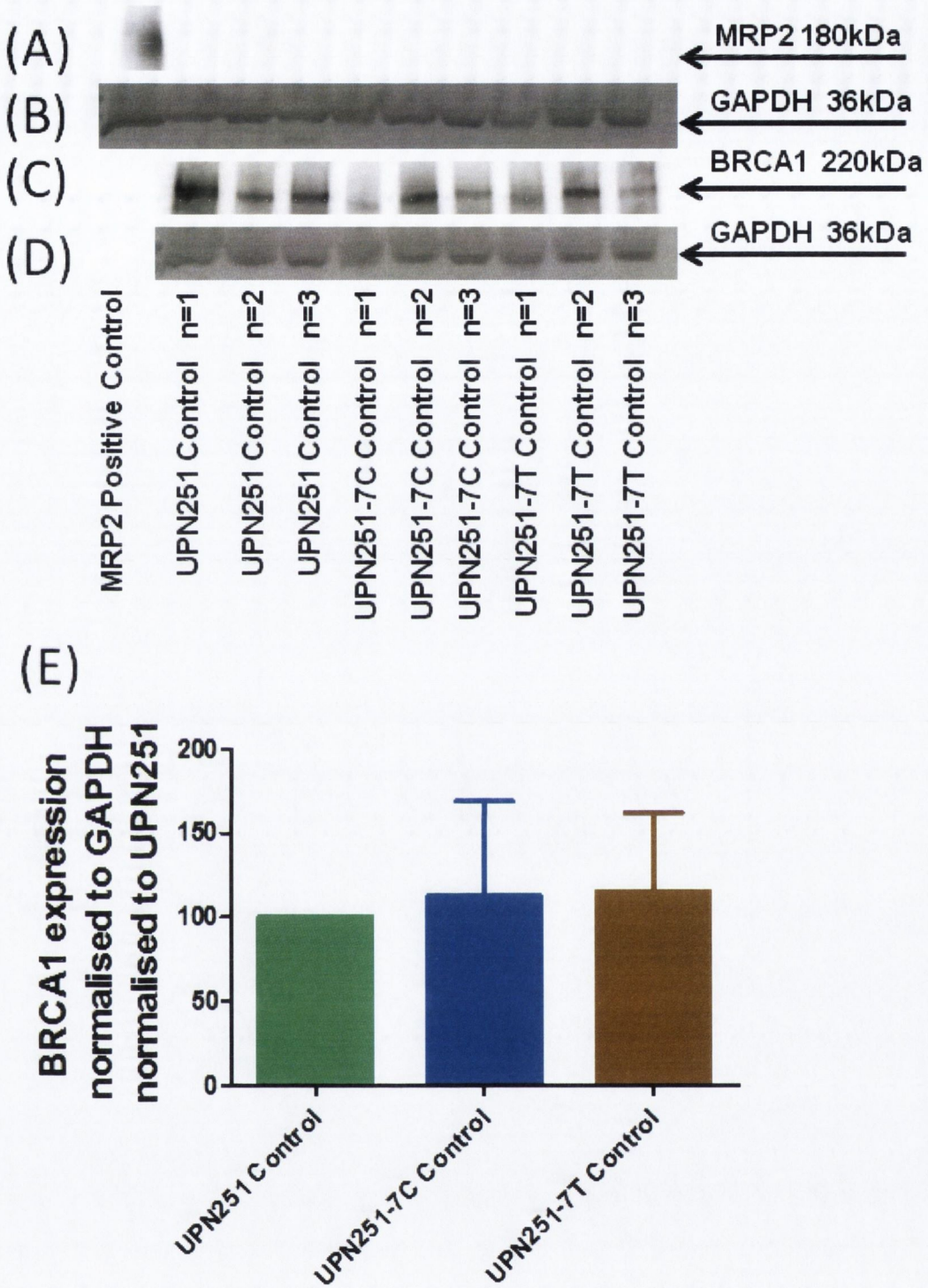

Figure 5.18 MRP2 (180kDa) & BRCA1 (220kDa) Western blot.

All protein samples were normalised to GAPDH and then UPN251 control. (A) MRP-2 (B) GAPDH loading control (C) BRCA1 (D) Graph of GAPDH loading control (E) BRCA1 protein expression normalised to GAPDH and then normalised to UPN251 control cells is shown on y-axis. Three biological replicates are shown.

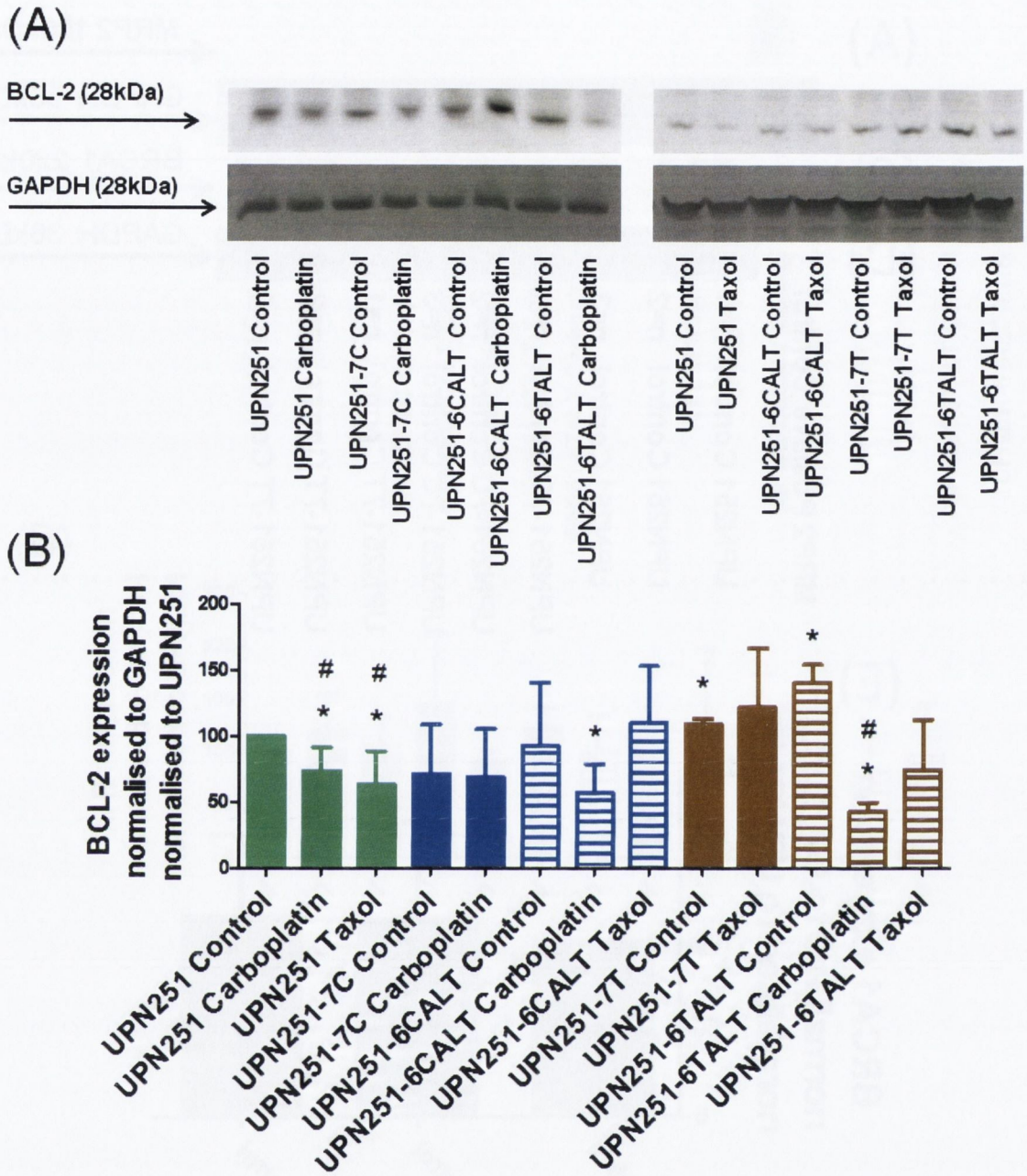

Figure 5.19 Bcl-2 (28kDa) Western blot.

Representative image of chemoluminescent photographs taken of target protein and GAPDH loading control. UPN251 cells and resistant sublines are given; both untreated (control) and treated with carboplatin (2µg/ml) or taxol (15ng/ml) for 3-day exposure to drug. (B) The target protein expression was normalised to GAPDH and then normalised to UPN251 control cells is shown on y-axis. This graph represents the mean and SD of at least 3 biological replicates.

*Indicates a significant change in protein expression compared to UPN251 control ($P<0.05$, student T-test).

# Indicates a significant change in protein expression compared to parental control ($P<0.05$, student T-test).

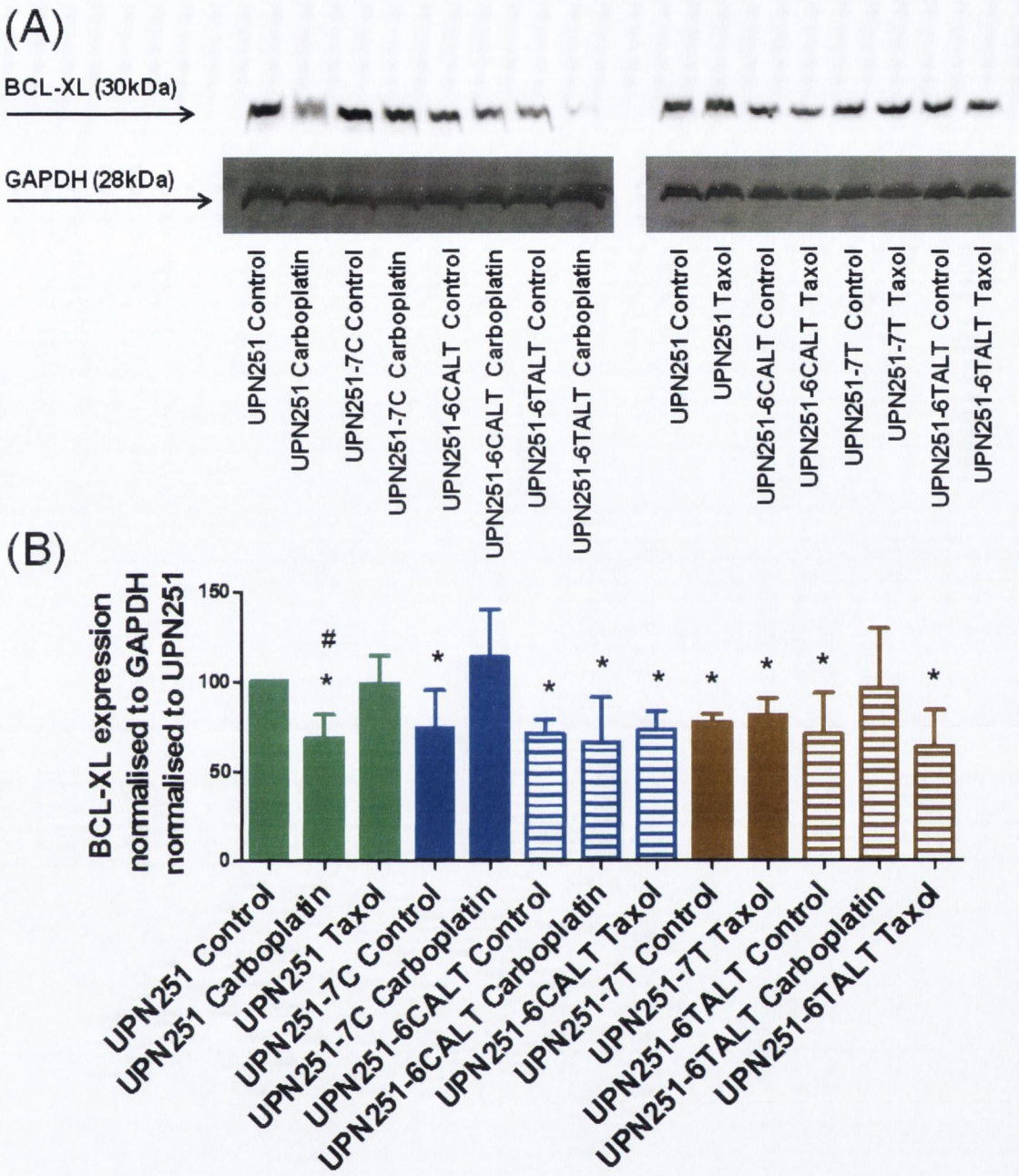

Figure 5.20 Bcl-XL (30kDa) Western blot.

Representative image of chemoluminescent photographs taken of target protein and GAPDH loading control. UPN251 cells and resistant sublines are given; both untreated (control) and treated with carboplatin (2µg/ml) or taxol (15ng/ml) for 3-day exposure to drug. (B) The target protein expression was normalised to GAPDH and then normalised to UPN251 control cells is shown on y-axis. This graph represents the mean and SD of at least 3 biological replicates.

*Indicates a significant change in protein expression compared to UPN251 control ($P<0.05$, student T-test).

# Indicates a significant change in protein expression compared to parental control ($P<0.05$, student T-test).

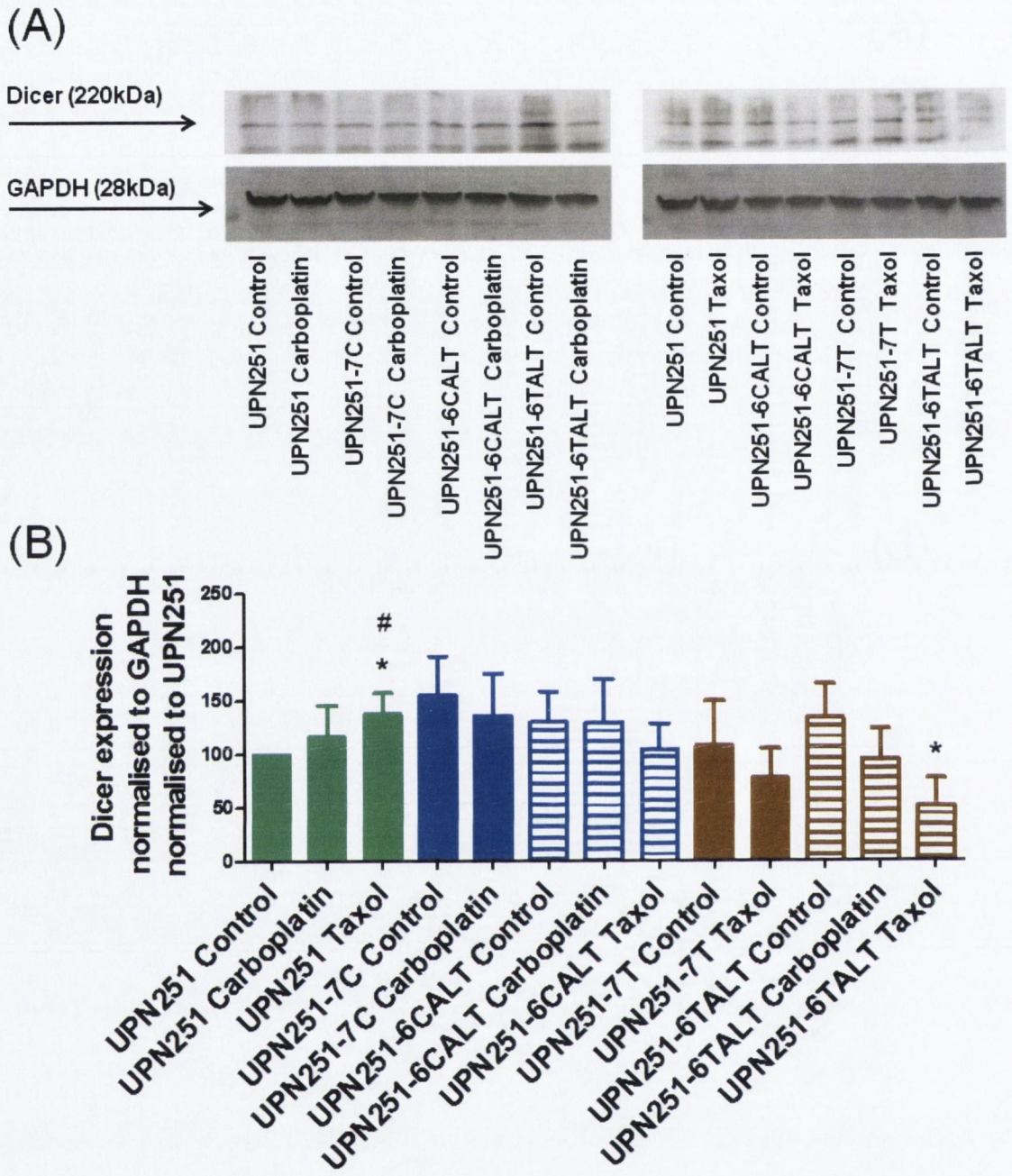

Figure 5.21 Dicer (220kDa) Western blot.

Representative image of chemoluminescent photographs taken of target protein and GAPDH loading control. UPN251 cells and resistant sublines are given; both untreated (control) and treated with carboplatin (2μg/ml) or taxol (15ng/ml) for 3-day exposure to drug. (B) The target protein expression was normalised to GAPDH and then normalised to UPN251 control cells is shown on y-axis. This graph represents the mean and SD of at least 3 biological replicates.

*Indicates a significant change in protein expression compared to UPN251 control ($P<0.05$, student T-test).

# Indicates a significant change in protein expression compared to parental control ($P<0.05$, student T-test).

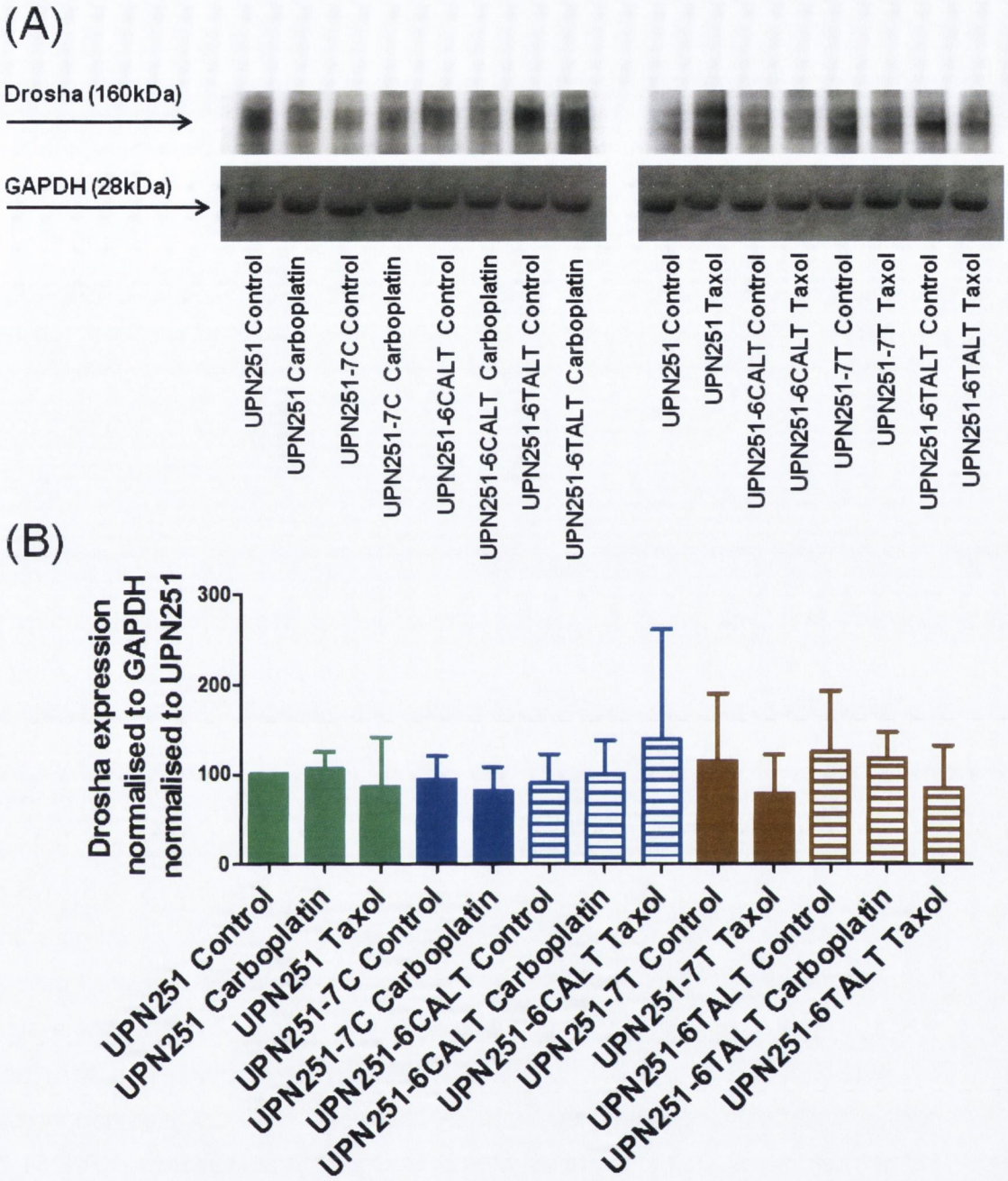

Figure 5.22 Drosha (160kDa) Western blot.

Representative image of chemoluminescent photographs taken of target protein and GAPDH loading control. UPN251 cells and resistant sublines are given; both untreated (control) and treated with carboplatin (2μg/ml) or taxol (15ng/ml) for 3-day exposure to drug. (B) The target protein expression was normalised to GAPDH and then normalised to UPN251 control cells is shown on y-axis. This graph represents the mean and SD of at least 3 biological replicates.

5.4 Discussion

5.4.1 Mechanisms of taxol resistance

As previously discussed, taxol-resistant cell models are very common in the literature. Many have been developed for ovarian cancer cell lines (*Duan et al. 1999b*; *Duan et al. 1999c*; *Hari et al. 2006*; *Parekh et al. 1997b*; *Zhang et al. 2012a*). As the majority of these models use different variations on the intermittent incremental inducement and increasing continuous administration strategies, this results in resistant sublines with high fold resistance and mechanisms of resistance not likely to be present in the clinic. Our work, using the pulsed strategy, provides a novel strategy in ovarian cancer with drug-resistant mechanisms that have the potential to mirror the clinical setting.

Over-expression of P-gp often arises as a mechanism of taxol resistance in cell models. P-gp is the main mechanism of taxol resistance in UPN251 derived resistance models treated with taxol. Cytotoxicity assays for P-gp substrates taxol, vinblastine and olaparib ± elacridar (Table 5.1 and Figure 5.1 and Figure 5.2), all show highly significant drops in IC_{50} when P-gp is inhibited with elacridar. Western blot data showed increased P-gp protein expression for sublines that had taxol treatment during selection (Figure 5.15). Therefore, it is likely that taxol is being actively pumped out of the cell by P-gp, causing taxol resistance. A change in apoptotic response to taxol treatment is a mechanism that contributes to the taxol-resistant phenotypes in this study. No change in the number of early apoptotic cells was seen when UPN251-7T (taxol resistant) cells were treated with 100ng/ml of taxol for 24 hours compared to untreated cells (Figure 5.9 (D)). However, UPN251 and UPN251-7C (taxol sensitive) cells saw a significant increase (fold increase = 3.8 and 3.5 respectively) in the number of early apoptotic cells in their populations after the same taxol treatment. All cell lines had increases in the number of cells in late stage apoptosis/necrosis, but UPN251 and UPN251-7C saw greater significant increases (Figure 5.9 (B)). This indicates an increase in apoptotic resistance in our cell lines in response to high dose taxol treatment.

Bcl-2 is a protein that is generally known to be an inhibitor of apoptosis (*Reed 1995*). Contributing to the evidence demonstrated by the apoptosis assay in this study, the protein expression of Bcl-2 was significantly increased in the UPN251-7T and UPN251-6TALT cells that had received taxol (15ng/ml) during its development (Figure 5.18). Taxol treatment (15ng/ml) of both cell lines saw no significant changes in Bcl-2 expression. However, non-resistant parental cells UPN251 did see a decrease of Bcl-2 in response to taxol (15ng/ml). The loss of the cells' ability to decrease Bcl-2 in response to taxol treatment may be a mechanism contributing to our taxol resistance

phenotype. This effect has been previously discussed in the literature where taxol treatment was able to reduce expression of the Bcl-2 protein in taxol sensitive ovarian cancer cells SKOV3-ip1 and not in taxol resistant SKOV3-ip2 cell lines (*Chen et al. 2013*). Increased expression of the Bcl-2 protein conveying resistance to taxol has been demonstrated in multiple myeloma cells (*Gazitt et al. 1998*; *Liu et al. 2003*). However, a decrease in Bcl-2 protein expression correlating to taxol resistance has also been seen in the literature in ovarian cancer cell lines (*Ferlini et al. 2003*; *Solar et al. 2008*). *Ferlini et al (2003)* gives evidence of a dual function of Bcl-2 in response to taxol, where it acts in the mitochondria and in microtubule turnover. This may be why up and down-regulation of Bcl-2 has been shown to confer resistance in different studies.

Circumvention of cell cycle arrest was a mechanism that contributed to our taxol-resistant phenotypes. Taxol is known to induce cell cycle arrest at the G2/M phase of the cell cycle, resulting in apoptosis as part of its mechanism of action (*Long et al. 1994*). At a high dose of 800ng/ml of taxol, UPN251-7T and UPN251-6TALT saw significantly less cells in mitosis than UPN251, UPN251-7C or UPN251-6CALT (Figure 5.6 (B)). At a lower concentration of 50ng/ml of taxol, all cell lines showed similar level of cells in mitosis. From the FACS cell cycle analysis assay in this study, it was shown that at a dose of 100ng/ml (double that of the doses that showed no affect in the mitosis assay) UPN251-7T had no changes in their cell cycle, while UPN251 and UPN251-7C both saw changes in cell number at different stages of the cell cycle (Figure 5.12 and Figure 5.14 (A-C)). Both UPN251 and UPN251-7C (taxol sensitive) had significant reductions in cells in the G1 phase of the cell cycle when treated with taxol while UPN251-7T remained the same. Also, UPN251-7C cells saw accumulation of cells in the G2/M phase of the cell cycle.

Reduction in growth rate may also be a mechanism by which cells overcome cell death in our models of taxol resistance (*Ohta et al. 1994*; *Wang et al. 2013*). All UPN251 resistant sublines took significantly longer to reach quadrupling time when treated with a range of 50-200ng/ml taxol in comparison to drug free controls ($p=0.03\text{-}0.2x10^{-3}$) (Figure 5.4 (B)). However, UPN251 had no significant changes for any taxol dose tested. As UPN251-7C (which is sensitive to taxol and only had exposure to carboplatin during development) also experienced a reduction in growth rate, it may be that this reduced growth rate is a general response to drug treatment and not a taxol specific mechanism. The cell line with the highest fold taxol resistance UPN251-7T also had reduction in growth rate in a range that encompassed lower doses of taxol (3.125-200ng/ml), ($p=0.04\text{-}0.2x10^{-3}$) when compared to untreated control cells. This may

indicate that taxol resistance in the UPN251 resistant sublines is coupled to a reduction in growth rate.

5.4.2 Mechanisms of carboplatin resistance

As discussed previously, carboplatin-resistant ovarian cancer cell models are rare in the literature. Therefore, the UPN251 carboplatin resistant cell models are novel and could reveal clinically relevant mechanisms of carboplatin resistance.

From the results of the GSH assays in this study (Figure 5.3), it became evident that only UPN251 showed a significant increase in total cellular GSH levels in response to carboplatin treatment. The developed UPN251 sublines had no significant increases compared to UPN251 with a carboplatin treatment of 2µg/ml. This suggests that elevated GSH plays a role in the parental cells initial response to carboplatin and that UPN251 resistance sublines utilise other mechanisms. Treatment with a 12.5µg/ml dose of BSO significantly decreases GSH in UPN251 and all sublines. This was the same dose of BSO used in our post selection drug screen with carboplatin (Table 5.1 and Figure 5.1 (A)). Small, but significant decreases in IC_{50} were noted in UPN251 sublines, but no difference in fold change was noted. This indicated that increased total cellular GSH may not be a major mechanism of carboplatin resistance in our developed models. An important point to note is that MRP expression can influence BSO treatment (*Akan et al. 2005*; *Rappa et al. 2003*). As MRP2 protein expression was absent in both UPN251 and resistant sublines, it is not likely that MRP transport influenced the results and conclusions drawn from this study.

$CuSO_4$ (Table 5.1 and Figure 5.1 (C)) had significantly higher IC_{50}'s for UPN251-7C and UN251-6CALT. This indicated a possible involvement of copper transporters ATP7A, ATP7B and CTR1 in carboplatin resistance (*Safaei et al. 2005*). However, Western blots for ATP7A and CTR1 showed little difference in protein expression (Figure 5.16 & 5.17 respectively). Instead, these proteins may be relocated to different parts of the cell, causing a resistance phenotype. An increase of ATP7A and ATP7B in the cellular membrane or a relocation of CTR1 to the golgi apparatus may lead to platinum resistance without a change in protein expression (*Stordal et al. 2012*).

A change in apoptotic response to carboplatin treatment was a mechanism that contributed to our carboplatin-resistant phenotypes. UPN251 cells saw a significant increase in the number of late apoptotic or necrotic cells in their populations after high dose carboplatin treatment (350µg/ml) (Figure 5.11 (B)). Both UPN251-7C and UPN251-7T did not demonstrate significant changes in cell number of late apoptotic or necrotic cells. It may have been expected to see a change in UPN251-7T (carboplatin

naïve) but toxicity assays of carboplatin and taxol (Table 5.1 and Figure 5.1) in this cell line showed that these cells were low level cross resistant to carboplatin. Also, UPN251-7T had a small elevation in cell number that was trending towards significance (p=0.09, fold increase=1.4), while UPN251-7C showed no change explaining this result. All cells had an increase in the number of cell undergoing early stage apoptosis with treatment of carboplatin (350µg/ml). However, UPN251 had the highest and most significant fold increase and UPN251-7C had the lowest and least significant increase. This indicates a moderate increase in apoptotic resistance in the cell lines in response to high-dose carboplatin treatment.

Bcl-2 over-expression has been linked with platinum resistance to ovarian cancer in the literature (*Kassim et al. 1999*). However, another study has shown that over-expression may be linked to sensitivity, not resistance to platinum drugs (*Beale et al. 2000*). Furthermore, ovarian cancer patients who simultaneously express BAX and Bcl-2 have been shown to have a longer progression-free and overall survival compared to patients who did not express Bcl-2 (*Schuyer et al. 2001*). In this study, there was a significant reduction of Bcl-2 in UPN251 and UPN251-6TALT after treatment with 2µg/ml of carboplatin when compared to untreated cells (Figure 5.19). The carboplatin resistant sublines, UPN251-7C and UPN251-6CALT, both saw no change in Bcl-2 protein expression. The difference in response of Bcl-2 levels to carboplatin treatment in UPN251 and UPN251-7C may indicate that the inability to reduce Bcl-2 levels have contributed to a carboplatin-resistance phenotype as in the taxol resistant cell models. The difference in UPN251-6CALT and UPN251-6TALT may indicate that different mechanisms of resistance have evolved due to different initial drug exposure during the selection strategy.

Bcl-XL is another protein (along with Bcl-2) that is generally known to be an inhibitor of apoptosis and up-regulation has been linked with chemoresistance and recurrence in ovarian cancer (*Williams et al. 2005*). Recently, the effects of inhibiting Bcl-XL with ABT-737 (A Bcl family inhibitor) in combination with carboplatin treatment sensitised a number of ovarian cancer cells to carboplatin by increasing apoptosis in response to treatment (*Witham et al. 2007*). However, not all cell lines responded in the same way. The effects of Bcl-XL expression on platinum and taxane resistance in ovarian cancer cell lines seemed to be cell line specific (*Dodier et al. 2006*). Modulation of Bcl-XL levels and its effect on apoptotic response to chemotherapeutics may depend on a cells genetic background (*Dodier et al. 2006*). In this study, there was consistent down-regulation of Bcl-XL levels across all of the untreated resistant sublines when compared to UPN251. Treatment with low dose carboplatin (2µg/ml) in UPN251

resulted in a significant decrease in Bcl-XL levels when compared to untreated parental cells, while there was no change across all the drug resistant phenotypes in response to carboplatin treatment. It may be that the loss of a cells ability to down-regulate Bcl-XL could contribute to its resistance phenotype as with Bcl-2. This theory is backed up by the literature where absence of Bcl-XL down-regulation in response to cisplatin (another platinum agent) has been associated with chemoresistance in ovarian cancer cell lines (*Villedieu et al. 2007*).

Resistance to cell cycle changes contributed to the carboplatin resistance phenotypes. The cell cycle of UPN251-7C, when treated with 350µg/ml of carboplatin for 24hours, remained unchanged when compared to untreated cells. UPN251 and UPN251-7T had significant changes in the number of cells at each stage (G1, S and G2/M) of the cell cycle when treated with the same dose of carboplatin.

5.4.3 Combined resistance to platinums and taxanes

Models of taxane-platinum resistance are rare in the literature. One study developed a taxane-platinum resistant model for non-small cell lung cancer by exposing the cells to cycles of taxol and carboplatin, two cytotoxic agents with different mechanisms of action (*Dalvi et al. 2012*). In the models up-regulation of ABCB1/MDR1, down-regulation of epithelial specific genes (suggesting cells were undergoing EMT), differential expression of epigenetic modulators and cancer testis family of GAGE genes, all contributed to the resistance phenotypes. Another study developed a dual carboplatin and docetaxel resistant subline from A2780 ovarian cancer cells which are cross resistant to both agents (*Armstrong et al. 2012*). The study also developed A2780 sublines that were resistant to each agent on their own and not cross resistant to the other agent. Gene profiling revealed that the dual model contained genetic changes that were not present in the singularly resistant models. This demonstrated that combined drug resistance may not be a simple combination of changes present in single-agent resistant cell lines, but can contain novel changes.

Our model presented this novel aspect of subline development in ovarian cancer for carboplatin and taxol, where sublines were exposed to alternating sequences of both drugs. As a result, UPN251-6CALT and UPN251-6TALT showed significant cross resistance to both carboplatin and taxol used in their development. They demonstrated a carboplatin fold resistance of 1.7 and 2 and a taxol fold resistance of 4.3 and 5.7 respectively (Table 5.1 and Figure 5.1). This was less than the UPN251 sublines selected with single agents, but these had no significant cross resistance to carboplatin or taxol except UPN251-7T, which was 1.5 fold resistant to carboplatin.

The cytotoxic agent, that our sublines were initially exposed to, influenced the mechanisms of resistance that arose. UPN251-6CALT and UPN251-6TALT both received 3 rounds of drugging with carboplatin and taxol. The only difference was that UPN251-6CALT received carboplatin in the first round, whereas UPN251-6TALT received taxol. As a result, UPN251-6CALT displayed significant fold resistance to $CuSO_4$ (2.3 fold, p=0.004), while UPN251-6TALT showed no significant fold resistance. Also, UPN251-6TALT showed significant sensitivity to oxaliplatin (p=0.01), while UPN251-6CALT had no significant fold change. This would indicate different resistance mechanisms being selected in these cells depending on initial drug exposure.

In the clinic for ovarian cancer, taxol is administered three hours before carboplatin in combination chemotherapy, every 3 weeks for 6 cycles (*Ozols et al. 2003*). Drugs are administered in this sequence to circumvent toxicity. Although our alternating models do not exactly mimic this administration, it is interesting to note that the sequence of taxol before carboplatin may produce specific mechanisms of resistance not seen in the opposite administration and vice-versa. This may be a consideration for future combinations of drugs administered to cancer patients. Cancer therapy is continually changing and evolving in order to improve survival from this lethal malignancy. Therefore, sequence dependant studies into acquired mechanisms of drug resistance may be an important factor to consider when designing new therapies or when improving existing regimes.

5.4.4 Resistance and miRNA biogenesis proteins

Dicer and drosha are not currently regarded as major contributors to ovarian cancer resistance. However, aberrant expression of miRNAs has been strongly associated with ovarian cancer resistance. Therefore, it was deemed interesting to see if aberrant expression of proteins involved in their biogenesis (dicer and drosha, two RNase III endonucleases which play a role in processing miRNA into its mature form) might be involved in conferring ovarian cancer chemoresistance. Western blots were carried out in order to investigate whether dicer and drosha had a role to play in ovarian cancer resistance to carboplatin or taxol. Suppression of dicer expression has been shown to confer a resistance to cisplatin and induce proliferation, migration and cell cycle progression in ovarian cancer cell lines (*Kuang et al. 2013*). In our study, no significant changes in expression were noted for dicer or drosha between the different sublines and UPN251. Also, no changes in expression occurred for both proteins when the cell lines were treated with carboplatin. However, with the addition of taxol, dicer was significantly increased in UPN251 and significantly decreased in UPN251-6TALT, when

compared to the UPN251 control cells. Furthermore, there was no difference in dicer protein expression between UPN251-6TALT untreated and taxol treated cells. For this reason, this study gives no compelling evidence that dicer and drosha expression were involved in the resistant phenotype.

5.4.5 Treatment options for platinum/taxane resistant ovarian cancers

None of the UPN251 resistant sublines saw any development of resistance to two of the PARP inhibitors tested in this study, CEP8983 and veliparib. Therefore, their mechanism of action was not affected by the multiple mechanisms of resistance that arose in the resistant sublines. For this reason, CEP8983 and veliparib may be good candidates for the treatment of platinum/taxane resistant ovarian cancer.

5.5 Conclusions

The over-expression of P-gp was the dominant mechanism of taxol resistance found in the UPN251 resistant sublines. However, this is not a major mechanism of resistance that presents in the clinic. This corroborates how cell lines are 'simple' models and how P-gp over-expression may be selected for more strongly *in-vitro*. This mechanism was complimented in the cell lines by a reduction in growth rate, apoptotic resistance (in part due to an inability to reduce Bcl-2 levels) and circumvention of G2/M arrest. These mechanisms may be more clinically relevant. The investigation of these mechanisms *in-vivo* will help to see if these mechanisms are prevalent in ovarian cancer patients, which may result in the development of targeted therapies. Markers identified, such as elevation in Bcl-2 after taxol treatment, could be used as markers of taxol resistance. This could to be further investigated by examining the levels of Bcl-2 in ovarian cancer patients, before and after taxol based treatment, and checking if Bcl-2 stability or loss of expression influences survival. As obtaining tumour tissue for different time points is not feasible, using serum samples could be an option.

Multiple mechanisms of carboplatin resistance were found to be present in the cell models. This included apoptotic resistance and resistance to changes in the cell cycle. Other major mechanisms identified in the literature, such as a rise in intracellular GSH, aberrant expression of copper transporters or alterations in copper metabolism, may only play minor roles in the carboplatin-resistant cell models. However, relocation of ATP7A and CTR1 might still contribute to their resistance, even without changes in protein expression. Again, it will be useful to further investigate these mechanisms *in-vivo*. For example, no reduction in Bcl-2/Bcl-XL expression levels in ovarian cancer

patients after carboplatin based treatment could be an indicator or carboplatin resistance.

The sequence of drug exposure was found to influence the resistance mechanism that developed in the resultant resistant sublines. UPN251-6CALT and UPN251-6TALT had different profiles of cross resistance to drugs; where their only difference was that one received carboplatin and one received taxol in the first round of development. Sequence dependant studies into acquired mechanisms of drug resistance may be an important factor to consider when designing new therapies or when improving existing regimes. New sequence studies of drug administration should investigate differences in resistance development along with adverse side effects, pharmacokinetic, pharmacodynamics, which are classically investigated.

As the development of resistance to carboplatin/taxol treatment is common in ovarian cancer, the introductions of new second line/salvage chemotherapy regimens that are not affected by this resistance are important. PARP inhibitors CEP8983 and veliparib may be useful in the treatment of platinum/taxane resistant ovarian cancer, as no cross resistance was seen in any of our resistant sublines. PARP inhibitors, such as olaparib, have shown promise in clinical trials to date for certain patients. CEP8983 and veliparib have been examined in a small number of small ovarian cancer resistant patient cohorts (*Kummar et al. 2012*; *Plummer et al. 2014*). Further studies involving these PARP inhibitors in resistant patient cohorts may be warranted in order to examine their potential in the treatment of platinum/taxane resistant ovarian cancer.

The UPN251 resistant sublines had been characterised as having a number of mechanisms of chemo-resistance, which were contributing to their resistance phenotypes. These mechanisms are likely to be clinically relevant due to their clinically relevant selection. However, less evidence has been found to identify what is causing resistance in the carboplatin resistant sublines. In chapter 6 novel markers of carboplatin and taxol resistance in ovarian cancer were investigated within the resistant sublines UPN251-7C and UPN251-7T, using Affymetrix gene and miRNA arrays. This was carried out in order to further elucidate the mechanisms of resistance that were present. As the resistant sublines were developed with clinical relevance in mind, the markers found by Affymetrix arrays have the potential to further understanding of resistance in the clinical setting. This has the potential to improve clinical therapy in ovarian cancer treatment by identifying new markers of resistance and the relevant pathways to target to circumvent resistance.

CHAPTER 6

Chemoresistant Ovarian Cancer Biomarker Discovery



TRINITY
COLLEGE
DUBLIN

Chapter 6 Chemoresistant ovarian cancer biomarker discovery

6.1 Introduction

This chapter dealt with the discovery of novel biomarkers which relate to chemoresistance in ovarian cancer. De-regulated genes and miRNAs in response to carboplatin or taxol treatment and changes over prolonged exposure to both agents were examined. This was achieved by utilising the developed resistant phenotypes of our UPN251 resistant sublines, selected for in Chapter 4. DNA microarray technology was used to discover de-regulated genes and miRNAs that are linked to chemoresistance.

6.1.1 Microarray technology

Microarray technology evolved from the technique of Southern blotting developed by Dr. Edward Southern in 1975, which was used to analyse DNA by the detection of specific DNA sequences (*Southern 1975*). DNA microarrays can be defined as a high-throughput multipurpose technology which is used to analyse gene expression of thousands of known and unknown genes in parallel or to detect polymorphisms and mutations in genomic DNA in DNA homology analysis studies. Thousands of DNA sequences (probes made up of short gene sections or other DNA elements) are immobilised to a solid surface (usually glass, silicon chips or nylon membrane). Complementary cDNA from samples is hybridised to its corresponding probes on the array. Detection of hybridisation to a specific probe is usually quantified by detection of fluorophore-silver or chemiluminescence-labelled targets indicating the amount of RNA sequences in the target sample. This technology allows for the parallel analysis of gene expression (*Heller 2002*).

Early 'simple' arrays were known as 'dot-blots' arrays and were developed in the 1980's with techniques based on Southern blotting (*Southern 2001*). These arrays were limited to the amount of DNA probes that could be bound to their surface and thus could only be used to examine a small number of genes. In 1995, DNA microarray technology was brought into the mainstream for most scientists after a publication in Science by Patrick Brown and colleagues. They used an automated method to print 45 *Arabidopsis thaliana* cDNAs onto a glass slide (*Schena et al. 1995*). DNA microarray technology expanded rapidly from these first models and progressed to the development of the current high-density microarrays which accommodate comprehensive transcriptome coverage. For example, the Affymetrix GeneChip®

Human Gene 2.0 ST Arrays used in this study have >30,000 coding transcripts and >11,000 long intergenic non-coding transcripts. They measure alternative splicing event/transcript variants and have probes designed to have maximum coverage of exons.

There are currently many different DNA microarray platforms commercially available, which differ in their fabrication and function (*Chon et al. 2011*; *Heller 2002*). The most common workflow associated with a DNA microarray experiment consists of RNA isolation from source tissue, conversion of RNA to cDNA (cDNA is more stable than RNA), labelling of cDNA, and hybridisation to the array. Arrays are then scanned using associated software and data is analysed (*Jayapal et al. 2006*). Key factors that should be considered when designing a microarray experiment include cost, number of replicates to be included, number and characteristics of samples from source material, and the questions that are to be answered by the data generated (*Jayapal et al. 2006*).

The study of gene expression using DNA microarrays has been used in a wide variety of different settings. It has been widely used in different aspects of cancer research including gene profiling of cancer types and subtypes, and biomarker discovery to aid prognosis, treatment and drug response. One of the first studies using DNA microarrays to have a major impact on cancer research was a study involving breast cancer (*Perou et al. 2000*). This study successfully distinguished between different classes of breast tumours and identified two new types of breast tumours that were overlooked by traditional classification methods. The authors also found expression patterns which were predictive of chemotherapy response. This was achieved by monitoring the expression of 8,102 different genes in 65 human breast tumour samples using DNA microarrays.

6.1.2 Gene expression analysis in ovarian cancer

Microarray technology has been widely used to help advance ovarian cancer research. The major areas investigated include identification of ovarian cancer subtypes, molecular profiling and biomarker discovery for early detection of ovarian cancer to aid prognosis, and as predicators of therapeutic response (*Chon et al. 2011*).

6.1.2.1 Molecular profiling and subtype identification

As ovarian cancer tumours are highly heterogeneous in nature the identification of different cancer types or subtypes becomes very useful. Different cancer subtypes have different characteristics, which may affect treatment and survival. Currently, in ovarian cancer, patients diagnosed broadly with ovarian cancer receive a standard

treatment regime depending on FIGO stage and previous exposure to platinum drugs (*Ozols 2005*). Molecular profiling of tumours has lead to better classification of tumour subtypes, which in turn allows for the customisation of treatments on a patient to patient basis. This can lead to an improved clinical outcome and response to therapy.

Molecular profiling has been very beneficial in the classification of ovarian cancer. Molecular signatures have been able to differentiate between normal ovarian tissue and ovarian carcinomas, between different histotypes of ovarian cancer, and have even identified a number of different subgroups within the serous ovarian carcinoma histotype (*Schwartz et al. 2002*; *Welsh et al. 2001*). It has been found that there are different signatures in gene expression that can separate high grade from low grade, and low malignant potential (LMP) serous ovarian tumours, suggesting that a tumour's genetic makeup could indicate its aggressiveness (*Bonome et al. 2005*; *Schwartz et al. 2002*). LMP tumours are distinct from high grade ovarian cancers, but have been shown to be similar to low-grade tumours (*Bonome et al. 2005*). This finding is strengthened by the evidence that high grade serous tumours are genetically distinct from low grade tumours, and are not simply a progression from low-grade to high grade phenotypes (*Singer et al. 2002*). Therefore, by targeting deregulated genes found in high-grade serous ovarian cancers, therapies may be developed that control disease progression. These examples show how gene profiling in ovarian cancer by microarray technology have advanced knowledge in ovarian cancer classification with beneficial results for ovarian cancer patients.

6.1.2.2 Biomarker for diagnosis and early detection

Correct diagnosis is essential for deploying the correct treatment strategy in cancer patients. This is because the tissue of origin is linked with standard treatments that are most effective for a particular cancer type. Cancer stage and grade can also effect treatment. Therefore, making a correct diagnosis of stage or grade is equally important. The use of diagnostic biomarkers can aid clinicians in making the correct diagnosis.

For example, in breast cancer, Mammaprint is a prognostic and predictive genetic profile that was developed in order to aid clinicians to accurately diagnose and treat the early stages of breast cancer (*van 't Veer et al. 2002*). Breast cancer patients that have the same stage, often have different treatment responses and overall outcome. The Mammaprint profile was designed to delineate between untreated patients who would benefit from endocrine treatment alone or with the addition of adjuvant chemotherapy. The profile was developed using DNA microarray data on 117 primary breast tumours. This test has since been approved by the FDA (*de Snoo et al. 2009*). Ovarian cancer

and colon cancer can also be difficult to distinguish between histologically. Gene signatures have been found using microarray technology, which can accurately separate the two pathologies. These pathologies have very different treatments (*Nishizuka et al. 2003*).

It has previously been discussed in chapter 1 (section 1.1.4), that ovarian cancer has a high mortality rate due to poor prognosis at an early stage. The discovery of diagnostic biomarkers by microarray studies has the potential to provide novel markers that could aid early detection and increase survival. HE4 is a promising serum biomarker that has been proposed to aid in ovarian cancer detection. Studies have shown that HE4 may be useful in combination with CA125 (routinely used) or in combination with other markers in a detection panel (*Moore et al. 2008*).

Prostasin is a potential prognostic biomarker that has stemmed from microarray experimentation (*Mok et al. 2001*).This study identified prostasin by comparing the genes expressed in three ovarian cancer cell lines to three normal human ovarian surface epithelial cell lines using microarrays. Prostasin gene expression was then tested in 64 patient serum samples with ovarian cancer and compared to 137 control samples and found to be up-regulated in the serum of ovarian cancer patients. It was found that the combination of prostasin and CA125 had a sensitivity of 92% and a specificity of 94% for ovarian cancer detection.

There has been a vast array of other proposed biomarkers from microarray studies, but relatively few have been investigated in large patient cohorts. Osteopontin is one such biomarker, which was discovered by microarray screening. It was further investigated and shown to be elevated in tissue and serum samples of cancer patients over healthy individuals. However, osteopontin only had 80.5% sensitivity in detecting early stage ovarian cancer (*Kim et al. 2002*; *Mok et al. 2001*; *Wong et al. 2001*). This is not sensitive enough for a standalone biomarker. Another example of a potential biomarker found by array technology is creatine kinase B, which is up-regulated in pre-operative patients with ovarian cancer compared to those with benign pelvic masses. It has been found to be significantly elevated in the sera of ovarian cancer patients, including those with stage 1 ovarian disease, compared to benign cases and normal controls (*Huddleston et al. 2005*). High grade stage 1 ovarian cancer has since been profiled using microarrays in order to discover early alterations in ovarian cancer pathogenesis (*Chien et al. 2009*). This was useful in order to find novel genes and pathways in ovarian cancer tissue that may drive carcinogenesis. These could be used as diagnostic biomarkers. Genes identified among the 285 differentially expressed genes comparing high grade stage one disease and borderline tumours, include FOLR3,

survivin, MCM3, SYNE1, AKAP14 and KNDC1. Pathways effected by these deregulated genes include cell-cycle regulation, cytoskeletal signalling, chromatin modification and inflammatory signalling (*Chien et al. 2009*).

However, proposed biomarkers have not had the prognostic power that clinician's have desired to date. Therefore, further studies are needed in this area with DNA microarrays providing an excellent platform for novel diagnostic biomarker discovery.

6.1.2.3 Biomarkers for prognosis, therapy and resistance

Microarrays can be used to generate gene signatures that will aid in cancer prognosis. This can facilitate clinicians in predicting outcomes that will help influence the selection of a specific therapy, which may be more beneficial to a particular patient subgroup. For example, some patients may not respond well a particular type of treatment and may be spared from undergoing harsh therapy, while other patients may generally have poor outcome to a treatment and a harsher therapy may be necessary. In many cases there is a lack of alternative treatment options. For this reason, clinicians turn to clinical trials for new therapies that stem from the examination of gene signatures. In ovarian cancer, this could mean deviation from the current standard carboplatin/taxol chemotherapy regime to other therapies with more favourable outcome for patients with specific gene signatures. Another application of gene signatures can be in the generation of biomarkers that are associated with the development of resistance. This gives us the opportunity to use these signatures to select adequate salvage chemotherapy. Using biomarker signatures in this way could improve response rates and overall survival in ovarian cancer patients. It could also help in the development of targeted treatments that circumvent the development of resistance.

One example of a study in ovarian cancer that provided prognostic biomarkers using microarrays was a study by *Spentzos et al. (2004),* who developed an Ovarian Cancer Prognostic Profile (OCPP) from 115 genes. There was a significant difference in survival between unfavourable and favourable groups when this profile was applied to the validation set of 34 patients. In the unfavourable group, genes associated with angiogenesis-related cytokines, tyrosine kinase receptors, and EMT were all over-expressed (*Spentzos et al. 2004*). Another study in ovarian cancer set out to discriminate between patients that have high risk of early recurrence after standard chemotherapy and those who were at a lower risk of recurrence (*Hartmann et al. 2005*). The team developed a 14 gene signature using cDNA microarrays containing 30,721 genes that could predict early recurrence at an accuracy of 86% with a 95% positive predictive value. Up-regulated genes included Protein kinase Cη, protein

tyrosine phosphatase receptor, and inhibitor of DNA binding 4. A number of studies have attempted to separate short term from long term survivors using gene profiles. One group has contributed substantially to this area of research using microarray technology (*Berchuck et al. 2005*; *Berchuck et al. 2009*). Not only were they able to generate a linear discriminate model that can distinguish between short and long-term survivors at 81% accuracy in late-stage ovarian cancer, but they noted that late-stage cancer with long-term survival shared signatures with most early-stage cancers in general. This data strengthens the view that aggressive and non-aggressive cancers arise separately and that there is a need to develop techniques to detect these virulent strains at an early stage (*Bonome et al. 2005*). The team also identified that the MAL gene, being the most de-regulated genes in their studies, was found to be a predictor of poor response.

Concerning the assessment of chemoresistance in ovarian cancer, a number of studies using microarrays have been undertaken examining gene signatures in this context. A small cohort study of 8 patients in 2004 used cDNA microarrays to generate signatures from chemo-naïve patients to try and predict their response to chemotherapy (*Selvanayagam et al. 2004*). Ovarian cancer patients received chemotherapy after surgery and were grouped according to chemotherapeutic response. The patients had different histological subtypes of ovarian cancer (serous, endometrial, clear cell and undifferentiated) and received platinum-based chemotherapy after surgery (carboplatin/taxol, cisplatin/taxol or cisplatin/cyclophosphamide). The team states that they were able to predict sensitivity or resistant outcome by applying a pattern-recognition algorithm to the gene signatures. Another study set out to identify genes that could predict platinum-chemotherapy resistance in ovarian cancer patients using a cohort of 96 primary specimens (*Helleman et al. 2006a*). 69 genes were differentially expressed between responders and non-responders, 9 of which were used to develop a signature that predicted platinum-resistance. This gene set had 89% sensitivity and 59% specificity in the validation set of 72 samples, which were better than predictions based on patient tumour characteristics. In order to better understand the platinum resistance phenotype, the evaluation of 14 cell lines in relation to their sensitivity/resistance to 4 different platinum drugs (carboplatin, cisplatin, oxaliplatin and AMD473) was carried out, which could ultimately contribute to novel drug development or specialized therapeutic regimes (*Roberts et al. 2005*). Using cDNA microarrays, Stat1 was identified as a positive predictive marker for cisplatin and AMD473 resistance. This study gave no overlap in gene signatures from the study by *Helleman*

et al. (2006a) above, which is likely to be due to the utilisation of cell lines in one study and tissue samples in the other (*Chon et al. 2011*).

As part of the Cancer Genome Atlas (TCGA) project, a gene signature was developed to predict outcomes in ovarian cancer patients (*The Cancer Genome Atlas Network 2011*). A 193 gene transcriptional signature was defined using an integrated expressional data set of 215 patient samples. 108 genes were correlated with poor survival and 85 genes were correlated with good survival, after univariate Cox regression analysis. This gene signature's predictive ability was tested on a set of 255 TCGA samples and on three independent expressional data sets. Kaplan Meier survival analysis indicated that this gene signature was significantly associated with survival in all of the validation sets tested.

More recently, a study set out to identify the major pathways and biomarkers associated with the development of intrinsic chemoresistance upon exposure to standard first-line carboplatin/taxol chemotherapy (*Koti et al. 2013*). A novel aspect of this study was that only ovarian cancer patients, who had an epithelial serous histotype, were included. Other studies have used a range of histologies, such as Selvanayagam et al. (2004), who had four different histologies in a patient cohort of eight individuals. For this common histotype, the team was able to identify a set of 204 differentially regulated genes that could separate resistant and sensitive groups. From this set of genes, pathway analysis revealed that the IGF1/PI3K/NFκB/ERK signalling networks were involved in resistance development of epithelial serous ovarian cancer.

Our research group has developed a gene expression profile using cDNA microarray technology that distinguishes between primary and recurrent serous ovarian cancer (*Laios et al. 2008b*). This signature contained 21 genes. 6 were up-regulated and 15 were down-regulated in recurrent, compared to primary, ovarian cancer. The data from this study puts forward an integrative model of recurrence in serous ovarian cancer where cells produce adhesion molecules and release cytokines, inflammatory mediators and growth factors during relapse. Adhesion molecules are used to regulate attachment, cytokines and inflammatory mediators to increase cell survival and growth factors bound to their associated receptors to induce proliferation. This is needed to help cells in transforming and conquering their surrounding environment.

In another study, our research group investigated the role of MyD88 and Toll-like receptor 4 (TLR4) as mediators of resistance in ovarian cancer and their possible utility as resistance biomarkers (*d'Adhemar et al. 2014*). Their expression was assessed by immunohistochemistry (IHC) in 198 paraffin-embedded ovarian cancer tissue samples.

In parallel, the expression of miR-21 and miR146a (known to regulate TLR4 and MyD88 expression) was assessed in the same samples and in a number of chemosensitive/resistant cancer cell lines. Functional analysis of the TLR4/MyD88 pathway was also analysed in the SKOV-3 ovarian cancer cell line. High expression of MyD88 was found to be significantly associated with reduced patient survival and found to be implicated in altered miRNA expression in tumours. Data also suggests that an intact and functioning TLR4/MyD88 pathway is required for cells to acquire chemoresistance in ovarian cancer. A reproducible method was devised as part of the study to assess MyD88 status by IHC. This has been optimised for cytological analysis of MyD88 in ascites fluid, which can assist ovarian cancer treatment in the future.

From the above evidence, gene expression signatures generated from microarrays have contributed significantly to the field of ovarian cancer treatment and therapy. However, more study is needed. More recently miRNAs as candidate biomarkers have been introduced to the field of cancer research. MiRNAs, which are post transcriptional regulators of gene expression, have shown to have promise as new cancer biomarkers and may play a role as biomarkers of resistance.

6.1.3 MiRNA expression analysis in ovarian cancer resistance

MiRNA expression has been linked to chemo-sensitivity and resistance in ovarian cancer. The *Sorrentino et al. (2008)* study endorses the use of miRNA profiling in the identification of resistant ovarian cancers cells. The team looked at one cisplatin and three taxol-resistant ovarian cancer cell lines. They found that MiR-30c, miR-130a and miR-335 were down-regulated in all resistant cell lines, pointing to significant involvement of these miRNAs in the development of chemo-resistance (*Sorrentino et al. 2008*). Downstream targeting has linked miR-130a to the activation of the M-CSF gene, which is known to confer resistance in ovarian cancer by enhancing invasiveness as a metastatic promoter and also acts as a marker for poor prognosis. In the same year, miR-214 up-regulation was linked to cell survival and cisplatin resistance in ovarian cancer. It was found that miR-214 targeted and down-regulated PTEN, a tumour suppressor gene. This caused the activation of the Akt pathway (*Yang et al. 2008a*).

27 miRNAs were linked to chemo-sensitivity in ovarian cancer through the study of *Boren et al. (2009)*, using cell line models. Of interest to our study, four miRNAs were differentially expressed in response to taxol treatment (3 up-regulated (miR-514, miR-126 and miR-99b) and one down-regulated (miR29c)). There were seven miRNAs differentially expressed with response to cisplatin chemotherapy (4 up-regulated (miR-

23b, miR-381, miR-340 and miR-520f) and three down-regulated (miR-331, miR-185 and miR-106a)) (*Boren et al. 2009*).

Another study carried out by *Eitan et al. (2009),* showed that increased expression of miR-23a, miR-27a, miR-30c, miR-199a-3p and let-7g, and decreased expression of miR-378 and miR-625, corresponded to resistance to platinum-based chemotherapy in ovarian cancer patients. This study also showed differential expression of 5 miRNA's that could be linked to different patterns in survival and recurrence-free survival. In particular, high expression miR-27a was linked with very poor prognosis (*Eitan et al. 2009*).

Other miRNAs recently found to be linked with cisplatin resistance in ovarian cancer include miR-125b, which targets Bak1. Down-regulation of Bak1 by miR-125b up-regulation results in the loss of apoptosis induced by cisplatin, leading to cisplatin resistance (*Kong et al. 2011*). MiR-376c has been shown to enhance cell survival by acting as a target for the activin receptor-like kinase 7 (ALK7). Over-expression of miR-376c inhibited cisplatin induced cell death, but use of an anti-miR-376c was shown to enhance the effects of cisplatin. As patients who responded well to chemotherapy had strong staining for ALK7 combined with low levels of miR-376c and patients who responded poorly had high miR-376c levels combined with low levels of ALK7 staining, it was deduced that mir-376 enhances chemo-resistance through the targeting of ALK7 (*Ye et al. 2011*).

Recently, miR-181a has been shown to promote TGF-β-mediated epithelial-to-mesenchymal transition by repression of the Smad7 protein. High expression of miR-181a was associated with shorter time to recurrence and poor outcome in ovarian cancer patients. Ectopic expression of miR-181a resulted in increased cellular survival, migration, invasion, platinum drug resistance and *in vivo* tumour burden and dissemination. Conversely, when miR-181a was inhibited by decoy vector suppression, the re-expression of Smad7 caused significant reversals of these phenotypes (*Parikh et al. 2014*).

Finally, a miRNA signature was investigated in relation to chemoresistance in ovarian cancer by examining tumour samples from 198 patients using miRNA arrays and qPCR in 2013 (*Vecchione et al. 2013*). Three miRNAs (miR-484, miR-642 and miR-217) were found to have the ability to predict chemoresistance to platinum/taxane chemotherapy in ovarian cancer in this set of ovarian tumour samples. Further analysis on miR-484 revealed its involvement in the regulation of the VEGFB and VEGFR2 pathways of angiogenesis. The authors conclude that these three miRNAs could classify response

to chemotherapy in a large multicenter cohort and that blocking VEGF via anti-VEGFA antibody may not be sufficient in improving survival in ovarian cancer patients without also blocking VEGFB signalling (*Vecchione et al. 2013*).

The above evidence shows that aberrant miRNA expression can cause the disruption of many cellular pathways, which are involved in conferring a resistant phenotype. Therefore, miRNAs have great potential as acting as novel biomarkers for ovarian cancer resistance. Further to this, two families of miRNAs have been identified as having a great influence on chemoresistance, which are discussed below.

6.1.3.1 The miR-200 family and resistance

The miR-200 family has been shown to be associated with treatment response to taxol containing chemotherapy regimes. This family is made up of five members that are found in two genomic clusters (miR-200a/b and miR-429 on chromosome 1 and miR-200c and miR-141 on chromosome 12).

Low expression of miR-200 family members, such as miR-200c, has been correlated to high βIII tubulin protein expression. High expression of βIII tubulin is a known mechanism of taxol resistance in ovarian cancer and is associated with poor prognosis, as discussed in section 1.6.2 (*Leskela et al. 2011*). Other studies that agree with this finding showed that increased miR200c expression was correlated with reduced βIII tubulin expression conferring taxol sensitivity (*Cochrane et al. 2010*; *Prislei et al. 2013*).

Expression studies from our group and others have found that aberrant expression levels of other family members are also correlated with ovarian cancer prognosis (*Gallagher et al. 2009*; *Iorio et al. 2007*; *Nam et al. 2008*; *Wyman et al. 2009*; *Yang et al. 2008a*). This family of miRNA could be used as biomarkers for response to taxol-based chemotherapy relapse and progression (*Leskela et al. 2011*).

6.1.3.2 The Let-7 family and resistance

The Let-7 family is made up of 10 mature miRNAs (let-7a-g/i, miR-98 and miR-202), which are spread over a number of clusters throughout the genome. Aberrant expression of these family members has been found to have a major involvement in chemoresistance. The majority of Let-7 family members act as tumour suppressors by inhibiting the translation of oncogenes, such as Myc, K-Ras and HMGA-2 and cell cycle regulators, such as cyclin D2, CDC25 and CDK6 (*Brueckner et al. 2007*; *Bussing et al. 2008*).

It has been found that patients who received platinum treatment in the absence of taxol, and who had high let-7a expression, showed better survival than those with low expression (*Lu et al. 2011*). Also, patients who received platinum therapy with taxol, who had low expression of let-7a, had better outcomes than those with high expression. This, and other results in the study, suggested that patients with low let-7a may benefit from taxol chemotherapy, while those with high expression may not (*Lu et al. 2011*). Also, low-expression of let-7b was found to be significantly associated with poor prognosis in serous ovarian cancer patients by microarray analysis (*Nam et al. 2008*).

Let-7i has been associated with the ability to predict chemotherapy responses. It was found by microarray analysis to be significantly reduced in expression in platinum-chemotherapy-resistant patients and was also significantly associated with shorter progression-free survival in advanced ovarian cancer patients. Loss of function and gain of function manipulations, through Let-7i inhibitors and retroviral over expression, showed that a reduction in Let-7i expression resulted in increased cisplatin resistance in ovarian and breast cancer cells (*Yang et al. 2008b*). More work on Let7i has led to the finding that a chimera containing MUC1 aptamer and Let-7i can be delivered into taxol resistant ovarian tumours cells. This releases Let7i, which re-sensitises the cells to the chemotherapy drug. This was tested on the OVCAR3 ovarian cancer cell line. It was found that Let7i specifically sensitised the role of taxol by inhibiting proliferation, inducing apoptosis and decreasing long-term survival. Therefore, this treatment, which releases Let7i into the cell, sensitizes the cells to taxol treatment (*Liu et al. 2012*).

Further evidence in relation to Let7 expression and prognosis lies with Lin28 and Lin28b, which are inhibitors of the Let-7 processing. High expression of these proteins, which will result in reduced expression of Let-7 family members, is correlated with shorter progression-free and overall survival (*Lu et al. 2009a*). Therefore, the Let-7 family is an important family of miRNAs in ovarian cancer resistance management. A number of different expression profile studies in ovarian cancer include the down-regulation of let-7 members in their aberrant expression profiles (*Dahiya et al. 2008*; *Iorio et al. 2007*; *Zhang et al. 2008a*).

6.1.3.3 Contributions by the Discovary consortium to miRNA resistance

The Discovary Consortium, that this project is involved with, has proposed miRNA models for molecular pathogenesis of recurrent ovarian cancer. Based on integrated transcriptome and miRNA analysis, down-regulation of miR-9 and up-regulation of miR-223 were found to have a potential role in recurrent ovarian cancer and could act as

biomarkers (*Laios et al. 2008a*). Both miRNAs were found to target the same pathways, including angiogenesis, Ras, integrin signalling and a pathway involving actin and tubulin. In this study, MiRNA sequencing has lead to the ability to clearly distinguish between primary and recurrent ovarian carcinomas. It was also found that Dicer, Drosha and eIF6 of the miRNA biosynthesis pathway did not seem to have a significant role in the aberrant expression of miRNA in recurrent ovarian cancer.

The consortium previously identified a number of targets that can differentiate between primary and recurrent ovarian cancer, using gene expression arrays. They found a total of 907 genes to be differentially expressed at $p < 0.01$, which was reduced to 182 genes using the more stringent false discover rate (FDR 0.1). Evidence from this study indicates that there is a multifactorial mechanism for recurrence and therefore there is a huge possibility that miRNAs can play a large role as regulators of gene expression (*Laios et al. 2008b*).

A summary of miRNAs that have been linked to chemotherapeutic resistance can be seen in Table 6.1.

Table 6.1 Overview of miRNAs associated with ovarian cancer chemoresistance.

This figure shows miRNAs identified from numerous studies. Some miRNAs were found to be up-regulated in one study, but down-regulated in another. In this case the expression state of the majority of associated studies is depicted. It gives high and low expression of miRNAs in ovarian cancer for chemotherapeutic resistant V's sensitive cases. This table was adapted from (*van Jaarsveld et al. 2010*). Other studies used in this thesis chapter were added in order to give a more comprehensive and up to date overview of miRNAs associated with chemotherapeutic resistance in ovarian cancer in tissue and cell line studies.

Agent	High Expression			Low Expression		
Platinum	Let-7g[1]	Pre-125b[3]	miR-340[2]	Let-7i[4]	Pre-107[3]	miR-331[2]
	miR-1b-1[4]	miR-152[4]	miR-376c[7]	pre-23a[3]	miR-130a[3]	miR-335[3]
	miR-22[4]	miR-181a[10]	miR-370[4]	pre-26a[3]	miR-130b[3]	miR-378[1]
	miR-23a[1]	miR-196a[4]	miR-381[2]	pre-29c[3]	miR-185[2]	miR-509[4]
	miR-23b[2]	miR-198[4]	miR-519e[4]	miR-30c[1]	pre-199a-2[3]	miR-625[1]
	miR-27a[1]	miR-199a-3p[1]	miR-520e[4]	pre-93[3]	pre-204[3]	
	miR-30c[1]	miR-214[4]	miR-520f[2]	pre-106[3]	pre-218[3]	
	miR-125b[6]	miR-216[4]	miR-521[4]	miR-106a[2,3]	miR-321[4]	
Taxol	Let-7a[5]	pre-197[3]		pre-10a[3]	miR-30c[3]	miR-130b[3]
	Let-7e[3]	miR-321[3]		pre-19b[3]	pre-92[3]	pre-137[3]
	miR-21[3]	miR-514[2]		pre-20[3]	pre-106[3]	miR-200c[8]
	pre-23b[3]			miR-20b[3]	pre-125a[3]	pre-204[3]
	miR-99b[2]			pre-26a[3]	pre-125b[3]	pre-218[3]
	miR-126[2]			miR-29c[2]	miR-130a[3]	miR-335[3]
Docetaxel	miR-99b[2]	miR-502[2]	miR-515-5p[2]			
	miR-371[2]	miR-514[2]	miR-518c-AS[2]			
Platinum/Taxane	miR-27a[1]			miR-9[11]	miR-217[9]	miR-484[9]
	miR-223[11]			miR-23a[1]	miR-378[1,2]	miR642[9]

1.(*Eitan et al. 2009*), 2.(*Boren et al. 2009*), 3.(*Sorrentino et al. 2008*), 4.(*Yang et al. 2008b*), 5.(*Lu et al. 2011*), 6.(*Kong et al. 2011*), 7.(*Ye et al. 2011*), 8.(*Leskela et al. 2011*), 9.(*Vecchione et al. 2013*), 10.(*Parikh et al. 2014*), 11.(*Laios et al. 2008a*).

6.1.4 Aims and objectives

This chapter examined the transcriptomic profiles of our carboplatin and taxol-resistant ovarian cancer sublines UPN251-7C and UPN251-7T, resistant to each agent respectively. The cell lines were subjected to mRNA and miRNA profiling in order to produce a combined signature of resistance for each chemotherapeutic agent. Gene and miRNA biomarkers discovered from this work were validated using qPCR in clinical samples (Chapter 7).

6.1.4.1 Hypotheses

The hypotheses examined in this chapter stated that:

- There exists a mRNA/miRNA signature for carboplatin and taxol resistance that can differentiate between chemoresistant and chemosensitive epithelial serous ovarian cancer.
- This signature can be used to identify key biomarkers that can be used in the prognosis and treatment of ovarian cancer patients and in the development of novel targeted therapies.

6.1.4.2 Objectives

This chapter aimed to produce mRNA/miRNA signatures for carboplatin and taxol resistance, derived from our resistant sub-lines of UPN251, produced in chapter 4. We aimed to identify biomarkers and pathways that could be linked to the development of carboplatin and taxol resistance in ovarian cancer, which will aid clinical diagnosis and contribute to the development of novel targeted therapies to circumvent resistance development in ovarian cancer.

6.2 Methods

6.2.1 Sample selection for Affymetrix analysis

UPN251-7C was selected as a model of carboplatin-resistant ovarian cancer and UPN251-7T was selected as a model of taxol-resistant ovarian cancer, based on the results found in chapter 4 and 5. These cell lines were the most resistant to carboplatin and taxol respectively and served as a good model for further evaluation. UPN251 parental cells were used as non-resistant control cells. All cell lines had drug treated and non-drug treated cells analyses for expression. The inclusion of drug treated cell lines allowed us to examine differences in drug response across the resistant cell lines and non-resistant parental cells. 24 arrays for both gene and miRNA expression were

processed in total. The same samples were used on both array platforms so that the data generated from each platform would be consistent and complement each other. Gene expression and miRNA expression are linked as miRNAs are post transcriptional regulators of gene expression (*Lewis et al. 2005*). This should be reflected in the expression profiles generated by both platforms. Three biological replicates were run for each condition listed below on each platform:

1. UPN251 (untreated)
2. UPN251_C (carboplatin treated (2µg/ml))
3. UPN251_TL (low dose taxol treated (15ng/ml))
4. UPN251-7C (untreated)
5. UPN251-7C_C (carboplatin treated (2ug/ml))
6. UPN251-7T (untreated)
7. UPN251-7T_TL (low dose taxol treated (15ng/ml))
8. UPN251-7T_TH (high dose taxol treated (60ng/ml))

The doses of carboplatin used were the same as in the selection strategy. However, a lower dose of taxol was used on UPN251 parental cells, as the selecting dose caused a high percentage of cell death during cell pellet harvesting. This was necessary in our selection strategy to drive selection of resistant cells. However, not enough cells survived in order to be able to extract a suitable amount of RNA in this case. Therefore, the low dose refers to the modified lower dose given to the cells to allow adequate survival for RNA extraction and the high dose refers to the dose given in the selection strategy.

6.2.2 Sample preparation for Affymetrix platform

Cells were pelleted and total RNA was extracted using the miRNeasy mini kit, as described in chapter 2. RNA yield was measured using a traditional spectrometer (BioPhotometer (Eppendorf, Germany)) at 260nm and RNA quality and integrity was assessed using the Agilent 2100 Bioanalyzer as described in chapter 2. Samples were then prepped for both gene and miRNA expression platforms, as per the Affymetrix gene expression analysis protocol and the Affymetrix miRNA expression analysis protocol described in chapter 2. Arrays were run for 3 biological replicates for each condition on each platform. The data was then analysed using the Expression consol software (Affymetrix, USA).

6.2.3 Quality control analysis for the Affymetrix platform

The mRNA arrays tested were examined using quality control methods that are outlined in the 'quality assessment white paper', downloadable from http://media.affymetrix.com/support/technical/whitepapers/exon_gene_arrays_qa_whitepaper.pdf, as part of the Affymetrix GeneChip® Gene and Exon Array Whitepaper Collection (*Affymetrix 2007*). The miRNA arrays tested were examined using FlashTag™ Biotin HSR RNA Labelling Kit manual. The arrays were visually inspected for uniform intensity and for correct alignment. Other quality control aspects were addressed using algorithms outlined in the 'quality assessment white paper' and FlashTag™ Biotin HSR RNA Labelling Kit manual. mRNA array metrics were analysed at three levels; probe level, probe set summarisations, and individual probe level. Also, three types of metrics were used in mRNA quality control; sample metrics, hybridisation metrics and labelling metrics. Some of these metrics had overlap with the miRNA array metrics as indicated below. MiRNA arrays also had specific quality control aspects, which will be discussed below.

6.2.3.1 Probe level metrics

I) pm_mean (mRNA/miRNA): This is the mean value of all the raw intensities from each PM probe on the array before any transformations of intensity occurs. This value was used to determine if certain chips were unusually dim or bright, which may affect other analysis parameters (e.g., unusually high median absolute deviations of residuals).

6.2.3.2 Probe set summarisations metrics

II) pos_vs_neg_auc (mRNA): This is the area under the curve (AUC) for a receiver operating characteristic plot, which compares the signal value of the positive controls to the signal value of the negative controls. It measured how well the probe set could distinguish between the signal from a positive control and negative control, assuming that negative controls are false positive and positive controls are true positives. An AUC of 1 translated as perfect separation of signals, while an AUC of 0.5 indicated no separation whatsoever. Typically, the analysis would return values of between 0.8-0.9, if separation of signal was adequate.

III) x_mean (mRNA): This is the mean signal value for all the probe sets analysed from category 'X'.

IV) x_mad_residual_mean (mRNA): This is the mean of the absolute deviation of the residuals from the median for all probe sets analysed from category 'X'. On a single

chip, different probes will return different intensities when hybridised to a common target. RMA and PLIER algorithms create models which account for individual feature responses. These models could be used to identify problematic chips by identifying whether a large number of probes were behaving differently or not. They looked at the difference between the actual value and the predicted value (the residual) for the intensity of given probes. If the residual for a given probe was very different to the median, then it gave a poor fit to the model. Calculating the mean of the absolute values of all the deviations produced, measured how well the probes on a given chip fitted the model. Unusually high mean absolute deviation of the residuals from the mean indicated problematic data for the chip.

V) x_rle_mean (mRNA/miRNA): This is the mean absolute relative log expression for all the probe sets analysed from category 'X'. It used the signal estimate from the probe set on a single chip and calculated the difference from the median signal of that probe set across all of the chips in the study. This was expected to be low in order to reflect low biological variability between samples.

6.2.3.3 Individual probe level metrics

VI) all_probeset (mRNA): This is all the probe sets analysed. It included the vast majority of the probe sets that would be used in downstream statistical analysis and represented the quality of the data most highly.

VII) bac_spike (mRNA/miRNA): This is the set of probe sets that hybridise to the pre-labelled bacterial spike controls (BioB, BioC, BioD and Cre). It was used to asses if the hybridisation of probes to the chip had worked adequately. There would be inherently more variability compared to other metrics due to the limited amount of spikes and probe sets.

VIII) polya_spike (mRNA): This is the set of polyadenylated RNA spikes (Lys, Phe, Thr and Dap). It was used to access problems with the target preparation. There would also be more variability compared to other metrics due to the limited amount of spikes and probe sets.

IX) neg_control (mRNA): This is the set of putative intron based probe sets from putative housekeeping genes. These four-probe probe sets were designed from intronic regions of probe sets, which were shown to have constitutive expression over many samples on 3'IVT arrays. They were used to calculate the false positive rate for the pos_vs_neg_auc metric.

X) pos_control (mRNA): This is the set of putative exon based probe sets from putative housekeeping genes. These four-probe probe sets were designed from exonic regions of probe sets, which were shown to have constitutive expression over many samples on 3'IVT arrays. They were used to calculate the true positive rate for the pos_vs_neg_auc metric. This category and the all_probset category most closely reflected the overall quality of the entire experiment including RNA, target prep, chip, hybridisation, scanning and gridding. They also reflected the quality of the data that was used in downstream statistical analysis.

6.2.3.4 MiRNA array specific probe metrics

Spike-in control probe sets indicate whether the FlashTag™ Biotin HSR RNA Labelling Kit was carried out successfully. The spike-in control probe sets were representative of synthetic miRNAs, which were present in vial 8 of the kit. They should have a signal >=1000 (<=9.96 for log2 signal). Spike_in control-2_st and Spike_in control-29_st were an indication of successful poly(A) tailing and ligation. Spike_in control-31_st is poly(A) RNA and indicated successful ligation. Spike_in control-36_st is poly(dA) DNA and indicated successful ligation and lack of RNases in the RNA sample.

6.2.4 Affymetrix gene and miRNA array data analysis

Bioconductor software libraries (www.bioconductor.org) were used in the analysis and comparisons of array data. Bioconductor is a highly active, open source and open developmental resource, which provides effective tools for the analysis and understanding of high-throughput genomic data. It is a collaborative project that provides a vast quantity of different packages, which are written in the R statistical programming language. One such package, the 'oligo' package (*Carvalho et al. 2010*), was used to import Affymetrix CEL file data. This data was then used to compute robust multichip average (RMA) expression values (*Bolstad et al. 2003*; *Irizarry et al. 2003a*; *Irizarry et al. 2003b*). This value was generated from a three step process, namely; background adjustment, quantile normalisation and summarisation. The 'made4' package was used for visualisation of RMA expression values (*Culhane et al. 2005*) and RankProd was used to identify expressional differences between gene chips (*Breitling et al. 2004*).

6.2.4.1 RMA method

The RMA method is a log scale linear additive model that removes background intensities and normalises probe level data across all the arrays (*Bolstad et al. 2003*; *Irizarry et al. 2003a*; *Irizarry et al. 2003b*). The background adjustment was used to

remove noise from the analysis and the data normalisation was used to allow comparisons to be taken between chips by correcting for differences in expression levels within and between chips. The RMA method used Turkey's median polish during data normalisation to estimate expression values, which were log base 2 transformed. Quantile normalisation corrects for any array biases introduced to the study by comparing expression levels between arrays for various quantiles. The process makes the distribution of probe intensities the same for each array, across a set of arrays. It removed variation that had been introduced to the study from sample preparation etc., without removing true variation between biological samples (*Irizarry et al. 2003b*). Summarisation was an important step in the RMA process, as each gene represented on each gene chip had a median of 21 probes associated with it. The summarisation step summarised the probe intensities for each probe set.

Some advantages associated with the RMA algorithm are that it is more precise, consistent and has a higher specificity than other models (*Irizarry et al. 2003a*). It generally produces smaller standard deviations for genes with low expression, while efficiently detecting differentially expressed probe sets (*Irizarry et al. 2003b*).

6.2.4.2 Differential gene and miRNA expression analysis

Differential expression analysis across the arrays was carried out using RankProd (*Breitling et al. 2004*). This software is a non-parametric statistical method used to identify significantly de-regulated probes. Its analysis is based on the calculation of rank products and estimation of false predictions. Its performance is superior to other platforms in cases where datasets have low numbers of samples or have a high level of noise (*Jeffery et al. 2006*). The software identified de-regulated genes as those with a fold-change in expression value of 2.0 or more, having a p-value of <0.05, adjusted for multiple testing. An adjusted p-value was used in this study to eliminate family-wise error rate (FWER). Ordinarily, a p-value will have five false positive predictions in every 100 predictions made. This is quite acceptable for small scale experiments, but in large scale experiments, such as microarray experiments, this will give an inflated false positive rate known as FWER. The Benjamini and Hochberg method of false-discovery rate (FDR) was used in this study to control FWER (*Benjamini et al. 1995*). This method accounted for the presence of errors and the number of errors made, defined as 'the expected proportion of errors among the rejected hypotheses'.

6.2.4.3 Analysis of target gene and miRNA lists

Genes and miRNAs that had a fold-change of 2 or more with an adjusted p-value (FDR<0.05) were deemed as significantly de-regulated. 10 different comparisons were generated in total and analysed for both genes and miRNAs;

A). UPN251 (untreated) v UPN251-7C (untreated)

This comparison identified stable changes in gene/miRNA expression that had occurred after the development of carboplatin resistance. This was achieved by comparing the de-regulated expression profiles of our carboplatin-resistant subline UPN251-7C to its parental cell line UPN251.

B). UPN251_C (2µg/ml carboplatin) v UPN251-7C_C (2µg/ml carboplatin)

This comparison investigated the stable changes of gene/miRNA expression that occurred between a carboplatin-resistant cell line and a non-carboplatin-resistant cell line when exposed to carboplatin treatment. This was achieved by comparing the de-regulated expression profiles of our carboplatin-resistant subline UPN251-7C to its parental cell line UPN251 after both were treated with a dose of 2µg/ml carboplatin for three days.

C). UPN251 (untreated) v UPN251-7T (untreated)

This comparison identified stable changes in gene/miRNA expression that had occurred after the development of taxol resistance. This was achieved by comparing the de-regulated expression profiles of our taxol-resistant subline UPN251-7T to its parental cell line UPN251.

D). UPN251_TL (15ng/ml taxol (low dose)) v UPN251-7T_TL (15ng/ml taxol (low dose))

This comparison investigated the stable changes of gene/miRNA expression that occurred between a taxol-resistant cell line and a non-taxol-resistant cell line when exposed to low dose taxol treatment. This was achieved by comparing the de-regulated expression profiles of our taxol-resistant subline UPN251-7T to its parental cell line UPN251 after both were treated with a dose of 15ng/ml taxol for three days.

E). UPN251_TL (15ng/ml taxol (low dose)) v UPN251-7T_TH (60ng/ml taxol (high dose))

This comparison investigated the stable changes of gene/miRNA expression that occurred between a taxol-resistant cell line and a non-taxol-resistant cell

line when exposed to high dose taxol treatment. This was achieved by comparing the de-regulated expression profiles of our taxol-resistant subline UPN251-7T to its parental cell line UPN251 treated with a dose of 60 and 15ng/ml taxol respectively for three days.

F). UPN251 (untreated) v UPN251_C (2µg/ml carboplatin)

This comparison identified the initial changes in gene/miRNA expression that took place when a non-carboplatin-resistant cell line was treated with carboplatin. This was achieved by comparing the de-regulated expression profiles of non-carboplatin-resistant cell line UPN251 to UPN251, when treated with 2µg/ml carboplatin for three days.

G). UPN251-7C (untreated) v UPN251-7C_C (2µg/ml carboplatin)

This comparison identified the initial changes in gene/miRNA expression that took place when a carboplatin-resistant cell line was treated with carboplatin. This was achieved by comparing the de-regulated expression profiles of the carboplatin resistant cell line UPN251-7C to UPN251-7C when treated with 2µg/ml carboplatin for three days.

H). UPN251 (untreated) v UPN251_TL (15ng/ml taxol (low dose))

This comparison identified the initial changes in gene/miRNA expression that took place when a non-taxol-resistant cell line was treated with taxol. This was achieved by comparing the de-regulated expression profiles of non-taxol-resistant cell line UPN251 to UPN251 when treated with 15ng/ml taxol for three days.

I). UPN251-7T (untreated) v UPN251-7T_TL (15ng/ml taxol (low dose))

This comparison identified the initial changes in gene/miRNA expression that took place when a taxol-resistant cell line was treated with low dose taxol. This was achieved by comparing the de-regulated expression profiles of the taxol resistant cell line UPN251-7T to UPN251-7T when treated with 15ng/ml taxol for three days.

J). UPN251-7T (untreated) v UPN251-7T_TL (60ng/ml taxol (high dose))

This comparison identified the initial changes in gene/miRNA expression that took place when a taxol-resistant cell line was treated with high dose taxol. This was achieved by comparing the de-regulated expression profiles of the taxol resistant cell line UPN251-7T to UPN251-7T when treated with 60ng/ml taxol for three days.

Furthermore, the following investigations were made between comparisons;

A v C – Examined which probes had de-regulation in the same and opposite directions between carboplatin-resistant cell lines compared to non-resistant parental cells and taxol-resistant cell lines compared to non-resistant parental cells. This investigation examined the differences and similarities in the gene/miRNAs that were deregulated in carboplatin and taxol resistance development.

B v D – Examined which probes had de-regulation in the same and opposite directions between carboplatin-resistant cell lines compared to non-resistant parental cells when both were treated with carboplatin and taxol-resistant cell lines compared to non-resistant parental cells when both were treated with taxol. This investigation examined the differences and similarities in the gene/miRNAs that were deregulated in response to carboplatin/taxol exposure in carboplatin and taxol resistance development.

A v F – Examined which probes had de-regulation in the same and opposite directions between cell lines that had carboplatin resistance compared to those that were carboplatin sensitive and non-carboplatin-resistant cells treated with carboplatin compared to treatment naïve cells. This investigation examined the differences and similarities in the gene/miRNAs that were deregulated in initial carboplatin response and carboplatin resistance development.

C v H – Examined which probes had de-regulation in the same and opposite directions between cell lines that had taxol resistance compared to those that didn't and non-taxol-resistant cells treated with taxol compared to treatment naïve cells. This investigation examined the differences and similarities in the gene/miRNAs that were deregulated in initial taxol response and taxol resistance development.

Genes/miRNAs that were deregulated in the same direction may indicate a common mechanism of resistance between platinums and taxanes and genes/miRNAs that were deregulated in the opposite direction may indicate their involvement in the inverse resistance relationship (Chapter 1, section 1.7.3).

The top five up and down-regulated genes and miRNAs were examined from each list. Gene annotation database DAVID (Database for Annotation, Visualization and Integrated Discovery) v6.7 was used for pathway analysis of de-regulated gene lists (*Huang et al. 2008*; *Huang et al. 2009*). DAVID provides a comprehensive set of annotation tools to allow researchers to gain biological understanding from large gene lists. It is capable of discovering enriched functionally related gene groups and visualising them on KEGG pathways. It can also list interacting proteins, explore gene names in batch, link gene-disease associations and redirect users to related literature,

to name a few useful functionalities. Another useful aspect of this database for our study was its pre-built Affymetrix chip background that allowed for improved gene list comparisons for this format. Individual gene and miRNA function and relevance was further analysed using PubMed literature searches.

6.2.4.3.1 MiRNA-Target interactions (MTIs) analysis

Genes and miRNAs shown to be significantly de-regulated were selected for further analysis in order to determine possible miRNA-Target Interactions (MTIs) between miRNA and gene lists of the same comparison. Several MTI databases exist for this purpose; MiRTarBase (*Hsu et al. 2014*), miRecords (Henry et al. 2014) and miRWalk (*Dweep et al. 2011*). These databases provide references for MTIs that have been validated experimentally via Western blot, reporter assay, microarray, and next generation sequencing experiments. MirRecords, miRWalk and other databases (miRTar (Lu et al. 2009b), Targetscan (*Garcia et al. 2011; Grimson et al. 2007; Lewis et al. 2005*) and starBase (*Li et al. 2014a*; *Yang et al. 2011*)) provide lists of MTIs that have been computationally predicted, using in-house software or by assembling lists of results from third party MTI prediction tools.

The expression levels of significantly de-regulated miRNAs and potential target genes across all the samples were examined by pair-wise Pearson correlation analysis. This correlation estimated the strength and direction of a linear relationship between two replicate groups. Therefore, the miRNA-gene pairs that had a negative Pearson correlation coefficient (r) were chosen to potentially interact. The strength of the interaction between each pair was indicated by the correlation coefficient. A direct indication of the strength in a relationship between interacting pairs was achieved by squaring the coefficient (r^2). The closer the r^2 value is to 1 the stronger the predicted interaction will be.

Following this, a number of MTI databases were interrogated for further evidence supporting a pair's interaction. Evidence of an MTI was accepted if the MTI has been experimentally validated (present in at least one of the above experimentally validated databases) or has been reliably computationally predicted (present in all of the computationally predicted databases above).

The results from this analysis were outlined in the form of network images and tables for each comparison (A-J). It must be noted that MTIs are not mutually exclusive. One miRNA can target multiple genes and one gene can also be targeted by multiple miRNAs. For this reason, a connected network of interactions is the best way to view MTIs.

6.3 Results - Affymetrix quality control and general clustering analysis

After the results of quality control and general clustering analysis, the results and discussion were combined under the following headings for clarity:

- Carboplatin resistance biomarker discovery
- Taxol resistance biomarker discovery
- First response biomarker discovery
- Comparisons of de-regulation between datasets

6.3.1 Array quality control

The quality control analysis for the mRNA and miRNA arrays involved carrying out a visual inspection and assessing different probe metrics described in section 6.2.3.

6.3.1.1 Visual quality control

All arrays, with the exception of one, passed the initial visual inspection. This involved checking for scratches on the surface or any 'patchy' staining or regions of unusually high or low intensity of staining. UPN251-7T_TH2 (mRNA array) had a dim region that was not noted on any of the other 23 gene array chips. Sample preparation was repeated for this sample and the chip was then re-run. Initial visual inspection was then passed on all 48 array chips. Further visual inspection involved examining the expression of the B2 oligo positive control (See Figure 6.1). This control oligonucleotide hybridised to specific locations on the chips. Checkerboard corners should be visible at each corner of the chip and at the corners of each internal grid. This ensured that the chip was correctly aligned. All chips passed this inspection process.

6.3.1.2 Probe metric quality control

Probe metrics were used to compute summary statistics for each array in a set and all of the arrays together. This allowed for the identification of outlier arrays which could skew downstream data analysis.

6.3.1.2.1 MRNA array probe metrics

There was a low level of variation across all metrics examined. A graph of the allprobesets_mad_residual_mean, allprobesets_rle_mean and pos_vs_neg_auc was created to examine whether there was similar expression of probesets across the

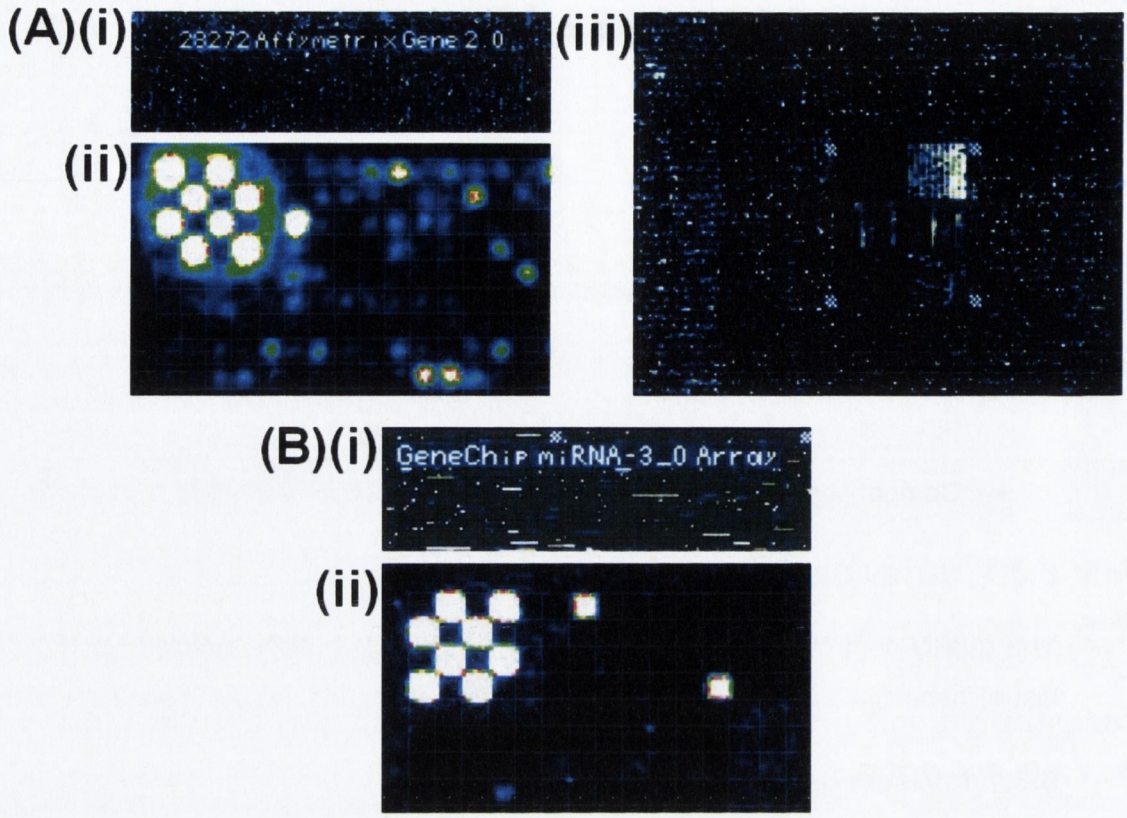

Figure 6.1 Visual quality control for HuGene 2.0 and miRNA-3.0 array chips.

(A) HuGene 2.0 (i) Array chip name (ii) Typical result for B2 oligo control expression of checker board corner on a gene chip (iii) Typical result of successful hybridisation of spike in controls (seen towards the centre of the gene chip). (B) miRNA-3.0 array (i) Array chip name (ii) Typical result for B2 oligo control expression of checker board corner on a miRNA chip.

The intensity of B2 oligo controls were examined in regions within the chips, at the edges of the chips and in checkerboard corners to ensure proper alignment of the chips grid and probes

arrays (Figure 6.2). The pos_vs_neg_auc value was between 0.8 and 0.9. This is a typical value that indicates adequate separation of positive and negative control signals across the arrays. The allprobesets_mad_residual_mean and allprobesets_rle_mean gave similar values across the datasets and did not indicate any outlier data. Box plots of the relative log expression (RLE) values were then generated (Figure 6.3). The median RLE value for all arrays varied closely around 0, indicating that there was no skewed data present following normalisation. The pm_mean was graphed (Figure 6.4) and also showed no outliers. The mean probe level intensity was similar across all arrays and indicated no source of skew for downstream analysis. At an individual probe level, the mean absolute deviations of residuals for the poly A spikes, positive control and back spikes were very similar across all arrays (Figure 6.5). This indicated that

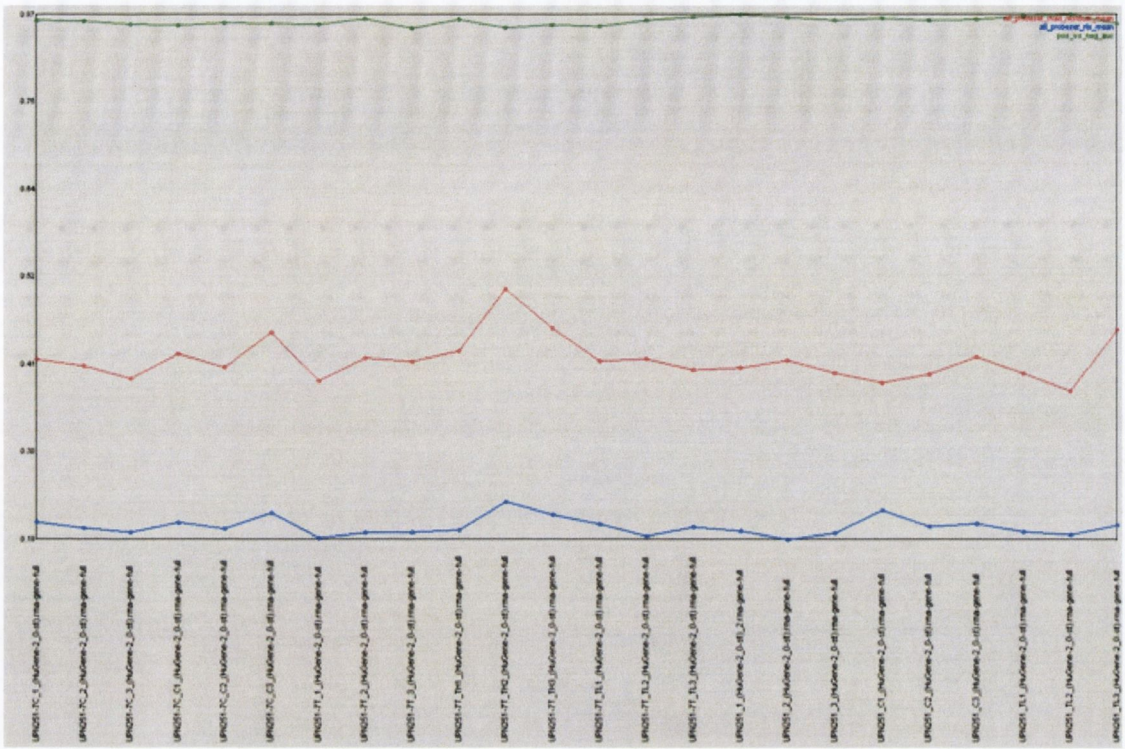

Figure 6.2 Probe summarisation quality control metrics.

pos_vs_neg_auc is given by the green line. This lies between 0.8 and 0.9 indicating good separation of positive and negative signals across the arrays. The allprobesets_mad_residual_mean (red) and allprobesets_rle_mean (blue) gave minimal variation between arrays indicating no outlying datasets.

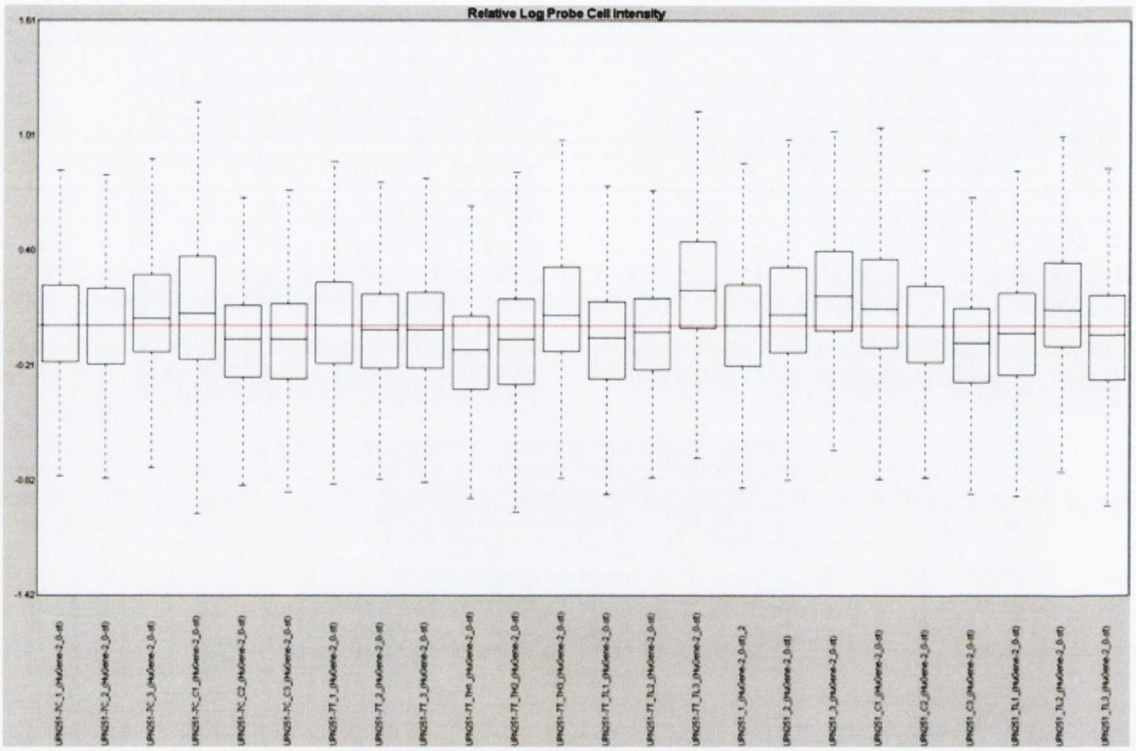

Figure 6.3 Box plots of the relative log expression values (mRNA arrays).

The mean absolute RLE is proportional to the width of the box plots. The middle bar of each box plot is the median RLE. The red line represents an RLE value of 0. As all median RLE values are close to 0 no outliers could be identified.

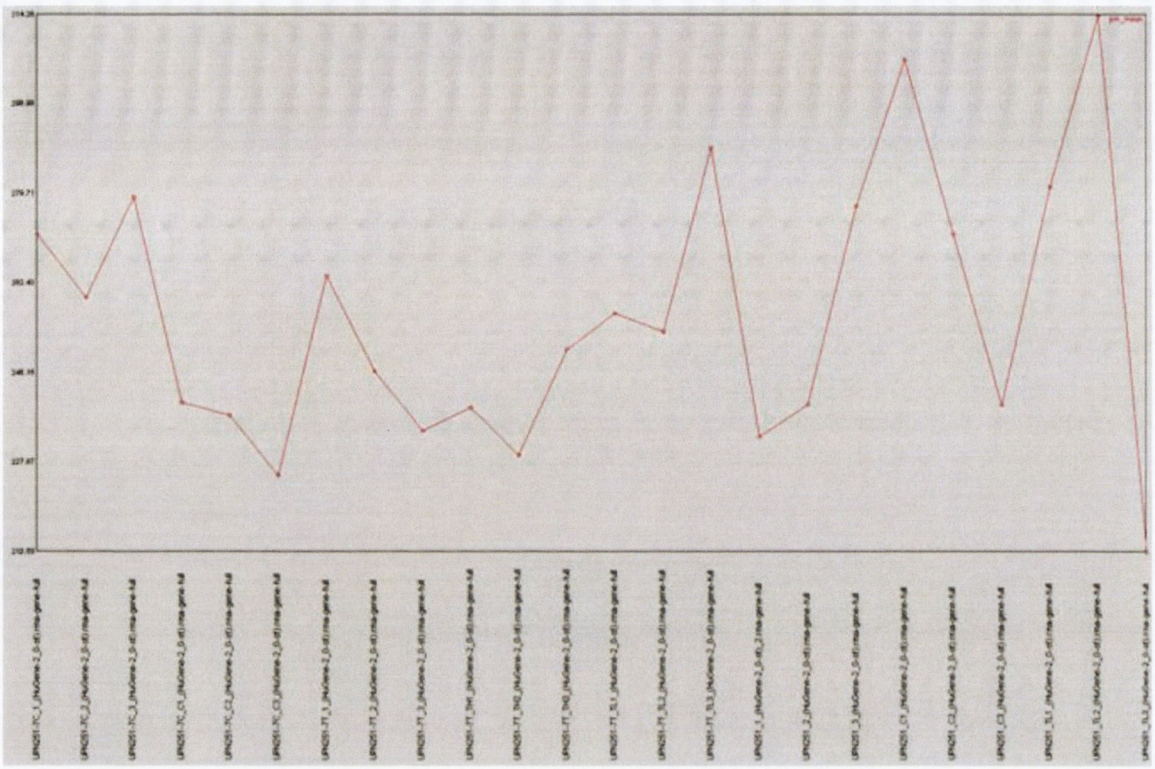

Figure 6.4 Probe level quality control metrics (mRNA).

The red line (pm_mean) indicates the mean probe level intensity prior to normalisation or background correction. This is used to indicate unusually dim or bright areas on a chip. As little variation occurs there is no indication that there are no abnormal values of pm_mean skewing the data.

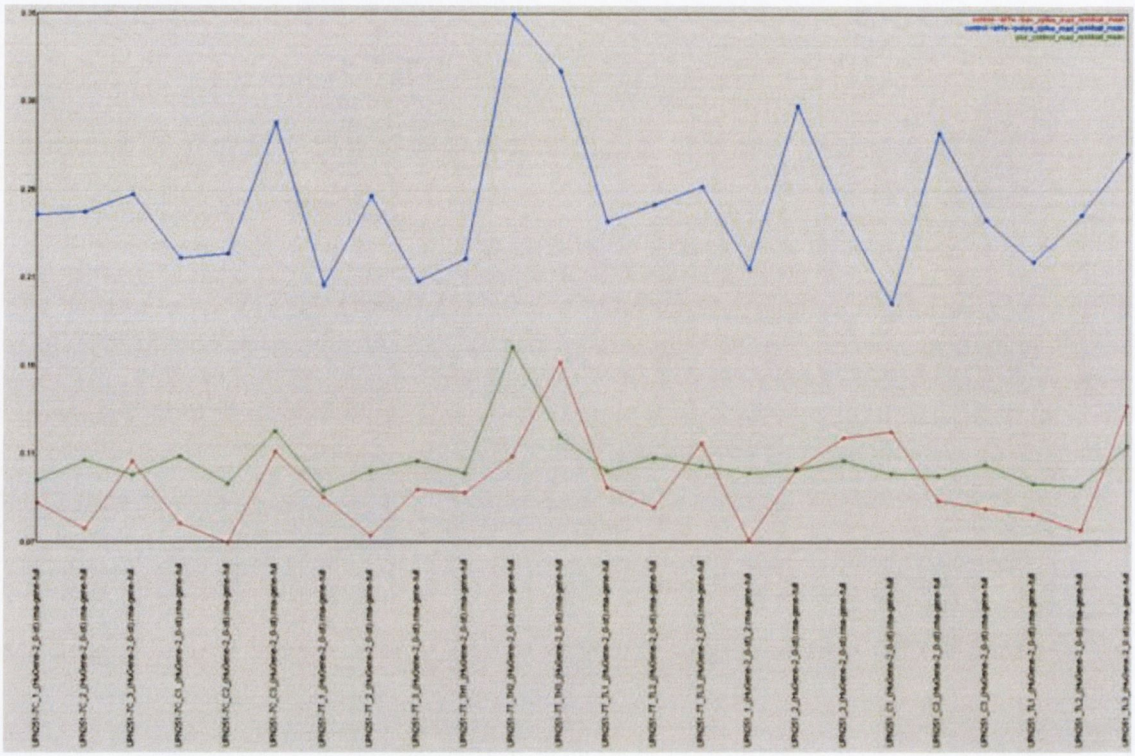

Figure 6.5 Individual probe level metrics.

Mean absolute deviations of residuals for the poly A spikes (blue), positive control (green) and bac spikes (red) were similar across all arrays. This indicates successful sample preparation and hybridisation.

there were no issues with the target preparation or hybridisation. Also, the hybridisation control probes appeared in the expected rank order in relation to their respective concentrations (Figure 6.6). This gave further assurance that there were no problems with sample preparation. Overall, from examining the quality control metrics, it could be confirmed that the mRNA array experiments were successful and that there were no outlier arrays that could cause skewed data analysis.

6.3.1.2.2 MiRNA array probe metrics

There was a low level of variation across all metrics examined. A box plot graph of the RLE is shown in Figure 6.7. The median RLE value for all arrays varied closely around 0, indicating that there was no skewed data present following normalisation. The pm_mean was graphed (Figure 6.8) and also showed no outliers. The mean probe level intensity was similar across all arrays with a small spread and indicated no source of skew for downstream analysis. The hybridisation control probes appeared in the expected rank order in relation to their respective concentrations (Figure 6.9). This gave assurances that there were no problems with sample preparation.

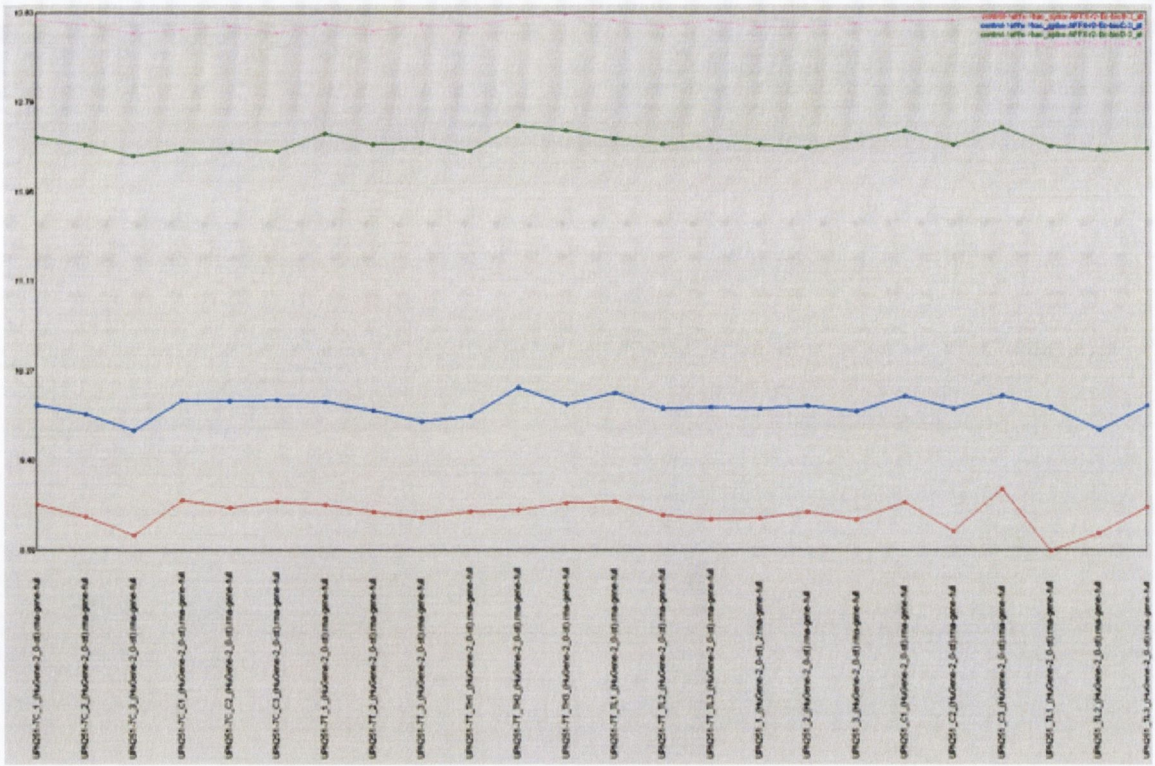

Figure 6.6 Rank order of bac spike controls.

The rank order of bac spikes controls gave good separation in the expected rank order as was expected from their relative concentration (BioB (red) < BioC (blue), BioD (green) and Cre (pink)). This strengthens evidence that there were no issues with the sample preparation.

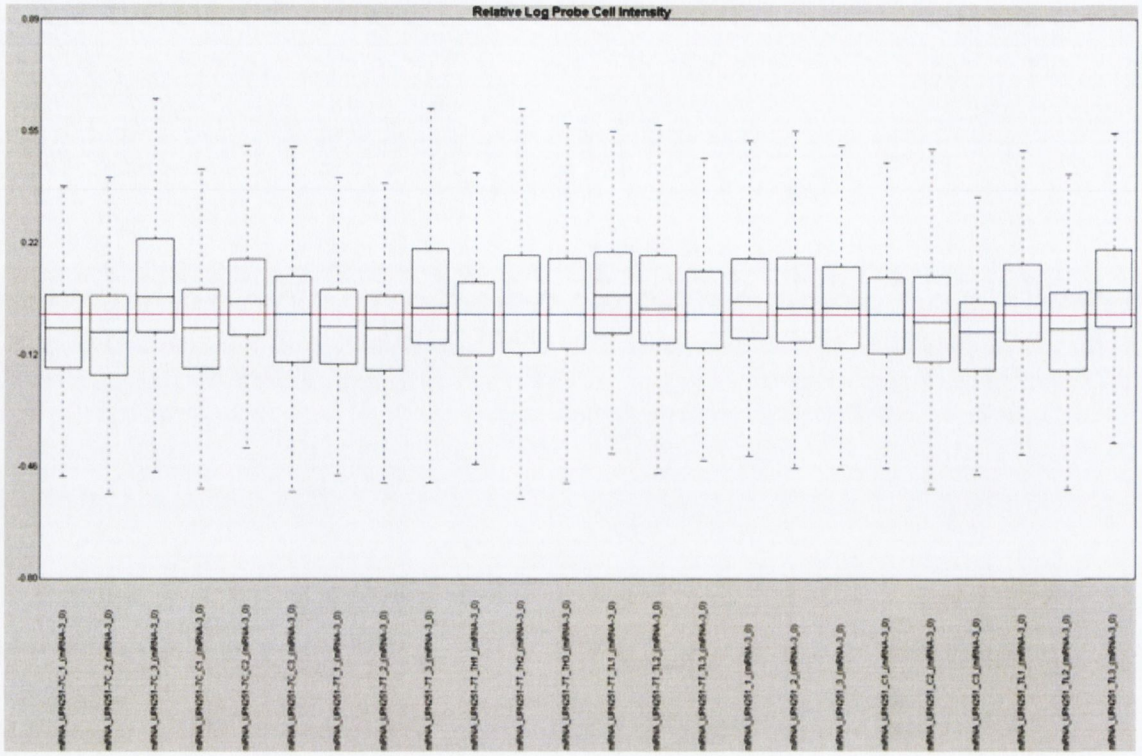

Figure 6.7 Box plots of the relative log expression values (miRNA arrays).

The mean absolute RLE is proportional to the width of the box plots. The middle bar of each box plot is the median RLE. The red line represents an RLE value of 0. As all median RLE values are close to 0 no outliers could be identified.

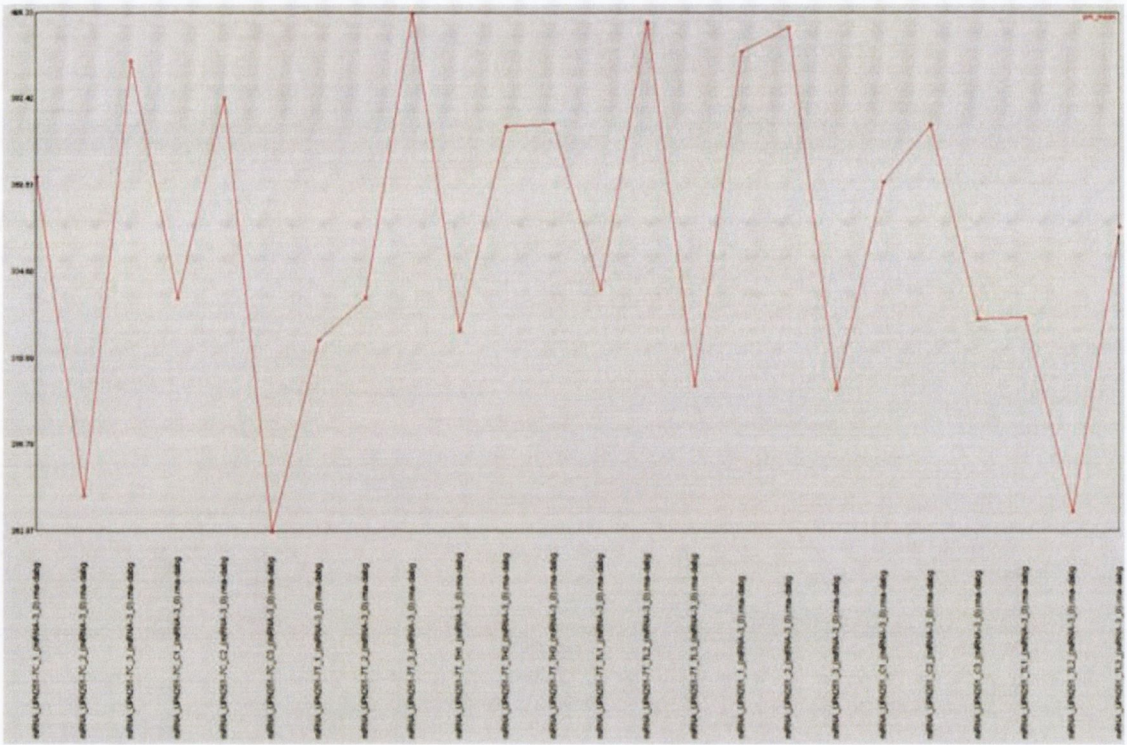

Figure 6.8 Probe level quality control metrics (miRNA).

The red line (pm_mean) indicates the mean probe level intensity prior to normalisation or background correction. This is used to indicate unusually dim or bright areas on a chip. As little variation occurs there is no indication that there are no abnormal values of pm_mean skewing the data.

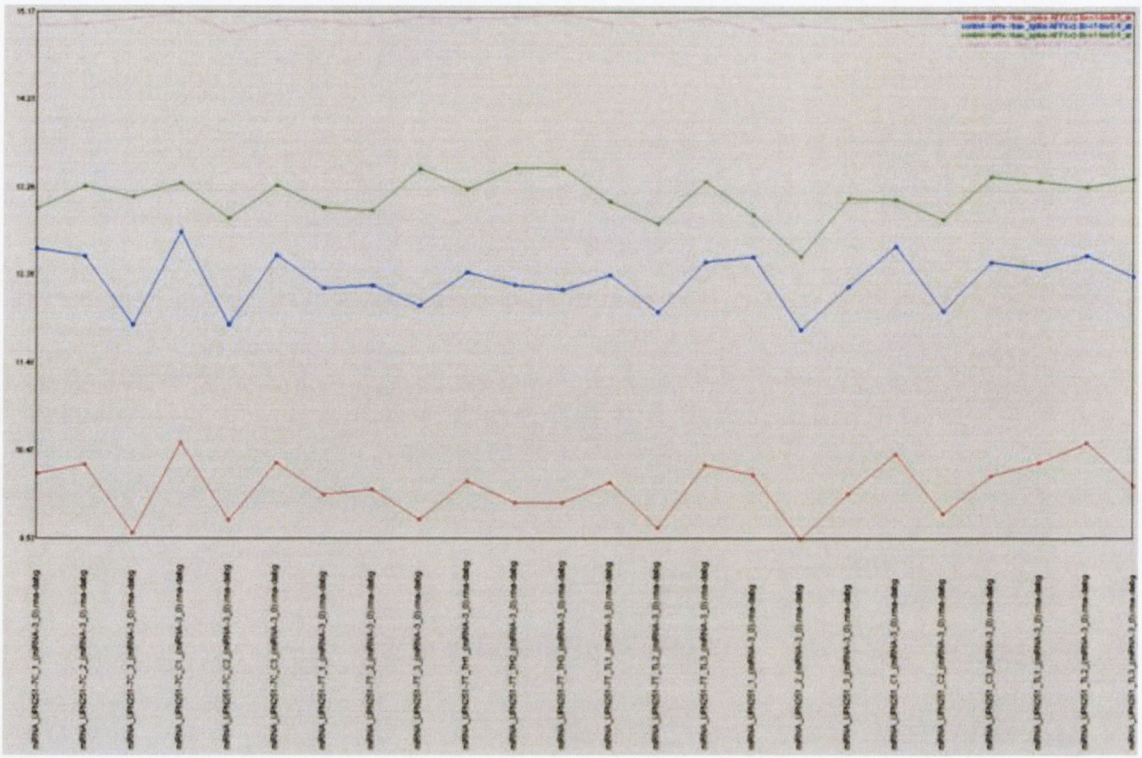

Figure 6.9 Rank order of bac spike controls.

The rank order of bac spikes controls gave good separation in the expected rank order as was expected from their relative concentration (BioB (red) < BioC (blue), BioD (green) and Cre (pink)). This strengthens evidence that there were no issues with the sample preparation.

The synthetic spike-in controls all showed little variation and spread and had a log2 signal value of <9.96 (Figure 6.10). This indicated that the poly(A) tailing and ligation was carried out successfully in the absence of RNase in samples.

Overall, from examining the quality control metrics, it could be confirmed that the miRNA array experiments were successful and that there were no outlier arrays that could cause skewed data analysis.

6.3.2 Summary characteristics analysis of datasets

A Pearson's correlation was carried out for all samples (gene and miRNA), which are shown in Figure 6.11 (A & B). Comparisons were taken between samples within a group and between sample groups. A coefficient score of 1 indicates perfect correlation between samples and are coloured red on the graph. Perfect correlation was only achieved when a sample was compared to itself. A coefficient score of <1 indicates less correlation between samples. This is shown in blue on the graph. It must be noted that there is very high correlation between all samples regardless of colour.

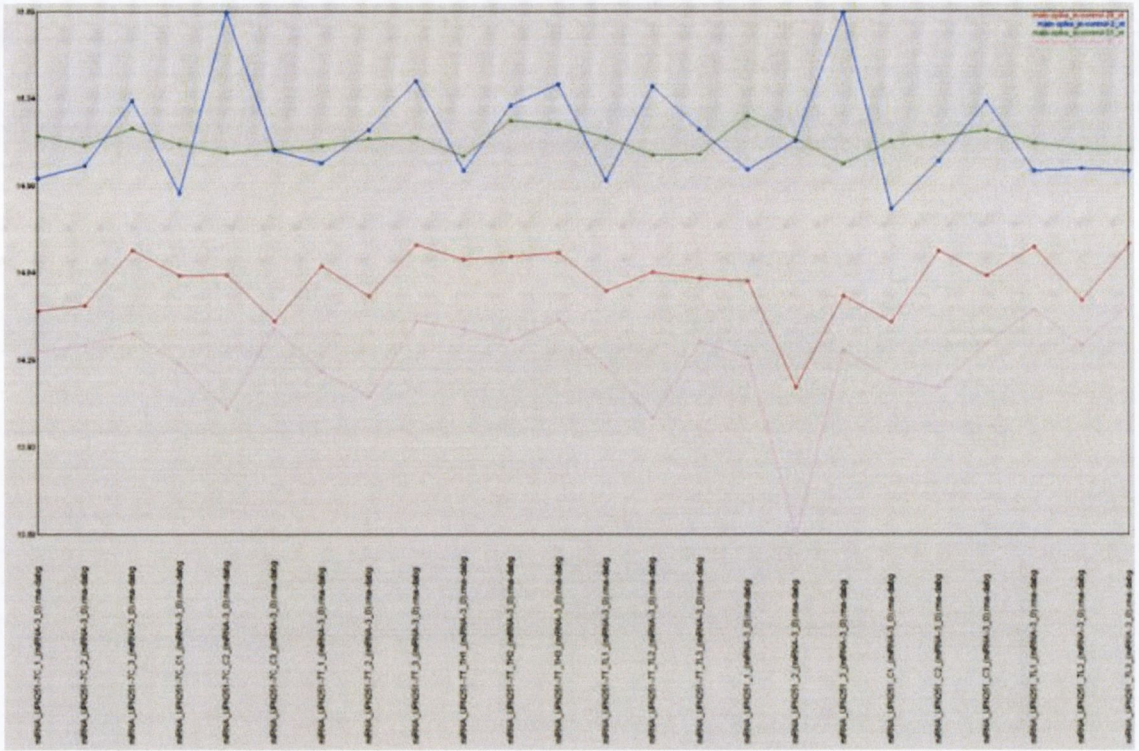

Figure 6.10 Spike-in control probe sets.

The log2 signal values of oligos 2, 29, 31 and 36 are shown. As all log2 values are >9.96, this is an indication that sample preparation was carried out successfully.

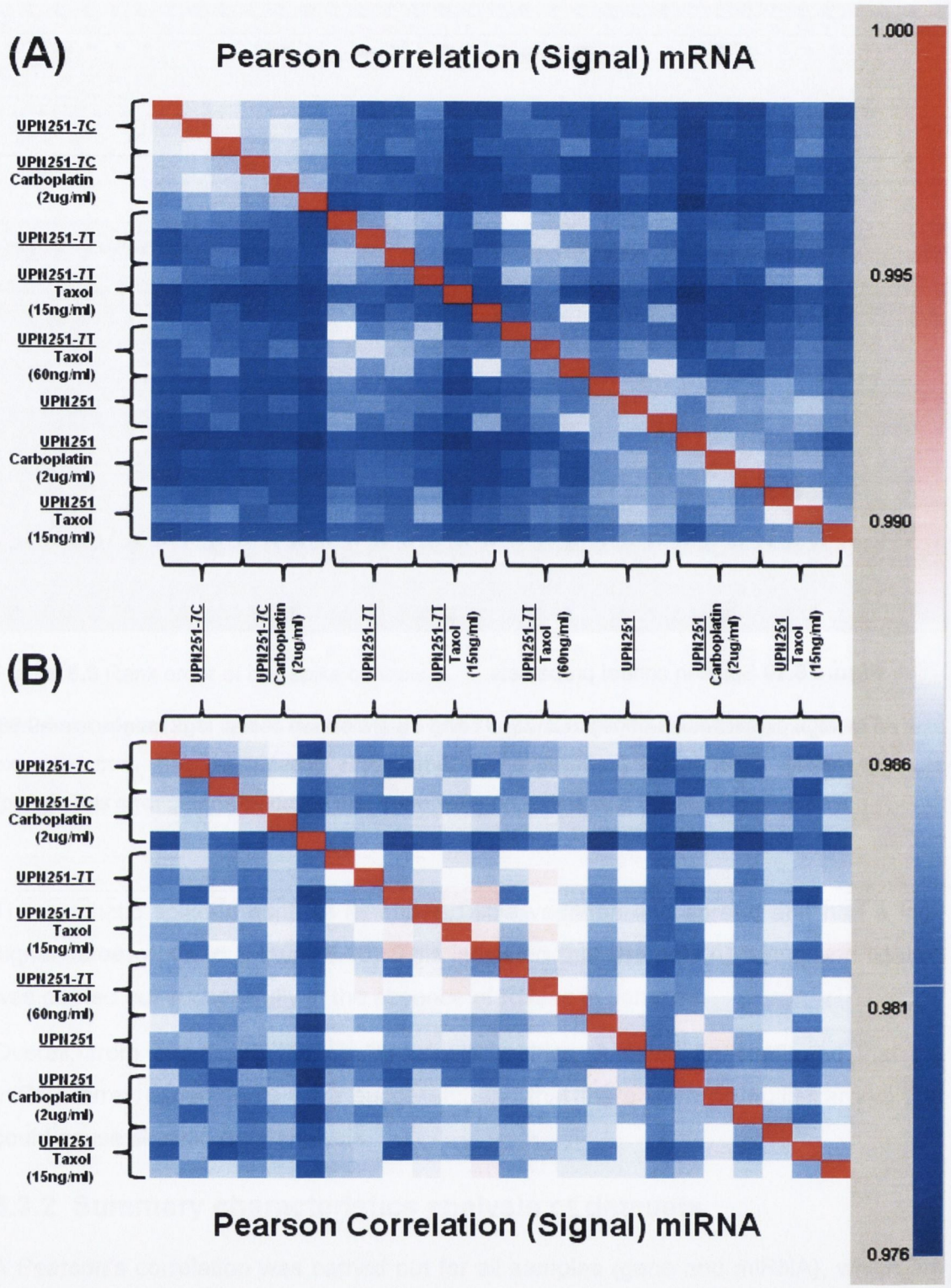

Figure 6.11 Pearson correlation of samples analysed using Affymetrix gene and miRNA arrays.

Pearson correlation was used to show how closely related the sample groups were to each other. Strong correlation is shown in red and weaker correlation is indicated in blue. (A) Pearson correlation between mRNA arrays (B) Pearson correlation between miRNA arrays.

The scale of correlation values range between 1 and 0.976. This is due to all samples being derived from the same cell line UPN251 and derived cell lines receiving relatively small drug concentrations of clinical relevance during selection in chapter 4. These subtle transcriptomic changes could be important in understanding the development of resistance in a clinical setting.

High correlation was seen in the miRNA comparisons between UPN251-7T treated with low and high doses of taxol, which would be expected (Figure 6.11 (B)). This pattern was also seen in our gene comparisons, but to a slightly lesser extent (Figure 6.11 (A)). From the gene comparisons, UPN251 (parental) samples differed most from UPN251-7C and UPN251-7T. This would be expected, as both resistant sublines would have acquired transcriptomic changes during the course of resistance development. UPN251-7C and UPN251-7T also differed, indicating that different transcriptomic changes were acquired depending on the selecting agent administered. These changes were not as prominent in the miRNA comparisons, but could still be seen with UPN251 differing from UPN251-7C to the greatest extent (Figure 6.11 (B)).

From a hierarchical clustering analysis we saw that UPN251, UPN251-7C and UPN251-7T samples cluster together for all of the gene chips ran (Figure 6.12). This indicated that the cell lines have become distinct in their gene signatures. The miRNA samples were not grouped together as neatly (Figure 6.13). This is probably due to miRNA expression being inherently more plastic and the miRNA chips containing a relatively small number of probes compared to the gene chips.

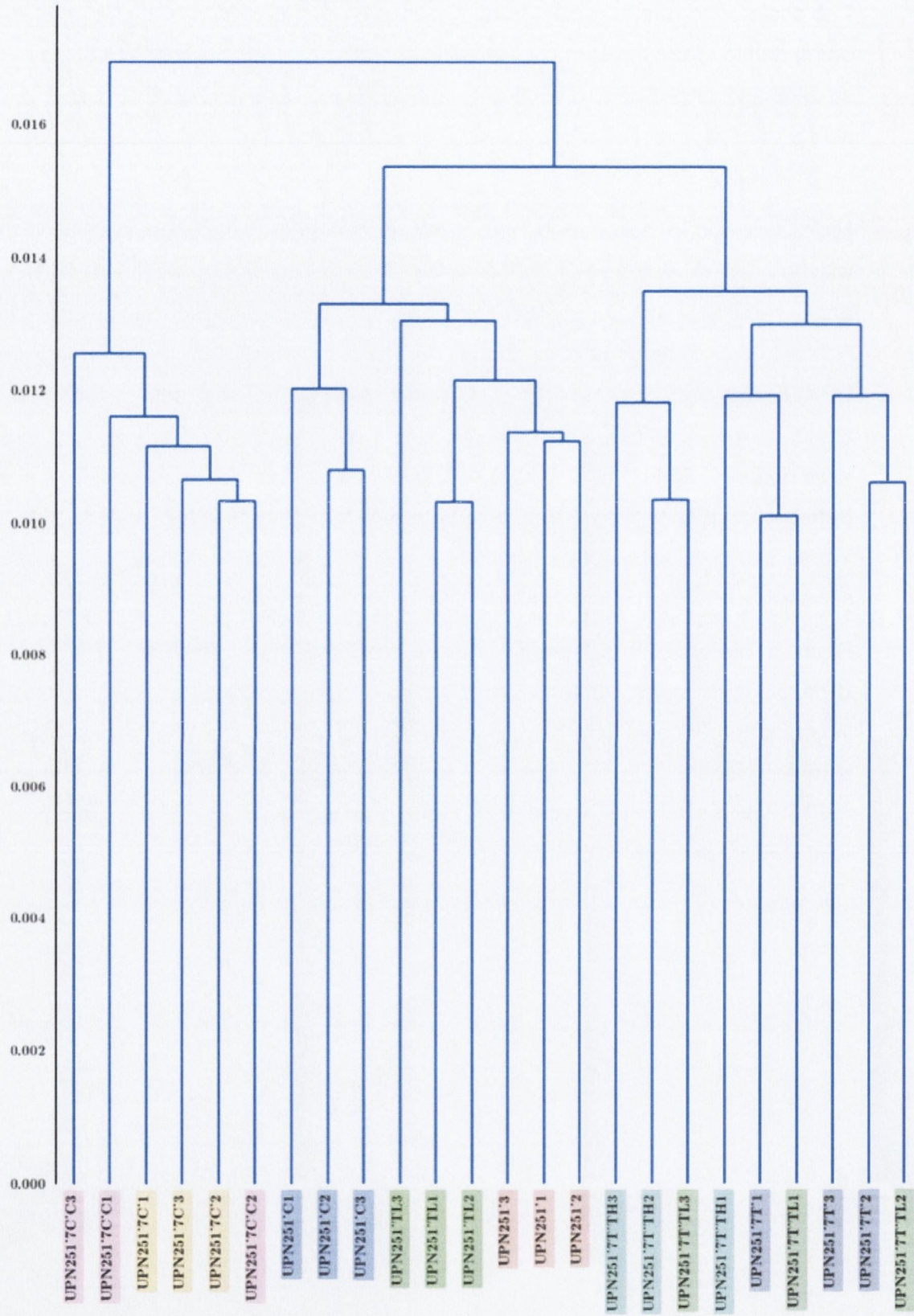

Figure 6.12 Clustering denogram of hierarchical clustering analysis of all samples run on the mRNA Affymetrix arrays.

The different cell lines clustered together showing separation between UPN251 parent cells and derived sublines UPN251-7C and UPN251-7T.

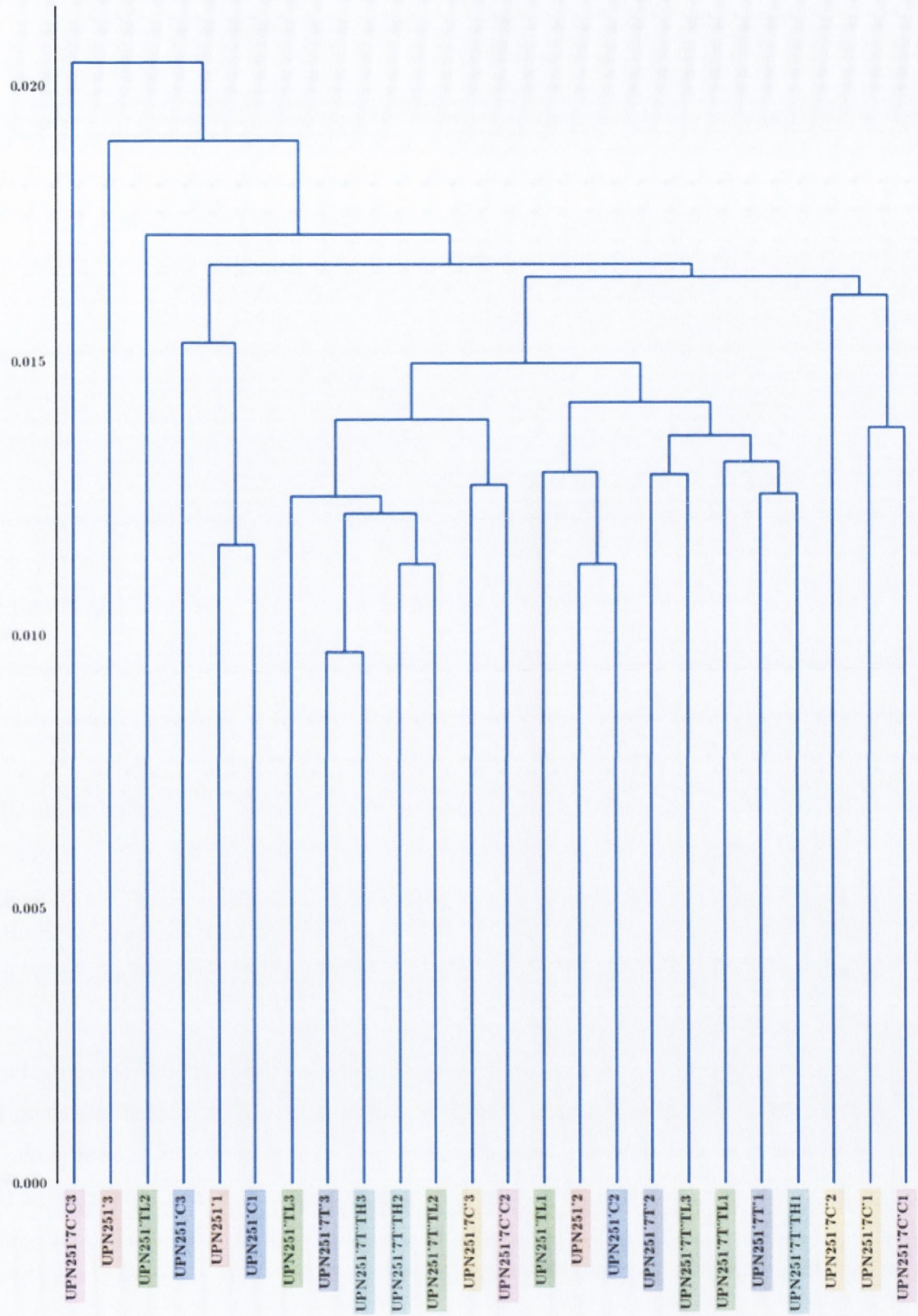

Figure 6.13 Clustering denogram of hierarchical clustering analysis of all samples run on the miRNA Affymetrix arrays.

The different cell lines clustered together showing separation between UPN251 parent cells and derived sublines UPN251-7C and UPN251-7T.

6.4 Results and discussion – Affymetrix gene/miRNA expression

A number of different comparisons were taken between lists of gene and miRNA to find differential expression between datasets. Analyses were separated into an analysis of carboplatin-resistant biomarkers, taxol-resistant biomarkers, biomarkers for carboplatin and taxol that were linked to first response to drug exposure and an investigation into the genes and miRNAs that were deregulated between the different comparisons.

The CEL file data from our Affymetrix analysis is attached in CD format to this manuscript in the Appendix A folder. The full lists of de-regulated components for all comparisons made between gene and miRNA chips are attached in CD format to this manuscript in the Appendix B folder.

6.4.1 Carboplatin resistance biomarker discovery

Two types of comparison between samples were made in order to discover carboplatin resistant biomarkers from both the gene and miRNA array data sets;

A. UPN251 Vs UPN251-7C

B. UPN251_C Vs UPN251-7C_C

Comparison A examined the differences in expression between parental UPN251 ovarian cancer cells and its carboplatin resistant subline UPN251-7C. Comparison B examined the differences in expression between parental UPN251 cells and its carboplatin resistant subline UPN251-7C, after the cells were exposed to the dose of carboplatin (2µg/ml) used to develop UPN251-7C's resistance phenotype in the cell selection strategy (Chapter 4).

Figures 6.14-6.17 gives a visual overview of the mRNA and miRNA data for each carboplatin comparison A and B. Each figure contains; (A) a clustering demograph of the hierarchical clustering analysis between replicates of both treatments being compared, (B) a volcano plot showing the significance and scale of fold change (Log 2) of each de-regulated probe in a comparison, (C) a chromosome location plot depicting the chromosomal locations of up-regulated and down-regulated probes and (D) a heat map showing the overall expressional changes between both treatments. This gives a visual overview of the data obtained from Affymetrix analyses for specific comparisons of de-regulated probes for easy reference. A large amount of data was simply depicted allowing for the rapid identification of any patterns that were present in the data.

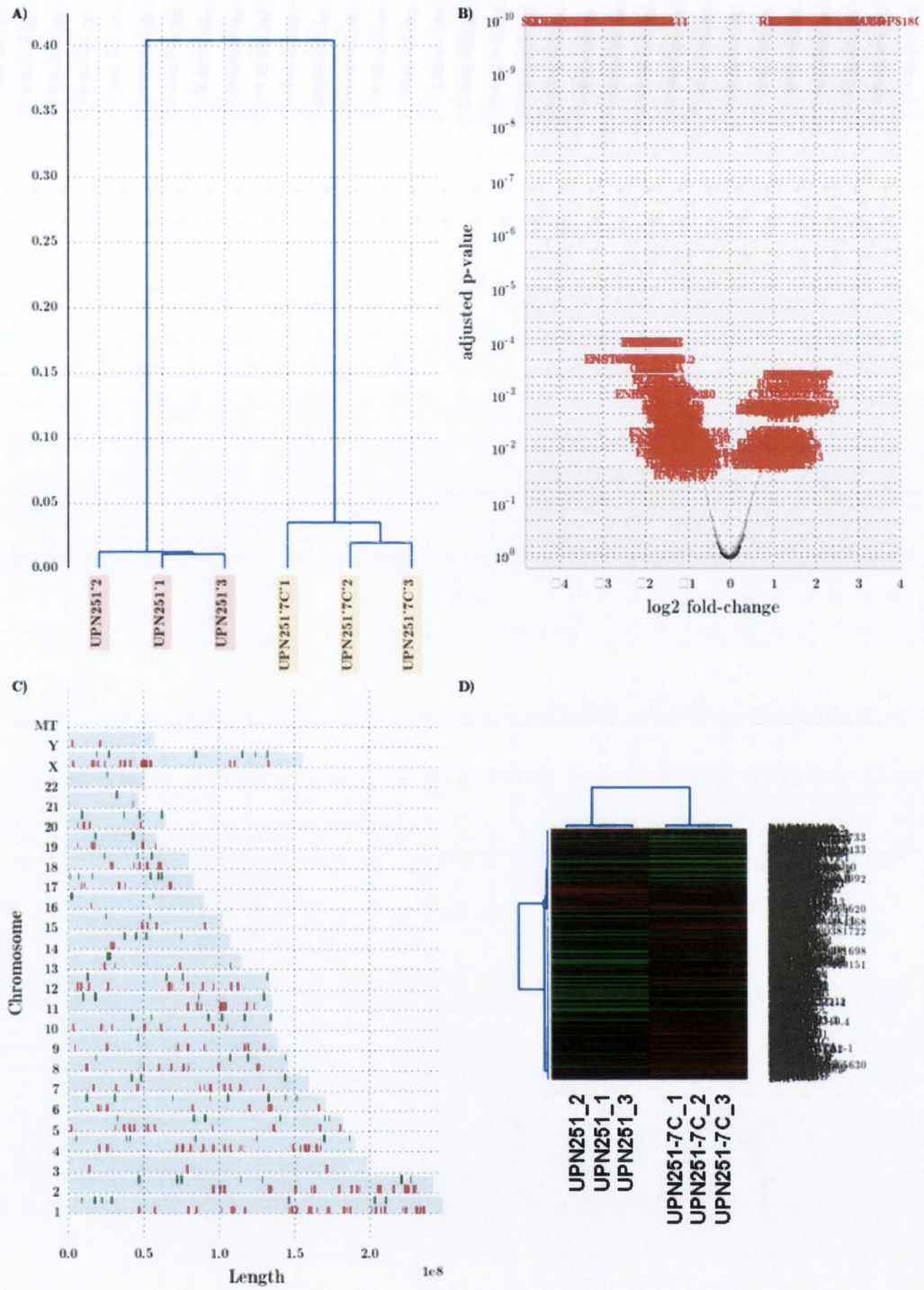

Figure 6.14 Overview of the deregulated gene expression from comparison A=UPN251 V UPN251-7C.

(A) Clustering demograph of hierarchical clustering analysis between replicates of both treatments. (B) Volcano plot. This shows the significance and scale of the fold change of each de-regulated gene. Adjusted P-value is given on Y-axis and Log 2 fold change is given on X-axis. (C) Chromosome location plot. Depicts the chromosomal locations of up-regulated (green) and down-regulated genes. (D) Heat map. This shows overall expressional changes between both treatments. High expression is given in (green) and low expression in (red).

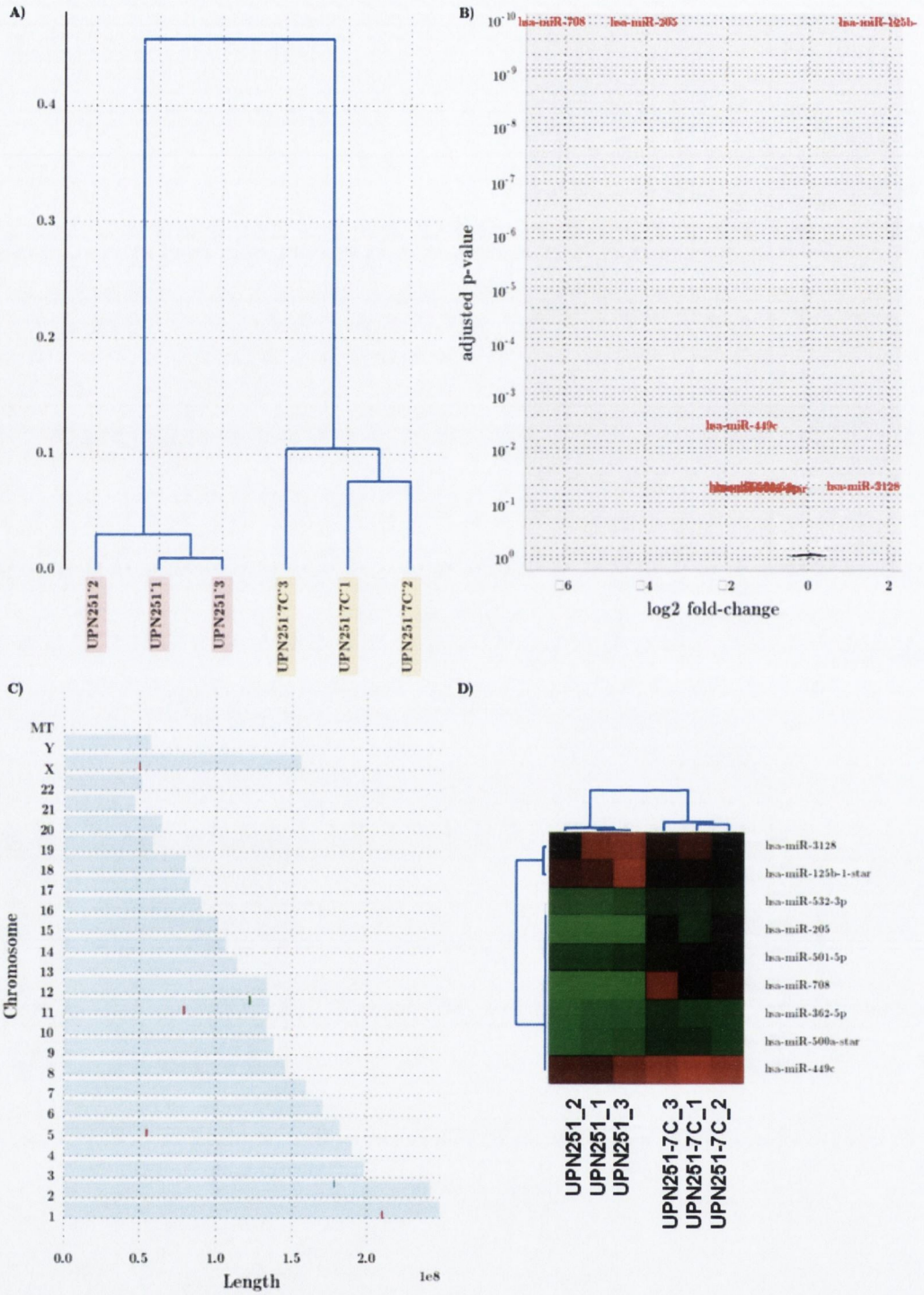

Figure 6.15 Overview of the deregulated miRNA expression from comparison A=UPN251 V UPN251-7C.

(A) Clustering demograph of hierarchical clustering analysis between replicates of both treatments. (B) Volcano plot. This shows the significance and scale of the fold change of each de-regulated miRNA. Adjusted P-value is given on Y-axis and Log 2 fold change is given on X-axis. (C) Chromosome location plot. Depicts the chromosomal locations of up-regulated (green) and down-regulated genes. (D) Heat map. This shows overall expressional changes between both treatments. High expression is given in (green) and low expression in (red).

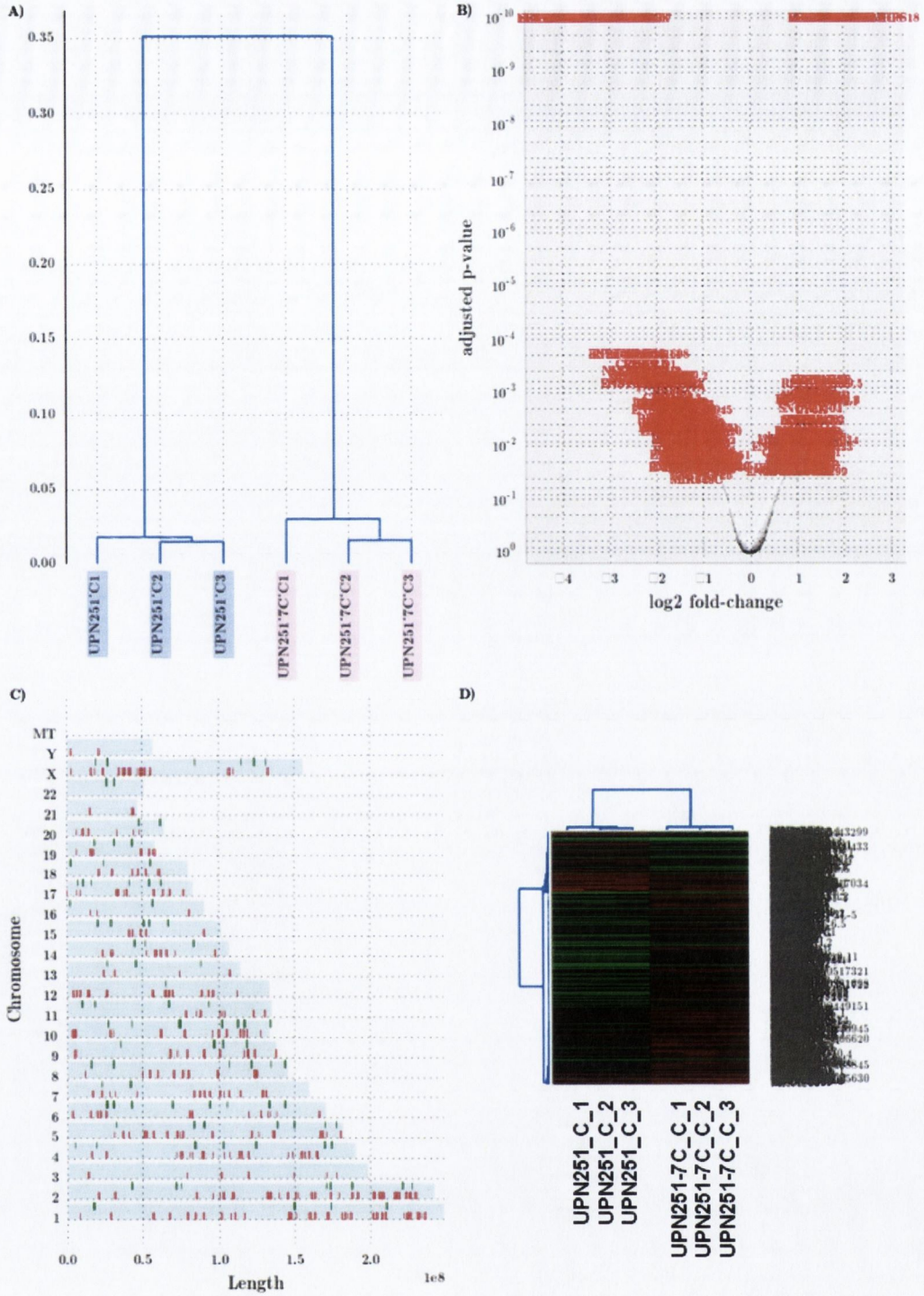

Figure 6.16 Overview of the deregulated gene expression from comparison B=UPN251_C V UPN251-7C_C.

(A) Clustering demograph of hierarchical clustering analysis between replicates of both treatments. (B) Volcano plot. This shows the significance and scale of the fold change of each de-regulated gene. Adjusted P-value is given on Y-axis and Log 2 fold change is given on X-axis. (C) Chromosome location plot. Depicts the chromosomal locations of up-regulated (green) and down-regulated genes. (D) Heat map. This shows overall expressional changes between both treatments. High expression is given in (green) and low expression in (red).

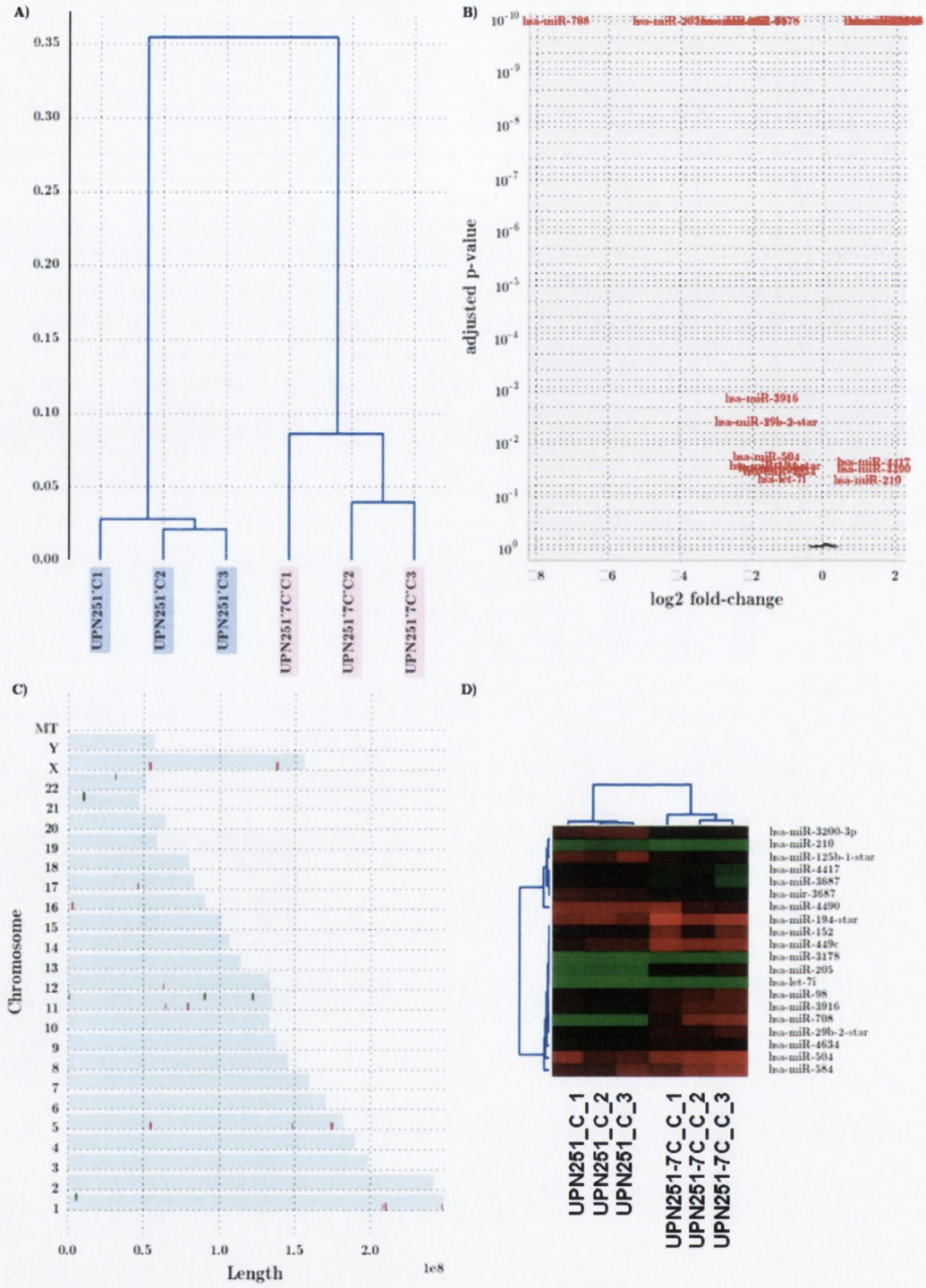

Figure 6.17 Overview of the deregulated miRNA expression from comparison B=UPN251_C V UPN251-7C_C.

(A) Clustering demograph of hierarchical clustering analysis between replicates of both treatments. (B) Volcano plot. This shows the significance and scale of the fold change of each de-regulated miRNA. Adjusted P-value is given on Y-axis and Log 2 fold change is given on X-axis. (C) Chromosome location plot. Depicts the chromosomal locations of up-regulated (green) and down-regulated genes. (D) Heat map. This shows overall expressional changes between both treatments. High expression is given in (green) and low expression in (red).

6.4.1.1 Top five deregulated genes and miRNAs

The top five most de-regulated genes and miRNAs from comparisons A and B are shown in Table 6.2. As a general trend, there were more down-regulated genes and miRNAs than up-regulated gene and miRNAs in the resistant cell lines UPN251-7C compared to UPN251 for both A and B comparisons. There were also greater fold decreases in expression than fold increases in UPN251-7C compared to UPN251 in A and B comparisons. All of the genes that appeared in the top 5 deregulated gene list of A and B comparisons also appeared in the other comparison's gene list at some level of fold change (i.e. all of the top five deregulated genes found in A were also found in B and vice versa). This indicated that the top genes that had been subjected to changes in transcriptional expression during initial exposure to carboplatin when chemo-naïve was the same genes that were affected by response to drug exposure in the newly developed carboplatin-resistant cell lines. Table 6.3 shows the genes and miRNAs that have been found to be involved in ovarian cancer and/or resistance.

A number of transcripts were found in both A and B comparisons' top 5 deregulated lists, comparing UPN251-7C to UPN251 under different conditions. PLAC8, EPHA7, CHST9 and miR-125b-1* were up-regulated and SERPINB7, DPP4, miR708, miR205 and miR449c were down-regulated in UPN251-7C. Only one of these genes, DPP4 (CD26), has been previously linked to epithelial ovarian cancer. In this study, decreased expression was linked to taxol resistance (*Kajiyama et al. 2010*). The same author had previously shown that up-regulation of DPP4 significantly lessens invasive potential in ovarian cancer cells both *in-vitro* and *in-vivo* by changing cell morphology from a fibroblastic to epitheloid pattern (*Kajiyama et al. 2002*).

Other transcripts from top 5 deregulated lists of A and B, comparing UPN251-7C to UPN251 (exploring expressional changes linked to carboplatin resistance), have also been linked with resistance in ovarian cancer. These were EEF1A2, GDF15 and LIN28B, which were up-regulated, and MAL, miR-98 and miR-152, which were down regulated in UPN251-7C compared to UPN251.

The literature supports that the over-expression of EEF1A2, GDF15 and LIN28B is associated with chemo-resistance (*Bock et al. 2010*; *Sun et al. 2008*; *Topp et al. 2014*; *Yan et al. 2013*). In addition, these studies found that over-expression of GDF15 and LIN28B are linked to poor prognosis in ovarian cancer. Up-regulation of MAL, which was found to be down-regulated in UPN251-7C compared to UPN251 in our study, has been found to be associated with platinum resistance in ovarian cancer (*Lee et al. 2010*). A number of studies in ovarian cancer patients have also shown that MAL

Table 6.2 Overview of deregulated genes and miRNA for carboplatin comparisons.

Top 5 deregulated genes and miRNAs are given for each comparison at 2 Fold (base 10) cut off FDR p<0.05. Probe 1-Probe 5 represents the top 5 up/down-regulated genes or miRNAs in a comparison.

		Total	> FC	Probe 1	FC	Probe 2	FC	Probe 3	FC	Probe 4	FC	Probe 5	FC
Comparison A: UPN251 V UPN251-7C (changes in carboplatin resistance development)													
UP-regulated	**Gene**	80	12.6	PLAC8	8.8	EPHA7	4.6	EEF1A2	4.1	GDF15	4.0	CHST9	3.9
	MiRNA	2	4.3	miR-125b-1*	4.3	miR-3128	2.6						
Down-regulated	**Gene**	249	8.1	SLC4A4	20.9	CDH6	20.8	SERPINB7	16.6	DPP4	15.7	BMPR1B	14.1
	MiRNA	7	79.5	miR-708	79.5	miR-205	16.7	miR-449c	3.1	miR-501-5p	2.6	miR-532-3p	2.3
Comparison B: UPN251_C V UPN251-7C_C (changes in response to carboplatin in carboplatin resistance development)													
Up-regulated	**Gene**	67	20.9	PLAC8	7.2	EPHA7	4.8	POF1B	4.8	LIN28B	4.1	CHST9	3.8
	MiRNA	11	4.3	miR-125b-1*	4.3	miR-3200-3p	3.9	miR-3687	3.7	miR-1272	2.7	miR-4417	2.7
Down-regulated	**Gene**	352	20.6	MAL	20.6	SERPINB7	19.1	MAMDC2	18.7	DPP4	15.5	TMEM47	13.7
	MiRNA	15	177.4	miR-708	177.4	miR-205	21.1	miR-449c	5.8	miR-152	5.6	miR-98	3.7

Total= Total number of up or down regulated probes from a comparison (For gene chips this will include more than protein coding genes which we are interested in for this study (e.g. non protein coding genes, Long non coding RNAs, snoRNA etc.) Only top 5 deregulated genes are given in the body of the table), >FC = the greatest fold increase or decrease by a single probe from a comparison (base 10 Fold Change), FC= Fold Change (base 10).

Table 6.3 Top five transcripts involved in ovarian cancer and/or resistance (carboplatin comparisons).

Gene/miRNA	Function	Literature (gene/miRNA expression or stated if otherwise)	Source and references
↑ PLAC8	Plasmacytoid dendritic cell activation	One of 2871 genes associated with doxorubicin resistance (endometrial cancer). Up-regulation is linked to apoptotic resistance.	Cell-lines : Endometrial cancer (KLE, HEC 1B, HEC 1A, RL 95-2 and AN3-Ca) (*Indermaur et al. 2010*), embryonic kidney (HEK 293T), Leukemia (CEM-C7(clone CKM1)), Jukart (clone 293T), epithelial (MFC-10A), breast cancer (MCF7) (*Mourtada-Maarabouni et al. 2013*)
↑ EPHA7	Protein-tryosine kinase (Developmental events)	Up-regulation is linked to resistance in other cancer types and it is linked to poor prognosis in other cancer types.	Patient tumour tissue (*Deng et al. 2011; Kim et al. 2010; Liu et al. 2013; Wang et al. 2008*)
↑ EEF1A2	Subunit of the elongation factor-1 complex	Up-regulation is involved in ovarian cancer progression and apoptotic resistance.	Cell lines: Immortalised OSE (I-80RZ and I-144RZ) (*Sun et al. 2008*)
↑ GDF15	Differentiation	Up-regulation is linked to poor chemotherapy response and reduced overall survival in ovarian cancer.	Patient tumour tissue (*Bock et al. 2010*)
↑ LIN28B	Cellular transformation	Up-regulation is linked to platinum resistance and poor prognosis in ovarian cancer.	Cell lines: ovarian cancer (0432 and Uci101) (*Yan et al. 2013*) patient tumour tissue (*Topp et al. 2014; Yan et al. 2013*) patient derived xenographs and mouse models (*Topp et al. 2014*)
↓ CDH6	cell-cell adhesion, cell differentiation and morphogenesis	Down-regulated in estrogen+ ovarian cancer in response to 17β-estradiol treatment.	Cell lines: Ovarian cancer (PEO4) (*Walker et al. 2007*) #Patient tumour samples (*Walker et al. 2007*)
↓ DDP4	Intrinsic membrane glycoprotein/ serine exopeptidase	Down-regulation is linked to taxol resistance in ovarian cancer.	Cell lines: Ovarian cancer (SKOV-3, NOS-2, TAOV, NOS-4, HRA, RMG-I, RMG-II, NOS1, ES-2, HEY and KOC-7C) (*Kajiyama et al. 2010*)
↓ BMPR1B	Mediates proliferation, differentiation and apoptosis	Down-regulation is linked to ovarian cancer development and poor prognosis.	Patient tumour tissue (*Ma et al. 2010*)

↓ MAL	Hydrophobic integral membrane protein (diverse functionality)	Up-regulation is linked to platinum resistance and poor prognosis in ovarian cancer. There is evidence of its involvement in acquired ovarian cancer resistance.	Cell lines: Ovarian cancer (OVCA432 (*Lee et al. 2010*),SKOV-3 (*d'Adhemar et al. 2014*)) patients tumour tissue (*Berchuck et al. 2005*; *Berchuck et al. 2009*; *d'Adhemar et al. 2014*; *Lee et al. 2010*)
↓ miR-205	Regulation of gene expression	Up-regulated in ovarian cancer and deregulated in other cancer types. MiR-205 in combination with let-7f has been proposed as a predictive biomarker for ovarian cancer prognosis.	Patient tumour tissue (*Iorio et al. 2007*; *Tsukamoto et al. 2014*; *Zhou et al. 2014*) and plasma (*Tsukamoto et al. 2014*; *Zheng et al. 2013*)
↓ miR-152	Regulation of gene expression	It has up (*Liu et al. 2014*) or down (*Xiang et al. 2014*) regulation in different studies involved in ovarian cancer resistance.	Cell lines: ovarian cancer (SKOV-3 and A2780) (*Xiang et al. 2014*) patient tumour tissue (*Liu et al. 2014*)
↓ miR-98	Regulation of gene expression	Down-regulated in ovarian cancer chemoresistance. Also, deregulated in platinum and hydroxycamptothecin resistance in lung and gastric cancer, respectively.	Cell lines: ovarian cancer (SKOV-3 (*Wendler et al. 2011*)), lung cancer(A549 (*Xiang et al. 2013*)), gastric cancer(BGC-823, SGC-7901, MGC-803, HGC-27, NCI-N87 and AGS (*Wu et al. 2011*))

Green indicates up-regulation and red indicated down regulation of a gene or miRNA. OSE=ovarian serous epithelium.

#Protein expression examined

gene expression was increased in patients with poor prognosis (*Berchuck et al. 2005; Berchuck et al. 2009)*. MAL is a hydrophobic integral membrane protein of the MAL family of proteolipids and has many cellular functions including T-cell signal transduction, myelin biogenesis and/or function in the nervous system and the formation, stabilisation and maintenance of glycosphingolipid-enriched membrane microdomains (*Bernard et al. 2013*). MAL is known to be required for TLR4 signalling by combining with MyD88 in the cytoplasm, initialling a signalling cascade (*Fitzgerald et al. 2001)*. Our research group has shown that myD88 expression is significantly associated with reduced patient survival and may be required for acquired ovarian cancer resistance (*d'Adhemar et al. 2014*).

As was seen in our study, miR-98 has been found to be down-regulated in ovarian cancer resistance in the literature. It was also found to be involved in the regulation of PGRMC1, which is elevated in ovarian cancer. PGRMC1 has been shown to be involved in the promotion of tumourigenesis and chemo-resistance (*Wendler et al. 2011*). It has a binding site for miR-98 and let7i (also down regulated in UPN251-7C compared to UPN251 in comparison B) in the 3' region of the gene which was shown in ovarian cancer SKOV3 cells.

Mir-152, which was down-regulated in UPN251-7C compared to UPN251 in our study, has been shown to be both up and down-regulated in different studies when linked to ovarian cancer resistance. One study found miR-152 to be expressed significantly higher in drug-resistant ovarian cancer tissue compared to drug-sensitive tissue (*Liu et al. 2014*). The second study found miR-152 and miR-185 to be significantly down-regulated in the cisplatin-resistant ovarian cell lines SKOV3/DDP and A2780/DDP, compared with their sensitive parental cell lines SKOV3 and A2780 (*Xiang et al. 2014*). The differences between our results and the literature and between different studies in the literature for MAL and miR-152 may be due to differences in sample origin.

Some genes and miRNAs from the top 5 lists of A and B, comparing UPN251-7C to UPN251 under different conditions (exploring expressional changes linked to carboplatin resistance), have not been linked with ovarian cancer in the literature, but have been found to be de-regulated in other cancer types. These include PLAC8, EPHA7, CHST9, miR-3687 and miR-4417, up-regulated in our study, and SLC4A4, SERPINB7, TMEM47, miR-708, miR-449C, miR-501-5p and miR-532-3p down-regulated in our study, in UPN251-7C compared to UPN251. Also, potentially novel targets may be those that have not been found to be linked to cancer through PubMed searches to date. These potential targets may have been linked to other diseases or syndromes or be newly discovered and relatively unstudied (which is the case in some

of the miRNAs found). From our carboplatin comparisons (A and B), we found a number of potentially novel ovarian cancer biomarkers, which appeared in our top five de-regulated lists that have not been linked to cancer in the literature to our knowledge. These included POF1B, miR-125b-1*, miR-3128, miR-3200-3p and miR-1272 which were up-regulated and MAMDC2, which was down-regulated in UPN251-7C compared to UPN251 in our carboplatin comparisons (A and B).

6.4.1.2 Pathway analysis by DAVID

Pathway analysis of A and B comparisons by DAVID v6.7 was carried out on our gene array data to predict pathways that our deregulated genes may be involved in. An overview of the pathways predicted by DAVID from comparisons A and B, comparing UPN251-7C to UPN251 (exploring expressional changes linked to carboplatin resistance), is shown in Table 6.4. Three pathways were found in both A and B, namely hematopoietic cell lineages, axon guidance and cytokine-cytokine receptor interactions. Three other pathways were found only in B. These were basal cell carcinoma, hedgehog signalling pathway, and pathways in cancer. Only two of the genes found in the pathway analysis were present in the top 5 de-regulated gene lists. Those were EPHA7 (Axon Guidance pathway) and BMPR1B (cytokine-cytokine receptor interactions), which have been discussed above in section 6.4.1.1 and Table 6.3.

6.4.1.2.1 Hematopoietic cell lineages

Hematopoietic cell lineages refer to a pathway of genes that are ordinarily involved in the blood-cell development process, where hematopoietic stem cells either self-renew or differentiate into a multilineage committed progenitor cell. The stage and specific lineage of a cell in the differentiation process is defined by a lineage-specific expression pattern of genes that code for surface markers, a number of which have been identified in our deregulated gene lists. The genes from our study are spread out across different stages and lineages of cells in this pathway. For this reason, it is unlikely to be of importance that this subset of genes from our list is involved in this blood cell development pathway. However, individually these genes may still be involved in ovarian cancer resistance and could be used as biomarkers. Hematopoietic cytokines, which regulate the growth and differentiation of hematopoietic progenitor cells, have been investigated in epithelial ovarian cancer as tumour markers (*Lawicki et al. 2012*). *Lawicki et al (2012)* found that CSF-1 could be used in ovarian cancer diagnosis to discriminate between cancerous and non-cancerous legions and could be used to compliment CA125. Table 6.5 gives an overview of the genes identified in the

Table 6.4 DAVID carboplatin resistance pathway analysis.

The de-regulated genes found in comparisons A (UPN251 V UPN251-7C) and B (UPN251_C V UPN251-7C_C) Carboplatin Analyses.

	Genes	De-regulated Genes
Common Pathways (Found in A and B comparisons)		
Hematopoietic Cell Lineages	**A ONLY**	N/A
	B ONLY	CD55, CSF1, IL6, ITGA6
	COMMON	ANPEP, CD9, IL1R1, IL7, ITGA2, KITLG,
Axon Guidance	**A ONLY**	SLIT2
	B ONLY	SEMA3A, SLIT3
	COMMON	EFNB2, EPHA7, NTN1, NTN4, NTNG1, ROBO1
Cytokine-Cytokine Receptor Interactions	**A ONLY**	TNFRSF19
	B ONLY	CCL2, CSF1, IL23A, TNFRSF9
	COMMON	BMP2, BMPR1B, CCL20, IL1R1, IL7, IL18R1, KITLG, TNFRSF11A
Pathways found only in B:		
Basal Cell Carcinoma & Hedgehog Signalling Pathway	**B ONLY**	BMP2, GLI3, HHIP
	A ALSO	SMO, WNT7A
Pathways in Cancer	**B ONLY**	FGF18, JUP, MMP9, LAMC2
	Other Pathways	BMP2, GLI3, HHIP, ITGA2 , ITGA6, KITLG, WNT7A

A ONLY= Genes only found in A comparison by DAVID pathway analysis for a given pathway, B ONLY= Genes only found in B comparison by DAVID pathway analysis for a given pathway, COMMON= Genes found in both A & B comparison by DAVID pathway analysis for a given pathway, A ALSO=genes were deregulated in A comparison also but were not picked up by DAVID pathway analysis, Other Pathways= Genes were also found in other pathways found by DAVID pathway analysis. (RED) genes are down regulated (Green) genes are up-regulated.

Table 6.5 Deregulated genes in the hematopoietic cell lineages pathway.

Gene	Deregulation	Literature	Ovarian cancer/resistance linked references
ANPEP	↓ A(3.9), B(5.5)	Deregulated in other cancer types (not previously in ovarian).	
CD9	↓ A(2.6), B(3.0)	Deregulation is linked to ovarian cancer but not yet chemoresistance.	*(Bauerschlag et al. 2013; Furuya et al. 2005; Houle et al. 2002; Hwang et al. 2012)*
CD55	↓ B(2.2)	Up-regulation mediates resistance to complement-mediated cytotoxicity (ovarian cancer cell). Also, deregulated in other cancer types.	*(Mamidi et al. 2013)*
CSF1	↓ B(2.0)	Deregulated in other cancer types (not previously in ovarian).	
IL1R1	↓ A(3.1), B(3.9)	Deregulated in other cancer types (not previously in ovarian).	
IL6	↓ B(2.2)	Up-regulation is linked to cisplatin and/or taxol resistance and poor prognosis in ovarian cancer cell lines, patient tumour tissue, serum and ascites.	*(Coward et al. 2011; Hong et al. 2007; Wang et al. 2010)*
IL7	↓ A(3.3), B(2.8), C(2.2)	Up-regulation is linked to ovarian cancer prognosis but not yet chemoresistance. Evidence from protein levels in patient tumour serum samples.	*(Lambeck et al. 2007; Xie et al. 2004)*
ITGA2	↓ A(4.6), B(4.5), D(2.1)	Deregulated in other cancer types (not previously in ovarian).	
ITGA6	↓ B(2.4), D(2.3)	Deregulated in other cancer types (not previously in ovarian).	
KITLG	↓ A(6.4), B(10.5)	Up-regulation is linked to cisplatin and/or taxol resistance in ovarian cancer cells.	*(Shaw et al. 2007; Zhang et al. 2008b)*

Deregulation=comparison (Fold Change); Comparison A=UPN251 V UPN251-7C (Genes/miRNA changes in carboplatin resistance development), Comparison B=UPN251_C V UPN251-7C_C (Genes/miRNA changes in response to carboplatin in carboplatin resistance development), Comparison C=UPN251 V UPN251-7T (Genes/miRNA changes in taxol resistance development), Comparison D=UPN251_TL V UPN251-7T_TL (Genes/miRNA changes in response to low dose taxol in taxol resistance development). ↑ = significant up-regulated expression. ↓ = significant down-regulated expression.

Hematopoietic cell lineages pathway that have been linked to ovarian cancer and/or resistance.

6.4.1.2.2 Axon guidance

The axon guidance pathway is an important step in the formation of the neuronal network. A number of guidance factors are involved in guiding axons such as ephrins, netrins, slits, and semaphorins. Guidance cues from these factors are read by growth cone receptors and signal transduction pathways downstream results in changes made to cytoskeletal organisation, which determines the orientation that the growth cones will grow. Studies have shown that guidance factors are expressed outside of the nervous system and that their expression may play an important role in cancer (*Chedotal et al. 2005*). Table 6.6 shows an overview of the genes identified in the axon guidance pathway that have been linked to ovarian cancer and/or resistance.

6.4.1.2.3 Cytokine-cytokine receptor interaction

Cytokines are soluble extracellular proteins or glycoproteins that play an integral role in intracellular regulation and mobilisation of cells. They are engaged in a number of processes including innate and adaptive immune response, cell growth, differentiation, angiogenesis, cell death, and development and repair processes of homeostasis. Cytokines are released by a huge number of different cell types in the body, usually in response to stimuli, and mediate responses in target cells by binding to cell surface target receptors. It has been well established that expression of cytokines and their receptors have a role to play in cancer and may have a role to play in the progression of ovarian cancer (*Balkwill 2004*; *Nash et al. 1999*). The expression of cytokines has been investigated in ovarian cancer cell lines, ascites fluid and biopsies from ovarian cancer patients in different studies (*Kulbe et al. 2012*; *Matte et al. 2012*). These studies revealed that there is a complex network of deregulated cytokines involved in ovarian cancer progression, which is influenced by cytokines in the extracellular microenvironment. They also indicate that the expression of cytokines and cytokine receptors within the cell mediate key cellular events. Table 6.7 gives an overview of the genes identified in the axon cytokine-cytokine receptor interaction pathway that have been linked to ovarian cancer and/or resistance.

6.4.1.2.4 Hedgehog signalling pathway

Members of the Hedgehog family of secreted proteins play a pivotal role in the development of diverse animal phyla, including human, where they control morphogenesis in a variety of tissues and organs. The Hedgehog family also mediates

Table 6.6 Deregulated genes in the axon guidance pathway.

Gene*	Deregulation	Literature	Ovarian cancer/resistance linked references
EFNB2	↓ A(4.6), B(7.8)	Deregulated in other cancer types (not previously in ovarian).	
NTN1	↓ A(2.5), B(2.8)	Up-regulated in ovarian cancer tissue and linked to apoptotic resistance. Also, deregulated and linked to poor prognosis in other cancer types.	*(Papanastasiou et al. 2011)*
NTN4	↓ A(2.9), B(3.6)	Deregulated in other cancer types (not previously in ovarian).	
NTNG1	↓ A(2.5), B(2.2), C(2.1)	Has not been previously identified in cancer.	
ROBO1	↓ A(2.0), B(2.0)	Deregulation is linked to ovarian cancer but not yet chemoresistance.	*(Dai et al. 2011; Dickinson et al. 2011)*
SEMA3A	↓ B(2.6), C(2.2), D(2.9), E(2.4)	It has not previously been identified in ovarian cancer but it has been shown to facilitate the circumvention of resistance mechanisms in other cancer types.	*(Maione et al. 2009)*
SLIT2	↓ A(2.2)	^Deregulation is linked to ovarian cancer but not yet chemoresistance.	*(Dai et al. 2011; Dickinson et al. 2011; Dong et al. 2012; Qiu et al. 2011).*
SLIT3	↓ B(2.0)	^Deregulation is linked to ovarian cancer but not yet chemoresistance.	*(Dai et al. 2011; Dickinson et al. 2011)*

Deregulation=comparison (Fold Change); Comparison A=UPN251 V UPN251-7C (Genes/miRNA changes in carboplatin resistance development), Comparison B=UPN251_C V UPN251-7C_C (Genes/miRNA changes in response to carboplatin in carboplatin resistance development), Comparison C=UPN251 V UPN251-7T (Genes/miRNA changes in taxol resistance development), Comparison D=UPN251_TL V UPN251-7T_TL (Genes/miRNA changes in response to low dose taxol in taxol resistance development), Comparison E=UPN251_TL V UPN251-7T_TH (Genes/miRNA changes in response to high dose taxol in taxol resistance development). ↑ = significant up-regulated expression. ↓ = significant down-regulated expression.

*Not included in table: EPHA7 (discussed in section 6.4.1.1)

^Protein and mRNA expression examined

Table 6.7 Deregulated genes in the cytokine-cytokine receptor interaction pathway.

Gene*	Deregulation	Literature	Ovarian cancer/resistance linked references
CCL2	↓ B(2.5)	Down-regulation is linked to cisplatin and/or taxol resistance and poor prognosis in ovarian cancer cell line and patient data.	*(Arnold et al. 2005; Fader et al. 2010; Furukawa et al. 2013; Wojnarowicz et al. 2008)*
CCL20	↓ A(2.1), B(3.8)	Expressed at low levels in ascites fluid of ovarian cancer patients and cell lines after IL1 and TNF exposure	*(Schutyser et al. 2002; Son et al. 2007)*
IL23A	↓ B(2.4), D(2.6)	Deregulation is linked to ovarian cancer development but not yet chemoresistance. Also, deregulated in other cancer types.	*(Backman et al. 2014)*
IL18R1	↓ A(3.9), B(3.0)	Has not previously been identified in cancer.	
TNFRSF9	↓ B(2.8)	Currently under investigation as a novel target in ovarian cancer treatment.	*(Wei et al. 2013a)*
TNFRSF11A	↓ A(2.0), B(3.1)	Down-regulation is linked to cisplatin resistance in ovarian cancer cells. Also, deregulated in other cancer types.	*(Yoon et al. 2010)*
TNFRSF19	↓ A(2.6), B(2.3)	Deregulation is linked to temozolomide resistance in Glioblastoma. Also, deregulated in other cancer types but not yet linked to ovarian cancer.	*(Loftus et al. 2013)*

Deregulation=comparison (Fold Change); A=UPN251 V UPN251-7C (Genes/miRNA changes in carboplatin resistance development), Comparison B=UPN251_C V UPN251-7C_C (Genes/miRNA changes in response to carboplatin in carboplatin resistance development), Comparison D=UPN251_TL V UPN251-7T_TL (Genes/miRNA changes in response to low dose taxol in taxol resistance development). ↑ = significant up-regulated expression. ↓ = significant down-regulated expression.

*Not included in table: BMPR1B and BMP2 (discussed in Table 6.3), CSF1, IL1R1, IL7 and KITLG (discussed in Table 6.5)

stem cell proliferation in adult tissue and aberrant expression of its members has been linked to multiple cancer types, (*Evangelista et al. 2006*) including ovarian cancer (*Chen et al. 2007*). The exact same genes that were found by DAVID in the hedgehog signalling pathway were found in the basal cell carcinoma pathway. This was because hedgehog signalling plays a big part in the development of this carcinoma (*Daya-Grosjean et al. 2005*). Table 6.8 gives an overview of the genes identified in the hedgehog signalling pathway that have been linked to ovarian cancer and/or resistance.

6.4.1.2.5 Pathways in cancer

In DAVID, the 'Pathways in cancer' pathway brings up genes that are well established as being involved in cancer. A number of genes have already been discussed from the previous pathway analyses. However, any gene not covered previously will be summarised in Table 6.9. In total this included five genes (FGF18, JUP, MMP9, and LAMC2), which were all down-regulated in UPN251-7C compared to UPN251.

6.4.1.3 MiRNA-Target interactions (MTIs) for carboplatin resistance analyses

Figure 6.18 shows the possible miRNA-Target interactions (MTIs) networks for our carboplatin comparisons A and B (exploring expressional changes linked to carboplatin resistance). Table 6.10 gives the strengths of each interaction pair in the form of an r^2 value from a Pearson correlation test.

Analysis of comparison A (Exploring the difference between carboplatin-sensitive and carboplatin resistant cells), revealed only one miRNA that had validated interactions between two genes from our deregulated gene and miRNA lists (see Figure 6.18 (A)). MiR-205 was down regulated, while GLI3 and CTGF were up-regulated in UPN251-7C compared to UPN251. MiR-205 has been shown to be frequently down-regulated in advanced cancers, but has also been shown to be up-regulated in cancer depending on the tissue of origin (*Iorio et al. 2007*). This suggests that miR-205 has many different targets that can contribute to a cancerous phenotype (*Tsukamoto et al. 2014*). Although miR-205 up-regulation has been seen in previous ovarian cancer studies (*Zheng et al. 2013*; *Zhou et al. 2014*), its down-regulation might contribute to ovarian cancer carboplatin resistance in this study by allowing the expression of GLI3, a molecule of the hedgehog signalling pathway (section 6.4.1.2.4). Gli3 is known to be a marker of poor prognosis in NSCLC (*Bai et al. 2013*) and chemoresistance in cervical cancer (*Wen et al. 2014*). Regarding CTGF, normal ovarian epithelial cells usually

Table 6.8 Deregulated genes in the hedgehog signalling pathway.

Gene*	Deregulation	Literature	Ovarian cancer/resistance linked references
GLI3	↑ B(2.3)	Deregulated in other cancer types (not previously in ovarian cancer). Also, up-regulation has been associated with chemoresistance in cervical cancer.	*(Wen et al. 2014)*
HHIP	↓ B(2.7), D(2.8)	Up-regulated in ovarian endometrioid carcinoma but has not yet been identified in epithelial serous.	*(Steg et al. 2006)*
SMO	↓A(2.3), B(2.2)	Up-regulation is linked to taxol resistance in ovarian cancer cell line and patient data.	*(Chen et al. 2007; Steg et al. 2012)*
WNT7A	↓A(2.1), B(2.4)	Deregulated in ovarian cancer patients and cell lines. Its Linked to poor prognosis but not yet chemoresistance in ovarian cancer.	*(Merritt et al. 2009; Yoshioka et al. 2012; Zhang et al. 2010)*

Deregulation=comparison (Fold Change); A=UPN251 V UPN251-7C (Genes/miRNA changes in carboplatin resistance development), Comparison B=UPN251_C V UPN251-7C_C (Genes/miRNA changes in response to carboplatin in carboplatin resistance development), Comparison D=UPN251_TL V UPN251-7T_TL (Genes/miRNA changes in response to low dose taxol in taxol resistance development). ↑ = significant up-regulated expression. ↓ = significant down-regulated expression.

*Not included in table: BMP2 (discussed in Table 6.3)

Table 6.9 Deregulated genes in the pathways in cancer pathway.

Gene*	Deregulation	Literature	Ovarian cancer/resistance linked references
FGF18	↓ B(2.5)	Up-regulation is linked to poor prognosis and carboplatin/taxol chemoresistance in ovarian cancer patients.	*(Meng et al. 2014; Wei et al. 2013b)*
JUP	↓ B(2.6), C(2.6), D(2.3), E(2.1)	Has been investigated in ovarian cancer patients but was not found to be predictive of prognosis or recurrence.	*(Faleiro-Rodrigues et al. 2004)*
LAMC2	↓ B(4.3), C(3.3), D(4.0), E(2.8)	Deregulated in other cancer types (not previously in serous ovarian cancer, but was found in mucinous).	*(Okuma et al. 2010)*
MMP9	↓ B(3.1), D(2.6)	Deregulation is linked to ovarian cancer prognosis and chemoresistance. It has also been investigated as a target for therapy.	*(Laios et al. 2008b; Laios et al. 2013; Latifi et al. 2012; Li et al. 2013)*

Deregulation=comparison (Fold Change); Comparison B=UPN251_C V UPN251-7C_C (Genes/miRNA changes in response to carboplatin in carboplatin resistance development), Comparison C=UPN251 V UPN251-7T (Genes/miRNA changes in taxol resistance development), Comparison D=UPN251_TL V UPN251-7T_TL (Genes/miRNA changes in response to low dose taxol in taxol resistance development), Comparison E=UPN251_TL V UPN251-7T_TH (Genes/miRNA changes in response to high dose taxol in taxol resistance development). ↑ = significant up-regulated expression. ↓ = significant down-regulated expression.

*Not included in table: BMP2 (discussed in Table 6.3), ITGA2, ITGA6 and KITLG (discussed in Table 6.5), GLI3 and HHIP (discussed in Table 6.8).

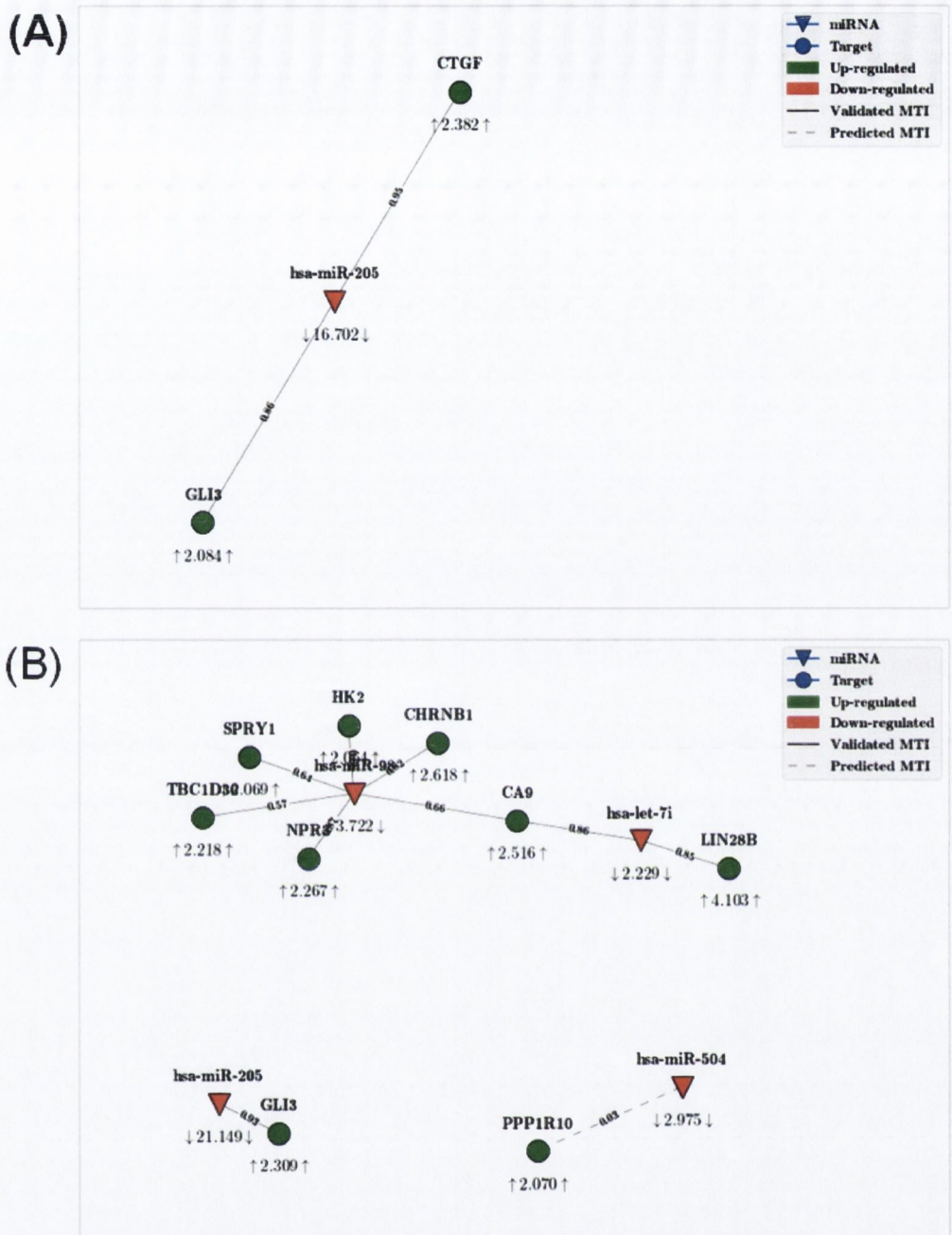

Figure 6.18 miRNA/mRNA interactions for comparisons A and B.

(A) Shows the possible interactions between mRNA and miRNA molecules in our cell lines for the de-regulated datasets of Comparison A (UPN251 V UPN251-7C) (B) Shows the possible interactions between mRNA and miRNA molecules in our cell lines for the de-regulated datasets of Comparison B (UPN251_C V UPN251-7C_C). The likelihood that a gene interacts with a miRNA is given as a r^2 value from a Pearson correlation test given on the line between each interaction and is based on their relative expressions from our Affymetrix array data. Please note that the distance of the lines is random and does not indicate strength of an interaction. Arrows/numbers represent the direction and fold of deregulation in UPN251-7C compared to UPN251.

Table 6.10 MiRNA-Target Interactions for carboplatin comparisons.

Validated or predicted status of in interaction is given along with the strength of the interaction in the form of an r^2 value from Pearson correlation analysis.

Comparison	miRNA	Gene	Status	R	r^2	Comparison	miRNA	Gene	Status	r	r^2
A	miR-205	CTGF	Validated	-0.98	0.95	B	Let-7i	CA9	Validated	-0.93	0.86
	miR-205	GLI3	Validated	-0.93	0.86		Let-7i	LIN28B	Validated	-0.92	0.85
							miR-98	CA9	Validated	-0.82	0.66
							miR-98	CHRNB1	Validated	-0.91	0.82
							miR-98	HK2	Validated	-0.81	0.66
							miR-98	NPR3	Validated	-0.93	0.87
							miR-98	SPRY1	Validated	-0.80	0.64
							miR-98	TBC1D30	Validated	-0.76	0.57
							miR-205	GLI3	Validated	-0.96	0.93
							miR-504	PPP1R10	Predicted	-0.17	0.03

Comparison A=UPN251 V UPN251-7C (Genes/miRNA changes in carboplatin resistance development), Comparison B=UPN251_C V UPN251-7C_C (Genes/miRNA changes in response to carboplatin in carboplatin resistance development), r=Pearson correlation coefficient value.

express CTGF. Its expression is frequently lost due to methylation during cancer progression (*Jacobson et al. 2012*). In early stage cancer, high expression has a protective effect with patients experiencing prolonged survival. However, in late stage ovarian cancer, where CTGF expression is restored, high expression is correlated to a malignant phenotype (*Kikuchi et al. 2007*). When CTGF acts as a tumour promoter, it promotes tumour invasion, cell survival and angiogenesis (*Jacobson et al. 2012*). Increased expression of GLI3 and CTGF by suppression of miR-205 may have contributed to UPN251-7Cs carboplatin resistant phenotype.

Again, the interaction of miR-205 and GLI3 was found in comparison B (Exploring the difference between carboplatin-sensitive and carboplatin resistant cells in response to carboplatin exposure (Figure 6.18 (B)). A predicted interaction between miR-504 and PPP1R10 was found, but this has not been experimentally validated. An interesting interaction from this analysis may be the expression of LIN28B repressing the expression of miRNA let-7i in UPN251-7C compared to UPN251. LIN28B is an inhibitor of the Let-7 processing system. High expression of LIN28B, which will result in reduced expression of Let-7 family members, is correlated with shorter progression free and overall survival in ovarian cancer (*Lu et al. 2009a*). Down-regulation of let-7i has been linked to cisplatin chemoresistance in ovarian cancer (*Yang et al. 2008b*). Knockdown and expressional studies in ovarian and breast cancer cell lines have confirmed that reduced expression of let-7i significantly increased cisplatin resistance. Microarray studies showed that decreased expression of let-7i in ovarian cancer patients correlated with shorter progression-free survival (*Yang et al. 2008b*). Also, our research group have found that there are reduced levels of let7i in the serum of ovarian cancer patients compared to benign cases (*Langhe et al. 2014*). These results indicate that let-7i may be a good candidate biomarker for platinum resistance in ovarian cancer. Our study indicates that this, in combination with LIN28B, may be a viable marker. The other gene that interacts with let-7i in our study is CA9, a transmembrane zinc metalloenzyme. Up-regulation of this gene, in combination with the up-regulation of VEGF, has been found to be a significant indicator of chemotherapy resistance and poor overall survival in serous ovarian cancer patients (*Williams et al. 2012*). In endometrioid and mucinous ovarian cancer, over-expression of CA9 is often seen. It has the potential to act as an independent indicator of poor patient survival (*Choschzick et al. 2011*). Our research group has shown CA9 to be down-regulated in ovarian cancer cell line A2780 in hypoxic conditions when treated with cisplatin (*McEvoy 2012*). CA9 also interacts with miR-98. However, our study predicts that this interaction is weaker than its interaction with let-7i. They had Pearson r^2 values of 0.66

and 0.86 respectively (see table 6.10). MiR-98 is another member of the let-7 family. Down-regulation, involving in the promotion of chemo-resistance in ovarian cancer, has been seen in the literature (*Wendler et al. 2011*). Aberrant miR-98 expression has also been shown to be involved in platinum resistance in lung cancer (*Xiang et al. 2013*). This interaction between miR-98 and CA9 may have a role to play in carboplatin chemoresistance in our cell lines. MiR-98 had a total of 5 validated targets found in our study in comparison B, comparing UPN251 to UPN251-7C after carboplatin exposure. It had the highest potential correlated interaction with NPR3 in our study, with a Pearson r^2 value of 0.87 (see Table 6.10). This gene encodes a natriuretic peptide receptor that is responsible for clearing circulating and extracellular natriuretic peptides through endocytosis of the receptor. High expression of this gene, in medulloblastoma patients, has been significantly associated with poor progression-free survival and overall survival (*Northcott et al. 2011*). This interaction may also play a role in our carboplatin resistance phenotype and may act as a potential biomarker in ovarian cancer platinum resistance.

6.4.2 Taxol resistance biomarker discovery

Three comparisons were made in order to discover biomarkers of taxol resistance from both the gene and miRNA array data sets;

C. UPN251 Vs UPN251-7T

D. UPN251_TL Vs UPN251-7T_TL

E. UPN251_TL Vs UPN251-7T_TH

Comparison C examined the differences in expression between parental UPN251 ovarian cancer cells and its taxol resistant subline UPN251-7T. Comparison D and E examined the differences in expression between parental UPN251 and its taxol resistant subline UPN251-7T, after the cells were exposed to a dose of taxol. In comparison D, a low dose of taxol (15ng/ml) was applied to both cell lines to examine expressional differences upon taxol exposure. In comparison, E UPN251-7T was exposed to a higher dose of taxol (60ng/ml), which was used to develop UPN251-7T's resistance phenotype in the cell selection strategy (Chapter 4). A lower dose of taxol (15ng/ml) was applied to UPN251 parental cells, as too much cell death occurred over a three day exposure to harvest enough RNA for array analysis.

Figures 6.19-6.24 gives a visual overview of the mRNA and miRNA data for each taxol comparison C, D and E. Each figure contains; (A) a clustering demograph of the

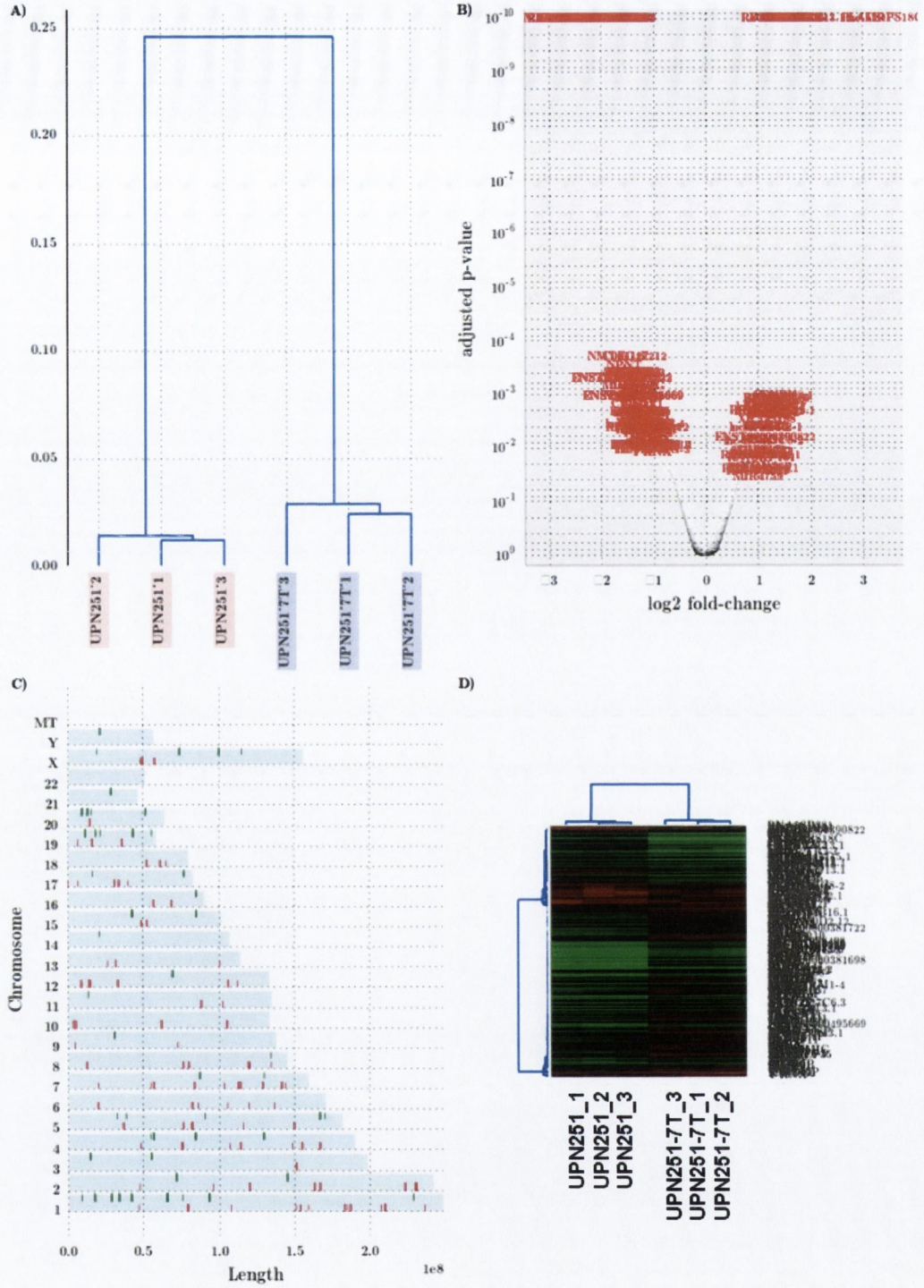

Figure 6.19 Overview of the deregulated gene expression from comparison C=UPN251 V UPN251-7T.

(A) Clustering demograph of hierarchical clustering analysis between replicates of both treatments. (B) Volcano plot. This shows the significance and scale of the fold change of each de-regulated gene. Adjusted P-value is given on Y-axis and Log 2 fold change is given on X-axis. (C) Chromosome location plot. Depicts the chromosomal locations of up-regulated (green) and down-regulated genes. (D) Heat map. This shows overall expressional changes between both treatments. High expression is given in (green) and low expression in (red).

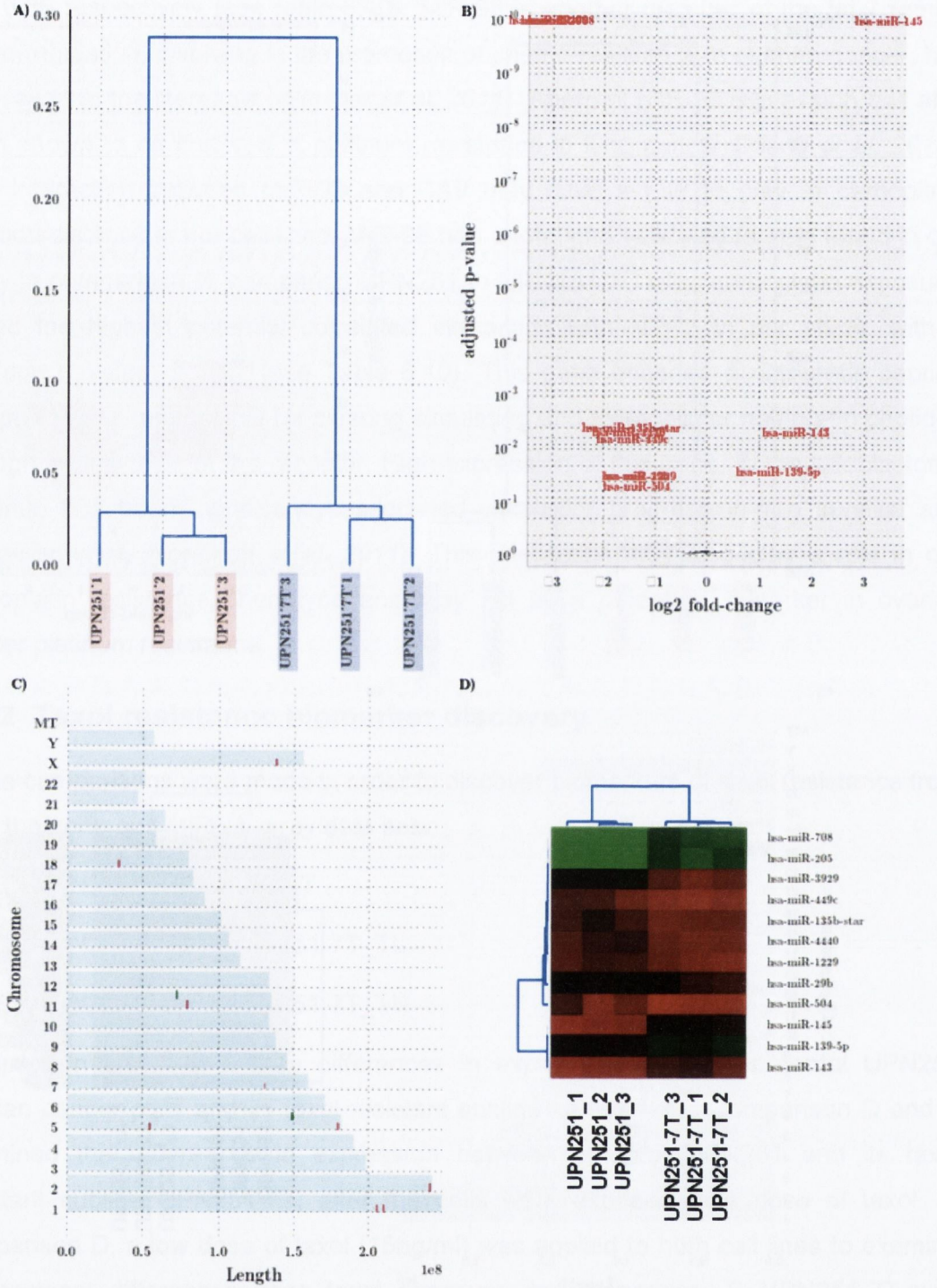

Figure 6.20 Overview of the deregulated miRNA expression from comparison C=UPN251 V UPN251-7T.

(A) Clustering demograph of hierarchical clustering analysis between replicates of both treatments. (B) Volcano plot. This shows the significance and scale of the fold change of each de-regulated miRNA. Adjusted P-value is given on Y-axis and Log 2 fold change is given on X-axis. (C) Chromosome location plot. Depicts the chromosomal locations of up-regulated (green) and down-regulated genes. (D) Heat map. This shows overall expressional changes between both treatments. High expression is given in (green) and low expression in (red).

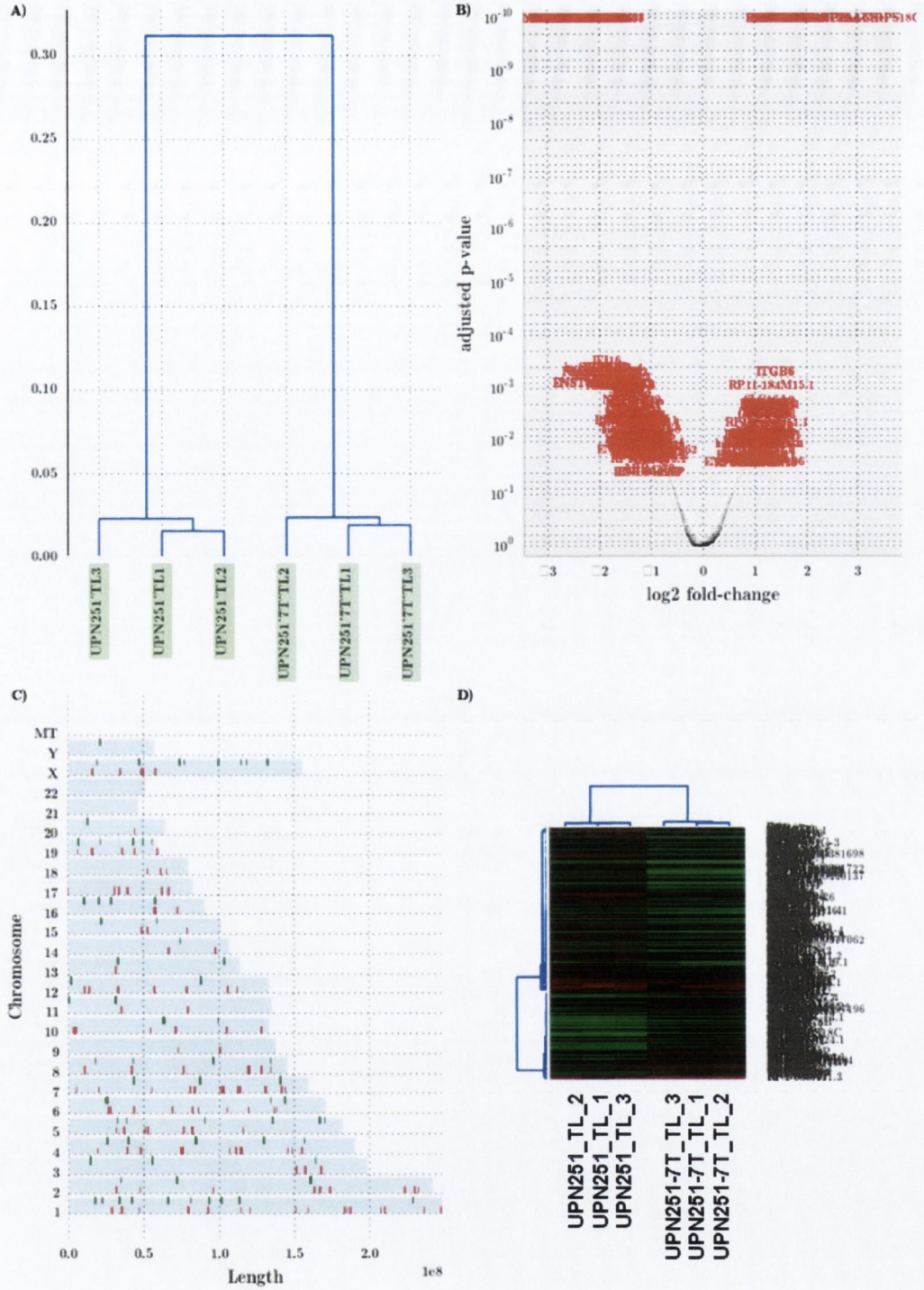

Figure 6.21 Overview of the deregulated gene expression from comparison D=UPN251_TL V UPN251-7T_TL.

(A) Clustering demograph of hierarchical clustering analysis between replicates of both treatments. (B) Volcano plot. This shows the significance and scale of the fold change of each de-regulated gene. Adjusted P-value is given on Y-axis and Log 2 fold change is given on X-axis. (C) Chromosome location plot. Depicts the chromosomal locations of up-regulated (green) and down-regulated genes. (D) Heat map. This shows overall expressional changes between both treatments. High expression is given in (green) and low expression in (red).

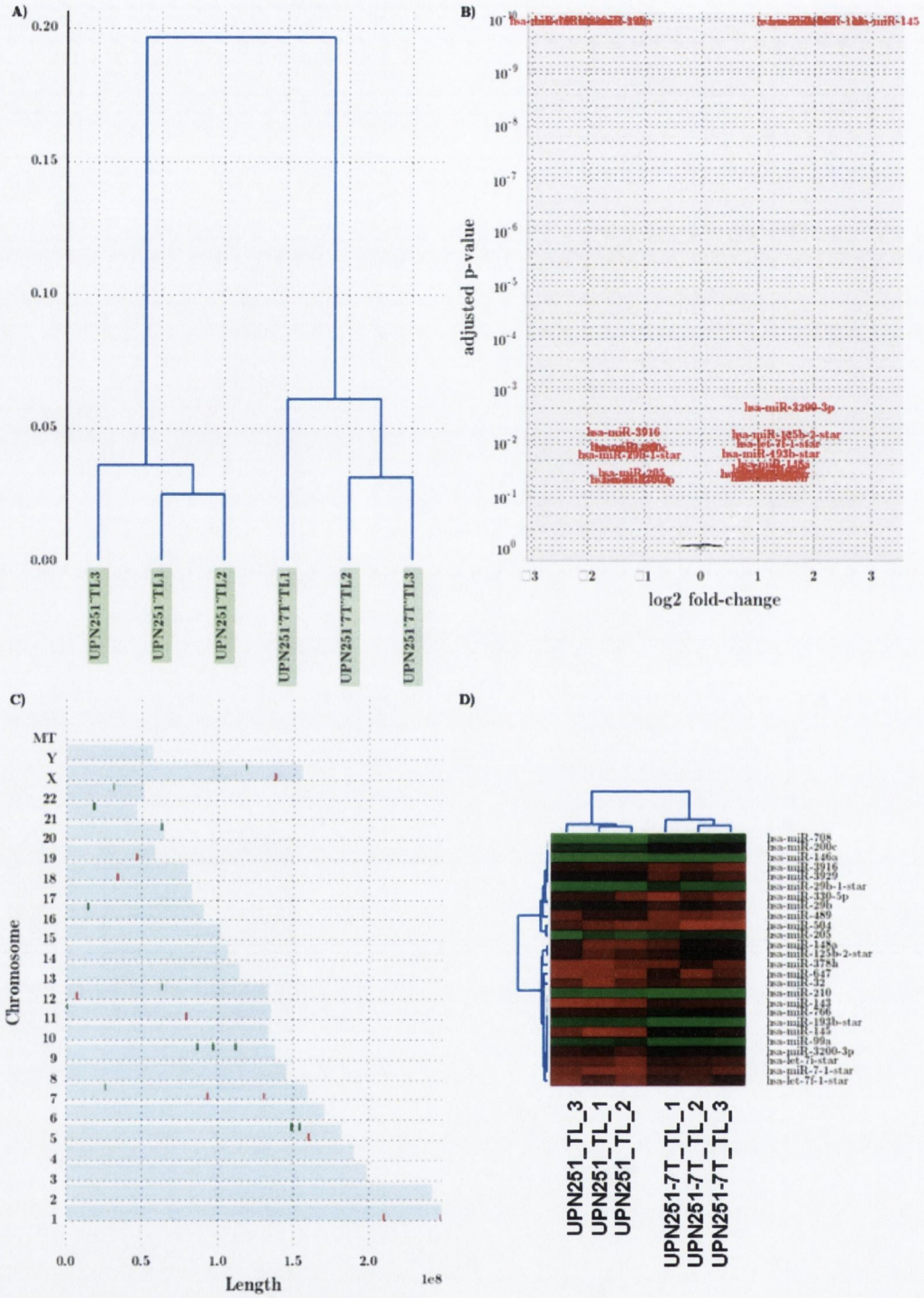

Figure 6.22 Overview of the deregulated miRNA expression from comparison D=UPN251_TL V UPN251-7T_TL.

(A) Clustering demograph of hierarchical clustering analysis between replicates of both treatments. (B) Volcano plot. This shows the significance and scale of the fold change of each de-regulated miRNA. Adjusted P-value is given on Y-axis and Log 2 fold change is given on X-axis. (C) Chromosome location plot. Depicts the chromosomal locations of up-regulated (green) and down-regulated genes. (D) Heat map. This shows overall expressional changes between both treatments. High expression is given in (green) and low expression in (red).

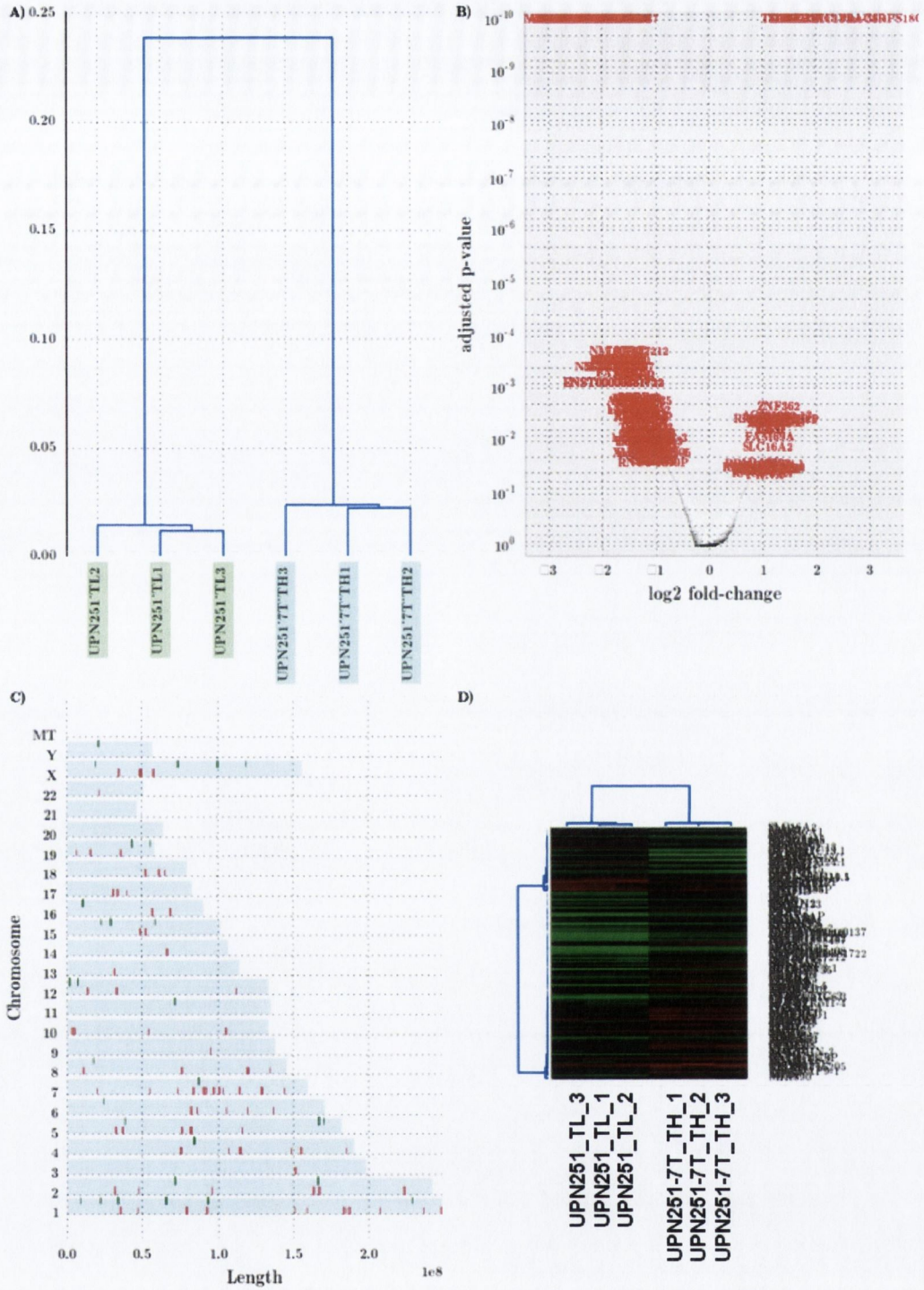

Figure 6.23 Overview of the deregulated gene expression from comparison E=UPN251_TL V UPN251-7T_TH.

(A) Clustering demograph of hierarchical clustering analysis between replicates of both treatments. (B) Volcano plot. This shows the significance and scale of the fold change of each de-regulated gene. Adjusted P-value is given on Y-axis and Log 2 fold change is given on X-axis. (C) Chromosome location plot. Depicts the chromosomal locations of up-regulated (green) and down-regulated genes. (D) Heat map. This shows overall expressional changes between both treatments. High expression is given in (green) and low expression in (red).

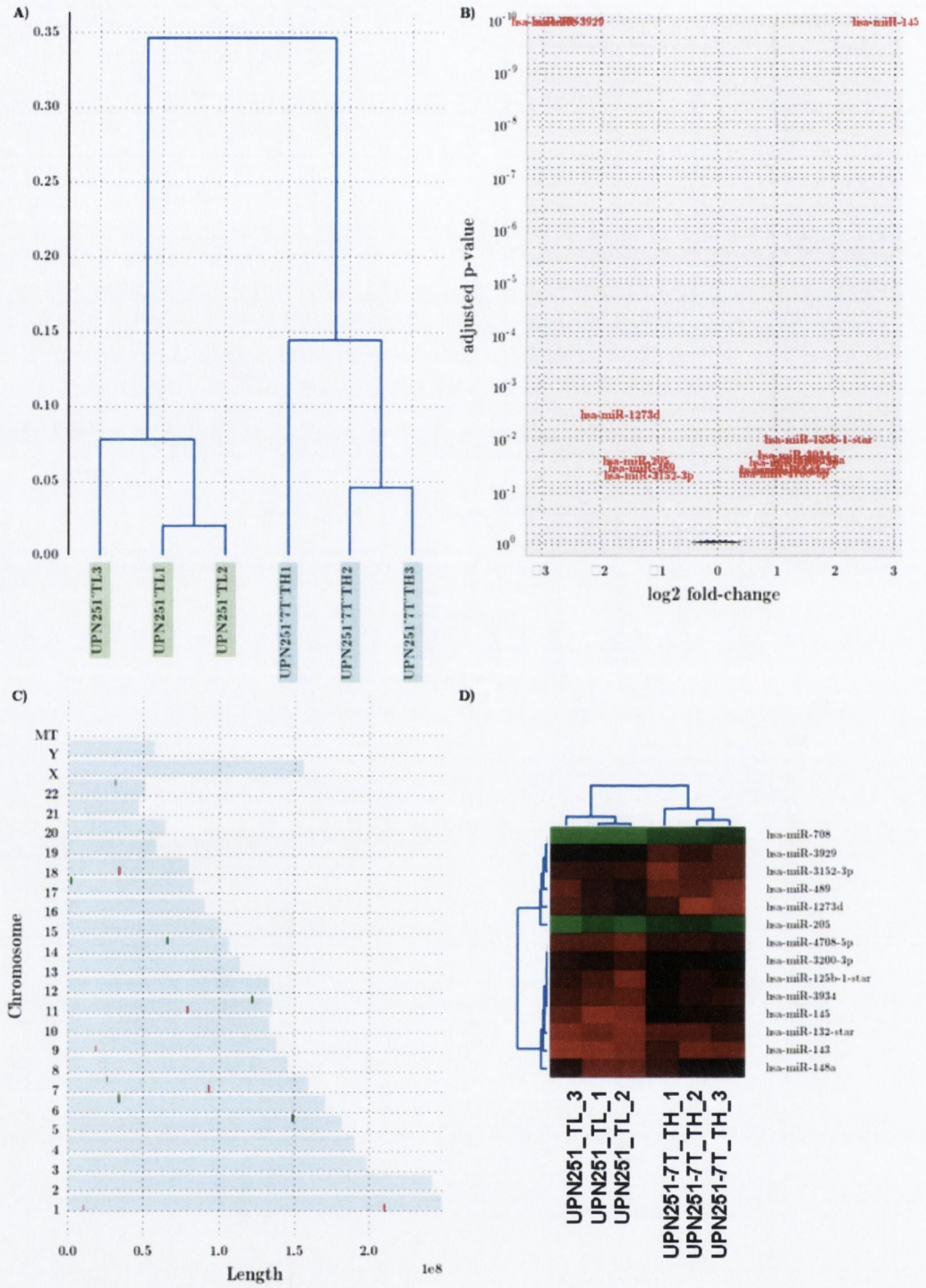

Figure 6.24 Overview of the deregulated miRNA expression from comparison E=UPN251_TL V UPN251-7T_TH.

(A) Clustering demograph of hierarchical clustering analysis between replicates of both treatments. (B) Volcano plot. This shows the significance and scale of the fold change of each de-regulated miRNA. Adjusted P-value is given on Y-axis and Log 2 fold change is given on X-axis. (C) Chromosome location plot. Depicts the chromosomal locations of up-regulated (green) and down-regulated genes. (D) Heat map. This shows overall expressional changes between both treatments. High expression is given in (green) and low expression in (red).

hierarchical clustering analysis between replicates of both treatments being compared, (B) a volcano plot showing the significance and scale of fold change (Log 2) of each de-regulated probe in a comparison, (C) a chromosome location plot depicting the chromosomal locations of up-regulated and down-regulated probes and (D) a heat map showing the overall expressional changes between both treatments. This gave a visual overview of the data obtained from Affymetrix analyses for specific comparisons of de-regulated probes for easy reference. A large amount of data was simply depicted allowing for the rapid identification of any patterns present in the data.

6.4.2.1 Top five deregulated genes and miRNAs

The top five most de-regulated genes and miRNAs between UPN251 and UPN251-7T from comparisons C, D and E are given in Table 6.11. As a general trend, there were more down-regulated genes than up-regulated genes in UPN251-7T compared to UPN251 in our comparisons, while a similar number of miRNAs were up- and down-regulated. There was a similar level of fold increased and decreased gene expression in our taxol comparisons, while the miRNA had much larger fold decreases than fold increases in UPN251-7T compared to UPN251. As in the carboplatin comparisons, all of the genes that appeared in the top 5 deregulated genes lists of C, D and E comparisons also appeared in the other comparisons gene list at some level of fold change (e.g. all of the top 5 deregulated genes found in C are also found in D and E comparisons). This indicates that the top genes that were subject to changes in expression during the development of taxol resistance were the same genes that were affected by response to drug exposure in the newly developed taxol-resistant cell lines.

Some of the genes and miRNAs that were found in our top five deregulated taxol comparisons were also found in the top five deregulated carboplatin comparison lists (Table 6.11 and 6.2 respectively). PLAC8 was highly up-regulated in all five carboplatin and taxol comparisons (comparing UPN251-7C/UPN251-7T to UPN251 under different conditions), while miR125b-1* was up-regulated in the top five lists of A, B and E comparisons. Both miR-205 and miR-708 were highly down-regulated in all of our comparisons (A-E, comparing UPN251-7C/UPN251-7T to UPN251 under different conditions). MiR-3200-3p was down-regulated in B, D and E's lists, implying that it may be involved in platinum/taxane drug response in chemoresistant sublines. As these genes and miRNAs have been previously discussed in the carboplatin resistance biomarker discovery section above (section 6.4.1), they will not be further discussed here.

Table 6.11 Overview of deregulated genes and miRNA for taxol comparisons.

Top 5 deregulated genes and miRNAs are given for each comparison at 2 Fold (base 10) cut off FDR p<0.05. Probe 1-Probe 5 represents the top 5 up/down-regulated genes or miRNAs in a comparison.

		Total	> FC	Probe1	FC	Probe2	FC	Probe3	FC	Probe4	FC	Probe5	FC
Comparison C: UPN251 V UPN251-7T (changes in taxol resistance development)													
UP-regulated	**Gene**	52	10.8	PLAC8	7.9	ABCB1	4.0	TENM2	3.5	MAP3K15	3.5	SRPX2	3.1
	MiRNA	3	11	miR-145	11.0	miR-143	3.3	miR-139-5p	2.6				
Down-regulated	**Gene**	118	8.9	MAL2	8.9	AREG	5.4	NID1	5.2	CRISPLD1	4.7	EDNRA	4.7
	MiRNA	9	8.9	miR-3929	8.9	miR-205	7.9	miR-708	7.2	miR-4440	2.9	miR-135b*	2.7
Comparison D: UPN251_TL V UPN251-7T_TL (changes in response to low dose taxol in taxol resistance development)													
Up-regulated	**Gene**	79	11.4	PLAC8	8.2	MAP3K15	4.5	ABCB1	3.7	TENM2	3.6	DYSF	3.3
	MiRNA	17	9.5	miR-145	9.5	miR-143	4.9	miR-766	3.4	miR-3200-3p	3.0	miR-210	3.0
Down-regulated	**Gene**	147	8.8	MAL2	8.8	AREG	8.0	EDNRA	6.4	CTSS	5.8	NID1	5.5
	MiRNA	12	6.7	miR-708	6.9	miR-3929	4.9	miR-29b	3.0	miR-146a	2.9	miR-135b*	2.7
Comparison E: UPN251_TL V UPN251-7T_TH (changes in response to high dose taxol in taxol resistance development)													
Up-regulated	**Gene**	34	10.0	PLAC8	7.0	MAP3K15	3.7	ABCB1	3.5	SRPX2	2.8	TENM2	2.6
	MiRNA	8	7.3	miR-145	7.3	miR-125b-1*	3.4	miR-148a	3.0	miR-3934	2.5	miR-3200-3p	2.5
Down-regulated	**Gene**	99	8.7	MAL2	8.7	AREG	7.7	EDNRA	5.6	NID1	4.8	CRISPLD1	4.3
	MiRNA	6	7.9	miR-708	7.8	miR-3929	5.9	miR-1273d	3.1	miR-205	2.6	miR489	2.4

Total= Total number of up or down regulated probes from a comparison (For gene chips this will include more than protein coding genes which we are interested in for this study (e.g. non protein coding genes, Long non coding RNAs, snoRNA etc.) Only top 5 deregulated genes are given in the body of the table), >FC = the greatest fold increase or decrease by a single probe from a comparison (base 10 Fold Change), FC= Fold Change (base 10).

Of the remaining transcripts, ABCB1, TENM2, MAP3K15, SRPX2, miR-145 and miR-143, were up-regulated and MAL2, AREG, NID1, CRISPLD1, EDNRA, miR-3929 and miR-135b* were down-regulated in the top 5 gene and miRNA lists of more than one taxol comparison (C, D or E). Table 6.12 gives an overview of all transcripts from our top five deregulated taxol comparisons (C, D and E) that are involved in ovarian cancer and/or resistance. The transcripts from our lists that have been linked to chemoresistance were ABCB1, SRPX2, miR-143, miR-145, miR-148a and miR-766 (up-regulated in UPN251-7T compared to UPN251) and AREG, CTSS, MAL2, miR-29b, miR-146a and miR-489 (down-regulated in UPN251-7T compared to UPN251). Those that were linked to chemoresistance in ovarian cancer were ABCB1, AREG, MAL2, miR-143, miR-145, miR-29b, miR-146a and miR-489.

P-glycoprotein (P-gp), the protein coded for by ABCB1 (MDR-1) gene, was found to be up-regulated in our taxol resistant subline UPN251-7T and down-regulated in our carboplatin resistant subline UPN251-7C when treated with carboplatin in chapter 5. This is reflected in our Affymetrix array data. ABCB1 mRNA was over-expressed in UPN251-7T compared to UPN251 in the C, D and E taxol comparisons and was under-expressed in UPN251-7C compared to UPN251 in the A and B carboplatin comparisons (exploring expressional changes linked to carboplatin resistance). As up-regulation of ABCB1 occurs with taxane resistance in our study and down-regulation of ABCB1 occurs in platinum resistance in our study, ABCB1/P-gp may have a role to play in the inverse resistance relationship between platinum and taxanes examined in chapter 4.

MAL2, a gene that codes for a multispan transmembrane protein of the MAL proteolipid family, has been found to be over-expressed in ovarian cancer by many independent microarray studies, but could not be linked to patient outcome (*Byrne et al. 2010*). However, MAL family members may be involved in acquired ovarian cancer resistance (*d'Adhemar et al. 2014*). Data from our group suggests that a functioning TLR4/MyD88 pathway is required for cells to acquire chemoresistance in ovarian cancer. Signalling from this pathway requires the interaction of MAL members with MyD88. For this reason MAL members may influence a resistance phenotype in ovarian cancer. Up-regulation of MAL2 specifically has also been linked to platinum resistance in pancreatic cancer (*Arumugam et al. 2009*).

AREG, like MAL2, has been shown to be up-regulated in cancer and cancer resistant phenotypes in the literature. However, MAL2 is down-regulated in UPN251-7T compared to UPN251 in our study. AREG over-expression has been found in ovarian cancer and has been linked to ovarian cancer progression and resistance

Table 6.12 Top five transcripts involved in ovarian cancer and resistance (taxol comparisons).

Gene/miRNA*	Function	Literature (gene/miRNA expression or stated if otherwise)	Source and references
↑ ABCB1	Transmembrane efflux pump.	Up-regulation is linked to taxol resistance and bad prognosis in ovarian cancer (*Chapter 1 section 1.6.1.*)	Cell lines: Ovarian cancer (SKOV-3(*Duan et al. 1999*), KF, SKOV-3, KOC7c (*Kamazawa et al. 2002*), ^2008 (*Parekh et al. 1997*)) Patient tumour tissue (*Kamazawa et al. 2002*; *Nakayama et al. 2002*)
↑ SRPX2	Brain development and possible role in angiogenesis.	Up-regulation is linked with chemotherapy resistance in leukaemia and un-favourable outcome in gastric cancer. It has not yet been linked to ovarian cancer.	Cell lines: leukaemia (UOC-B1) (*Kurosawa et al. 1999*) Patient gastric tumour tissue (*Yamada et al. 2014*)
↓ MAL2	Multispan transmembrane protein.	Up-regulation is linked with platinum resistance in pancreatic cancer. It is up-regulated in ovarian cancer tumour tissue#. Members of the MAL family have been linked with intrinsic chemoresistance in ovarian cancer.	Cell lines: ovarian cancer (SKOV-3 (*d'Adhemar et al. 2014*)) pancreatic cancer (L3.6pl, BxPC-3, CFPAC-1, SU86.86, PANC-1, Hs766T, AsPC-1, MIAPaCa-2 and MPanc96 (*Arumugam et al. 2009*)) Patient tumour tissue (*Byrne et al. 2010*; *d'Adhemar et al. 2014*)
↓ AREG	Autocrine growth factor.	Up-regulation is linked to chemoresistance and progression in ovarian cancer. It is also associated with resistance to a number of other chemotherapeutic agents in different cancer types.	Cell lines: ovarian cancer# (SKOV-3, CAOV3) Mouse xenografts models# and patient tissue (*Panupinthu et al. 2014*). Review: (*Berasain et al. 2014*)
↓ NID1	Cell interactions with the extracellular matrix.	Up-regulation is linked with ovarian cancer development.	Patient serum *(Zhang et al. 2012)*
↓ EDNRA	Receptor for endothelin-1 (involved in vasoconstriction).	Down-regulation is linked to better prognosis in ovarian and colon cancer.	Patient tumour tissue *(Rachidi et al. 2013)*
↓ CTSS	lysosomal cysteine	Up-regulation is linked to CPT-11 resistance to in colorectal cancer.	Cell lines: colorectal cancer (HCT116, LoVo, Colo205

	proteinase.		and HUVEC) *(Burden et al. 2012)* Patient xenografts *(Burden et al. 2012)*
↑ miR-145	Regulation of gene expression	Down-regulation has been linked to taxol resistance in ovarian cancer. Also, it is down regulated in ovarian cancer patients, compared to healthy individuals. However, it is highly up-regulated in ovarian cancer patients that are relapsers compared to those who are non-relapsers.	Cell lines: ovarian cancer (IGROV1, OVCAR3, ES2 and SKOV-3 (*Wu et al. 2013*) SKOV-3 and A2780 (*Zhu et al. 2014*)) Patient tumour tissue, serum (*Chung et al. 2013*; *Wu et al. 2013*) and ascites (*Chung et al. 2013*)
↑ miR-143	Regulation of gene expression	Down-regulated in ovarian cancer patients, compared to healthy individuals. However, it is highly up-regulated in ovarian cancer patients that are relapsers compared to those who are non-relapsers.	Patient tumour tissue (*Chung et al. 2013*; *Marchini et al. 2011*), serum and ascites (*Chung et al. 2013*)
↑ miR-139-5p	Regulation of gene expression	Down-regulated in ovarian cancer compared to normal ovarian tissue.	Patient tumour tissue *(Miles et al. 2012)*
↑ miR-766	Regulation of gene expression	Up-regulation is linked to chemotherapy response to 5-fluorouracil in cutaneous squamous cell and oesophageal carcinoma.	Patient tumour tissue *(Sand et al. 2012)*
↑ miR-210	Regulation of gene expression	Up-regulation is linked to recurrence, poor survival and metastasis in other cancer types. Also, up-regulation is seen in hypoxic conditions in ovarian cancer, promoting tumour growth and inhibiting apoptosis.	Cell lines: leukaemia (Reh and RS4;11) (*Mei et al. 2014*) Patient tumour tissue (*Greither et al. 2010*; *Hong et al. 2012*; *Li et al. 2014*; *Mei et al. 2014*; *Qiu et al. 2013*)
↑ miR-148a	Regulation of gene expression	Up-regulation is linked to cisplatin chemosensitivity in oesophageal adenocarcinoma and squamous cell carcinoma. Also, up-regulated in the majority of ovarian cancers.	Cell lines: ovarian cancer (SKOV-3 and OVCAR3) (*Zhou et al. 2012*) squamous cell carcinoma (KYSE410) and adenocarcinoma (OE19) (*Hummel et al. 2011*) Patient tissue (*Zhou et al. 2012*)
↓ miR-29b	Regulation of gene expression	Down-regulation is linked to chemotherapy resistance and poor prognosis in ovarian cancer.	Cell lines: ovarian cancer (ES2 and AMOC2) (*Sugio et al. 2014*) Patient tumour tissue (*Dai et al. 2014*; *Flavin et al.*

			2009; *Sugio et al. 2014*)
↓ miR-146a	Regulation of gene expression	Down-regulation is linked to poor overall survival in primary ovarian tumours. However, up-regulation in omental lesions is linked to increased survival and chemoresistance.	Cell lines: ovarian cancer (SKOV3) (*d'Adhemar et al. 2014*) Patient tumour tissue (*d'Adhemar et al. 2014*)) and omental lesions (*Vang et al. 2013*)
↓ miR-489	Regulation of gene expression	Down-regulation is linked to cisplatin chemoresistance in ovarian cancer.	Cell lines: ovarian cancer (SKOV-3 and OVCAR8) *(Wu et al. 2014)*

Green indicates up-regulation and red indicated down regulation of a gene or miRNA.

*Table excludes PLAC8 and miR-205 previously shown in Table 6.3

#Protein expression examined

^Protein and mRNA expression examined

(*Panupinthu et al. 2014*). AREG up-regulation has also been associated with resistance to a wide number of treatments including cisplatin, gefitinib, doxorubicin and sorafenib and hormonal treatments in various cancers (*Berasain et al. 2014*).

MiRNAs miR-145 and miR-143 have been shown to be co-down-regulated in endometrioid carcinoma and under-expressed in many cancers, acting as broad tumour suppressors in the literature (*Zhang et al. 2013*). The down-regulation of miR-145 is linked to taxol resistance in studies that examined ovarian cancer cell lines, patient tissue and serum samples (*Wu et al. 2013*; *Zhu et al. 2014*). Furthermore, the down-regulation of miR-143 and miR-145 has also been shown to occur in the serum of ovarian cancer patients, compared to healthy individuals (*Chung et al. 2013*). However, both miR-143 and miR-145 have been shown to be more highly up-regulated in ovarian cancer patients that are relapsers compared to those who are non-relapsers in a retrospective study of two independent tumour tissue collections (*Marchini et al. 2011*). This may indicate their suitability as a marker of prognosis in ovarian cancer and explain their up-regulation in UPN251-7T compared to UPN251 in our study.

Down-regulation of miR-29b has been strongly linked with taxol resistance and poor survival in ovarian cancer patients (*Dai et al. 2014*; *Sugio et al. 2014*). Lower expression of miR-29b and high expression of ATG9A and MAPK10, other known targets of miR-29b, has also been associated with shorter survival in ovarian cancer patients after chemotherapy (*Dai et al. 2014*). Our research group has shown that miR-29b is down-regulated in a significant proportion of ovarian cancer patients and that high miR-29b expression is linked with reduced disease-free survival (DFS) (*Flavin et al. 2009*). This may be an interesting candidate for the study of ovarian cancer resistance markers.

MiR-146a may have varied success as a candidate biomarker. It has been shown to act as both a tumour suppressor and tumour promoter under different conditions (*Li et al. 2014b*). Low expression of miR-146a in primary ovarian tumours is associated with poor overall patient survival, while increased expression of miR-146a in omental lesions result in increased survival and drug resistance (*Vang et al. 2013*). Our group has shown that miR-146a expression is significantly increased in MyD88 negative ovarian cancer cells (*d'Adhemar et al. 2014*). MyD88 positive ovarian cancer cells that had less miR-146a expression was associated with significantly reduced patient survival. This complimented the work from this study, as reduced expression of miR-146a was linked to taxane chemoresistance in our cell line UPN251-7T.

MiR-489 may be a useful candidate biomarker. Reduced expression was seen in cisplatin resistant ovarian cancer cell lines compared to non-resistant parental cells (*Wu et al. 2014*). Forced re-expression of miR-489 in SKOV3/CDDP and OVCAR3/CCDP ovarian cancer cell lines, resulted in cisplatin sensitivity. Similar results were seen with adriamycin resistant breast cancer cell lines MCF-7/WT, where re-expression of miR-489 resulted in adriamycin sensitivity (*Jiang et al. 2014*).

The remaining genes and miRNAs were either found to be deregulated in ovarian cancer (and/or other cancer types), but not linked to resistance (EDNRA, NID1, MiR-139-5p, miR-210), other cancer types (TENM2, CTSS, DYSF and miR-766), other diseased states (MAP3K15 and CRISPLD1) or were not found by literature searches (miR-135b*, miR-1273d, miR-3929, miR-3934 and miR-4440).

6.4.2.2 Pathway analysis by DAVID

Pathway analysis of C, D and E comparisons (exploring expressional changes linked to taxol resistance) by DAVID v6.7 was carried out on our gene array data to predict pathways that our deregulated genes may be involved in. Only comparison D (examining changes in expression between taxol-sensitive and resistant cells upon low dose taxol exposure) had enough genes listed to link groups of genes to specific pathways. C and E comparisons returned no results. An overview of the pathways predicted by DAVID from comparison D is given in Table 6.13. Four pathways were found in D namely; extra cellular matrix (ECM)-receptor interaction, small cell lung cancer, arrhythogenic right ventricle cardiomyopathy (ARVC) and pathways in cancer. A number of genes from this analysis were also returned by the pathway analysis of the carboplatin comparisons A and B. Those genes are indicated in Table 6.13 and will not be further discussed in this section.

6.4.2.2.1 Extra cellular matrix (ECM)-receptor interaction

Interactions between the extracellular matrix, via cell surface molecules, drive cellular changes such as adhesion, migration, differentiation, proliferation and apoptosis. These processes are known to be involved in cancer progression (*van Dijk et al. 2013*). Three genes from this pathway (GP6, ITGB6 and LAMB3), which were identified by DAVID, were only found in comparison D. All of the genes found in DAVID's small cell lung cancer pathway were also found in the ECM-receptor interaction pathway, so they will only be discussed here.

Laminin-5 chains LAMC2 and LAMA3 have previously been discussed in section 6.4.1.2.5. LAMB3 found in the ECM-receptor interaction pathway, along with LAMC2, is

Table 6.13 DAVID pathway analysis of deregulated genes found in comparisons D (Taxol).

De-regulated Genes	
Pathways in Comparison D (UPN251_TL V UPN251-7T_TL)	
ECM-receptor Interaction	GP6, ITGA2 , ITGA6, ITGB6, LAMB3, LAMC2
Small Cell Lung Cancer	ITGA2, ITGA6, LAMB3, LAMC2
Arrhythogenic Right Ventricle Cardiomyopathy (ARVC)	ITGA2, ITGA6, ITGB6, JUP, PKP2
Pathways in Cancer	HHIP, IL8, ITGA2, ITGA6, JUP, LAMB3, LAMC2, MMP9, WNT2B, WNT5A
Carboplatin (A and B) and Taxol (C,D and E) Analysis	
Genes From Taxol Analysis Also in Carboplatin Analysis	HHIP, ITGA2, ITGA6, JUP, LAMC2, MMP9
Genes Unique to Taxol Analysis	GP6, IL8, ITGB6, LAMB3, PKP2, WNT2B, WNT5A

(RED) genes are down regulated (Green) genes are up-regulated.

part of the same family of basement membrane proteins. It is the beta-2 chain, part of the multifunction cell adhesion molecule Laminin-5, which is composed of LAMB3 and two other chains (alpa-3 (LAMA3) and gamma-2 (LAMC2)). In the literature, LAMB3 has not been linked to serous ovarian carcinoma to date (As with LAMC2 and LAMA3). In prostate cancer, the expression of LAMB3 was found to be reduced during cancer development even though it has elevated expression in normal and cancerous tissue (*Reis et al. 2013*). Aberrant expression of GP6, which is up-regulated in UPN251-7T compared to UPN251 in our study, has not been linked with ovarian cancer or other cancer types in the literature, to our knowledge. Therefore, it may be a candidate novel resistance biomarker in ovarian cancer. Finally, Integrin ITGB6 was not found to be described in ovarian cancer in the literature. However, its up-regulation in UPN251-7T compared to UPN251 in comparison D may be a resistance linked adaptation to taxol drug response. In glioma patients, up-regulation has been shown to be linked with poor prognosis (*Schittenhelm et al. 2013*). This compliments our findings.

6.4.2.2.2 Arrhythogenic right ventricle cardiomyopathy (ARVC)

Arrhythogenic right ventricle cardiomyopathy (ARVC) is an inherited heart muscle disease which may result in arrhythmia, heart failure and sudden death (*Awad et al. 2008*). There was only one gene found in this list that had not been found previously in other DAVID pathway analyses. This gene was PKP2 and it was down-regulated in UPN251-7T compared to UPN251 in comparisons C, D and E (examining changes in expression between taxol-sensitive and resistant cells upon low dose taxol exposure). This gene is a member of the arm-repeat (armadillo) and plankophilin gene families and its gene product may regulate beta-catenin signalling. Up-regulation of PKP2 has been found in bladder cancer cell lines being linked with cell invasion capabilities (*Takahashi et al. 2012*). However, it has also been found to be down-regulated in gastric cancer tissue when compared to normal controls (*Demirag et al. 2011*). This study found a correlation between decreased expression and a shorter DFS. This indicates its possible utility as a prognostic marker.

6.4.2.2.3 Pathways in cancer

In DAVID, the 'Pathways in cancer' pathway brings up genes that are well established as being involved in cancer. A number of genes returned in the 'Pathways in cancer' pathway for comparison D, have already been discussed from being identified in previous pathway analyses. These include HHIP, ITGA2, JUP, LAMB3, LAMC2 and MMP9. Any genes not covered previously were discussed below. In total this included three genes, two of which are up-regulated (WNT2B and WNT5A) and one which is down regulated (IL8) in UPN251-7T compared to UPN251 when exposed to low dose taxol.

WNT2B and WNT5A are both genes that are part of the wingless-type MMTV integration site (WNT) family, which are known to function in many developmental processes, including cell growth and differentiation (*Willert et al. 2012*). Genes in this family have been linked to carcinogenesis. WNT2B, which is up-regulated in UPN251-7T compared to UPN251 in comparison D, has been shown to be involved in ovarian cancer resistance (*Wang et al. 2012*). Silencing of WNT2B expression by siRNA treatment in A2780 and C13K ovarian cancer cell lines resulted in sensitivity to cisplatin and taxol treatment respectively. Evidence concerning WNT5A's role in ovarian cancer is conflicting. Two studies have shown that increased expression of WNT5A is linked to poor prognosis in ovarian cancer patients (*Badiglian et al. 2009*; *Peng et al. 2011*). Contrary to these studies, *Bilter et al. (2011)* showed that loss of WNT5A is a predictor of poor patient outcome in ovarian cancer. They also demonstrated that WNT5A

signalling suppressing growth in ovarian cancer cells by triggering cellular senescence (*Bitler et al. 2011*).

IL8 is secreted by several cell types and is a key mediator of inflammatory response. IL8 is under-expressed in UPN251-7T compared to UPN251 in our study. In ovarian cancer, IL8 has been shown to be elevated in cyst fluid, serum, ascites and tumour tissue of ovarian cancer patients (*Fasciani et al. 2001*; *Kassim et al. 2004*; *Merritt et al. 2008a*; *Nowak et al. 2010*). Increased expression is correlated to poor prognosis and taxol chemoresistance (*Kassim et al. 2004*; *Penson et al. 2000*; *Uslu et al. 2005*). IL-8 is over-expressed in most human cancers and has been strongly linked to tumour progression and metastasis (*Tanaka et al. 2005*). From the literature, it is not clear why decreased expression of IL-8 is seen in our taxol treated, taxol resistant cell lines (UPN251-7T) compared to parental, non resistant cells (UPN251) treated with taxol. This may be a cell line specific response to taxol chemotherapy.

6.4.2.3 MiRNA-Target interactions (MTIs) for taxol resistance analyses

Figure 6.25 shows the possible miRNA-Target interactions (MTIs) networks for our taxol comparisons C, D and E (examining changes in expression between taxol-sensitive and resistant cells upon low dose taxol exposure and or treatment naïve). Table 6.14 gives the strengths of each interaction pair in the form of an r^2 value from a Pearson correlation test. In comparison C (examining expressional differences in taxol-sensitive and taxol resistant cells) three miRNAs were found to have possible interactions with different genes (Figure 6.25 (A)). MiR-139-5p and ANK2 had a predicted interaction, but this has not been validated experimentally. MiR-143 had a validated interaction with MACC1 from our list. Also, miR-145 had validated interactions with LIN28B and LAMC2. As previously discussed, both miR-143 and miR-145 have been found to be co-down-regulated in endometrioid carcinoma and under-expressed in many cancers, acting as broad tumour suppressors in the literature (*Zhang et al. 2013*). However, they have been shown to be more highly up-regulated in ovarian cancer patients that are relapsers compared to those that are non-relapsers in a retrospective study of two independent tumour tissue collections (*Marchini et al. 2011*). This could explain the up-regulation of these two miRNAs in our study of taxol chemoresistance. Also previously discussed, over-expression of LIN28B is linked with prognosis in ovarian cancer and chemoresistance (*Topp et al. 2014*; *Yan et al. 2013*) and LAMC2 over-expression is implicated in a number of cancer types with a possible function in tumour migration and invasion (*Okuma et al. 2010*). However, these two genes are down-regulated in these interactions in UPN251-7T compared to UPN251.

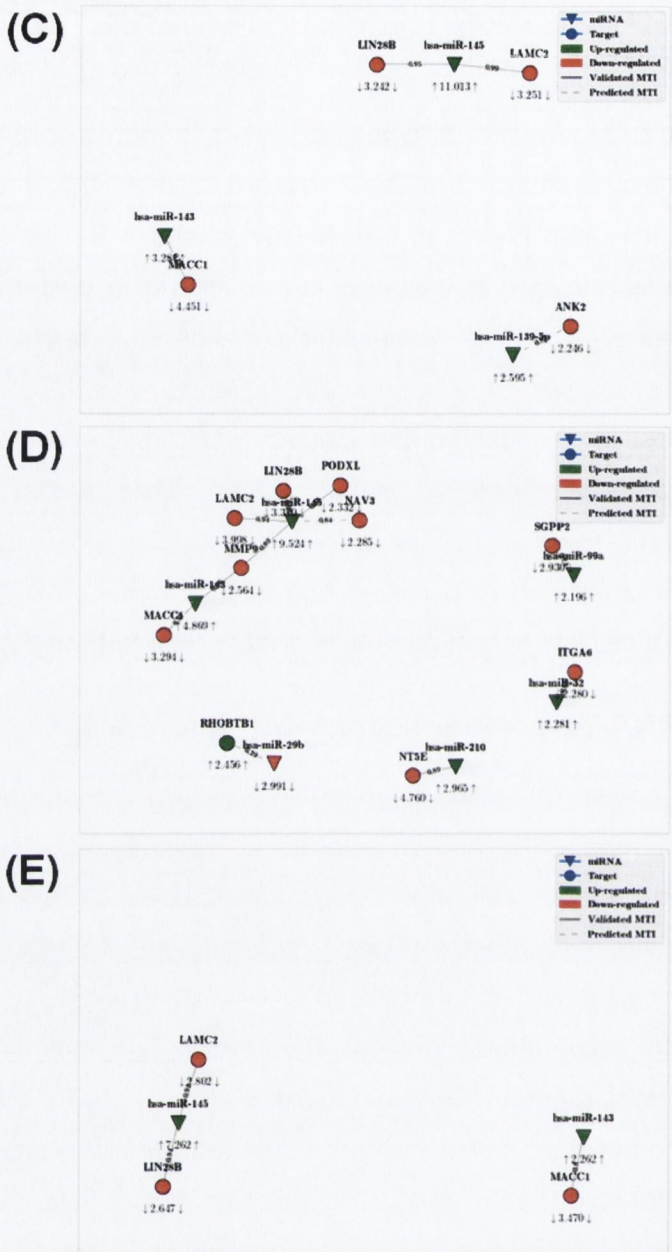

Figure 6.25 miRNA/mRNA interactions for taxol comparisons C, D and E.

(A) Shows the possible interactions between mRNA and miRNA molecules in our cell lines for the de-regulated datasets of Comparison C (UPN251 V UPN251-7T) (B) Shows the possible interactions between mRNA and miRNA molecules in our cell lines for the de-regulated datasets of Comparison D (UPN251_TL V UPN251-7T_TL) (E) Shows the possible interactions between mRNA and miRNA molecules in our cell lines for the de-regulated datasets of Comparison E (UPN251_TL V UPN251-7T_TH). The likelihood that a gene interacts with a miRNA is given as a r^2 value from a Pearson correlation test given on the line between each interaction and is based on their relative expressions from our Affymetrix array data. Please note that the distance of the lines is random and does not indicate strength of an interaction. Arrows/numbers represent the direction and fold of deregulation in UPN251-7T compared to UPN251.

Table 6.14 MiRNA-Target Interactions for taxol comparisons.

Validated or predicted status of in interaction is given along with the strength of the interaction in the form of an r^2 value from Pearson correlation analysis.

Comparison	miRNA	Gene	Status	R	r^2	Comparison	miRNA	Gene	Status	r	r^2
C	miR-139-5p	ANK2	Predicted	-0.91	0.83	D	miR-29b	RHOBTB1	Predicted	-0.63	0.40
	miR-143	MACC1	Validated	-0.88	0.78		miR-32	ITGA6	Validated	-0.83	0.69
	miR-145	LAM2C	Validated	-0.99	0.99		miR-99a	SGPP2	Validated	-0.86	0.74
	miR-145	LIN28B	Validated	-0.98	0.95		miR-143	MACC1	Validated	-0.98	0.97
							miR-143	MMP9	Validated	-0.98	0.96
							miR-145	LAMC2	Validated	-0.97	0.94
E	miR-143	MACC1	Validated	-0.90	0.80		miR-145	LIN28B	Validated	-0.95	0.91
	miR-145	LAM2C	Validated	-0.96	0.91		miR-145	MMP9	Validated	-0.94	0.89
	miR-145	LIN28B	Validated	-0.97	0.94		miR-145	NAV3	Predicted	-0.92	0.84
							miR-145	PODXL	Validated	-0.92	0.85
							miR-210	NT5E	Validated	-0.94	0.89

Comparison C=UPN251 V UPN251-7T (Genes/miRNA changes in taxol resistance development), Comparison D=UPN251_TL V UPN251-7T_TL (Genes/miRNA changes in response to low dose taxol in taxol resistance development), Comparison E=UPN251_TL V UPN251-7T_TH (Genes/miRNA changes in response to high dose taxol in taxol resistance development), r=Pearson correlation coefficient value.

MACC1 is a recently discovered gene that was initially shown to promote metastasis in colorectal cancer. MACC1 up-regulation has been shown to be an independent prognostic indicator of recurrence and disease-free survival in colorectal cancer patients (*Stein et al. 2009*). In ovarian cancer, higher expression was seen in cancer tissue compared to normal ovarian tissues and benign cancer tissues (*Zhang et al. 2011a*; *Zhang et al. 2011b*). Higher expression was associated with advanced stage, poor differentiation and lymph node metastasis. Suppression of MACC1 in ovarian cancer cell line OVCAR3 has been found to suppress the malignant biological behaviour of ovarian cancer in these cells (*Sheng et al. 2014*). This gene, along with LIN28B and LAMC2, are down regulated in UPN251-7T compared to UPN251 in our study for comparison C, which is contrary to evidence in the literature. Their down-regulated interaction, with over-expressed miR-143 and miR-145, may be a cell line specific mechanism taxol resistance present in our in our taxol resistant subline UPN251-7T.

The same validated interactions between miR-143 and miR145, which were seen in comparison C, also occurred in both D and E comparisons (examining expressional differences in taxol-sensitive and taxol resistant cells in response to taxol exposure, Figure 6.25 (A-C)). Therefore, these interactions may be involved in response to taxol exposure in taxol resistant cell lines and the generation of a long-term taxol resistant phenotype. Other interactions also occurred in comparison D. MiR-145 also interacted with MMP9, PODXL and NAV3 (NAV3 being a predicted interaction). MMP9 also interacted with miR-143. It had high r^2 values for both miRNAs (0.96 for miR-143 and 0.89 for miR-145, Table 6.14). As previously discussed, conflicting results have been seen in the literature concerning MMP9. Over-expression of MMP9 in ovarian cancer has been correlated with poor prognosis, good prognosis or to have no prognostic value in different studies (*Li et al. 2013*). Down-regulation of MMP9, through interactions with miR-143 and miR-145, may contribute to our taxol resistance phenotype in UPN251-7T. MiR-29b has a predicted interaction with RHOBTB1 in comparison D, but this is not experimentally validated. Of the remaining possible interactions in comparison D, up-regulated miR-210 as a target of suppressed NT5E (CD73) gives the highest r^2 value at 0.89 (Table 6.14). Up-regulation of miR-210 has been associated with recurrence, poor survival and metastasis in a number of cancer types including pancreatic, breast and glioblastoma (*Greither et al. 2010*; *Hong et al. 2012*; *Qiu et al. 2013*). Also, in ovarian cancer, miR-210 elevations have been seen in hypoxic conditions promoting tumour growth and inhibiting apoptosis *in vitro* (*Li et al. 2014b*). However, its target NT5E has been shown to confer shorter life expectancy in

patients with solid tumours when it is up-regulated, not down-regulated, as was seen in UPN251-7T compared to UPN251 in comparison D. Therefore, our results contradict the literature, meaning that NT5E may not be a viable marker for taxol resistance in clinical samples.

6.4.3 First response biomarker discovery

In order to examine which genes and miRNAs were de-regulated upon initial drug exposure in our non-resistant parental cells (UPN251) and carboplatin and taxol resistant sublines (UPN251-7C and UPN251-7T respectively), a number of comparisons were made between the deregulated gene and miRNA datasets. This allowed us to see the different genes and miRNAs which were affected by drug exposure in non-resistant and resistant cell lines for the doses of carboplatin (2μg/ml) and taxol (60ng/ml) used in our selection strategy (Chapter 4). Five comparisons were made in order to examine first response biomarkers;

F. UPN251 Vs UPN251_C

G. UPN251-7C Vs UPN251-7C_C

H. UPN251 Vs UPN251_TL

I. UPN251-7T Vs UPN251-7T_TL

J. UPN251-7T Vs UPN251-7T_TH

Comparison F examined the initial expressional changes that occurred in parental UPN251 cells, after exposure to 2μg/ml carboplatin. Comparison G examined the initial expressional changes that occurred in carboplatin resistant UPN251-7C cells, after exposure to 2μg/ml carboplatin. Comparison H examined the initial expressional changes that occurred in parental UPN251 cells, after exposure to 15ng/ml taxol. Comparison I examined the initial expressional changes that occurred in taxol resistant UPN251-7T cells, after exposure to 15ng/ml taxol. Finally, comparison J examined the initial expressional changes that occurred in taxol resistant UPN251-7T cells, after exposure to 60ng/ml taxol.

Table 6.15 gives an overview of the top five de-regulated genes and miRNAs in all five first response comparisons (F-J). The majority of expressional changes occurred in parental UPN251 cells after exposure to carboplatin (Comparison F). These cells were sensitive to carboplatin, so exposure to carboplatin had caused transcriptional changes in response to the stress of carboplatin exposure. Less transcriptional changes occurred in carboplatin resistant cell line UPN251-7C, when exposed to the same dose

Table 6.15 Overview of deregulated genes and miRNA for first response comparisons.

Top 5 deregulated genes and miRNAs are given for each comparison at 2 Fold (base 10) cut off FDR p<0.05. Probe 1-Probe 5 represents the top 5 up/down-regulated genes or miRNAs in a comparison.

		Total	> FC	Probe1	FC	Probe2	FC	Probe3	FC	Probe4	FC	Probe5	FC
Comparison F: UPN251 V UPN251_C (initial changes in parental cells treated with carboplatin)													
UP-regulated	**Gene**	40	4.3	PTPN22	3.8	CPA4	3.4	IL8	3.4	PLAT	2.9	F2RL2	2.5
	MiRNA	2	3.6	miR-3916	3.6	miR-584	3.1						
Down-regulated	**Gene**	12	2.9	HIST1H3F	2.9	HIST1H4B	2.8	HIST1H2BB	2.7	KCNIP1	2.6	HIST1H2BM	2.5
	MiRNA	0	N/A										
Comparison G: UPN251-7C V UPN251-7C_C (initial changes in carboplatin resistant cells treated with carboplatin)													
Up-regulated	**Gene**	5	3.4										
	MiRNA	0	N/A										
Down-regulated	**Gene**	3	3.5										
	MiRNA	2	2.6	miR-4274	2.6	miR-1238	2.6						
Comparison H: UPN251 V UPN251_TL (initial changes in parental cells treated with low dose taxol)													
Up-regulated	**Gene**	8	2.7	KRTAP2-4	2.7	OR2B6	2.5	NT5E	2.2				
	MiRNA	0	N/A										
Down-regulated	**Gene**	9	3.0	SLC17A1	3	MMP7	2.5	VCAM1	2.2	ITGB6	2.1		
	MiRNA	6	3.9	miR-205	3.9	miR-1285	2.7	miR-125b-2*	2.7	MiR-644*	2.6	miR-3187-5p	2.4
Comparison I: UPN251-7T V UPN251-7T_TL (initial changes in taxol resistant cells treated with low dose taxol)													
Up-regulated	**Gene**	0	N/A										
	MiRNA	2	2.6	miR-32	2.6	Let-7f-1*	2.4						
Down-regulated	**Gene**	0	N/A										
	MiRNA	0	N/A										
Comparison J: UPN251-7T V UPN251-7T_TH (initial changes in taxol resistant cells treated with high dose taxol)													
Up-regulated	**Gene**	4	2.7										
	MiRNA	1	2.9	miR-4708-5p	2.9								
Down-regulated	**Gene**	4	3.2	EDN2	3.2	ACSM2A	2.5	CNN1	2.3				
	MiRNA	1	2.3	miR-181c	2.3								

Total= Total number of up or down regulated probes from a comparison (For gene chips this will include more than protein coding genes which we are interested in for this study (e.g. non protein coding genes, Long non coding RNAs, snoRNA etc.) Only top 5 deregulated genes are given in the body of the table), >FC = the greatest fold increase or decrease by a single probe from a comparison (base 10 Fold Change), FC= Fold Change (base 10).

of carboplatin. These cells had made expressional changes during the selection strategy that allowed them to deal with the stress of carboplatin exposure without making further changes. Very few transcriptional changes occurred in comparison I, where UPN251-7T was exposed to 15ng/ml taxol at the two fold cut-off value. Two miRNAs (miR-32 and miR-7f-1*) were over-expressed in UPN251-7T treated with 15ng/ml taxol compare to treatment naïve cells. These cells did not seem to be stressed with this dose of taxol. It may be that sufficient amount of change had already occurred in these cells to resist this dose, without having to evoke more changes. The higher taxol dose (60ng/ml comparison J) also evokes little change in UPN251-7T. Therefore, it may have made enough changes to its phenotype to sufficiently deal with this higher dose also.

The de-regulated genes and miRNAs in this section will not be heavily discussed, however, a few interesting observations were made. F2RL2 was up-regulated in UPN251 carboplatin treated compared to treatment naïve cells in comparison F, but found to be down-regulated in UPN251-7C carboplatin treated compared to UPN251 carboplatin treated in comparison B. This implies that carboplatin sensitive cells up-regulate F2RL2, while carboplatin resistant cell lines down-regulate or don't change their expression of F2RL2, in response to carboplatin exposure. This gene encodes a protein of the protease-activated receptor, which has essential roles to play in homeostasis and thrombosis. This gene has not been linked with ovarian cancer in the literature, but was found to be down-regulated in rectal cancer patients during pre-operative radiotherapy by microarray expression studies (*Supiot et al. 2013*). MiR-3916 and miR-584 show the same pattern of expression in our comparisons with miR3916 also being down-regulated in UPN251-7T compared to UPN251 when treated with taxol in comparison D. MiR-3916 was not found in literature searches, while miR-584 has been found to act as a tumour suppressor. MiR-584 has been shown to have reduced expression in different cancer types (*Fils-Aime et al. 2013*; *Ueno et al. 2011*). These genes and miRNAs could act as interesting novel biomarkers of resistance in ovarian cancer.

Histone proteins drive epigenetic modification, a mechanism which can contribute to cancer development and progression when disrupted (*Sawan et al. 2010*). A number of genes coding for histones were found to be down-regulated in comparison F, but up-regulated in comparison B (HIST1H3F, HIST1H4B and HIST1H2BB). This implies that carboplatin-sensitive cells down-regulate these histones, while carboplatin resistant cell lines up-regulate or don't change their expression of these histones in response to carboplatin exposure. Literature searches involving HIST1H3F, HIST1H4B and

HIST1H2BB did not find any information linking these histones to ovarian cancer. Therefore, they have the potential to act as novel biomarkers for ovarian cancer resistance.

Similar expressional patterns were seen with H (UPN251's response to taxol) that were seen in F (UPN251's response to carboplatin). NT5E (CD73) was up-regulated in UPN251 when exposed to taxol compared to treatment naïve cells in the comparison H, while NT5E was down-regulated in UPN251-7T compared to UPN251 in the comparisons C-E. High expression of NT5E has been shown to confer shorter life expectancy in patients with solid tumours playing a role in neovascularisation, invasiveness and metastasis (*Xiong et al. 2014*). High expression has been put forward as a marker of aggressiveness in ER-negative breast cancer and chemoresistance to doxorubicin in triple negative breast cancer (*Loi et al. 2013*). Again, NT5E may have the potential to act as a novel biomarker for ovarian cancer resistance.

SLC17A1, VCAM1, ITGB6 and miR-125b-2* are all down-regulated in UPN251 treated with taxol compared to treatment naïve cells in comparison H, yet they are all up-regulated in UPN251-7T compared to UPN251 treated with taxol in comparison D. Interestingly, VCAM1 expression in mice models with ovarian cancer have been shown to be reduced in tumours that are carboplatin sensitive when treated with carboplatin, but remain elevated in tumours that are carboplatin resistant when treated with carboplatin (*Scalici et al. 2013*). This was seen in our study with taxol. UPN251 saw decreased expression of VCAM1 with taxol exposure compared to treatment naïve (comparison H) and UPN251-7T saw elevated VCAM1 expression in response to taxol exposure compared to UPN251 (Comparison D). Elevated VCAM1 is associated with poor prognosis, poor response to surgery and chemotherapy resistance in ovarian cancer (*Huang et al. 2013*). This gene encodes a protein which is a cell surface sialoglycoprotein expressed in cytokine-activated endothelial cells and is involved in leukocyte-endothelial cell adhesion and signal transduction (*Yamada et al. 2010*). SLC17A1, miR-125-2* and ITGB6 have not been reported on in ovarian cancer in the literature, to our knowledge.

6.4.4 Comparisons of de-regulation between datasets

The following investigations were taken in order to examine which genes and miRNA had been de-regulated in the same and opposite directions between the different comparisons describes in sections 6.4.1-6.4.3. The following investigations were undertaken:

- Comparison A (UPN251 V UPN251-7C) v Comparison C (UPN251 V UPN251-7T): To examine the differences and similarities in the gene/miRNAs that were deregulated in carboplatin and taxol resistance development.
- Comparison B (UPN251_C V UPN251-7C_C) v comparison D (UPN251_TL V UPN251-7T_TL): To examine the differences and similarities in the gene/miRNAs that were deregulated in response to carboplatin/taxol exposure in carboplatin and taxol resistance development.
- Comparison A (UPN251 V UPN251-7C) v Comparison F (UPN251 V UPN251_C): To examine the differences and similarities in the gene/miRNAs that were deregulated in initial carboplatin response and carboplatin resistance development.
- Comparison C (UPN251 V UPN251-7T) v Comparison H (UPN251 V UPN251_TL): To examine the differences and similarities in the gene/miRNAs that were deregulated in initial taxol response and taxol resistance development.

Table 6.16 gives an overview of the genes and miRNAs identified in these investigations. From the first investigation (Comparison A v C) we can see which genes and miRNAs were commonly up and down-regulated in both carboplatin and taxol resistant sublines (UPN251-7C and UPN251-7T respectively). These genes may be involved in platinum and taxane cross-resistance or may be involved in a general drug resistance phenotype. The genes and miRNAs that were de-regulated in opposite directions may be involved in the inverse resistance relationship between platinum and taxane drugs (Chapter 1, section 1.7.3). A systematic review of the literature has revealed that the most likely genetic players in the inverse resistance relationship are BRCA1 (Investigated in chapter 4), C-erbB2, Survivin, Bcl-Xl, Her-2, MAGE2, MAGE6, MRP1, PGK1, ABCB1, FHIT, GSTP1, p21, p53, p53wt, RB and Xrcc2 (*Stordal et al. 2009*). These genetic markers do not overlap with our first investigation (Comparison A v C), which gave four probes de-regulated in the opposite direction (Three protein coding genes (CD24P4, TENM2 and LIN28B) and one non-coding RNA (Y RNA)). These genes may also contribute to the inverse resistance relationship.

From our second investigation (Comparison B v D) we could see which genes and miRNAs were commonly up and down-regulated in both carboplatin and taxol resistant sublines (UPN251-7C and UPN251-7T respectively) when exposed to their respective selecting agent (carboplatin and taxol). These genes and miRNAs may be involved in platinum and taxane cross-resistance and drug response or may be involved in a

Table 6.16 Comparison of de-regulated probes (gene and miRNA) between datasets.

Examining which genes and miRNA had de-regulation in the same and opposite directions between different comparisons. Intersections were found using VENNY an online interactive tool for generating Venn diagrams (*Oliveros 2007*).

	De-regulated Probes
A - UPN251 V UPN251-7C (changes in carboplatin resistance development) V C - UPN251 V UPN251-7T (changes in taxol resistance development)	
Commonly Up-regulated	PLAC8, CTB-147C13.1, GDF15, MAP3K15, AC005392.13, AC004603.4, DYSF, CENPV, NPR3
Commonly Down-regulated	SERPINB7, DPP4, NPNT, AREG, ANK3, GAGE12J, MAL, CCDC68, MAMDC2, IFI44L, RAB27B, NID1, MMP7, EDNRA, IFI16, CRISPLD1, FBN1, CLEC4E, CYP4F11, LAMC2, MIR205HG, FAM129A, CTSS, C1orf116, FOXP2, RELN, IL7, FLRT3, SLC38A5, PLA2G4A, FAM46A, C3, MYO5C, IFI44, ID4, SLC1A3, RAB38, ALOX5AP, PID1, ALDH2, SLC1A1, TLL1, NTNG1, SLFN11, TSPAN1, TSPAN33, SGPP2, MAN1A1, INA, Y_RNA, IRF6, miR-708, miR-205, miR-449c
Up in A & Down in C	CD24P4, TENM2
Up in C & Down in A	LIN28B, Y_RNA
B - UPN251_C V UPN251-7C_C V (changes in response to carboplatin in carboplatin resistance development) D - UPN251_TL V UPN251-7T_TL (changes in response to low dose taxol in taxol resistance development)	
Commonly Up-regulated	PLAC8, CTB-147C13.1, MAP3K15, RNA5SP221, NPR3, miR-3200-3p, miR-210
Commonly Down-regulated	MAL, SERPINB7, MAMDC2, DPP4, TMEM47, IFI44L, AREG, FBN1, NPNT, NID1, GAGE12J, CCDC68, CTSS, C3, IFI16, ALOX5AP, IFI44, CYP4F11, CRISPLD1, EDNRA, ITGA2, LAMC2, SLC38A5, C1orf116, XDH, FAM129A, TNFAIP3, MMP9, FAM46A, SLC1A3, PID1, HHIP, PLA2G4A, SEMA3A, JUP, MYO5C, LINC00704, SLFN11, ITGA6, IL23A, AC108004.2, ALDH2, PODXL, MAN1A1, TLR2, AC112518.3, SGPP2, UCA1, miR-708, miR-205, miR-3916, miR-504
Up in B & Down in D	CD24P4, VCAM1, GUCY1B3, SLC34A2, SLC17A1, GPC4, TENM2, ABCB1
Up in D & Down in B	LIN28B
A - UPN251 V UPN251-7C (changes in carboplatin resistance development) V F - UPN251 V UPN251_C (Initial changes in parental cells treated with carboplatin)	
Commonly Up-regulated	RP11-255G12.3, GDF15, ANKRD1, SAA1
Commonly Down-regulated	MAP2K6, AC005725.1
Up in A & Down in F	MAMDC2, C3, ACTBL2, ALOX5AP
Up in F & Down in A	
C - UPN251 V UPN251-7T V (changes in taxol resistance development) H - UPN251 V UPN251_TL) Initial changes in parental cells treated with low dose taxol)	
Commonly Up-regulated	
Commonly Down-regulated	MMP7, MIR205HG, Y_RNA, miR-205, miR-4440
Up in C & Down in H	
Up in H & Down in C	NT5E

general drug response. The genes and miRNAs that were de-regulated in opposite directions may also be involved in the inverse resistance relationship between platinum and taxane drugs. Nine candidate protein coding genes were identified from our second investigation (CD24P4, VCAM1, GUCY1B3, SLC34A2, SLC17A1, GPC4, TENM2, ABCB1 and LIN28B). Of these genes, one overlapped with the literature review by *Stordal et al. (2009).* This gene was ABCB1, which is involved in taxane resistance by actively pumping the drug out of the cell. This may be a strong candidate for further investigation into the inverse resistance phenotype. Further evidence linking ABCB1 to the inverse resistance phenotype from our study is that ABCB1 mRNA was over-expressed in UPN251-7T in C, D and E comparisons and was under-expressed in UPN251-7C in A and B comparisons.

The final two investigations (Comparison A v F) and (Comparison C v H) look at which genes and miRNAs were commonly up and down-regulated between a resistant subline (UPN251-7C and UPN251-7T respectively) and their parental cell line (UPN251) treated with the same selecting agent used to develop resistance in the resistant subline (carboplatin and taxol respectively, table 6.16). The probes which were commonly up and down-regulated indicate the genes or miRNAs which are initially de-regulated in response to a selecting agent, which are still utilised by the resistant subline to convey its resistance phenotype. Again the genes and miRNAs that were de-regulated in opposite directions may be involved in the inverse resistance relationship between platinum and taxane drugs.

6.5 Conclusions

To date, single markers of prognosis and resistance have had limited success in the clinic. This study, using a clinically relevant selection strategy has the potential to provide an array of novel markers to test in clinical samples. However, due to the complexity of ovarian cancer at a molecular level it is unlikely that a single marker will have sufficient predictive power to be used in the clinic for prognosis or detection of resistant disease. It is more likely that the development of a transcriptomic signature of expression will have more success. The markers identified by this study may have predictive power by being incorporated into such a signature.

From the results of the Affymetrix gene and miRNA analyses using the resistant cell lines UPN251-7C and UPN251-7T, a number of potential carboplatin and taxol resistance biomarkers for ovarian cancer were identified.

Some genes and miRNAs were up- and down-regulated in the same or opposite direction, from what is reported in the literature. Those gene/miRNAs that were

deregulated in the opposite direction to those observed in ovarian cancer patients in the literature might be experiencing cell line specific de-regulation, which may not be transferable to the clinic as a biomarker. Cancer cell lines do not always translate directly to what is occurring in the clinic. However, they are useful for preliminary studies.

Genes and miRNAs deregulated in the same direction as is seen in the literature for ovarian and other cancer types have a better chance of transferring to the clinic as a biomarker. In this study, some of these markers had been linked to ovarian cancer resistance and/or poor overall/progression free survival previously in the literature from patients and/or cell lines data. Therefore, these markers may be useful on their own or in combination with other markers as ovarian cancer resistance biomarkers. These include; EEF1A2, GDF15, LIN28B, DPP4, BMP2, BMPR1B, KITLG, TNFRSF11A, CCL2, WNT2B, WNT5A, IL8, MMP7, VCAM1, Let-7i, miR-146a, miR-152, miR-98, miR-143, miR-29b and miR-489. Other markers have been found to be de-regulated in ovarian cancer in the literature, but have not yet been linked to resistance. Therefore, these markers may have potential utility as biomarkers of resistance in ovarian cancer. These include; IL7, SLIT2/3, ROBO1, CCL20 and miR-205. Other markers have been linked to chemo-resistance and/or poor overall/progression free survival in other cancer types and, therefore, may also play a role in ovarian cancer. These include; EPHA7, SEMA3A, GLI3, SRPX2, and miR-210 and miR-181c. The remaining markers with potential as resistance biomarkers are novel markers. These have been found to be deregulated in other cancer types or have not yet been studied in cancer. These include; MAP3K15, CTSS, SERPINB7, LAMB3, ITGB6, EDN2, miR-708, miR-532-3p, miR-125b-1*, miR-3128, miR-3200-3p, miR-3687, miR1272, miR-4417, miR-501-5p, miR-766, miR-3200, miR-3949, miR-3929, miR-4440, miR-3916, miR-1273, miR-4708-5p, miR-4274 and miR-1285. It is possible that the de-regulation of these genes and miRNAs are a cell line specific response to drug treatment and resistance development. This is the reason that biomarkers need to be validated in clinical samples.

The numerous pathways that the top de-regulated genes were involved in for both carboplatin and taxol resistance included apoptosis, tissue differentiation and maintenance, cell growth, cellular transformation, signal transduction, angiogenesis, embryogenesis, inflammation, interaction with extracellular matrix, cell adhesion and cell migration. Further to these pathways, pathway analysis by DAVID identified a number of pathways in which a number of de-regulated genes were found to be involved. These pathways included axon guidance, cytokine-cytokine receptor

interactions, hedgehog signalling, extra cellular matrix interactions, ARVC and pathways in cancer. All of these pathways have the potential to confer a chemo-resistant phenotype when de-regulated. This corroborates how complex signalling and interacting pathways contributed to carboplatin resistance in UPN251-7C and taxol resistance in UPN251-7T. This infers that complex interactions are occurring in ovarian cancer patients. This is further evidence that the development of transcriptomic signatures to identify resistant cancer would be better than the identification of single markers.

As gene arrays have had limited success in identifying markers of resistance in ovarian cancer, adding another layer to complexity in the form of miRNAs could lead to more success in the future of resistance biomarker discovery. Identifying mRNA and miRNAs from the same samples represents a novel approach to biomarker identification. This approach was taken in the present study. A number of MTIs were identified in this study that may have contributed to the UPN251 sublines resistance phenotype. The most interesting of these interactions were the down-regulation of miR-205 and up-regulation on GLI3 and the up-regulation of LIN28B and the down-regulation of let7-i. Identifying miRNAs that target gene products in pathways involved in resistance could be a good way of identifying novel targets for new therapies. In combination, interacting mRNA/miRNAs could provide more robust markers of prognosis and resistance, than mRNA markers on their own.

In addition, P-gp was further confirmed to be the dominant mechanism of taxol resistance in the taxol resistant subline UPN251-7T. It may also play a role in the inverse resistance relationship between platinums and taxanes along with CD24P4, GPC4, GUCY1B3, LIN28B, SLC17A1, SLC34A2, TENM2 and VCAM1. These could be useful in a panel of biomarkers to identify inverse resistance in patient samples. Such a panel could identify patients that are likely to respond to platinum or taxane salvage chemotherapy. Therefore, this panel could be used to optimise an individual patient's chemotherapy schedule and be used to monitor a patient's response to treatment.

CHAPTER 7

Resistance Biomarkers Clinical Validation



TRINITY
COLLEGE
DUBLIN

Chapter 7 Resistance biomarkers clinical validation

7.1 Introduction

Ovarian cancer is the leading cause of death from a gynaecological malignancy. Incidences of cancers throughout Europe show that ovarian cancer was the 5th most common cancer for all European women in 2012 (*Ferlay et al. 2013*). Standard chemotherapy approaches, such as the combination of taxol and carboplatin, often fail and patients relapse with chemoresistant ovarian cancer. Currently, approximately 75% of treated patients suffer from recurrence after treatment with cytoreductive surgery and platinum/taxane combination chemotherapy with a median survival of 2 years following the recurrence. All relapsed patients eventually die from their disease (*Ozols 2005)*.

The discovery of platinum/taxane resistance biomarkers is important in order to identify patients that are likely to relapse in response to this treatment. This will allow clinicians to use alternate treatments strategies which are more likely to increase the patient's disease free survival (DFS) or overall survival (OS) if they are diagnosed as resistant to platinum/taxane chemotherapy. Also, the identification of markers that contribute to a platinum/taxane resistance phenotype will help elucidate the underlying mechanisms of ovarian cancer resistance, allowing for the development of novel personalised treatments that can target or circumvent resistance mechanisms.

7.1.1 Aims and objectives

In this chapter, a subset of potential resistance biomarkers, identified from Affymetrix gene and miRNA chip analyses in chapter 6, were screened in ovarian cancer patient samples in order to identify markers that may have clinical utility in the diagnosis of platinum/taxane resistant disease. The expression of this subset of markers was tested in fresh frozen tissue samples from ovarian cancer patients by qPCR. The patient samples were classified into three groups, based on their sensitivity to platinum/taxane chemotherapy obtained from follow-up data. The samples were split into groups of responders, who were deemed platinum/taxane sensitive (patients who relapsed 12 months after completion of 1st line chemotherapy), non-responders, who were deemed platinum/taxane resistant (patients who relapsed within the first 6 months after completion of 1st line chemotherapy), and partial responders, who were deemed partially resistant to platinum/taxane chemotherapy (patients who relapsed between 6 and 12 months following completion of 1st line chemotherapy) (*Salzberg et al. 2005*).

The expression of these markers within the sample groups of this pilot study indicated whether or not further investigation in a larger cohort of patient samples would be valuable in the search for resistance biomarkers in ovarian cancer.

7.1.1.1 Hypotheses

The hypothesis examined in this chapter was:

- A number of mRNA/miRNA biomarkers for carboplatin and taxol resistance can differentiate between chemoresistant and chemosensitive epithelial serous ovarian cancer, the most common and aggressive histological subtype of ovarian cancer.

7.1.1.2 Objectives

The objective was to identify one or more mRNA/miRNA biomarkers for predicting response of ovarian cancer patients to standard platinum/taxane chemotherapy.

7.2 Methods

A selection of potential resistance biomarkers that were identified in chapter 6 were tested in fresh frozen tissue samples from ovarian cancer patients that were treated and biopsied in St. James's Hospital. Large and small RNA fractions were extracted from the tissue samples using the miRNeasy® Mini Kit (Qiagen Ltd, UK) as outlined in chapter 2 section 2.1.12. qPCR was carried out on the RNA extracted samples as outlined in chapter 2 section 2.1.16.

7.2.1 Patient sample details

32 fresh frozen tissue samples from the biobank at St. James's Hospital were selected for this study. All samples were obtained from chemo-naïve patients who were diagnosed with advanced (FIGO stage 3-4) serous papillary adenocarcinoma of the ovary. All samples were taken from patients undergoing primary surgery before 1st line adjuvant platinum containing chemotherapy. The patients' BRCA1 status was unknown. Informed consent was obtained from all patients prior to surgery and the use of the patient samples was approved by the Joint St James's Hospital/Adelaide and Meath Hospital Dublin Research Ethics Committee. The patients' clinicopathological details were assembled from the St. James's hospital archives. A summary of the relevant patient details for this study are given in Table 7.1. Survival data was calculated from patient records, which allowed us to determine disease-free survival (DFS), progression free survival (PFS), and overall survival (OS) for each patient in the study. DFS in cancer treatment is defined as the length of time after completion of 1st

Table 7.1 Patient details for pilot study.

Patient #	FIGO STAGE	Debulking Status	Chemotherapy	DFS	PFS	OS	Response Status
2	3C	Optimal	Carboplatin/taxol	2	7	16	NR
4	3C	Optimal	Carboplatin/taxol	18	23	46	R
5	3C	Optimal	Carboplatin/taxol	30	39	75	R
6	3C	Optimal	Carboplatin/taxol	19	23	48	R
7	3C	Suboptimal	Taxol then carboplatin	1	10	13	NR
9	4	Optimal	Carboplatin/taxol	18	23	32	R
10	3A	Unknown	Carboplatin	0	3	3	NR
11	3C	Optimal	Carboplatin/taxol	44	48	65+	R
12	3B	Optimal	Carboplatin/taxol	0	4	4	NR
15	3C	Optimal	Carboplatin/taxol	2	7	23+	NR
16	3B	Optimal	Carboplatin/taxol	34+	41+	40+	R
17	3B	Optimal	Carboplatin/taxol	21+	26+	26+	R
18	3C	Optimal	Carboplatin/taxol	22	27	36	R
19	3C/4	Optimal	Carboplatin/taxol	10	15	27	PR
20	4	Suboptimal	Carboplatin/taxol	4	9	9+	NR
21	4	Suboptimal	Carboplatin	3	7	7+	NR
22	3C	Optimal	Carboplatin/taxol	20	26	26+	R
23	3C/4C	Unknown	Carboplatin/taxol	5	10	33	NR
25	3C	Unknown	Carboplatin/taxol	38	44	50	R
28	3C	Optimal	Carboplatin/taxol	57+	63	63+	R
30	3C	Optimal	Carboplatin/taxol	11	17	63	PR
33	3C	Suboptimal	Carboplatin	0	5	9	NR
34	3C	Optimal	Carboplatin/taxol	39	44	71	R
35	3C	Optimal	Carboplatin/taxol	4	8	11	NR
36	3C	Unknown	Carboplatin	0		9	NR
37	3C	Optimal	Carboplatin/taxol	42	48	66	R
39	3C	Suboptimal	Carboplatin/taxol	7	11	11+	PR
40	4	Unknown	Cisplatin/taxol	20	25	96	R
43	4	Unknown	Carboplatin/taxol	0	3	19	NR
44	3	Unknown	Carboplatin	10	17	27	PR
46	3C	Unknown	Carboplatin/taxol	0	3	5	NR
47	3C	Unknown	Carboplatin/taxol	16	20	52	R

PFS, DFS and OS are given in months

+ indicates that an event has not yet occurred at this time point (The last entry in the patient's records) but may still occur in the future. This data was censored for analysis.

line chemotherapy that there was no sign or symptoms of the patient's cancer (i.e. the date chemotherapy was finished to date of first recurrence). A cancer patient's PFS is defined as the length of time from the start of treatment to recurrence (i.e. the date of surgery to the date of relapse or follow-up if relapse did not occur). A cancer patient's OS is defined as the length of time after a patient's surgery that the patient is still alive (i.e. the date of surgery to the date of death).

Response data was determined from a patient's DFS and was used to group patients according to their platinum chemosensitivity status. Responders to chemotherapy (platinum sensitive) were defined as having a DFS of > 12 months, non-responders to chemotherapy (platinum resistant) were defined as having a DFS < 6 month, and partial responders (partially platinum resistant) were defined as having a DFS of between 6 and 12 months (*Chien et al. 2013*; *Pfisterer et al. 2006a*). In total 15 responders (R), 13 non-responders (NR) and 4 partial responders (PR) were recruited into our pilot study.

7.2.2 Biomarker selection for clinical validation

A three pronged approach was taken as a risk reduction strategy in order to select potential ovarian cancer resistance biomarkers. These biomarkers were identified by Affymetrix analysis of carboplatin and taxol resistant cell lines, carried out in chapter 6 (UPN251-7C and UPN251-7T respectively). The chemoresistant cell lines were initially developed in chapter 4.

Firstly, from chapter 6, the top five de-regulated genes and miRNAs and the de-regulated genes identified by DAVID pathway analysis from carboplatin and taxol resistance related comparisons (A-E), were investigated by literature searches using PubMed to identify previous work carried out on the potential biomarkers relating to cancer resistance. This allowed the identification of aspects of the potential biomarkers that may support their clinical utility, using evidence from the literature. A detailed definition of comparisons (A-E), referenced in this section, is given in Chapter 6 section 6.2.4.3. Briefly;

A). UPN251 (untreated) v UPN251-7C (untreated)

B). UPN251_C (2µg/ml carboplatin) v UPN251-7C_C (2µg/ml carboplatin)

C). UPN251 (untreated) v UPN251-7T (untreated)

D). UPN251_TL (15ng/ml taxol (low dose)) v UPN251-7T_TL (15ng/ml taxol (low dose))

E). UPN251_TL (15ng/ml taxol (low dose)) v UPN251-7T_TH (60ng/ml taxol (high dose))

Secondly, the deregulated comparisons were subjected to miRNA-target interactions (MTIs) analysis, as described in chapter 6 section 6.2.4.3.1. This allowed the identification of validated and predicted MTIs that occurred in the de-regulated comparisons. This interacting pair may present us with an attractive target for therapeutic intervention or a stronger prognostic resistance biomarker than a solitary mRNA or miRNA.

Finally, all of the top five deregulated probes, probes identified by DAVID and probes identified by MTIs analysis were assessed using OVMARK; an online tool for correlating transcriptomic data to ovarian cancer survival (*Madden et al. 2014*). OVMARK is an algorithm that allows for the identification of gene/miRNA subsets that are associated with disease progression in ovarian cancer. The algorithm integrates gene expression microarray data (often containing miRNA expression data) and clinical data to correlate clinical outcome using differential gene and miRNA expression levels. In total, the algorithm incorporates data from 14 datasets on 7 different microarray platforms to report on approximately 17,000 genes and 341 miRNAs in up to 2,129 patient samples (*Bonome et al. 2008*; *Crijns et al. 2009*; *Denkert et al. 2009*; *Ferriss et al. 2012*; *Konstantinopoulos et al. 2010*; *Konstantinopoulos et al. 2011*; *Mateescu et al. 2011*; *Mok et al. 2009*; *Spentzos et al. 2005*; *The Cancer Genome Atlas Network 2011*; *Tothill et al. 2008*; *Yoshihara et al. 2010*; *Yoshihara et al. 2012*).

In our study, both survival options (DFS and OS) were selected separately when analysing our targets with OVMARK. Targets were analysed in the full patient and the platinum/taxane cohort using a median cut-off value. The cut-off value refers to the expression level used to determine the groups for high and low expression of a given marker within the individual datasets analysed by OVMARK. The median was used as the cut-off value in our analyses. When a sample was assigned to the high or low expression group within its database, the 14 datasets were combined and global survival analysis was performed. OVMARK treats each dataset separately when determining the high or low expression groups, as the target of interest will vary greatly across different platforms/experiments. The full patient cohort contains all patient samples available for a given marker to be tested from the 14 datasets. The platinum treatment and taxane treatment cohorts only contain samples from patients where the study states that they have been treated with platinum or taxane chemotherapy respectively. A combined target analysis was also carried out. Using this option, patient samples with the two targets of interest, which are both over-expressed, are compared

to all of the remaining patient samples in a selected cohort. By selecting the inverse option, patient samples with one marker over-expressed and the other marker under-expressed were compared to remaining patients in a selected cohort.

Targets which, when analysed in OVMARK, had a significant log-rank p-value and a hazard ratio (HR), which complemented the direction of de-regulation of our marker on the Affymetrix platform (chapter 6), were considered as interesting candidate biomarkers. P-values were adjusted for multiple testing using the Benjamini-Hochberg method (*Benjamini et al. 1995*). The HR was calculated by Cox regression analysis. A HR value of >1 indicated that the target expression when up-regulated in ovarian cancer patients is associated with poor prognosis. Conversely, a hazard ratio of <1 indicated that the target expression when up-regulated is associated with good prognosis. For example, a HR of 2 implies that patients with high expression of a tested marker will do twice as poorly as those with low expression. The opposite is true for patients with a HR of 0.5. When using OVMARK, it is important to remember that the risk estimate is always based on increased expression of a marker.

7.2.3 Kaplan-Meier survival analysis

The relationships between gene/miRNA expression and PFS and OS were examined using Kaplan-Meier survival curves, using the GraphPad Prism 5 Software. This programme allows for censoring when an event has not occurred (e.g. death or recurrence) (*Bland 1998*). A number of assumptions are made when using this method. It is firstly assumed that the survival probabilities are the same for subjects recruited early and late into a study. This did not apply to our study as all patients were monitored independently for follow-up. Samples were collected and flash frozen at the time of surgery and stored in a bio-bank until required for experimentation. Therefore, early and late recruitment does not apply. The second assumption states that censored patients have the same survival prospects as those who are followed. In our study, the patient data was censored if the patient had not yet progressed or died. The third and final assumption states that it is assumed that events occur at the time specified. This is accurate for certain events, for example, the date of death in a patient is unequivocal. For other events it was not so clear cut. For example, the time of patient progression can be more complicated as the exact time of progression is not always clear from patient records. In ovarian cancer management, CA125 levels are routinely checked at six month intervals. A rise in CA125 can be an indicator of disease recurrence. However, some clinicians only conclude that a patient has recurred when they become symptomatic. For this reason, it is not always clear when exactly a patient

has recurred. The time of recurrence in our study was determined as being the time when a recurrence was identified by radiology and logged into patient notes by their consultant. The survival curves generated by the Kaplan-Meier method were generated using a product limit formula and compared using the log rank test (*Bland 2004*). This is a non-parametric hypothesis based test used in comparing survival distributions of two groups and can be applied to censored data. It uses the same assumptions as those used to generate the survival curves (*Bland 2004*). If an individual's patient data was censored, it was considered to be at risk of an event (e.g. recurrence or death) at the time of censoring, but not in subsequent time points (*Bland 2004*). The Kaplan-Meier curves in this study were based on gene/miRNA expression, so that expression of a marker could be linked to survival in our cohort of patients. For the Kaplan Meier analysis, the HR is defined as being a ratio of the slopes of the survival curves. It compares two patient groups, computing the HR from all the data present (not at any one time point). For example, if the HR is 2, then the rate of an event (DFS/OS) in one treatment group is twice that of the other. It is assumed that the population HR is consistent over time, with any differences being due to random sampling (assumption of the proportional hazards). One caution is that if the HR is not consistent over time, the value that prism reports will not be useful.

7.3 Results

7.3.1 Selection of targets for clinical validation

Four genes (LIN28B, SRPX2, CCL20 and GLI3) and two miRNAs (let-7i and miR-205) were selected for further validation in our pilot study using patient samples. The rational for selecting each target is described below. Table 7.2 demonstrates the results of each target when analysed with OVMARK (an online tool which combines array expression data from different studies). Both the full-patient and the taxane/platinum cohorts were assessed separately. Samples were also analysed in pairs by OVMARK to see if they would improve DFS or OS compared to each target individually. Pairing the targets did not improve the log-rank p-value or the HR in most combinations. However, one pairing resulted in an improvement. The combination of GLI3 over-expression and CCL20 under-expression gave a significant p-value of 0.03 and a HR of 1.199 (1.013 - 1.42) in the all-patient cohort for DFS.

A detailed definition of comparisons (A-E) referenced in the following sections is given in Chapter 6 section 6.2.4.3

Table 7.2 OVMARK results for candidate platinum/taxane resistance biomarkers.

Target	Affymetrix de-regulated expression: Comparisons (FC)	All Patients DFS	Poor Prognosis	All Patients OS	Poor Prognosis	Pt & Taxol Treated DFS	Poor Prognosis	Pt & Taxol Treated OS	Poor Prognosis
CCL20	↓ A(2.1), B(3.8)	n=996 p=0.1417 HR=0.897 (0.776-1.037)	↓	n=1990 p=0.07537 HR=0.895 (0.792-1.011)	↓	n=451 p=0.6009 HR=0.944 (0.760-1.172)	↓	n=454 **p=0.02001** HR=0.715 (0.538-0.950)	↓
GLI3	↑ B(2.3)	n=996 p=0.05833 HR=1.149 (0.995-1.328)	↑	n=1833 p=0.14 HR=1.102 (0.969-1.253)	↑	n=451 **p=0.04021** HR=1.253 (1.01-1.554)	↑	n=454 p=0.1346 HR=1.24 (0.935-1.644)	↑
LIN28B	↑ A(3.0), B(4.3) ↓ C(3.2), D(3.4), E(2.6)	n=811 **p=0.01** HR=1.236 (1.05-1.455)	↑	n=910 **p=0.001644** HR=1.35 (1.119-1.629)	↑	n=451 **p=0.04488** HR=1.249 (1.005-1.552)	↑	n=454 p=0.1458 HR=1.233 (0.929-1.635)	↑
SRPX2	↑ C(3.1), D(2.9), E(2.8)	n=996 p=0.09885 HR=1.129 (0.977-1.304)	↑	n=1990 **p=0.003354** HR=1.199 (1.062-1.355)	↑	n=451 p=0.2012 HR=1.151 (0.928-1.428)	↑	n=454 p=0.09227 HR=1.273 (0.961-1.688)	↑
Let-7i	↓ B(2.2)	Not in OVMARK	-	Not in OVMARK	-	Not in OVMARK	-	Not in OVMARK	-
miR-205	↓A(16.7),B(21.1),C(7.9) D(2.3), E(2.6)	n=329 p=0.1479 HR=0.820 (0.627-1.073)	↓	n=417 p=0.1387 HR=0.794 (0.585-1.078)	↓	n=191 p=0.08398 HR=0.737 (0.521-1.043)	↓	n=194 p=0.422 HR=0.831 (0.518-1.333)	↓

↑ = up-regulated expression, ↓ = down-regulated expression. Arrows in bold indicate a significant change in OVMARK.

7.3.1.1 LIN28B

LIN28B was selected for a number of reasons. Firstly, it was up-regulated in UPN251-7C compared to UPN251 in both carboplatin resistance related comparisons (A and B) and down-regulated in UPN251-7T compared to UPN251 in all the taxol resistance related comparisons (C-E). This gave an interesting target that was highly deregulated in our comparisons and that may play a role in the inverse resistance relationship between platinum and taxane chemotherapy (Chapter 1 section 1.7.3). It was also found to be one of the top five deregulated genes in carboplatin resistance related comparison B. Secondly, LIN28B interacts with let7i, which was down-regulated in UPN251-7C compared to UPN251 in comparison B. LIN28B is a known inhibitor of the let-7 processing system. LIN28B binds to the terminal loops of let-7 family miRNA precursors resulting in the negative regulation of its members (*Heo et al. 2008*; *Rybak et al. 2008*). Over-expression of LIN28B promotes cellular transformation *in vitro* and is associated with advanced disease in a number of tumour types, including Wilms', Kidney, germ cell, and ovarian tumours (*Viswanathan et al. 2009*). It has been shown that high expression of LIN28B, which results in reduced expression of Let-7 family members, is correlated with shorter progression-free and overall survival in ovarian cancer in the literature (*Lu et al. 2009a*). Over-expression of LIN28B has also been linked with poor prognosis and chemoresistance in ovarian cancer (*Topp et al. 2014*; *Yan et al. 2013*). In the study by *Topp et al. (2014),* patient derived xenografts (PDX) were produced from chemo-naïve ovarian cancer patients with the high-grade serous disease. Four PDXs were platinum sensitive, three were platinum resistant, and three were platinum refractory. All three of the platinum-refractory PDXs over-expressed LIN28B. In contrast, none of the platinum-sensitive PDXs over-expressed LIN28B (*Topp et al. 2014*). *Yan et al. (2013)* linked the down-regulation of PSP94 to chemoresistance in ovarian cancer through the modulation of LIN28B/Let-7 signalling. However, we did not observe deregulation of the PSP94 gene. The existing literature provided strong evidence of LIN28B's potential as a candidate biomarker for chemoresistance in ovarian cancer. Finally, OVMARK analysis showed that the over-expression of LIN28B was associated with poor DFS in the all patient and platinum/taxane patient cohorts (p=0.01 and 0.04 respectively) and poor OS in the all patients cohort (p=0.002, Table 7.2). From the above evidence, further investigation of LIN28B in our patient cohort was warranted. This would extend existing knowledge of LIN28B's affects on survival and chemoresistance and would allow the investigation of LIN28B in combination with let7-i as a more robust biomarker compared to LIN28B alone.

7.3.1.2 SRPX2

SRPX2 was highly up-regulated in UPN251-7T compared to UPN251 in all three taxol resistance related comparisons (C-E). To our knowledge, SRPX2 has not been studied in ovarian cancer resistance, but has been linked to having a possible role in chemotherapy resistance in leukaemia. SRPX2 was first described as a downstream target gene for E2A-HLA which is associated with a form of leukaemia that does not respond to chemotherapy (*Kurosawa et al. 1999*). SRPX2 over-expression has been noted in a number of cancer cell lines including gastric, colorectal, lung, mesothelioma and glioma, and has been shown to affect cellular migration and adhesion (*Tanaka et al. 2009*). It has also been linked with unfavourable outcome in gastric cancer, making this an interesting novel candidate biomarker for chemoresistance in ovarian cancer (*Yamada et al. 2014*). Results from OVMARK analysis showed that up-regulation of SRPX2 was associated with poor OS in the all patients cohort (p=0.003, Table 7.2).

7.3.1.3 CCL20

CCL20 was down-regulated in UPN251-7C compared to UPN251 in both carboplatin resistance related comparisons from chapter 6 (A and B). DAVID pathway analysis identified CCL20 to be part of the cytokine-cytokine receptor interaction pathway (section 6.4.1.2.3). The expression of cytokines and their receptors have a role to play in cancer (*Balkwill 2004*) and may have a role to play in the progression of ovarian cancer (*Nash et al. 1999*). The expression of cytokines has been investigated in ovarian cancer cell lines, ascites fluid and biopsies from ovarian cancer patients in different studies (*Kulbe et al. 2012*; *Matte et al. 2012*). Low concentrations of CCL20 have been found in ascites fluid from ovarian cancer patients. Its concentration is much lower than other cytokines, such as IL8 or CCL18 (*Schutyser et al. 2002*). CCL20 is also expressed at a moderately low level in SKOV-3 ovarian cancer cell lines after exposure to pro-inflammatory chemokines IL1 and TNF (*Son et al. 2007*). In colorectal cancer, increased expression of CCL20 and its receptor CCR6 are seen in patients who receive pre-operative FOLFOX chemotherapy (*Rubie et al. 2011*). This increase in expression is short lived. Increased expression has also been linked to the inducement of cellular differentiation and migration in breast pancreatic and colorectal cancer through the up-regulation of MMP9 (down-regulated in UPN251-7C compared to UPN251 in our study) (*Brand et al. 2006*; *Campbell et al. 2005*; *Marsigliante et al. 2013*). CCL20 was observed to have decreased expression in carboplatin-resistant cell line UPN251-7C, compared to carboplatin-naïve parental cells UPN251. This may indicate that the effects of CCL20 expression are tissue specific or that a response of

an increase in CCL20 expression to chemotherapy might be lost in chemoresistant ovarian cancer cells. For this reason, decreased expression of CCL20 may be linked with chemo-resistance. OVMARK analysis indicated that low expression of CCL20 was associated with poor OS in the platinum/taxane chemotherapy cohort of ovarian cancer patients (p=0.02, Table 7.2). To our knowledge, this chemokine has not been investigated as a chemoresistant marker in ovarian cancer and might be a potential biomarker for chemoresistance, based on the evidence above.

7.3.1.4 GLI3

GLI3 was found to be up-regulated in UPN251-7C compared to UPN251 in comparison B (related to carboplatin resistance). GLI3 was identified by DAVID pathway analysis as part of the hedgehog signalling pathway. Aberrant expression of hedgehog family members has been linked to multiple cancer types (*Evangelista et al. 2006*), including ovarian cancer (*Chen et al. 2007*). GLI3 over-expression was seen in the cytoplasm of endometrioid carcinoma tumour tissue when compared to normal endometrium from a patient cohort of 271 (*Kim et al. 2009*). Up-regulation of GLI3 has been found in a number of different cancer types and in NSCLC over-expression is associated with poor prognosis and may play an important role in tumourigenesis (*Bai et al. 2013*). In the context of chemoresistance, over-expression of GLI3 in cervical cancer has been shown to inhibit apoptosis and cell cycle arrest (*Wen et al. 2014*). From the MTIs analysis, GLI3 was shown to interact with miR-205, which is down-regulated in UPN251-7C and UPN251-7T compared to UPN251 in all carboplatin and taxol related resistance comparisons (A-E). Also, OVMARK analysis indicated that GLI3 up-regulation was significantly associated with poor DFS in the platinum/taxane cohort of ovarian cancer patients (p=0.04, Table 7.2). The above evidence pointed towards GLI3's potential as an ovarian cancer chemoresistance biomarker.

7.3.1.5 Let-7i

Let-7i of the let-7 family was down-regulated in UPN251-7C compared to UPN251 in carboplatin resistance related comparison B. In ovarian cancer, let-7i has been found to have the ability to predict chemotherapy responses. Its expression was significantly reduced in platinum resistant patients and was also significantly associated with shorter PFS in advanced ovarian cancer patients (*Yang et al. 2008b*). In the same study, loss of function and gain of function manipulations through Let-7i inhibitors and retroviral over expression showed that a reduction in Let-7i expression resulted in increased cisplatin resistance in ovarian and breast cancer cells (*Yang et al. 2008b*). Our group has shown that let7i is down-regulated in the serum of ovarian cancer patients (*Langhe*

et al. 2014). In addition, patients who developed chemoresistant ovarian cancer saw no detectable expression of let-7i from serum samples. MTIs analysis found that LIN28B (section 7.3.1.1) was a validated target of let-7i. Therefore, let-7i in combination with LIN28B may act as a robust biomarker panel of carboplatin-resistant in ovarian cancer. Also, let-7i delivery into taxol resistant ovarian cancer tumours re-sensitises the cells to taxol chemotherapy (*Liu et al. 2012*). This was tested on the OVCAR3 ovarian cancer cell line. Let7i specifically sensitised the role of taxol by inhibiting proliferation, inducing apoptosis, and decreasing long term survival. Therefore, this treatment releasing Let7i, sensitises the cells to taxol chemotherapy (*Liu et al. 2012*). No information was available through analysis with OVMARK, as this miRNA was not screened for in the microarray experiments utilised by the online tool. Evidence from the literature and its interaction with LIN28B by MTI analysis, makes this an attractive potential biomarker to test in our pilot study.

7.3.1.6 MiR-205

MiR-205 was down-regulated in UPN251-7C and UPN251-7T compared to UPN251 in all of the carboplatin and taxol resistance related comparisons (A-E) in chapter 6. It was found to be part of the top-five deregulated miRNA lists of four of these comparisons (A, B, C and E). In the literature, miR-205 has been shown to be frequently down-regulated in advanced cancers (*Iorio et al. 2007*). However, it has also been shown to be up-regulated in cancer, depending on the tissue of origin. This may suggest that miR-205 has more than one target mRNA and that it could function as an oncogene or tumour suppressor gene, depending on the cellular context (*Tsukamoto et al. 2014*). A number of studies have shown miR-205 to be up-regulated in ovarian cancer tissue and plasma (*Zheng et al. 2013*; *Zhou et al. 2014*). Down-regulation of miR-205 in the current study may be a result of resistance development as miR-205 seems to be ordinarily up-regulated in ovarian cancer tissue compared to normal ovarian tissue. From MTIs analysis, miR-205 has been shown to have a predicted interaction with GLI3. Therefore, GLI3 could act as a more robust biomarker panel in combination with miR-205 than either marker on their own. However, OVMARK analysis on miR-205 does not give significant correlations with DFS or OS in either the full patient or platinum/taxane cohorts. Its scale of deregulation in our Affymetrix analysis (chapter 6), its interaction with GLI3, and evidence in the literature of its down-regulation in cancer all contribute in making this an attractive potential biomarker. Also, miR-205 in combination with let-7f has been suggested in the literature as a predictive biomarker panel for ovarian cancer prognosis that could complement CA125 (*Zheng et*

al. 2013). Our study suggests that miR-205 may have the ability to predict chemotherapy resistance in combination with GLI3.

7.3.2 Target expression analysis

32 patient samples were analysed for the expression of CCL20, GLI3, LIN28B and SRPX genes and let-7i and miR-205 miRNAs by qPCR. In total, 15 patient samples were classed as responders (R) to chemotherapy, 13 were classified as non-responders (NR) to chemotherapy, and 4 were classified as partial responders (PR) to chemotherapy (Table 7.1). The average fold expression of each target (gene/miRNA) within the NR, PR and a combination of NR and PR groups relative to the R group is given in Table 7.3 and shown diagrammatically in Figure 7.1. In general, fold changes of markers in the chemoresistant groups had high standard deviations (SDs). This was because, in most cases the groups contained a number of samples that had both up and down-regulated expression of a single target when compared to the chemosensitive R group. Table 7.4 shows that in the chemoresistant NR group, each target had a nearly equal amount of patient samples with up and down-regulated expression relative to the non-chemoresistant R group. This is most likely due to the variability of biological samples. This trend was not seen for every target in the partially-chemoresistant PR group, but this is likely to be due to the small amount of patient samples in this group (Table 7.4). Significant changes were only observed in LIN28B between sample groups (Table 7.3, Figure 7.1). Significance was assessed by carrying out two tailed T-tests (un-equal variance) between sample group's ΔCT values for the target of interest. Figure 7.2 shows the spread, mean and median of ΔCT values for each target within each patient group. LIN28B was significantly down-regulated in the PR and PR+NR groups in relation to the R group ($p=0.03$ and 0.04 respectively). The analysis of LIN28B excluded samples that had no detectable expression of LIN28B by qPCR. These samples were deemed to not express LIN28B. In total, 15 out of 32 samples did not express LIN28B (Table 7.4). Validation of this finding needs confirmation in a larger patient cohort.

7.3.3 Survival analysis

In order to link target (gene/miRNA) expression to survival, Kaplan Meier survival graphs were generated for DFS and OS. In LIN28B, three scenarios were examined to account for the samples that did not express LIN28B by qPCR. One scenario compares samples of up-regulated expression to down-regulated expression, excluding samples that did not express LIN28B from the analysis. The second scenario treats the samples that were not expressed as down-regulated and included them in

Table 7.3 Mean fold change of target (gene/miRNA) in patient chemotherapy-response groups relative to responders group.

Target (gene/miRNA)	NR (n=13)		PR (n=4)		NR + PR (n=17)	
	Mean Fold ± SD	P	Mean Fold ± SD	P	Mean Fold ± SD	P
CCL20	2.7 ± 4.7	0.74	39.7 ± 76.3	0.35	11.4 ± 37.0	0.34
GLI3	1.8 ± 2.6	0.67	0.4 ± 0.3	0.20	1.5 ± 2.4	0.50
LIN28B ^	0.5 ± 0.7 (n=7)	0.06	0.2 ± 0.2* (n=3)	**0.03**	0.4 ± 0.6* (n=10)	**0.05**
SRPX2	3.3 ± 7.4	0.41	0.7 ± 0.4	0.06	2.7 ± 6.5	0.54
Let-7i	2.0 ± 2.3	0.87	1.7 ± 1.2	0.67	2.0 ± 2.0	0.81
miR-205	3.2 ± 7.4	0.32	6.7 ± 11	0.81	4.0 ± 8.1	0.35

^Only includes patient's samples that had detectable expression of target by qPCR. Samples that were not detected were excluded.

*Indicates a significant difference between ΔCT values of responder group and ΔCT values of selected group ($p<0.05$ students t-test (un-equal variance)).

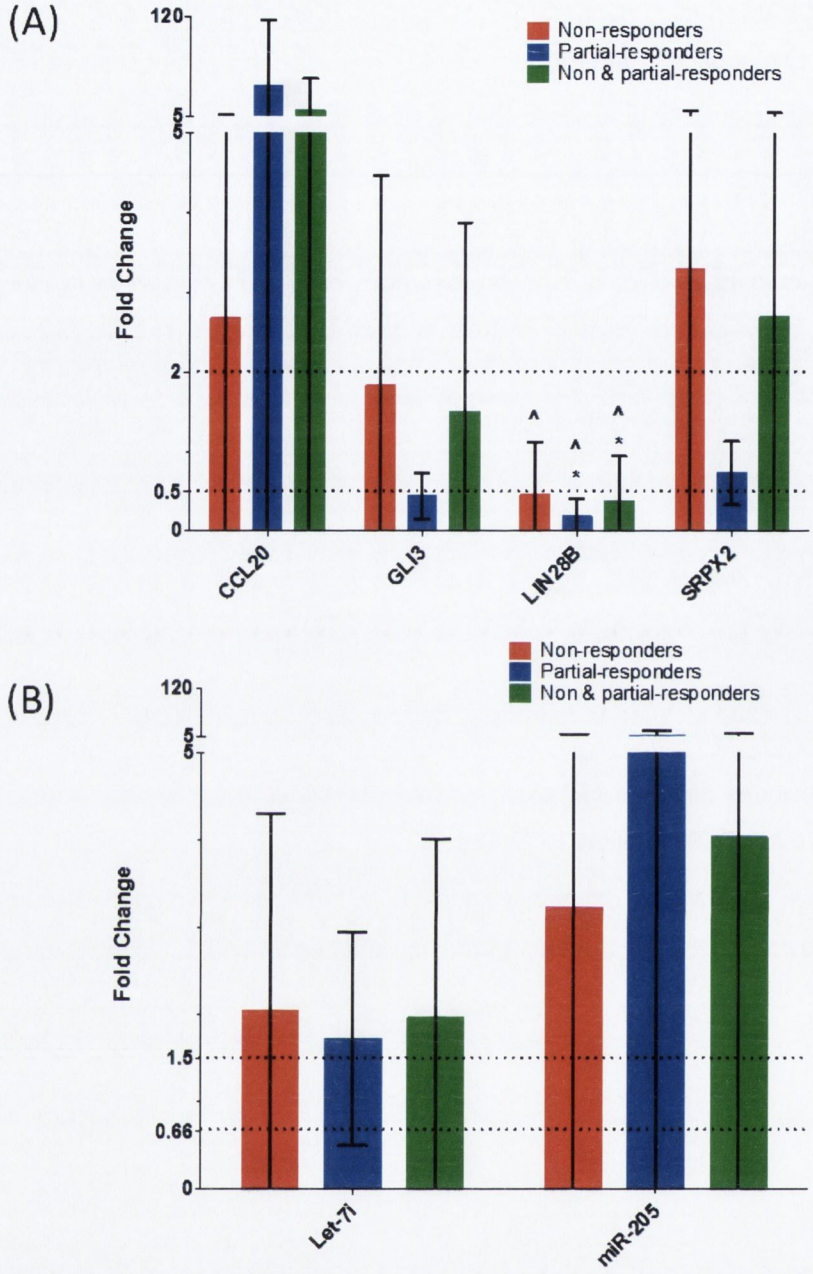

Figure 7.1 Fold change of qPCR target expression in non-responder (NR) and partial-responder (PR) patient groups relative to the responder (R) patient group.

Fold change is given on y-axis and targets grouped into (NR), (PR) and (NR + PR) is shown on the x-axis. (A) Gene targets. Significant up-regulation of genes are fold changes >2 and significant down-regulation of genes are fold changes <0.5. (B) MiRNA targets. Significant up-regulation of miRNAs are fold changes >1.5 and significant down-regulation of miRNAs are fold changes <0.66.

^Only includes patient's samples that had detectable expression of target by qPCR. Samples that were not detected were excluded.

* Indicates a significant difference in fold expression between patient group of interest and responders ($P<0.05$, student T-test (non-equal variance)).

Table 7.4 Number of significant fold changes in NR or PR when compared to R.

This table indicates the amount of patient samples that had significant up or down-regulated expression in non and partial-responders groups relative to the average ΔCT values of the responders group. It also indicates the amount of samples that were not found to be expressed by qPCR in each sample group.

	CCL20			GLI3			LIN28B			SRPX2			let-7i			miR-205			N
	↑	↓	NE	↑	↓	NE	↑	↓	NE	↑	↓	NE	↑	↓	NE	↑	↓	NE	
NR	5	4	0	3	4	0	0	5	6	4	4	0	6	5	0	5	5	0	13
PR	2	0	0	0	3	0	0	3	1	0	2	0	2	1	0	2	2	0	4
R	-	-	0	-	-	0	-	-	8	-	-	0	-	-	0	-	-	0	15

↑ = significant up-regulated expression, ↓ = significant down-regulated expression, NE = not expressed, NR = non-responder, PR = partial-responder, R = Responder, N = total number of samples in each group

For gene targets, significant fold up-regulation = >2 fold and significant fold down-regulation = <0.5 fold.

For miRNA targets, significant fold up-regulation = >1.5 fold and significant fold down-regulation = <0.66 fold.

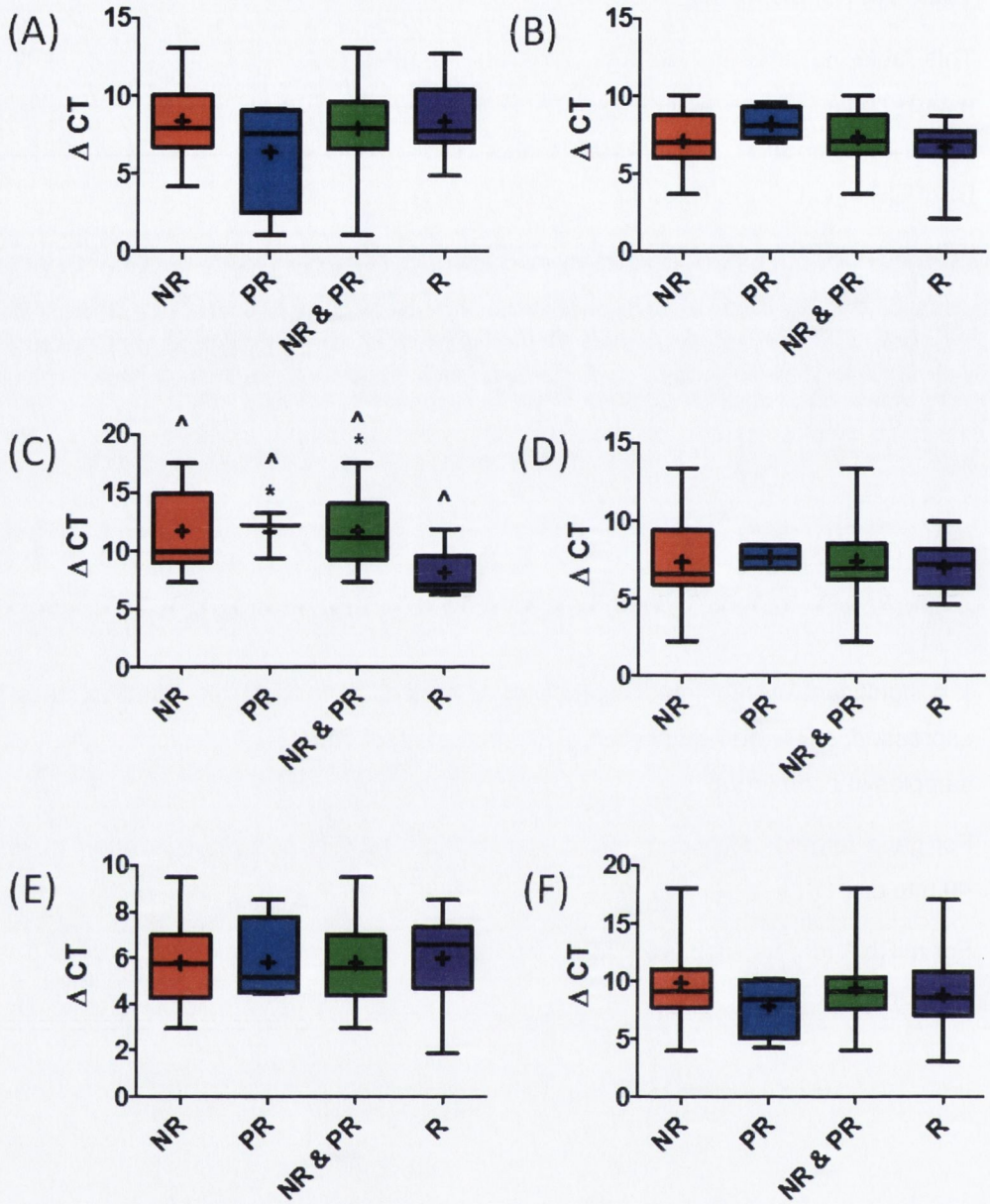

Figure 7.2 Δ CT values of qPCR targets in patient samples grouped by chemotherapy response.

X-axis depicts Δ CT values and Y-axis depicts patient groups. (A) CCL20 (B) GLI3 (C) LIN28B (D) SRPX2 (E) let-7i (F) miR-205. + represents the group mean. Bar within box depicts the group median. Whiskers represent the min and max sample Δ CT values. The box extends from the 25th to 75th percentile of group Δ CT values. Higher Δ CT values indicate lower target expression while lower Δ CT values indicate higher target expression.

^Only includes patient's samples that had detectable expression of target by qPCR. Samples that were not detected were excluded.

* Indicates a significant difference in fold expression between patient group of interest and responders ($P<0.05$, student T-test (non-equal variance)).

the analysis. The last scenario compared all samples that had any detectable expression of LIN28B by qPCR to samples that had no detectable expression of LIN28B by qPCR.

No significant differences in DFS or OS were seen between high and low expressers of any target by Kaplan Meier analysis when the median value was used as a cut-off value to separate the samples into high and low expressers. Significant differences were seen when the cut-off value was set as the top 25% of samples for over-expressers and bottom 25% of samples for under-expressers. The following Kaplan Meier results were based on this analysis.

Figure 7.3 and Figure 7.4 show the results of Kaplan Meier analysis for differences in DFS in our samples, comparing high and low levels of target expression. CCL20 (Figure 7.3 (A)), SRPX2 (Figure 7.3 (B)), let-7i (Figure 7.3 (C)) and miR-205 (Figure 7.3 (D)) were shown to have no significant difference in DFS between high and low-expressers of the examined target. GLI3 (Figure 7.4 (A)) and LIN28B (Figure 7.4 (B-D)) did show significant differences in DFS. Low expression of GLI3 was significantly associated with poor DFS (p=0.009, 1 df (Log-rank test), HR=0.1210 (0.02480-0.5907)). The HR of 0.1 indicates that patients with low expression of GLI3 are 10 times more likely to progress than those with high GLI3 expression. Median DFS in the GLI3 up-regulated group was 25 months, while the median survival in the GLI3 down-regulated group was 7.5 months. Also, down-regulated expression of LIN28B was associated with poor DFS when the non-expressed samples were removed from the study (p=0.0067, 1 df (Log-rank Test), HR=0.05537 (0.006830-0.4489), Figure 7.4 (B)). The HR of 0.06 indicates that patients with low expression of LIN28B are approximately 17 times more likely to progress than those with high LIN28B expression. Median DFS in the LIN28B up-regulated group was 24.5 months and the median DFS in the LIN28B down-regulated group was 2.5 months. The other scenarios for LIN28B (not expressed as down-regulated, Figure 7.4 (C) and expressers compared to non-expressers, Figure 7.4 (D)) did not show any significant differences in DFS.

Figure 7.5 and Figure 7.6 shows the results of Kaplan Meier analysis for differences in OS comparing high and low levels of target expression. CCL20 (Figure 7.5 (A)), SRPX2 (Figure 7.5 (B)), let-7i (Figure 7.5 (C)), miR-205 (Figure 7.5 (D)) and LIN28B (Figure 7.6 (B-D)) were all shown to have no significant difference in OS between high and low-expressers of the examined target. Only GLI3 showed a significant difference in OS between high and low-expressers of the target (Figure 7.6 (A)). Low expression of GLI3 was significantly associated with poor OS (p=0.0289, 1 df (Log-rank Test),

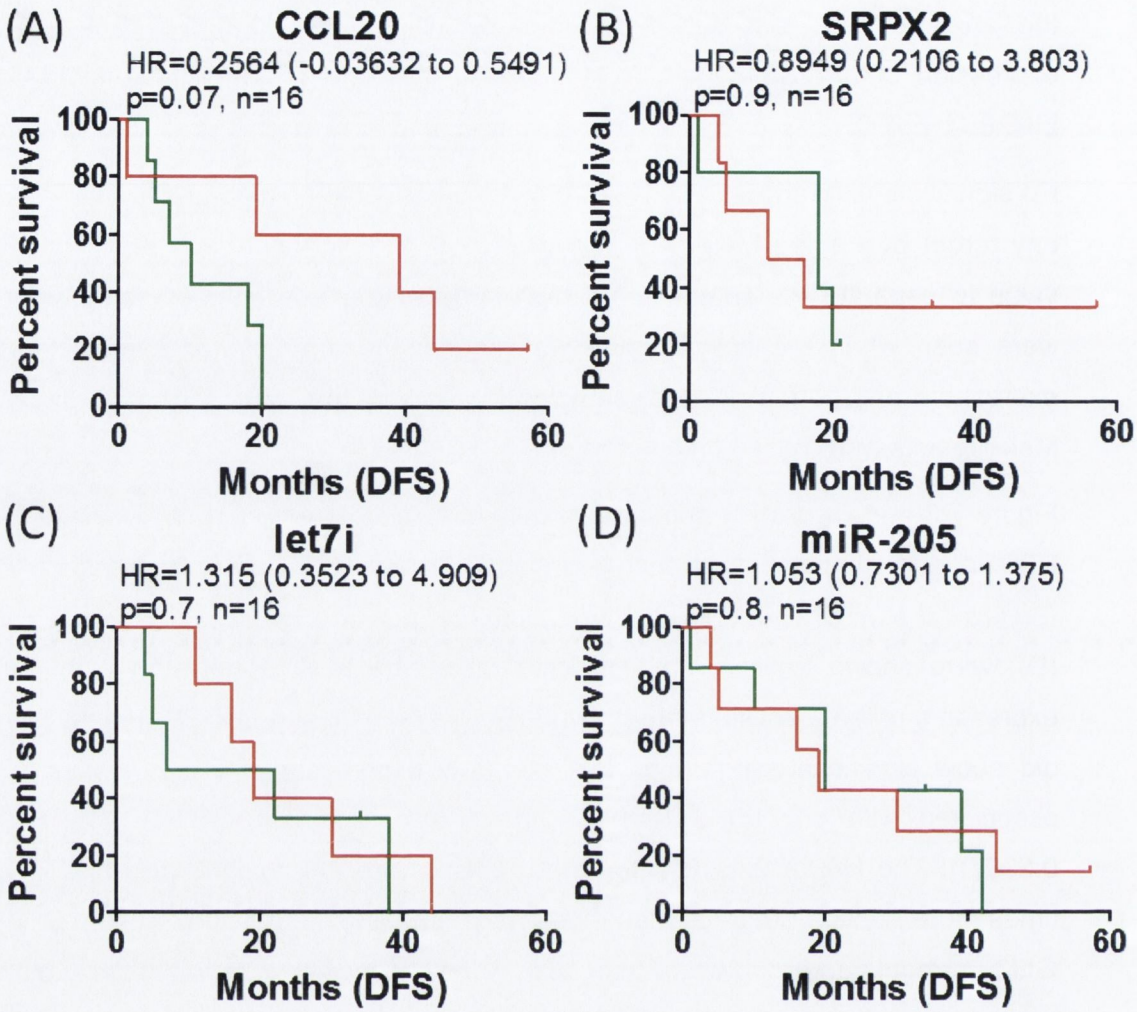

Figure 7.3 Kaplan Meier survival curves depicting disease free survival (DFS) in patient samples grouped and compared by expressional data.

X-axis depicts the time taken in months for a patient to relapse after surgery. Y-axis depicts the percentage survival of patients. The green line represents up-regulation and the red line represents down-regulation of a given target. (A) up-regulation compared to down-regulation of CCL20. (B) up-regulation compared to down-regulation of SRPX2. (C) up-regulation compared to down-regulation of let-7i. (D) up-regulation compared to down-regulation of miR-205.

The cut-off value for high and low sample expression defines high expression of a marker to be the top 25% expression level and low expression to be the bottom 25% expression level.

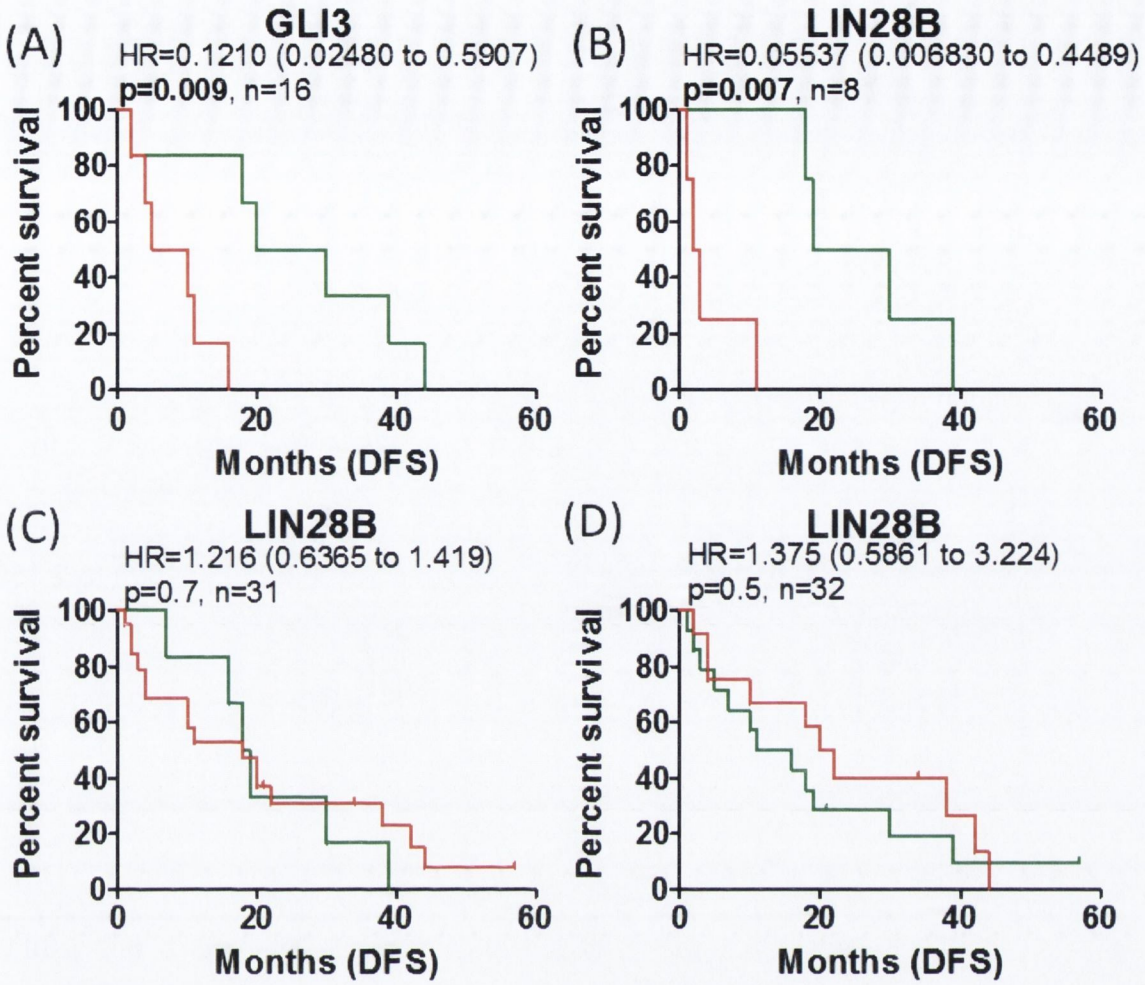

Figure 7.4 Kaplan Meier survival curves depicting disease free survival (DFS) in patient samples grouped and compared by expressional data.

X-axis depicts the time taken in months for a patient to relapse after surgery. Y-axis depicts the percentage survival of patients. The green line represents up-regulation and the red line represents down-regulation of a given target. (A) up-regulation compared to down-regulation of GLI3. (B) up-regulation compared to down-regulation of LIN28B without non-expressed patient samples not detected by qPCR. (C) up-regulation compared to down-regulation of LIN28B where non-expressed are grouped as down-regulated. (D) Expressed samples (green) compared to non-expressed samples of LIN28B (red) by qPCR.

The cut-off value for high and low sample expression defines high expression of a marker to be the top 25% expression level and low expression to be the bottom 25% expression level.

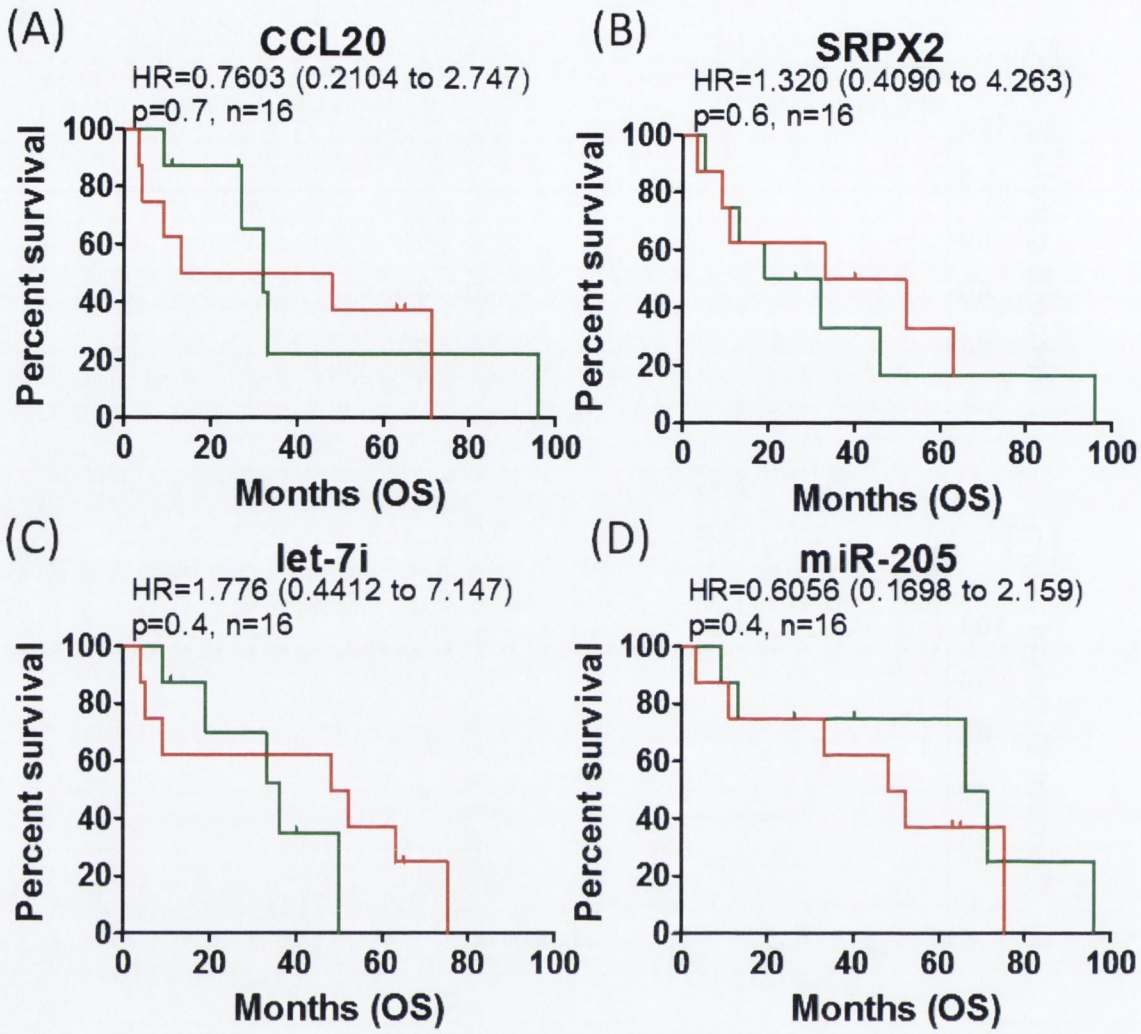

Figure 7.5 Kaplan Meier survival curves depicting overall survival (OS) in patient samples grouped and compared by expressional data.

X-axis depicts the time taken in months for a patient to relapse after surgery. Y-axis depicts the percentage survival of patients. The green line represents up-regulation and the red line represents down-regulation of a given target. (A) up-regulation compared to down-regulation of CCL20. (B) up-regulation compared to down-regulation of SRPX2. (C) up-regulation compared to down-regulation of let-7i. (D) up-regulation compared to down-regulation of miR-205.

The cut-off value for high and low sample expression defines high expression of a marker to be the top 25% expression level and low expression to be the bottom 25% expression level.

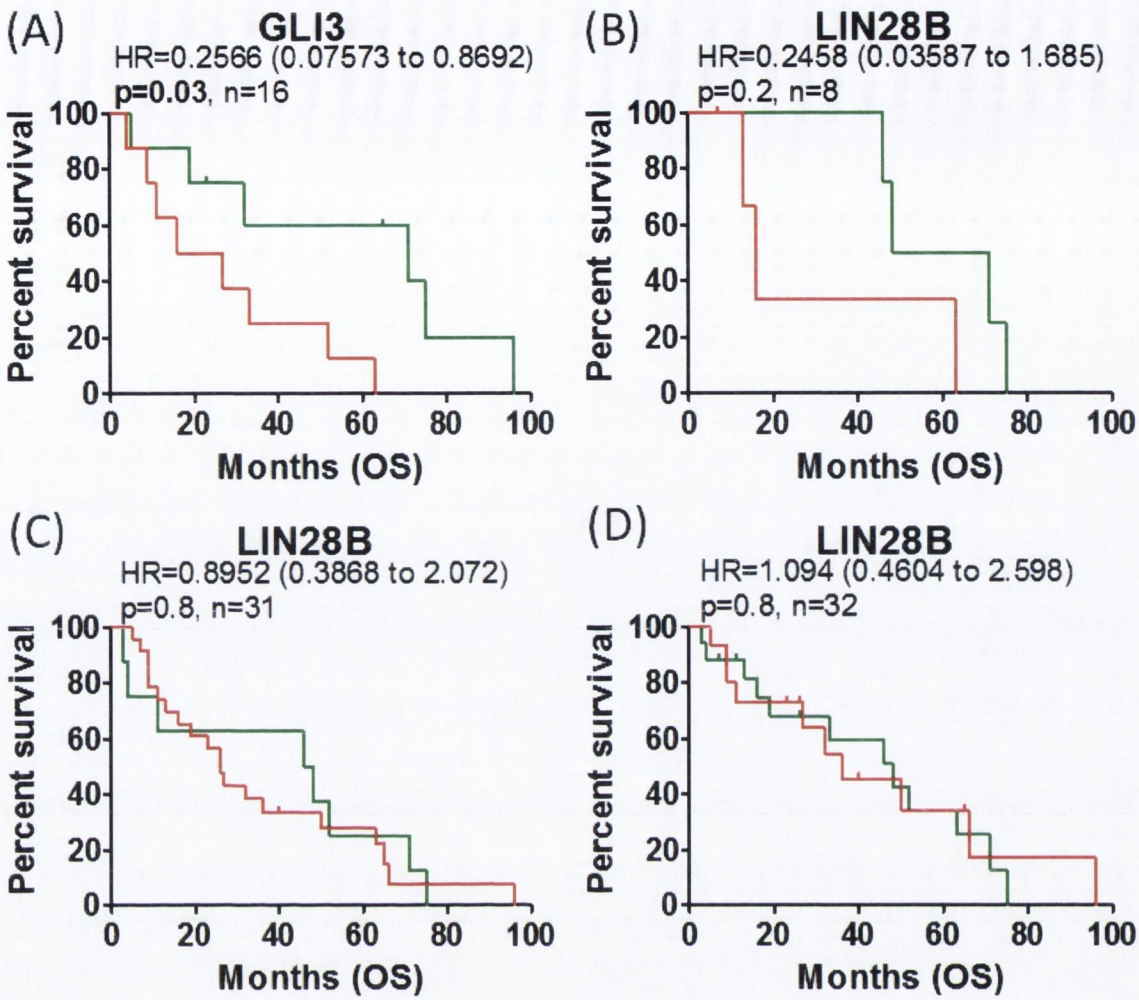

Figure 7.6 Kaplan Meier survival curves depicting overall survival (OS) in patient samples grouped and compared by expressional data.

X-axis depicts the time taken in months for a patient to relapse after surgery. Y-axis depicts the percentage survival of patients. The green line represents up-regulation and the red line represents down-regulation of a given target. (A) up-regulation compared to down-regulation of GLI3. (B) up-regulation compared to down-regulation of LIN28B without non-expressed patient samples not detected by qPCR. (C) up-regulation compared to down-regulation of LIN28B where non-expressed are grouped as down-regulated. (D) Expressed samples (green) compared to non-expressed samples of LIN28B (red) by qPCR.

The cut-off value for high and low sample expression defines high expression of a marker to be the top 25% expression level and low expression to be the bottom 25% expression level.

HR=0.2566 (0.07573-0.8692)). The HR of 0.3 indicates that patients with low expression of GLI3 are approximately 3.3 times more likely to suffer death than those with high GLI3 expression. Median OS in the GLI3 up-regulated group was 71 months, while the median survival in the GLI3 down-regulated group was only 21.5 months.

Kaplan Meier analysis of the data was also carried out in optimally debulked patients to determine if debulking status influenced the findings. However, no influence was observed.

Furthermore, significant differences in DFS and OS were examined between patient samples that had different expression patterns of a gene and a miRNA that had a predicted miRNA-target interaction (MTI) (Figure 7.7). There was no difference in DFS or OS when comparing samples that had up-regulated expression of LIN28B and down-regulated expression of let-7i to samples that had down-regulated expression of LIN28B and up-regulated expression of let-7i (Figure 7.7 (A & B)). Similarly, there was no difference in DFS or OS, when comparing samples that had up-regulated expression of GLI3 and down-regulated expression of miR-205 to samples that had down-regulated expression of GLI3 and up-regulated expression of miR-205 (Figure 7.7 (C & D)).

Finally, an algorithm was devised using all 6 gene/miRNA targets (CCL20, GLI3, LIN28B, SRPX2, let-7i and miR-205) that could be used as a predictor of chemotherapy response. This was achieved by examining the direction of fold change of all the targets in a given sample from the chemoresistant groups (NR and PR) relative to the non-chemoresistant group R and determining how many of these targets were expressed in the direction that was predictive of poor response from OVMARK analysis (Table 7.2). Table 7.5 shows the expected direction of fold change in chemoresistant samples for all the targets examined (from Affymetrix data (Chapter 6) and OVMARK analysis (Table 7.2)) and the actual direction of fold change that was observed in our biological samples. In total, from the 17 chemoresistant samples examined, 23 instances of a target being expressed in the expected direction occurred, while 44 instances of a target being expressed in an unexpected direction occurred. In 26 instances, a target had no significant change and in 7 instances, no expression of a target was found using qPCR. The samples were then grouped into an expected and an unexpected group or excluded from further analysis. The two groups were defined as follows;

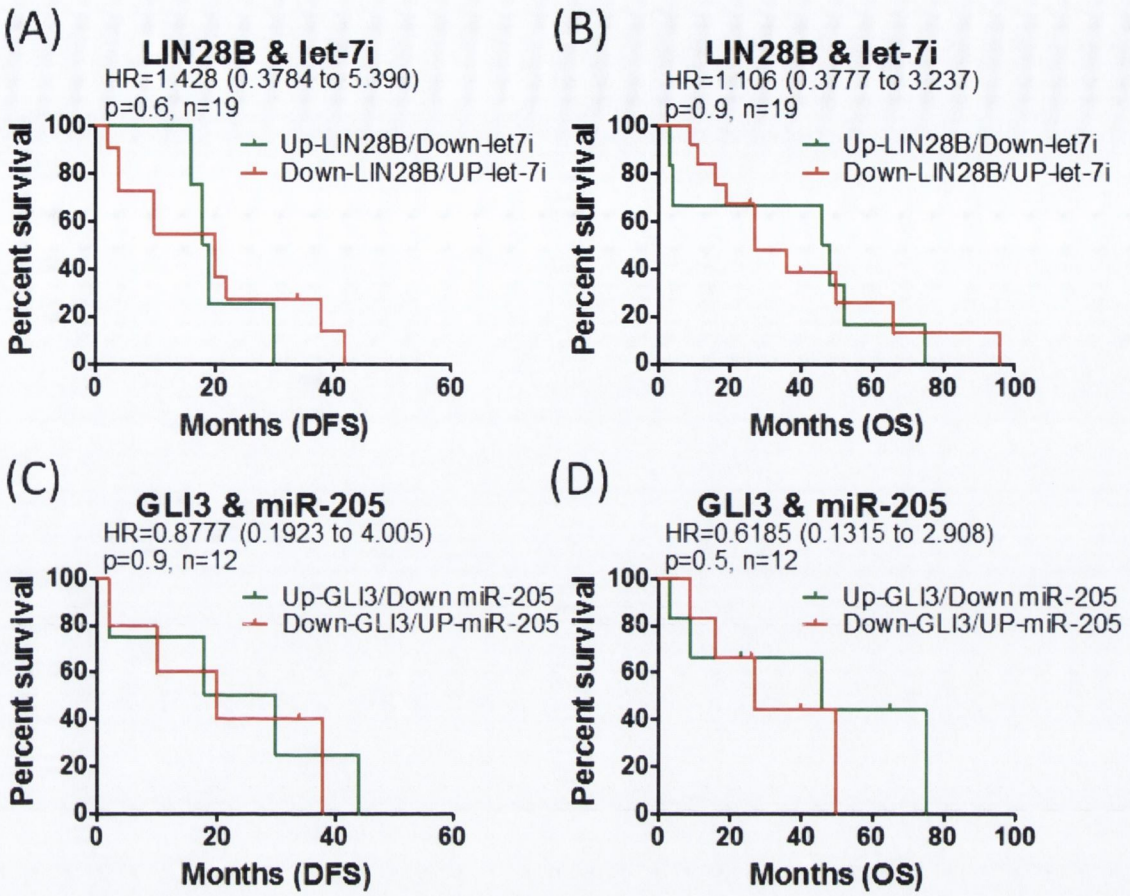

Figure 7.7 Kaplan Meier analysis of DFS and OS between different expression patterns of a miRNA and predicted target gene.

X-axis depicts the time taken in months for a patient to relapse after surgery. Y-axis depicts the percentage survival of patients. (A) PFS in samples with up-regulated expression of LIN28B and down-regulated expression of let-7i compared to down-regulated expression of LIN28B and up-regulated expression of let-7i. (B) OS in samples with up-regulated expression of LIN28B and down-regulated expression of let-7i compared to down-regulated expression of LIN28B and up-regulated expression of let-7i. (C) PFS in samples with up-regulated expression of GLI3 and down-regulated expression of miR-205 compared to down-regulated expression of GLI3 and up-regulated expression of miR-205. (D) OS in samples with up-regulated expression of GLI3 and down-regulated expression of miR-205 compared to down-regulated expression of GLI3 and up-regulated expression of miR-205.

Table 7.5 Fold change direction and survival.

The number of targets (genes/miRNAs) expressed in the expected and unexpected direction of fold expression in a given sample was examined. Fold change in the PR and NR patient samples were relative to the R group. Extent of fold change is indicated in brackets. The samples DFS and OS were given for comparison purposes.

Sample	↓ CCL20 ↓	↑ SRPX2 ↑	↑ LIN28B ↑	↓ Let-7i ↓	↑ GLI3 ↑	↓ miR-205 ↓	Expected	Un-expected	DFS	OS
19 (PR)	-	-	↓ (0.1)	↑ (2.4)	-	↑ (23.1)	0	3	10	26
30 (PR)	-	↓ (0.4)	↓ (0.03)	↓ (0.2)	↓ (0.1)	↓ (0.4)	2	3	11	63
39 (PR)	↑ (154.1)	↓ (0.4)	↓ (0.5)	↑ (2.9)	↓ (0.4)	↓ (0.6)	0	5	7	11
44 (PR)	↑ (3.4)	-	NE	-	↓ (0.4)	↑ (2.7)	0	4	10	27
2 (NR)	-	-	↓ (0.02)	↓ (0.6)	↓ (0.2)	↑ (2.1)	1	2	2	16
7 (NR)	↓ (0.3)	↑ (2.4)	↓ (0.01)	-	-	↑ (4.9)	3	1	1	13
10 (NR)	↓ (0.03)	↓ (0.01)	-	↓ (0.5)	-	↓ (0.002)	3	1	0	3
12 (NR)	↓ (0.3)	-	-	↓ (0.1)	↓ (0.3)	↓ (0.6)	3	1	0	4
15 (NR)	-	-	↓ (0.001)	↑ (1.5)	↑ (2.1)	↓ (0.6)	2	2	2	23+
20 (NR)	↑ (3.5)	-	↓ (0.4)	↑ (4.1)	-	↑ (1.8)	0	4	4	9
21 (NR)	-	-	↓ (0.3)	-	-	↓ (0.3)	1	1	3	7+

23 (NR)	↑ (17.9)	↓ (0.1)	NE	↑ (3.5)	↓ (0.1)	↓ (0.003)	0	5	5	33
33 (NR)	↑ (3.4)	↑ (3.9)	NE	↓ (0.5)	-	-	2	1	0	9
35 (NR)	↑ (3.1)	↓ (0.3)	NE	↑ (1.5)	↓ (0.2)	-	0	4	4	11
36 (NR)	↓ (0.3)	↓ (0.1)	NE	↑ (3.2)	↓ (0.2)	↑ (27.6)	1	4	0	9
43 (NR)	↑ (2.0)	↑ (27.6)	NE	↑ (8.2)	↑ (8.2)	↑ (2.1)	2	3	0	19
46 (NR)	-	↑ (2.1)	NE	↓ (0.5)	↑ (7.0)	-	3	0	0	5
Total							23	44		

↑ target ↑ = expected up-regulated expression, ↓ target ↓ = expected down-regulated expression, ↑ = significant up-regulated expression, ↓ = significant down-regulated expression, - = not significantly different, NE = not expressed, NR = non-responder, PR = partial-responder, R = Responder, Total = total number of expected and un-expected directional expression in samples, DFS = disease free survival, OS = overall survival

Expected

- 3 or more targets expressed in the expected direction
- 1 or less targets expressed in the unexpected direction

- Unexpected
  - 3 or more targets expressed in an unexpected direction
  - 1 or less targets expressed in an expected direction

The expected group contained 4 samples and the unexpected group contained 7 samples from our pilot study. The remaining samples were excluded from this analysis, as they did not meet the criteria of the expected or unexpected groups. OS and PFS were compared between the expected and unexpected groups. From this comparison, it was found that patient samples from the expected group had a significantly worse DFS and OS than patient samples that were part of the unexpected group ($p=0.007$ and 0.02 respectively (student T-test (un-equal variance))) (Figure 7.8). The expected group was shown to have significantly lower DFS ($p=0.01$, 1 df (Log-rank Test)) and lower OS ($p=0.04$, 1 df (Log-rank Test)). The HR ratios for these comparisons were not calculated as they would not be accurate due to the low number of cases in each group being assessed. The median DFS was 1 and 6 months and the median OS was 4.5 and 11 months for expected and unexpected groups respectively.

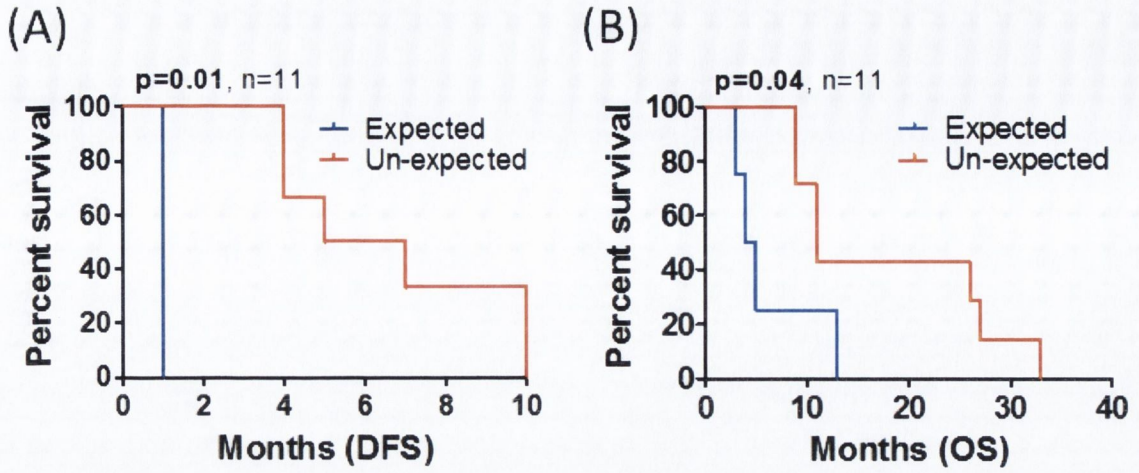

Figure 7.8 Analysis of DFS and OS between samples in the expected group and the un-expected group.

Expected group=3 or more markers in an expected direction of expression and 1 or less markers in an un-expected direction predictive for poor prognosis by OVMARK analysis.

Un-expected group=3 or more markers in an un-expected direction of expression and 1 or less markers in an expected direction predictive for poor prognosis by OVMARK analysis.

X-axis depicts the time taken in months for a patient to relapse after surgery. Y-axis depicts the percentage survival of patients. (A) PFS between expected (n=4) and un-expected (n=7) (B) OS between expected (n=4) and un-expected (n=7).

7.4 Discussion

Chemoresistance is one of the major problems facing ovarian cancer management. The identification of biomarkers that can accurately predict patients who will be resistant to standard platinum/taxane chemotherapy or who will have a poor outcome is important in the fight to improve patient survival. This will allow clinicians to make informed decisions about alternate treatments that may have greater benefit to individual patients' needs. Novel therapies could be designed to target biomarkers that are found to be linked to resistance. In this way, these therapies could inhibit the development of resistance or circumvent mechanisms of resistance that have evolved. We investigated the clinical utility of 6 potential gene/miRNA biomarkers CCL20, GLI3, LIN28B, SRPX2, let-7i and miR-205. Kaplan Meier analysis of these targets using the top and bottom 25% of expressers are discussed below. This analysis was carried out as a pilot study containing a small sample size of 32 patients.

7.4.1 LIN28B as a marker of diagnosis and resistance

Of the 6 gene/miRNA markers investigated in clinical samples, our study indicated that the down-regulation of LIN28B may be linked with chemoresistance in ovarian cancer. However, it was difficult to draw definitive conclusions as all response groups (NR, PR and R) had samples that had no detectable expression of LIN28B by qPCR (Table 7.4). It is only when we examined a subset of samples (samples that expressed LIN28B to some degree by qPCR (n=17)), that a significant reduction in expression was seen in chemoresistant groups (PR (n=3) + NR (n=7)) compared to the non-chemoresistant R group (Table 7.3, Figure 7.1). This subset of LIN28B expressers had reduced DFS in those patients that expressed the gene at lower levels compared to those that had higher expression (p=0.0067, 1 df (Log-rank Test), HR=0.05537 (0.006830-0.4489), Figure 7.4 (B)). The HR value of 0.6 indicated that patients with low expression of LIN28B were 17 times more likely to progress than those with high expression. The LIN28B gene is primarily expressed in fetal tissues and is not ordinarily expressed in adult tissues. However, it does become re-expressed in cancerous tissues. For this reason, it may be reasonable to deduce that samples in our study that have no detectable expression by qPCR may be classed as low-expressers of LIN28B, and those that have any detectable expression by qPCR may be classed as high-expressers. For this reason, the expression of LIN28B and survival was re-evaluated using these criteria on our full set of patient samples. Unfortunately, no significant difference in DFS or OS was seen in this case (Figure 7.4 & 7.6 (D)).

The literature and results from OVMARK analysis (Table 7.2) contradicted the findings from our small cohort of samples linking low LIN28B expression to reduced DFS. It has been shown that up-regulation of LIN28B is associated with advanced carcinomas including Wilms' Kidney, germ cell, and ovarian tumours (*Viswanathan et al. 2009*). In ovarian cancer patients, high expression of LIN28B has been found to be significantly associated with reduced PFS and OS compared to patients having low LIN28B expression (p=0.0017 and p=0.0022, respectively) (*Lu et al. 2009a*). The study by *Lu et al. (2009a)* utilises a larger cohort of patient samples when carrying out Kaplan Meier analysis (High expressers of LIN28B (n=59) and low expressers of LIN28B (n=82)). The team also found that high expression of LIN28B was associated with a larger residual tumours and suboptimal debulking status. Samples numbers were insufficient to investigate this in our study. *Lu et al. (2009a)* also found that LIN28B expression was not associated with the stage and grade of a tumour. It was not possible to evaluate this in our study, as we confined our samples to advanced cases (FIGO 3-4) of ovarian cancer. As this study used different grades, stages and histotypes of ovarian cancer,

this could explain the difference in results obtained from *Lu et al. (2009a)* and our study.

Other studies also link over-expression of LIN28B to poor prognosis and chemoresistance in ovarian cancer (*Topp et al. 2014*; *Yan et al. 2013*). UPN251-7C had up-regulated expression of LIN28B and down-regulated expression of let-7i when compared to non-resistant UPN251 parental cells. LIN28B is a known inhibitor of the Let-7 processing system binding to the terminal loops of Let-7 family miRNA precursors, resulting in the negative regulation of its members (*Heo et al. 2008*; *Rybak et al. 2008*). Considering this system of interaction, our study investigated whether opposed expression of these two markers (i.e. up-regulation of one marker and down regulation of the other and vice versa) influenced DFS and OS in our patient cohort. No significant differences were found in either DFS or OS (Figure 7.7 (A & B)). For this reason, we cannot conclude that these markers in combination improve their singular predictive power.

In summary, the results from our small subset of patients (excluding samples that did not express LIN28B), linking low LIN28B expression to chemoresistance and reduced DFS, could not be confidently confirmed. This was due to LIN28B not being expressed in many of our samples by qPCR across response groups, non-expressed samples of LIN28B showing no difference in DFS and OS compared to samples expressing LIN28B and the literature indicating from a large cohort study that high-expression of LIN28B was significantly associated with PFS and OS.

7.4.2 GLI3 as a marker of diagnosis and resistance

Although no significant differences in GLI3 expression were seen between chemoresistant and chemosensitive patient groups (Table 7.3, Figure 7.1), GLI3 expression levels within our samples could be linked with DFS and OS. Patients that expressed low levels of GLI3 in our study had worse DFS than those who expressed high levels of GLI3 (p=0.009, 1 df (Log-rank Test), HR=0.1210 (0.02480-0.5907), Figure 7.4 (A)). The HR of 0.1 indicated that patients with low expression of GLI3 had 10 times greater chance of progressing than those with high GLI3 expression. Also, patients with low expression levels of GLI3 had a worse OS than those who expressed high levels of GLI3 (p=0.0289, 1 df (Log-rank Test), HR=0.2566 (0.07573-0.8692), Figure 7.6 (A)). The HR of 0.3 indicated that patients with low expression of GLI3 had a 3.3 times greater chance of dying than those with high GLI3 expression. Our carboplatin resistant cell line UPN251-7C had up-regulated expression of GLI3 and down-regulated expression of miR-205 when compared to non-resistant UPN251

parental cells (chapter 6). MTI analysis showed a validated interaction between GLI3 and miR-205. Considering this interaction, our study investigated whether opposed expression of these two markers (i.e. up-regulation of one marker and down regulation of the other and vice versa) influenced DFS and OS in our patient cohort. No significant differences were found in either DFS or OS (Figure 7.7 (C & D)). For this reason, we cannot conclude that these markers in combination improve their singular predictive power.

The results obtained from our OVMARK analysis showed that up-regulation of GLI3 was associated with poor DFS, the opposite of what is shown by our cohort of patients. In the literature, GLI3 over-expression is seen in the cytoplasm of endometrioid carcinoma tumour tissue when compared to normal endometrium from a patient cohort of 271 (*Kim et al. 2009*). Our analysis by OVMARK contained samples from both epithelial serous patients and endometrioid patients. As up-regulation of GLI3 occurs in endometrioid carcinoma, this may have skewed the results given by OVMARK to point towards an up-regulated expression being linked with poor prognosis in advanced ovarian cancer. Our patient cohort only included patients with serous epithelial ovarian cancer. This may account for the differences in results. Down-regulation of GLI3 contributing to poor prognosis may be specific to serous ovarian cancer. The finding that up-regulation of GLI3 may be involved in platinum resistance from our Affymetrix work on UPN251-7C (chapter 6) may have been a cell line specific result. Cell lines are not a perfect system for examining gene expression in a clinically relevant context and can differ to that of patient samples.

It has been shown that GLI3, along with having a key role in the activation of hedgehog signalling (Identified by DAVID, chapter 6), controls a diverse range of cellular behaviours by cross-talk with other cell signalling pathways, such as the WNT/β-catenin pathway (*Sengupta et al. 2007*). In colon cancer, GLI3 (up-regulated in colon cancer cells compared to normal tissue) has been shown to promote cell proliferation by interacting with p53. Knockdown of GLI3 causes disruption of MDM2-p53 interaction and increases p53-dependant cell growth inhibition in colon cancer cells (*Kang et al. 2012*). In colorectal cancer, up-regulation of GLI3 promotes anchorage-independent growth and tumorigenicity by causing the up-regulation of genes related to adhesion, independent of p53 status (*Iwasaki et al. 2013*). In cervical cancer, GLI3 over-expression by reduction in miR-506, a tumour suppressor targeting GLI3, has been shown to suppress apoptosis and cell cycle arrest and confer resistance to chemotherapy (*Wen et al. 2014*). In addition to this, GLI3 has been shown to modulate angiogenesis and endothelial cell migration in mammalian adults (*Renault et al. 2009*).

The above evidence highlights the fact that GLI3 is a complex signalling molecule playing a role in a diverse number of signalling pathways (in addition to hedgehog signalling). This suggests that GLI3 may contribute to various physiological and pathological conditions in a number of ways. The mechanism by which GLI3 down-regulation is conferring poor PFS and OS in our serous ovarian cancer patient cohort is unknown. In the majority of cancer types, up-regulation of GLI3 has been associated with poor prognosis and cancer progression. To our knowledge, no other survival or expressional studies have been carried out for GLI3 in serous epithelial ovarian cancer. Further studies in serous ovarian cancer with a larger patient cohort are warranted for GLI3 in order to increase knowledge of GLI3 expression in ovarian cancer and resistance and to confirm our result of down-regulated expression of GLI3 being associated with poor prognosis. One caveat to this result is that as a prognostic tool detecting low levels of expression is more difficult than detecting high levels of expression in a clinical setting.

Gene expression does not necessarily translate to the protein level. There are many points of regulation between gene expression and translation into protein (including post transcriptional regulation). These points of regulation affect RNA processing, RNA stability, Translation and protein stability (*Vogel et al. 2012*). For this reason, immunohistochemistry analysis would be beneficial in order to confirm this finding.

7.4.3 Potential biomarkers (alone and in combination)

When the markers were assessed Individually, GLI3 could be confidently linked to predicting poor DFS and OS survival in patients with low GLI3 expression. None of the markers tested including GLI3 had any significant changes in fold expression when comparing chemoresistant groups (non-responders to chemotherapy (NR)) to the non-chemoresistant group (responders to chemotherapy (R)). Both groups contained samples that had high and low expression of tested markers resulting in fold changes with high SD and no significance (Table 7.3, Figure 7.1). LIN28B showed a significant fold reduction in expression in the partially chemoresistant group (partial responders to chemotherapy (PR)) when compared to the non-chemoresistant group. The partially chemoresistant group was small (n=4) and the analysis excluded one sample which had no expression of LIN28B by qPCR. Other groups also had a number of samples that had no expression of LIN28B (Table 7.4). Due to the small sample size of the PR group and difficulties in analysing data from LIN28B due to samples with no detectable expression, the reduction in fold expression by LIN28B could not be confidently regarded as a true result.

By examining all of the markers tested together (6 in total), we noted that 4 samples (out of the 17 resistant and partially resistant samples) had 3 or more markers with fold changes in the direction of expression that was expected to confer resistance (from Affymetrix analysis of resistant cell lines (chapter 6) and OVMARK analysis (Table 7.2)) when compared to non-chemoresistant samples (expected group). These samples also contained 1 or less target expressed in an unexpected direction. These 4 samples from the expected group had a median DFS of 1 month and a median OS of 6 months. 7 samples were also found that had 3 or more markers, with fold changes in the direction of expression, that was not expected to confer resistance (unexpected sample group) when compared to non-chemoresistant samples. These samples also contained 1 or less target expressed in an expected direction. When we compared the expected and unexpected groups, it was found that the expected group had a significantly worse prognosis (Figure 7.8). This indicated that this biomarker signature could be useful in identifying patients that will have poor prognosis when treated with conventional platinum/taxane chemotherapy. It would be beneficial to test this result in a larger patient cohort in order to confirm these findings.

This biomarker signature approach could potentially be used by clinicians to identify particularly aggressive cases of ovarian cancer. This could help shape a patient's treatment regime. If the patient's tumour expresses enough of this panel of markers in an expected direction, it could be classified as having poor prognosis with conventional chemotherapy. Therefore, other approaches could be employed to lengthen PFS and OS.

7.5 Conclusions

The down-regulation of LIN28B may play a role in chemoresistance in our patient cohort. This result was made difficult to interpret as a number of samples had no detectable expression across both chemoresistant and non-chemoresistant groups (which were excluded from our original analysis). A fold reduction in expression between partially chemoresistant/chemoresistant patients and non-chemoresistant patients was seen along with a significant reduction in DFS in patients with low LIN28B expression (excluding patient samples with no detectable LIN28B expression by qPCR). However, when samples with no detectable LIN28B expression were compared against samples that had detectable expression of LIN28B, no change in OS or DFS was seen. Therefore, this result is not clear-cut. Affymetrix analysis of carboplatin resistant cell lines UPN251-7C (chapter 6) and evidence from the literature pointed towards up-regulated expression of LIN28B being involved in resistance and

poor prognosis. This is the opposite of what was found in our small patient cohort. For this reason, LIN28B may not be an ideal marker to bring forward for further validation.

GLI3 displayed an association with poor DFS and OS in patients that had low GLI3 expression. This result, along with evidence from the literature that GLI3 has been found to be deregulated in other cancer types, makes it an attractive potential biomarker. This result warrants further investigation in a larger cohort of patients, containing at least 135 individuals for statistical power, to confirm its validity as a possible prognostic biomarker. If successful, GLI3 could help clinicians to select an appropriate treatment on a patient to patient basis. In general, this helps us move away from the standard chemotherapy approach currently employed for all patients with late stage epithelial ovarian cancer.

Further to this, an algorithm for a biomarker signature containing our 6 investigated targets (CCL20, GLI3, LIN28B, SRPX2, let-7i and miR-205) was devised, which may be useful in predicting patients with poor response to platinum/taxane chemotherapy, resulting in short DFS and OS. In breast cancer, a panel of markers has been successfully integrated into the clinic as a predictor of relapse in ER positive breast cancer. Oncotype DX® uses a panel of 21 genes to score the likelihood of breast cancer recurrence after standard treatment. This shows how a panel of markers, like our panel, can be useful in the clinical setting to improve treatment options. Again, this finding should also be verified in a larger patient cohort as with GLI3 alone in a study containing approximately 135 individuals.

CHAPTER 8

General Discussion



TRINITY
COLLEGE
DUBLIN

Chapter 8 General discussion

8.1 Introduction

Ovarian cancer is the leading cause of death from a gynaecological malignancy. European cancer incidence statistics show that ovarian cancer was the 5th most common cancer for all European women in 2012. There was a reported estimate of more than 65,000 new cases and approximately 42,000 deaths (*Ferlay et al. 2013*). This gives a mortality rate of approximately 65% in Europe. Ireland had in excess of 350 reported cases in 2012 with mortality figures exceeding 260 (*Ferlay et al. 2013*). This gives Ireland a mortality rate that is greater than the European average at approximately 75%. This highlights the huge need for research to be invested into the area of ovarian cancer in order to improve these statistics.

With this in mind, two of the most pressing areas of research in ovarian cancer are early detection and screening and chemoresistance. A high mortality rate in ovarian cancer is partly due to poor diagnosis. When detected early, the 5-year survival rate for ovarian cancer patients is approximately 90%. However, when diagnosed at late stage, ovarian cancer patients have a 5-year survival rate of approximately 33% (*Clarke-Pearson 2009*). To date, no suitable screening program has been established to detect ovarian cancer at an early stage. Therefore, ovarian cancer typically presents at late stage and, as a result, higher mortality rates are experienced. Another factor contributing to high mortality in ovarian cancer is the development of chemoresistant disease. The current standard for treatment of ovarian cancer at late stage (FIGO III-IV) is surgical debulking followed by an intravenous combination of platinum and taxane based chemotherapy (usually carboplatin and taxol) (*Cannistra 2004*). Approximately 75% of treated patients will have recurrence of disease after treatment with cytoreductive surgery and combination chemotherapy due to the development of chemoresistant disease. Relapsed patients have a median survival of 2 years following the recurrence and will all eventually die from their disease (*Ozols 2005*). The main focus of this thesis was to uncover a greater understanding of the mechanisms of chemoresistance in order to contribute significantly to the improved treatment of ovarian cancer patients in the clinical setting.

8.2 A novel investigation of chemoresistance in ovarian cancer

One of the greatest risk factors associated with epithelial ovarian cancer is a family history of the disease. This is most often linked to germline BRCA1/2 mutations where

incidence in ovarian cancer patients is estimated to be as high as 18.3% (*Hennessy et al. 2010*). A woman with a BRCA1 germline mutation has a 39-46% chance of developing ovarian cancer (*Hennessy et al. 2009*). The status of BRCA1 expression has also been shown to influence chemotherapy response. Down-regulation of BRCA1 causes sensitivity to DNA damaging agents, such as platinums and resistance to microtubule-interfering agents, such as taxol (*Foulkes 2006*; *Lafarge et al. 2001*; *Yuan et al. 1999*). Up-regulation of BRCA1 causes resistance to DNA damaging agents and sensitivity to microtubule-interfering agents (*Husain et al. 1998*; *Righetti et al. 1996*; *Tassone et al. 2003*). This is the basis for the 'inverse resistance relationship' that has been observed between acquired platinum and taxane resistance cell models, where BRCA1 was found to be a major genetic player driving this relationship (*Stordal et al. 2009*; *Stordal et al. 2007b*).

In this study, our research team devised a comparative selection strategy to allow the effects of resistance development on the inverse resistance relationship between platinum and taxane chemotherapy to be investigated in relation to BRCA1 status. The information obtained from monitoring resistance development in the selection strategy would provide evidence for whether ovarian cancer patients with BRCA1 defects in the clinical setting would respond differently to carboplatin and taxol treatment, when compared to those with functional BRCA1. If found to be different, BRCA1 screening of ovarian cancer patients could be beneficial in order to identify patient that will respond better to conventional chemotherapy, having slower development of resistance. Patients that develop resistance quicker to conventional chemotherapy, as indicated by BRCA1 status, may benefit more from alternate treatment regimes.

Our goal was achieved by exposing OVCAR8 (BRCA1-methylated) and UPN251 (BRCA1-wildtype) cell lines to different combinations of single agent carboplatin (platinum) and taxol (taxane) treatments over several months. The time taken for cells to recover and the extent of resistance developed over time allowed us to draw conclusions about how the development of resistance is effected by BRCA1 in relation to the inverse resistance relationship between platinums and taxanes (chapter 4).

It must be noted that cell line models have certain pros and cons associated with them. Some of the advantages of cell models, that influenced the decision to use them in this study, were that they are; readily available, widely used and easy to handle/maintain/manipulate at a relatively low cost. Also, they initially have a high degree of similarity with the initial tumour. Some disadvantages are that they can be genomically unstable, which may lead to a change in cellular characteristics, and they are maintained in a different environment than the tumour from which they were

originally derived. Therefore, cell models do not receive the same signals that the original tumour receives from its surrounding microenvironment and may act differently to certain stimuli. However, cell models are regarded as a good starting point for translational studies and drug testing. Results from cell line models are usually extrapolated to *in-vivo* models for further testing to confirm findings (*Ferreira et al. 2013*).

Also, in the selection strategy, the effects of alternating doses of platinums and taxanes on the cell lines was investigated to see if this slowed down resistance development due to the inverse resistance relationship. This novel approach to cell line development is unique and, to the author's knowledge, has not been investigated previously. If alternating treatments slowed down resistance development, then introducing this to the clinic to replace conventional combined administration could lead to improve survival in ovarian cancer patients.

One of the most novel aspects of this study was the stringent focus on maintaining clinical relevance throughout its duration. As the projects main focus was to better understand resistance mechanisms in ovarian cancer with the ultimate aim of improving treatment, it was important to keep all aspects of the study as clinically relevant as possible. For this reason, the selection strategy was devised as a low dose, pulsed strategy using drugs administered routinely in ovarian cancer treatment to mirror the clinical setting of chemotherapy administration, where patients receive 3-6 cycles of carboplatin/taxol chemotherapy every 3-4 weeks by intravenous bolus injection (chapter 4) (*Hennessy et al. 2009*; *Ozols 2005*). The majority of cellular models in the literature used to model carboplatin and taxol resistance have used an intermittent incremental inducement strategy or an increasing continuous administration strategy (*Duan et al. 1999a*; *Duan et al. 1999b*; *Hari et al. 2006*; *Li et al. 2004*; *Parekh et al. 1997b*; *Zhang et al. 2012a*). Although these strategies produce stable resistance, they use doses of drug that are too high for the clinical setting and produce higher fold resistance than is observed in the clinic (*McDermott et al. 2014*). Therefore, the resulting mechanisms of resistance that arose from the pulsed model in this study had the potential to produce clinically relevant changes that could be characterised and related to ovarian cancer patients. Also, models of carboplatin resistance are rare in the literature, which gives this study novel insight into carboplatin resistance in ovarian cancer.

Although there are many established mechanisms of platinum and taxane resistance in the literature, there is still a poor understanding of resistance in ovarian cancer. Some of the most prevalent mechanisms of platinum resistance that have been established to

date include, decreased accumulation and deactivation of the drug within the cell, loss or decrease in mismatch repair (MMR), increased repair of DNA adducts, inhibition of apoptosis and mutations in p53 (*Piccart et al. 2001*; *Rabik et al. 2007*; *Stordal et al. 2007a*; *Vasey 2003*). Similarly, some of the most prevalent mechanisms of taxol resistance to date include the expression of different isotypes of the β-tubulin subunit, mutation in the gene which codes for β-tubulin causing altered dynamics, and altered binding of taxanes to microtubules (*Kavallaris 2010*) and the over-expression of the ABCB1 gene which codes for the P-glycoprotein protein (P-gp, p170) (*Gottesman et al. 2002*). Further to this, transcriptomic changes in the transcriptome may also contribute to the development of taxane resistance mechanisms.

After the development of cellular resistance, the cell lines, derived from the selection strategy (chapter 4), were tested for a number of these commonly established mechanisms of carboplatin and taxol resistance (chapter 5). A drug screen using cell viability assays, a cellular glutathione (GSH) assay, growth assays, cell cycle and mitosis assays, apoptosis assays and western blotting were all utilised to characterise the resistant cells. Established mechanisms of resistance could then be linked to the clinically relevant resistant sublines. This, in turn, allowed us to speculate what mechanism of resistance may be developing within recurrent ovarian cancer patient tumours. In order to further elucidate the clinically relevant mechanisms of resistance that arose in the resistant sublines, gene chip technology was used in order to profile changes in both gene and miRNA expression in two of the most carboplatin and taxol resistant sublines (UPN251-7C and UPN251-7T), when compared to non-resistant parental cells (chapter 6).

The establishment of viable resistance biomarkers in ovarian cancer would be extremely beneficial in improving treatment in ovarian cancer. In the literature, gene profiling studies have been performed for numerous aspects of ovarian cancer including molecular profiling, subtype identification, diagnosis, early detection, prognosis and therapy (*Berchuck et al. 2005*; *Berchuck et al. 2009*; *Bonome et al. 2005*; *Chien et al. 2009*; *Hartmann et al. 2005*; *Huddleston et al. 2005*; *Mok et al. 2001*; *Moore et al. 2008*; *Nishizuka et al. 2003*; *Schwartz et al. 2002*; *Spentzos et al. 2004*; *The Cancer Genome Atlas Network 2011*; *Welsh et al. 2001*). The main aim of this study was to better understand chemoresistance in ovarian cancer. A number of gene profiling and biomarker discovery studies have also been undertaken in the area of chemoresistance; a number of which that have been conducted by our research group (*d'Adhemar et al. 2014*; *Helleman et al. 2006a*; *Koti et al. 2013*; *Laios et al. 2008b*; *Roberts et al. 2005*; *Selvanayagam et al. 2004*). Recently, the profiling of miRNAs in

ovarian cancer has also aimed at providing biomarkers for many aspects of the disease. MiRNAs are post transcriptional regulators of gene expression and are shown to be aberrantly expressed in cancer, presenting the opportunity to characterise these changes in expression (*Di Leva et al. 2010*; *Lewis et al. 2005*). Measurement of miRNA expression is much more sensitive than that of mRNA expression. MiRNAs frequently target entire pathways, and for this reason may be superior drug targets than genes or proteins (*Pritchard et al. 2012*). A number of studies have investigated miRNA expression with regards to ovarian cancer chemoresistance (*Boren et al. 2009*; *Cochrane et al. 2010*; *Eitan et al. 2009*; *Kong et al. 2011*; *Laios et al. 2008a*; *Leskela et al. 2011*; *Liu et al. 2012*; *Lu et al. 2011*; *Nam et al. 2008*; *Prislei et al. 2013*; *Yang et al. 2008a*; *Yang et al. 2008b*; *Ye et al. 2011*). These studies have taken place shortly before or during the commencement of this research project highlighting the current interest in this topic.

A number of factors separate our profiling study from previous studies (chapter 6). It has recently been stated that a robust overview of ovarian cancer resistance biomarkers could be obtained from the combination of mRNA and miRNA expression profiling (*Miles et al. 2012*). This article was published after the commencement of this research project. Our study does just that by profiling both gene and miRNA changes that occur between chemoresistant ovarian cancer cell lines and their non-chemoresistant parental cells. The top deregulated genes/miRNAs were examined from the Affymetrix arrays and DAVID pathway analysis was carried out on the gene datasets to identify deregulated pathways. Also miRNA-target interaction (MTI) analysis was carried out between the gene and miRNA datasets in order to identify systems of interaction within the cells. From this analysis we could see if any of the top deregulated genes or genes identified by DAVID, had interacting target miRNAs. Paired gene/miRNAs could provide novel drug targets that could potentially knock down key pathways involved in ovarian cancer resistance.

Another novel aspect of this experiment was that the cell lines utilised in this study were developed in a clinically relevant fashion (as previously described) and therefore have the ability to identify clinically relevant biomarkers from two different molecular levels in the cell that interact (mRNA/miRNA). Furthermore, the identified biomarkers with the most promise were then screened by qPCR in a pilot study containing tumour specimens from ovarian cancer patients with different responses to chemotherapy, allowing us to see if the biomarker was an accurate predictor of resistance (chapter 7). This bridged the gap from our laboratory derived cell models to the clinical setting by testing the discovered resistance biomarkers in ovarian cancer patient samples.

8.3 Contributions to the current knowledge on ovarian cancer resistance

This study has added substantially to the current knowledge of ovarian cancer resistance. It has provided a novel method of measuring cell confluence to the cellular research community. It has broadened our understanding of taxol and carboplatin resistance in a clinically relevant framework and it has delivered a number of novel findings relating to the discovery of biomarkers for ovarian cancer resistance.

8.3.1 Development of the novel area fraction output method

As part of the cell selection strategy the need for a method that could objectively measure the point in time when cells in drugged flasks reached confluence, without disturbing growth was observed. This was required by our research group in order to accurately measure the time taken for cells to recover from drugging after each round of selection in the author's selection strategy. The values returned from this method were used as a parameter to help elucidate the time taken for drug resistance to develop in the developing resistant cell line models. The manuscript for this method has been accepted for publication by MethodsX, a peer-reviewed journal.

The resulting method of area fraction (AF) output provides a fast, accurate, cheap, non-destructive and non-invasive method of measuring cell number as an estimate for cell confluence. It is ideal for adherent cells in cell-culture flasks that require undisturbed continued growth. It provides an objective measure of when cells reach confluence. The method was validated against cell counting using a haemocytometer, known to be an accurate measure of cell number (Figure 3.4). It is limited to adherent cell lines that grow in a monolayer. Other common methods of measuring cell number or confluence such as colorimetric assays, membrane integrity assays and the use of microscopic systems can be expensive, destructive, invasive, and laborious and often use indirect measurements (*Allen et al. 1994*; *Anoopkumar-Dukie et al. 2005*; *Brinkmann et al. 2002*; *Curl et al. 2004*; *Jones et al. 1985*; *Juneau et al. 2013*; *Louis et al. 2011*; *Molder et al. 2008*; *Mosmann 1983*; *Muir et al. 1990*; *O'Brien et al. 2000*; *Ribble et al. 2005*; *Tennant 1964*). This makes the AF method ideal for laboratories on a small budget. It can be adapted easily for equipment that is readily available and inexpensive. This technique could be applied to several biological fields that routinely require measurements of cell confluence such as oncology, stem cell biology and immunology. The technique is particularly geared towards measuring cytotoxicity and effects of drug administration to cells.

8.3.2 BRCA1 and the inverse resistance relationship

Current knowledge on the inverse resistance relationship states that the majority of cellular models, that had acquired drug resistance and reported sensitivities to platinums or taxanes, had an inverse resistance relationship between cisplatin and taxol as well as other combinations of drugs, such as carboplatin and taxol used in this study (*Stordal et al. 2007b*). It was found that clinical responses to platinums and taxanes in ovarian cancer mirror that of cellular models, displaying this inverse resistance relationship. The mechanisms behind this inverse resistance relationship are poorly understood, but systematic review has indicated that BRCA1 was most associated with the inverse resistance relationship between cisplatin and taxol (*Stordal et al. 2009*).

This study contributes to the current knowledge of the inverse resistance relationship. Our results found that, both resistance to carboplatin and taxol developed quicker and more stably in UPN251 (BRC1-wildtype) compared to OVCAR8 (BRCA1-methylated), (Figure 4.6). This was not expected as it was hypothesised that, due to the inverse resistance relationship, carboplatin resistance would develop quicker than taxol resistance in cells expressing BRCA1 and that the opposite would be true in cells not expressing BRCA1. Also, taxol resistance developed quicker in BRCA1-wildtype and BRCA1-methylated cells models, irrespective of BRCA1 status (Figure 4.8). These results are outlined in a manuscript recently accepted by Experimental Cell Research, a peer-reviewed journal.

Furthermore, it was hypothesised that, due to the inverse resistance relationship, cells receiving alternating treatments of carboplatin and taxol should develop resistance slower or not at all when compared to single-agent treatments. This would have the potential to evolve ovarian cancer treatment if found to hold true. However, the results were ambiguous, depending on the logic used to draw conclusions. It can be shown to be true or false under different conditions (Figure 4.8). For this reason, we cannot currently provide strong evidence for this sequence of treatment being superior to the current standard platinum/taxane combination chemotherapy. However, from the drug screen carried out on the cell lines prior to resistance development, PARP inhibitors CEP8983 and veliparib can put forward as possible candidate drugs for the treatment of carboplatin/taxol resistant ovarian cancer. No cross resistance was seen by either PARP inhibitor, in any of the carboplatin or taxol resistant UPN251 sublines developed (Table 5.1, Figure 5.2).

In addition to BRCA1, a number of additional genes were put forward from our study as having a possible involvement in the inverse resistance relationship between platinum and taxane resistance. ABCB1, CD24P4, GPC4, GUCY1B3, SLC17A1, SLC34A2, TENM2 and VCAM1 were all found to be up-regulated in carboplatin resistant cells and down-regulated in taxol resistant cells under different conditions when compared to non-resistant cells by Affymetrix gene chip analysis (Table 6.16). Similarly, LIN28B was up-regulated in taxol resistant cells and down-regulated in carboplatin resistant cells (Table 6.16). P-glycoprotein (P-gp), the product of the ABCB1 gene, has been previously put forward as a player in this relationship (*Stordal et al. 2009*). Up-regulation of the P-gp protein in taxol resistance and down-regulation in carboplatin resistance is also seen by Western blotting in our study in the same cell lines (Figure 5.15). This evidence strengthens the findings by *Stordal et.al (2009)* and provides additional genes that have the potential to mediate the inverse resistance relationship. In order to confirm this result, further investigation of these markers in *in-vivo* studies is warranted. For example, the development of platinum and taxane resistant ovarian cancer xenografts could be carried out to see if these markers show the same inverse expressional patterns between taxol and carboplatin resistance, as seen in this study.

8.3.3 Mechanisms of resistance in ovarian cancer

Resistance in ovarian cancer remains a hot topic of research. This thesis has made significant contributions in this area. As the present study was designed to be clinically relevant in all aspects, the mechanisms of resistance that arose in the cell lines had the potential to mirror the mechanism of resistance that arise in ovarian cancer patients.

8.3.3.1 Taxol Resistance

The over-expression of P-gp was the dominant mechanism of taxol resistance found in our UPN251 resistant sublines. Cytotoxicity assays for P-gp substrates taxol, vinblastine and olaparib ± elacridar all show highly significant drops in IC_{50} when P-gp is inhibited with elacridar (Table 5.1, Figure 5.1 and Figure 5.2) (Lawlor et al. 2014). Western blot data showed increased P-gp protein expression for sublines that had taxol treatment during selection (Figure 5.15). Finally, the ABCB1 gene that codes for P-gp is part of the top five significantly up-regulated genes returned by our Affymetrix gene chip analysis of UPN251-7T taxol resistant cells (Table 6.11). Therefore, it is likely that taxol is being actively pumped out of the cell by P-gp causing taxol resistance (*Juliano et al. 1976*; *Ueda et al. 1987*). Up-regulation of this protein is linked with poor prognosis for patients with ovarian and breast cancers, sarcomas and other malignant diseases (*Hoffmann et al. 2010*; *Nakayama et al. 2002*; *Rodrigues et al.*

2008). However, other studies have indicated that strong P-gp over-expression is uncommon in the clinic, even if it is strongly correlated with poor outcome and relapse (*Materna et al. 2004*; *McGown et al. 1994*; *Penson et al. 2004*). With this in mind, further investigation into the other mechanisms of taxol resistance contributing to the cells resistant phenotype was examined.

Apoptotic resistance was found to be another mechanism of taxol resistance in our cells as was shown by FACS apoptosis assays (Figure 5.8 & 5.9). This was, in part, due to an inability to reduce Bcl-2 levels, which was observed by Western blotting in the taxol-resistant cell lines, but not in taxol-sensitive cells (Figure 5.19). Another recent study has shown a similar result in ovarian cancer cells. Taxol treatment was able to reduce expression of the Bcl-2 protein in taxol-sensitive ovarian cancer cells SKOV3-ip1 and not in taxol resistant SKOV3-ip2 cell lines (*Chen et al. 2013*). Circumvention of G2/M arrest was another mechanism by which the UPN251 taxol-resistant cell lines modulated apoptosis to survive (Figure 5.6). Taxol is known to induce cell cycle arrest at the G2/M phase of the cell cycle, resulting in apoptosis as part of its mechanism of action (*Long et al. 1994*). From the results of the our mitosis assay on the UPN251 resistant sublines, at a high dose of taxol, UPN251-7T and UPN251-6TALT saw significantly less cells in mitosis than UPN251, UPN251-7C or UPN251-6CALT. Further to this, two genes that play a role in the modulation of apoptosis were found to be highly deregulated in our taxol resistant UPN251-7T cells by Affymetrix gene chip analysis. These genes were PLAC8 and MAP3K15 (ASK3), both up-regulated compared to non-resistant parental cells (Table 6.11). PLAC8 is an important target gene of the proto-oncogene c-Myc, where PLAC8 regulation is responsible for conferring resistance to apoptotic stimuli (*Mourtada-Maarabouni et al. 2013*). Its over-expression has been shown to protect cancer cell lines from apoptosis, while PLAC8 knockdown induces apoptosis (*Mourtada-Maarabouni et al. 2013*). It has also been associated with doxorubicin resistance (*Indermaur et al. 2010*). MAP3K15, on the other hand, has no publications relating to cancer by searches made in PubMed. The protein encoded by this gene is a member of the mitogen-activated protein kinase (MAPK) family, playing an essential role in apoptotic cell death triggered by cellular stresses.

Taxol resistant cells have also been shown to have a reduction in growth rate, which contributes to their taxol resistant phenotype (*Ohta et al. 1994*; *Wang et al. 2013*). Via growth assays, all UPN251 resistant sublines took significantly longer to reach quadrupling time when treated with a range of taxol concentrations compared to drug free controls, whereas, UPN251 had no significant changes for any taxol dose tested

(Figure 5.4 and Figure 5.5). The cell line with the highest fold taxol resistance, UPN251-7T, also had reduction in growth rate at lower doses of taxol than any of the other UPN251 derived sublines. The AREG gene was found to be highly deregulated in the UPN251 resistant cell lines by Affymetrix analysis (Table 6.11). The AREG protein encoded by this gene is a member of the epidermal growth factor family and interacts with the EGF/TGF-alpha receptor to promote the growth of normal epithelial cells. It has been shown to inhibit the growth of aggressive cancer cell lines. AREG over-expression has been found in ovarian cancer and has been linked to ovarian cancer progression and resistance (*Panupinthu et al. 2014*). However, it was found to be down-regulated in UPN251-7T. AREG deregulation may still contribute to the reduction in growth rate observed in the UPN251 cells to circumvent resistance. A summary of the taxol resistance mechanisms found in our taxol resistant cell line UPN251-7T is shown in Figure 8.1.

Other pathways involved in taxol resistance, identified by the top deregulated genes in our taxol resistant cell lines, include angiogenesis, membrane regeneration and repair, intracellular transport, cell interactions with the extracellular matrix and vasoconstriction. DAVID pathway analysis also found a number of pathways in which a number of genes were deregulated namely; ECM-receptor interaction, small cell lung cancer, arrhythogenic right ventricle cardiomyopathy (ARVC) and pathways in cancer (Table 6.13).

8.3.3.2 Carboplatin resistance

The mechanisms of resistance in the UPN251 carboplatin resistant cell lines appeared to be a complex mixture, involving the deregulation of many genes and miRNAs affecting many signalling pathways.

A number of the classical mechanisms of resistance already established in the literature were ruled as having major roles to play in our carboplatin-resistant phenotypes. Rises in intracellular GSH was ruled out by the results of our GSH assay, which showed the resistant cell lines to have no significant rise in intracellular GSH levels in response to carboplatin (Figure 5.3) (*Chen et al. 2010*). Also, aberrant expression of copper transporters or alterations in copper metabolism was found not to have a major role in the author's carboplatin-resistant phenotypes (*Safaei et al. 2005*). The possible role of copper transports in the author's carboplatin resistant model was first indicated by the carboplatin resistant cells having cross resistance to $CuSO_4$ (Table 5.1, Figure 5.1 (C)). Protein expression by Western blotting (Figure 5.16 & 5.17) and mRNA expression by Affymetrix gene chip analysis of ATP7A and CTR1

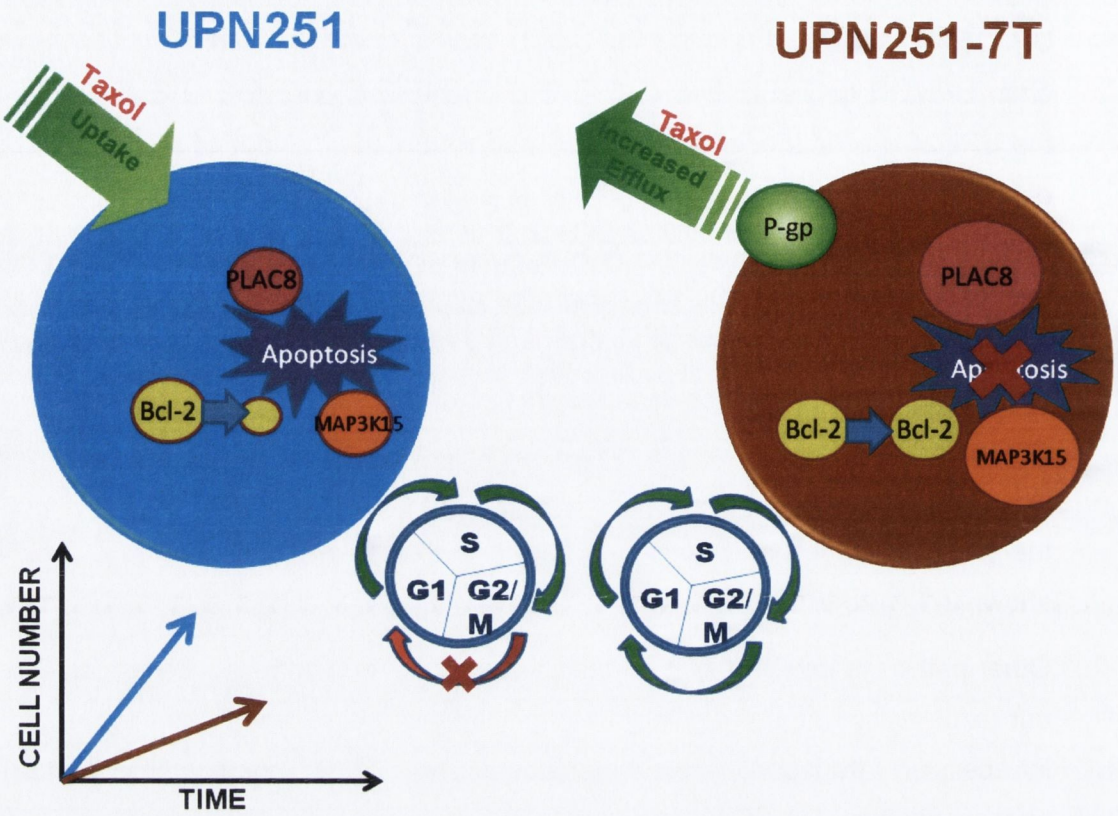

Figure 8.1 Characterisation of resistance mechanisms in taxol-resistant cell line UPN251-7T.

Mechanisms include increased efflux of taxol via over-expression of P-gp, increased expression of PLAC8 and MAP3K15 and inability to decrease Bcl-2 resulting in resistance to apoptosis, circumvention of G2/M arrest and a reduction in growth rate.

(chapter 6) indicated no significant changes between carboplatin resistant cells and non resistant parental cells. However, relocation of ATP7A and CTR1 might still contribute to their resistant phenotypes, even without changes in protein or gene expression (*Stordal et al. 2012*).

As with taxol resistance, a reduction in apoptosis played a role in our carboplatin resistant cell lines, as was indicated by FACS apoptosis assays (Figure 5.10 & 5.11). Also, an inability to reduce the levels of both bcl-2 and bcl-XL in carboplatin-resistant cell lines appears to be contributing to a carboplatin-resistance phenotype. By Western blotting, bcl-2 was reduced following carboplatin exposure in non-resistant parental cells when compared to an un-treated control (Figure 5.19). It was not reduced in the most highly resistant UPN251 subline UPN251-7C after carboplatin exposure. This follows the same theory of resistance as was seen in our taxol resistance model for bcl-2. Treatment with carboplatin in UPN251 gives a significant drop in Bcl-XL protein

expression levels by Western blotting, when compared to untreated parental cells (Figure 5.20). However, no change was seen across all the drug-resistant phenotypes in response to carboplatin treatment when compared to their untreated counterparts. It may be that the loss of a cell's ability to down-regulate Bcl-XL was contributing to a carboplatin resistance phenotype, as seen with Bcl-2. This theory is backed up by the literature where by the absence of Bcl-XL down-regulation in response to cisplatin (another platinum agent) has been associated with chemoresistance in ovarian cancer cell lines (*Villedieu et al. 2007*). MAP3K15 and PLAC8, which confers apoptotic and chemotherapy resistance when over-expressed, were also found to be highly up-regulated in the carboplatin-resistant UPN251-7C cells by Affymetrix gene chip analysis, as was found in the taxol-resistant cell lines (Table 6.2). Therefore, this may be a general response to cellular stresses experienced by the cells after drug exposure. Two bone morphogenetic proteins (BMPs) were down-regulated in our UPN251-7C cell lines by Affymetrix analysis (BMPR1B and BMP2). The signalling of BMP genes are involved in apoptosis and, therefore, may be contributing to apoptotic resistance to carboplatin in our cell lines (*Miyazono et al. 2001*; *Wozney 1998*).

Resistance to cell cycle changes contribute to the carboplatin-resistance phenotypes in our models. The cell cycle of UPN251-7C, when treated with a high dose of carboplatin for 24hours, remained unchanged when compared to untreated cells (Figure 5.13 & 5.14). UPN251 and UPN251-7T had significant changes in the number of cells at each stage of the cell cycle (G1, S and G2/M) when treated with the same dose of carboplatin. A summary of the carboplatin resistance mechanisms found in the carboplatin resistant cell line UPN251-7C is shown in Figure 8.2.

Other pathways involved in carboplatin resistance, identified by the top deregulated genes in the UPN251 taxol-resistant cell lines include regulation of developmental events, tissue differentiation, cell maintenance, morphogenesis, cell-cell interaction, signal transduction, cellular transformation, cell migration, bicarbonate secretion and absorption, regulation of intracellular pH and T-cell signal transduction. Also, DAVID pathway analysis found a number of pathways in which a number of genes were deregulated, namely; hematopoietic cell lineages, axon guidance, Cytokine-cytokine receptor interactions, basal cell carcinoma, hedgehog signalling pathway, and pathways in cancer (Table 6.4).

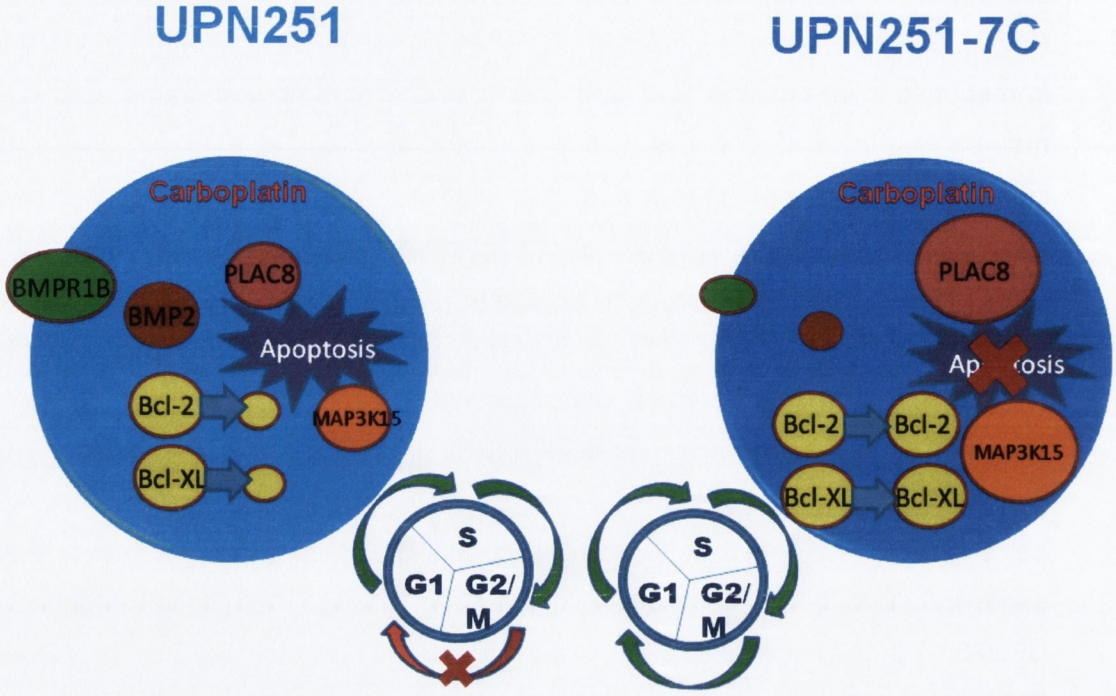

Figure 8.2 Characterisation of resistance mechanisms in carboplatin-resistant cell line UPN251-7C.

Mechanisms include increased expression of PLAC8 and MAP3K15, reduced expression of BMPR1B and BMP2 and inability to decrease Bcl-2/Bcl-XL resulting in resistance to apoptosis and resistance to changes in the cell cycle when exposed to high dose carboplatin.

8.3.3.3 Combined platinum and taxol resistance models and their effects on resistance development

Models of taxane-platinum resistance are rare in the literature. One such study developed a taxane-platinum resistant model for non-small cell lung cancer (NSCLC) by exposing the cells to cycles of taxol and carboplatin, as was done with our alternating cell lines UPN251-6CALT and UPN251-6TALT (*Dalvi et al. 2012*). These NSCLC models displayed over-expression of P-gp (ABCB1) and showed characteristics of cell undergoing EMT. Another study developed a dual carboplatin and docetaxel resistant cell line from A2780 ovarian cancer cell lines, which are cross resistant to both agents (*Armstrong et al. 2012*). The study also developed A2780 sublines that were resistant to each agent individually, but were not cross-resistant to the other agent. Gene profiling revealed that the dual model contained genetic changes

not present in the singularly resistant models demonstrating that combined drug resistance may not be a simple combination of changes present in single-agent resistant cell lines, but can contain novel changes.

Results from this study allowed for novel observations to be made concerning models receiving alternating doses of drugs with different mechanisms of action. It was concluded that the cytotoxic agent that a cell-line was exposed to first influenced the mechanisms of resistance that developed in the cells thereafter. From the drug screen on our cell lines receiving alternating treatments of carboplatin and taxol, UPN251-6CALT displayed significant fold resistance to $CuSO_4$, while UPN251-6TALT showed no significant fold resistance (Table 5.1, Figure 5.1 (C)). Also, UPN251-6TALT showed significant sensitivity to oxaliplatin, while UPN251-6CALT had no significant fold change. The only difference was that UPN251-6CALT received carboplatin in the first round, whereas, UPN251-6TALT received taxol. This would indicate that different resistance mechanisms were being selected in these cells, depending on initial drug exposure. This may be a consideration for future combinations of drugs administered to cancer patients. Cancer therapy is continually changing and evolving in order to improve survival from this lethal malignancy. Therefore, sequence dependant studies into acquired mechanisms of drug resistance may be an important factor to consider when designing new therapies, or when improving existing regimes. Again, it must be mentioned that cell line models can be genetically unstable, leading to changes that may not necessarily be representative of, in this case, the development of resistance in ovarian cancer patient tumours (*Ferreira et al. 2013*). Therefore, further confirmation of this result by *in-vivo* studies is warranted.

8.3.4 Ovarian cancer resistance biomarkers

From the Affymetrix analysis of carboplatin and taxol resistant cell lines UPN251-7C and UPN251-7T, a number of potential gene and miRNA resistance biomarkers were identified for ovarian cancer (chapter 6). A number of gene/miRNAs were found to be de-regulated in the same direction as was seen in the literature for ovarian and other types of carcinoma making them interesting candidates for follow up analysis. A number of the top deregulated genes/miRNAs, relating to carboplatin and taxol resistance, and those identified by DAVID, have been linked to ovarian cancer resistance and/or poor OS/PFS by previous studies in patients or cell lines. Therefore, these markers may be useful on their own or in combination with other markers as ovarian cancer resistance biomarkers. These include; EEF1A2, GDF15, LIN28B, DPP4, BMP2, BMPR1B, KITLG, TNFRSF11A, CCL2, WNT2B, WNT5A, IL8, MMP7,

VCAM1, Let-7i, miR-146a, miR-152, miR-98, miR-143, miR-145, miR-29b and miR-489 (*Arnold et al. 2005*; *Badiglian et al. 2009*; *Bitler et al. 2011*; *Bock et al. 2010*; *d'Adhemar et al. 2014*; *Fader et al. 2010*; *Huang et al. 2013*; *Kajiyama et al. 2010*; *Kassim et al. 2004*; *Li et al. 2014b*; *Liu et al. 2014*; *Ma et al. 2010*; *Marchini et al. 2011*; *Peng et al. 2011*; *Penson et al. 2000*; *Shaw et al. 2007*; *Sugio et al. 2014*; *Sun et al. 2008*; *Topp et al. 2014*; *Uslu et al. 2005*; *Wang et al. 2012*; *Wendler et al. 2011*; *Wojnarowicz et al. 2008*; *Wu et al. 2014*; *Yan et al. 2013*; *Yang et al. 2008b*; *Yoon et al. 2010*; *Zhang et al. 2008b*; *Zhu et al. 2014*). A selection of these markers have only been found to be de-regulated in ovarian cancer in the literature, but have not yet been linked to resistance and, therefore, may have potential utility as markers of resistance in ovarian cancer. These include; IL7, SLIT2/3, ROBO1, CCL20 and miR-205 (*Dai et al. 2011*; *Dickinson et al. 2011*; *Dong et al. 2012*; *Iorio et al. 2007*; *Lambeck et al. 2007*; *Qiu et al. 2011*; *Schutyser et al. 2002*; *Son et al. 2007*; *Tsukamoto et al. 2014*; *Xie et al. 2004*; *Zheng et al. 2013*; *Zhou et al. 2014*). Another subset of markers have been found to be linked to chemo-resistance and/or poor overall/progression free survival in other cancer types and, therefore, may have effect in ovarian cancer. These include; EPHA7, SEMA3A, GLI3, SRPX2, miR-210 and miR-181c (*Bai et al. 2013*; *Cui et al. 2013*; *Deng et al. 2011*; *Greither et al. 2010*; *Hong et al. 2012*; *Kim et al. 2010a*; *Kurosawa et al. 1999*; *Liu et al. 2013a*; *Maione et al. 2009*; *Maione et al. 2012*; *Mei et al. 2014*; *Qiu et al. 2013*; *Wang et al. 2008*; *Wen et al. 2014*; *Yamada et al. 2014*). Also, a large number of novel markers were identified for ovarian cancer. These have been found to be deregulated in other cancer types or do not have publications in the literature linking them to cancer. These include; MAP3K15, CTSS, SERPINB7, LAMB3, ITGB6, EDN2, miR-708, miR-532-3p, miR-125b-1*, miR-3128, miR-3200-3p, miR-3687, miR1272, miR-4417, miR-501-5p, miR-766, miR-3200, miR-3949, miR-3929, miR-4440, miR-3916, miR-1273, miR-4708-5p, miR-4274 and miR-1285.

Further to the Affymetrix analysis, a small subset of potential markers to examine in ovarian cancer patient tumour samples with different responses to platinum/taxol combination chemotherapy were selected as a pilot study (CCL20, GLI3, LIN28B, SRPX2, let-7i and miR-205). From this study, it was found that down-regulation of LIN28B may be involved in chemoresistance in ovarian cancer. It was also found that GLI3 expression was correlated with patient outcomes. Low expression of GLI3 was linked with poor DFS and OS in the ovarian cancer patient cohort (Figure 7.4 & 7.6). This is a novel marker for ovarian cancer. However, deregulation of GLI3 has been previously associated with patient outcome and resistance in other cancer types (*Kim et al. 2009*; *Wen et al. 2014*). Also, a biomarker signature containing the six

investigated targets that may be predictive of patients with short DFS and OS was put forward (Table 7.5, Figure 7.8).

8.3.5 Summary of contributions to current knowledge

A summary of the contributions made by this project to the current knowledge of ovarian cancer resistance is given below:

- The development of a novel rapid, affordable, non invasive method of measuring confluence in adherent cell lines directly in tissue culture flasks;
- The development and characterisation of novel singularly and dual carboplatin and taxol resistant cell lines in a clinically relevant framework;
- We provided novel insights into the development of chemoresistance in relation to BRCA1 status;
- We provided novel insights into dual carboplatin and taxol resistant mechanisms;
- The discovery of novel gene/miRNA biomarkers for ovarian cancer platinum/taxane resistance;
- The identification of clinically relevant pathways involved in carboplatin and taxol resistance via gene/miRNA screening;
- The identification of genes that may play a role in the inverse resistance between platinum and taxane chemotherapy;
- The discovery of GLI3 and our novel biomarker panel (CL20, GLI3, LIN28b, SRPX2, Let-7i and miR-205), which could act as prognostic biomarkers in ovarian cancer. They have been shown to be predictive of DFS and OS in ovarian cancer patient tumour samples.

8.4 Future directions

Further studies relating to this research project could include:

- Clinical validation of more potential resistance biomarkers identified by Affymetrix expression data
    - Pilot studies in small patient cohort
    - Studies in larger patients cohorts for markers with promise
- Further clinical validation of the currently identified biomarkers in larger patient cohorts
- Further validation of potential targets by examination in other resistant cell line panels
- Clinical validation of lincRNA identified by Affymetrix expression data
- Evaluation of promising biomarkers at a protein level
- Affymetrix analysis of carboplatin and taxol cross-resistant cell lines
- Further characterisation of carboplatin and taxol resistant cell lines

This study has identified multiple biomarkers through Affymetrix array data that have the potential to separate non-chemoresistant and chemoresistant disease in ovarian cancer. Only a small subset of these markers was chosen to test further in a pilot study of 32 ovarian cancer patients.

Markers previously linked to ovarian cancer resistance and/or OS/PFS by previous studies in patients or cell lines would be useful to pursue further in ovarian cancer patient samples. They could be tested on their own or in combination to find biomarkers or signatures that predict chemotherapy resistance or response to chemotherapy. Similarly, markers that have been previously linked to ovarian cancer in the literature but have not yet been linked to resistance would be useful to pursue further in patient samples. This study has discovered a number of biomarkers that are novel to ovarian cancer resistance. Both gene and miRNA biomarkers have been found that are novel to ovarian cancer or have not yet been linked to any type of carcinoma. The majority of these are newly discovered miRNAs. The characterisation of these biomarkers in patient samples could potentially identify new biomarkers of resistance or diagnosis that are effective in the clinical setting for ovarian cancer. Other biomarkers

that could be pursued are those that have been previously linked with resistance in other cancer types, but have not yet been investigated in ovarian cancer.

After the testing of these potential biomarkers in a small sample pilot study, interesting markers should be examined in larger patient cohorts for further clinical validation. From our study, GLI3 and the biomarker panel of six targets (CCL20, GLI3, LIN28B, SRPX2, let-7i and miR-205) have shown promise as diagnostic biomarkers. These need to be tested in larger patient cohorts for further validation. Also, as mRNA expression levels in the cell do not necessarily correlate to protein expression, the investigation of these biomarkers by IHC in patient samples at the protein level is an important validation that should be carried out.

Potential markers, such as GLI3 and PLAC8 (involved in carboplatin resistance in our study), could also be examined in other chemoresistant ovarian cancer cell line panels to see how prevalent these markers are in resistant ovarian cancer cells. A cell line panel of 41 ovarian cancer cells is available for study by our research team (*Stordal et al. 2013*). The markers could be tested in more intrinsically carboplatin resistant cell lines, such as OCC1 or OVCAR433 (Figure 4.1), to see if they mimic the expression from the UPN251 acquired resistance models. This could indicate differences and similarities between acquired and intrinsic resistance. For example, high expression of PLAC8 may indicate circumvention of apoptosis in these cells by a similar mechanism. Therefore, It may also be interesting to look at other markers involved in apoptotic signalling that were deregulated in our cell lines such as bcl-2, bcl-XL, BMPR1B and BMP2 in OCC1 or OVCAR433. The effects of knocking down any of these markers that may be over-expressed would be expected to sensitise cells to carboplatin treatment. Similarly, in the case of low expression of markers, the cells could be transfected with the marker in question in order to see if the cells are sensitised to carboplatin. Markers could also be studied in other cell systems of acquired resistance such as IGROV1 (cisplatin sensitive) and IGROV-CDDP (cisplatin resistant) (*Ma et al. 1998*; *Stordal et al. 2012*).

The Affymetrix GeneChip® Human Gene 2.0 ST arrays not only return expression levels of mRNA molecules that code for protein, but they also contain long intergenic non-coding RNA transcripts (lincRNA) that do not code for protein. Recently, greater than 10,000 transcripts have been discovered, however, only a small percentage of these have functional annotations found to date. However, there is a large body of evidence that points towards aberrant expression of lincRNAs being linked with cancer (*Esteller 2011*). As an example, a recent study in ovarian cancer identified lincRNA HOTAIR over-expression in epithelial serous ovarian cancer patients as being

associated with reduced DFS and OS (*Qiu et al. 2014*). Expression was also correlated to FIGO stage, histological grade and metastasis. Examination of the aberrantly expressed lincRNAs from our study returned by the Affymetrix gene chip analysis on the carboplatin and taxol resistant cell lines could provide novel biomarkers for ovarian cancer chemoresistance.

The study by *Armstrong et.al (2012)* has given evidence that cell lines produced with a dual resistance to two cytotoxic agents, produce novel genetic changes during resistance development. These changes are not seen in cell lines developed in parallel that are resistant to one agent, but not cross resistant to the other. The study developed a dual carboplatin and docetaxel resistant cell line from A2780 ovarian cancer cell lines, which are cross resistant to both agents. Gene profiling revealed that the dual model contained genetic changes that were not present in the singularly resistant models. This demonstrated that combined drug resistance may not be a simple combination of changes present in single-agent resistant cell lines, but can contain novel changes. For this reason, it would be interesting to profile our carboplatin and taxol cross-resistant cell lines UPN251-6CALT and UPN251-6TALT using the Affymetrix gene and miRNA chips. By comparing and contrasting the deregulated targets with our current panel of markers it would be possible to deduce if novel mechanisms of resistance had arisen in the dual resistant models compared to the singularly resistant models. This may provide stronger clinically relevant biomarkers than the markers produced from the present study.

The chemoresistant UPN251 sublines could be further characterised with additional experimentation in order to further elucidate the mechanism of platinum and taxane resistance that have resulted in their resistant phenotypes. For example, platinum adduct assays could be performed to monitor the extent to which harmful DNA damaging platinum adducts form on DNA strands after carboplatin treatment in the UPN251 chemoresistant cell line panel. Decreased accumulation or increased repair of platinum adducts after platinum treatment is an established mechanism of resistance in ovarian cancer cells (*Johnson et al. 1997*). Western blotting for newly discovered gene targets from Affymetrix array data could be carried out in the cell lines to see if mRNA levels correlate to protein expression.

Finally, functional analysis of promising gene/miRNA biomarkers can be tested in the author's cell lines by knockdown and over-expression experiments investigating their effects on chemoresistance. This again could be replicated in other resistant cell line panels such as IGROV-CDDP or other intrinsically resistant cell lines (*Ma et al. 1998*;

Stordal et al. 2013). This could indicate if the gene/miRNAs could act as therapeutic targets in ovarian cancer patients.

8.5 Publications and conference proceedings

8.5.1 Publications

1) **Busschots, S.**, O' Toole, S., Hennessy, B.T., O'Leary, J.J. and Stordal, B. 2014. Carboplatin and taxol resistance develops more rapidly in functional BRCA1 compared to dysfunctional BRCA1 ovarian cancer cells. Experimental Cell Research. pii: S0014-4827(14)00527-8. doi: 10.1016/j.yexcr.2014.12.001.

2) **Busschots, S.**, O' Toole, S., Hennessy, B.T., O'Leary, J.J. and Stordal, B. 2014. Non-invasive and non-destructive measurements of confluence in cultured adherent cell lines. Methods X, 2, 8-13.

3) Lawlor, D., Martin, P., **Busschots, S.**, Thery, J., O'Leary, J.J., Hennessy, B.T. and Stordal, B. 2014. Parp Inhibitors as P-Glycoprotein Substrates. Journal of Pharmaceutical Sciences, 103, (6), 1913-1920.

4) Mc Dermott, M., Eustace, A.J., **Busschots, S.**, Breen, L., Crown, J., Clynes, M., O'Donovan, N. and Stordal, B. 2014. *In vitro* development of chemotherapy and targeted therapy drug-resistant cancer cell lines: A practical guide with case studies. Frontiers in Oncology, 4, (40).

5) Stordal, B., Timms, K., Farrelly, A., Renaud, M., Thery, J., **Busschots, S.**, Williams, D., Potter, J., Tran, T., Korpanty, G., Cremona, M., Carey, M., Li, J., Li, Y., Aslan, O., O'Leary, J.J., Mills, G.B. and Hennessy, B.T. 2013. BRCA1/2 mutation analysis in 41 ovarian cell lines reveals only one functionally deleterious BRCA1 mutation. Molecular Oncology, 7, (3) 567-579.

8.5.2 Conference proceedings

1) **Steven Busschots**, Sharon O' Toole, Bryan T. Hennessey, John J. O'Leary and Britta Stordal. Developing platinum and taxane resistant ovarian cancer cell lines: Investigating the role of BRCA1. 11th International Symposium on Platinum Coordination Compounds in Cancer Chemotherapy, Verona, Italy - Poster. (November 2012).

2) **Steven Busschots**, Sharon O' Toole, Bryan T. Hennessey, John J. O'Leary and Britta Stordal. Developing platinum and taxane resistant ovarian cancer cell lines: Investigating the role of BRCA1. 5th School of Medicine Postgraduate Research Day, Trinity College Dublin – Poster. (September 2012).

3) **Steven Busschots**, Sharon O' Toole, Bryan T. Hennessey, John J. O'Leary and Britta Stordal. Investigating the role of BRCA1 in the development of platinum and taxane resistant ovarian cancer cell lines. British Gynaecological Cancer Society Meeting, Belfast, UK– Poster. (June 2013).

4) **Steven Busschots**, Sharon O' Toole, Bryan T. Hennessey, John J. O'Leary and Britta Stordal. D. Developmental role of BRCA1 on platinum and taxane resistant models for ovarian cancer: MDR related mechanisms. The role of MDR proteins in pharmacokinetics and toxicology. Masurian Lake District, Ryn, Poland – Poster Presentation (September 2013)

5) **Steven Busschots**, Sharon O' Toole, Bryan T. Hennessey, John J. O'Leary and Britta Stordal. D. Developmental role of BRCA1 on platinum and taxane resistant models for ovarian cancer: MDR related mechanisms. Irish Association for Cancer Research. Galway Bay Hotel, Salthill, Galway, Ireland – Poster Presentation (February 2014)

6) **Steven Busschots**, Sharon O' Toole, Bryan T. Hennessey, John J. O'Leary and Britta Stordal. Developmental role of BRCA1 on platinum and taxane resistant models for ovarian cancer: MDR related mechanisms. United States and Canadian Academy of Pathology 103rd annual meeting. San Diego, California, USA – Poster Presentation (March 2014)

7) **Steven Busschots**, Cathy Spillane, Gordon Blackshields, Sharon O' Toole, Bryan T. Hennessey, John J. O'Leary and Britta Stordal. Novel cell lines mirror the complexity of resistance mechanisms in ovarian cancer. Trinity College Dublin's 9th International Cancer Conference. Biomedical Sciences Institute, Trinity College Dublin, Ireland – Poster Presentation (September 2014)

8.6 Conclusions

As a whole, this study has produced a number of useful findings and results that relate to ovarian cancer chemoresistance. This includes the establishment of a novel method for measuring cell confluence that is fast, accurate, cheap, non-destructive and non-invasive. The method measures cell confluence in adherent cells in cell culture flasks requiring undisturbed continued growth. It provides an objective, consistent measure of when cells reach confluence that could be applied to several biological fields, such as oncology, stem cell biology and immunology. This method has been accepted for publication by MethodsX, a peer-reviewed journal.

This study has produced a number of novel carboplatin and taxol resistant ovarian cancer cell models in a clinically relevant fashion. During their development, new insights into the inverse resistance relationship between acquired platinum and taxane resistance were discovered that have contributed to current knowledge. It was discovered that resistance to both carboplatin and taxol developed quicker and more stably in UPN251 (BRC1-wildtype) compared to OVCAR8 (BRCA1-methylated) and that taxol resistance developed quicker in BRCA1-wildtype and BRCA1-methylated cells models, irrespective of BRCA1 status. These results have been accepted for publication in Experimental Cell Research, a peer-reviewed journal. Also, from the Affymetrix array data, a number of additional novel genes that may contribute to the inverse resistance relationship were identified, which included; CD24P4, GPC4, GUCY1B3, SLC17A1, SLC34A2, TENM2 and VCAM1.

The characterisation of the UPN251 resistant sublines has provided novel insights into the development of acquired carboplatin and taxol resistance in ovarian cancer. In the UPN251 taxol resistant models, over-expression of P-gp was the main mechanism driving taxol resistance. Inhibition of apoptosis was a contributing factor, with taxol resistant cells losing their ability to reduce Bcl-2 levels, circumventing G2/M arrest and having deregulation of molecules involved in apoptotic signalling including PLAC8 and MAP3K15 (ASK3). Also, a reduction in growth rate contributed to taxol resistance in the models (Figure 8.1). Other pathways found to have deregulated gene were pathways of angiogenesis, membrane regeneration and repair, intracellular transport, cell interactions with the extracellular matrix, vasoconstriction, ECM-receptor interaction, small cell lung cancer and arrhythogenic right ventricle cardiomyopathy (ARVC).

In the UPN251 carboplatin-resistant models, reduction in apoptosis played a role in acquired carboplatin resistance with an inability to reduce levels of bcl-2 and bcl-XL in response to carboplatin exposure. Along with this, the over-expression of PLAC8 and

MAP3K15 and deregulation of BMPR1B and BMP2 were further possible mechanisms for apoptotic inhibition. Resistance to changes in the cell cycle induced by carboplatin exposure also contributed to a carboplatin resistant phenotype (Figure 8.2). Other pathways found to have deregulated elements were pathways of regulation of developmental events, tissue differentiation, cell maintenance, morphogenesis, cell-cell interaction, signal transduction, cellular transformation, cell migration, bicarbonate secretion and absorption, regulation of intracellular pH, T-cell signal transduction, hematopoietic cell lineages, axon guidance, Cytokine-cytokine receptor interactions, basal cell carcinoma, and hedgehog signalling.

From investigations into the taxol and carboplatin cross resistant cell models, we were able to conclude that, in the dual resistance models, the cytotoxic agent that a cell-line was exposed to first influenced the mechanisms of resistance that developed in the cells thereafter. UPN251-6CALT and UPN251-6TALT had different profiles of $CuSO_4$ and oxaliplatin resistance. Also, as PARP inhibitors CEP8983 and veliparib did not develop resistance in any of our carboplatin or taxol models (both cross resistant and singularly resistant), they have been recommended as possible candidate drugs for the treatment of carboplatin/taxol resistant ovarian cancer by the results of this study. A number of the findings related to the development of carboplatin and taxol resistance have also been accepted for publication in Experimental Cell Research in the same manuscript mentioned previously.

Finally, this study has contributed significantly to the subject of ovarian cancer resistance through the discovery of genes and miRNAs that have the potential to act as biomarkers for platinum and taxane resistant in ovarian cancer. Some of these genes/miRNAs have been previously linked with ovarian cancer resistance and/or poor OS/PFS, making them strong candidates for further investigation. Other markers have been found to be de-regulated in ovarian cancer in the literature, but have not yet been linked to resistance and, therefore, may have potential utility as markers of resistance in ovarian cancer. Others have been found to be linked to chemoresistance and/or poor OS/PFS in other cancer types and, therefore, may have utility in ovarian cancer. Additionally a large number of novel markers were identified for ovarian cancer. These have been found to be deregulated in other cancer types or do not have publications in the literature linking them to cancer.

Further investigation of potential resistance makers in a small pilot study identified GLI3 and a panel of six markers (CCL20, GLI3, LIN28B, SRPX2, let-7i and miR-205) as having predictive power for patient outcomes including DFS and OS.

All of the above findings have contributed substantially to the current knowledge on ovarian cancer chemoresistance and have the potential to contribute to the improvement of ovarian cancer treatment in the future.

References

Abal, M., Andreu, J. M., and Barasoain, I. 2003. Taxanes: microtubule and centrosome targets, and cell cycle dependent mechanisms of action. Current Cancer Drug Targets., 3, (3) 193-203.

Abedini, M. R., Muller, E. J., Brun, J., Bergeron, R., Gray, D. A., and Tsang, B. K. 2008. Cisplatin Induces p53-Dependent FLICE-Like Inhibitory Protein Ubiquitination in Ovarian Cancer Cells. Cancer Research, 68, (12) 4511-4517.

Affymetrix. 2007. Quality Assessment of Exon and Gene Arrays. Affymetrix GeneChip® Gene and Exon Array Whitepaper Collection.

Akan, I., Akan, S., Akca, H., Savas, B., and Ozben, T. 2005. Multidrug resistance-associated protein 1 (MRP1) mediated vincristine resistance: effects of N-acetylcysteine and Buthionine sulfoximine. Cancer Cell International, 5, (1) 22-

Akiyama, S., Fojo, A., Hanover, J. A., Pastan, I., and Gottesman, M. M. 1985. Isolation and genetic characterization of human KB cell lines resistant to multiple drugs. Somatic Cell Molecular Genetics, 11, (2) 117-126.

Allen, M., Millett, P., Dawes, E., and Rushton, N. 1994. Lactate dehydrogenase activity as a rapid and sensitive test for the quantification of cell numbers in vitro. Clinical Materials, 16, (4) 189-194.

Alvarez, M., Paull, K., Monks, A., Hose, C., Lee, J. S., Weinstein, J., Grever, M., Bates, S., and Fojo, T. 1995. Generation of a drug resistance profile by quantitation of mdr-1/P-glycoprotein in the cell lines of the National Cancer Institute Anticancer Drug Screen. Journal of Clinical Investigation, 95, (5) 2205-2214.

Ambros, V., Bartel, B., Bartel, D. P., Burge, C. B., Carrington, J. C., Chen, X., Dreyfuss, G., Eddy, S. R., Griffiths-Jones, S., Marshall, M., Matzke, M., Ruvkun, G., and Tuschl, T. 2003. A uniform system for microRNA annotation. RNA, 9, (3) 277-279.

Andrews, P. A., Velury, S., Mann, S. C., and Howell, S. B. 1988. cis-Diamminedichloroplatinum(II) Accumulation in Sensitive and Resistant Human Ovarian Carcinoma Cells. Cancer Research, 48, (1) 68-73.

Anoopkumar-Dukie, S., Carey, J. B., Conere, T., O'Sullivan, E., van Pelt, F. N., and Allshire, A. 2005. Resazurin assay of radiation response in cultured cells. British Journal of Radiology, 78, (934) 945-947.

Armstrong, D. K. 2002. Relapsed ovarian cancer: challenges and management strategies for a chronic disease. Oncologist, 7 Suppl 5, 20-28.

Armstrong, S. R., Narendrula, R., Guo, B., Parissenti, A. M., McCallum, K. L., Cull, S., and Lanner, C. 2012. Distinct genetic alterations occur in ovarian tumor cells selected for combined resistance to carboplatin and docetaxel. Journal of Ovarian Research, 5, (1) 40-40.

Arnold, J. M., Huggard, P. R., Cummings, M., Ramm, G. A., and Chenevix-Trench, G. 2005. Reduced expression of chemokine (C-C motif) ligand-2 (CCL2) in ovarian adenocarcinoma. British Journal of Cancer, 92, (11) 2024-2031.

Arumugam, T., Ramachandran, V., Fournier, K. F., Wang, H., Marquis, L., Abbruzzese, J. L., Gallick, G. E., Logsdon, C. D., McConkey, D. J., and Choi, W. 2009. Epithelial to Mesenchymal Transition Contributes to Drug Resistance in Pancreatic Cancer. Cancer Research, 69, (14) 5820-5828.

Ashkenazi, A. 2002. Targeting death and decoy receptors of the tumour-necrosis factor superfamily. Nature Reviews Cancer, 2, (6) 420-430.

Audeh, M. W., Carmichael, J., Penson, R. T., Friedlander, M., Powell, B., Bell-McGuinn, K. M., Scott, C., Weitzel, J. N., Oaknin, A., Loman, N., Lu, K., Schmutzler, R. K., Matulonis, U., Wickens, M., and Tutt, A. 2010. Oral poly(ADP-ribose) polymerase inhibitor olaparib in patients with BRCA1 or BRCA2 mutations and recurrent ovarian cancer: a proof-of-concept trial. Lancet, 376, (9737) 245-251.

Awad, M. M., Calkins, H., and Judge, D. P. 2008. Mechanisms of disease: molecular genetics of arrhythmogenic right ventricular dysplasia/cardiomyopathy. Nature Clinical Practice.Cardiovascular Medicine, 5, (5) 258-267.

Backman, S., Kollara, A., Haw, R., Stein, L., and Brown, T. J. 2014. Glucocorticoid-induced reversal of interleukin-1beta-stimulated inflammatory gene expression in human oviductal cells. PLoS ONE, 9, (5)

Badiglian, F. L., Oshima, C. T., De Oliveira, L. F., De Oliveira, C. H., De Sousa, D. R., Gomes, T. S., and Goncalves, W. J. 2009. Canonical and noncanonical Wnt pathway: a comparison among normal ovary, benign ovarian tumor and ovarian cancer. Oncology Reports, 21, (2) 313-320.

Bai, X. Y., Lin, J. Y., Zhang, X. C., Xie, Z., Yan, H. H., Chen, Z. H., Xu, C. R., An, S. J., Sheng, G. M., and Wu, Y. L. 2013. High expression of truncated GLI3 is associated with poor overall survival in patients with non-small cell lung cancer. Cancer Biomarkers: Section A of Disease Markers, 13, (1) 37-47.

Baldwin, R. L., Nemeth, E., Tran, H., Shvartsman, H., Cass, I., Narod, S., and Karlan, B. Y. 2000. BRCA1 Promoter Region Hypermethylation in Ovarian Carcinoma: A Population-based Study. Cancer Research, 60, (19) 5329-5333.

Balkwill, F. 2004. Cancer and the chemokine network. Nature Reviews Cancer, 4, (7) 540-550.

Bankhead, C. R., Collins, C., Stokes-Lampard, H., Rose, P., Wilson, S., Clements, A., Mant, D., Kehoe, S. T., and Austoker, J. 2008. Identifying symptoms of ovarian cancer: a qualitative and quantitative study. BJOG: An International Journal of Obstetrics & Gynaecology, 115, (8) 1008-1014.

Bartel, D. P. 2004. MicroRNAs: genomics, biogenesis, mechanism, and function. Cell, 116, (2) 281-297.

Bast, R. C., Jr., Klug, T. L., St, J. E., Jenison, E., Niloff, J. M., Lazarus, H., Berkowitz, R. S., Leavitt, T., Griffiths, C. T., Parker, L., Zurawski, V. R., Jr., and Knapp, R. C. 1983. A radioimmunoassay using a monoclonal antibody to monitor the course of epithelial ovarian cancer. The New England Journal of Medicine, 309, (15) 883-887.

Bast, R. C., Hennessy, B., and Mills, G. B. 2009. The biology of ovarian cancer: new opportunities for translation. Nature Reviews Cancer, 9, (6) 415-428.

Bauerschlag, D., Brautigam, K., Moll, R., Sehouli, J., Mustea, A., Salehin, D., Krajewska, M., Reed, J. C., Maass, N., Hampton, G. M., and Meinhold-Heerlein, I. 2013. Systematic analysis and validation of differential gene expression in ovarian serous adenocarcinomas and normal ovary. Journal of Cancer Research and Clinical Oncology, 139, (2) 347-355.

Beale, P. J., Rogers, P., Boxall, F., Sharp, S. Y., and Kelland, L. R. 2000. BCL-2 family protein expression and platinum drug resistance in ovarian carcinoma. British Journal of Cancer, 82, (2) 436-440.

Beltsos, A. N. and Odem, R. R. 1996. Ovulation induction and ovarian malignancy. Seminars in Reprodive Endocrinology, 14, (4) 367-374.

Ben David, Y., Chetrit, A., Hirsh-Yechezkel, G., Friedman, E., Beck, B. D., Beller, U., Ben-Baruch, G., Fishman, A., Levavi, H., Lubin, F., Menczer, J., Piura, B., Struewing, J. P., Modan, B., and for the National Israeli Study of Ovarian Cancer. 2002. Effect of BRCA Mutations on the Length of Survival in Epithelial Ovarian Tumors. Journal of Clinical Oncology, 20, (2) 463-466.

Benard, J., Da, S. J., De Blois, M. C., Boyer, P., Duvillard, P., Chiric, E., and Riou, G. 1985. Characterization of a human ovarian adenocarcinoma line, IGROV1, in tissue culture and in nude mice. Cancer Research, 45, (10) 4970-4979.

Benjamini, Y. and Hochberg, Y. 1995. Controlling the False Discovery Rate: A Practical and Powerful Approach to Multiple Testing. Journal of the Royal Statistical Society.Series B (Methodological), 57, (1) 289-300.

Berasain, C. and Avila, M. A. 2014. Amphiregulin. Seminars in Cell & Developmental Biology, 28, 31-41.

Berchuck, A., Iversen, E. S., Lancaster, J. M., Pittman, J., Luo, J., Lee, P., Murphy, S., Dressman, H. K., Febbo, P. G., West, M., Nevins, J. R., and Marks, J. R. 2005. Patterns of Gene Expression That Characterize Long-term Survival in Advanced Stage Serous Ovarian Cancers. Clinical Cancer Research, 11, (10) 3686-3696.

Berchuck, A., Iversen, E. S., Luo, J., Clarke, J. P., Horne, H., Levine, D. A., Boyd, J., Alonso, M. A., Secord, A. A., Bernardini, M. Q., Barnett, J. C., Boren, T., Murphy, S. K., Dressman, H. K., Marks, J. R., and Lancaster, J. M. 2009. Microarray Analysis of Early Stage Serous Ovarian Cancers Shows Profiles Predictive of Favorable Outcome. Clinical Cancer Research, 15, (7) 2448-2455.

Bernard, N. J. and O'Neill, L. A. 2013. Mal, more than a bridge to MyD88. IUBMB.Life, 65, (9) 777-786.

Bhalla, K., Huang, Y., Tang, C., Self, S., Ray, S., Mahoney, M. E., Ponnathpur, V., Tourkina, E., Ibrado, A. M., Bullock, G., and . 1994. Characterization of a human myeloid leukemia cell line highly resistant to taxol. Leukemia, 8, (3) 465-475.

Bianco, P. R., Tracy, R. B., and Kowalczykowski, S. C. 1998. DNA strand exchange proteins: a biochemical and physical comparison. Frontiers in Bioscience, 3, D570-D603.

Biedler, J. L. and Riehm, H. 1970. Cellular Resistance to Actinomycin D in Chinese Hamster Cells in Vitro: Cross-Resistance, Radioautographic, and Cytogenetic Studies. Cancer Research, 30, (4) 1174-1184.

Binkhathlan, Z. and Lavasanifar, A. 2013. P-glycoprotein inhibition as a therapeutic approach for overcoming multidrug resistance in cancer: current status and future perspectives. Current Cancer Drug Targets, 13, (3) 326-346.

Birkbak, N. J., Wang, Z. C., Kim, J. Y., Eklund, A. C., Li, Q., Tian, R., Bowman-Colin, C., Li, Y., Greene-Colozzi, A., Iglehart, J. D., Tung, N., Ryan, P. D., Garber, J. E., Silver, D. P., Szallasi, Z., and Richardson, A. L. 2012. Telomeric Allelic Imbalance Indicates Defective DNA Repair and Sensitivity to DNA-Damaging Agents. Cancer Discovery, 2, (4) 366-375.

Bissery, M. C., Nohynek, G., Sanderink, G. J., and Lavelle, F. 1995. Docetaxel (Taxotere): a review of preclinical and clinical experience. Part I: Preclinical experience. Anticancer Drugs, 6, (3) 339-8.

Bitler, B. G., Nicodemus, J. P., Li, H., Cai, Q., Wu, H., Hua, X., Li, T., Birrer, M. J., Godwin, A. K., Cairns, P., and Zhang, R. 2011. Wnt5a Suppresses Epithelial Ovarian Cancer by Promoting Cellular Senescence. Cancer Research, 71, (19) 6184-6194.

Bland, J. M. A. 1998. Survival probabilities (the Kaplan-Meier method). British Medical Journal, 317, (7172) 1572-1580.

Bland, J. M. A. 2004. The logrank test. British Medical Journal, 328, (7447) 1073-1073.

Bock, A. J., Stavnes, H. T., Kempf, T., Trope, C. G., Berner, A., Davidson, B., and Staff, A. C. 2010. Expression and clinical role of growth differentiation factor-15 in ovarian carcinoma effusions. International Journal of Gynecological Cancer, 20, (9) 1448-1455.

Bolstad, B. M., Irizarry, R. A., Astrand, M., and Speed, T. P. 2003. A comparison of normalization methods for high density oligonucleotide array data based on variance and bias. Bioinformatics, 19, (2) 185-193.

Bonome, T., Levine, D. A., Shih, J., Randonovich, M., Pise-Masison, C. A., Bogomolniy, F., Ozbun, L., Brady, J., Barrett, J. C., Boyd, J., and Birrer, M. J. 2008. A gene signature predicting for survival in suboptimally debulked patients with ovarian cancer. Cancer Research, 68, (13) 5478-5486.

Bonome, T., Lee, J. Y., Park, D. C., Radonovich, M., Pise-Masison, C., Brady, J., Gardner, G. J., Hao, K., Wong, W. H., Barrett, J. C., Lu, K. H., Sood, A. K., Gershenson, D. M., Mok, S. C., and Birrer, M. J. 2005. Expression Profiling of Serous Low Malignant Potential, Low-Grade, and High-Grade Tumors of the Ovary. Cancer Research, 65, (22) 10602-10612.

Boren, T., Xiong, Y., Hakam, A., Wenham, R., Apte, S., Chan, G., Kamath, S. G., Chen, D. T., Dressman, H., and Lancaster, J. M. 2009. MicroRNAs and their target messenger RNAs associated with ovarian cancer response to chemotherapy. Gynecologic Oncology, 113, (2) 249-255.

Borst, P., Evers, R., Kool, M., and Wijnholds, J. 2000. A Family of Drug Transporters: the Multidrug Resistance-Associated Proteins. Journal of the National Cancer Institute, 92, (16) 1295-1302.

Boyerinas, B., Park, S. M., Murmann, A. E., Gwin, K., Montag, A. G., Zillhardt, M., Hua, Y. J., Lengyel, E., and Peter, M. E. 2012. Let-7 modulates acquired resistance of ovarian cancer to Taxanes via IMP-1-mediated stabilization of multidrug resistance 1. International Journal of Cancer, 130, (8) 1787-1797.

Brand, S., Olszak, T., Beigel, F., Diebold, J., Otte, J. M., Eichhorst, S. T., Goke, B., and Dambacher, J. 2006. Cell differentiation dependent expressed CCR6 mediates ERK-1/2, SAPK/JNK, and Akt signaling resulting in proliferation and migration of colorectal cancer cells. Journal of Cellular Biochemistry, 97, (4) 709-723.

Breen, L., Murphy, L., Keenan, J., and Clynes, M. 2008. Development of taxane resistance in a panel of human lung cancer cell lines. Toxicology in vitro : an international journal published in association with BIBRA, 22, (5) 1234-1241.

Breitling, R., Armengaud, P., Amtmann, A., and Herzyk, P. 2004. Rank products: a simple, yet powerful, new method to detect differentially regulated genes in replicated microarray experiments. FEBS Letters, 573, (1–3) 83-92.

Brewster, W. R. 2005. Temporal trends in ovarian cancer: incidence and mortality across Europe. Nature Reviews Clinical Oncology, 2, (6) 286-287.

Brinkmann, M., Lutkemeyer, D., Gudermann, F., and Lehmann, J. 2002. New technologies for automated cell counting based on optical image analysis ;The Cellscreen'. Cytotechnology, 38, (1-3) 119-127.

Bristow, R. E., Tomacruz, R. S., Armstrong, D. K., Trimble, E. L., and Montz, F. J. 2002. Survival Effect of Maximal Cytoreductive Surgery for Advanced Ovarian Carcinoma During the Platinum Era: A Meta-Analysis. Journal of Clinical Oncology, 20, (5) 1248-1259.

Brotin, E., Meryet-Figuiere, M., Simonin, K., Duval, R. E., Villedieu, M., Leroy-Dudal, J., Saison-Behmoaras, E., Gauduchon, P., Denoyelle, C., and Poulain, L. 2010. Bcl-XL and MCL-1 constitute pertinent targets in ovarian carcinoma and their concomitant inhibition is sufficient to induce apoptosis. International Journal of Cancer, 126, (4) 885-895.

Brown, R. and Plumb, J. A. 2004. Demethylation of DNA by decitabine in cancer chemotherapy. Expert Reviews in Anticancer Therapy, 4, (4) 501-510.

Brueckner, B., Stresemann, C., Kuner, R., Mund, C., Musch, T., Meister, M., Sultmann, H., and Lyko, F. 2007. The Human let-7a-3 Locus Contains an Epigenetically Regulated MicroRNA Gene with Oncogenic Function. Cancer Research, 67, (4) 1419-1423.

Bugreev, D. V., Mazina, O. M., and Mazin, A. V. 2006. Rad54 protein promotes branch migration of Holliday junctions. Nature, 442, (7102) 590-593.

Burchenal, J. H. and Robinson, E. 1950. The induction of resistance to 4-amino-N10-methylpteroylglutamic acid in a strain of transmitted mouse leukemia. Science, 111, (2875) 116-116.

Burden, R. E., Gormley, J. A., Kuehn, D., Ward, C., Kwok, H. F., Gazdoiu, M., McClurg, A., Jaquin, T. J., Johnston, J. A., Scott, C. J., and Olwill, S. A. 2012. Inhibition of Cathepsin S by Fsn0503 enhances the efficacy of chemotherapy in colorectal carcinomas. Biochimie, 94, (2) 487-493.

Burger, R. A., Brady, M. F., Bookman, M. A., Fleming, G. F., Monk, B. J., Huang, H., Mannel, R. S., Homesley, H. D., Fowler, J., Greer, B. E., Boente, M., Birrer, M. J., and Liang, S. X. 2011. Incorporation of Bevacizumab in the Primary Treatment of Ovarian Cancer. New England Journal of Medicine, 365, (26) 2473-2483.

Burges, A. and Schmalfeldt, B. 2011. Ovarian cancer: diagnosis and treatment. Deutsches Arzteblatt International, 108, (38) 635-641.

Bussing, I., Slack, F. J., and Grobhans, H. 2008. let-7 microRNAs in development, stem cells and cancer. Trends in Molecular Medicine, 14, (9) 400-409.

Byrne, J. A., Maleki, S., Hardy, J. R., Gloss, B. S., Murali, R., Scurry, J. P., Fanayan, S., Emmanuel, C., Hacker, N. F., Sutherland, R. L., Defazio, A., and O'Brien, P. M. 2010. MAL2 and tumor protein D52 (TPD52) are frequently overexpressed in ovarian carcinoma, but differentially associated with histological subtype and patient outcome. BMC Cancer, 10,

Cabral, F., Wible, L., Brenner, S., and Brinkley, B. R. 1983. Taxol-requiring mutant of Chinese hamster ovary cells with impaired mitotic spindle assembly. The Journal of Cell Biology, 97, (1) 30-39.

Calin, G. A., Dumitru, C. D., Shimizu, M., Bichi, R., Zupo, S., Noch, E., Aldler, H., Rattan, S., Keating, M., Rai, K., Rassenti, L., Kipps, T., Negrini, M., Bullrich, F., and Croce, C. M. 2002. Frequent deletions and down-regulation of micro- RNA genes miR15 and miR16 at 13q14 in chronic lymphocytic leukemia. Proceedings of the National Academy of Sciences, 99, (24) 15524-15529.

Callahan, M. J., Crum, C. P., Medeiros, F., Kindelberger, D. W., Elvin, J. A., Garber, J. E., Feltmate, C. M., Berkowitz, R. S., and Muto, M. G. 2007. Primary Fallopian Tube Malignancies in BRCA-Positive Women Undergoing Surgery for Ovarian Cancer Risk Reduction. Journal of Clinical Oncology, 25, (25) 3985-3990.

Calvert, A. H., Newell, D. R., Gumbrell, L. A., O'Reilly, S., Burnell, M., Boxall, F. E., Siddik, Z. H., Judson, I. R., Gore, M. E., and Wiltshaw, E. 1989. Carboplatin dosage: prospective evaluation of a simple formula based on renal function. Journal of Clinical Oncology, 7, (11) 1748-1756.

Campbell, A. S., Albo, D., Kimsey, T. F., White, S. L., and Wang, T. N. 2005. Macrophage inflammatory protein-3alpha promotes pancreatic cancer cell invasion. Journal of Surgical Research, 123, (1) 96-101.

Cannistra, S. A. 2004. Cancer of the Ovary. New England Journal of Medicine, 351, (24) 2519-2529.

Carvalho, B. S. and Irizarry, R. A. 2010. A framework for oligonucleotide microarray preprocessing. Bioinformatics, 26, (19) 2363-2367.

Cass, I., Baldwin, R. L., Varkey, T., Moslehi, R., Narod, S. A., and Karlan, B. Y. 2003. Improved survival in women with BRCA-associated ovarian carcinoma. Cancer, 97, (9) 2187-2195.

Cass, I., Holschneider, C., Datta, N., Barbuto, D., Walts, A. E., and Karlan, B. Y. 2005. BRCA-mutation-associated fallopian tube carcinoma: a distinct clinical phenotype? Obstetrics Gynecology, 106, (6) 1327-1334.

Cassinelli, G., Supino, R., Perego, P., Polizzi, D., Lanzi, C., Pratesi, G., and Zunino, F. 2001. A role for loss of p53 function in sensitivity of ovarian carcinoma cells to taxanes. International Journal of Cancer, 92, (5) 738-747.

Cepeda, V., Fuertes, M. A., Castilla, J., Alonso, C., Quevedo, C., and Perez, J. M. 2007. Biochemical mechanisms of cisplatin cytotoxicity. Anticancer Agents in Medical Chemistry, 7, (1) 3-18.

Chedotal, A., Kerjan, G., and Moreau-Fauvarque, C. 2005. The brain within the tumor: new roles for axon guidance molecules in cancers. Cell Death Differenciation, 12, (8) 1044-1056.

Chen, H. H. and Kuo, M. T. 2010. Role of glutathione in the regulation of Cisplatin resistance in cancer chemotherapy. Metal Based Drugs, 2010, (1) 1-7.

Chen, H., Landen, C. N., Li, Y., Alvarez, R. D., and Tollefsbol, T. O. 2013. Epigallocatechin gallate and sulforaphane combination treatment induce apoptosis in paclitaxel-resistant ovarian cancer cells through hTERT and Bcl-2 down-regulation. Experimental Cell Research, 319, (5) 697-706.

Chen, L., Nievera, C. J., Lee, A. Y.-L., and Wu, X. 2008a. Cell Cycle-dependent Complex Formation of BRCA1-CtIP-MRN Is Important for DNA Double-strand Break Repair. Journal of Biological Chemistry, 283, (12) 7713-7720.

Chen, X., Ba, Y., Ma, L., Cai, X., Yin, Y., Wang, K., Guo, J., Zhang, Y., Chen, J., Guo, X., Li, Q., Li, X., Wang, W., Zhang, Y., Wang, J., Jiang, X., Xiang, Y., Xu, C., Zheng, P., Zhang, J., Li, R., Zhang, H., Shang, X., Gong, T., Ning, G., Wang, J., Zen, K., Zhang, J., and Zhang, C. Y. 2008b. Characterization of microRNAs in serum: a novel class of biomarkers for diagnosis of cancer and other diseases. Cell Research, 18, (10) 997-1006.

Chen, X., Horiuchi, A., Kikuchi, N., Osada, R., Yoshida, J., Shiozawa, T., and Konishi, I. 2007. Hedgehog signal pathway is activated in ovarian carcinomas, correlating with cell proliferation: It's inhibition leads to growth suppression and apoptosis. Cancer Science, 98, (1) 68-76.

Chendrimada, T. P., Gregory, R. I., Kumaraswamy, E., Norman, J., Cooch, N., Nishikura, K., and Shiekhattar, R. 2005. TRBP recruits the Dicer complex to Ago2 for microRNA processing and gene silencing. Nature, 436, (7051) 740-744.

Cheng, H., Shi, S., Cai, X., Long, J., Xu, J., Liu, C., and Yu, X. 2012. microRNA signature for human pancreatic cancer invasion and metastasis. Experimental and Therepuetic Medicine, 4, (2) 181-187.

Cheng, J. Q., Jiang, X., Fraser, M., Li, M., Dan, H. C., Sun, M., and Tsang, B. K. 2002. Role of X-linked inhibitor of apoptosis protein in chemoresistance in ovarian cancer: possible involvement of the phosphoinositide-3 kinase/Akt pathway. Drug resistance updates : reviews and commentaries in antimicrobial and anticancer chemotherapy, 5, (3) 131-146.

Chien, J., Kuang, R., Landen, C., and Shridhar, V. 2013. Platinum-sensitive recurrence in ovarian cancer: the role of tumor microenvironment. Genes and Development, 3, 251-

Chien, J., Fan, J. B., Bell, D. A., April, C., Klotzle, B., Ota, T., Lingle, W. L., Gonzalez Bosquet, J., Shridhar, V., and Hartmann, L. C. 2009. Analysis of gene expression in stage I serous tumors identifies critical pathways altered in ovarian cancer. Gynecologic Oncology, 114, (1) 3-11.

Cho, K. R. and Shih, I. 2009. Ovarian cancer. Annual Review of Pathology, 4, 287-313.

Chon, H. S. and Lancaster, J. M. 2011. Microarray-based gene expression studies in ovarian cancer. Cancer Control, 18, (1) 8-15.

Choschzick, M., Oosterwijk, E., Muller, V., Woelber, L., Simon, R., Moch, H., and Tennstedt, P. 2011. Overexpression of carbonic anhydrase IX (CAIX) is an independent unfavorable prognostic marker in endometrioid ovarian cancer. Virchows Archive: An International Journal of Pathology, 459, (2) 193-200.

Choudhuri, S. and Klaassen, C. D. 2006. Structure, Function, Expression, Genomic Organization, and Single Nucleotide Polymorphisms of Human ABCB1 (MDR1), ABCC (MRP), and ABCG2 (BCRP) Efflux Transporters. International Journal of Toxicology, 25, (4) 231-259.

Chung, Y. W., Bae, H. S., Song, J. Y., Lee, J. K., Lee, N. W., Kim, T., and Lee, K. W. 2013. Detection of microRNA as novel biomarkers of epithelial ovarian cancer from the serum of ovarian cancer patients. International Journal of Gynaecological Cancer, 23, (4) 673-679.

Clarke-Pearson, D. L. 2009. Screening for Ovarian Cancer. New England Journal of Medicine, 361, (2) 170-177.

Clynes, M., Redmond, A., Moran, E., and Gilvarry, U. 1992. Multiple drug-resistance in variant of a human non-small cell lung carcinoma cell line, DLKP-A. Cytotechnology, 10, (1) 75-89.

Cobbold, C., Ponnambalam, S., Francis, M. J., and Monaco, A. P. 2002. Novel membrane traffic steps regulate the exocytosis of the Menkes disease ATPase. Human Molecular Genetics, 11, (23) 2855-2866.

Cochrane, D. R., Howe, E. N., Spoelstra, N. S., and Richer, J. K. 2010. Loss of miR-200c: A Marker of Aggressiveness and Chemoresistance in Female Reproductive Cancers. Journal of Oncology, 2010, (1) 1-9.

Cole, S. P., Sparks, K. E., Fraser, K., Loe, D. W., Grant, C. E., Wilson, G. M., and Deeley, R. G. 1994. Pharmacological characterization of multidrug resistant MRP-transfected human tumor cells. Cancer Research, 54, (22) 5902-5910.

Collaborative Group on Epidemiological Studies of Ovarian Cancer. 2008. Ovarian cancer and oral contraceptives: collaborative reanalysis of data from 45 epidemiological studies including 23257 women with ovarian cancer and 87303 controls. The Lancet, 371, (9609) 303-314.

Connell, P. P., Jayathilaka, K., Haraf, D. J., Weichselbaum, R. R., Vokes, E. E., and Lingen, M. W. 2006. Pilot study examining tumor expression of RAD51 and clinical outcomes in human head cancers. International Journal of Oncology, 28, (5) 1113-1119.

Constantinou, A., Chen, X. B., McGowan, C. H., and West, S. C. 2002. Holliday junction resolution in human cells: two junction endonucleases with distinct substrate specificities. The EMBO Journal, 21, (20) 5577-5585.

Covens, A., Carey, M., Bryson, P., Verma, S., Fung Kee Fung, M., and Johnston, M. 2002. Systematic Review of First-Line Chemotherapy for Newly Diagnosed Postoperative Patients with Stage II, III, or IV Epithelial Ovarian Cancer. Gynecologic Oncology, 85, (1) 71-80.

Coward, J., Kulbe, H., Chakravarty, P., Leader, D., Vassileva, V., Leinster, D. A., Thompson, R., Schioppa, T., Nemeth, J., Vermeulen, J., Singh, N., Avril, N., Cummings, J., Rexhepaj, E., Jirstr+Âm, K., Gallagher, W. M., Brennan, D. J., McNeish, I. A., and Balkwill, F. R. 2011. Interleukin-6 as a Therapeutic Target in Human Ovarian Cancer. Clinical Cancer Research, 17, (18) 6083-6096.

Craik, A. C., Veldhoen, R. A., Czernick, M., Buckland, T. W., Kyselytzia, K., Ghosh, S., Lai, R., Damaraju, S., Underhill, D. A., Mackey, J. R., and Goping, I. S. 2010. The BH3-only protein Bad confers breast cancer taxane sensitivity through a nonapoptotic mechanism. Oncogene, 29, (39) 5381-5391.

Cramer, D. W. and Welch, W. R. 1983. Determinants of ovarian cancer risk. II. Inferences regarding pathogenesis. Journal of the Natonal Cancer Institute, 71, (4) 717-721.

Creighton, C. J., Benham, A. L., Zhu, H., Khan, M. F., Reid, J. G., Nagaraja, A. K., Fountain, M. D., Dziadek, O., Han, D., Ma, L., Kim, J., Hawkins, S. M., Anderson, M. L., Matzuk, M. M., and Gunaratne, P. H. 2010. Discovery of novel microRNAs in female reproductive tract using next generation sequencing. PLoS ONE, 5, (3) e9637-e9637.

Crijns, A. P., Fehrmann, R. S., de, J. S., Gerbens, F., Meersma, G. J., Klip, H. G., Hollema, H., Hofstra, R. M., te Meerman, G. J., de Vries, E. G., and van der Zee, A. G. 2009. Survival-related profile, pathways, and transcription factors in ovarian cancer. PLoS Med, 6, (2) e24-

Cui, M., Yue, L., Fu, Y., Yu, W., Hou, X., and Zhang, X. 2013. Association of microRNA-181c expression with the progression and prognosis of human gastric carcinoma. Hepatogastroenterology, 60, (125) 961-964.

Culhane, A. C., Thioulouse, J., Perriere, G., and Higgins, D. G. 2005. MADE4: an R package for multivariate analysis of gene expression data. Bioinformatics, 21, (11) 2789-2790.

Curl, C. L., Harris, T., Harris, P. J., Allman, B. E., Bellair, C. J., Stewart, A. G., and Delbridge, L. M. 2004. Quantitative phase microscopy: a new tool for measurement of cell culture

growth and confluency in situ. Pflugers Archiv: European Journal of Physiology, 448, (4) 462-468.

d'Adhemar, C. J., Spillane, C. D., Gallagher, M. F., Bates, M., Costello, K. M., Barry-O'Crowley, J., Haley, K., Kernan, N., Murphy, C., Smyth, P. C., O'Byrne, K., Pennington, S., Cooke, A. A., Ffrench, B., Martin, C. M., O'Donnell, D., Hennessy, B., Stordal, B., Finn, S., McCann, A., Gleeson, N., D'Arcy, T., Flood, B., O'Neill, L. A., Sheils, O., O'Toole, S., and O'Leary, J. J. 2014. The MyD88+ phenotype is an adverse prognostic factor in epithelial ovarian cancer. PLoS ONE, 9, (6) e100816-e100816.

Dabholkar, M., Vionnet, J., Bostick-Bruton, F., Yu, J. J., and Reed, E. 1994. Messenger RNA levels of XPAC and ERCC1 in ovarian cancer tissue correlate with response to platinum-based chemotherapy. The Journal of Clinical Investigation, 94, (2) 703-708.

Dahiya, N., Sherman-Baust, C. A., Wang, T. L., Davidson, B., Shih, I., Zhang, Y., Wood, W., III, Becker, K. G., and Morin, P. J. 2008. MicroRNA expression and identification of putative miRNA targets in ovarian cancer. PLoS ONE, 3, (6) e2436-e2436.

Dai, C., Jiang, Y., Li, Y., Wang, K., Liu, P., Patankar, M., and Zheng, J. 2011. Expression and roles of Slit/Robo in human ovarian cancer. Histochemistry and Cell Biology, 135, (5) 475-485.

Dai, F., Zhang, Y., and Chen, Y. 2014. Involvement of miR-29b signaling in the sensitivity to chemotherapy in patients with ovarian carcinoma. Human Pathology, 45, (6) 1285-1293.

Dalvi, M. P., Behrens, C., Suraokar, M., Girard, L., Xie, Y., Wistuba, I., and Minna, J. D. 2012. Abstract 821: Developing a molecular understanding of non small cell lung cancer (NSCLC) resistance to platin-taxane chemotherapy. Cancer Research, 72, (8 Supplement) 821-821.

Davar, D., Beumer, J. H., Hamieh, L., and Tawbi, H. 2012. Role of PARP inhibitors in cancer biology and therapy. Current Medical Chemistry, 19, (23) 3907-3921.

Davey, R. A., Longhurst, T. J., Davey, M. W., Belov, L., Harvie, R. M., Hancox, D., and Wheeler, H. 1995. Drug resistance mechanisms and MRP expression in response to epirubicin treatment in a human leukaemia cell line. Leukemia Research, 19, (4) 275-282.

David, P. 2004. MicroRNAs: Genomics, Biogenesis, Mechanism, and Function. Cell, 116, (2) 281-297.

Daya-Grosjean, L. and Couve-Privat, S. 2005. Sonic hedgehog signaling in basal cell carcinomas. Cancer Letters, 225, (2) 181-192.

De Donato, M., Mariani, M., Petrella, L., Martinelli, E., Zannoni, G. F., Vellone, V., Ferrandina, G., Shahabi, S., Scambia, G., and Ferlini, C. 2012. Class III Beta-tubulin and the cytoskeletal gateway for drug resistance in ovarian cancer. Journal of Cellular Physiology, 227, (3) 1034-1041.

de Snoo, F., Bender, R., Glas, A., and Rutgers, E. 2009. Gene expression profiling: Decoding breast cancer. Surgical Oncology, 18, (4) 366-378.

Demirag, G. G., Sullu, Y., Gurgenyatagi, D., Okumus, N. O., and Yucel, I. 2011. Expression of plakophilins (PKP1, PKP2, and PKP3) in gastric cancers. Diagnostic Pathology, 6, (1)

Deng, N. and Feng, Y. 2011. Expression of EphA7 and MTDH and clinicopathological significance in the squamous cell cancer of the tongue. Zhong.Nan.Da.Xue.Xue.Bao.Yi.Xue.Ban., 36, (12) 1195-1198.

Denkert, C., Budczies, J., Darb-Esfahani, S., Gyorffy, B., Sehouli, J., Konsgen, D., Zeillinger, R., Weichert, W., Noske, A., Buckendahl, A. C., Muller, B. M., Dietel, M., and Lage, H. 2009. A prognostic gene expression index in ovarian cancer - validation across different independent data sets. The Journal of Pathology, 218, (2) 273-280.

Derry, W. B., Wilson, L., Khan, I. A., Luduena, R. F., and Jordan, M. A. 1997. Taxol Differentially Modulates the Dynamics of Microtubules Assembled from Unfractionated and Purified Beta-Tubulin Isotypes. Biochemistry, 36, (12) 3554-3562.

Dhillon, K. K., Swisher, E. M., and Taniguchi, T. 2011. Secondary mutations of BRCA1/2 and drug resistance. Cancer Science, 102, (4) 663-669.

Di Leva, G. and Croce, C. M. 2010. Roles of small RNAs in tumor formation. Trends in Molecular Medicine, 16, (6) 257-267.

Di Leva, G. and Croce, C. M. 2013. The Role of microRNAs in the Tumorigenesis of Ovarian Cancer. Frontiers in Oncology, 3, 153-153.

Diaz, J. F. and Andreu, J. M. 1993. Assembly of purified GDP-tubulin into microtubules induced by taxol and taxotere: reversibility, ligand stoichiometry, and competition. Biochemistry, 32, (11) 2747-2755.

Dickinson, R. E., Fegan, K. S., Ren, X., Hillier, S. G., and Duncan, W. C. 2011. Glucocorticoid regulation of SLIT/ROBO tumour suppressor genes in the ovarian surface epithelium and ovarian cancer cells. PLoS ONE, 6, (11) e27792-e27792.

Dodier, P. and Piche, A. 2006. Bcl-XL is functionally non-equivalent for the regulation of growth and survival in human ovarian cancer cells. Gynecologic Oncology, 100, (2) 254-263.

Doherty, B., Lawlor, D., Gillet, J. P., Gottesman, M., O'Leary, J. J., and Stordal, B. 2014. Collateral sensitivity to cisplatin in KB-8-5-11 drug-resistant cancer cells. Anticancer Research, 34, (1) 503-507.

Dong, R., Yu, J., Pu, H., Zhang, Z., and Xu, X. 2012. Frequent SLIT2 Promoter Methylation in the Serum of Patients with Ovarian Cancer. Journal of International Medical Research, 40, (2) 681-686.

Downing, K. H. 2000. Structural basis for the interaction of tubulin with proteins and drugs that affect microtubule dynamics. Annual Reviews of Cell and Devopmental Biology, 16, 89-111.

Drew, R. and Miners, J. O. 1984. The effects of buthionine sulphoximine (BSO) on glutathione depletion and xenobiotic biotransformation. Biochemical Pharmacology, 33, (19) 2989-2994.

Drey, L. L., Graber, M. C., and Bieschke, J. 2013. Counting unstained, confluent cells by modified bright-field microscopy. Biotechniques, 55, (1) 28-33.

du Bois, A., Luck, H. J., Buser, K., Meerpohl, H. G., Sessa, C., Klaassen, U., Meden, H., Bochtler, H., and Diergarten, K. 1997. Extended phase II study of paclitaxel as a 3-h infusion in patients with ovarian cancer previously treated with platinum. European Journal of Cancer, 33, (3) 379-384.

du Bois, A., Luck, H. J., Meier, W., Adams, H. P., Mobus, V., Costa, S., Bauknecht, T., Richter, B., Warm, M., Schroder, W., Olbricht, S., Nitz, U., Jackisch, C., Emons, G., Wagner, U., Kuhn, W., Pfisterer, J., and For the Arbeitsgemeinschaft Gynakologische Onkologie (AGO) Ovarian Cancer Study Group. 2003. A Randomized Clinical Trial of Cisplatin/Paclitaxel Versus Carboplatin/Paclitaxel as First-Line Treatment of Ovarian Cancer. Journal of the National Cancer Institute, 95, (17) 1320-1329.

Duan, Z., Feller, A. J., Penson, R. T., Chabner, B., and Seiden, M. V. 1999a. Discovery of Differentially Expressed Genes Associated with Paclitaxel Resistance Using cDNA Array Technology: Analysis of Interleukin (IL) 6, IL-8, and Monocyte Chemotactic Protein 1 in the Paclitaxel-resistant Phenotype. Clinical Cancer Research, 5, (11) 3445-3453.

Duan, Z., Feller, A. J., Toh, H. C., Makastorsis, T., and Seiden, M. V. 1999b. TRAG-3, a novel gene, isolated from a taxol-resistant ovarian carcinoma cell line. Gene, 229, (1-2) 75-81.

Duan, Z., Feller, A. J., Penson, R. T., Chabner, B., and Seiden, M. V. 1999c. Discovery of Differentially Expressed Genes Associated with Paclitaxel Resistance Using cDNA Array Technology: Analysis of Interleukin (IL) 6, IL-8, and Monocyte Chemotactic Protein 1 in the Paclitaxel-resistant Phenotype. Clinical Cancer Research, 5, (11) 3445-3453.

Dweep, H., Sticht, C., Pandey, P., and Gretz, N. 2011. miRWalk — Database: Prediction of possible miRNA binding sites by walking the genes of three genomes. Journal of Biomedical Informatics, 44, (5) 839-847.

Dzantiev, L., Constantin, N., Genschel, J., Iyer, R. R., Burgers, P. M., and Modrich, P. 2004. A Defined Human System That Supports Bidirectional Mismatch-Provoked Excision. Molecular cell, 15, (1) 31-41.

Edwards, S. L., Brough, R., Lord, C. J., Natrajan, R., Vatcheva, R., Levine, D. A., Boyd, J., Reis-Filho, J. S., and Ashworth, A. 2008. Resistance to therapy caused by intragenic deletion in BRCA2. Nature, 451, (7182) 1111-1115.

Eitan, R., Kushnir, M., Lithwick-Yanai, G., David, M. B., Hoshen, M., Glezerman, M., Hod, M., Sabah, G., Rosenwald, S., and Levavi, H. 2009. Tumor microRNA expression patterns associated with resistance to platinum based chemotherapy and survival in ovarian cancer patients. Gynecologic Oncology, 114, (2) 253-259.

Elbashir, S. M., Lendeckel, W., and Tuschl, T. 2001a. RNA interference is mediated by 21- and 22-nucleotide RNAs. Genes and Development, 15, (2) 188-200.

Elbashir, S. M., Martinez, J., Patkaniowska, A., Lendeckel, W., and Tuschl, T. 2001b. Functional anatomy of siRNAs for mediating efficient RNAi in Drosophila melanogaster embryo lysate. The EMBO Journal, 20, (23) 6877-6888.

Emoto, M., Oshima, K., Ishiguro, M., Iwasaki, H., Kawarabayashi, T., and Kikuchi, M. 1999. Establishment and characterization of a serous papillary adenocarcinoma cell line of the human ovary in a serum-free culture. Pathology Research and Practice, 195, (4) 237-242.

Erickson, B. K., Conner, M. G., and Landen, J. 2013. The role of the fallopian tube in the origin of ovarian cancer. American Journal of Obstetrics and Gynecology, 209, (5) 409-414.

Esteller, M. 2011. Non-coding RNAs in human disease. Nature Reviews Genetics, 12, (12) 861-874.

Esteller, M., Corn, P. G., Baylin, S. B., and Herman, J. G. 2001. A Gene Hypermethylation Profile of Human Cancer. Cancer Research, 61, (8) 3225-3229.

Evangelista, M., Tian, H., and de Sauvage, F. J. 2006. The Hedgehog Signaling Pathway in Cancer. Clinical Cancer Research, 12, (20) 5924-5928.

Fader, A. N., Rasool, N., Vaziri, S. A., Kozuki, T., Faber, P. W., Elson, P., Biscotti, C. V., Michener, C. M., Rose, P. G., Rojas-Espaillat, L., Belinson, J. L., Ganapathi, M. K., and Ganapathi, R. 2010. CCL2 expression in primary ovarian carcinoma is correlated with

chemotherapy response and survival outcomes. Anticancer Research, 30, (12) 4791-4798.

Faleiro-Rodrigues, C., Macedo-Pinto, I., Pereira, D., and Lopes, C. S. 2004. Loss of beta-catenin is associated with poor survival in ovarian carcinomas. International Journal of Gynecological Pathology, 23, (4) 337-346.

Fan, S., El-Deiry, W. S., Bae, I., Freeman, J., Jondle, D., Bhatia, K., Fornace, A. J., Magrath, I., Kohn, K. W., and O'Connor, P. M. 1994. p53 Gene Mutations Are Associated with Decreased Sensitivity of Human Lymphoma Cells to DNA Damaging Agents. Cancer Research, 54, (22) 5824-5830.

Fan, S., Smith, M. L., Rivert, D. J., Duba, D., Zhan, Q., Kohn, K. W., Fornace, A. J., and O'Connor, P. M. 1995. Disruption of p53 Function Sensitizes Breast Cancer MCF-7 Cells to Cisplatin and Pentoxifylline. Cancer Research, 55, (8) 1649-1654.

Fasciani, A., D'Ambrogio, G., Bocci, G., Luisi, S., Artini, P. G., and Genazzani, A. R. 2001. Vascular endothelial growth factor and interleukin-8 in ovarian cystic pathology. Fertility and Sterility, 75, (6) 1218-1221.

Fathalla, M. F. 1971. Incessant ovulation--a factor in ovarian neoplasia? Lancet, 2, (7716) 163-163.

Feeley, K. M. and Wells, M. 2001. Precursor lesions of ovarian epithelial malignancy. Histopathology, 38, (2) 87-95.

Ferlay, J., Soerjomataram, H., Ervik, M., Dikshit, R., Eser, S., Mathers, C., Rebelo, M., Parkin, D. M., Forman, D., and Bray, F. 2013. GLOBOCAN 2012 v1.0, Cancer Incidence and Mortality Worldwide: IARC CancerBase No. 11. http://globocan.iarc.fr, accessed on 31/01/2014.

Ferlini, C., Raspaglio, G., Mozzetti, S., Distefano, M., Filippetti, F., Martinelli, E., Ferrandina, G., Gallo, D., Ranelletti, F. O., and Scambia, G. 2003. Bcl-2 Down-Regulation Is a Novel Mechanism of Paclitaxel Resistance. Molecular Pharmacology, 64, (1) 51-58.

Ferrandina, G., Zannoni, G. F., Martinelli, E., Paglia, A., Gallotta, V., Mozzetti, S., Scambia, G., and Ferlini, C. 2006. Class III Beta-Tubulin Overexpression Is a Marker of Poor Clinical Outcome in Advanced Ovarian Cancer Patients. Clinical Cancer Research, 12, (9) 2774-2779.

Ferreira, C. G., Tolis, C., and Giaccone, G. 1999. p53 and chemosensitivity. Annals of Oncology, 10, (9) 1011-1021.

Ferreira, D., Adega, F., and Chaves, R. 2013. The Importance of Cancer Cell Lines as in vitro Models in Cancer Methylome Analysis and Anticancer Drugs Testing. (6)

Ferriss, J. S., Kim, Y., Duska, L., Birrer, M., Levine, D. A., Moskaluk, C., Theodorescu, D., and Lee, J. K. 2012. Multi-gene expression predictors of single drug responses to adjuvant chemotherapy in ovarian carcinoma: predicting platinum resistance. PLoS ONE, 7, (2) e30550-

Fils-Aime, N., Dai, M., Guo, J., El-Mousawi, M., Kahramangil, B., Neel, J. C., and Lebrun, J. J. 2013. MicroRNA-584 and the Protein Phosphatase and Actin Regulator 1 (PHACTR1), a New Signaling Route through Which Transforming Growth Factor-beta Mediates the Migration and Actin Dynamics of Breast Cancer Cells. Journal of Biological Chemistry, 288, (17) 11807-11823.

Fink, D., Nebel, S., Norris, P. S., Baergen, R. N., Wilczynski, S. P., Costa, M. J., Haas, M., Cannistra, S. A., and Howell, S. B. 1998. Enrichment for DNA mismatch repair-deficient cells during treatment with cisplatin. International Journal of Cancer, 77, (5) 741-746.

Fink, D., Nebel, S., Aebi, S., Zheng, H., Cenni, B., Nehme, A., Christen, R. D., and Howell, S. B. 1996. The Role of DNA Mismatch Repair in Platinum Drug Resistance. Cancer Research, 56, (21) 4881-4886.

Fishel, R. and Kolodner, R. D. 1995. Identification of mismatch repair genes and their role in the development of cancer. Current Opinion in Genetics & Development, 5, (3) 382-395.

Fitzgerald, K. A., Palsson-McDermott, E. M., Bowie, A. G., Jefferies, C. A., Mansell, A. S., Brady, G., Brint, E., Dunne, A., Gray, P., Harte, M. T., McMurray, D., Smith, D. E., Sims, J. E., Bird, T. A., and O'Neill, L. A. J. 2001. Mal (MyD88-adapter-like) is required for Toll-like receptor-4 signal transduction. Nature, 413, (6851) 78-83.

Flavin, R., Smyth, P., Barrett, C., Russell, S., Wen, H., Wei, J., Laios, A., O'Toole, S., Ring, M., Denning, K., Li, J., Aherne, S., Sammarae, D., Aziz, N. A., Alhadi, A., Finn, S. P., Loda, M., B, S., Sheils, O., and O'Leary, J. J. 2009. miR-29b Expression Is Associated With Disease-Free Survival in Patients With Ovarian Serous Carcinoma. International Journal of Gynecological Cancer, 19, (4)

Flavin, R. J., Smyth, P. C., Finn, S. P., Laios, A., O'Toole, S. A., Barrett, C., Ring, M., Denning, K. M., Li, J., Aherne, S. T., Aziz, N. A., Alhadi, A., Sheppard, B. L., Loda, M., Martin, C., Sheils, O. M., and O'Leary, J. J. 2008. Altered eIF6 and Dicer expression is associated with clinicopathological features in ovarian serous carcinoma patients. Modern Pathology, 21, (6) 676-684.

Fleming, J. S., Beaugie, C. R., Haviv, I., Chenevix-Trench, G., and Tan, O. L. 2006. Incessant ovulation, inflammation and epithelial ovarian carcinogenesis: Revisiting old hypotheses. Molecular and Cellular Endocrinology, 247, (1–2) 4-21.

Foulkes, W. 2006. BRCA1 and BRCA2: Chemosensitivity, Treatment Outcomes and Prognosis. Familial Cancer, 5, (2) 135-142.

Fuertes, M. A., Alonso, C., and Perez, J. M. 2003a. Biochemical modulation of Cisplatin mechanisms of action: enhancement of antitumor activity and circumvention of drug resistance. Chemical Reviews, 103, (3) 645-662.

Fuertes, M. A., Castilla, J., Alonso, C., and Perez, J. M. 2003b. Cisplatin biochemical mechanism of action: from cytotoxicity to induction of cell death through interconnections between apoptotic and necrotic pathways. Current Medical Chemistry, 10, (3) 257-266.

Fung, E. T. 2010. A Recipe for Proteomics Diagnostic Test Development: The OVA1 Test, from Biomarker Discovery to FDA Clearance. Clinical Chemistry, 56, (2) 327-329.

Furlong, F., Fitzpatrick, P., O'Toole, S., Phelan, S., McGrogan, B., Maguire, A., O'Grady, A., Gallagher, M., Prencipe, M., McGoldrick, A., McGettigan, P., Brennan, D., Sheils, O., Martin, C., Kay, W., O'Leary, J., and McCann, A. 2012. Low MAD2 expression levels associate with reduced progression-free survival in patients with high-grade serous epithelial ovarian cancer. The Journal of Pathology, 226, (5) 746-755.

Furukawa, S., Soeda, S., Kiko, Y., Suzuki, O., Hashimoto, Y., Watanabe, T., Nishiyama, H., Tasaki, K., Hojo, H., Abe, M., and Fujimori, K. 2013. MCP-1 promotes invasion and adhesion of human ovarian cancer cells. Anticancer Research, 33, (11) 4785-4790.

Furuya, M., Kato, H., Nishimura, N., Ishiwata, I., Ikeda, H., Ito, R., Yoshiki, T., and Ishikura, H. 2005. Down-regulation of CD9 in human ovarian carcinoma cell might contribute to peritoneal dissemination: morphologic alteration and reduced expression of beta1 integrin subsets. Cancer Research, 65, (7) 2617-2625.

Gallagher, M., Flavin, R., Elbaruni, S., McInerney, J., Smyth, P., Salley, Y., Vencken, S., O'Toole, S., Laios, A., Lee, M., Denning, K., Li, J., Aherne, S., Lao, K., Martin, C.,

Sheils, O., and O'Leary, J. 2009. Regulation of microRNA biosynthesis and expression in 2102Ep embryonal carcinoma stem cells is mirrored in ovarian serous adenocarcinoma patients. Journal of Ovarian Research, 2, (1) 19-19.

Ganansia-Leymarie, V., Bischoff, P., Bergerat, J. P., and Holl, V. 2003. Signal transduction pathways of taxanes-induced apoptosis. Current Medical Chemistry: Anticancer Agents, 3, (4) 291-306.

Garcia, D. M., Baek, D., Shin, C., Bell, G. W., Grimson, A., and Bartel, D. P. 2011. Weak seed-pairing stability and high target-site abundance decrease the proficiency of lsy-6 and other microRNAs. Nature Structural and Molecular Biology, 18, (10) 1139-1146.

Garzon, R., Calin, G. A., and Croce, C. M. 2009. MicroRNAs in Cancer. Annual Review of Medicine, 60, 167-179.

Gaver, R. C., Colombo, N., Green, M. D., George, A. M., Deeb, G., Morris, A. D., Canetta, R. M., Speyer, J. L., Farmen, R. H., and Muggia, F. M. 1988. The disposition of carboplatin in ovarian cancer patients. Cancer Chemotherapy and Pharmacology, 22, (3) 263-270.

Gazitt, Y., Rothenberg, M. L., Hilsenbeck, S. G., Fey, V., Thomas, C., and Montegomrey, W. 1998. Bcl-2 overexpression is associated with resistance to paclitaxel, but not gemcitabine, in multiple myeloma cells. International Journal of Oncology, 13, (4) 839-848.

Genschel, J. and Modrich, P. 2003. Mechanism of 52-Directed Excision in Human Mismatch Repair. Molecular cell, 12, (5) 1077-1086.

Giaccone, G. 2000. Clinical perspectives on platinum resistance. Drugs, 59 Suppl 4, 9-17.

Giaccone, G., Huizing, M., Postmus, P. E., ten Bokkel Huinink, W. W., Koolen, M., van, Z. N., Vermorken, J. B., Beijnen, J. H., Dalesio, O., Pinedo, H. M., and . 1995. Dose-finding and sequencing study of paclitaxel and carboplatin in non-small cell lung cancer. Seminars In Oncology, 22, (4 Suppl 9) 78-82.

Giannakakou, P., Sackett, D. L., Kang, Y. K., Zhan, Z., Buters, J. T. M., Fojo, T., and Poruchynsky, M. S. 1997. Paclitaxel-resistant Human Ovarian Cancer Cells Have Mutant Beta-Tubulins That Exhibit Impaired Paclitaxel-driven Polymerization. Journal of Biological Chemistry, 272, (27) 17118-17125.

Gifford, G., Paul, J., Vasey, P. A., Kaye, S. B., and Brown, R. 2004. The Acquisition of hMLH1 Methylation in Plasma DNA after Chemotherapy Predicts Poor Survival for Ovarian Cancer Patients. Clinical Cancer Research, 10, (13) 4420-4426.

Gillet, J. P., Varma, S., and Gottesman, M. M. 2013. The clinical relevance of cancer cell lines. Journal of the National Cancer Institute, 105, (7) 452-458.

Gillies, R. J., Didier, N., and Denton, M. 1986. Determination of cell number in monolayer cultures. Analytical Biochemistry, 159, (1) 109-113.

Glynn, S. A., Gammell, P., Heenan, M., O'Connor, R., Liang, Y., Keenan, J., and Clynes, M. 2004. A new superinvasive in vitro phenotype induced by selection of human breast carcinoma cells with the chemotherapeutic drugs paclitaxel and doxorubicin. British Journal of Cancer, 91, (10) 1800-1807.

Go, R. S. and Adjei, A. A. 1999. Review of the Comparative Pharmacology and Clinical Activity of Cisplatin and Carboplatin. Journal of Clinical Oncology, 17, (1) 409-409.

Godwin, A. K., Meister, A., O'Dwyer, P. J., Huang, C. S., Hamilton, T. C., and Anderson, M. E. 1992. High resistance to cisplatin in human ovarian cancer cell lines is associated with

marked increase of glutathione synthesis. Proceedings of the National Academy of Sciences, 89, (7) 3070-3074.

Goff, B. A., Mandel, L. S., Drescher, C. W., Urban, N., Gough, S., Schurman, K. M., Patras, J., Mahony, B. S., and Andersen, M. R. 2007. Development of an ovarian cancer symptom index. Cancer, 109, (2) 221-227.

Gottesman, M. M., Fojo, T., and Bates, S. E. 2002. Multidrug resistance in cancer: role of ATP-dependent transporters. Nature Reviews Cancer, 2, (1) 48-58.

Gregory, R. I., Chendrimada, T. P., Cooch, N., and Shiekhattar, R. 2005. Human RISC Couples MicroRNA Biogenesis and Posttranscriptional Gene Silencing. Cell, 123, (4) 631-640.

Greither, T., Grochola, L. F., Udelnow, A., Lautenschlager, C., Wurl, P., and Taubert, H. 2010. Elevated expression of microRNAs 155, 203, 210 and 222 in pancreatic tumors is associated with poorer survival. International Journal of Cancer, 126, (1) 73-80.

Grimson, A., Farh, K. K., Johnston, W. K., Garrett-Engele, P., Lim, L. P., and Bartel, D. P. 2007. MicroRNA targeting specificity in mammals: determinants beyond seed pairing. Molecular and Cellular Biology, 27, (1) 91-105.

Grishok, A., Pasquinelli, A. E., Conte, D., Li, N., Parrish, S., Ha, I., Baillie, D. L., Fire, A., Ruvkun, G., and Mello, C. C. 2001. Genes and Mechanisms Related to RNA Interference Regulate Expression of the Small Temporal RNAs that Control C. elegans Developmental Timing. Cell, 106, (1) 23-34.

Gudermann, F., Ziemeck, P., and Lehmann, J. 1997. CeDEX: Automated Cell Density Determination. 301-305.

Guo, F., Tian, J., Lin, Y., Jin, Y., Wang, L., and Cui, M. 2013. Serum microRNA-92 expression in patients with ovarian epithelial carcinoma. The Journal of International Medical Research, 41, (5) 1456-1461.

Hall, J. M., Lee, M. K., Newman, B., Morrow, J. E., Anderson, L. A., Huey, B., and King, M. C. 1990. Linkage of early-onset familial breast cancer to chromosome 17q21. Science, 250, (4988) 1684-1689.

Hamilton, W., Peters, T. J., Bankhead, C., and Sharp, D. 2009. Risk of ovarian cancer in women with symptoms in primary care: population based case-control study. British Medical Journal, 339, b2998-b2998.

Hammond, J. W., Cai, D., and Verhey, K. J. 2008. Tubulin modifications and their cellular functions. Current Opinion in Cell Biology, 20, (1) 71-76.

Hammond, S. M., Bernstein, E., Beach, D., and Hannon, G. J. 2000. An RNA-directed nuclease mediates post-transcriptional gene silencing in Drosophila cells. Nature, 404, (6775) 293-296.

Han, J., Lee, Y., Yeom, K. H., Kim, Y. K., Jin, H., and Kim, V. N. 2004. The Drosha-DGCR8 complex in primary microRNA processing. Genes Development, 18, (24) 3016-3027.

Han, J., Lee, Y., Yeom, K. H., Nam, J. W., Heo, I., Rhee, J. K., Sohn, S. Y., Cho, Y., Zhang, B. T., and Kim, V. N. 2006. Molecular Basis for the Recognition of Primary microRNAs by the Drosha-DGCR8 Complex. Cell, 125, (5) 887-901.

Hanahan, D. and Weinberg, R. A. 2000. The Hallmarks of Cancer. Cell, 100, (1) 57-70.

Hankinson, S. E., Hunter, D. J., Colditz, G. A., Willett, W. C., Stampfer, M. J., Rosner, B., Hennekens, C. H., and Speizer, F. E. 1993. Tubal ligation, hysterectomy, and risk of ovarian cancer. A prospective study. JAMA, 270, (23) 2813-2818.

Hao, X., Zhou, Z., Ye, S., Zhou, T., Lu, Y., Ma, D., and Wang, S. 2010. Effect of Mad2 on paclitaxel-induced cell death in ovarian cancer cells. Journal of Huazhong University of Science and Technology -- Medical Sciences --, 30, (5) 620-625.

Hari, M., Loganzo, F., Annable, T., Tan, X., Musto, S., Morilla, D. B., Nettles, J. H., Snyder, J. P., and Greenberger, L. M. 2006. Paclitaxel-resistant cells have a mutation in the paclitaxel-binding region of Beta-tubulin (Asp26Glu) and less stable microtubules. Molecular Cancer Therapeutics, 5, (2) 270-278.

Hartlerode, A. J. and Scully, R. 2009. Mechanisms of double-strand break repair in somatic mammalian cells. Biochemical Journal, 423, (2) 157-168.

Hartmann, L. C., Lu, K. H., Linette, G. P., Cliby, W. A., Kalli, K. R., Gershenson, D., Bast, R. C., Stec, J., Iartchouk, N., Smith, D. I., Ross, J. S., Hoersch, S., Shridhar, V., Lillie, J., Kaufmann, S. H., Clark, E. A., and Damokosh, A. I. 2005. Gene Expression Profiles Predict Early Relapse in Ovarian Cancer after Platinum-Paclitaxel Chemotherapy. Clinical Cancer Research, 11, (6) 2149-2155.

Heintz, A. P., Odicino, F., Maisonneuve, P., Quinn, M. A., Benedet, J. L., Creasman, W. T., Ngan, H. Y., Pecorelli, S., and Beller, U. 2006. Carcinoma of the ovary. FIGO 26th Annual Report on the Results of Treatment in Gynecological Cancer. International Journal of Gynaecology and Obstetrics, 95 Suppl 1, S161-S192.

Helleday, T., Lo, J., van Gent, D. C., and Engelward, B. P. 2007. DNA double-strand break repair: From mechanistic understanding to cancer treatment. DNA Repair, 6, (7) 923-935.

Helleman, J., Jansen, M. P., Span, P. N., van Staveren, I. L., Massuger, L. F., Meijer-van Gelder, M. E., Sweep, F. C., Ewing, P. C., van der Burg, M. E., Stoter, G., Nooter, K., and Berns, E. M. 2006a. Molecular profiling of platinum resistant ovarian cancer. International Journal of Cancer, 118, (8) 1963-1971.

Helleman, J., van Staveren, I., Dinjens, W., van Kuijk, P., Ritstier, K., Ewing, P., van der Burg, M., Stoter, G., and Berns, E. 2006b. Mismatch repair and treatment resistance in ovarian cancer. BMC Cancer, 6, (1) 201-201.

Heller, M. J. 2002. DNA microarray technology: devices, systems, and applications. Annual Review of Biomedical Engineering, 4, 129-153.

Hennessy, B. T., Coleman, R. L., and Markman, M. 2009. Ovarian cancer. The Lancet, 374, (9698) 1371-1382.

Hennessy, B. T. J., Timms, K. M., Carey, M. S., Gutin, A., Meyer, L. A., Flake, D. D., Abkevich, V., Potter, J., Pruss, D., Glenn, P., Li, Y., Li, J., Gonzalez-Angulo, A. M., McCune, K. S., Markman, M., Broaddus, R. R., Lanchbury, J. S., Lu, K. H., and Mills, G. B. 2010. Somatic Mutations in BRCA1 and BRCA2 Could Expand the Number of Patients That Benefit From Poly (ADP Ribose) Polymerase Inhibitors in Ovarian Cancer. Journal of Clinical Oncology, 28, (22) 3570-3576.

Henry, V. J., Bandrowski, A. E., Pepin, A. S., Gonzalez, B. J., and Desfeux, A. 2014. OMICtools: an informative directory for multi-omic data analysis. Database, 2014,

Heo, I., Joo, C., Cho, J., Ha, M., Han, J., and Kim, V. N. 2008. Lin28 mediates the terminal uridylation of let-7 precursor MicroRNA. Molecular cell, 32, (2) 276-284.

Higby, D. J., Wallace, H. J., Jr., Albert, D. J., and Holland, J. F. 1974. Diaminodichloroplatinum: a phase I study showing responses in testicular and other tumors. Cancer, 33, (5) 1219-5.

Himmelstein, K. J., Patton, T. F., Belt, R. J., Taylor, S., Repta, A. J., and Sternson, L. A. 1981. Clinical kinetics on intact cisplatin and some related species. Clinical Pharmacology and Therapeutics, 29, (5) 658-664.

Ho, S. M. 2003. Estrogen, progesterone and epithelial ovarian cancer. Reproductive Biology and Endocrinology, 1, 73-73.

Hoffmann, A. C., Wild, P., Leicht, C., Bertz, S., Danenberg, K. D., Danenberg, P. V., Stohr, R., Stockle, M., Lehmann, J., Schuler, M., and Hartmann, A. 2010. MDR1 and ERCC1 expression predict outcome of patients with locally advanced bladder cancer receiving adjuvant chemotherapy. Neoplasia, 12, (8) 628-636.

Holzer, A. K., Katano, K., Klomp, L. W. J., and Howell, S. B. 2004. Cisplatin Rapidly Down-regulates Its Own Influx Transporter hCTR1 in Cultured Human Ovarian Carcinoma Cells. Clinical Cancer Research, 10, (19) 6744-6749.

Hong, D. S., Angelo, L. S., and Kurzrock, R. 2007. Interleukin-6 and its receptor in cancer. Cancer, 110, (9) 1911-1928.

Hong, F., Li, Y., Xu, Y., and Zhu, L. 2013. Prognostic significance of serum microRNA-221 expression in human epithelial ovarian cancer. The Journal of International Medical Research, 41, (1) 64-71.

Hong, L., Yang, J., Han, Y., Lu, Q., Cao, J., and Syed, L. 2012. High expression of miR-210 predicts poor survival in patients with breast cancer: A meta-analysis. Gene, 507, (2) 135-138.

Houle, C. D., Ding, X. Y., Foley, J. F., Afshari, C. A., Barrett, J. C., and Davis, B. J. 2002. Loss of expression and altered localization of KAI1 and CD9 protein are associated with epithelial ovarian cancer progression. Gynecologic Oncology, 86, (1) 69-78.

Hsu, S. D., Tseng, Y. T., Shrestha, S., Lin, Y. L., Khaleel, A., Chou, C. H., Chu, C. F., Huang, H. Y., Lin, C. M., Ho, S. Y., Jian, T. Y., Lin, F. M., Chang, T. H., Weng, S. L., Liao, K. W., Liao, I. E., Liu, C. C., and Huang, H. D. 2014. miRTarBase update 2014: an information resource for experimentally validated miRNA-target interactions. Nucleic Acids Research, 42, (Database issue) D78-D85.

Hu, X., Macdonald, D. M., Huettner, P. C., Feng, Z., El Naqa, I. M., Schwarz, J. K., Mutch, D. G., Grigsby, P. W., Powell, S. N., and Wang, X. 2009. A miR-200 microRNA cluster as prognostic marker in advanced ovarian cancer. Gynecologic Oncology, 114, (3) 457-464.

Huang, D. W., Sherman, B. T., and Lempicki, R. A. 2008. Systematic and integrative analysis of large gene lists using DAVID bioinformatics resources. Nature Protocols, 4, (1) 44-57.

Huang, D. W., Sherman, B. T., and Lempicki, R. A. 2009. Bioinformatics enrichment tools: paths toward the comprehensive functional analysis of large gene lists. Nucleic Acids Research, 37, (1) 1-13.

Huang, J., Zhang, J., Li, H., Lu, Z., Shan, W., Mercado-Uribe, I., and Liu, J. 2013. VCAM1 expression correlated with tumorigenesis and poor prognosis in high grade serous ovarian cancer. American Journal of Translational Research, 5, (3) 336-346.

Huang, Y., Ibrado, A. M., Reed, J. C., Bullock, G., Ray, S., Tang, C., and Bhalla, K. 1997. Co-expression of several molecular mechanisms of multidrug resistance and their significance for paclitaxel cytotoxicity in human AML HL-60 cells. Leukemia (08876924), 11, (2) 253-253.

Huddleston, H. G., Wong, K. k., Welch, W. R., Berkowitz, R. S., and Mok, S. C. 2005. Clinical applications of microarray technology: creatine kinase B is an up-regulated gene in

epithelial ovarian cancer and shows promise as a serum marker. Gynecologic Oncology, 96, (1) 77-83.

Huizing, M. T., Giaccone, G., van Warmerdam, L. J., Rosing, H., Bakker, P. J., Vermorken, J. B., Postmus, P. E., van, Z. N., Koolen, M. G., ten Bokkel Huinink, W. W., van der Vijgh, W. J., Bierhorst, F. J., Lai, A., Dalesio, O., Pinedo, H. M., Veenhof, C. H., and Beijnen, J. H. 1997. Pharmacokinetics of paclitaxel and carboplatin in a dose-escalating and dose-sequencing study in patients with non-small-cell lung cancer. The European Cancer Centre. Journal of Clinical Oncology, 15, (1) 317-329.

Hummel, R., Watson, D. I., Smith, C., Kist, J., Michael, M. Z., Haier, J., and Hussey, D. J. 2011. Mir-148a improves response to chemotherapy in sensitive and resistant oesophageal adenocarcinoma and squamous cell carcinoma cells. Journal of Gastrointestinal Surgery, 15, (3) 429-438.

Husain, A., He, G., Venkatraman, E. S., and Spriggs, D. R. 1998. BRCA1 Up-Regulation Is Associated with Repair-mediated Resistance to cis-Diamminedichloroplatinum(II). Cancer Research, 58, (6) 1120-1123.

Hwang, J. R., Jo, K., Lee, Y., Sung, B. J., Park, Y. W., and Lee, J. H. 2012. Upregulation of CD9 in ovarian cancer is related to the induction of TNF-alpha gene expression and constitutive NF-kappaB activation. Carcinogenesis, 33, (1) 77-83.

Hyafil, F., Vergely, C., Du, V. P., and Grand-Perret, T. 1993. In vitro and in vivo reversal of multidrug resistance by GF120918, an acridonecarboxamide derivative. Cancer Research, 53, (19) 4595-4602.

ICON3. 2002. Paclitaxel plus carboplatin versus standard chemotherapy with either single-agent carboplatin or cyclophosphamide, doxorubicin, and cisplatin in women with ovarian cancer: the ICON3 randomised trial. The Lancet, 360, (9332) 505-515.

Ikeda, H., Matsushita, M., Waisfisz, Q., Kinoshita, A., Oostra, A. B., Nieuwint, A. W. M., de Winter, J. P., Hoatlin, M. E., Kawai, Y., Sasaki, M. S., D'Andrea, M. R., Kawakami, Y., and Joenje, H. 2003. Genetic Reversion in an Acute Myelogenous Leukemia Cell Line from a Fanconi Anemia Patient with Biallelic Mutations in BRCA2. Cancer Research, 63, (10) 2688-2694.

Indermaur, M. D., Xiong, Y., Kamath, S. G., Boren, T., Hakam, A., Wenham, R. M., Apte, S. M., and Lancaster, J. M. 2010. Genomic-directed targeted therapy increases endometrial cancer cell sensitivity to doxorubicin. American Journal of Obstetrics and Gynecology, 203, (2) 158-158.

Iorio, M. V., Visone, R., Di, L. G., Donati, V., Petrocca, F., Casalini, P., Taccioli, C., Volinia, S., Liu, C. G., Alder, H., Calin, G. A., Menard, S., and Croce, C. M. 2007. MicroRNA signatures in human ovarian cancer. Cancer Research, 67, (18) 8699-8707.

Ip, S. C. Y., Rass, U., Blanco, M. G., Flynn, H. R., Skehel, J. M., and West, S. C. 2008. Identification of Holliday junction resolvases from humans and yeast. Nature, 456, (7220) 357-361.

Irizarry, R. A., Bolstad, B. M., Collin, F., Cope, L. M., Hobbs, B., and Speed, T. P. 2003a. Summaries of Affymetrix GeneChip probe level data. Nucleic Acids Research, 31, (4) e15-e15.

Irizarry, R. A., Hobbs, B., Collin, F., Beazer-Barclay, Y. D., Antonellis, K. J., Scherf, U., and Speed, T. P. 2003b. Exploration, normalization, and summaries of high density oligonucleotide array probe level data. Biostatistics, 4, (2) 249-264.

Iwasaki, H., Nakano, K., Shinkai, K., Kunisawa, Y., Hirahashi, M., Oda, Y., Onishi, H., and Katano, M. 2013. Hedgehog Gli3 activator signal augments tumorigenicity of colorectal cancer via upregulation of adherence-related genes. Cancer Science, 104, (3) 328-336.

Jaccard, N., Griffin, L. D., Keser, A., Macown, R. J., Super, A., Veraitch, F. S., and Szita, N. 2014. Automated method for the rapid and precise estimation of adherent cell culture characteristics from phase contrast microscopy images. Biotechnology & Bioengineering, 111, (3) 504-517.

Jacobs, I., Oram, D., Fairbanks, J., Turner, J., Frost, C., and Grudzinskas, J. G. 1990. A risk of malignancy index incorporating CA 125, ultrasound and menopausal status for the accurate preoperative diagnosis of ovarian cancer. British Journal of Obstetrics and Gynaecology, 97, (10) 922-929.

Jacobs, I. and Bast, R. C. 1989. The CA 125 tumour-associated antigen: a review of the literature. Human Reproduction, 4, (1) 1-12.

Jacobson, A. and Cunningham, J. 2012. Connective tissue growth factor in tumor pathogenesis. Fibrogenesis & Tissue Repair, 5, (Suppl 1) S8-S8.

Jacquemont, C. and Taniguchi, T. 2007. Proteasome Function Is Required for DNA Damage Response and Fanconi Anemia Pathway Activation. Cancer Research, 67, (15) 7395-7405.

Jamieson, E. R. and Lippard, S. J. 1999. Structure, Recognition, and Processing of Cisplatin–DNA Adducts. Chemical Reviews, 99, (9) 2467-2498.

Jayapal, M. and Melendez, A. J. 2006. DNA Microarray Technology for Target Identification and Validation. Clinical and Experimental Pharmacology and Physiology, 33, (5-6) 496-503.

Jeffery, I. B., Higgins, D. G., and Culhane, A. C. 2006. Comparison and evaluation of methods for generating differentially expressed gene lists from microarray data. BMC Bioinformatics, 7,

Jensen, A., Sharif, H., Frederiksen, K., and Kjaer, S. K. 2009. Use of fertility drugs and risk of ovarian cancer: Danish Population Based Cohort Study. British Medical Journal, 338, b249-b249.

Jensen, R. B., Carreira, A., and Kowalczykowski, S. C. 2010. Purified human BRCA2 stimulates RAD51-mediated recombination. Nature, 467, (7316) 678-683.

Jiang, L., He, D., Yang, D., Chen, Z., Pan, Q., Mao, A., Cai, Y., Li, X., Xing, H., Shi, M., Chen, Y., Bruce, I. C., Wang, T., Jin, L., Qi, X., Hua, D., Jin, J., and Ma, X. 2014. MiR-489 regulates chemoresistance in breast cancer via epithelial mesenchymal transition pathway. FEBS Letters, 588, (11) 2009-2015.

Joerger, M., Huitema, A. D. R., van den Bongard, D. H. J. G., Schellens, J. H. M., and Beijnen, J. H. 2006. Quantitative Effect of Gender, Age, Liver Function, and Body Size on the Population Pharmacokinetics of Paclitaxel in Patients with Solid Tumors. Clinical Cancer Research, 12, (7) 2150-2157.

Johnson, S. W., Laub, P. B., Beesley, J. S., Ozols, R. F., and Hamilton, T. C. 1997. Increased platinum-DNA damage tolerance is associated with cisplatin resistance and cross-resistance to various chemotherapeutic agents in unrelated human ovarian cancer cell lines. Cancer Research, 57, (5) 850-856.

Jones, K. H. and Senft, J. A. 1985. An improved method to determine cell viability by simultaneous staining with fluorescein diacetate-propidium iodide. Journal of Histochemistry & Cytochemistry, 33, (1) 77-79.

Jordan, A., Hadfield, J. A., Lawrence, N. J., and McGown, A. T. 1998. Tubulin as a target for anticancer drugs: agents which interact with the mitotic spindle. Medical Research Reviews, 18, (4) 259-296.

Jordan, P. and Carmo, F. 2000. Molecular mechanisms involved in cisplatin cytotoxicity. Cellular and Molecular Life Sciences, 57, (8) 1229-1235.

Jordan, S. J., Whiteman, D. C., Purdie, D. M., Green, A. I. C., and Webb, P. M. 2006. Does smoking increase risk of ovarian cancer? A systematic review. Gynecologic Oncology, 103, (3) 1122-1129.

Judson, I. and Kelland, L. R. 2000. New developments and approaches in the platinum arena. Drugs, 59 Suppl 4, 29-36.

Judson, P. L., Watson, J. M., Gehrig, P. A., Fowler, W. C., and Haskill, J. S. 1999. Cisplatin Inhibits Paclitaxel-induced Apoptosis in Cisplatin-resistant Ovarian Cancer Cell Lines: Possible Explanation for Failure ofCombination Therapy. Cancer Research, 59, (10) 2425-2432.

Juliano, R. L. and Ling, V. 1976. A surface glycoprotein modulating drug permeability in Chinese hamster ovary cell mutants. Biochimica et Biophysica Acta (BBA) - Biomembranes, 455, (1) 152-162.

Juneau, P. M., Garnier, A., and Duchesne, C. 2013. Selection and Tuning of a Fast and Simple Phase-Contrast Microscopy Image Segmentation Algorithm for Measuring Myoblast Growth Kinetics in an Automated Manner. Microscopy and Microanalysis, 19, (04) 855-866.

Kajiyama, H., Kikkawa, F., Suzuki, T., Shibata, K., Ino, K., and Mizutani, S. 2002. Prolonged Survival and Decreased Invasive Activity Attributable to Dipeptidyl Peptidase IV Overexpression in Ovarian Carcinoma. Cancer Research, 62, (10) 2753-2757.

Kajiyama, H., Shibata, K., Ino, K., Mizutani, S., Nawa, A., and Kikkawa, F. 2010. The expression of dipeptidyl peptidase IV (DPPIV/CD26) is associated with enhanced chemosensitivity to paclitaxel in epithelial ovarian carcinoma cells. Cancer Science, 101, (2) 347-354.

Kamazawa, S., Kigawa, J., Kanamori, Y., Itamochi, H., Sato, S., Iba, T., and Terakawa, N. 2002. Multidrug Resistance Gene-1 Is a Useful Predictor of Paclitaxel-Based Chemotherapy for Patients with Ovarian Cancer. Gynecologic Oncology, 86, (2) 171-176.

Kang, H. N., Oh, S. C., Kim, J. S., and Yoo, Y. A. 2012. Abrogation of Gli3 expression suppresses the growth of colon cancer cells via activation of p53. Experimental Cell Research, 318, (5) 539-549.

Kano, Y., Akutsu, M., Tsunoda, S., Suzuki, K., and Yazawa, Y. 1996. In vitro schedule-dependent interaction between paclitaxel and cisplatin in human carcinoma cell lines. Cancer Chemotherapy and Pharmacology., 37, (6) 525-530.

Kars, M. D., Ozlem, D. I., Gunduz, U., Ural, A., Arpaci, F., and Molnar, J. 2006. Development of Rational In Vitro Models for Drug Resistance in Breast Cancer and Modulation of MDR by Selected Compounds. Anticancer Research, 26, (6B) 4559-4568.

Kassim, S. K., Ali, H. S., Sallam, M. M., Fayed, S. T., Seada, L. S., abd-Elkawy, E., Seada, M. A., and Khalifa, A. 1999. Increased bcl-2 expression is associated with primary resistance to chemotherapy in human epithelial ovarian cancer. Clinical Biochemistry, 32, (5) 333-338.

Kassim, S. K., El-Salahy, E. M., Fayed, S. T., Helal, S. A., Helal, T., Azzam, E. E., and Khalifa, A. 2004. Vascular endothelial growth factor and interleukin-8 are associated with poor prognosis in epithelial ovarian cancer patients. Clinical Biochemistry, 37, (5) 363-369.

Katano, K., Kondo, A., Safaei, R., Holzer, A., Samimi, G., Mishima, M., Kuo, Y. M., Rochdi, M., and Howell, S. B. 2002. Acquisition of Resistance to Cisplatin Is Accompanied by Changes in the Cellular Pharmacology of Copper. Cancer Research, 62, (22) 6559-6565.

Kavallaris, M., Kuo, D. Y., Burkhart, C. A., Regl, D. L., Norris, M. D., Haber, M., and Horwitz, S. B. 1997. Taxol-resistant epithelial ovarian tumors are associated with altered expression of specific beta-tubulin isotypes. The Journal of Clinical Investigation, 100, (5) 1282-1293.

Kavallaris, M. 2010. Microtubules and resistance to tubulin-binding agents. Nature Reviews Cancer, 10, (3) 194-204.

Kavanagh, J. J., Gershenson, D. M., Choi, H., Lewis, L., Patel, K., Brown, G. L., Garcia, A., and Spriggs, D. R. 2005. Multi-institutional phase 2 study of TLK286 (TELCYTA, a glutathione S-transferase P1-1 activated glutathione analog prodrug) in patients with platinum and paclitaxel refractory or resistant ovarian cancer. International Journal of Gynaecological Cancer, 15, (4) 593-600.

Kennedy, R. D., Quinn, J. E., Johnston, P. G., and Harkin, D. P. 2002. BRCA1: mechanisms of inactivation and implications for management of patients. The Lancet, 360, (9338) 1007-1014.

Kessel, D., Botterill, V., and Wodinsky, I. 1968. Uptake and Retention of Daunomycin by Mouse Leukemic Cells as Factors in Drug Response. Cancer Research, 28, (5) 938-941.

Ketting, R. F., Fischer, S. E., Bernstein, E., Sijen, T., Hannon, G. J., and Plasterk, R. H. 2001. Dicer functions in RNA interference and in synthesis of small RNA involved in developmental timing in C. elegans. Genes and Development, 15, (20) 2654-2659.

Kikuchi, R., Tsuda, H., Kanai, Y., Kasamatsu, T., Sengoku, K., Hirohashi, S., Inazawa, J., and Imoto, I. 2007. Promoter Hypermethylation Contributes to Frequent Inactivation of a Putative Conditional Tumor Suppressor Gene Connective Tissue Growth Factor in Ovarian Cancer. Cancer Research, 67, (15) 7095-7105.

Kim, J. H., Skates, S. J., Uede, T., Wong, K. K., Schorge, J. O., Feltmate, C. M., Berkowitz, R. S., Cramer, D. W., and Mok, S. C. 2002. Osteopontin as a potential diagnostic biomarker for ovarian cancer. JAMA, 287, (13) 1671-1679.

Kim, J. C., Kim, S. Y., Cho, D. H., Roh, S. A., Choi, E. Y., Jo, Y. K., Jung, S. H., Na, Y. S., Kim, T. W., and Kim, Y. S. 2010a. Genome-wide identification of chemosensitive single nucleotide polymorphism markers in colorectal cancers. Cancer Science, 101, (4) 1007-1013.

Kim, K. H., Kim, J. M., Choi, Y. L., Shin, Y. K., Lee, H. C., Seong, I. O., Kim, B. K., Chae, S. W., Chung, Y. S., and Kim, S. H. 2009. Expression of sonic hedgehog signaling molecules in normal, hyperplastic and carcinomatous endometrium. Pathology International, 59, (5) 279-287.

Kim, K., Jo, M., Suh, D., Yoon, M., Shin, D., Lee, J., and Choi, K. 2012a. Expression and significance of the TLR4/MyD88 signaling pathway in ovarian epithelial cancers. World Journal of Surgical Oncology, 10, (1)

Kim, T. H., Kim, Y. K., Kwon, Y., Heo, J. H., Kang, H., Kim, G., and An, H. J. 2010b. Deregulation of miR-519a, 153, and 485-5p and its clinicopathological relevance in ovarian epithelial tumours. Histopathology, 57, (5) 734-743.

Kim, V. N. 2005. Small RNAs: classification, biogenesis, and function. Molecules and Cells, 19, (1) 1-15.

Kim, Y. K. and Kim, V. N. 2007. Processing of intronic microRNAs. The EMBO Journal, 26, (3) 775-783.

Kim, Y. W., Bae, S. M., Kim, I. W., Liu, H. B., Bang, H. J., Chaturvedi, P. K., Battogtokh, G., Lim, H., and Ahn, W. S. 2012b. Multiplexed bead-based immunoassay of four serum biomarkers for diagnosis of ovarian cancer. Oncology Reports, 28, (2) 585-591.

King, M. C., Marks, J. H., and Mandell, J. B. 2003. Breast and ovarian cancer risks due to inherited mutations in BRCA1 and BRCA2. Science, 302, (5645) 643-646.

Kirschner, M. W. 1978. Microtubule assembly and nucleation. International Reviews in Cytology, 54, 1-71.

Kong, F., Sun, C., Wang, Z., Han, L., Weng, D., Lu, Y., and Chen, G. 2011. miR-125b confers resistance of ovarian cancer cells to cisplatin by targeting pro-apoptotic Bcl-2 antagonist killer 1. Journal of Huazhong University of Science and Technology -- Medical Sciences --, 31, (4) 543-549.

Konstantinopoulos, P. A., Cannistra, S. A., Fountzilas, H., Culhane, A., Pillay, K., Rueda, B., Cramer, D., Seiden, M., Birrer, M., Coukos, G., Zhang, L., Quackenbush, J., and Spentzos, D. 2011. Integrated analysis of multiple microarray datasets identifies a reproducible survival predictor in ovarian cancer. PLoS ONE, 6, (3) e18202-

Konstantinopoulos, P. A., Spentzos, D., Karlan, B. Y., Taniguchi, T., Fountzilas, E., Francoeur, N., Levine, D. A., and Cannistra, S. A. 2010. Gene expression profile of BRCAness that correlates with responsiveness to chemotherapy and with outcome in patients with epithelial ovarian cancer. Journal of Clinical Oncology, 28, (22) 3555-3561.

Kool, M., de, H. M., Scheffer, G. L., Scheper, R. J., van Eijk, M. J., Juijn, J. A., Baas, F., and Borst, P. 1997. Analysis of expression of cMOAT (MRP2), MRP3, MRP4, and MRP5, homologues of the multidrug resistance-associated protein gene (MRP1), in human cancer cell lines. Cancer Research, 57, (16) 3537-3547.

Korita, P. V., Wakai, T., Shirai, Y., Matsuda, Y., Sakata, J., Takamura, M., Yano, M., Sanpei, A., Aoyagi, Y., Hatakeyama, K., and Ajioka, Y. 2010. Multidrug resistance-associated protein 2 determines the efficacy of cisplatin in patients with hepatocellular carcinoma. Oncology Reports, 23, (4) 965-972.

Koti, M., Gooding, R., Nuin, P., Haslehurst, A., Crane, C., Weberpals, J., Childs, T., Bryson, P., Dharsee, M., Evans, K., Feilotter, H., Park, P., and Squire, J. 2013. Identification of the IGF1/PI3K/NF kappaB/ERK gene signalling networks associated with chemotherapy resistance and treatment response in high-grade serous epithelial ovarian cancer. BMC Cancer, 13, (1) 549-549.

Krajewski, S., Blomqvist, C., Franssila, K., Krajewska, M., Wasenius, V. M., Niskanen, E., Nordling, S., and Reed, J. C. 1995. Reduced Expression of Proapoptotic Gene BAX Is Associated with Poor Response Rates to Combination Chemotherapy and Shorter Survival in Women with Metastatic Breast Adenocarcinoma. Cancer Research, 55, (19) 4471-4478.

Krueger, A., Baumann, S., Krammer, P. H., and Kirchhoff, S. 2001. FLICE-Inhibitory Proteins: Regulators of Death Receptor-Mediated Apoptosis. Molecular and Cellular Biology, 21, (24) 8247-8254.

Kuang, Y., Cai, J., Li, D., Han, Q., Cao, J., and Wang, Z. 2013. Repression of Dicer is associated with invasive phenotype and chemoresistance in ovarian cancer. Oncology Letters, 5, (4) 1149-1154.

Kulbe, H., Chakravarty, P., Leinster, D. A., Charles, K. A., Kwong, J., Thompson, R. G., Coward, J. I., Schioppa, T., Robinson, S. C., Gallagher, W. M., Galletta, L., Salako, M. A., Smyth, J. F., Hagemann, T., Brennan, D. J., Bowtell, D. D., and Balkwill, F. R. 2012. A Dynamic Inflammatory Cytokine Network in the Human Ovarian Cancer Microenvironment. Cancer Research, 72, (1) 66-75.

Kummar, S., Ji, J., Morgan, R., Lenz, H. J., Puhalla, S. L., Belani, C. P., Gandara, D. R., Allen, D., Kiesel, B., Beumer, J. H., Newman, E. M., Rubinstein, L., Chen, A., Zhang, Y., Wang, L., Kinders, R. J., Parchment, R. E., Tomaszewski, J. E., and Doroshow, J. H. 2012. A phase I study of veliparib in combination with metronomic cyclophosphamide in adults with refractory solid tumors and lymphomas. Clinical Cancer Research, 18, (6) 1726-1734.

Kurman, R. J. 2013. Origin and molecular pathogenesis of ovarian high-grade serous carcinoma. Annals of Oncology, 24, (suppl 10) x16-x21.

Kurman, R. J. and Shih, I. M. 2011. Molecular pathogenesis and extraovarian origin of epithelial ovarian cancer—Shifting the paradigm. Human Pathology, 42, (7) 918-931.

Kurosawa, H., Goi, K., Inukai, T., Inaba, T., Chang, K. S., Shinjyo, T., Rakestraw, K. M., Naeve, C. W., and Look, A. T. 1999. Two candidate downstream target genes for E2A-HLF. Blood, 93, (1) 321-332.

Lafarge, S., Sylvain, V., Ferrara, M., and Bignon, Y. J. 2001. Inhibition of BRCA1 leads to increased chemoresistance to microtubule-interfering agents, an effect that involves the JNK pathway. Oncogene, 20, (45) 6597-6606.

Laios, A., Mohamed, B. M., Kelly, L., Flavin, R., Finn, S., McEvoy, L., Gallagher, M., Martin, C., Sheils, O., Ring, M., Davies, A., Lawson, M., Gleeson, N., D'Arcy, T., d'Adhemar, C., Norris, L., Langhe, R., Saadeh, F. A., O'Leary, J. J., and O'Toole, S. A. 2013. Pre-Treatment of Platinum Resistant Ovarian Cancer Cells with an MMP-9/MMP-2 Inhibitor Prior to Cisplatin Enhances Cytotoxicity as Determined by High Content Screening. International Journal of Molecular Science, 14, (1) 2085-2103.

Laios, A., O'Toole, S., Flavin, R., Martin, C., Kelly, L., Ring, M., Finn, S. P., Barrett, C., Loda, M., Gleeson, N., D'Arcy, T., McGuinness, E., Sheils, O., Sheppard, B., and O' Leary, J. 2008a. Potential role of miR-9 and miR-223 in recurrent ovarian cancer. Molecular Cancer, 7, 35-35.

Laios, A., O'Toole, S. A., Flavin, R., Martin, C., Ring, M., Gleeson, N., D'Arcy, T., McGuinness, E. P., Sheils, O., Sheppard, B. L., and O' Leary, J. J. 2008b. An integrative model for recurrence in ovarian cancer. Molecular Cancer Therapeutics, 7, 8-8.

Lambeck, A. J., Crijns, A. P., Leffers, N., Sluiter, W. J., ten Hoor, K. A., Braid, M., van der Zee, A. G., Daemen, T., Nijman, H. W., and Kast, W. M. 2007. Serum cytokine profiling as a diagnostic and prognostic tool in ovarian cancer: a potential role for interleukin 7. Clinical Cancer Research, 13, (8) 2385-2391.

Landen, C. N., Birrer, M. J., and Sood, A. K. 2008. Early Events in the Pathogenesis of Epithelial Ovarian Cancer. Journal of Clinical Oncology, 26, (6) 995-1005.

Langdon, S. P., Lawrie, S. S., Hay, F. G., Hawkes, M. M., McDonald, A., Hayward, I. P., Schol, D. J., Hilgers, J., Leonard, R. C., and Smyth, J. F. 1988. Characterization and properties of nine human ovarian adenocarcinoma cell lines. Cancer Research, 48, (21) 6166-6172.

Langhe, R., Norris, L., Saadeh, F. A., Blackshields, G., Varley, R., Harrison, A., Gleeson, N., Spillane, C. D., Martin, C., O' Donnell, M., Darcy, T., O' Leary, J. J., and O' Toole, S. 2014. Novel Serum MicroRNA Panel To Discriminate Benign From Malignant Ovarian Disease. Cancer Letters, In Press.

Latifi, A., Luwor, R. B., Bilandzic, M., Nazaretian, S., Stenvers, K., Pyman, J., Zhu, H., Thompson, E. W., Quinn, M. A., Findlay, J. K., and Ahmed, N. 2012. Isolation and characterization of tumor cells from the ascites of ovarian cancer patients: molecular phenotype of chemoresistant ovarian tumors. PLoS ONE, 7, (10) e46858-e46858.

Law , L. W. 1951. Resistance in leukemic cells to a guanine analog, 8-azaguanine. Proceedings of the Society for Experimental Biology and Medicine, 78, (2) 499-502.

Lawicki, S., Gacuta-Szumarska, E., Bedkowska, G. E., and Szmitkowski, M. 2012. Hematopoietic cytokines as tumor markers in gynecological malignancies. A multivariate analysis in epithelial ovarian cancer patients. Growth Factors, 30, (6) 357-366.

Lawlor, D., Martin, P., Busschots, S., Thery, J., O'Leary, J. J., Hennessy, B. T., and Stordal, B. 2014. PARP Inhibitors as P-glyoprotein Substrates. Journal of Pharmaceutical Sciences, 103, (6) 1913-1920.

Lee, C. H., Subramanian, S., Beck, A. H., Espinosa, I., Senz, J., Zhu, S. X., Huntsman, D., van de Rijn, M., and Gilks, C. B. 2009. MicroRNA profiling of BRCA1/2 mutation-carrying and non-mutation-carrying high-grade serous carcinomas of ovary. PLoS ONE, 4, (10) e7314-e7314.

Lee, J. H. and Paull, T. T. 2004. Direct activation of the ATM protein kinase by the Mre11/Rad50/Nbs1 complex. Science, 304, (5667) 93-96.

Lee, K., Klein-Szanto, A. J. P., and Kruh, G. D. 2000. Analysis of the MRP4 Drug Resistance Profile in Transfected NIH3T3 Cells. Journal of the National Cancer Institute, 92, (23) 1934-1940.

Lee, P. S., Teaberry, V. S., Bland, A. E., Huang, Z., Whitaker, R. S., Baba, T., Fujii, S., Secord, A. A., Berchuck, A., and Murphy, S. K. 2010. Elevated MAL expression is accompanied by promoter hypomethylation and platinum resistance in epithelial ovarian cancer. International Journal of Cancer, 126, (6) 1378-1389.

Lee, R. C., Feinbaum, R. L., and Ambros, V. 1993. The C. elegans heterochronic gene lin-4 encodes small RNAs with antisense complementarity to lin-14. Cell, 75, (5) 843-854.

Lee, Y., Jeon, K., Lee, J. T., Kim, S., and Kim, V. N. 2002. MicroRNA maturation: stepwise processing and subcellular localization. The EMBO Journal, 21, (17) 4663-4670.

Lee, Y., Ahn, C., Han, J., Choi, H., Kim, J., Yim, J., Lee, J., Provost, P., Radmark, O., Kim, S., and Kim, V. N. 2003. The nuclear RNase III Drosha initiates microRNA processing. Nature, 425, (6956) 415-419.

Leeper, K., Garcia, R., Swisher, E., Goff, B., Greer, B., and Paley, P. 2002. Pathologic Findings in Prophylactic Oophorectomy Specimens in High-Risk Women. Gynecologic Oncology, 87, (1) 52-56.

Lentz, G. M., Lobo, R. A., Gershenson, D. M., and Katz, V. L. 2014. Comprehensive Gynecology. 6, 1-936.

Leskela, S., Leandro-Garcia, L. J., Mendiola, M., Barriuso, J., Inglada-Perez, L., Munoz, I., Martinez-Delgado, B., Redondo, A., de Santiago, J., Robledo, M., Hardisson, D., and Rodriguez-Antona, C. 2011. The miR-200 family controls Beta-tubulin III expression and is associated with paclitaxel-based treatment response and progression-free survival in ovarian cancer patients. Endocrine-Related Cancer, 18, (1) 85-95.

Lewis, B. P., Burge, C. B., and Bartel, D. P. 2005. Conserved Seed Pairing, Often Flanked by Adenosines, Indicates that Thousands of Human Genes are MicroRNA Targets. Cell, 120, (1) 15-20.

Lewis, B. P., Shih, I. h., Jones-Rhoades, M. W., Bartel, D. P., and Burge, C. B. 2003. Prediction of Mammalian MicroRNA Targets. Cell, 115, (7) 787-798.

Li, J., Feng, Q., Kim, J. M., Schneiderman, D., Liston, P., Li, M., Vanderhyden, B., Faught, W., Fung, M. F. K., Senterman, M., Korneluk, R. G., and Tsang, B. K. 2001. Human Ovarian Cancer and Cisplatin Resistance: Possible Role of Inhibitor of Apoptosis Proteins. Endocrinology, 142, (1) 370-380.

Li, J. H., Liu, S., Zhou, H., Qu, L. H., and Yang, J. H. 2014a. starBase v2.0: decoding miRNA-ceRNA, miRNA-ncRNA and protein–RNA interaction networks from large-scale CLIP-Seq data. Nucleic Acids Research, 42, (D1) D92-D97.

Li, L., Huang, K., You, Y., Fu, X., Hu, L., Song, L., and Meng, Y. 2014b. Hypoxia-induced miR-210 in epithelial ovarian cancer enhances cancer cell viability via promoting proliferation and inhibiting apoptosis. International Journal of Oncology, 44, (6) 2111-2120.

Li, L., Luan, Y., Wang, G., Tang, B., Li, D., Zhang, W., Li, X., Zhao, J., Ding, H., Reed, E., and Li, Q. Q. 2004. Development and characterization of five cell models for chemoresistance studies of human ovarian carcinoma. International Journal of Molecular Medicine, 14, (2) 257-264.

Li, L. N., Zhou, X., Gu, Y., and Yan, J. 2013. Prognostic value of MMP-9 in ovarian cancer: a meta-analysis. Asian Pacific Journal of Cancer Prevention, 14, (7) 4107-4113.

Li, M., Balch, C., Montgomery, J. S., Jeong, M., Chung, J. H., Yan, P., Huang, T. H., Kim, S., and Nephew, K. P. 2009. Integrated analysis of DNA methylation and gene expression reveals specific signaling pathways associated with platinum resistance in ovarian cancer. BMC Medical Genomics, 2,

Liang, X. J., Shen, D. W., Garfield, S., and Gottesman, M. M. 2003. Mislocalization of membrane proteins associated with multidrug resistance in cisplatin-resistant cancer cell lines. Cancer Research, 63, (18) 5909-5916.

Liang, Y., O'Driscoll, L., McDonnell, S., Doolan, P., Oglesby, I., Duffy, K., O'Connor, R., and Clynes, M. 2004. Enhanced in vitro invasiveness and drug resistance with altered gene expression patterns in a human lung carcinoma cell line after pulse selection with anticancer drugs. International Journal of Cancer, 111, (4) 484-493.

Litman, T., Brangi, M., Hudson, E., Fetsch, P., Abati, A., Ross, D. D., Miyake, K., Resau, J. H., and Bates, S. E. 2000. The multidrug-resistant phenotype associated with overexpression of the new ABC half-transporter, MXR (ABCG2). Journal of Cell Science, 113, (11) 2011-2021.

Liu, D. C. and Yang, Z. L. 2013a. MTDH and EphA7 are markers for metastasis and poor prognosis of gallbladder adenocarcinoma. Diagnostic Cytopathology, 41, (3) 199-205.

Liu, H. X., Cartegni, L., Zhang, M. Q., and Krainer, A. R. 2001. A mechanism for exon skipping caused by nonsense or missense mutations in BRCA1 and other genes. Nature Genetics, 27, (1) 55-58.

Liu, J. R., Opipari, A. W., Tan, L., Jiang, Y., Zhang, Y., Tang, H., and Nunez, G. 2002. Dysfunctional Apoptosome Activation in Ovarian Cancer. Cancer Research, 62, (3) 924-931.

Liu, L., Zou, J., Wang, Q., Yin, F. Q., Zhang, W., and Li, L. 2014. Novel microRNAs expression of patients with chemotherapy drug-resistant and chemotherapy-sensitive epithelial ovarian cancer. Tumor Biology, 1-5.

Liu, N., Zhou, C., Zhao, J., and Chen, Y. 2012. Reversal of Paclitaxel Resistance in Epithelial Ovarian Carcinoma Cells by a MUC1 Aptamer-let-7i Chimera. Cancer Investigation, 30, (8) 577-582.

Liu, Q. and Gazitt, Y. 2003. Potentiation of dexamethasone-, paclitaxel-, and Ad-p53-induced apoptosis by Bcl-2 antisense oligodeoxynucleotides in drug-resistant multiple myeloma cells. Blood, 101, (10) 4105-4114.

Liu, Z., Qiu, M., Tang, Q. L., Liu, M., Lang, N., and Bi, F. 2010. Establishment and biological characteristics of oxaliplatin-resistant human colon cancer cell lines. Chinese Journal of Cancer, 29, (7) 661-667.

Liu, Z., Gersbach, E., Zhang, X., Xu, X., Dong, R., Lee, P., Liu, J., Kong, B., Shao, C., and Wei, J. J. 2013b. miR-106a Represses the Rb Tumor Suppressor p130 to Regulate Cellular Proliferation and Differentiation in High-Grade Serous Ovarian Carcinoma. Molecular Cancer Research, 11, (11) 1314-1325.

Loftus, J. C., Dhruv, H., Tuncali, S., Kloss, J., Yang, Z., Schumacher, C. A., Cao, B., Williams, B. O., Eschbacher, J. M., Ross, J. T. D., and Tran, N. L. 2013. TROY (TNFRSF19) Promotes Glioblastoma Survival Signaling and Therapeutic Resistance. Molecular Cancer Research, 11, (8) 865-874.

Loi, S., Pommey, S., Haibe-Kains, B., Beavis, P. A., Darcy, P. K., Smyth, M. J., and Stagg, J. 2013. CD73 promotes anthracycline resistance and poor prognosis in triple negative breast cancer. Proceedings of the National Academy of Science of the U.S.A., 110, (27) 11091-11096.

Long, B. H. and Fairchild, C. R. 1994. Paclitaxel inhibits progression of mitotic cells to G1 phase by interference with spindle formation without affecting other microtubule functions during anaphase and telephase. Cancer Research, 54, (16) 4355-4361.

Lorenzi, P. L., Reinhold, W. C., Varma, S., Hutchinson, A. A., Pommier, Y., Chanock, S. J., and Weinstein, J. N. 2009. DNA fingerprinting of the NCI-60 cell line panel. Molecular Cancer Therapeutics, 8, (4) 713-724.

Louis, K. S. and Siegel, A. C. 2011. Cell viability analysis using trypan blue: manual and automated methods. Methods in Molecalar Biology, 740, 7-12.

Lu, J., Getz, G., Miska, E. A., Alvarez-Saavedra, E., Lamb, J., Peck, D., Sweet-Cordero, A., Ebert, B. L., Mak, R. H., Ferrando, A. A., Downing, J. R., Jacks, T., Horvitz, H. R., and Golub, T. R. 2005. MicroRNA expression profiles classify human cancers. Nature, 435, (7043) 834-838.

Lu, L., Katsaros, D., Shaverdashvili, K., Qian, B., Wu, Y., de la Longrais, I. A. R., Preti, M., Menato, G., and Yu, H. 2009a. Pluripotent factor lin-28 and its homologue lin-28b in epithelial ovarian cancer and their associations with disease outcomes and expression of let-7a and IGF-II. European journal of cancer (Oxford, England : 1990), 45, (12) 2212-2218.

Lu, L., Schwartz, P., Scarampi, L., Rutherford, T., Canuto, E. M., Yu, H., and Katsaros, D. 2011. MicroRNA let-7a: A potential marker for selection of paclitaxel in ovarian cancer management. Gynecologic Oncology, 122, (2) 366-371.

Lu, Y., Xiao, J., Lin, H., Bai, Y., Luo, X., Wang, Z., and Yang, B. 2009b. A single anti-microRNA antisense oligodeoxyribonucleotide (AMO) targeting multiple microRNAs offers an improved approach for microRNA interference. Nucleic Acids Research, 37, (3) e24-e24.

Lund, E., Guttinger, S., Calado, A., Dahlberg, J. E., and Kutay, U. 2004. Nuclear export of microRNA precursors. Science, 303, (5654) 95-98.

Ma, J., Maliepaard, M., Kolker, H. J., Verweij, J., and Schellens, J. H. 1998. Abrogated energy-dependent uptake of cisplatin in a cisplatin-resistant subline of the human ovarian cancer cell line IGROV-1. Cancer Chemotherapy and Pharmacology, 41, (3) 186-192.

Ma, Y., Ma, L., Guo, Q., and Zhang, S. 2010. Expression of bone morphogenetic protein-2 and its receptors in epithelial ovarian cancer and their influence on the prognosis of ovarian cancer patients. Journal of Experimental & Clinical Cancer Research, 29, (1)

Madden, S. F., Clarke, C., Stordal, B., Gallagher, W. M., Crown, J., Clynes, M., and Hennessy, B. T. 2014. *OvMark*: An Integrated Approach to Mining Publically Available Transcriptomic Datasets Relating to Ovarian Cancer Outcomes. Molecular Cancer, In Press.

Maione, F., Capano, S., Regano, D., Zentilin, L., Giacca, M., Casanovas, O., Bussolino, F., Serini, G., and Giraudo, E. 2012. Semaphorin 3A overcomes cancer hypoxia and metastatic dissemination induced by antiangiogenic treatment in mice. Journal of Clinical Investigation, 122, (5) 1832-1848.

Maione, F., Molla, F., Meda, C., Latini, R., Zentilin, L., Giacca, M., Seano, G., Serini, G., Bussolino, F., and Giraudo, E. 2009. Semaphorin 3A is an endogenous angiogenesis inhibitor that blocks tumor growth and normalizes tumor vasculature in transgenic mouse models. Journal of Clinical Investigation, 119, (11) 3356-3372.

Malinge, J. M., Giraud-Panis, M. J. p., and Leng, M. 1999. Interstrand cross-links of cisplatin induce striking distortions in DNA. Journal of Inorganic Biochemistry, 77, (1-2) 23-29.

Mamidi, S., Cinci, M., Hasmann, M., Fehring, V., and Kirschfink, M. 2013. Lipoplex mediated silencing of membrane regulators (CD46, CD55 and CD59) enhances complement-dependent anti-tumor activity of trastuzumab and pertuzumab. Molecular Oncology, 7, (3) 580-594.

Manfredi, J. J. and Horwitz, S. B. 1984. Taxol: an antimitotic agent with a new mechanism of action. Pharmacology & Therapeutics, 25, (1) 83-125.

Maraz, A., Furak, J., Palfoldi, R., Eller, J., Szanto, E., Kahan, Z., Thurzo, L., Molnar, J., Tiszlavicz, L., and Hideghety, K. 2011. Roles of BCL-2 and MDR1 Expression in the Efficacy of Paclitaxel-based Lung Cancer Chemoradiation. Anticancer Research, 31, (4) 1431-1436.

Marchini, S., Cavalieri, D., Fruscio, R., Calura, E., Garavaglia, D., Nerini, I. F., Mangioni, C., Cattoretti, G., Clivio, L., Beltrame, L., Katsaros, D., Scarampi, L., Menato, G., Perego, P., Chiorino, G., Buda, A., Romualdi, C., and D'Incalci, M. 2011. Association between miR-200c and the survival of patients with stage I epithelial ovarian cancer: a retrospective study of two independent tumour tissue collections. Lancet Oncology, 12, (3) 273-285.

Markman, M. and Bookman, M. A. 2000. Second-Line Treatment of Ovarian Cancer. The Oncologist, 5, (1) 26-35.

Markman, M., Moon, J., Wilczynski, S., Lopez, A. M., Rowland, J., Michelin, D. P., Lanzotti, V. J., Anderson, G. L., and Alberts, D. S. 2010. Single agent carboplatin versus carboplatin plus pegylated liposomal doxorubicin in recurrent ovarian cancer: Final survival results of a SWOG (S0200) phase 3 randomized trial. Gynecologic Oncology, 116, (3) 323-325.

Marsigliante, S., Vetrugno, C., and Muscella, A. 2013. CCL20 induces migration and proliferation on breast epithelial cells. Journal of Cellular Physiology, 228, (9) 1873-1883.

Mateescu, B., Batista, L., Cardon, M., Gruosso, T., de, F. Y., Mariani, O., Nicolas, A., Meyniel, J. P., Cottu, P., Sastre-Garau, X., and Mechta-Grigoriou, F. 2011. miR-141 and miR-

200a act on ovarian tumorigenesis by controlling oxidative stress response. Nature Medicine, 17, (12) 1627-1635.

Matei, D. E., Schilder, J. M., and Michael, H. 2006. Germ Cell Tumors of the Ovary. 467-476.

Materna, V., Pleger, J., Hoffmann, U., and Lage, H. 2004. RNA expression of MDR1/P-glycoprotein, DNA-topoisomerase I, and MRP2 in ovarian carcinoma patients: correlation with chemotherapeutic response. Gynecologic Oncology, 94, (1) 152-160.

Matte, I., Lane, D., Laplante, C., Rancourt, C., and Piche, A. 2012. Profiling of cytokines in human epithelial ovarian cancer ascites. American Journal of Cancer Research, 2, (5) 566-580.

McDermott, M., Eustace, A. J., Busschots, S., Breen, L., Crown, J., Clynes, M., O'Donovan, N., and Stordal, B. 2014. In vitro Development of Chemotherapy and Targeted Therapy Drug-Resistant Cancer Cell Lines: A Practical Guide with Case Studies. Frontiers in Oncology, 4,

McEvoy, L. 2012. Developing Novel Therapeutic Approaches in Chemoresistant Ovarian Cancer Patients. PhD thesis, Trinity College Dublin, Dublin, Ireland.

McGlynn, P. and Lloyd, R. G. 2002. Recombinational repair and restart of damaged replication forks. Nature Reviews Molecular Cell Biology, 3, (11) 859-870.

McGown, A. T., Murphy, D., Swindell, R., Crowther, D., and Fox, B. W. 1994. Correlation of drug resistance-associated parameters in ovarian tumor biopsies. International Journal of Gynaecological Cancer, 4, (4) 241-249.

McGuire, W. P., Hoskins, W. J., Brady, M. F., Kucera, P. R., Partridge, E. E., Look, K. Y., Clarke-Pearson, D. L., and Davidson, M. 1996. Cyclophosphamide and Cisplatin Compared with Paclitaxel and Cisplatin in Patients with Stage III and Stage IV Ovarian Cancer. New England Journal of Medicine, 334, (1) 1-6.

McNatty, K. P., Makris, A., DeGrazia, C., Osathanondh, R., and Ryan, K. J. 1979. The production of progesterone, androgens, and estrogens by granulosa cells, thecal tissue, and stromal tissue from human ovaries in vitro. The Journal Clinical Endocrinology Metabolism, 49, (5) 687-699.

Mei, Y., Gao, C., Wang, K., Cui, L., Li, W., Zhao, X., Liu, F., Wu, M., Deng, G., Ding, W., Jia, H., and Li, Z. 2014. Effect of microRNA-210 on prognosis and response to chemotherapeutic drugs in pediatric acute lymphoblastic leukemia. Cancer Science, 105, (4) 463-472.

Meng, Q. H., Xu, E., Hildebrandt, M. A. T., Liang, D., Lu, K., Ye, Y., Wagar, E. A., and Wu, X. 2014. Genetic Variants in the Fibroblast Growth Factor Pathway as Potential Markers of Ovarian Cancer Risk, Therapeutic Response, and Clinical Outcome. Clinical Chemistry, 60, (1) 222-232.

Menon, U., Gentry-Maharaj, A., Hallett, R., Ryan, A., Burnell, M., Sharma, A., Lewis, S., Davies, S., Philpott, S., Lopes, A., Godfrey, K., Oram, D., Herod, J., Williamson, K., Seif, M. W., Scott, I., Mould, T., Woolas, R., Murdoch, J., Dobbs, S., Amso, N. N., Leeson, S., Cruickshank, D., Mcguire, A., Campbell, S., Fallowfield, L., Singh, N., Dawnay, A., Skates, S. J., Parmar, M., and Jacobs, I. 2009. Sensitivity and specificity of multimodal and ultrasound screening for ovarian cancer, and stage distribution of detected cancers: results of the prevalence screen of the UK Collaborative Trial of Ovarian Cancer Screening (UKCTOCS). The Lancet Oncology, 10, (4) 327-340.

Merritt, M. A., Parsons, P. G., Newton, T. R., Martyn, A. C., Webb, P. M., Green, A. C., Papadimos, D. J., and Boyle, G. M. 2009. Expression profiling identifies genes involved in neoplastic transformation of serous ovarian cancer. BMC Cancer, 9, 378-387.

Merritt, W. M., Lin, Y. G., Spannuth, W. A., Fletcher, M. S., Kamat, A. A., Han, L. Y., Landen, C. N., Jennings, N., De, G. K., Langley, R. R., Villares, G., Sanguino, A., Lutgendorf, S. K., Lopez-Berestein, G., Bar-Eli, M. M., and Sood, A. K. 2008a. Effect of interleukin-8 gene silencing with liposome-encapsulated small interfering RNA on ovarian cancer cell growth. Journal of the Natonal Cancer Institute, 100, (5) 359-372.

Merritt, W. M., Lin, Y. G., Han, L. Y., Kamat, A. A., Spannuth, W. A., Schmandt, R., Urbauer, D., Pennacchio, L. A., Cheng, J. F., Nick, A. M., Deavers, M. T., Mourad-Zeidan, A., Wang, H., Mueller, P., Lenburg, M. E., Gray, J. W., Mok, S., Birrer, M. J., Lopez-Berestein, G., Coleman, R. L., Bar-Eli, M., and Sood, A. K. 2008b. Dicer, Drosha, and Outcomes in Patients with Ovarian Cancer. New England Journal of Medicine, 359, (25) 2641-2650.

Meyers, M., Hwang, A., Wagner, M. W., and Boothman, D. A. 2004. Role of DNA mismatch repair in apoptotic responses to therapeutic agents. Environmental and Molecular Mutagenesis, 44, (4) 249-264.

Miles, G. D., Seiler, M., Rodriguez, L., Rajagopal, G., and Bhanot, G. 2012. Identifying microRNA/mRNA dysregulations in ovarian cancer. BMC Research Notes, 5,

Milross, C. G., Peters, L. J., Hunter, N. R., Mason, K. A., and Milas, L. 1995. Sequence-dependent antitumor activity of paclitaxel (taxol) and cisplatin in vivo. International Journal of Cancer, 62, (5) 599-604.

Miranda, K. C., Huynh, T., Tay, Y., Ang, Y. S., Tam, W. L., Thomson, A. M., Lim, B., and Rigoutsos, I. 2006. A pattern-based method for the identification of MicroRNA binding sites and their corresponding heteroduplexes. Cell, 126, (6) 1203-1217.

Mistry, P., Kelland, L. R., Abel, G., Sidhar, S., and Harrap, K. R. 1991. The relationships between glutathione, glutathione-S-transferase and cytotoxicity of platinum drugs and melphalan in eight human ovarian carcinoma cell lines. British Journal of Cancer, 64, (2) 215-220.

Mitchell, P. S., Parkin, R. K., Kroh, E. M., Fritz, B. R., Wyman, S. K., Pogosova-Agadjanyan, E. L., Peterson, A., Noteboom, J., O'Briant, K. C., Allen, A., Lin, D. W., Urban, N., Drescher, C. W., Knudsen, B. S., Stirewalt, D. L., Gentleman, R., Vessella, R. L., Nelson, P. S., Martin, D. B., and Tewari, M. 2008. Circulating microRNAs as stable blood-based markers for cancer detection. Proceedings of the National Academy of Science of the U.S.A., 105, (30) 10513-10518.

Miyazono, K., Kusanagi, K., and Inoue, H. 2001. Divergence and convergence of TGF-beta/BMP signaling. Journal of Cellular Physiology, 187, (3) 265-276.

Modan, B., Hartge, P., Hirsh-Yechezkel, G., Chetrit, A., Lubin, F., Beller, U., Ben-Baruch, G., Fishman, A., Menczer, J., Struewing, J. P., Tucker, M. A., Ebbers, S. M., Friedman, E., Piura, B., and Wacholder, S. 2001. Parity, Oral Contraceptives, and the Risk of Ovarian Cancer among Carriers and Noncarriers of a BRCA1 or BRCA2 Mutation. New England Journal of Medicine, 345, (4) 235-240.

Moggs, J. G., Szymkowski, D. E., Yamada, M., Karran, P., and Wood, R. D. 1997. Differential Human Nucleotide Excision Repair of Paired and Mispaired Cisplatin-DNA Adducts. Nucleic Acids Research, 25, (3) 480-490.

Mohle, J., Whittemore, A., Pike, M., and Darby, S. 1985. Gonadotrophins and ovarian cancer risk. Journal of the Natonal Cancer Institute, 75, (1) 178-180.

Mok, S. C., Bonome, T., Vathipadiekal, V., Bell, A., Johnson, M. E., Wong, K. K., Park, D. C., Hao, K., Yip, D. K., Donninger, H., Ozbun, L., Samimi, G., Brady, J., Randonovich, M., Pise-Masison, C. A., Barrett, J. C., Wong, W. H., Welch, W. R., Berkowitz, R. S., and Birrer, M. J. 2009. A gene signature predictive for outcome in advanced ovarian cancer

identifies a survival factor: microfibril-associated glycoprotein 2. Cancer Cell, 16, (6) 521-532.

Mok, S. C., Chao, J., Skates, S., Wong, K. k., Yiu, G. K., Muto, M. G., Berkowitz, R. S., and Cramer, D. W. 2001. Prostasin, a Potential Serum Marker for Ovarian Cancer: Identification Through Microarray Technology. Journal of the National Cancer Institute, 93, (19) 1458-1464.

Molder, A., Sebasta, M., Gustafsson, M., Gisselson, L., Wingren, A. G., and Alm, K. 2008. Non-invasive, label-free cell counting and quantitative analysis of adherent cells using digital holography. Journal of Microscopy, 232, (2) 240-247.

Monteiro, A. N., August, A., and Hanafusa, H. 1996. Evidence for a transcriptional activation function of BRCA1 C-terminal region. Proceedings of the National Academy of Science of the U.S.A., 93, (24) 13595-13599.

Moore, R. G., Brown, A. K., Miller, M. C., Skates, S., Allard, W. J., Verch, T., Steinhoff, M., Messerlian, G., DiSilvestro, P., Granai, C. O., and Bast, J. 2008. The use of multiple novel tumor biomarkers for the detection of ovarian carcinoma in patients with a pelvic mass. Gynecologic Oncology, 108, (2) 402-408.

Moore, R. G., Jabre-Raughley, M., Brown, A. K., Robison, K. M., Miller, M. C., Allard, W. J., Kurman, R. J., Bast, R. C., and Skates, S. J. 2010. Comparison of a novel multiple marker assay vs the Risk of Malignancy Index for the prediction of epithelial ovarian cancer in patients with a pelvic mass. American Journal of Obstetrics and Gynecology, 203, (3) 228-228.

Mor, G., Visintin, I., Lai, Y., Zhao, H., Schwartz, P., Rutherford, T., Yue, L., Bray-Ward, P., and Ward, D. C. 2005. Serum protein markers for early detection of ovarian cancer. Proceedings of the National Academy of Science of the U.S.A., 102, (21) 7677-7682.

Mosmann, T. 1983. Rapid colorimetric assay for cellular growth and survival: Application to proliferation and cytotoxicity assays. Journal of Immunological Methods, 65, (1–2) 55-63.

Moudi, M., Go, R., Yien, C. Y., and Nazre, M. 2013. Vinca alkaloids. International Journal of Preventative Medicine, 4, (11) 1231-1235.

Mourtada-Maarabouni, M., Watson, D., Munir, M., Farzaneh, F., and Williams, G. T. 2013. Apoptosis suppression by candidate oncogene PLAC8 is reversed in other cell types. Current Cancer Drug Targets, 13, (1) 80-91.

Mross, K., Hollannder, N., Hauns, B., Schumacher, M., and Maier-Lenz, H. 2000. The pharmacokinetics of a 1-h paclitaxel infusion. Cancer Chemotherapy and Pharmacology, 45, (6) 463-470.

Muir, D., Varon, S., and Manthorpe, M. 1990. An enzyme-linked immunosorbent assay for bromodeoxyuridine incorporation using fixed microcultures. Analytical Biochemistry, 185, (2) 377-382.

Muller, C. Y. 2010. Doctor, should I get this new ovarian cancer test-OVA1? Obstetrics Gynecology, 116, (2 Pt 1) 246-247.

Murphy, C. G. and Moynahan, M. E. 2010. BRCA gene structure and function in tumor suppression: a repair-centric perspective. Cancer Journal (Sudbury, Mass.), 16, (1) 39-47.

Murphy, M. A. and Wentzensen, N. 2011. Frequency of mismatch repair deficiency in ovarian cancer: a systematic review This article is a US Government work and, as such, is in

the public domain of the United States of America. International Journal of Cancer, 129, (8) 1914-1922.

Nakayama, K., Kanzaki, A., Ogawa, K., Miyazaki, K., Neamati, N., and Takebayashi, Y. 2002. Copper-transporting P-type adenosine triphosphatase (ATP7B) as a cisplatin based chemoresistance marker in ovarian carcinoma: comparative analysis with expression of MDR1, MRP1, MRP2, LRP and BCRP. International Journal of Cancer, 101, (5) 488-495.

Nakayama, K., Miyazaki, K., Kanzaki, A., Fukumoto, M., and Takebayashi, Y. 2001. Expression and cisplatin sensitivity of copper-transporting P-type adenosine triphosphatase (ATP7B) in human solid carcinoma cell lines. Oncology Reports, 8, (6) 1285-1287.

Nam, E. J., Yoon, H., Kim, S. W., Kim, H., Kim, Y. T., Kim, J. H., Kim, J. W., and Kim, S. 2008. MicroRNA Expression Profiles in Serous Ovarian Carcinoma. Clinical Cancer Research, 14, (9) 2690-2695.

Naniwa, J., Kigawa, J., Kanamori, Y., Itamochi, H., Oishi, T., Shimada, M., Shimogai, R., Kawaguchi, W., Sato, S., and Terakawa, N. 2007. Genetic diagnosis for chemosensitivity with drug-resistance genes in epithelial ovarian cancer. International Journal of Gynaecological Cancer, 17, (1) 76-82.

Nash, M. A., Ferrandina, G., Gordinier, M., Loercher, A., and Freedman, R. S. 1999. The role of cytokines in both the normal and malignant ovary. Endocrine-Related Cancer, 6, (1) 93-107.

National Cancer Institute. 2014. Ovarian Cancer. http://www.cancer.gov.

Nishimura, M., Jung, E. J., Shah, M. Y., Lu, C., Spizzo, R., Shimizu, M., Han, H. D., Ivan, C., Rossi, S., Zhang, X., Nicoloso, M. S., Wu, S. Y., Almeida, M. I., Bottsford-Miller, J., Pecot, C. V., Zand, B., Matsuo, K., Shahzad, M. M., Jennings, N. B., Rodriguez-Aguayo, C., Lopez-Berestein, G., Sood, A. K., and Calin, G. A. 2013. Therapeutic Synergy between microRNA and siRNA in Ovarian Cancer Treatment. Cancer Discovery, 3, (11) 1302-1315.

Nishizuka, S., Chen, S. T., Gwadry, F. G., Alexander, J., Major, S. M., Scherf, U., Reinhold, W. C., Waltham, M., Charboneau, L., Young, L., Bussey, K. J., Kim, S., Lababidi, S., Lee, J. K., Pittaluga, S., Scudiero, D. A., Sausville, E. A., Munson, P. J., Petricoin, E. F., Liotta, L. A., Hewitt, S. M., Raffeld, M., and Weinstein, J. N. 2003. Diagnostic Markers That Distinguish Colon and Ovarian Adenocarcinomas: Identification by Genomic, Proteomic, and Tissue Array Profiling. Cancer Research, 63, (17) 5243-5250.

Nogales, E. 2001. Structural Insights Into Microtubule Function. Annual Review of Biophysics and Biomolecular Structure, 30, (1) 397-420.

Norquist, B., Wurz, K. A., Pennil, C. C., Garcia, R., Gross, J., Sakai, W., Karlan, B. Y., Taniguchi, T., and Swisher, E. M. 2011. Secondary Somatic Mutations Restoring BRCA1/2 Predict Chemotherapy Resistance in Hereditary Ovarian Carcinomas. Journal of Clinical Oncology, 29, (22) 3008-3015.

Northcott, P. A., Korshunov, A., Witt, H., Hielscher, T., Eberhart, C. G., Mack, S., Bouffet, E., Clifford, S. C., Hawkins, C. E., French, P., Rutka, J. T., Pfister, S., and Taylor, M. D. 2011. Medulloblastoma Comprises Four Distinct Molecular Variants. Journal of Clinical Oncology, 29, (11) 1408-1414.

Nowak, M., Glowacka, E., Szpakowski, M., Szyllo, K., Malinowski, A., Kulig, A., Tchorzewski, H., and Wilczynski, J. 2010. Proinflammatory and immunosuppressive serum, ascites and cyst fluid cytokines in patients with early and advanced ovarian cancer and benign ovarian tumors. Neuro Endocrinology Letters, 31, (3) 375-383.

O' Driscoll, L., Walsh, N., Larkin, A., Ballot, J., Ooi, W. S., Gullo, G., O'Connor, R., Clynes, M., Crown, J., and Kennedy, S. 2007. MDR1/P-glycoprotein and MRP-1 drug efflux pumps in pancreatic carcinoma. Anticancer Research, 27, (4B) 2115-2120.

O'Brien, J., Wilson, I., Orton, T., and Pognan, F. 2000. Investigation of the Alamar Blue (resazurin) fluorescent dye for the assessment of mammalian cell cytotoxicity. European Journal of Biochemistry, 267, (17) 5421-5426.

O'Connor, R. 2007. The Pharmacology of Cancer Resistance. Anticancer Research, 27, (3A) 1267-1272.

Oberlies, N. H. and Kroll, D. J. 2004. Camptothecin and Taxol: Historic Achievements in Natural Products Research. Journal of Natural Products, 67, (2) 129-135.

Oguri, S., Sakakibara, T., Mase, H., Shimizu, T., Ishikawa, K., Kimura, K., and Smyth, R. D. 1988. Clinical pharmacokinetics of carboplatin. The Journal of Clinical Pharmacology, 28, (3) 208-215.

Ohishi, Y., Oda, Y., Basaki, Y., Kobayashi, H., Wake, N., Kuwano, M., and Tsuneyoshi, M. 2007. Expression of beta-tubulin isotypes in human primary ovarian carcinoma. Gynecologic Oncology, 105, (3) 586-592.

Ohta, S., Nishio, K., Kubota, N., Ohmori, T., Funayama, Y., Ohira, T., Nakajima, H., Adachi, M., and Saijo, N. 1994. Characterization of a taxol-resistant human small-cell lung cancer cell line. Japanese Journal of Cancer Research: Gann, 85, (3) 290-297.

Okuma, E., Ohishi, Y., Oda, Y., Aishima, S., Kurihara, S., Nishimura, I., Yasunaga, M., Kobayashi, H., Wake, N., and Tsuneyoshi, M. 2010. Cytoplasmic and stromal expression of laminin gamma 2 chain correlates with infiltrative invasion in ovarian mucinous neoplasms of gastro-intestinal type. Oncology Reports, 24, (6) 1569-1576.

Oliveros, J. C. 2007. VENNY. An interactive tool for comparing lists with Venn Diagrams. http://bioinfogp.cnb.csic.es/tools/venny/index.html.

Osmak, M., Bizjak, L., Jernej, B., and Kapitanovi-ç, S. 1995. Characterization of carboplatin-resistant sublines derived from human larynx carcinoma cells. Mutation Research Letters, 347, (3–4) 141-150.

Outwater, E. K., Wagner, B. J., Mannion, C., McLarney, J. K., and Kim, B. 1998. Sex cord-stromal and steroid cell tumors of the ovary. RadioGraphics, 18, (6) 1523-1546.

Ozols, R. F. 2005. Treatment goals in ovarian cancer. International Journal of Gynecological Cancer, 15, 3-11.

Ozols, R. F., Bundy, B. N., Greer, B. E., Fowler, J. M., Clarke-Pearson, D., Burger, R. A., Mannel, R. S., DeGeest, K., Hartenbach, E. M., and Baergen, R. 2003. Phase III Trial of Carboplatin and Paclitaxel Compared With Cisplatin and Paclitaxel in Patients With Optimally Resected Stage III Ovarian Cancer: A Gynecologic Oncology Group Study. Journal of Clinical Oncology, 21, (17) 3194-3200.

Pal, T., Permuth-Wey, J., Betts, J. A., Krischer, J. P., Fiorica, J., Arango, H., LaPolla, J., Hoffman, M., Martino, M. A., Wakeley, K., Wilbanks, G., Nicosia, S., Cantor, A., and Sutphen, R. 2005. BRCA1 and BRCA2 mutations account for a large proportion of ovarian carcinoma cases. Cancer, 104, (12) 2807-2816.

Panday, V., Huinink, W., Vermorken, J. B., Rosing, H., Koopman, F. J., Swart, M., Schellens, J. H. M., and Beijnen, J. H. 1999. Pharmacokinetics of paclitaxel administered as a 3-hour or 96-hour infusion. Pharmacological Research, 40, (1) 67-74.

Panupinthu, N., Yu, S., Zhang, D., Zhang, F., Gagea, M., Lu, Y., Grandis, J. R., Dunn, S. E., Lee, H. Y., and Mills, G. B. 2014. Self-reinforcing loop of amphiregulin and Y-box binding protein-1 contributes to poor outcomes in ovarian cancer. Oncogene, 33, (22) 2846-2856.

Papanastasiou, A. D., Pampalakis, G., Katsaros, D., and Sotiropoulou, G. 2011. Netrin-1 overexpression is predictive of ovarian malignancies. Oncotarget, 2, (5)

Parekh, H., Wiesen, K., and Simpkins, H. 1997a. Acquisition of taxol resistance via P-glycoprotein- and non-P-glycoprotein-mediated mechanisms in human ovarian carcinoma cells. Biochemical Pharmacology, 53, (4) 461-470.

Parekh, H., Wiesen, K., and Simpkins, H. 1997b. Acquisition of taxol resistance via P-glycoprotein- and non-P-glycoprotein-mediated mechanisms in human ovarian carcinoma cells. Biochemical Pharmacology, 53, (4) 461-470.

Parikh, A., Lee, C., Joseph, P., Marchini, S., Baccarini, A., Kolev, V., Romualdi, C., Fruscio, R., Shah, H., Wang, F., Mullokandov, G., Fishman, D., D'Incalci, M., Rahaman, J., Kalir, T., Redline, R. W., Brown, B. D., Narla, G., and DiFeo, A. 2014. microRNA-181a has a critical role in ovarian cancer progression through the regulation of the epithelial–to–mesenchymal transition. Nature Communications, 5,

Pasalich, M., Su, D., Binns, C. W., and Lee, A. H. 2013. Reproductive factors for ovarian cancer in southern Chinese women. Journal of Gynecological Oncology, 24, (2) 135-140.

Pasetto, L. M., D'Andrea, M. R., Brandes, A. A., Rossi, E., and Monfardini, S. 2006. The development of platinum compounds and their possible combination. Critical reviews in oncology/hematology, 60, (1) 59-75.

Pasquinelli, A. E., Reinhart, B. J., Slack, F., Martindale, M. Q., Kuroda, M. I., Maller, B., Hayward, D. C., Ball, E. E., Degnan, B., Muller, P., Spring, J., Srinivasan, A., Fishman, M., Finnerty, J., Corbo, J., Levine, M., Leahy, P., Davidson, E., and Ruvkun, G. 2000. Conservation of the sequence and temporal expression of let-7 heterochronic regulatory RNA. Nature, 408, (6808) 86-89.

Pathania, S., Nguyen, J., Hill, S., Scully, R., Adelmant, G., Marto, J., Feunteun, J., and Livingston, D. 2011. BRCA1 Is Required for Postreplication Repair after UV-Induced DNA Damage. Molecular cell, 44, (2) 235-251.

Paulusma, C. C., van Geer, M. A., Evers, R., Heijn, M., Ottenhoff, R., Borst, P., and Oude Elferink, R. P. 1999. Canalicular multispecific organic anion transporter/multidrug resistance protein 2 mediates low-affinity transport of reduced glutathione. The Biochemical Journal, 338 (Pt 2), 393-401.

Peleg-Shulman, T. and Gibson, D. 2001. Cisplatin-protein adducts are efficiently removed by glutathione but not by 5'-guanosine monophosphate. Journal of the American Chemical Society, 123, (13) 3171-3172.

Peng, C., Zhang, X., Yu, H., Wu, D., and Zheng, J. 2011. Wnt5a as a predictor in poor clinical outcome of patients and a mediator in chemoresistance of ovarian cancer. International Journal of Gynaecological Cancer, 21, (2) 280-288.

Pennington, K., Pulaski, H., Pennington, M., and Liu, J. R. 2010. Too much of a good thing: suicide prevention promotes chemoresistance in ovarian carcinoma. Current Cancer Drug Targets, 10, (6) 575-583.

Penson, R. T., Kronish, K., Duan, Z., Feller, A. J., Stark, P., Cook, S. E., Duska, L. R., Fuller, A. F., Goodman, A. K., Nikrui, N., MacNeill, K. M., Matulonis, U. A., Preffer, F. I., and Seiden, M. V. 2000. Cytokines IL-1beta, IL-2, IL-6, IL-8, MCP-1, GM-CSF and

TNFalpha in patients with epithelial ovarian cancer and their relationship to treatment with paclitaxel. International Journal of Gynaecological Cancer, 10, (1) 33-41.

Penson, R. T., Oliva, E., Skates, S. J., Glyptis, T., Fuller, J., Goodman, A., and Seiden, M. V. 2004. Expression of multidrug resistance-1 protein inversely correlates with paclitaxel response and survival in ovarian cancer patients: a study in serial samples. Gynecologic Oncology, 93, (1) 98-106.

Perou, C. M., Sorlie, T., Eisen, M. B., van de Rijn, M., Jeffrey, S. S., Rees, C. A., Pollack, J. R., Ross, D. T., Johnsen, H., Akslen, L. A., Fluge, O., Pergamenschikov, A., Williams, C., Zhu, S. X., Lonning, P. E., Borresen-Dale, A. L., Brown, P. O., and Botstein, D. 2000. Molecular portraits of human breast tumours. Nature, 406, (6797) 747-752.

Perren, T. J., Swart, A. M., Pfisterer, J., Ledermann, J. A., Pujade-Lauraine, E., Kristensen, G., Carey, M. S., Beale, P., Cervantes, A. s., Kurzeder, C., Bois, A. d., Sehouli, J., Kimmig, R., St+ñhle, A., Collinson, F., Essapen, S., Gourley, C., Lortholary, A., Selle, F. d. r., Mirza, M. R., Leminen, A., Plante, M., Stark, D., Qian, W., Parmar, M. K. B., and Oza, A. M. 2011. A Phase 3 Trial of Bevacizumab in Ovarian Cancer. New England Journal of Medicine, 365, (26) 2484-2496.

Pfisterer, J. and Ledermann, J. A. 2006a. Management of platinum-sensitive recurrent ovarian cancer. Seminars In Oncology, 33, (2 Suppl 6) S12-S16.

Pfisterer, J., Plante, M., Vergote, I., du Bois, A., Hirte, H., Lacave, A. J., Wagner, U., Stahle, A., Stuart, G., Kimmig, R., Olbricht, S., Le, T., Emerich, J., Kuhn, W., Bentley, J., Jackisch, C., Luck, H. J., Rochon, J., Zimmermann, A. H., and Eisenhauer, E. 2006b. Gemcitabine Plus Carboplatin Compared With Carboplatin in Patients With Platinum-Sensitive Recurrent Ovarian Cancer: An Intergroup Trial of the AGO-OVAR, the NCIC CTG, and the EORTC GCG. Journal of Clinical Oncology, 24, (29) 4699-4707.

Piccart, M. J., Lamb, H., and Vermorken, J. B. 2001. Current and future potential roles of the platinum drugs in the treatment of ovarian cancer. Annals of Oncology, 12, (9) 1195-1203.

Piccart, M. J., Bertelsen, K., James, K., Cassidy, J., Mangioni, C., Simonsen, E., Stuart, G., Kaye, S., Vergote, I., Blom, R., Grimshaw, R., Atkinson, R. J., Swenerton, K. D., Trope, C., Nardi, M., Kaern, J., Tumolo, S., Timmers, P., Roy, J. A., Lhoas, F., Lindvall, B., Bacon, M., Birt, A., Andersen, J. E., Zee, B., Paul, J., Baron, B., and Pecorelli, S. 2000. Randomized Intergroup Trial of Cisplatin–Paclitaxel Versus Cisplatin–Cyclophosphamide in Women With Advanced Epithelial Ovarian Cancer: Three-Year Results. Journal of the National Cancer Institute, 92, (9) 699-708.

Piek, J. M. J., van Diest, P. J., Zweemer, R. P., Jansen, J. W., Poort-Keesom, R. J. J., Menko, F. H., Gille, J. J. P., Jongsma, A. P. M., Pals, G., Kenemans, P., and Verheijen, R. H. M. 2001. Dysplastic changes in prophylactically removed Fallopian tubes of women predisposed to developing ovarian cancer. The Journal of Pathology, 195, (4) 451-456.

Piek, J. M. J., Verheijen, R. H. M., Kenemans, P., Massuger, L. F., Bulten, H., and van Diest, P. J. 2003. BRCA1/2-related ovarian cancers are of tubal origin: a hypothesis. Gynecologic Oncology, 90, (2)

Pil, P. M. and Lippard, S. J. 1992. Specific binding of chromosomal protein HMG1 to DNA damaged by the anticancer drug cisplatin. Science, 256, (5054) 234-237.

Plummer, R., Stephens, P., Aissat-Daudigny, L., Cambois, A., Moachon, G., Brown, P. D., and Campone, M. 2014. Phase 1 dose-escalation study of the PARP inhibitor CEP-9722 as monotherapy or in combination with temozolomide in patients with solid tumors. Cancer Chemotherapy and Pharmacology, 74, (2) 257-265.

Prislei, S., Martinelli, E., Mariani, M., Raspaglio, G., Sieber, S., Ferrandina, G., Shahabi, S., Scambia, G., and Ferlini, C. 2013. MiR-200c and HuR in ovarian cancer. BMC Cancer, 13, 72-72.

Pritchard, C. C., Cheng, H. H., and Tewari, M. 2012. MicroRNA profiling: approaches and considerations. Nature Reviews Genetics, 13, (5) 358-369.

Przybycin, C. G., Kurman, R. J., Ronnett, B. M., Shih, I., and Vang, R. 2010. Are all pelvic (nonuterine) serous carcinomas of tubal origin? The American Journal of Surgical Pathology, 34, (10) 1407-1416.

Qiu, H., Zhu, J., Yu, J., Pu, H., and Dong, R. 2011. SLIT2 is epigenetically silenced in ovarian cancers and suppresses growth when activated. Asian Pacific Journal of Cancer Prevention, 12, (3) 791-795.

Qiu, J. j., Lin, Y. y., Ye, L. c., Ding, J. x., Feng, W. w., Jin, H. y., Zhang, Y., Li, Q., and Hua, K. q. 2014. Overexpression of long non-coding RNA HOTAIR predicts poor patient prognosis and promotes tumor metastasis in epithelial ovarian cancer. Gynecologic Oncology, 134, (1) 121-128.

Qiu, S., Lin, S., Hu, D., Feng, Y., Tan, Y., and Peng, Y. 2013. Interactions of miR-323/miR-326/miR-329 and miR-130a/miR-155/miR-210 as prognostic indicators for clinical outcome of glioblastoma patients. Journal of Translational Medicine, 11, 10-10.

Quinn, J. E., James, C. R., Stewart, G. E., Mulligan, J. M., White, P., Chang, G. K. F., Mullan, P. B., Johnston, P. G., Wilson, R. H., and Harkin, D. P. 2007. BRCA1 mRNA Expression Levels Predict for Overall Survival in Ovarian Cancer after Chemotherapy. Clinical Cancer Research, 13, (24) 7413-7420.

Rabik, C. A. and Dolan, M. E. 2007. Molecular mechanisms of resistance and toxicity associated with platinating agents. Cancer Treatment Reviews, 33, (1) 9-23.

Rachidi, S. M., Qin, T., Sun, S., Zheng, W. J., and Li, Z. 2013. Molecular profiling of multiple human cancers defines an inflammatory cancer-associated molecular pattern and uncovers KPNA2 as a uniform poor prognostic cancer marker. PLoS ONE, 8, (3) e57911-e57911.

Rakovitch, E., Mellado, W., Hall, E. J., Pandita, T. K., Sawant, S., and Geard, C. R. 1999. Paclitaxel sensitivity correlates with P53 status and DNA fragmentation, but not G2/M accumulation. International Journal of Radiation Oncology*Biology*Physics, 44, (5) 1119-1124.

Ramachandra, M., Ambudkar, S. V., Chen, D., Hrycyna, C. A., Dey, S., Gottesman, M. M., and Pastan, I. 1998. Human P-Glycoprotein Exhibits Reduced Affinity for Substrates during a Catalytic Transition State. Biochemistry, 37, (14) 5010-5019.

Rao, S., Orr, G. A., Chaudhary, A. G., Kingston, D. G. I., and Horwitz, S. B. 1995. Characterization of the Taxol Binding Site on the Microtubule. Journal of Biological Chemistry, 270, (35) 20235-20238.

Rappa, G., Gamcsik, M. P., Mitina, R. L., Baum, C., Fodstad, O., and Lorico, A. 2003. Retroviral transfer of MRP1 and gamma-glutamyl cysteine synthetase modulates cell sensitivity to L-buthionine-S,R-sulphoximine (BSO): new rationale for the use of BSO in cancer therapy. European Journal of Cancer, 39, (1) 120-128.

Raymond, E., Chaney, S. G., Taamma, A., and Cvitkovic, E. 1998. Oxaliplatin: A review of preclinical and clinical studies. Annals of Oncology, 9, (10) 1053-1071.

Reed, J. C. 1995. Bcl-2 family proteins: regulators of chemoresistance in cancer. Toxicology Letters, 82–83, 155-158.

Reedijk J. 1987. The mechanism of action of platinum anti-tumor drugs. Pure and Applicable chemistry, 59, (2) 181-192.

Rein, B. J., Gupta, S., Dada, R., Safi, J., Michener, C., and Agarwal, A. 2011. Potential markers for detection and monitoring of ovarian cancer. Journal of Oncology, 2011, 475983-475983.

Reinecke, P., Schmitz, M., Schneider, E. M., Gabbert, H. E., and Gerharz, C. D. 2000. Multidrug resistance phenotype and paclitaxel (Taxol) sensitivity in human renal carcinoma cell lines of different histologic types. Cancer Investigation, 18, (7) 614-625.

Reis, S. T., Timoszczuk, L. S., Pontes-Junior, J., Viana, N., Silva, I. A., Dip, N., Srougi, M., and Leite, K. R. 2013. The role of micro RNAs let7c, 100 and 218 expression and their target RAS, C-MYC, BUB1, RB, SMARCA5, LAMB3 and Ki-67 in prostate cancer. Clinics (Sao Paulo), 68, (5) 652-657.

Renault, M. A., Roncalli, J. +., Tongers, J. +., Misener, S., Thorne, T., Jujo, K., Ito, A., Clarke, T., Fung, C., Millay, M., Kamide, C., Scarpelli, A., Klyachko, E., and Losordo, D. W. 2009. The Hedgehog Transcription Factor Gli3 Modulates Angiogenesis. Circulation Research, 105, (8) 818-826.

Resnick, K. E., Alder, H., Hagan, J. P., Richardson, D. L., Croce, C. M., and Cohn, D. E. 2009. The detection of differentially expressed microRNAs from the serum of ovarian cancer patients using a novel real-time PCR platform. Gynecologic Oncology, 112, (1) 55-59.

Ribble, D., Goldstein, N. B., Norris, D. A., and Shellman, Y. G. 2005. A simple technique for quantifying apoptosis in 96-well plates. BMC Biotechnology, 5, (12)

Rice, J. C., Ozcelik, H., Maxeiner, P., Andrulis, I., and Futscher, B. W. 2000. Methylation of the BRCA1 promoter is associated with decreased BRCA1 mRNA levels in clinical breast cancer specimens. Carcinogenesis, 21, (9) 1761-1765.

Righetti, S. C., Torre, G. D., Pilotti, S., Menard, S., Ottone, F., Colnaghi, M. I., Pierotti, M. A., Lavarino, C., Cornarotti, M., Oriana, S., Bohm, S., Bresciani, G. L., Spatti, G., and Zunino, F. 1996. A Comparative Study of p53 Gene Mutations, Protein Accumulation, and Response to Cisplatin-based Chemotherapy in Advanced Ovarian Carcinoma. Cancer Research, 56, (4) 689-693.

Riman, T., Dickman, P. W., Nilsson, S., Correia, N., Nordlinder, H., Magnusson, C. M., and Persson, I. R. 2002. Risk Factors for Invasive Epithelial Ovarian Cancer: Results from a Swedish Case-Control Study. American Journal of Epidemiology, 156, (4) 363-373.

Riman, T., Nilsson, S., and Persson, I. R. 2004. Review of epidemiological evidence for reproductive and hormonal factors in relation to the risk of epithelial ovarian malignancies. Acta Obstetricia et Gynecologica Scandinavica, 83, (9) 783-795.

Risch, H. A. 1998. Hormonal Etiology of Epithelial Ovarian Cancer, With a Hypothesis Concerning the Role of Androgens and Progesterone. Journal of the National Cancer Institute, 90, (23) 1774-1786.

Risch, H. A., McLaughlin, J. R., Cole, D. E. C., Rosen, B., Bradley, L., Kwan, E., Jack, E., Vesprini, D. J., Kuperstein, G., Abrahamson, J. L. A., Fan, I., Wong, B., and Narod, S. A. 2001. Prevalence and Penetrance of Germline BRCA1 and BRCA2 Mutations in a Population Series of 649 Women with Ovarian Cancer. The American Journal of Human Genetics, 68, (3) 700-710.

Roberts, D., Schick, J., Conway, S., Biade, S., Laub, P. B., Stevenson, J. P., Hamilton, T. C., O'Dwyer, P. J., and Johnson, S. W. 2005. Identification of genes associated with platinum drug sensitivity and resistance in human ovarian cancer cells. British Journal of Cancer, 92, (6) 1149-1158.

Roberts, D., Wodinsky, I., and Hall, T. C. 1965. Studies on Folic Reductase. Cancer Research, 25, (11 Part 1) 1899-1903.

Rodrigues, F. F., Santos, R. E., Melo, M. B., Silva, M. A., Oliveira, A. L., Rozenowicz, R. L., Ulson, L. B., and Aoki, T. 2008. Correlation of polymorphism C3435T of the MDR-1 gene and the response of primary chemotherapy in women with locally advanced breast cancer. Genetics and Molecular Research, 7, (1) 177-183.

Rodriguez, A., Griffiths-Jones, S., Ashurst, J. L., and Bradley, A. 2004. Identification of Mammalian microRNA Host Genes and Transcription Units. Genome Research, 14, (10a) 1902-1910.

Romero, I. and Bast, R. C., Jr. 2012. Minireview: human ovarian cancer: biology, current management, and paths to personalizing therapy. Endocrinology, 153, (4) 1593-1602.

Rosenberg, B., Renshaw, E., Vancamp, L., Hartwick, J., and Drobnik, J. 1967. Platinum-Induced Filamentous Growth in Escherichia coli. The Journal of Bacteriology, 93, (2) 716-721.

Rosenberg, L., Palmer, J. R., Zauber, A. G., Warshauer, M. E., Lewis, J. L., Strom, B. L., Harlap, S., and Shapiro, S. 1994. A Case-Control Study of Oral Contraceptive Use and Invasive Epithelial Ovarian Cancer. American Journal of Epidemiology, 139, (7) 654-661.

Rowinsky, E. K. 1997. The development and clinical utility of the taxane class of antimicrotubule chemotherapy agents. Annual Review of Medicine, 48, 353-374.

Roy, S., Kenny, E., Kennedy, S., Larkin, A., Ballot, J., Perez, D., V, Crown, J., and O'Driscoll, L. 2007. MDR1/P-glycoprotein and MRP-1 mRNA and protein expression in non-small cell lung cancer. Anticancer Research, 27, (3A) 1325-1330.

Rubie, C., Frick, V. O., Ghadjar, P., Wagner, M., Justinger, C., Graeber, S., Sperling, J., Kollmar, O., and Schilling, M. K. 2011. Effect of preoperative FOLFOX chemotherapy on CCL20/CCR6 expression in colorectal liver metastases. World Journal of Gastroenterology, 17, (26) 3109-3116.

Rubin, S. C., Blackwood, M. A., Bandera, C., Behbakht, K., Benjamin, I., Rebbeck, T. R., and Boyd, J. 1998. BRCA1, BRCA2, and hereditary nonpolyposis colorectal cancer gene mutations in an unselected ovarian cancer population: relationship to family history and implications for genetic testing. American Journal of Obstetrics and Gynecology, 178, (4) 670-677.

Rustin, G. J., Nelstrop, A. E., McClean, P., Brady, M. F., McGuire, W. P., Hoskins, W. J., Mitchell, H., and Lambert, H. E. 1996. Defining response of ovarian carcinoma to initial chemotherapy according to serum CA 125. Journal of Clinical Oncology, 14, (5) 1545-1551.

Rustin, G. J. S., Bast, R. C., Kelloff, G. J., Barrett, J. C., Carter, S. K., Nisen, P. D., Sigman, C. C., Parkinson, D. R., and Ruddon, R. W. 2004. Use of CA-125 in Clinical Trial Evaluation of New Therapeutic Drugs for Ovarian Cancer. Clinical Cancer Research, 10, (11) 3919-3926.

Rutledge, M. L., Robey-Cafferty, S. S., Silva, E. G., and Bruner, J. M. 1990. Monoclonal antibody C219 detection of the multidrug-resistant protein P-glycoprotein in routinely processed tissues: a study of 36 cases of ovarian carcinoma. Modern Pathology, 3, (3) 298-301.

Rybak, A., Fuchs, H., Smirnova, L., Brandt, C., Pohl, E. E., Nitsch, R., and Wulczyn, F. G. 2008. A feedback loop comprising lin-28 and let-7 controls pre-let-7 maturation during neural stem-cell commitment. Nature Cell Biology, 10, (8) 987-993.

Safaei, R. and Howell, S. B. 2005. Copper transporters regulate the cellular pharmacology and sensitivity to Pt drugs. Critical reviews in oncology/hematology, 53, (1) 13-23.

Saini, H. K., Griffiths-Jones, S., and Enright, A. J. 2007. Genomic analysis of human microRNA transcripts. Proceedings of the National Academy of Science of the U.S.A., 104, (45) 17719-17724.

Sakai, T., Toguchida, J., Ohtani, N., Yandell, D. W., Rapaport, J. M., and Dryja, T. P. 1991. Allele-specific hypermethylation of the retinoblastoma tumor-suppressor gene. American Journal of Human Genetics, 48, (5) 880-888.

Sakai, W., Swisher, E. M., Jacquemont, C. +., Chandramohan, K. V., Couch, F. J., Langdon, S. P., Wurz, K., Higgins, J., Villegas, E., and Taniguchi, T. 2009. Functional Restoration of BRCA2 Protein by Secondary BRCA2 Mutations in BRCA2-Mutated Ovarian Carcinoma. Cancer Research, 69, (16) 6381-6386.

Sakai, W., Swisher, E. M., Karlan, B. Y., Agarwal, M. K., Higgins, J., Friedman, C., Villegas, E., Jacquemont, C., Farrugia, D. J., Couch, F. J., Urban, N., and Taniguchi, T. 2008. Secondary mutations as a mechanism of cisplatin resistance in BRCA2-mutated cancers. Nature, 451, (7182) 1116-1120.

Sakamoto, M., Kondo, A., Kawasaki, K., Goto, T., Sakamoto, H., Miyake, K., Koyamatsu, Y., Akiya, T., Iwabuchi, H., Muroya, T., Ochiai, K., Tanaka, T., Kikuchi, Y., and Tenjin, Y. 2001. Analysis of gene expression profiles associated with cisplatin resistance in human ovarian cancer cell lines and tissues using cDNA microarray. Human Cell, 14, (4) 305-315.

Salehi, F., Dunfield, L., Phillips, K. P., Krewski, D., and Vanderhyden, B. C. 2008. Risk Factors for Ovarian Cancer: An Overview with Emphasis on Hormonal Factors. Journal of Toxicology and Environmental Health, Part B, 11, (3-4) 301-321.

Salzberg, M., Thurlimann, B., Bonnefois, H., Fink, D., Rochlitz, C., von, M. R., and Senn, H. 2005. Current concepts of treatment strategies in advanced or recurrent ovarian cancer. Oncology, 68, (4-6) 293-298.

Samimi, G., Fink, D., Varki, N. M., Husain, A., Hoskins, W. J., Alberts, D. S., and Howell, S. B. 2000. Analysis of MLH1 and MSH2 Expression in Ovarian Cancer before and after Platinum Drug-based Chemotherapy. Clinical Cancer Research, 6, (4) 1415-1421.

Samimi, G., Safaei, R., Katano, K., Holzer, A. K., Rochdi, M., Tomioka, M., Goodman, M., and Howell, S. B. 2004. Increased Expression of the Copper Efflux Transporter ATP7A Mediates Resistance to Cisplatin, Carboplatin, and Oxaliplatin in Ovarian Cancer Cells. Clinical Cancer Research, 10, (14) 4661-4669.

Sancar, A. 1996. DNA Excision Repair. Annual Review of Biochemistry, 65, (1) 43-81.

Sancar, A., Lindsey-Boltz, L. A., Unsal-Kacmaz, K., and Linn, S. 2004. Molecular mechanisms of mammalian DNA repair and the DNA damage checkpoints. Annual Review of Biochemistry, 73, 39-85.

Sand, M., Skrygan, M., Georgas, D., Sand, D., Hahn, S. A., Gambichler, T., Altmeyer, P., and Bechara, F. G. 2012. Microarray analysis of microRNA expression in cutaneous squamous cell carcinoma. Journal of Dermatological Science, 68, (3) 119-126.

Sauna, Z. E. and Ambudkar, S. V. 2000. Evidence for a requirement for ATP hydrolysis at two distinct steps during a single turnover of the catalytic cycle of human P-glycoprotein. Proceedings of the National Academy of Sciences, 97, (6) 2515-2520.

Savic, V., Yin, B., Maas, N. L., Bredemeyer, A. L., Carpenter, A. C., Helmink, B. A., Yang-Iott, K. S., Sleckman, B. P., and Bassing, C. H. 2009. Formation of Dynamic ¦-H2AX

Domains along Broken DNA Strands Is Distinctly Regulated by ATM and MDC1 and Dependent upon H2AX Densities in Chromatin. Molecular cell, 34, (3) 298-310.

Sawan, C. and Herceg, Z. 2010. Histone Modifications and Cancer. Volume 70, (3) 57-85.

Scalici, J. M., Thomas, S., Harrer, C., Raines, T. A., Curran, J., Atkins, K. A., Conaway, M. R., Duska, L., Kelly, K. A., and Slack-Davis, J. K. 2013. Imaging VCAM-1 as an Indicator of Treatment Efficacy in Metastatic Ovarian Cancer. Journal of Nuclear Medicine, 54, (11) 1883-1889.

Schena, M., Shalon, D., Davis, R. W., and Brown, P. O. 1995. Quantitative monitoring of gene expression patterns with a complementary DNA microarray. Science, 270, (5235) 467-470.

Schilder, R. J., Hall, L., Monks, A., Handel, L. M., Fornace, A. J., Jr., Ozols, R. F., Fojo, A. T., and Hamilton, T. C. 1990. Metallothionein gene expression and resistance to cisplatin in human ovarian cancer. International Journal of Cancer, 45, (3) 416-422.

Schildkraut, J. M., Schwingl, P. J., Bastos, E., Evanoff, A., and Hughes, C. 1996. Epithelial ovarian cancer risk among women with polycystic ovary syndrome. Obstetrics Gynecology, 88, (4 Pt 1) 554-559.

Schinkel, A. H., Mayer, U., Wagenaar, E., Mol, C. A., van, D. L., Smit, J. J., van der Valk, M. A., Voordouw, A. C., Spits, H., van, T. O., Zijlmans, J. M., Fibbe, W. E., and Borst, P. 1997. Normal viability and altered pharmacokinetics in mice lacking mdr1-type (drug-transporting) P-glycoproteins. Proceedings of the National Academy of Science of the U.S.A., 94, (8) 4028-4033.

Schittenhelm, J., Schwab, E. I., Sperveslage, J., Tatagiba, M., Meyermann, R., Fend, F., Goodman, S. L., and Sipos, B. 2013. Longitudinal expression analysis of alphav integrins in human gliomas reveals upregulation of integrin alphavbeta3 as a negative prognostic factor. Journal of Neuropathology & Experimental Neurology, 72, (3) 194-210.

Schneider, C. A., Rasband, W. S., and Eliceiri, K. W. 2012. NIH Image to ImageJ: 25 years of image analysis. Nature Methods, 9, (7) 671-675.

Schondorf, T., Kurbacher, C. M., Gohring, U. J., Benz, C., Becker, M., Sartorius, J., Kolhagen, H., Mallman, P., and Neumann, R. 2002. Induction of MDR1-gene expression by antineoplastic agents in ovarian cancer cell lines. Anticancer Research, 22, (4) 2199-2203.

Schouten, L. J., Rivera, C., Hunter, D. J., Spiegelman, D., Adami, H. O., Arslan, A., Beeson, W. L., van den Brandt, P. A., Buring, J. E., Folsom, A. R., Fraser, G. E., Freudenheim, J. L., Goldbohm, R. A., Hankinson, S. E., Lacey, J. V., Leitzmann, M., Lukanova, A., Marshall, J. R., Miller, A. B., Patel, A. V., Rodriguez, C., Rohan, T. E., Ross, J. A., Wolk, A., Zhang, S. M., and Smith-Warner, S. A. 2008. Height, Body Mass Index, and Ovarian Cancer: A Pooled Analysis of 12 Cohort Studies. Cancer Epidemiology Biomarkers & Prevention, 17, (4) 902-912.

Schutyser, E., Struyf, S., Proost, P., Opdenakker, G., Laureys, G. v., Verhasselt, B., Peperstraete, L., Van de Putte, I., Saccani, A., Allavena, P., Mantovani, A., and Van Damme, J. 2002. Identification of Biologically Active Chemokine Isoforms from Ascitic Fluid and Elevated Levels of CCL18/Pulmonary and Activation-regulated Chemokine in Ovarian Carcinoma. Journal of Biological Chemistry, 277, (27) 24584-24593.

Schuyer, M., van der Burg, M. E., Henzen-Logmans, S. C., Fieret, J. H., Klijn, J. G., Look, M. P., Foekens, J. A., Stoter, G., and Berns, E. M. 2001. Reduced expression of BAX is associated with poor prognosis in patients with epithelial ovarian cancer: a multifactorial analysis of TP53, p21, BAX and BCL-2. British Journal of Cancer, 85, (9) 1359-1367.

Schwartz, D. R., Kardia, S. L. R., Shedden, K. A., Kuick, R., Michailidis, G., Taylor, J. M. G., Misek, D. E., Wu, R., Zhai, Y., Darrah, D. M., Reed, H., Ellenson, L. H., Giordano, T. J., Fearon, E. R., Hanash, S. M., and Cho, K. R. 2002. Gene Expression in Ovarian Cancer Reflects Both Morphology and Biological Behavior, Distinguishing Clear Cell from Other Poor-Prognosis Ovarian Carcinomas. Cancer Research, 62, (16) 4722-4729.

Sciff, P. B., Fant, J., and Horwitz, S. B. 1979. Promotion of microtubule assembly in vitro by taxol. Nature, 277, (5698) 665-667.

Selvakumaran, M., Pisarcik, D. A., Bao, R., Yeung, A. T., and Hamilton, T. C. 2003. Enhanced Cisplatin Cytotoxicity by Disturbing the Nucleotide Excision Repair Pathway in Ovarian Cancer Cell Lines. Cancer Research, 63, (6) 1311-1316.

Selvanayagam, Z. E., Cheung, T. H., Wei, N., Vittal, R., Kit Lo, K. W., Yeo, W., Kita, T., Ravatn, R., Hung Chung, T. K., Wong, Y. F., and Chin, K. V. 2004. Prediction of chemotherapeutic response in ovarian cancer with DNA microarray expression profiling. Cancer Genetics and Cytogenetics, 154, (1) 63-66.

Sengupta, A., Banerjee, D., Chandra, S., Banerji, S. K., Ghosh, R., Roy, R., and Banerjee, S. 2007. Deregulation and cross talk among Sonic hedgehog, Wnt, Hox and Notch signaling in chronic myeloid leukemia progression. Leukemia, 21, (5) 949-955.

Shah, P. P., Hutchinson, L. E., and Kakar, S. S. 2009. Emerging role of microRNAs in diagnosis and treatment of various diseases including ovarian cancer. Journal of Ovarian Research, 2, (1) 11-11.

Sharma, N., Ramachandran, S., Bowers, M., Yegappan, M., Brown, R., Aziz, S., Chapman, R., and Yu, B. W. 2000. Multiple factors other than p53 influence colon cancer sensitivity to paclitaxel. Cancer Chemotherapy and Pharmacology, 46, (4) 329-337.

Shaw, T. J. and Vanderhyden, B. C. 2007. AKT mediates the pro-survival effects of KIT in ovarian cancer cells and is a determinant of sensitivity to imatinib mesylate. Gynecologic Oncology, 105, (1) 122-131.

Shen, D. W., Akiyama, S., Schoenlein, P., Pastan, I., and Gottesman, M. M. 1995. Characterisation of high-level cisplatin-resistant cell lines established from a human hepatoma cell line and human KB adenocarcinoma cells: cross-resistance and protein changes. British Journal of Cancer, 71, (4) 676-683.

Sheng, X. J., Li, Z., Sun, M., Wang, Z. H., Zhou, D. M., Li, J. Q., Zhao, Q., Sun, X. F., and Liu, Q. C. 2014. MACC1 induces metastasis in ovarian carcinoma by upregulating hepatocyte growth factor receptor c-MET. Oncology Letters, 8, (2) 891-897.

Siddik, Z. H. 2003. Cisplatin: mode of cytotoxic action and molecular basis of resistance. Oncogene, 22, (47) 7265-7279.

Silasi, D. A., Alvero, A. B., Illuzzi, J., Kelly, M., Chen, R., Fu, H. H., Schwartz, P., Rutherford, T., Azodi, M., and Mor, G. 2006. MyD88 predicts chemoresistance to paclitaxel in epithelial ovarian cancer. The Yale Journal of Biological Medicine, 79, (3-4) 153-163.

Silver, D. P. and Livingston, D. M. 2012. Mechanisms of BRCA1 Tumor Suppression. Cancer Discovery, 2, (8) 679-684.

Singer, G., Kurman, R. J., Chang, H. W., Cho, S. K. R., and Shih, I. M. 2002. Diverse Tumorigenic Pathways in Ovarian Serous Carcinoma. The American Journal of Pathology, 160, (4) 1223-1228.

Skates, S. J., Menon, U., MacDonald, N., Rosenthal, A. N., Oram, D. H., Knapp, R. C., and Jacobs, I. J. 2003. Calculation of the Risk of Ovarian Cancer From Serial CA-125

Values for Preclinical Detection in Postmenopausal Women. Journal of Clinical Oncology, 21, (10 suppl) 206-210.

Skates, S. J., Pauler, D. K., and Jacobs, I. J. 2001. Screening Based on the Risk of Cancer Calculation From Bayesian Hierarchical Changepoint and Mixture Models of Longitudinal Markers. Journal of the American Statistical Association, 96, (454) 429-439.

Smith, V., Rowlands, M. G., Barrie, E., Workman, P., and Kelland, L. R. 2002. Establishment and Characterization of Acquired Resistance to the Farnesyl Protein Transferase Inhibitor R115777 in a Human Colon Cancer Cell Line. Clinical Cancer Research, 8, (6) 2002-2009.

Solar, P., Feldman, L., Jeong, J. Y., Busingye, J. R., and Sytkowski, A. J. 2008. Erythropoietin treatment of human ovarian cancer cells results in enhanced signaling and a paclitaxel-resistant phenotype. International Journal of Cancer, 122, (2) 281-288.

Son, D. S., Parl, A. K., Montgomery Rice, V., and Khabele, D. 2007. Keratinocyte chemoattractant (KC)/human growth-regulated oncogene (GRO) chemokines and pro-inflammatory chemokine networks in mouse and human ovarian epithelial cancer cells. Cancer Biology & Therapy, 6, (8) 1308-1318.

Song, I. S., Chen, H. H. W., Aiba, I., Hossain, A., Liang, Z. D., Klomp, L. W. J., and Kuo, M. T. 2008. Transcription Factor Sp1 Plays an Important Role in the Regulation of Copper Homeostasis in Mammalian Cells. Molecular Pharmacology, 74, (3) 705-713.

Sorrentino, A., Liu, C. G., Addario, A., Peschle, C., Scambia, G., and Ferlini, C. 2008. Role of microRNAs in drug-resistant ovarian cancer cells. Gynecologic Oncology, 111, (3) 478-486.

Soti, C., Racz, A., and Csermely, P. 2002. A Nucleotide-dependent Molecular Switch Controls ATP Binding at the C-terminal Domain of Hsp90. Journal of Biological Chemistry, 277, (9) 7066-7075.

Southern, E. M. 1975. Detection of specific sequences among DNA fragments separated by gel electrophoresis. Journal of Molecular Biology, 98, (3) 503-517.

Southern, E. M. 2001. DNA microarrays. History and overview. Methods in Molecalar Biology, 170, 1-15.

Spentzos, D., Levine, D. A., Kolia, S., Otu, H., Boyd, J., Libermann, T. A., and Cannistra, S. A. 2005. Unique gene expression profile based on pathologic response in epithelial ovarian cancer. Journal of Clinical Oncology, 23, (31) 7911-7918.

Spentzos, D., Levine, D. A., Ramoni, M. F., Joseph, M., Gu, X., Boyd, J., Libermann, T., and Cannistra, S. A. 2004. Gene Expression Signature With Independent Prognostic Significance in Epithelial Ovarian Cancer. Journal of Clinical Oncology, 22, (23) 4700-4710.

Steg, A., Wang, W., Blanquicett, C., Grunda, J. M., Eltoum, I. A., Wang, K., Buchsbaum, D. J., Vickers, S. M., Russo, S., Diasio, R. B., Frost, A. R., LoBuglio, A. F., Grizzle, W. E., and Johnson, M. R. 2006. Multiple Gene Expression Analyses in Paraffin-Embedded Tissues by TaqMan Low-Density Array. The Journal of Molecular Diagnostics, 8, (1) 76-83.

Steg, A. D., Katre, A. A., Bevis, K. S., Ziebarth, A., Dobbin, Z. C., Shah, M. M., Alvarez, R. D., and Landen, C. N. 2012. Smoothened Antagonists Reverse Taxane Resistance in Ovarian Cancer. Molecular Cancer Therapeutics, 11, (7) 1587-1597.

Stein, U., Walther, W., Arlt, F., Schwabe, H., Smith, J., Fichtner, I., Birchmeier, W., and Schlag, P. M. 2009. MACC1, a newly identified key regulator of HGF-MET signaling, predicts colon cancer metastasis. Nature Medicine, 15, (1) 59-67.

Stiekema, A., Lok, C. A. R., Kenter, G. G., van Driel, W. J., Vincent, A. D., and Korse, C. M. 2014. A predictive model combining human epididymal protein 4 and radiologic features for the diagnosis of ovarian cancer. Gynecologic Oncology, 132, (3) 573-577.

Stojic, L., Brun, R., and Jiricny, J. 2008. Mismatch repair and DNA damage signalling. DNA Repair, 3, (8-9) 1091-1101.

Stordal, B. and Davey, R. 2009. A systematic review of genes involved in the inverse resistance relationship between cisplatin and paclitaxel chemotherapy: role of BRCA1. Current Cancer Drug Targets, 9, (3) 354-365.

Stordal, B. and Davey, M. 2007a. Understanding cisplatin resistance using cellular models. IUBMB Life, 59, (11) 696-699.

Stordal, B., Davey, M., and Davey, R. 2006. Oxaliplatin induces drug resistance more rapidly than cisplatin in H69 small cell lung cancer cells. Cancer Chemotherapy and Pharmacology, 58, (2) 256-265.

Stordal, B., Hamon, M., McEneaney, V., Roche, S., Gillet, J. P., O'Leary, J. J., Gottesman, M., and Clynes, M. 2012. Resistance to Paclitaxel in a Cisplatin-Resistant Ovarian Cancer Cell Line Is Mediated by P-Glycoprotein. PLoS ONE, 7, (7) e40717-e40717.

Stordal, B., Pavlakis, N., and Davey, R. 2007b. A systematic review of platinum and taxane resistance from bench to clinic: An inverse relationship. Cancer Treatment Reviews, 33, (8) 688-703.

Stordal, B., Pavlakis, N., and Davey, R. 2007c. Oxaliplatin for the treatment of cisplatin-resistant cancer: A systematic review. Cancer Treatment Reviews, 33, (4) 347-357.

Stordal, B., Timms, K., Farrelly, A., Gallagher, D., Busschots, S., Renaud, M. l., Thery, J., Williams, D., Potter, J., Tran, T., Korpanty, G., Cremona, M., Carey, M., Li, J., Li, Y., Aslan, O., O'Leary, J. J., Mills, G. B., and Hennessy, B. T. 2013. BRCA1/2 mutation analysis in 41 ovarian cell lines reveals only one functionally deleterious BRCA1 mutation. Molecular Oncology, 7, (3) 567-579.

Strobel, T., Tai, Y. T., Korsmeyer, S., and Cannistra, S. A. 1998. BAD partly reverses paclitaxel resistance in human ovarian cancer cells. Oncogene, 17, (19) 2419-2427.

Sugio, A., Iwasaki, M., Habata, S., Mariya, T., Suzuki, M., Osogami, H., Tamate, M., Tanaka, R., and Saito, T. 2014. BAG3 upregulates Mcl-1 through downregulation of miR-29b to induce anticancer drug resistance in ovarian cancer. Gynecologic Oncology, 134, (3) 615-623.

Suh, K. S., Remache, Y. K., Patel, J. S., Chen, S. H., Haystrand, R., Ford, P., Shaikh, A. M., Wang, J., and Goy, A. H. 2009. Informatics-guided procurement of patient samples for biomarker discovery projects in cancer research. Cell Tissue Bank., 10, (1) 43-48.

Suh, K. S., Park, S. W., Castro, A., Patel, H., Blake, P., Liang, M., and Goy, A. 2010. Ovarian cancer biomarkers for molecular biosensors and translational medicine. Expert Review of Molecular Diagnostics, 10, (8) 1069-1083.

Sun, Y., Wong, N., Guan, Y., Salamanca, C. M., Cheng, J. C., Lee, J. M., Gray, J. W., and Auersperg, N. 2008. The eukaryotic translation elongation factor eEF1A2 induces neoplastic properties and mediates tumorigenic effects of ZNF217 in precursor cells of human ovarian carcinomas. International Journal of Cancer, 123, (8) 1761-1769.

Supiot, S., Gouraud, W., Campion, L., Jezequel, P., Buecher, B., Charrier, J., Heymann, M. F., Mahe, M. A., Rio, E., and Cherel, M. 2013. Early dynamic transcriptomic changes during preoperative radiotherapy in patients with rectal cancer: a feasibility study. World Journal of Gastroenterology, 19, (21) 3249-3254.

Suzukake, K., Petro, B. J., and Vistica, D. T. 1982. Reduction in glutathione content of L-PAM resistant L1210 Cells confers drug sensitivity. Biochemical Pharmacology, 31, (1) 121-124.

Svoboda, M., Wlcek, K., Taferner, B., Hering, S., Stieger, B., Tong, D., Zeillinger, R., Thalhammer, T., and Jager, W. 2011. Expression of organic anion-transporting polypeptides 1B1 and 1B3 in ovarian cancer cells: Relevance for paclitaxel transport. Biomedicine & Pharmacotherapy, 65, (6) 417-426.

Swisher, E. M., Sakai, W., Karlan, B. Y., Wurz, K., Urban, N., and Taniguchi, T. 2008. Secondary BRCA1 Mutations in BRCA1-Mutated Ovarian Carcinomas with Platinum Resistance. Cancer Research, 68, (8) 2581-2586.

Tabuchi, Y., Matsuoka, J., Gunduz, M., Imada, T., Ono, R., Ito, M., Motoki, T., Yamatsuji, T., Shirakawa, Y., Takaoka, M., Haisa, M., Tanaka, N., Kurebayashi, J., Jordan, V. C., and Naomoto, Y. 2009. Resistance to paclitaxel therapy is related with Bcl-2 expression through an estrogen receptor mediated pathway in breast cancer. International Journal of Oncology, 34, (2) 313-319.

Taguchi, T., Kato, Y., Baba, Y., Nishimura, G., Tanigaki, Y., Horiuchi, C., Mochimatsu, I., and Tsukuda, M. 2004. Protein levels of p21, p27, cyclin E and Bax predict sensitivity to cisplatin and paclitaxel in head and neck squamous cell carcinomas. Oncology Reports, 11, (2) 421-426.

Takahashi, H., Nakatsuji, H., Takahashi, M., Avirmed, S., Fukawa, T., Takemura, M., Fukumori, T., and Kanayama, H. 2012. Up-regulation of plakophilin-2 and Down-regulation of plakophilin-3 are correlated with invasiveness in bladder cancer. Urology, 79, (1) 240-248.

Takenaka, T., Yoshino, I., Kouso, H., Ohba, T., Yohena, T., Osoegawa, A., Shoji, F., and Maehara, Y. 2007. Combined evaluation of Rad51 and ERCC1 expressions for sensitivity to platinum agents in non-small cell lung cancer. International Journal of Cancer, 121, (4) 895-900.

Tan, D. S. P., Rothermundt, C., Thomas, K., Bancroft, E., Eeles, R., Shanley, S., Ardern-Jones, A., Norman, A., Kaye, S. B., and Gore, M. E. 2008. BRCAness Syndrome in Ovarian Cancer: A Case-Control Study Describing the Clinical Features and Outcome of Patients With Epithelial Ovarian Cancer Associated With BRCA1 and BRCA2 Mutations. Journal of Clinical Oncology, 26, (34) 5530-5536.

Tanaka, K., Arao, T., Maegawa, M., Matsumoto, K., Kaneda, H., Kudo, K., Fujita, Y., Yokote, H., Yanagihara, K., Yamada, Y., Okamoto, I., Nakagawa, K., and Nishio, K. 2009. SRPX2 is overexpressed in gastric cancer and promotes cellular migration and adhesion. International Journal of Cancer, 124, (5) 1072-1080.

Tanaka, T., Bai, Z., Srinoulprasert, Y., Yang, B. G., Hayasaka, H., and Miyasaka, M. 2005. Chemokines in tumor progression and metastasis. Cancer Science, 96, (6) 317-322.

Tassone, P., Tagliaferri, P., Perricelli, A., Blotta, S., Quaresima, B., Martelli, M. L., Goel, A., Barbieri, V., Costanzo, F., Boland, C. R., and Venuta, S. 2003. BRCA1 expression modulates chemosensitivity of BRCA1-defective HCC1937 human breast cancer cells. British Journal of Cancer, 88, (8) 1285-1291.

Tegze, B., Szallasi, Z., Haltrich, I., Penzvalto, Z., Toth, Z., Liko, I., and Gyorffy, B. 2012. Parallel evolution under chemotherapy pressure in 29 breast cancer cell lines results in dissimilar mechanisms of resistance. PLoS ONE, 7, (2)

Teicher, B. A., Cucchi, C. A., Lee, J. B., Flatow, J. L., Rosowsky, A., and Frei, E. 1986. Alkylating Agents: In Vitro Studies of Cross-Resistance Patterns in Human Cell Lines. Cancer Research, 46, (9) 4379-4383.

Tennant, J. R. 1964. Evaluation of the trypan blue Technique for determination of cell viability. Transplantation, 2, 685-694.

Teodoridis, J. M., Hall, J., Marsh, S., Kannall, H. D., Smyth, C., Curto, J., Siddiqui, N., Gabra, H., McLeod, H. L., Strathdee, G., and Brown, R. 2005. CpG Island Methylation of DNA Damage Response Genes in Advanced Ovarian Cancer. Cancer Research, 65, (19) 8961-8967.

Tesniere, A., Schlemmer, F., Boige, V., Kepp, O., Martins, I., Ghiringhelli, F., Aymeric, L., Michaud, M., Apetoh, L., Barault, L., Mendiboure, J., Pignon, J. P., Jooste, V., van, E. P., Ducreux, M., Zitvogel, L., Piard, F., and Kroemer, G. 2010. Immunogenic death of colon cancer cells treated with oxaliplatin. Oncogene, 29, (4) 482-491.

The Cancer Genome Atlas Network. 2011. Integrated genomic analyses of ovarian carcinoma. Nature, 474, (7353) 609-615.

Thigpen, J. T., Aghajanian, C. A., Alberts, D. S., Campos, S. M., Gordon, A. N., Markman, M., McMeekin, D. S., Monk, B. J., and Rose, P. G. 2005. Role of pegylated liposomal doxorubicin in ovarian cancer. Gynecologic Oncology, 96, (1) 10-18.

Titus-Ernstoff, L., Perez, K., Cramer, D. W., Harlow, B. L., Baron, J. A., and Greenberg, E. R. 2001. Menstrual and reproductive factors in relation to ovarian cancer risk. British Journal of Cancer, 84, (5) 714-721.

Topman, G., Sharabani-Yosef, O., and Gefen, A. 2011. A method for quick, low-cost automated confluency measurements. Microscopy and microanalysis : the official journal of Microscopy Society of America, Microbeam Analysis Society, Microscopical Society of Canada, 17, (6) 915-922.

Topp, M. D., Hartley, L., Cook, M., Heong, V., Boehm, E., McShane, L., Pyman, J., McNally, O., Ananda, S., Harrell, M., Etemadmoghadam, D., Galletta, L., Alsop, K., Mitchell, G., Fox, S. B., Kerr, J. B., Hutt, K. J., Kaufmann, S. H., Australian Ovarian, C. S., Swisher, E. M., Bowtell, D. D., Wakefield, M. J., and Scott, C. L. 2014. Molecular correlates of platinum response in human high-grade serous ovarian cancer patient-derived xenografts. Molecular Oncology, 8, (3) 656-668.

Tothill, R. W., Tinker, A. V., George, J., Brown, R., Fox, S. B., Lade, S., Johnson, D. S., Trivett, M. K., Etemadmoghadam, D., Locandro, B., Traficante, N., Fereday, S., Hung, J. A., Chiew, Y. E., Haviv, I., Gertig, D., Defazio, A., and Bowtell, D. D. 2008. Novel molecular subtypes of serous and endometrioid ovarian cancer linked to clinical outcome. Clinical Cancer Research, 14, (16) 5198-5208.

Trimbos, J. B., Parmar, M., Vergote, I., Guthrie, D., Bolis, G., Colombo, N., Vermorken, J. B., Torri, V., Mangioni, C., Percorelli, S., Lissoni, A., and Swart, A. M. 2003a. International Collaborative Ovarian Neoplasm Trial 1 and Adjuvant ChemoTherapy In Ovarian Neoplasm Trial: Two Parallel Randomized Phase III Trials of Adjuvant Chemotherapy in Patients With Early-Stage Ovarian Carcinoma. Journal of the National Cancer Institute, 95, (2) 105-112.

Trimbos, J. B., Vergote, I., Bolis, G., Vermorken, J. B., Mangioni, C., Madronal, C., Franchi, M., Tateo, S., Zanetta, G., Scarfone, G., Giurgea, L., Timmers, P., Coens, C., Pecorelli, S., and For the EORTC-ACTION Collaborators. 2003b. Impact of Adjuvant Chemotherapy

and Surgical Staging in Early-Stage Ovarian Carcinoma: European Organisation for Research and Treatment of Cancer Adjuvant ChemoTherapy in Ovarian Neoplasm Trial. Journal of the National Cancer Institute, 95, (2) 113-125.

Tsukamoto, O., Miura, K., Mishima, H., Abe, S., Kaneuchi, M., Higashijima, A., Miura, S., Kinoshita, A., Yoshiura, K. i., and Masuzaki, H. 2014. Identification of endometrioid endometrial carcinoma-associated microRNAs in tissue and plasma. Gynecologic Oncology, 132, (3) 715-721.

Tutt, A., Robson, M., Garber, J. E., Domchek, S. M., Audeh, M. W., Weitzel, J. N., Friedlander, M., Arun, B., Loman, N., Schmutzler, R. K., Wardley, A., Mitchell, G., Earl, H., Wickens, M., and Carmichael, J. 2010. Oral poly(ADP-ribose) polymerase inhibitor olaparib in patients with BRCA1 or BRCA2 mutations and advanced breast cancer: a proof-of-concept trial. Lancet, 376, (9737) 235-244.

Tworoger, S. S., Fairfield, K. M., Colditz, G. A., Rosner, B. A., and Hankinson, S. E. 2007. Association of Oral Contraceptive Use, Other Contraceptive Methods, and Infertility with Ovarian Cancer Risk. American Journal of Epidemiology, 166, (8) 894-901.

Ueda, K., Cardarelli, C., Gottesman, M. M., and Pastan, I. 1987. Expression of a full-length cDNA for the human "MDR1" gene confers resistance to colchicine, doxorubicin, and vinblastine. Proceedings of the National Academy of Science of the U.S.A., 84, (9) 3004-3008.

Ueno, K., Hirata, H., Shahryari, V., Chen, Y., Zaman, M. S., Singh, K., Tabatabai, Z. L., Hinoda, Y., and Dahiya, R. 2011. Tumour suppressor microRNA-584 directly targets oncogene Rock-1 and decreases invasion ability in human clear cell renal cell carcinoma. British Journal of Cancer, 104, (2) 308-315.

Uslu, R., Sanli, U. A., Dikmen, Y., Karabulut, B., Ozsaran, A., Sezgin, C., Muezzinoglu, G. G., Omay, S. B., and Goker, E. 2005. Predictive value of serum interleukin-8 levels in ovarian cancer patients treated with paclitaxel-containing regimens. International Journal of Gynaecological Cancer, 15, (2) 240-245.

Vaksman, O., Stavnes, H. T., Kaern, J., Trope, C. G., Davidson, B., and Reich, R. 2011. miRNA profiling along tumour progression in ovarian carcinoma. Journal of Cellular and Molecular Medicine, 15, (7) 1593-1602.

van 't Veer, L. J., Dai, H., van de Vijver, M. J., He, Y. D., Hart, A. A. M., Mao, M., Peterse, H. L., van der Kooy, K., Marton, M. J., Witteveen, A. T., Schreiber, G. J., Kerkhoven, R. M., Roberts, C., Linsley, P. S., Bernards, R., and Friend, S. H. 2002. Gene expression profiling predicts clinical outcome of breast cancer. Nature, 415, (6871) 530-536.

van Dijk, M., Goransson, S. A., and Stromblad, S. 2013. Cell to extracellular matrix interactions and their reciprocal nature in cancer. Experimental Cell Research, 319, (11) 1663-1670.

Van Gelder, R. N., von Zastrow, M. E., Yool, A., Dement, W. C., Barchas, J. D., and Eberwine, J. H. 1990. Amplified RNA synthesized from limited quantities of heterogeneous cDNA. Proceedings of the National Academy of Sciences, 87, (5) 1663-1667.

van Jaarsveld, M. T. M., Helleman, J., Berns, E. M. J. J., and Wiemer, E. A. C. 2010. MicroRNAs in ovarian cancer biology and therapy resistance. The International Journal of Biochemistry & Cell Biology, 42, (8) 1282-1290.

Vandier, D., Calvez, V., Massade, L., Gouyette, A., Mickley, L., Fojo, T., and Rixe, O. 2000. Transactivation of the Metallothionein Promoter in Cisplatin-Resistant Cancer Cells: a Specific Gene Therapy Strategy. Journal of the National Cancer Institute, 92, (8) 642-647.

Vang, R., Shih, I., and Kurman, R. J. 2009. Ovarian low-grade and high-grade serous carcinoma: pathogenesis, clinicopathologic and molecular biologic features, and diagnostic problems. Advances in Anatomic Pathology, 16, (5) 267-282.

Vang, S., Wu, H. T., Fischer, A., Miller, D. H., MacLaughlan, S., Douglass, E., Comisar, L., Steinhoff, M., Collins, C., Smith, P. J., Brard, L., and Brodsky, A. S. 2013. Identification of ovarian cancer metastatic miRNAs. PLoS ONE, 8, (3) e58226-

Vasey, P. A. 2003. Resistance to chemotherapy in advanced ovarian cancer: mechanisms and current strategies. British Journal of Cancer, 89, (S3) S23-S28.

Vasey, P. A., Jones, N. A., Jenkins, S., Dive, C., and Brown, R. 1996. Cisplatin, camptothecin, and taxol sensitivities of cells with p53-associated multidrug resistance. Molecular Pharmacology, 50, (6) 1536-1540.

Vasey, P. A., Jayson, G. C., Gordon, A., Gabra, H., Coleman, R., Atkinson, R., Parkin, D., Paul, J., Hay, A., Kaye, S. B., and On behalf of the Scottish Gynaecological Cancer Trials Group. 2004. Phase III Randomized Trial of Docetaxel–Carboplatin Versus Paclitaxel–Carboplatin as First-line Chemotherapy for Ovarian Carcinoma. Journal of the National Cancer Institute, 96, (22) 1682-1691.

Vecchione, A., Belletti, B., Lovat, F., Volinia, S., Chiappetta, G., Giglio, S., Sonego, M., Cirombella, R., Onesti, E. C., Pellegrini, P., Califano, D., Pignata, S., Losito, S., Canzonieri, V., Sorio, R., Alder, H., Wernicke, D., Stoppacciaro, A., Baldassarre, G., and Croce, C. M. 2013. A microRNA signature defines chemoresistance in ovarian cancer through modulation of angiogenesis. Proceedings of the National Academy of Sciences, 110, (24) 9845-9850.

Vermorken, J. B., van der Vijgh, W. J., Klein, I., Hart, A. A., Gall, H. E., and Pinedo, H. M. 1984. Pharmacokinetics of free and total platinum species after short-term infusion of cisplatin. Cancer Treatment Reports, 68, (3) 505-513.

Villedieu, M., Louis, M. H., Dutoit, S., Brotin, E., Lincet, H., Duigou, F., Staedel, C., Gauduchon, P., and Poulain, L. 2007. Absence of Bcl-xL down-regulation in response to cisplatin is associated with chemoresistance in ovarian carcinoma cells. Gynecologic Oncology, 105, (1) 31-44.

Vilming Elgaaen, B., Olstad, O., Haug, K. B., Brusletto, B., Sandvik, L., Staff, A., Gautvik, K., and Davidson, B. 2014. Global miRNA expression analysis of serous and clear cell ovarian carcinomas identifies differentially expressed miRNAs including miR-200c-3p as a prognostic marker. BMC Cancer, 14, (1)

Viswanathan, S. R., Powers, J. T., Einhorn, W., Hoshida, Y., Ng, T. L., Toffanin, S., O'Sullivan, M., Lu, J., Phillips, L. A., Lockhart, V. L., Shah, S. P., Tanwar, P. S., Mermel, C. H., Beroukhim, R., Azam, M., Teixeira, J., Meyerson, M., Hughes, T. P., Llovet, J. M., Radich, J., Mullighan, C. G., Golub, T. R., Sorensen, P. H., and Daley, G. Q. 2009. Lin28 promotes transformation and is associated with advanced human malignancies. Nature Genetics, 41, (7) 843-848.

Vogel, C. and Marcotte, E. M. 2012. Insights into the regulation of protein abundance from proteomic and transcriptomic analyses. Nature Reviews Genetics, 13, (4) 227-232.

Walker, G., MacLeod, K., Williams, A. R. W., Cameron, D. A., Smyth, J. F., and Langdon, S. P. 2007. Estrogen-regulated gene expression predicts response to endocrine therapy in patients with ovarian cancer. Gynecologic Oncology, 106, (3) 461-468.

Wang, H., Fan, L., Xia, X., Rao, Y., Ma, Q., Yang, J., Lu, Y., Wang, C., Ma, D., and Huang, X. 2012. Silencing Wnt2B by siRNA interference inhibits metastasis and enhances chemotherapy sensitivity in ovarian cancer. International Journal of Gynaecological Cancer, 22, (5) 755-761.

Wang, J. X., He, Y. L., Zhu, S. T., Yang, S., and Zhang, S. T. 2011. Aberrant methylation of the 3q25 tumor suppressor gene PTX3 in human esophageal squamous cell carcinoma. World Journal of Gastroenterology, 17, (37) 4225-4230.

Wang, L. G., Liu, X. M., Kreis, W., and Budman, D. R. 1999. The effect of antimicrotubule agents on signal transduction pathways of apoptosis: a review. Cancer Chemotherapy and Pharmacology, 44, (5) 355-361.

Wang, L. F., Fokas, E., Juricko, J., You, A., Rose, F., Pagenstecher, A., Engenhart-Cabillic, R., and An, H. X. 2008. Increased expression of EphA7 correlates with adverse outcome in primary and recurrent glioblastoma multiforme patients. BMC Cancer, 8, (1)

Wang, N. N., Zhao, L. J., Wu, L. N., He, M. F., Qu, J. W., Zhao, Y. B., Zhao, W. Z., Li, J. S., and Wang, J. H. 2013. Mechanistic analysis of taxol-induced multidrug resistance in an ovarian cancer cell line. Asian Pacific Journal of Cancer Prevention, 14, (9) 4983-4988.

Wang, T. H., Wang, H. S., and Soong, Y. K. 2000. Paclitaxel-induced cell death. Cancer, 88, (11) 2619-2628.

Wang, Y., Fei, D., Vanderlaan, M., and Song, A. 2004. Biological activity of bevacizumab, a humanized anti-VEGF antibody in vitro. Angiogenesis, 7, (4) 335-345.

Wang, Y., Yin, S., Blade, K., Cooper, G., Menick, D. R., and Cabral, F. 2005. Mutations at Leucine 215 of Beta-Tubulin Affect Paclitaxel Sensitivity by Two Distinct Mechanisms. Biochemistry, 45, (1) 185-194.

Wang, Y., Niu, X. L., Qu, Y., Wu, J., Zhu, Y. Q., Sun, W. J., and Li, L. Z. 2010. Autocrine production of interleukin-6 confers cisplatin and paclitaxel resistance in ovarian cancer cells. Cancer Letters, 295, (1) 110-123.

Watanabe, Y., Koi, M., Hemmi, H., Hoshai, H., and Noda, K. 2001. A change in microsatellite instability caused by cisplatin-based chemotherapy of ovarian cancer. British Journal of Cancer, 85, (7) 1064-1069.

Wei, H., Zhao, L., Li, W., Fan, K., Qian, W., Hou, S., Wang, H., Dai, M., Hellstrom, I., Hellstrom, K. E., and Guo, Y. 2013a. Combinatorial PD-1 blockade and CD137 activation has therapeutic efficacy in murine cancer models and synergizes with cisplatin. PLoS ONE, 8, (12) e84927-e84927.

Wei, W., Mok, S. C., Oliva, E., Kim, S. H., Mohapatra, G., and Birrer, M. J. 2013b. FGF18 as a prognostic and therapeutic biomarker in ovarian cancer. Journal of Clinical Investigation, 123, (10) 4435-4448.

Weiss, R. B. 1992. The anthracyclines: will we ever find a better doxorubicin? Seminars In Oncology, 19, (6) 670-686.

Weiss, R. B. and Christian, M. C. 1993. New cisplatin analogues in development. A review. Drugs, 46, (3) 360-377.

Welsh, C., Day, R., McGurk, C., Masters, J. R. W., Wood, R. D., and K+Åberle, B. 2004. Reduced levels of XPA, ERCC1 and XPF DNA repair proteins in testis tumor cell lines. International Journal of Cancer, 110, (3) 352-361.

Welsh, J. B., Zarrinkar, P. P., Sapinoso, L. M., Kern, S. G., Behling, C. A., Monk, B. J., Lockhart, D. J., Burger, R. A., and Hampton, G. M. 2001. Analysis of gene expression profiles in normal and neoplastic ovarian tissue samples identifies candidate molecular markers of epithelial ovarian cancer. Proceedings of the National Academy of Sciences, 98, (3) 1176-1181.

Wen, S. Y., Lin, Y., Yu, Y. Q., Cao, S. J., Zhang, R., Yang, X. M., Li, J., Zhang, Y. L., Wang, Y. H., Ma, M. Z., Sun, W. W., Lou, X. L., Wang, J. H., Teng, Y. C., and Zhang, Z. G. 2014. miR-506 acts as a tumor suppressor by directly targeting the hedgehog pathway transcription factor Gli3 in human cervical cancer. Oncogene, March 2014,

Wendler, A., Keller, D., Albrecht, C., Peluso, J. J., and Wehling, M. 2011. Involvement of let-7/miR-98 microRNAs in the regulation of progesterone receptor membrane component 1 expression in ovarian cancer cells. Oncology Reports, 25, (1) 273-279.

Willert, K. and Nusse, R. 2012. Wnt proteins. Cold Spring Harbor Perspectives in Biology, 4, (9)

Williams, E., Martin, S., Moss, R., Durrant, L., and Deen, S. 2012. Co-expression of VEGF and CA9 in ovarian high-grade serous carcinoma and relationship to survival. Virchows Archive: An International Journal of Pathology, 461, (1) 33-39.

Williams, J., Lucas, P. C., Griffith, K. A., Choi, M., Fogoros, S., Hu, Y. Y., and Liu, J. R. 2005. Expression of Bcl-xL in ovarian carcinoma is associated with chemoresistance and recurrent disease. Gynecologic Oncology, 96, (2) 287-295.

Witham, J., Valenti, M. R., De-Haven-Brandon, A. K., Vidot, S., Eccles, S. A., Kaye, S. B., and Richardson, A. 2007. The Bcl-2/Bcl-XL family inhibitor ABT-737 sensitizes ovarian cancer cells to carboplatin. Clinical Cancer Research, 13, (23) 7191-7198.

Wojnarowicz, P. M., Breznan, A., Arcand, S. L., Filali-Mouhim, A., Provencher, D. M., Mes-Masson, A. M., and Tonin, P. N. 2008. Construction of a chromosome 17 transcriptome in serous ovarian cancer identifies differentially expressed genes. International Journal of Gynaecological Cancer, 18, (5) 963-975.

Wong, K. K., Cheng, R. S., and Mok, S. C. 2001. Identification of differentially expressed genes from ovarian cancer cells by MICROMAX cDNA microarray system. Biotechniques, 30, (3) 670-675.

Wozney, J. M. 1998. The bone morphogenetic protein family: multifunctional cellular regulators in the embryo and adult. European Journal of Oral Sciences, 106 Suppl 1, 160-166.

Wu, H., Xiao, Z., Zhang, H., Wang, K., Liu, W., and Hao, Q. 2014. MiR-489 modulates cisplatin resistance in human ovarian cancer cells by targeting Akt3. Anticancer Drugs, 25, (7) 799-809.

Wu, H., Xiao, Z., Wang, K., Liu, W., and Hao, Q. 2013. MiR-145 is downregulated in human ovarian cancer and modulates cell growth and invasion by targeting p70S6K1 and MUC1. Biochemical and Biophysical Research Communications, 441, (4) 693-700.

Wu, L. and Hickson, I. D. 2003. The Bloom's syndrome helicase suppresses crossing over during homologous recombination. Nature, 426, (6968) 870-874.

Wu, X. m., Shao, X. q., Meng, X. x., Zhang, X. n., Zhu, L., Liu, S. x., Lin, J., and Xiao, H. s. 2011. Genome-wide analysis of microRNA and mRNA expression signatures in hydroxycamptothecin-resistant gastric cancer cells. Acta Pharmacol Sin, 32, (2) 259-269.

Wyman, S. K., Parkin, R. K., Mitchell, P. S., Fritz, B. R., O'Briant, K., Godwin, A. K., Urban, N., Drescher, C. W., Knudsen, B. S., and Tewari, M. 2009. Repertoire of microRNAs in epithelial ovarian cancer as determined by next generation sequencing of small RNA cDNA libraries. PLoS ONE, 4, (4) e5311-e5311.

Wynder, E. L., Dodo, H., and Barber, H. R. K. 1969. Epidemiology of cancer of the ovary. Cancer, 23, (2) 352-370.

Xiang, Q., Tang, H., Yu, J., Yin, J., Yang, X., and Lei, X. 2013. MicroRNA-98 sensitizes cisplatin-resistant human lung adenocarcinoma cells by up-regulation of HMGA2. Pharmazie, 68, (4) 274-281.

Xiang, Y., Ma, N., Wang, D., Zhang, Y., Zhou, J., Wu, G., Zhao, R., Huang, H., Wang, X., Qiao, Y., Li, F., Han, D., Wang, L., Zhang, G., and Gao, X. 2014. MiR-152 and miR-185 co-contribute to ovarian cancer cells cisplatin sensitivity by targeting DNMT1 directly: a novel epigenetic therapy independent of decitabine. Oncogene, 33, (3) 378-386.

Xiao, H., Verdier-Pinard, P., Fernandez-Fuentes, N., Burd, B., Angeletti, R., Fiser, A., Horwitz, S. B., and Orr, G. A. 2006. Insights into the mechanism of microtubule stabilization by Taxol. Proceedings of the National Academy of Science of the U.S.A., 103, (27) 10166-10173.

Xie, X., Ye, D., Chen, H., Lu, W., Cheng, B., and Zhong, H. 2004. Interleukin-7 and suppression of local peritoneal immunity in ovarian carcinoma. International Journal of Gynecology and Obstetrics, 85, (2) 151-158.

Xiong, L., Wen, Y., Miao, X., and Yang, Z. 2014. NT5E and FcGBP as key regulators of TGF-1-induced epithelial-mesenchymal transition (EMT) are associated with tumor progression and survival of patients with gallbladder cancer. Cell Tissue Res, 355, (2) 365-374.

Xu, Y. Z., Xi, Q. H., Ge, W. L., and Zhang, X. Q. 2013. Identification of serum microRNA-21 as a biomarker for early detection and prognosis in human epithelial ovarian cancer. Asian Pacific Journal of Cancer Prevention, 14, (2) 1057-1060.

Yamada, T., Oshima, T., Yoshihara, K., Sato, T., Nozaki, A., Shiozawa, M., Ota, M., Yoshikawa, T., Akaike, M., Numata, K., Rino, Y., Kunisaki, C., Tanaka, K., Imada, T., and Masuda, M. 2014. Impact of overexpression of Sushi repeat-containing protein X-linked 2 gene on outcomes of gastric cancer. Journal of Surgical Oncology, 109, (8) 836-840.

Yamada, Y., Arao, T., Matsumoto, K., Gupta, V., Tan, W., Fedynyshyn, J., Nakajima, T. E., Shimada, Y., Hamaguchi, T., Kato, K., Taniguchi, H., Saito, Y., Matsuda, T., Moriya, Y., Akasu, T., Fujita, S., Yamamoto, S., and Nishio, K. 2010. Plasma concentrations of VCAM-1 and PAI-1: a predictive biomarker for post-operative recurrence in colorectal cancer. Cancer Science, 101, (8) 1886-1890.

Yan, B., Ma, J., Zhang, J., Guo, Y., Riedel, H., Mueller, M. D., Remick, S. C., and Yu, J. J. 2013. PSP94 contributes to chemoresistance and its peptide derivative PCK3145 represses tumor growth in ovarian cancer. Oncogene, November 2013,

Yan, X. D., Li, M., Yuan, Y., Mao, N., and Pan, L. Y. 2007. Biological comparison of ovarian cancer resistant cell lines to cisplatin and Taxol by two different administrations. Oncology Reports, 17, (5) 1163-1169.

Yang, H., Kong, W., He, L., Zhao, J. J., O'Donnell, J. D., Wang, J., Wenham, R. M., Coppola, D., Kruk, P. A., Nicosia, S. V., and Cheng, J. Q. 2008a. MicroRNA Expression Profiling in Human Ovarian Cancer: miR-214 Induces Cell Survival and Cisplatin Resistance by Targeting PTEN. Cancer Research, 68, (2) 425-433.

Yang, J. H., Li, J. H., Shao, P., Zhou, H., Chen, Y. Q., and Qu, L. H. 2011. starBase: a database for exploring microRNA–mRNA interaction maps from Argonaute CLIP-Seq and Degradome-Seq data. Nucleic Acids Research, 39, (suppl 1) D202-D209.

Yang, N., Kaur, S., Volinia, S., Greshock, J., Lassus, H., Hasegawa, K., Liang, S., Leminen, A., Deng, S., Smith, L., Johnstone, C. N., Chen, X. M., Liu, C. G., Huang, Q., Katsaros, D., Calin, G. A., Weber, B. L., Butzow, R., Croce, C. M., Coukos, G., and Zhang, L. 2008b. MicroRNA Microarray Identifies Let-7i as a Novel Biomarker and Therapeutic Target in Human Epithelial Ovarian Cancer. Cancer Research, 68, (24) 10307-10314.

Yang, T. T., Sinai, P., and Kain, S. R. 1996. An Acid Phosphatase Assay for Quantifying the Growth of Adherent and Nonadherent Cells. Analytical Biochemistry, 241, (1) 103-108.

Yang, X. L. and Wang, A. H. J. 1999. Structural studies of atom-specific anticancer drugs acting on DNA. Pharmacology and Therapeutics, 83, (3) 181-215.

Yang, X., Fraser, M., Moll, U. M., Basak, A., and Tsang, B. K. 2006. Akt-Mediated Cisplatin Resistance in Ovarian Cancer: Modulation of p53 Action on Caspase-Dependent Mitochondrial Death Pathway. Cancer Research, 66, (6) 3126-3136.

Yang, Y., Zhang, Q., Xu, F., Wu, L., He, Q., and Li, X. 2012. Tumor suppressor gene BLU is frequently downregulated by promoter hypermethylation in myelodysplastic syndrome. Journal of Cancer Research and Clinical Oncology, 1-9.

Yap, T. A., Sandhu, S. K., Carden, C. P., and de Bono, J. S. 2011. Poly(ADP-ribose) polymerase (PARP) inhibitors: Exploiting a synthetic lethal strategy in the clinic. CA: Cancer Journal for Clinicians, 61, (1) 31-49.

Ye, G., Fu, G., Cui, S., Zhao, S., Bernaudo, S., Bai, Y., Ding, Y., Zhang, Y., Yang, B. B., and Peng, C. 2011. MicroRNA 376c enhances ovarian cancer cell survival by targeting activin receptor-like kinase 7: implications for chemoresistance. Journal of Cell Science, 124, (3) 359-368.

Yin, S., Bhattacharya, R., and Cabral, F. 2010. Human Mutations That Confer Paclitaxel Resistance. Molecular Cancer Therapeutics, 9, (2) 327-335.

Yin, S., Cabral, F., and Veeraraghavan, S. 2007. Amino acid substitutions at proline 220 of beta-tubulin confer resistance to paclitaxel and colcemid. Molecular Cancer Therapeutics, 6, (10) 2798-2806.

Ying, S. Y., Chang, C. P., and Lin, S. L. 2010. Intron-mediated RNA interference, intronic microRNAs, and applications. Methods in Molecalar Biology, 629, 205-237.

Ying, W., Wang, S., Shi, J., and Sun, Y. 2012. ER-/ER+ breast cancer cell lines exhibited different resistance to paclitaxel through pulse selection. Medical Oncology, 29, (2) 495-502.

Yoon, J., Kim, E. S., Lee, S. J., Park, C. W., Cha, H. J., Hong, B. H., and Choi, K. Y. 2010. Apoptosis-related mRNA expression profiles of ovarian cancer cell lines following cisplatin treatment. Journal of Gynecological Oncology, 21, (4) 255-261.

Yoshihara, K., Tajima, A., Yahata, T., Kodama, S., Fujiwara, H., Suzuki, M., Onishi, Y., Hatae, M., Sueyoshi, K., Fujiwara, H., Kudo, Y., Kotera, K., Masuzaki, H., Tashiro, H., Katabuchi, H., Inoue, I., and Tanaka, K. 2010. Gene expression profile for predicting survival in advanced-stage serous ovarian cancer across two independent datasets. PLoS ONE, 5, (3) e9615-

Yoshihara, K., Tsunoda, T., Shigemizu, D., Fujiwara, H., Hatae, M., Fujiwara, H., Masuzaki, H., Katabuchi, H., Kawakami, Y., Okamoto, A., Nogawa, T., Matsumura, N., Udagawa, Y., Saito, T., Itamochi, H., Takano, M., Miyagi, E., Sudo, T., Ushijima, K., Iwase, H., Seki, H., Terao, Y., Enomoto, T., Mikami, M., Akazawa, K., Tsuda, H., Moriya, T., Tajima, A., Inoue, I., and Tanaka, K. 2012. High-risk ovarian cancer based on 126-gene expression signature is uniquely characterized by downregulation of antigen presentation pathway. Clinical Cancer Research, 18, (5) 1374-1385.

Yoshioka, S., King, M. L., Ran, S., Okuda, H., MacLean, J. A., McAsey, M. E., Sugino, N., Brard, L., Watabe, K., and Hayashi, K. 2012. WNT7A Regulates Tumor Growth and Progression in Ovarian Cancer through the WNT/Beta-Catenin Pathway. Molecular Cancer Research, 10, (3) 469-482.

Young, L., Sung, J., Stacey, G., and Masters, J. R. 2010. Detection of Mycoplasma in cell cultures. Nature Protocols, 5, (5) 929-934.

Yu, L. and Wang, Z. 2004. Difference in expression of Bcl-2 and Bcl-xl genes in cisplatin-sensitive and cisplatin-resistant human in ovarian cancer cell lines. Journal of Huazhong University of Science and Technology -- Medical Sciences --, 24, (2) 151-153.

Yuan, S. S., Lee, S. Y., Chen, G., Song, M., Tomlinson, G. E., and Lee, E. Y. 1999. BRCA2 is required for ionizing radiation-induced assembly of Rad51 complex in vivo. Cancer Research, 59, (15) 3547-3551.

Zajchowski, D. A., Karlan, B. Y., and Shawver, L. K. 2012. Treatment-Related Protein Biomarker Expression Differs between Primary and Recurrent Ovarian Carcinomas. Molecular Cancer Therapeutics, 11, (2) 492-502.

Zamble, D. B., Mu, D., Reardon, J. T., Sancar, A., and Lippard, S. J. 1996. Repair of cisplatin--DNA adducts by the mammalian excision nuclease. Biochemistry, 35, (31) 10004-10013.

Zhang, C. C., Yang, J. M., Bash-Babula, J., White, E., Murphy, M., Levine, A. J., and Hait, W. N. 1999. DNA Damage Increases Sensitivity to Vinca Alkaloids and Decreases Sensitivity to Taxanes through p53-dependent Repression of Microtubule-associated Protein 4. Cancer Research, 59, (15) 3663-3670.

Zhang, J., Zhao, J., Zhang, W., Liu, G., Yin, D., Li, J., Zhang, S., and Li, H. 2012a. Establishment of paclitaxel-resistant cell line and the underlying mechanism on drug resistance. International Journal of Gynecological Cancer, 22, (9) 1450-1456.

Zhang, L., Huang, J., Yang, N., Greshock, J., Megraw, M. S., Giannakakis, A., Liang, S., Naylor, T. L., Barchetti, A., Ward, M. R., Yao, G., Medina, A., O'brien-Jenkins, A., Katsaros, D., Hatzigeorgiou, A., Gimotty, P. A., Weber, B. L., and Coukos, G. 2006. microRNAs exhibit high frequency genomic alterations in human cancer. Proceedings of the National Academy of Science of the U.S.A., 103, (24) 9136-9141.

Zhang, L., Volinia, S., Bonome, T., Calin, G. A., Greshock, J., Yang, N., Liu, C. G., Giannakakis, A., Alexiou, P., Hasegawa, K., Johnstone, C. N., Megraw, M. S., Adams, S., Lassus, H., Huang, J., Kaur, S., Liang, S., Sethupathy, P., Leminen, A., Simossis, V. A., Sandaltzopoulos, R., Naomoto, Y., Katsaros, D., Gimotty, P. A., DeMichele, A., Huang, Q., Butzow, R., Rustgi, A. K., Weber, B. L., Birrer, M. J., Hatzigeorgiou, A. G., Croce, C. M., and Coukos, G. 2008a. Genomic and epigenetic alterations deregulate microRNA expression in human epithelial ovarian cancer. Proceedings of the National Academy of Sciences, 105, (19) 7004-7009.

Zhang, R., Shi, H., Chen, Z., Wu, Q., Ren, F., and Huang, H. 2011a. Effects of metastasis-associated in colon cancer 1 inhibition by small hairpin RNA on ovarian carcinoma OVCAR-3 cells. Journal of Experimental & Clinical Cancer Research, 30,

Zhang, R. T., Shi, H. R., Huang, H. L., Chen, Z. M., Liu, H. N., and Yuan, Z. F. 2011b. Expressions of MACC1, HGF, and C-met protein in epithelial ovarian cancer and their significance. Nan.Fang Yi.Ke.Da.Xue.Xue.Bao., 31, (9) 1551-1555.

Zhang, S., Balch, C., Chan, M. W., Lai, H. C., Matei, D., Schilder, J. M., Yan, P. S., Huang, T. H. M., and Nephew, K. P. 2008b. Identification and Characterization of Ovarian Cancer-Initiating Cells from Primary Human Tumors. Cancer Research, 68, (11) 4311-4320.

Zhang, X. L., Peng, C. J., Peng, J., Jiang, L. Y., Ning, X. M., and Zheng, J. H. 2010. Prognostic role of Wnt7a expression in ovarian carcinoma patients. Neoplasma, 57, (6) 545-551.

Zhang, X., Dong, Y., Ti, H., Zhao, J., Wang, Y., Li, T., and Zhang, B. 2013. Down-regulation of miR-145 and miR-143 might be associated with DNA methyltransferase 3B overexpression and worse prognosis in endometrioid carcinomas. Human Pathology, 44, (11) 2571-2580.

Zhang, Y., Xu, B., Liu, Y., Yao, H., Lu, N., Li, B., Gao, J., Guo, S., Han, N., Qi, J., Zhang, K., Cheng, S., Wang, H., Zhang, X., Xiao, T., Wu, L., and Gao, Y. 2012b. The ovarian cancer-derived secretory/releasing proteome: A repertoire of tumor markers. Proteomics, 12, (11) 1883-1891.

Zheng, H., Zhang, L., Zhao, Y., Yang, D., Song, F., Wen, Y., Hao, Q., Hu, Z., Zhang, W., and Chen, K. 2013. Plasma miRNAs as diagnostic and prognostic biomarkers for ovarian cancer. PLoS ONE, 8, (11) e77853-e77853.

Zhou, C., Huang, P., and Liu, J. 2005. The carboxyl-terminal of BRCA1 is required for subnuclear assembly of RAD51 after treatment with cisplatin but not ionizing radiation in human breast and ovarian cancer cells. Biochemical and Biophysical Research Communications, 336, (3) 952-960.

Zhou, C., Smith, J. L., and Liu, J. 2003. Role of BRCA1 in cellular resistance to paclitaxel and ionizing radiation in an ovarian cancer cell line carrying a defective BRCA1. Oncogene, 22, (16) 2396-2404.

Zhou, J., Liu, H., Chen, Y., Wen, J., Li, L., and Wu, X. 2014. Expression and significance of VEGF, miR-205 and target protein Ezrin and Lamin A/C in ovarian cancer. Zhong.Nan.Da.Xue.Xue.Bao.Yi.Xue.Ban., 39, (2) 142-150.

Zhou, X., Zhao, F., Wang, Z. N., Song, Y. X., Chang, H., Chiang, Y., and Xu, H. M. 2012. Altered expression of miR-152 and miR-148a in ovarian cancer is related to cell proliferation. Oncology Reports, 27, (2) 447-454.

Zhu, X., Li, Y., Xie, C., Yin, X., Liu, Y., Cao, Y., Fang, Y., Lin, X., Xu, Y., Xu, W., Shen, H., and Wen, J. 2014. miR-145 sensitizes ovarian cancer cells to paclitaxel by targeting Sp1 and Cdk6. International Journal of Cancer, 135, (6) 1286-1296.

Zhu, Y., Huang, J. M., Zhang, G. N., Zha, X., and Deng, B. F. 2012. Prognostic significance of MyD88 expression by human epithelial ovarian carcinoma cells. Journal of Translational Medicine, 10, (1)